

2012 Atomic, Molecular, and Optical Sciences Research Meeting



**Bolger Conference Center
Potomac, Maryland
October 28-31, 2012**



U.S. DEPARTMENT OF
ENERGY

Office of
Science

Office of Basic Energy Sciences
Chemical Sciences, Geosciences &
Biosciences Division

Foreword

This volume summarizes the 32st annual Research Meeting of the Atomic, Molecular and Optical Sciences (AMOS) Program sponsored by the U. S. Department of Energy (DOE), Office of Basic Energy Sciences (BES), and comprises descriptions of the current research sponsored by the AMOS program. The participants of this meeting include the DOE laboratory and university principal investigators (PIs) within the BES AMOS Program. The purpose is to facilitate scientific interchange among the PIs and to promote a sense of program identity.

The BES/AMOS program is vigorous and innovative, and enjoys strong support within the Department of Energy. This is due entirely to our scientists, the outstanding research they perform, and the relevance of this research to DOE missions. FY 2012 has been an exciting year for BES and the research community. Continuing initiatives included the Early Career Research Program, the Energy Frontier Research Centers and the Energy Innovation Hubs. As illustrated in this volume, the AMOS community continues to explore new scientific frontiers relevant to the DOE mission and the strategic challenges facing our nation and the world.

We are deeply indebted to the members of the scientific community who have contributed their valuable time toward the review of proposals and programs, either by mail review of grant applications, panel reviews, or on-site reviews of our multi-PI programs. These thorough and thoughtful reviews are central to the continued vitality of the AMOS program.

We are privileged to serve in the management of this research program. In performing these tasks, we learn from the achievements of, and share the excitement of, the research of the scientists and students whose work is summarized in the abstracts published on the following pages.

Many thanks to the staff of the Oak Ridge Institute for Science and Education (ORISE), in particular Connie Lansdon and Tim Ledford, and to the Bolger Conference Center for assisting with the meeting. We also thank Diane Marceau, Robin Felder, and Michaelena Kyler-King in the Chemical Sciences, Geosciences, and Biosciences Division for their indispensable behind-the-scenes efforts in support of the BES/AMOS program. We also appreciate Mark Pederson's coordination of computational resources and interactions with related DOE program offices.

Jeffrey L. Krause
Michael P. Casassa
Chemical Sciences, Geosciences, and Biosciences Division
Office of Basic Energy Sciences
Department of Energy

Cover Art Courtesy of Bolger Conference Center

This document was produced under contract number DE-AC05-06OR23100 between the U.S. Department of Energy and Oak Ridge Associated Universities.

The research grants and contracts described in this document are supported by the U.S. DOE Office of Science, Office of Basic Energy Sciences, Chemical Sciences, Geosciences and Biosciences Division.

Agenda

2012 Meeting of the Atomic, Molecular and Optical Sciences Program
Office of Basic Energy Sciences
U. S. Department of Energy

Bolger Center, Potomac, Maryland, October 28-31, 2012

Sunday, October 28

3:00-6:00 pm **** Registration ****
6:00 pm **** Reception (No Host) ****
6:30 pm **** Dinner ****

Monday, October 29

7:30 am **** Breakfast ****

8:30 am *Welcome and Introductory Remarks*
Jeff Krause, BES/DOE

Session I Chair: **Lou DiMauro**

9:00 am *Attosecond Electron Dynamics in Atoms and Molecules*
Steve Leone, Lawrence Berkeley National Laboratory

9:30 am *Electron Correlation Effects in Intense Laser-Atom Processes*
Tony Starace, University of Nebraska

10:00 am *Probing Liquid Phase Molecular Dynamics with Ultrafast X-rays*
Bob Schoenlein, Lawrence Berkeley National Laboratory

10:30 am **** Break ****

11:00 am *Toward Controlled Electronic Dynamics in Complex Systems*
Tamar Seideman, Northwestern University

11:30 am *Seeded vs. SASE: Ultraintense X-ray Interactions in Atoms*
Linda Young, Argonne National Laboratory

12:00 noon *Nucleobase Photoprotection Studied by Soft X-rays*
Markus Gühr, SLAC National Accelerator Laboratory

12:30 pm **** Lunch ****

Session II Chair: **Anne Marie March**

- 4:00 pm *Strong-field Coherent Control of Molecules*
Brett Esry, Kansas State University
- 4:30 pm *Ultrafast Electron Diffraction from Aligned Molecules*
Martin Centurion, University of Nebraska
- 5:00 pm *Understanding and Controlling Strong-Field Laser Interactions with Polyatomic Molecules*
Marcos Dantus, Michigan State University
- 5:30 pm *Controlling Molecular Rotations of Asymmetric Top Molecules: Methods and Applications*
Vinod Kumarappan, Kansas State University
- 6:00 pm ***** Reception (No Host) *****
- 6:30 pm ***** Dinner *****

Tuesday, October 30

7:30 am ***** Breakfast *****

Session III Chair: **Dave DeMille**

- 8:30 am *Experiments in Ultracold Collisions and Ultracold Molecules*
Phil Gould, University of Connecticut
- 9:00 am *Reactive Scattering of Ultracold Molecules*
John Bohn, University of Colorado
- 9:30 am *Formation of Ultracold Molecules*
Robin Côté, University of Connecticut
- 10:00 am ***** Break *****
- 10:30 am *Combining Dissociative Ionization Pump Probe Spectroscopy and Ab Initio Calculations to Explore Excited State Dynamics in Polyatomic Molecules*
Spiridoula Matsika, Temple University
- 11:00 am *Imaging of Electronic Wave Functions during Chemical Reactions*
Pierre Agostini, Ohio State University
- 11:30 am *Correlated Electron Motion and Laser Dressing*
Chris Greene, University of Colorado
- 12:00 noon *First Principles Dynamics of Ultrafast Chemistry*
Todd Martinez, SLAC National Accelerator Laboratory
- 12:30 pm ***** Lunch *****

Session IV Chair: **Christian Buth**

- 4:00 pm *Spatial Frequency X-ray Heterodyne Imaging of Micro and Nano Structured Materials and their Time-resolved Dynamics*
Christoph Rose-Petruck, Brown University
- 4:30 pm *Photo-induced Molecular Transitions to the Continuum Investigated with the COLTRIMS Method*
Thorsten Weber, Lawrence Berkeley National Laboratory
- 5:00 pm *Imaging Molecules using Multi-particle Coincidence*
Allen Landers, Auburn University
- 5:30 pm *Capturing Electron Dynamics in Atoms and Molecules using VMI and COLTRIMS*
Henry Kapteyn and Margaret Murnane, University of Colorado
- 6:00 pm **** Reception (No Host) ****
- 6:30 pm **** Dinner ****

Wednesday, October 31

- 7:30 am **** Breakfast ****

Session V Chair: **Gilles Doumy**

- 8:30 am *Photoionizing Atoms inside a Fullerene Cage*
Ron Phaneuf, University of Nevada
- 9:00 am *Properties of Actinide Ions from Measurements of Rydberg Ion Fine Structure*
Steve Lundeen, Colorado State University
- 9:30 am *Molecular Scattering Aspects of HHG*
Erwin Poliakoff, Louisiana State University
- 10:00 am **** Break ****
- 10:30 am *Time-Resolved Studies of Energy Transfer in Luminescent Lanthanide Complexes*
Jerry Seidler, University of Washington
- 11:00 am *Optical Control of Metal Nanowires to Enable Single-Particle X-ray Diffraction*
Matt Pelton, Argonne National Laboratory
- 11:30 am *Closing Remarks*
Jeff Krause, BES/DOE
- 11:45 am **** Lunch ****
- 1:00 pm Discussion
- 3:00 pm Adjourn

Table of Contents

Laboratory Research Summaries (by Institution)

AMO Physics and Optical Control of Nanoparticles at Argonne National Laboratory	1
<i>Hidden Resonances and Nonlinear X-ray Processes at High Intensities</i> Elliot Kanter	2
<i>Pulse Duration Measurements at LCLS</i> Gilles Doumy	2
<i>Angle-resolved Measurement of Laser-assisted Auger Decay in Neon at LCLS</i> Gilles Doumy	3
<i>Seeded vs. SASE: Ultra High-Intensity, Hard X-ray Interactions with Atoms</i> Linda Young	4
<i>Ultrafast Absorption of Intense X-rays by Nitrogen Molecules</i> Christian Buth	5
<i>Time-dependent Resonance Fluorescence</i> Christian Buth	6
<i>Capturing Ultrafast Dynamics of Molecules with X-ray Absorption, X-ray Emission, and X-ray Scattering</i> Anne Marie March	7
<i>Time-Resolved X-ray Absorption and Emission Spectroscopy of Photoexcited Ferro-cyanide Ions in Aqueous Solution</i> Ann Marie March	8
<i>Laser-initiated Rearrangement of Bromiodomethane in Solution</i> Ann Marie March	9
<i>Progress toward the Short Pulse X-ray Facility at the Advanced Photon Source</i> Linda Young	10
<i>High-order Harmonic Generation Enhanced by X-rays</i> Christian Buth	10
<i>Optical Control of X-ray Lasing</i> Christian Buth	12
<i>Laser-Dressed Resonant Auger Decay Induced by X-rays</i> Steve Southworth	13

<i>Exploring Laser Aligned Molecules in Solution</i> Anne Marie March	14
<i>X-ray Scattering from Laser-Aligned Molecules – Experiment</i> Gilles Doumy	14
<i>Charge Redistribution and Ion Fragmentation in Deep Inner-shell Vacancy Decay</i> Bob Dunford	15
<i>Optical Control of Metal Nanowires to enable Single-particle X-ray Diffraction</i> Matt Pelton and Norbert Scherer	16
J.R. Macdonald Laboratory - Overview 2012	23
<i>Structure and Dynamics of Atoms, Ions, Molecules, and Surfaces: Molecular Dynamics with Ion and Laser Beams</i> Itzik Ben-Itzhak	25
<i>Structure and Dynamics of Atoms, Ions, Molecules and Surfaces: Atomic Physics with Ion Beams, Lasers and Synchrotron Radiation</i> Lew Cocke	29
<i>Strong-field Coherent Control of Molecules</i> Brett Esry	33
<i>Light-wave Control and Attosecond Tracing of Electron Dynamics in Atoms, Molecules and Nanosystems</i> Matthias Kling	37
<i>Controlling Rotations of Asymmetric Top Molecules: Methods and Applications</i> Vinod Kumarappan	41
<i>Strong Field Rescattering Physics and Attosecond Physics</i> Chii-Dong Lin	45
<i>Spatio-temporal Imaging of Light-induced Dynamics: From Strong-field Physics to Ultrafast Photochemistry</i> Artem Rudenko	49
<i>Structure and Dynamics of Atoms, Ions, Molecules and Surfaces: Atomic Physics with Ion Beams, Lasers and Synchrotron Radiation</i> Uwe Thumm	53
<i>Strong-Field Time-Dependent Spectroscopy</i> Carlos Trallero	57

Atomic, Molecular and Optical Sciences at Los Alamos National Laboratory	61
<i>Engineered Electronic and Magnetic Interactions in Nanocrystal Quantum Dots</i> Victor Klimov	61
Atomic, Molecular and Optical Sciences at LBNL	65
<i>Inner-Shell Photoionization and Dissociative Electron Attachment to Small Molecules</i> Ali Belkacem and Thorsten Weber	66
<i>Electron-Atom and Electron-Molecule Collision Processes</i> Tom Rescigno, Bill McCurdy, and Dan Haxton	70
Ultrafast X-ray Science Laboratory at LBNL	75
<i>Soft X-ray High Harmonic Generation and Applications in Chemical Physics</i> Oliver Gessner	75
<i>Ultrafast X-ray Studies of Condensed Phase Molecular Dynamics</i> Robert Schoenlein	77
<i>Time-Resolved Studies and Nonlinear Interaction of Femtosecond X-rays with Atoms and Molecules</i> Thorsten Weber and Ali Belkacem	78
<i>Attosecond Atomic and Molecular Science</i> Steve Leone and Dan Neumark	80
<i>Theory and Computation</i> Bill McCurdy, Martin Head-Gordon, and Dan Haxton	81
<i>Ultrafast X-ray Studies of Intramolecular and Interfacial Charge Migration</i> Oliver Gessner	87
 SLAC Ultrafast Chemical Science Program	 89
<i>ATO: High Harmonic Generation and Electronic Structure</i> Phil Bucksbaum and Markus Gühr	93

<i>NLX: Ultrafast X-ray Optical Science and Strong Field Control</i> David Reis	97
<i>NPI: Non-Periodic Imaging</i> Mike Bogan	100
<i>SFA: Strong-field Laser Matter Interactions</i> Phil Bucksbaum	104
<i>SFA: Solution Phase Chemical Dynamics</i> Kelly Gaffney	108
<i>UTS: Ultrafast Theory and Simulation</i> Todd J. Martínez	112
<i>Understanding Photochemistry using Extreme Ultraviolet and Soft X-ray Time Resolved Spectroscopy</i> Markus Gühr	115

University Research Summaries (by PI)

<i>Coherent Control of Electron Dynamics</i> Andreas Becker	119
<i>Probing Complexity using the LCLS and the ALS</i> Nora Berrah	123
<i>Reactive Scattering of Ultracold Molecules</i> John Bohn	127
<i>Ultrafast Electron Diffraction from Aligned Molecules</i> Martin Centurion	131
<i>Atomic and Molecular Physics in Strong Fields</i> Shih-I Chu	135
<i>Formation of Ultracold Molecules</i> Robin Côté	139
<i>Optical Two-Dimensional Spectroscopy of Disordered Semiconductor Quantum Wells and Quantum Dots</i> Steve Cundiff	143
<i>Understanding and Controlling Strong-Field Laser Interactions with Polyatomic Molecules</i> Marcos Dantus	147
<i>Picosecond X-ray Diagnostics for Third and Fourth Generation Synchrotron Sources</i> Matt DeCamp	151
<i>Production and Trapping of Ultracold Polar Molecules</i> Dave DeMille	155
<i>Spatial-temporal imaging during Chemical Reactions</i> Lou DiMauro and Pierre Agostini and Terry Miller	159
<i>Attosecond and Ultra-fast X-ray Science</i> Lou DiMauro and Pierre Agostini	163
<i>Ultracold Molecules: Physics in the Quantum Regime</i> John Doyle	167
<i>Atomic Electrons in Strong Radiation Fields</i> Joe Eberly	169

<i>Algorithms for X-ray Imaging of Single Particles</i> Veit Elser	173
<i>Reaction Imaging and the Molecular Coulomb Continuum</i> Jim Feagin	177
<i>Studies of Autoionizing States Relevant to Dielectronic Recombination</i> Tom Gallagher	181
<i>Experiments in Ultracold Collisions and Ultracold Molecules</i> Phil Gould	185
<i>Physics of Correlated Systems</i> Chris Greene	189
<i>Using Strong Optical Fields to Manipulate and Probe Coherent Molecular Dynamics</i> Bob Jones	193
<i>Molecular Dynamics Probed by Coherent Electrons and X-rays</i> Henry Kapteyn and Margaret Murnane	197
<i>Imaging Multi-particle Atomic and Molecular Dynamics</i> Allen Landers	201
<i>Properties of Actinide Ions from Measurements of Rydberg Ion Fine Structure</i> Steve Lundeen	205
<i>Theory of Atomic Collisions and Dynamics</i> Joe Macek	209
<i>Photoabsorption by Free and Confined Atoms and Ions</i> Steve Manson	213
<i>Combining High Level Ab Initio Calculations with Laser Control of Molecular Dynamics</i> Spiridoula Matsika and Tom Weinacht	217
<i>Electron-Driven Processes in Polyatomic Molecules</i> Vince McKoy	221
<i>Electron/Photon Interactions with Atoms/Ions</i> Alfred Msezane	225
<i>Theory and Simulations of Nonlinear X-ray Spectroscopy of Molecules</i> Shaul Mukamel	229
<i>Nonlinear Photoacoustic Spectroscopies Probed by Ultrafast EUV Light</i> Keith Nelson and Margaret Murnane	233

<i>Antenna-Coupled Light-Matter Interactions</i>	
Lukas Novotny	237
<i>Electron and Photon Excitation and Dissociation of Molecules</i>	
Ann Orel	241
<i>Low-Energy Electron Interactions with Liquid Interfaces and Biological Targets</i>	
Thom Orlando	245
<i>Structure from Fleeting Illumination of Faint Spinning Objects in Flight</i>	
Abbas Ourmazd and Peter Schwander	249
<i>Energetic Photon and Electron Interactions with Positive Ions</i>	
Ron Phaneuf	253
<i>Molecular Photoionization Studies of Nucleobases and Correlated Systems</i>	
Erwin Poliakoff and Robert Lucchese	257
<i>Control of Molecular Dynamics: Algorithms for Design and Implementation</i>	
Hersch Rabitz and Tak-San Ho	261
<i>Coherent and Incoherent Transitions</i>	
Francis Robicheaux	265
<i>Generation of Bright Soft X-ray Laser Beams</i>	
Jorge Rocca	269
<i>Spatial Frequency X-ray Heterodyne Imaging of Micro and Nano Structured Materials and their Time-resolved Dynamics</i>	
Christoph Rose-Petruck	273
<i>Toward Controlled Electronic Dynamics in Complex Systems</i>	
Tamar Seideman	277
<i>Inelastic X-ray Scattering under Extreme and Transitional Conditions</i>	
Jerry Seidler	281
<i>Dynamics of Few-Body Atomic Processes</i>	
Tony Starace	285
<i>Femtosecond and Attosecond Laser-Pulse Energy Transformation and Concentration in Nanostructured Systems</i>	
Mark Stockman	289
<i>Laser-Produced Coherent X-ray Sources</i>	
Don Umstadter	293

<i>New Scientific Frontiers with Ultracold Molecules</i>	
Jun Ye	297
Principal Investigator Index	299
Participants	301

Laboratory Research Summaries
(by institution)

AMO Physics and Optical Control of Nanoparticles at Argonne National Laboratory

Christian Buth, Gilles Doumy, Robert Dunford, Elliot Kanter,
Bertold Krässig, Anne Marie March, Steve Southworth, Linda Young

X-ray Science Division

Argonne National Laboratory, Argonne, IL 60439

cbuth@anl.gov, gdoumy@aps.anl.gov, dunford@anl.gov, kanter@anl.gov
kraessig@anl.gov, amarch@anl.gov, southworth@anl.gov, young@anl.gov

Matthew Pelton

Center for Nanoscale Materials

Argonne National Laboratory, Argonne, IL 60439

pelton@anl.gov

Norbert Scherer

Chemistry Department

University of Chicago, Chicago, IL 60637

nfschere@uchicago.edu

1 OVERVIEW

The Atomic, Molecular, and Optical Physics program aims at a quantitative understanding of x-ray interactions with atoms and molecules from the weak-field limit explored at the Advanced Photon Source (APS) to the strong-field regime accessible at the Linac Coherent Light Source (LCLS). Single photon x-ray processes can be dramatically altered in the presence of strong optical fields, and we exploit ultrafast x-ray sources to study these effects. Conversely, the atomic or molecular response to strong optical fields is itself of great interest due to the discovery of phenomena such as high-order harmonic generation and attosecond pulse generation. The use of tunable, polarized x-rays to probe such processes *in situ* can lead to new physical insights and quantitative structural information not accessible by other techniques. Theory is a key component of our program by predicting phenomena that motivate experiments and by simulating and interpreting measured results. Nonlinear and multiple-photon phenomena in x-ray and inner-shell interactions are explored using the intense, femtosecond x-ray pulses generated at the LCLS free-electron laser. The APS remains our primary source of intense, tunable, polarized x rays both for time-resolved laser-pump/x-ray-probe experiments and for basic studies of x-ray interactions with atoms, molecules, and complex systems such as solvated molecules. To exploit the full x-ray flux available at the APS, we are developing high-repetition-rate laser systems for pump-probe experiments at MHz pulse rates. This capability enables measurements of laser-induced, transient electronic and atomic structures with high sensitivity. High-repetition-rate techniques will also be exploited for pump-probe experiments with ~ 2 ps x-ray pulses that will be generated at Short Pulse X-ray (SPX) beamlines as a major component of the APS Upgrade project. Optical lasers can also trap, orient, and order nanoparticles, providing a new route towards manipulation and assembly of nanomaterials. X-ray diffraction is the only technique that has the capability of providing three-dimensional, *in situ* information about the structure, orientation, and arrangement of molecules and nanoparticles as they inter-

act with light. Hence, we are developing laser-control methods to manipulate nanoparticles in combination with x-ray imaging at the APS.

2 INTENSE X-RAY PHYSICS

Hidden resonances and nonlinear x-ray processes at high intensities

(E. P. Kanter, B. Krässig, R. Santra,^{1,2} S. H. Southworth, L. Young, J. Bozek³, L. DiMauro⁴, N. Berrah⁵, P. Bucksbaum⁶, D. Reis⁶)

The first experiments at LCLS all studied photon-matter interactions in a continuum, in principle, far removed from resonances [1, 2, 3, 4, 5, 15]. In this later followup study, we instead investigated resonant nonlinear x-ray processes in atomic Ne at high x-ray intensity. At high photon energies resonant absorption by inner-shell electrons dominates all x-ray photoprocesses, with cross sections $\sim 100\times$ greater than those for non-resonant valence ionization. On an inner-shell resonance, absorption/stimulated emission cycles (Rabi flopping) can be the dominant photoinduced process and resonances can be used to enhance x-ray multiphoton processes. At photon energies less than the binding energy of the 1s electron, resonant two-photon absorption has a significantly larger cross section than non-resonant two-photon absorption; though both generate the same final state of the system - an atom with a 1s hole plus an s- or d- wave photoelectron. Capitalizing on this resonance phenomenon, we studied two-photon absorption in neon at 848 eV, where, as we demonstrated in a recent publication [16], the first photon ionizes the Ne 2p electron and the second photon excites the Ne⁺ 1s-2p resonance. Ne⁺ 1s⁻¹ *K-LL* Auger electrons are the signature of this resonant two-photon creation of a 1s hole. This generation of a 2p hole orbital is advantageous for observing/studying the Rabi-cycling phenomenon; the Ne⁺ 1s-2p dipole matrix element is $5.6\times$ larger than that for the 1s-3p transition in Ne.

We followed the response of the neon atom on this two photon resonance at 848 eV as a function of x-ray FEL pulse duration. For short x-ray pulses, the signature of 1s hole creation is weak, but as the pulse width is raised, the Auger line appears and, at high intensity, is broadened as Rabi-oscillations become important in comparison to the normal diagram line (¹D) measured far above threshold. Indeed, as expected for the 1s-3p transition, no such broadening was detected. In addition to demonstrating the ability to control an inner-shell decay process, this work has important ramifications for the broader XFEL community. We have discovered previously unexplored x-ray resonances in ionic species created by the high fluence of the LCLS beam. Such resonances, with consequently large cross sections, can contribute significantly to unexpected sample damage in all experiments at such x-ray intensities and merits further study. We plan further studies aimed at exploring such sample damage in heavier systems with seeded beams.

Pulse duration measurements at LCLS

(G. Doumy, S. Düsterer,⁷ A. L. Cavalieri,¹ M. Meyer,⁸ R. Keinberger⁹ and other collaborators)

The LCLS x-ray free electron laser is capable of producing very intense x-ray pulses believed to be as short as a few tens of femtoseconds. Those properties have already revolutionized the field of ultrafast time resolved x-ray science, in spite of the current lack of exact determination of the pulse duration characteristics. Any measuring scheme is rendered even more challenging by the SASE (Self Amplified Spontaneous Emission) operating mode of LCLS, which makes it a purely chaotic source and ultimately requires a single shot measurement of every shot to get a full characterization of the source properties. In addition, the SASE operation produces an inherent temporal jitter between the x-ray pulses and any other laser source operating in parallel, which limits greatly the resolution of pump-probe techniques commonly used in time-resolved measurements.

The main route followed by our large collaboration to get a handle on those properties consists in transferring the time properties of the x-ray pulses to electron wave-packets produced during

ionization of a gas target or subsequent Auger decay. The simultaneous presence of a strong laser field (operating in the visible, IR or THz region) modifies the energy spectrum of those electrons wave-packets in a deterministic way. It is then possible to extract from the measured final energy distribution some of the properties of the x-ray pulses, as well as the jitter between the x-rays and the strong laser field.

In the case of a long x-ray pulse duration compared to the oscillation of the laser electric field, only statistical information can be obtained. Such an experiment was made using Auger electrons from Neon atoms after *K*-edge ionization, with a laser operating at 800 nm. The main conclusion of the study is that the laser-x-ray timing jitter is significant (~ 150 fs) and that the x-ray pulse duration is on average significantly shorter than the electron bunch duration used to generate the x-ray pulses in the XFEL, e.g., 120 fs instead of 175 fs [17].

When the x-ray pulse duration is comparable with (or shorter than) the oscillation period of the laser, it is possible to use a streaking mode, where there is a one-to-one correspondence between the measured photoelectron energy and the time of emission. This method can in principle yield single-shot, every-shot temporal characterization, and was tested with the LCLS operating in its low bunch-charge mode, where the pulses are expected to be less than 5 fs, using an IR laser operating at 2.4 microns. Unfortunately the timing jitter limits the technique by making it impossible to know the exact field conditions when the streaking happens. Statistical information on an upper value of the pulse duration can nonetheless be extracted, which confirmed that the pulse duration was indeed less than 4 fs [30].

The jitter limitation is essentially eliminated when using a laser-derived single cycle terahertz source, due to its much longer period. First attempts at using this method at LCLS have demonstrated its potential for a large range of pulse durations, but the resolution is currently experimentally limited to approximately 50 fs. This version of the technique not only gives access to the pulse duration, but also to the shot-to-shot timing relative to the laser used to generate the THz radiation.

The behavior of the LCLS x-ray free electron laser can be exquisitely tuned by careful manipulation of the electron beam characteristics before it enters the row of undulators to create the x-ray pulses. In particular, a clever way to vary the x-ray pulse duration consists in inserting a slotted foil in one of the bunch compressors where the electron bunch is spread transversely. The part of the electron beam that goes through the slot is unmodified and participates in lasing as usual, while the rest experiences a spoiled emittance and does not participate in the subsequent lasing process. This should allow continuous variation of the pulse duration.

In addition, a foil with two slots exists, which should allow for creating two x-ray pulses with a fixed, but adjustable, delay. A full characterization of such a system is nonetheless necessary, since it is not known whether two pulses are always created, or what their relative strength is, and any integrated measurement (e.g. total energy) would be unable to provide any insight into it. Terahertz streaking, as described above, would be a good way to access those properties on every shot. Three shifts of beamtime have been awarded in December 2012 for such measurements.

Angle-resolved measurement of laser-assisted Auger decay in neon at LCLS

(G. Doumy, M. Meyer,⁸ N.M. Kabachnik,⁸ A. L. Cavalieri,¹ and other collaborators)

When a gas target is ionized by a short, intense x-ray pulse like the ones produced at the LCLS, in the presence of a strong laser field, sidebands are known to appear in the electron spectrum. These sidebands arise due to interaction of the photo- or Auger electrons with the laser field and are associated with absorption or emission of a few ir photons by the outgoing electrons. For the decay of an inner-shell vacancy, this phenomenon is known as laser-assisted Auger decay (LAAD).

In experiments realized at LCLS [24] on the *K-LL* Auger decay in Neon in the presence of an

the simple second-row elements, e.g. neon, in that intermediate electron shells can be addressed selectively. In this photon energy regime at ultrahigh intensities, broadband SASE pulses are predicted to initiate then facilitate chain reaction ionization via successive resonance excitation, whereas narrowband seeded pulses cannot. Understanding electron dynamics in transition metal atoms is also of vital importance for establishing the reliability of multiple wavelength anomalous dispersion (MAD) phase retrieval methodologies at high intensity. Therefore, we plan to characterize ultraintense x-ray interactions with nickel atoms using ion time-of-flight and x-ray emission spectroscopies for three relevant photon energy regimes as a function of bandwidth, pulse energy, and pulse duration. The nickel atom is an ideal target as the range for self-seeded LCLS operation (7.1–9.5 keV) spans the nickel K -edge (8.333 keV).

Ultrafast absorption of intense x rays by nitrogen molecules

(C. Buth, J.-C. Liu,¹² M. H. Chen,¹³ R. N. Coffee,³ N. Berrah,⁵ and other collaborators)

We study theoretically nitrogen molecules (N_2) in ultrashort and intense x rays from the free electron laser (FEL) Linac Coherent Light Source (LCLS). Specifically, we examine ion yields and the average charge state and compare with experimental data from LCLS. The description of the interaction is set out from atomic rate equations. The equations are formulated using all one-x-ray-photon absorption cross sections and the Auger and radiative decay widths of multiply-ionized nitrogen atoms. We use a series of phenomenological models reaching beyond a single atom: first, symmetric sharing of charges is considered; second, a fragmentation matrix model is developed [Fig. 2a] and Ref. [25]. The hints from these models are used to devise a third model based on molecular rate equations which are centered around the formation and decay of single and double core holes, the metastable states of N_2^{2+} , and molecular fragmentation [Fig. 2b]. The crucial role of the progression in the actual pulse energy is revealed, the lifetime of the metastable states is approximately found, and the role of double core holes and charge redistribution are exhibited.

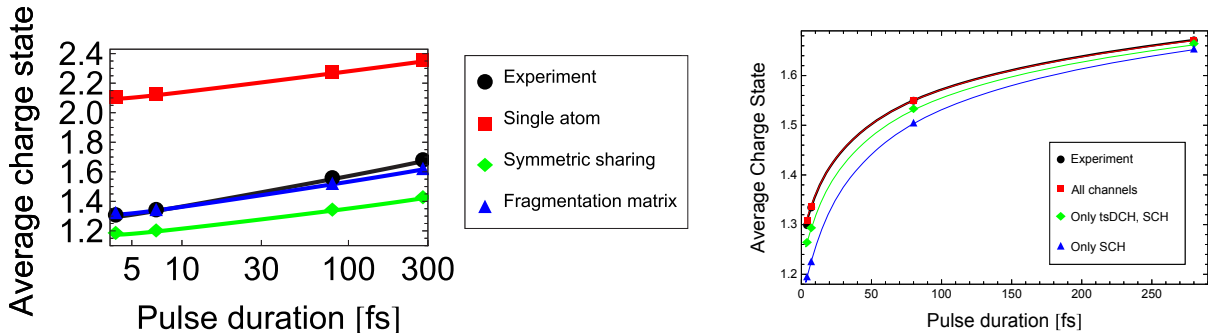


Figure 2: Average charge state of nitrogen molecules (N_2) in ultrafast and intense x rays. (a) Single-atom, symmetric sharing, and fragmentation-matrix models compared with experimental data. Actual LCLS pulse energies are fractions of the nominal pulse energy of 0.26 mJ: 31% (280 fs), 25% (80 fs), 16% (7 fs) and for 0.15 mJ: 26% (4 fs). Figure adapted from Ref. [25]. (b) Molecular rate equation model compared with experimental data involving all channels [single core holes (SCHs), double core holes on a single site (ssDCHs) and on two sites (tsDCHs)] and only a subset. Actual pulse energies are of 0.26 mJ: 38% (280 fs), 30% (80 fs), 16% (7 fs) and of 0.15 mJ: 24% (4 fs).

Further, we study nuclear dynamics induced by multiple ionization in N_2 [33]. We use the fact that the intense LCLS pulses cause multiple core-level photoabsorption with subsequent Auger decay processes. The timing dynamics of the photoabsorption and dissociation processes is mapped onto the kinetic energy of the fragments. This allows us to find the average internuclear separation

for molecular photoionization steps and obtain the average time interval between the photoabsorption events. Using multiphoton ionization as a tool of intrapulse pump-probe scheme, we demonstrate the change in the progression of the ionization and nuclear dynamics as we vary the LCLS pulse duration.

Time-dependent resonance fluorescence

(S. M. Cavaletto,¹⁴ C. Buth, Z. Harman,¹⁴ E. P. Kanter, S. H. Southworth, L. Young, and C. H. Keitel¹⁴)

Resonance fluorescence is one of the cornerstones of quantum optics. The spectrum of resonance fluorescence is experimentally measured by detecting the energy distribution of photons that are scattered by an ensemble of atoms or ions driven by a near-resonant electric field. The simplest case, namely a two-level system driven by monochromatic light, has been extensively studied at optical frequencies. In this case, nonlinear effects such as dynamic Stark splitting take place for strong driving: the intense driving field induces Rabi oscillations of the atomic system, whose frequency is related to the intensity of the field itself. This nonlinear effect clearly manifests itself in the so-called Mollow triplet in the spectrum of resonance fluorescence for continuous-wave light.

For x-ray transitions the ultrafast nature of Auger decay and the lack of sufficiently intense x-ray radiation sources represented for long time an obstacle to the study of strong-field effects at short wavelengths. Emerging x-ray sources of unprecedented brilliance such as the Linac Coherent Light Source (LCLS), the first x-ray Free Electron Laser (FEL), induce nonlinear phenomena at x-ray frequencies and, in particular, Rabi flopping, for whose demonstration resonance fluorescence represents a good candidate. The measurement and understanding of x-ray Rabi oscillations is an important step towards x-ray control of inner-shell dynamics. Present FELs based on the Self-Amplified Spontaneous Emission (SASE) principle produce ultrashort pulses with a chaotic shape. The recent development of optical laser- and self-seeding methods improves the coherence properties of the pulses.

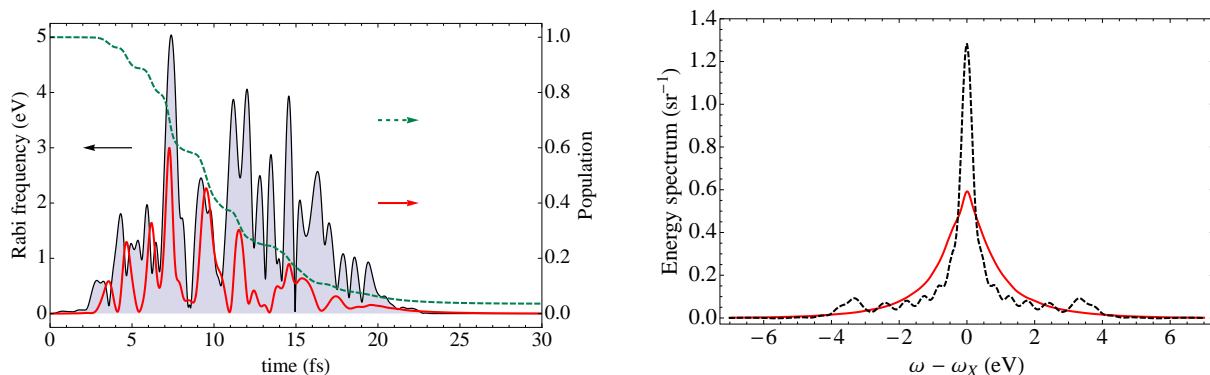


Figure 3: Calculated evolution in time for Ne^+ ions driven by a single SASE pulse tuned to the $1s2p^{-1} \rightarrow 1s^{-1}2p$ resonance at 848 eV. The black, solid line shows the instantaneous Rabi frequency, the red, solid curve the population of the excited level and the green, dashed curve the total population of the two-level system. (b) Resonance fluorescence energy spectrum: the red, solid curve is the average spectrum over 500 SASE pulses of intensity $I = 1.5 \times 10^{17} \text{ W/cm}^2$, the black, dashed curve is the spectrum obtained by driving the system with a single, coherent, Gaussian pulse of intensity $I = 2.6 \times 10^{17} \text{ W/cm}^2$.

In Ref. [27], we develop a four-level model to describe the interaction of an atomic system with time-dependent pulses, by further including spontaneous decay of the excited level and destruction processes of the system such as Auger decay and photoionization. We apply the model to compute

the spectrum of resonance fluorescence of Ne^+ ions driven by strong x rays tuned to the transition at 848 eV [16]. The Auger-decay width is 0.27 eV, i.e., the Auger decay of the system takes place in a few femtoseconds.

For SASE pulses, we plot in Fig. 3a a possible realization of the time-dependent pulse (black line) and the corresponding evolution in time of the system (total population as the green line, population of the excited state as the red one). The evolution of the system and the oscillations, which appear as the red line, are related both to the chaotic nature and to the high intensity of the field. This gives rise to the average spectrum for 500 independent SASE pulses, which is depicted in Fig. 3b as the red line. The predicted width of the resonance fluorescence spectrum is larger than the natural width of the system, which would be measured at synchrotron facilities: this increased width is a consequence of Rabi oscillations induced by the intense x rays. A clearer signature of Rabi flopping is predicted for coherent x-ray pulses. The obtained multipeak spectrum, shown in the black line in Fig. 3b, displays frequency contributions clearly related to the Rabi oscillations induced by the external field [32].

Combining x rays with an optical laser offers prospects for controlling the interaction with the x rays. A large amount of such coherent phenomena were studied and observed in three-level systems of V-, Λ -, and Ξ -type. This supports us in investigating the effects induced in the emitted x-ray resonance fluorescence spectrum by the presence of an optical driving field, such as for example an optical frequency comb. We explore possibilities to imprint the properties of optical pulses onto the x-ray spectrum of resonance fluorescence. First results of optical control and modification of the x-ray spectrum are encouraging. Furthermore, our schemes of resonance fluorescence may also offer a way for the retrieval of SASE pulse properties.

3 X-RAY PROBES OF MOLECULAR DYNAMICS

Capturing ultrafast dynamics of molecules with x-ray absorption, x-ray emission, and x-ray scattering

(A. M. March, G. Doumy, E. P. Kanter, S. H. Southworth, R. W. Dunford, D. Ray, L. Young, M. K. Haldrup,¹⁵ G. Vankó,¹⁶ W. Gawelda,⁸ M. M. Nielsen,¹⁵ C. Bressler,⁸ and other collaborators)

With an international collaboration of experts in the use of x-ray absorption (XAS), x-ray emission (XES), and x-ray diffuse scattering (XDS) techniques, we studied the dynamics of Fe(II) spin crossover molecules in solution, utilizing the full flux of the APS storage ring by carrying out pump-probe experiments at 3.26 MHz. Our setup (see Fig. 4) combined a crystal spectrometer (for XES), a fast scintillator (for XAS), and a gateable area detector (for XDS) and made use of our high repetition rate laser system and x-ray microprobe setup at 7ID-D [21]. We successfully demonstrated simultaneous acquisition of time-resolved XES and XAS data and of XES and XDS data. Acquisition of time-resolved data using the flux demanding techniques of XES and XDS was made possible by our efficient use of the available flux at the APS.

The molecules studied, $[\text{Fe}(\text{bipy})_3]^{2+}$ and $[\text{Fe}(\text{terpy})_2]^{2+}$ in aqueous solution, reside in a low-spin ground state. Upon absorption of an optical photon, they undergo a spin-state transition to a short-lived high-spin state. Time-resolved XAS and XES were sensitive to the electronic configuration changes between the low-spin ground state and the high-spin excited state, while time-resolved XDS revealed the structural changes accompanying this transformation. The time scales for the dynamics of the excited state decay measured by the three techniques were found to be in excellent agreement. XES was used to extract a reliable excited state fraction, which provided an additional constraint for the fitting routines used to analyze the XDS data. In addition to the expected increase in the Fe-N bond length between ground state and excited state, the scattering data revealed sensitivity to changes in the solvent cage following laser excitation of the solute molecule. An in-

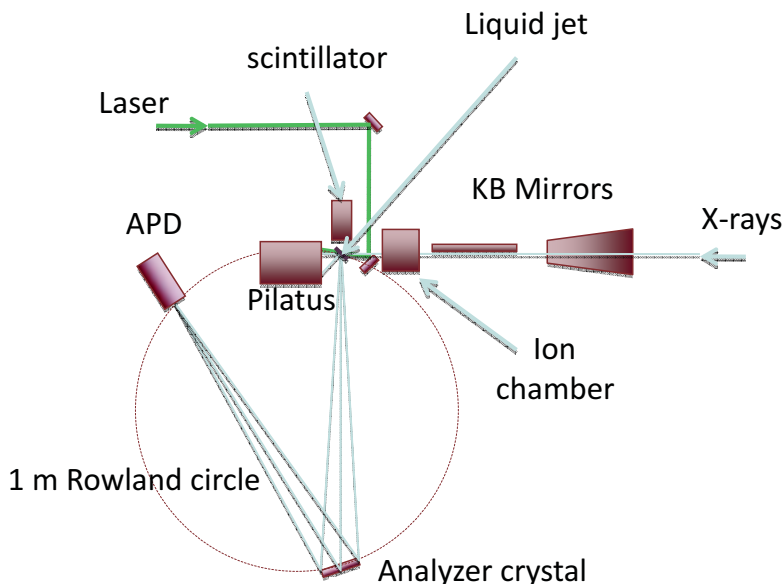


Figure 4: Experimental setup for measurements of time-resolved x-ray absorption, x-ray emission, and x-ray scattering from laser-pumped aqueous solutions of the spin crossover molecules $[\text{Fe}(\text{bipy})_3]^{2+}$ and $[\text{Fe}(\text{terpy})_2]^{2+}$. See Refs. [34, 35].

crease in the bulk solvent density on the 100 ps time scale was observed, and comparison with DFT and MD computations indicates it may be due to the expulsion of ~ 2 water molecules from the solvent shell into the bulk solvent following the conversion of the solute molecule to the HS state. The finding that such dynamics can be directly investigated by diffuse x-ray scattering underscores the new possibilities opened up by increasing the available x-ray flux by orders of magnitude, as well as the benefits of using a “tickle and probe” approach, where smaller laser pulse energies are used for the pump pulse, thus not drowning out small signals by thermal effects. These results have recently been submitted for publication [34]. Details of the XES measurements, including time-resolved resonant inelastic x-ray scattering (RIXS) data, will also be published [35].

Time-resolved x-ray absorption and emission spectroscopy of photoexcited ferrocyanide ions in aqueous solution

(A. M. March, G. Doumy, S. H. Southworth, E. P. Kanter, B. Krässig, R. W. Dunford, D. Ray, L. Young, A. Galler,⁸ A. Bordage,¹⁶ C. Bressler,⁸ B. Vankó,¹⁶ and W. Gawelda⁸)

As a continuation of our work with our international collaborators, we will develop a versatile time-resolved x-ray emission spectroscopy (XES) setup using the previously developed high repetition rate setup at 7ID-D for studies of photochemical processes in condensed phase molecular systems. The aim is to expand the time-resolved XES techniques we demonstrated with the measurements on Fe(II) spin-crossover complexes, namely $K\alpha$ (1s-2p) and $K\beta_{1,3}$ (1s-3p) spectroscopy, to include the even more flux demanding valence-to-core spectroscopies, $K\beta''/K\beta_{2,5}$. In the case of Fe, $K\beta$ XES, both $K\beta_{1,3}$ and $K\beta''/K\beta_{2,5}$ (valence to core) have been shown to be sensitive to the electronic configuration (3p-3d exchange correlation, spin, oxidation state) and also to ligand properties (identity, hybridization and protonation). Static measurements have been compared with DFT calculations to yield quantitative results. Time-resolved measurements have not been carried out due to inefficient use of 3rd generation synchrotron flux. We will study the dynamics of a model system $[\text{Fe}(\text{II})(\text{CN})_6]^{4-}$ (ferrocyanide) in an aqueous solution after laser excitation using

x-ray absorption spectroscopy (XAS) and x-ray emission spectroscopy (XES). We will study the system with 10 ps laser pulses at 355 nm, where the photoexcited state evolves into the pentacyano-aquo complex $[\text{Fe}(\text{II})(\text{CN})_5\text{H}_2\text{O}]^{3-}$ via ligand dissociation, and also at 266 nm where the excited state can lead to photoinjection of an electron into the solvent, concomitant to the oxidation state change of the iron center, yielding $[\text{Fe}(\text{III})(\text{CN})_6]^{3-}$. The aim is to gain better insight into the ligand abstraction and charge injection processes that take place in the ferrocyanide system.

Laser-initiated rearrangement of bromiodomethane in solution

(A. M. March, G. Doumy, E. P. Kanter, L. S. Cederbaum,¹⁷ N. Kryzhevoi,¹⁷ C. Buth, and S. H. Southworth)

Halomethanes have warranted a great deal of study due to their role in the earth’s atmospheric ozone depletion, but also due to their relative simplicity that makes them model systems to study photochemistry upon laser excitation. In particular, CH_2BrI , with its two different carbon-halogen bonds, is a model system for studying selective bond dissociation upon electronic excitation. By exciting the molecules with laser light at 266 nm, we can selectively break the carbon-iodine bond. Previous studies, both experimental and theoretical, indicated that a major path of recombination involves the formation of iso- $\text{CH}_2\text{Br-I}$, where the iodine atom attaches to the bromine atom of the CH_2Br radical. Identifying this major structural change, and studying the effect of the solvent on the structure and the kinetics, is a problem for which ultrafast x-ray probes are ideally suited, due to their ability to provide atomic scale resolution as well as ultrashort time resolution.

We have implemented fourth harmonic generation (266 nm) of our high repetition rate DUETTO laser situated at Sector 7ID-D at the APS. This has allowed us to efficiently excite CH_2BrI in solution at a repetition rate of 592 kHz and 384 kHz. In combination with our fast flowing liquid jet, this ensures that each x-ray shot probes a fresh region of sample, which is necessary due to the production of irreversible photoproducts at every shot. We were able to perform time resolved x-ray absorption spectroscopy (TR-XANES) both at the Br K -edge and at the I L_1 -edge. Experiments were done using three different solvents (ethanol, acetonitrile and cyclohexane) of diverse properties in order to examine the effect of solvation on the dynamics of molecular recombination. A clear transient signal is observed on the pre-edge region in all solvents, but identification of the species responsible for this transient feature is difficult. The leading hypothesis attributes the measured signals to the production and disappearance of the two radicals resulting from the bond cleavage. Dynamics of recombination are complex and depend significantly on the nature of the solvent (polarity, proticity).

The experimental investigation of the laser-initiated rearrangement of bromiodomethane in solution poses interesting questions for theory. As a first problem, there is the identification of some of the intermediate products and byproducts in the x-ray absorption spectrum of CH_2BrI . In order to gain deeper insights in the absorption spectrum of CH_2BrI , we have performed state-of-the-art quantum chemical computations on ground-state CH_2BrI and the CH_2Br radical to determine the lowest lying core-excitation energies and oscillator strengths. This will yield the x-ray absorption cross section in the pre-edge region. The computations are centered on a restricted-active space (RAS) description of the compounds for the ground state and the lowest-lying core excited state that include all valence electrons of the compounds and all electrons of the bromine atom. The RAS wave function model is then used as a basis to perform a multireference configuration interaction (MRCI) computation to yield higher accuracy and higher lying excited states. Particular (computational) challenges in the project are an accurate treatment of many-electron effects, scalar relativistic effects, and spin-orbit splitting.

Progress toward the Short Pulse X-ray Facility at the Advanced Photon Source

(L. Young, P. Evans,¹⁸ E. Dufresne, Y. Li, D. Keavney, R. Reininger, S. H. Southworth, G. Doumy, A. M. March, D. A. Reis,⁶ Ch. Bressler,⁸ L. X. Chen,¹⁹ S. Johnson,²⁰ A. Lindenberg,²¹ H. Dürr,²¹ D. Fritz³)

The Short Pulse X-ray Facility (SPX) at the Advanced Photon Source (APS) is designed to provide high-average-flux, tunable, polarized x-ray pulses of \sim picosecond duration at a repetition rate of 6.5 MHz in both the hard and soft x-ray regimes. The flux scales linearly with pulse duration; presently with 100 ps pulses at a storage ring current of 100 mA the monochromatic flux ($\Delta E/E \sim 0.5 \times 10^{-5}$) is $\sim 10^{13}$ photons/s at 10 keV. Due to the advantageous timing structure of the APS, 24 bunches spaced by 153 ns, the entire x-ray flux is readily usable for time-domain studies, in contrast to other US synchrotron light sources with interpulse spacings of ~ 2 ns. Short pulses are produced by introducing a vertical chirp to the electron pulses with an rf cavity and removing the chirp in a second cavity downstream by 2 sectors. Feedback to these cavities to ensure that the electron orbit around the remainder of the ring is unperturbed will be derived from 360 independent beam monitors; achievement of this degree of control in a storage ring is unprecedented.

Three independently operating beamlines (and 6 endstations) are initially envisioned: a) the hard x-ray scattering and spectroscopy beamline, fully tunable between 4.5–35 keV with adjustable bandwidth (10^{-4} – 10^{-2}), pulse duration (2–100 ps), repetition rate (6.5 MHz, 271 kHz, 5 kHz) and focal spot size ($\sim 5 \mu\text{m}$); b) hard x-ray imaging and microscopy beamline which captures the full fan of the time-dispersed radiation (1 mrad) over a photon energy range ~ 5 –25 keV and allows exploration of novel techniques such as time-dispersed diffractive imaging, in addition to a microscope with spotsize of ~ 100 nm; c) soft x-ray spectroscopy beamline on a bending magnet (200–2000 eV, $\Delta E/E \sim 0.5 \times 10^{-3}$, 1–10 ps, rapidly switchable circular polarization, 10 μm spotsize).

This year, preliminary design of these beamlines within the context of the APS Upgrade has proceeded. This has included optical ray tracing for the beamlines, specification of the x-ray optical components and associated instrumentation, such as specialized pump lasers, detectors, and a zone-plate based microscope.

An initial version of the SPX, dubbed SPX0, is scheduled for installation in early 2014. This affords the opportunity to perform ~ 10 picosecond experiments at multiple locations around the storage ring and the first test of synchronization and pulse characterization using a variety of techniques.

4 CONTROL OF X-RAY AND INNER-SHELL PROCESSES

High-order harmonic generation enhanced by x rays

(C. Buth, M. C. Kohler,¹⁴ F. He,¹⁴ J. Ullrich,¹⁴ J.-C. Liu,¹² K. Z. Hatsagortsyan,¹⁴ and C. H. Keitel¹⁴)

We consider high-order harmonic generation (HHG) in simultaneous intense near-infrared (NIR) laser light and brilliant x rays (see Fig. 5). The impact of the x rays on HHG is studied for two cases: first, HHG light is produced by an initial tunnel ionization of a valence electron; it propagates in the continuum and eventually recombines with the hole under emission of a high-harmonic photon. The x rays, e.g., from the Linac Coherent Light Source (LCLS), are tuned to resonantly excite a core electron into the transient valence vacancy that is created in the course of the HHG process. Depending on the probability to find the core electron in the valence and the core, the returning continuum electron recombines with the valence and the core, emitting HHG radiation that is characteristic for the combined process. We devise a two-electron quantum theory for a single atom assuming no Coulomb interaction between the two electrons. The theory has been applied to krypton on the $3d \rightarrow 4p$ resonance and to neon on the $1s \rightarrow 2p$ resonance in the respective cations.

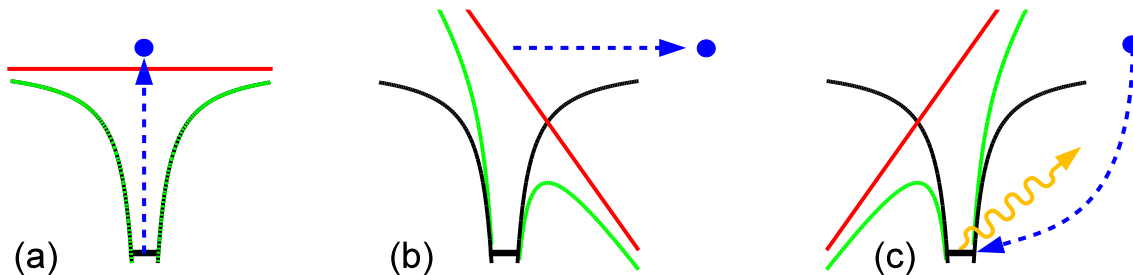


Figure 5: Schematic of the three-step model for the HHG process modified by x-ray induced ionization of a core electron: (a) x-ray absorption ejects a core electron (b) which is subsequently driven through the continuum by the NIR light; (c) upon returning to the parent ion it may recombine with the core hole and release its excess energy in terms of a high harmonic of the NIR laser plus the x-ray photon energy. The NIR laser has only a noticeable influence on continuum electrons and barely influences core electrons. The converse holds true for the interaction with the x rays.

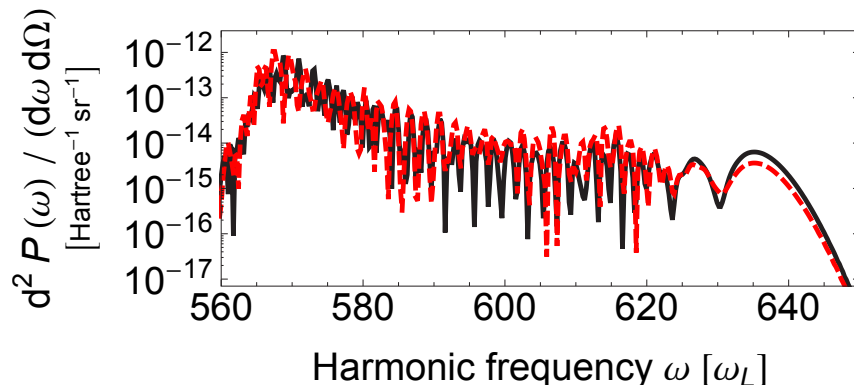


Figure 6: Harmonic photon number spectra (HPNS) for Ne 1s core electrons using two SASE pulses. The solid, black line is from the black SASE pulse and the dashed, red line from the red pulse. The x-ray intensity was chosen such that the ionization rate is the same as the tunnel ionization rate by the NIR laser. The NIR laser vector potential has a cosine square pulse envelope with a FWHM duration of 1.5 optical cycles and a peak intensity of 7×10^{14} W/cm² for 800 nm central wavelength.

HHG light of about kiloelectronvolt photon energy has been generated in the latter case with an efficiency that is comparable to HHG from the valence electrons at 10^{16} W/cm² x-ray intensity in both cases [26, 18].

Second, we consider HHG by a NIR laser with x rays tuned above an inner-shell absorption edge. Thereby, a tightly bound inner-shell electron is transferred into the continuum. Then, NIR light takes over and drives the liberated electron through the continuum until it eventually returns to the cation leading in some cases to recombination and emission of a high-harmonic photon that is upshifted by the x-ray photon energy. In contrast to the previous case, a single-active electron theory adequately describes this scenario that takes into account the destruction of the system by the NIR and x-ray light. We apply it to 1s electrons of neon atoms and obtain HHG spectra for different SASE x-ray pulses (see Fig. 6). A time-frequency analysis reveals the changes in the emission process due to the different x-ray pulse structure. The x-ray boosted high harmonic light is used to generate a single attosecond pulse in the kiloelectronvolt regime.

Estimates of the phase matching conditions in a macroscopic medium indicate that HHG with

x rays provides a high photon yield for suitably chosen NIR laser and x-ray parameters. A detailed one-dimensional pulse propagation is under investigation. It is based on a solution of the Maxwell equations [43] where propagation equations for the NIR, FEL x rays, and high harmonic light are used. The x-ray-boostered single-atom dipole moment is employed as a source term. As HHG is the basis of attoscience and x-ray sources, our prediction opens perspectives for nonlinear x-ray physics, attosecond x rays, and HHG-based spectroscopy involving core orbitals.

Optical control of x-ray lasing

(G. Darvasi,¹⁴ C. H. Keitel,¹⁴ and C. Buth)

X-ray free-electron lasers (FELs) have a large impact on x-ray science by achieving femtosecond pulses with unprecedented intensities. However, present-day facilities have a number of shortcomings, namely, their radiation has a chaotic pulse profile and short coherence times. A scheme for a neon-based atomic inner-shell x-ray laser (XRL) was proposed, and x-ray lasing has been predicted to occur when intense x rays from an x-ray free electron laser core-ionize atoms [44]. Recent measurements at the Linac Coherent Light Source (LCLS) confirm these theoretical predictions [45] In core-ionized atoms, electrons in higher-lying shells may fill the core vacancy and in the course of this emit x rays spontaneously. During the copropagation of a beam of FEL radiation and spontaneously emitted x rays through a macroscopic medium, the spontaneously emitted radiation stimulates emission, i.e., lasing in the x-ray regime.

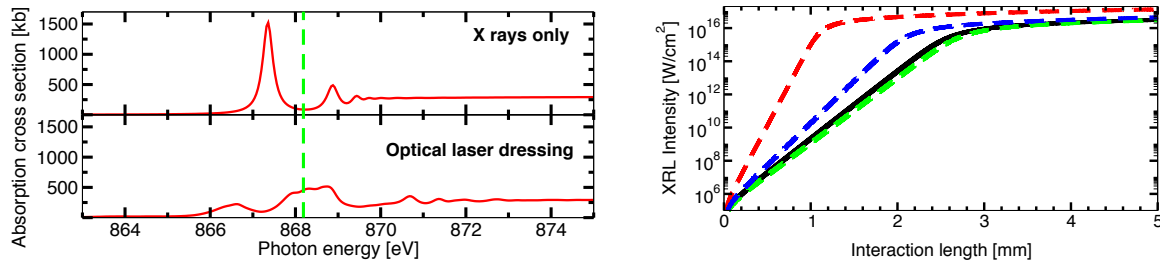


Figure 7: (a) X-ray photoabsorption cross section of neon near the K edge with optical laser dressing and without it. Here, θ_{LX} is the angle between the polarization vectors of the optical laser and the x rays. The optical laser operates at a wavelength of 800 nm and an intensity of 10^{13} W/cm². (b) Output of x-ray lasing in neon depending on the propagation distance in the medium and the relative position of the optical laser pulse with respect to the FEL x rays. Please see Ref. [31] for details.

Based on this FEL-x-ray-only scheme, we propose an optically controlled XRL that produces temporally and spatially coherent, sub-femtosecond pulses that are controlled by and synchronized to an optical laser with femtosecond precision. The optical laser is used to modify the x-ray absorption cross section in a way that absorption is substantially enhanced for a chosen x-ray energy when the optical laser is present [38, 6] and has the x-ray photon energy indicated by the green-dashed line in Fig. 7a. Then, the degree of core ionization and thus x-ray lasing depends on the presence of the optical laser, and x-ray lasing is controlled by it.

We have investigated optical control of x-ray lasing in Ref. [31]. Our study demonstrates the ability to optically control an XRL. Sample outputs are shown in Fig. 7b for a series of overlaps between the x-ray pulse and the optical pulse. This allows one to spatially structure x-ray laser pulses by a spatially structured optical laser pulse. Furthermore, attosecond x-ray pulses can be generated by a nonlinear compression of the FEL x-ray pulse during the propagation in the medium. We envision that our XRL will enable one to control atomic and molecular dynamics in two-color pump-probe experiments.

Laser-dressed resonant Auger decay induced by x rays

(A. Picón, G. Doumy, B. Krässig, S. H. Southworth, and C. Buth)

An intense optical laser may have considerable influence on x-ray transitions [38, 6] and was shown to induce a multipeak structure in the Auger electron spectrum, the so-called sidebands, due to a laser-dressed continuum. Several studies have already proven the fundamental character and importance of laser-dressed Auger decay in attosecond science and in x-ray pulse duration characterization at free electron lasers. Laser-dressed resonant Auger decay, however, has not received similar attention. In this case, the optical field may resonantly couple two core-excited states in the Rydberg manifold as well as laser-dress the continuum, as indicated in Fig. 8a.

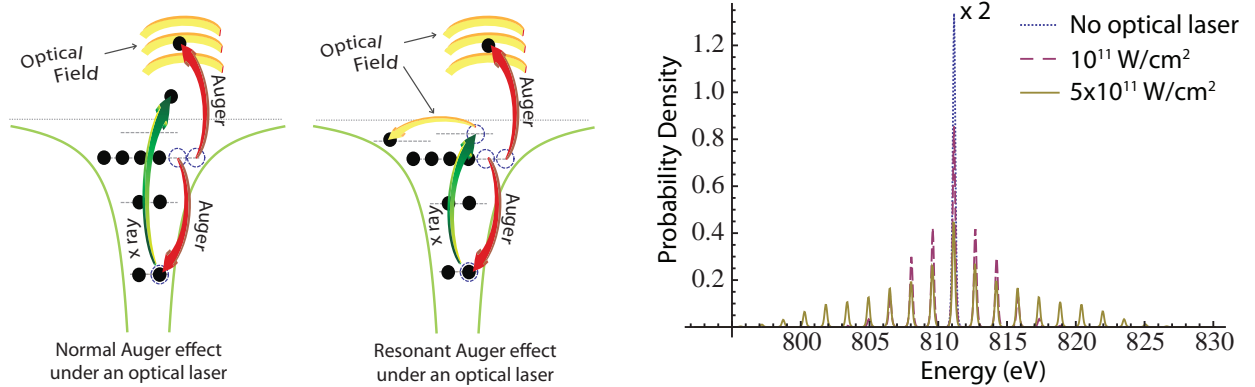


Figure 8: (a) Normal and resonant laser-dressed Auger effects are depicted. In the resonant case, the intense optical laser, besides dressing the continuum, also couples two core-excited states in the Rydberg manifold. (b) Laser-dressed resonant Auger electron spectrum of Ne due to the decay of the $1s^{-1}3p$ excitation. Blue-dotted line, Auger electron spectrum without optical laser at an energy of 811 eV; the probability density is multiplied by two. When the optical laser dresses the continuum, a multipeak structure starts to show as the one shown as red-dashed line for an optical intensity of 10^{11} W/cm² and yellow-solid line for an optical intensity of 5×10^{11} W/cm². The peaks are separated by photon energy of the optical laser. In this numerical simulation an 800 nm laser was used (photon energy 1.55 eV).

We have theoretically and numerically studied resonant Auger decay on the $1s \rightarrow 1s^{-1}3p$ excitation by x rays in neon when an intense optical laser is present based on the framework of Refs. [38, 6, 42]. X rays couple the $1s$ and $1s^{-1}3p$ states while the optical field couples the $1s^{-1}3p$ and $1s^{-1}3s$ core-excited states and dresses the continuum. We describe the interaction of the system with x rays and the intense optical field and calculate the resonant Auger electron spectrum beyond the two-step approximation. We analyzed two main configurations: when the linear polarization of the x rays and the optical field are perpendicular or parallel for different parameters of both the optical field and the x rays: pulse duration, optical laser intensity, pulse shape, and optical photon energy. In the perpendicular configuration, due to selection rules, no transfer of population between $1s^{-1}3p$ and $1s^{-1}3s$ states is possible. Then, the intense optical laser only dresses the continuum and induces sidebands (see Fig. 8b). However, in the parallel configuration, the results show a clear signature in the Auger electron spectrum of the optical coupling between the $1s^{-1}3p$ and $1s^{-1}3s$ states, responsible for the effect of electromagnetically induced transparency (EIT) for x rays [38, 6]. Such coupling allows us to manipulate the core-excited states population before the atom undergoes Auger decay, affecting the lineshape of the Auger electron spectrum.

Exploring laser aligned molecules in solution

(P. J. Ho, A. M. March, G. Doumy, E. P. Kanter, D. Ray, S. H. Southworth)

Intense optical laser pulses have been used to align molecules in the gas phase. However, such strong-field alignment effects have not been demonstrated and observed before for molecules in liquid solutions. We attempted to demonstrate this strong-field effect by adiabatically aligning dibromobenzene solvated in a nonpolar (CCl_4) solvent using our high repetition rate laser in 130-ps mode and measuring the alignment signals via resonant x-ray absorption at the Br K -edge. The experimental efforts were guided by theoretical studies of resonant x-ray absorption of laser-aligned solvated dibromobenzene molecules. In these studies, the rotational dynamics of the solvated dibromobenzene molecules were modeled as Brownian rotational motion in an intense aligning laser pulse using the Fokker-Planck equation, and the effects of the aligning laser on the solvent were neglected. These calculations showed that in order to get a good degree of alignment the laser pulse duration must be greater than the diffusion time of the solvated molecules, and a colder solvent can provide a higher degree of molecular alignment. In particular, for dibromobenzene molecules solvated in CCl_4 at room temperature, the calculations predicted a 3% signal in the transient x-ray absorption anisotropy measured with two perpendicular laser polarizations. Motivated by these theoretical results, an experiment was performed at APS. A ~ 10 mM dibromobenzene/ CCl_4 solution was circulated in a liquid jet, the fundamental wavelength (1064 nm) of the high repetition rate laser was focused to ~ 20 μm spot on the sample, and microfocused x-rays (~ 8 μm spot) probed the central region of the laser focal volume. We found, however, that even at a moderate laser intensity ($< 10^{11}$ W/cm²), presumed avalanche ionization led to the formation of plumes from the liquid jet, which disrupted our measurement on long time scales, prohibiting us from acquiring necessary laser-off measurements. A solution may be to lower the repetition rate of the laser, which would have detrimental effects on our data collection time, and therefore signal-to-noise, or try a molecule with an even larger anisotropic polarizability. Also, we could explore the response of different solvents to high fluence, moderate intensity laser fields, to find candidates that would be suitable for this measurement.

X-ray scattering from laser-aligned molecules—experiment

(G. Doumy, P. J. Ho, E. P. Kanter, B. Krässig, A. M. March, D. Ray, S. H. Southworth, L. Young, T. J. Graber,²² R. W. Henning²²)

This work builds upon our previous demonstration of an x-ray microprobe of laser-aligned bromotrifluoromethane (CF_3Br) molecules [39]. As in the previous work, the duration of the x-ray probe pulse is ~ 100 ps, which is of similar magnitude as molecular rotational periods, and TW laser pulses with ~ 100 ps duration at 1 kHz are used to produce quasi-adiabatic molecular alignment in a gaseous sample cooled by supersonic expansion. Whereas in our previous work the x-ray probe was based on resonant x-ray absorption and fluorescence detection, the goal of this work is to collect diffraction patterns of coherently scattered x-rays from laser aligned ensembles of molecules, guided by theoretical predictions made in our group [11, 40, 41].

The cross section for coherent x-ray scattering is orders of magnitude lower than that of resonant absorption, as in the work of Ref. [39], or that of electron scattering, as in Ref. [47]. A demonstration of coherent x-ray scattering from a molecular beam requires significantly higher x-ray flux and sample density than in the work of Ref. [39]. We use beamline 14-ID-B at the Advanced Photon Source, which has two in-line undulators and produces x-ray pulses of 10^{10} photons per pulse in pink beam operation ($\Delta E/E \sim 2\%$) and a pulsed Even-Lavie valve as a molecular beam source.

In the past year we changed the placement of the pulsed valve inside our experimental setup such that the x-ray beam intersects the unskimmed molecular beam at about 10 mm from the expansion nozzle. In measurements without the alignment laser we characterized our target densities based on

Br- K fluorescence emission for x-ray energies above the Br K -ionization threshold on a fluorescence detector at 90 degrees from the x-ray beam. With our test mixture of 5% CF₃Br seeded in helium, we obtained CF₃Br number densities up to 10¹⁴/cm³ for backing pressures of <400 psi. The diameter of the molecular beam is \sim 4 mm FWHM at 10 mm from the nozzle. We recorded CCD images of 2π coherent x-ray scattering patterns for CF₃Br at 12-keV x-ray energy and various number densities of the sample. We found the scattering patterns with our 5% CF₃Br in helium mixture to deviate considerably from the theoretical expectation when the backing pressure was increased beyond 20 psi (6×10^{12} /cm³ number density of CF₃Br), which we interpret as an indication for the formation of (CF₃Br) _{n} clusters or helium droplets around the CF₃Br molecules in our molecular beam. On the other hand, unseeded CF₃Br at 22 psi backing pressure and 10¹⁴/cm³ sample density is in good agreement with the theoretical prediction. The background of x-rays from scattering off the collimating slits masks the signal of molecular scattering in the CCD images by \sim 60:1.

Charge redistribution and ion fragmentation in deep inner-shell vacancy decay

(R. W. Dunford, S. H. Southworth, E. P. Kanter, B. Krässig, D. Ray, L. Young, C. Buth, R. Santra,^{1,2} S.-K. Son,¹ and O. Vendrell¹)

X-ray absorption by an atomic inner-shell electron produces a highly excited vacancy state that relaxes on the attosecond/femtosecond time scale by ejecting fluorescent photons and Auger electrons. In this “vacancy cascade” process, holes are transferred from inner to outer electronic shells of the atom. In a free atom, such as Xe gas, x-ray absorption by a 1s electron leads to highly charged final states, e.g., a charge state in the range of +4 to +12. A range of charge states is produced due to alternative decay pathways - electron emission increases the charge state while photon emission does not. The molecular damage triggered by such events can potentially be used in new radiotherapy techniques based on the insertion of iodinated compounds into tumorous regions, which are then exposed to synchrotron radiation above the K -edge of the heavy atom [48]. An understanding of decay processes in electronically excited molecules is also particularly important in plasma physics and astrophysics and can be an important source of low energy electrons and energetic reactive ions [49] that produce radiation damage in biological systems [50].

In earlier work [28] we observed molecular effects in vacancy cascades of the molecule XeF₂. Our method was to compare the total charge produced in atomic Xe to that produced in XeF₂ following deep inner-shell ionization of Xe. The yields of the final charge states were measured in coincidence with x-ray fluorescence. Some interesting results were found. The first was that the dominant breakup modes were symmetric, i.e. the two fluorine ions emerged each carrying the same charge. Another was that the total charge produced in the XeF₂ molecule was larger than that produced in the isolated Xe atom. These results led to theoretical work by R. Santra *et al.* who argued that the increased charge was an indication of an interatomic-Coulombic-decay-like (ICD-like) process. In addition, using an independent ion model, they found that the symmetric charge distributions minimize the total ionization energy in XeF₂. Experimental and theoretical results indicate that the F atoms participate in the decay cascade within the first few femtoseconds after core-hole formation and that fragmentation begins during the decay process.

In order to fully test the theoretical model, the Kinetic Energy Release (KER) associated with a given breakup mode must be known. In the earlier experiment we were only able to measure the KER averaged over all Xe charge states and this was not sufficient. This provided the motivation for us to assemble a new apparatus with a position-sensitive ion detector, which allows a complete reconstruction of each ion fragmentation event and we are now able to more fully test the theoretical calculations. In addition to gaining a further understanding of the ICD process in the hard x-ray regime, the new apparatus will also be used to explore the more general question of what are the most probable breakup modes for a molecule following deep inner-shell photoionization of a heavy

atom constituent.

In two recent beamtimes at the Advanced Photon Source (APS), we have completed a more detailed study to compare photoionization of XeF_2 with atomic Xe. In addition we have begun to study other systems starting with the simple binary molecule IBr. For IBr, the APS has the capability for creating *K*-shell holes in either the Br atom at 13 keV or in the I atom at 33 keV. So these data will provide a comparison of the breakup patterns resulting from quite different excitation modes. Data analysis is in progress, but it is already apparent that the improved apparatus with its faster electronics, multi-hit position-sensitive detector, and increased detection efficiency have removed the ambiguities in the charge-state distributions that limited the earlier study of XeF_2 .

5 X-RAY IMAGING OF LASER CONTROLLED NANOPARTICLES

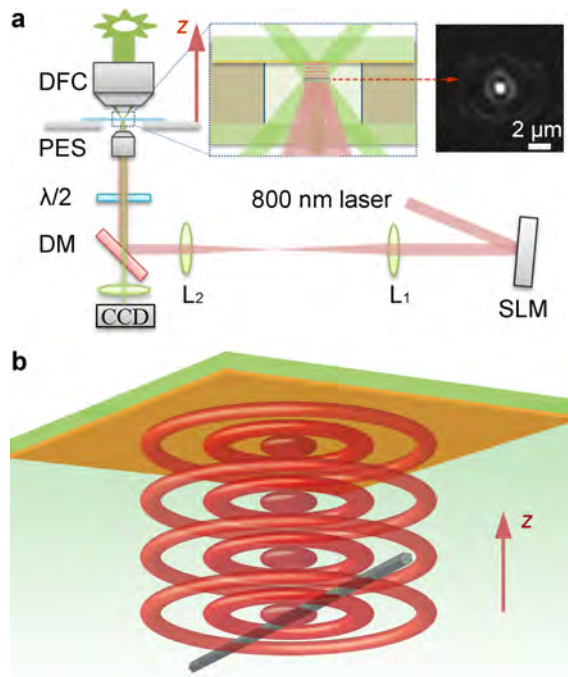


Figure 9: (a) Schematic of the experimental setup used for three-dimensional manipulation of silver nanowires. The inset shows a cross-section of the optical Bessel beam used for optical trapping. (b) Illustration of the retroreflected Bessel-beam trap, with a trapped silver nanowire.

Optical control of metal nanowires to enable single-particle x-ray diffraction

(Matthew Pelton, Julian Sweet, Norbert F. Scherer, and Zijie Yan)

Silver and gold nanowires have the potential to serve as key elements in nanoscale photonic circuits, allowing optical fields to be relayed over distances of several micrometers while being confined on the nanometer scale in transverse directions. In particular, chemically synthesized metal nanowires are nearly free of bulk crystalline defects, and thus offer plasmon transport that is limited only by intrinsic losses in the metal. In order for these nanowires to serve as functional elements in nanophotonic systems, it will be necessary to position and align them in three dimensions with nanometer-scale precision. Optical forces provide a flexible, non-contact method for single-nanowire manipulation. Moreover, it should be possible to use x-ray diffraction to image a single metal nanowire held in an optical trap. This will make it possible to image three-dimensional

strain distributions and defects in the nanowires, providing insight into their optical properties and into the nucleation and growth processes involved in their synthesis. The metal nanowires scatter optical photons and x-ray photons strongly, simplifying both optical and x-ray experiments, while still allowing them to serve as models for x-ray diffraction measurements on individual optically-trapped molecules.

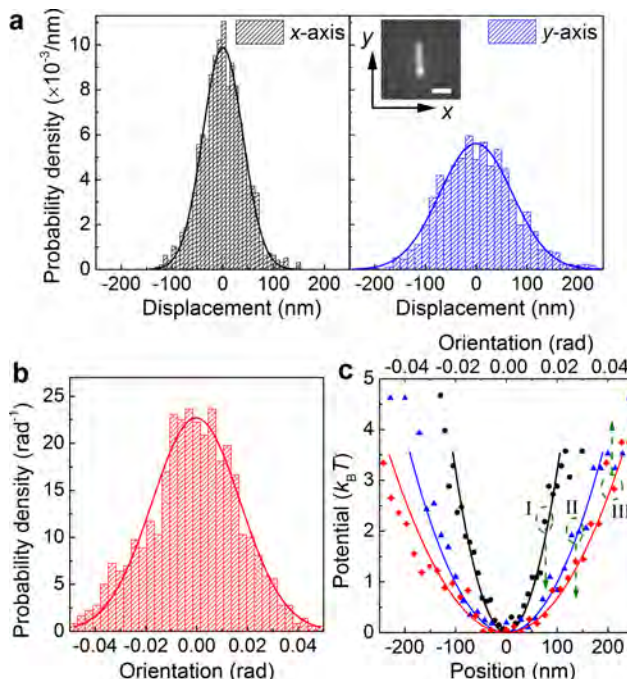


Figure 10: Measured probability distributions for (a) displacement and (b) orientation of a trapped silver nanowire. (c) Trapping potentials inferred from the probability densities. The three curves are color coded according to the probability distributions from which they are derived.

One major challenge with optical trapping of metal nanowires comes from their strong optical scattering. The optical gradient forces that are responsible for trapping are easily overwhelmed by radiation pressure due to scattering and absorption by the nanowires. We therefore developed a new optical-trapping configuration that enables, for the first time, three-dimensional optical manipulation and orientation of individual metal nanowires. First, we characterized optical forces on metal nanowires by trapping and manipulating individual silver nanowires in two dimensions next to a glass surface, using structured optical fields that were generated by a spatial light modulator [36]. We found that, for linearly polarized light at a wavelength of 800 nm, the nanowires are attracted towards the maxima of optical intensity along the surface and are oriented perpendicular to the polarization direction. This can be understood in terms of excitation of plasmon resonances in the metal nanowires. In order to trap the nanowires in three dimensions, we used a retroreflection geometry to cancel radiation pressure in the beam propagation direction: after the trapping light passes through the sample, it is reflected back on itself using a flat mirror. This requires a large depth of focus, so that the diameter of the reflected beam is nearly identical to that of the incident beam. Such a large Rayleigh range is provided by a zero-order Bessel beam, which can be generated by the spatial light modulator. The trapping configuration is illustrated in Fig. 9. Using this Bessel-mirror trap, we could position individual nanowires with precision better than 100 nm and could orient them with precision of approximately 1° , as illustrated in Fig. 10 [37].

In order to demonstrate the feasibility of x-ray characterization of these trapped nanowires, we measured coherent x-ray diffraction from individual nanowires that have been immobilized on a substrate. Silver nanowires were rapidly damaged by intense x-ray flux, but gold nanowires remained undamaged for at least several hours. On the other hand, the position of the gold nanowires on the substrate was found to vary slowly as they were illuminated by the x-rays. This instability was eventually eliminated by depositing a thin metal layer below the nanowires, to remove charges that build up during illumination, and by embedding the nanowires in a layer of amorphous silicon dioxide, deposited after all organic material has been thoroughly removed from the nanowires. This allowed us to collect coherent-diffraction data from individual gold nanowires with a high signal/noise ratio; analysis of the data is ongoing.

6 Affiliations of collaborators

¹Center for Free-Electron Laser Science, DESY, Hamburg, Germany

²University of Hamburg, Germany

³Linac Coherent Light Source, SLAC National Accelerator Laboratory, Menlo Park, CA

⁴Ohio State University, Columbus, OH

⁵Western Michigan University, Kalamazoo, MI

⁶Pulse Center, SLAC National Accelerator Laboratory, Menlo Park, CA

⁷FLASH at DESY, Hamburg, Germany

⁸European XFEL, Hamburg, Germany

⁹Max Planck Institute for Quantum Optics, Garching, Germany

¹⁰Paul Scherrer Institute, Villigen, Switzerland

¹¹Stanford Synchrotron Radiation Laboratory, SLAC NAL, Menlo Park, CA

¹²North China Electric Power University, Beijing, China

¹³Lawrence Livermore National Laboratory, Livermore, CA

¹⁴Max-Planck-Institut für Kernphysik, Heidelberg, Germany

¹⁵Technical University of Denmark

¹⁶Wigner Research Centre for Physics, Hungarian Academy Sciences, Budapest, Hungary

¹⁷Institute of Physical Chemistry, Heidelberg University, Germany

¹⁸University of Wisconsin, Madison, WI

¹⁹Northwestern University, Evanston, IL

²⁰ETH-Zurich, Switzerland

²¹Stanford Institute for Materials and Energy Science, SLAC NAL, Menlo Park, CA

²²BioCARS, University of Chicago, IL

References

Publications 2010–2012

- [1] L. Young, E. P. Kanter, B. Krässig, Y. Li, A. M. March, S. T. Pratt, R. Santra, S. H. Southworth, N. Rohringer, L. F. DiMauro, G. Doumy, C. A. Roedig, N. Berrah, L. Fang, M. Hoener, P. H. Bucksbaum, J. P. Cryan, S. Ghimire, J. M. Glowonia, D. A. Reis, J. D. Bozek, C. Bostedt, and M. Messerschmidt, “Femtosecond electronic response of atoms to ultra-intense x-rays,” *Nature* **466**, 56 (2010).
- [2] M. Hoener, L. Fang, O. Kornilov, O. Gessner, S. T. Pratt, M. Gühr, E. P. Kanter, C. Blaga, C. Bostedt, J. D. Bozek, P. H. Bucksbaum, C. Buth, M. Chen, R. Coffee, J. Cryan, L. DiMauro, M. Glowonia, E. Hosler, E. Kukkk, S. R. Leone, B. McFarland, M. Messerschmidt, B. Murphy, V. Petrovic, D. Rolles, and N. Berrah, “Ultraintense x-ray induced ionization, dissociation, and frustrated absorption in molecular nitrogen,” *Phys. Rev. Lett.* **104**, 253002 (2010).
- [3] L. Fang, M. Hoener, O. Gessner, F. Tarantelli, S. T. Pratt, O. Kornilov, C. Buth, M. Ghr, E. P. Kanter, C. Bostedt, J. D. Bozek, P. H. Bucksbaum, M. Chen, R. Coffee, J. Cryan, M. Glowonia, E. Kukkk, S. R.

- Leone, and N. Berrah, “Double core-hole production in N_2 : beating the Auger clock,” *Phys. Rev. Lett.* **105**, 083005 (2010).
- [4] J. M. Glowia, J. P. Cryan, J. Andreasson, A. Belkacem, N. Berrah, C. I. Blaga, C. Bostedt, J. Bozek, L. F. DiMauro, L. Fang, J. Frisch, O. Gessner, M. Ghr, J. Hajdu, M. P. Hertlein, M. Hoener, G. Huang, O. Kornilov, J. P. Marangos, A. M. March, B. K. McFarland, H. Merdji, V. S. Petrovic, C. Raman, D. Ray, D. Reis, M. Trigo, J. L. White, W. White, R. Wilcox, L. Young, R. N. Coffee, and P. H. Bucksbaum, “Time-resolved pump-probe experiments at the LCLS,” *Opt. Exp.* **18**, 17620 (2010).
- [5] J. P. Cryan, J. M. Glowia, J. Andreasson, A. Belkacem, N. Berrah, C. I. Blaga, C. Bostedt, J. Bozek, C. Buth, L. F. DiMauro, L. Fang, O. Gessner, M. Guehr, J. Hajdu, M. P. Hertlein, M. Hoener, O. Kornilov, J. P. Marangos, A. M. March, B. K. McFarland, H. Merdji, V. S. Petrovic, C. Raman, D. Ray, D. Reis, F. Tarantelli, M. Trigo, J. L. White, W. White, L. Young, P. H. Bucksbaum, and R. N. Coffee, “Auger electron angular distribution of double core-hole states in the molecular reference frame,” *Phys. Rev. Lett.* **105**, 083004 (2010).
- [6] T. E. Glover, M. P. Hertlein, S. H. Southworth, T. K. Allison, J. van Tilborg, E. P. Kanter, B. Krässig, H. R. Varma, B. Rude, R. Santra, A. Belkacem, and L. Young, “Controlling x-rays with light,” *Nat. Phys.* **6**, 69 (2010).
- [7] L. Greenman, P. J. Ho, S. Pabst, E. Kamarchik, D. A. Mazziotti, and R. Santra, “Implementation of the time-dependent configuration-interaction singles method for atomic strong-field processes,” *Phys. Rev. A* **82**, 023406 (2010).
- [8] E. Goulielmakis, Z.-H. Loh, A. Wirth, R. Santra, N. Rohringer, V. S. Yakovlev, S. Zherebtsov, T. Pfeifer, A. M. Azzeer, M. F. Kling, S. R. Leone, and F. Krausz, “Real-time observation of valence electron motion,” *Nature* **466**, 739 (2010).
- [9] A. Grigoriev, P. G. Evans, M. Trigo, D. Reis, L. Young, R. W. Dunford, E. P. Kanter, B. Krässig, R. Santra, S. H. Southworth, L. X. Chen, D. M. Tiede, K. Attenkofer, G. Jennings, X. Zhang, T. Graber, and K. Moffat, “Picosecond Structural Dynamics at the Advanced Photon Source,” *Synch. Rad. News* **23**, 18 (2010).
- [10] S. Pabst, P. J. Ho, and R. Santra, “Computational studies of x-ray scattering from three-dimensionally-aligned asymmetric-top molecules,” *Phys. Rev. A* **81**, 043425 (2010).
- [11] S. Pabst and R. Santra, “Alignment of asymmetric-top molecules using multiple-pulse trains,” *Phys. Rev. A* **81**, 065401 (2010).
- [12] L. Young, C. Buth, R. W. Dunford, P. J. Ho, E. P. Kanter, B. Krässig, E. R. Peterson, N. Rohringer, R. Santra, and S. H. Southworth, “Using strong electromagnetic fields to control x-ray processes,” *Rev. Mex. Fis. S* **56**, 11 (2010).
- [13] C. Buth, R. Santra, and L. Young, “Refraction and absorption of x rays by laser-dressed atoms,” *Rev. Mex. Fis. S* **56**, 59 (2010).
- [14] P. J. Ho and R. Santra, “Theory of x-ray diffraction from laser-aligned molecules,” *Rev. Mex. Fis. S* **56**, 88 (2010).
- [15] G. Doumy, C. Roedig, S.-K. Son, C. I. Blaga, A. D. Chiara, R. Santra, N. Berrah, C. Bostedt, J. D. Bozek, P. H. Bucksbaum, J. Cryan, L. Fang, S. Ghimire, J. M. Glowia, M. Hoener, E. P. Kanter, B. Krässig, M. Kuebel, M. Messerschmidt, G. G. Paulus, D. A. Reis, N. Rohringer, L. Young, P. Agostini, and L. F. DiMauro, “Nonlinear Atomic Response to Intense Ultrashort X Rays,” *Phys. Rev. Lett.* **106**, 083002 (2011).
- [16] E. P. Kanter, B. Krässig, Y. Li, A. M. March, P. Ho, N. Rohringer, R. Santra, S. H. Southworth, L. F. DiMauro, G. Doumy, C. A. Roedig, N. Berrah, L. Fang, M. Hoener, P. H. Bucksbaum, S. Ghimire, D. A. Reis, J. D. Bozek, C. Bostedt, M. Messerschmidt, and L. Young, “Unveiling and Driving Hidden Resonances with High-Fluence, High-Intensity X-Ray Pulses,” *Phys. Rev. Lett.* **107**, 233001 (2011).
- [17] S. Düsterer, P. Radcliffe, C. Bostedt, J. Bozek, A. L. Cavalieri, R. Coffee, J. T. Costello, D. Cubaynes, L. F. DiMauro, Y. Ding, G. Doumy, F. Grüner, W. Helml, W. Schweinberger, R. Kienberger, A. R. Maier, M. Messerschmidt, V. Richardson, C. Roedig, T. Tschentscher, and M. Meyer, “Femtosecond x-ray pulse length characterization at the Linac Coherent Light Source free-electron laser,” *New J. Phys.* **13**, 093024 (2011).
- [18] C. Buth, M. C. Kohler, J. Ullrich, and C. H. Keitel, “High-order harmonic generation enhanced by XUV light,” *Opt. Lett.* **36**, 3530 (2011).
- [19] S. Pabst, L. Greenman, P. J. Ho, D. A. Mazziotti, and R. Santra, “Decoherence in attosecond photoion-

- ization,” *Phys. Rev. Lett.* **106**, 053003 (2011).
- [20] S.-K. Son, L. Young, and R. Santra, “Impact of hollow-atom formation on coherent x-ray scattering at high intensity,” *Phys. Rev. A* **83**, 033402 (2011); **83**, 069906(E) (2011).
- [21] A. M. March, A. Stickrath, G. Doumy, E. P. Kanter, B. Krässig, S. H. Southworth, K. Attenkofer and C. A. Kurtz, L. X. Chen, and L. Young, “Development of high-repetition-rate laser pump/x-ray probe methodologies for synchrotron facilities,” *Rev. Sci. Instrum.* **82**, 073110 (2011).
- [22] E. Silver, J. D. Gillaspay, P. Gokhale, E. P. Kanter, N. S. Brickhouse, R. W. Dunford, K. Kirby, T. Lin, J. McDonald, D. Schneider, S. Seifert, and L. Young, “Work Towards Experimental Evidence Of Hard X-Ray Photoionization In Highly Charged Krypton,” *AIP Conference Proceedings* **1336**, 146 (2011).
- [23] R. W. Dunford and R. J. Holt, “Parity nonconservation in hydrogen,” *Hyp. Int.* **Online**, (2011).
- [24] M. Meyer, P. Radcliffe, T. Tschentscher, J. T. Costello, A. L. Cavalieri, I. Grguras, A. R. Maier, R. Kienberger, J. Bozek, C. Bostedt, S. Schorb, R. Coffee, M. Messerschmidt, C. Roedig, E. Sistrunk, L. F. Di Mauro, G. Doumy, K. Ueda, S. Wada, S. Düsterer, A. K. Kazansky, and N. M. Kabachnik, “Angle-Resolved Electron Spectroscopy of Laser-Assisted Auger Decay Induced by a Few-Femtosecond X-Ray Pulse,” *Phys. Rev. Lett.* **108**, 063007 (2012).
- [25] C. Buth, J.-C. Liu, M. H. Chen, J. P. Cryan, L. Fang, J. M. Glowina, M. Hoener, R. N. Coffee, and N. Berrah, “Ultrafast absorption of intense x rays by nitrogen molecules,” *J. Chem. Phys.* **136**, 214310 (2012).
- [26] M. C. Kohler, C. Müller, C. Buth, A. B. Voitkiv, K. Z. Hatsagortsyan, J. Ullrich, T. Pfeiffer, C. H. Keitel, “Electron correlation and interference effects in strong-field processes,” in *Multiphoton Processes and Attosecond Physics*, K. Yamanouchi and K. Midorikawa, Springer Proceedings in Physics **125**, Springer, Berlin, 2012.
- [27] S. M. Cavaletto, C. Buth, Z. Harman, E. P. Kanter, S. H. Southworth, L. Young, and C. H. Keitel, “Resonance fluorescence in ultrafast and intense x-ray free-electron-laser pulses,” *Phys. Rev. A*, in press (2012).
- [28] R. W. Dunford, S. H. Southworth, D. Ray, E. P. Kanter, B. Krässig, L. Young, D. A. Arms, E. M. Dufresne, D. A. Walko, O. Vendrell, S.-K. Son, and R. Santra, “Evidence for interatomic Coulombic decay in Xe *K*-shell-vacancy decay of XeF₂,” *Phys. Rev. A*, in press (2012).
- [29] C. Buth *et al.*, “Attosecond pulses at kiloelectronvolt photon energies from high-order harmonic generation with core electrons,” arXiv:1203:4127, submitted (2012).
- [30] W. Helml *et al.*, “Direct time domain measurement of the world’s shortest X-ray pulses,” submitted (2012).
- [31] G. Darvasi, C. H. Keitel, and C. Buth, submitted (2012).
- [32] B. W. Adams, C. Buth, S. M. Cavaletto, J. Evers, Z. Harman, C. H. Keitel, A. Pálffy, A. Picón, R. Röhlberger, Y. Rostovtsev, K. Tamasaku, *J. Mod. Opt.*, submitted (2012).
- [33] L. Fang, T. Osipov, B. Murphy, F. Tarantelli, E. Kukk, J. Cryan, P. H. Bucksbaum, R. N. Coffee, M. Chen, C. Buth, and N. Berrah, “Multiphoton ionization as a tool to reveal molecular dynamics with intense short x-ray free electron laser pulses,” submitted (2012).
- [34] K. Haldrup, G. Vankó, W. Gawelda, A. Galler, G. Doumy, A. M. March, E. P. Kanter, A. Bordage, A. Dohn, T. B. van Driel, K. S. Kjaer, H. T. Lemke, S. E. Canton, J. Uhlig, V. Sundström, L. Young, S. H. Southworth, M. M. Nielsen, and C. Bressler, “Guest-Host Interactions Investigated By Time-Resolved X-Ray Spectroscopies and Scattering at MHz Rates: Solvation Dynamics and Photoinduced Spin Transition in Aqueous [Fe(bipy)₃]²⁺,” *J. Phys. Chem.*, submitted (2012).
- [35] G. Vankó, A. Bordage, P. Glatzel, E. Gallo, M. Rovezzi, W. Gawelda, A. Galler, C. Bressler, G. Doumy, A. M. March, E. P. Kanter, L. Young, S. H. Southworth, S. E. Canton, J. Uhlig, V. Sundström, K. Haldrup, T. Brandt van Driel, M. M. Nielsen, K. S. Kjaer, and H. T. Lemke, “Spin-state studies with XES and RIXS: From static to ultrafast,” special issue “Progress in RIXS” of the *J. Electron. Spectrosc. Relat. Phenom.*, accepted (2012).
- [36] Z. Yan, J. Sweet, J. E. Jureller, M. J. Guffey, M. Pelton, and N. F. Scherer, “Controlling the position and orientation of single silver nanowires on a surface using structured optical fields,” *ACS Nano*, DOI: 10.1021/nn302795j, published online (2012).
- [37] Z. Yan, J. E. Jureller, J. Sweet, M. J. Guffey, M. Pelton, and N. F. Scherer, “Three-dimensional optical trapping and manipulation of single silver nanowires,” *Nano Lett.*, accepted (2012).

Other cited references

- [38] C. Buth, R. Santra, and L. Young, “Electromagnetically induced transparency for x rays,” *Phys. Rev. Lett.* **98**, 253001 (2007).
- [39] E. R. Peterson, C. Buth, D. A. Arms, R. W. Dunford, E. P. Kanter, B. Krässig, E. C. Landahl, S. T. Pratt, R. Santra, S. H. Southworth, and L. Young, “An x-ray probe of laser-aligned molecules,” *Appl. Phys. Lett.* **92**, 094106 (2008).
- [40] P. J. Ho, D. Starodub, D. K. Saldin, V. L. Shneerson, A. Ourmazd, and R. Santra, “Molecular structure determination from x-ray scattering patterns of laser-aligned symmetric-top molecules,” *J. Chem. Phys.* **131**, 131101 (2009).
- [41] P. J. Ho and R. Santra, “Theory of x-ray diffraction from laser-aligned symmetric-top molecules,” *Phys. Rev. A* **78**, 053409 (2008).
- [42] C. Buth and K. J. Schafer, “Theory of Auger decay by laser-dressed atoms,” *Phys. Rev. A* **80**, 033410 (2009).
- [43] E. Priori, G. Cerullo, M. Nisoli, S. Stagira, S. De Silvestri, P. Villoresi, L. Poletto, P. Cecherini, C. Altucci, R. Bruzzese, and C. de Lisio, “Nonadiabatic three-dimensional model of high-order harmonic generation in the few-optical-cycle regime,” *Phys. Rev. A* **61**, 063801 (2000).
- [44] N. Rohringer and R. London, “Atomic inner-shell x-ray laser pumped by an x-ray free-electron laser,” N. Rohringer and R. London, *Phys. Rev. A* **80**, 013809 (2009) and *Phys. Rev. A* **82**, 049902(E) (2010).
- [45] N. Rohringer, D. Ryan, R. A. London, M. Purvis, F. Albert, J. Dunn, J. D. Bozek, C. Bostedt, A. Graf, R. Hill, S. P. Hau-Riege, and J. J. Rocca, “Atomic inner-shell X-ray laser at 1.46 nanometres pumped by an X-ray free-electron laser,” *Nature* **481**, 488 (2012).
- [46] J. Amann *et al.*, *Nature Photonics*, online August 2012.
- [47] C. J. Hensley, J. Yang, and M. Centurion, “Imaging of isolated molecules with ultrafast electron pulses,” submitted (2012).
- [48] S. Corde *et al.*, *Brit. J. Cancer* **91**, 544 (2004).
- [49] M. Mucke *et al.*, *Nature Phys.* **6**, 143 (2010).
- [50] L. Caron *et al.*, *Phys. Rev. A* **80**, 012705 (2009).

J.R. MACDONALD LABORATORY – OVERVIEW 2012

The J.R. Macdonald Laboratory focuses on the interaction of intense laser pulses with matter – specifically, observing and controlling single atoms and molecules on short time scales. The eventual goal is to work at the natural time scale for electrons moving in matter. Doing so will add to our existing capability to trace nuclear motion in molecules using femtosecond laser pulses. All of these activities build toward the ultimate goal of understanding the dynamical processes of reactions well enough to control them. To this end, we are advancing theoretical modeling and computational approaches as well as experimental techniques and taking advantage of our expertise in particle imaging techniques (such as COLTRIMS, VMI, MDI, etc.). Most of our research projects are associated with one of the two themes: “Attosecond Physics” and “Control”. The boundary between these themes, however, is sometimes not well defined. A few examples are briefly mentioned below, while further details of typical projects are provided in the individual contributions of the PIs: *I. Ben-Itzhak, C.L. Cocke, B.D. Esry, M.F. Kling, V. Kumarappan, C.D. Lin, U. Thumm, C. Trallero*, and our newest faculty member, *Artem Rudenko*.

Attosecond physics: The goal of the efforts under this theme is to follow, on their natural timescale, electronic motion in atoms and molecules. However, attosecond pulses can also serve as very precise triggers or probes of the femtosecond-scale nuclear motion in molecules. Moreover, the underlying high harmonic generation (HHG) mechanism, used to create attosecond pulses, provides essential information about the target and has been the focus of some of our theoretical and experimental studies. We have experimentally demonstrated that the directionality of emitted electrons can be temporally controlled on an attosecond time scale through the interference of opposite parity atomic orbitals. We have investigated the spectral splitting of high harmonics generated in a semi-infinite gas cell by performing an extreme ultraviolet (EUV) and near-infrared (NIR) cross-correlation experiment. In collaboration with the Ohio State group, we have demonstrated femtosecond temporal and sub-angstrom spatial resolution in bond relaxation following tunneling ionization of O₂ and N₂ by mid-infrared lasers. We have theoretically examined photoelectron and transient absorption spectra generated by attosecond pulses coupled to intense IR lasers in a gas medium. We have studied high harmonic generation from well-aligned molecules ranging from well-studied diatomic molecules to more complex asymmetric-top molecules. In collaboration with Robert Lucchese and Erwin Poliakoff, we have utilized HHG for coherent spectroscopy of large molecular systems and explored the impact of macroscopic conditions. We have presented a pump-probe scheme to enhance carrier-envelope phase (CEP) effects by an order of magnitude and have demonstrated its utility for H₂⁺. Experimentally, in collaboration with Gerhard Paulus and others, we have developed and implemented single-shot CEP tagging in conjunction with 3-dimensional imaging techniques as an alternative to the detection of CEP-effects using CEP stabilization. We have achieved attosecond control of correlated electron emission in non-sequential double ionization of atoms, molecules, and nanoparticles.

Control: Methods for controlling the motion of heavy particles in small molecules continue to be developed. Theoretically, our work shows that CEP effects, two-color control, and the physics of overlapping attosecond pulse trains and infrared pulses are all manifestations of multi-color control and can all be treated with exactly the same analytical framework. In particular, our formulation shows that these effects arise from interference between different multiphoton pathways. Our experimental two-color control of strong-field dissociation of D₂⁺ and HD⁺ serves as a good demonstration of the theory. We have demonstrated control over the reaction products of HD⁺ dissociation, that is enhancing H⁺+D over H+D⁺ and vice versa. In collaboration with

Reinhard Dörner, we have controlled Ar_2^+ dissociation in a pump-probe two-color field ($\omega_2 \neq 2\omega_1$). Theoretically, we have modeled the time-resolved IR-light-induced fragmentation dynamics in diatomic molecules and in XUV-pump and XUV-probe pulses. We have experimental and theoretical evidence for dissociation of a metastable molecular dication by a multiphoton transition to the vibrational continuum driven by commonly neglected permanent-dipole transitions. In collaboration with Eric Wells and others, we have implemented 3D velocity map imaging (VMI) as a feedback to the genetic-learning algorithm for controlling a reaction product in a strong laser field. We have implemented theoretically and experimentally a multi-pulse scheme for the 3D alignment of asymmetric top molecules. We have recently developed an optical technique for characterizing the degree of alignment of molecules.

In addition to our laser-related research, we have conducted some studies using our high- and low-energy accelerators. Some of this work is conducted in collaboration with visiting scientists (for example, S. Lundeen).

Like the visitors benefiting from the use of our facilities, we pursue several outside collaborations at other facilities and with other groups (e.g., ALS, Århus, FLASH, University of Frankfurt, University of Jena, LBNL, Max-Planck Institutes for Quantum Optics and Kernphysik, Ohio State University, Texas A&M, Tokyo, Weizmann Institute, and others).

Finally, it is worth mentioning the changes our group and laboratory are undergoing at present. With DOE funding, we have purchased a high-repetition-rate, high-power, CE phase-locked laser from KM Labs that has been operating since early August in our lab. Specifically, this laser provides about an order of magnitude improvement in count rate (10-20 kHz, 790 nm, 2 mJ/pulse, ~21 fs FWHM, CEP stable) over KLS, which is essential for most of our multi-parameter coincidence measurements (like COLTRIMS, MDI, etc). Moreover, the shorter pulses (than currently available from KLS) will allow us to generate pulses shorter than the 5.5 fs we currently produce by compression in hollow core fiber using the KLS. In addition to the added laser capabilities, this new laser system alleviates the shortage of beam time – hopefully allowing for more collaborations involving visiting scientists.

In addition to the new laser capabilities, our lab has seen an amazing improvement in infrastructure during the past year. The University has invested in excess of half a million dollars to upgrade two laboratory spaces for housing new lasers. The new PULSAR laser is now operational in one of the renovated spaces.

On the personnel side, a new AMO faculty member, *Artem Rudenko*, has just joined our group. His expertise with free-electron lasers, ultrafast lasers, and COLTRIMS will be an asset to our experimental efforts.

This hire completes our recent personnel changes, and we are looking forward to the future and have started planning the addition of a third laser – a high power, long wavelength system, based on an upgrade of an existing laser, previously supported by a MURI grant. We envision three young faculty members, *Vinod*, *Carlos* and *Matthias*, taking charge of the operation, scheduling, maintenance and upgrade of the three main laser systems, each responsible for one of them, while experiments conducted by all are allocated to the laser that fits them best.

**Structure and Dynamics of Atoms, Ions, Molecules, and Surfaces:
Molecular Dynamics with Ion and Laser Beams**

*Itzik Ben-Itzhak, J. R. Macdonald Laboratory, Kansas State University
Manhattan, KS 66506; ibi@phys.ksu.edu*

Scope: The goal of this part of the JRML program is to study and control molecular dynamics under the influence of ultrashort intense laser pulses or the swift Coulomb field of ions. To this end we typically use molecular ion beams as the subject of our studies and have a close collaboration between theory and experiment.¹ Examples of our recent work are given below.

Multiphoton permanent dipole transitions in NO²⁺, *B. Jochim, M. Zohrabi, B. Gaire, U. Ablikim, Tereza Uhlíková, K.D. Carnes, E. Wells, B.D. Esry, and I. Ben-Itzhak* – Metastable molecular ions offer unique opportunities as demonstrated recently in Pub. [8] by the use of vibrationally cold CO²⁺ to observe above threshold dissociation (ATD) structure in the kinetic energy release (KER) spectrum.

Another molecular dication we find interesting is the long-lived NO²⁺. Similar to CO²⁺, this molecular ion “cools” vibrationally in flight to the interaction region, since states above $v=12$ in the X²Σ⁺ ground state are depleted by predissociation (see Fig. 1(a), Ref. [1] and Pub. [26]).

At moderate laser intensities, we expect only the lowest two electronic states to play a role in NO²⁺ dissociation. We expect that one 800 nm (1.6 eV) photon should excite most of the populated vibrational levels for $v \geq 6$ in the X²Σ⁺ potential well to the A²Π vibrational continuum, thereby leading to their prompt dissociation. The X²Σ⁺ ($v = 5$) state will be excited to the short-lived $v_f = 8$ or 9 states of A²Π ($\tau \sim 45$ ns and 14 ps, respectively), which will dissociate enabling detection. Lower vibrational levels, however, will be excited to A²Π ($v_f < 8$) states, which live long enough to reach the detector before dissociation.

One should note that the one-photon transitions discussed above involve $\Delta\Lambda = 1$. Therefore, fragments aligned perpendicular to the laser polarization are expected (see, e.g. Ref. [2]). In contrast, X²Σ⁺ → B²Σ⁺ dissociative transitions, which require the absorption of four or five photons depending on the initial v , are expected to align strongly along the laser polarization as $\Delta\Lambda = 0$ in this case.

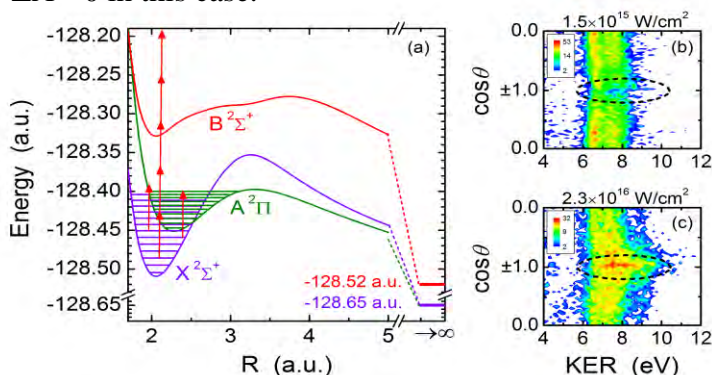


Figure 1. (a) Born-Oppenheimer potential energy curves for the lowest doublet states of NO²⁺ calculated by Baková *et al.* [1] along with their vibrational levels computed with the Phase-Amplitude method [3]. Only $v \leq 12$ states of X²Σ⁺ have population remaining when probed with the laser (see text). (b)&(c) Density plots of N⁺O⁺ coincidences as a function of KER and $\cos\theta$ for the peak intensities indicated (see text). Adapted from Ref. [4].

Our results indicate that most of these predictions are correct [4]. Specifically, at intensities below $\sim 10^{15}$ W/cm² the angular distribution favors dissociation perpendicular to the polarization. Higher intensity pulses ($\sim 10^{16}$ W/cm²), on the other hand, yield a prominent contribution from molecules breaking parallel to the polarization. This changeover is shown in Figs. 1(b)–(c).

This strongly-aligned feature is one of the intriguing outcomes of our study, since it is due to purely permanent-dipole, multiphoton transitions to the vibrational continuum of X²Σ⁺.

Moreover, through the combination of our methods and this unique system, we have strong evidence that this often-neglected process is responsible for the aligned feature. Experimentally, the measured KER fits that expected for two- to three-photon $X^2\Sigma^+(v_i) \rightarrow X^2\Sigma^+(E)$ transitions better than for four- to five-photon $X^2\Sigma^+(v_i) \rightarrow B^2\Sigma^+(E)$ transitions. Theoretically, TDSE calculations by Brett Esry’s group show that $X^2\Sigma^+(v_i) \rightarrow B^2\Sigma^+$ transition probabilities are about four orders of magnitude smaller than those for the $X^2\Sigma^+(v_i) \rightarrow X^2\Sigma^+(E)$ permanent dipole transitions of interest. This project was presented by our graduate student, Bethany Jochim, as an invited award talk at DAMOP 2012, and it is being prepared for publication [4].

Channel asymmetry in HD^+ controlled by a single pulse, *M. Zohrabi, U. Ablikim, B. Gaire, B. Rigsbee, K.D. Carnes, B.D. Esry, and I. Ben-Itzhak* – This project was part of our wider effort to control the dissociation of the benchmark HD^+ molecule into either $H^+ + D$ or $H + D^+$. That is, we aimed to impose channel asymmetry using as our control parameters the pulse bandwidth and chirp, or alternatively the two-color [5-6] or carrier-envelope phase (see B.D. Esry’s abstract).

Our first step towards observing and controlling channel asymmetry A_c in HD^+ involved the intriguing zero-photon dissociation (ZPD) process [7-9]. As Fig 2(Left) shows, we observed a preference for dissociation in 7 fs FTL pulses to the energetically lower $H^+ + D$ channel at very low KER in accord with our ground state dissociation (GSD) findings [10]. Based on our GSD experience, we expected the difference between the two channels to diminish with increasing KER. This expectation was borne out as shown in the inset of Fig. 2(Left) for ZPD KER up to ~ 0.25 eV. The asymmetry is due to channel mixing by a strong non-adiabatic coupling between the lowest energy curves around $R = 12$ a.u. [10,11].

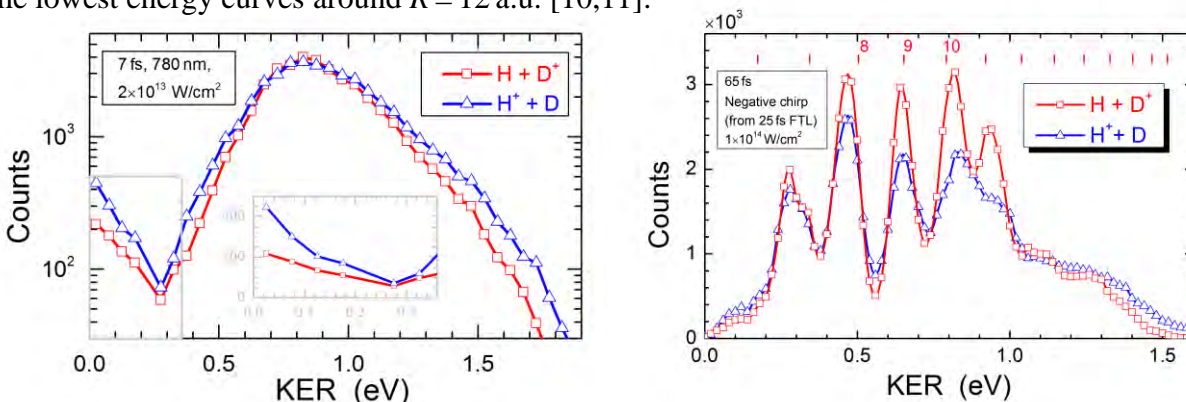


Figure 2. The KER distribution of HD^+ dissociation into $H^+ + D$ and $H + D^+$ showing channel asymmetry in (Left) 7 fs FTL pulses—inset shows a zoomed-in view of the ZPD low-KER (adapted from Ref [9]), and in (Right) 65 fs negatively chirped pulses—the channel asymmetry strongly depends on the vibrational level (adapted from Ref [12]).

Surprisingly, though, Fig. 2(Right) shows that the channel asymmetry persists over a wide range of KER well beyond that associated with ZPD. Repeating the experiment with a 65 fs pulse to obtain vibrational resolution [12] reveals significantly different channel asymmetry for each vibrational state, as shown in Fig. 2(Right).

Preliminary calculations by Esry’s group and other measurements suggest that this channel asymmetry depends strongly on essentially all of the parameters of the system, appearing in a wide variety of pulses. Further theoretical and experimental work is in progress to bring this project to completion.

Collisions: In addition to our laser studies, we have conducted a few collision experiments between keV molecular ion beams and atomic targets. For example, at present we focus on

alignment and orientation dependences of collision induced dissociation in slow $\text{HeD}^+ + \text{Ar}$ collisions with our upgraded setup. This project was presented as an invited talk in CAARI 2012.

Future plans: We will continue interrogating benchmark molecular ion beams, such as H_2^+ and H_3^+ , in particular taking advantage of the new capabilities of the PULSAR laser, specifically exploring challenging two-color, pump-probe and CEP dependence (see Pub. [23]) experiments. We will carry on our studies of more complex molecules including triatomic molecules and also continue some collision studies that will merge with our laser studies in the near future.

References:

1. R. Baková *et al.* J. Chem. Phys. **128**, 144301 (2008).
2. A.M. Sayler *et al.* Phys. Rev. A **75** 063420 (2007).
3. E.Y. Sidkey and I. Ben-Itzhak, Phys. Rev. A **60**, 3586 (1999).
4. B. Jochim *et al.* (2012) – in preparation.
5. B. Sheehy, B. Walker, and L. F. DiMauro, Phys. Rev. Lett. **74**, 4799 (1995).
6. E. Charron, A. Giusti-Suzor, and F. H. Mies, Phys. Rev. Lett. **75**, 2815 (1995).
7. J.H. Posthumus *et al.*, J. Phys. B **33**, L563 (2000).
8. J.H. Posthumus *et al.*, Phys. Rev. Lett. **101**, 233004 (2008).
9. B. Gaire *et al.*, Phys. Rev. Lett. – submitted.
10. E. Wells *et al.* Phys. Rev. Lett. **86**, 4803 (2001).
11. B.D. Esry and H.R. Sadeghpour, Phys. Rev. A **60**, 3604 (1999).
12. M. Zohrabi *et al.* – in preparation.

Publications of DOE sponsored research in the last 3 years:

28. “Frustrated tunneling ionization during strong-field fragmentation of D_3^+ ”, J. McKenna, A.M. Sayler, B. Gaire, Nora G. Johnson, B.D. Esry, K.D. Carnes, and I. Ben-Itzhak, New J. Phys. (2012) – *accepted*
27. “Fragmentation of molecular-ion beams in intense ultrashort laser pulses”, Itzik Ben-Itzhak, Fragmentation Processes - Topics in Atomic and Molecular Physics, edited by Colm T. Whelan (Cambridge University Press, 2012) p. 86 (in print) – *Invited*
26. “Attosecond control of orbital parity mix interferences and the relative phase of even and odd harmonics in an attosecond pulse train”, G. Laurent, W. Cao, H. Li, Z. Wang, I. Ben-Itzhak, and C. L. Cocke, Phys. Rev. Lett. **109**, 083001 (2012).
25. “Study of asymmetric electron emission in two-color ionization of helium (XUV-IR)”, G. Laurent, W. Cao, I. Ben-Itzhak, and C.L. Cocke, in *Multiphoton Processes and Attosecond Physics* (Proceedings of the 12th International Conference on Multiphoton Processes (ICOMP12) and the 3rd International Conference on Attosecond Physics, edited by Kaoru Yamanouchi and Katsumi Midorikawa, Springer Proceedings in Physics, Vol. **125** (2012) p. 173.
24. “Tracing nuclear-wave-packet dynamics in singly and doubly charged states of N_2 and O_2 with XUV-pump–XUV-probe experiments”, M. Magrakvelidze, O. Herrwerth, Y.H. Jiang, A. Rudenko, M. Kurka, L. Foucar, K.U. Kühnel, M. Kübel, Nora G. Johnson, C.D. Schröter, S. Düsterer, R. Treusch, M. Lezius, I. Ben-Itzhak, R. Moshhammer, J. Ullrich, M.F. Kling, and U. Thumm, Phys. Rev. A **86**, 013415 (2012).
23. “Attosecond tracing of correlated electron-emission in nonsequential double ionization”, B. Bergues, M. Kübel, N.G. Johnson, B. Fischer, N. Camus, K.J. Betsch, O. Herrwerth, A. Senftleben, A.M. Sayler, T. Rathje, I. Ben-Itzhak, R.R. Jones, G.G. Paulus, F. Krausz, R. Moshhammer, J. Ullrich, and M.F. Kling, Nature Communications **3**, 813 (2012).
22. “Spectral splitting and quantum path study of high-harmonic generation from a semi-infinite gas cell”, W. Cao, G. Laurent, Cheng Jin, H. Li, Z. Wang, C.D. Lin, I. Ben-Itzhak, and C.L. Cocke, J. Phys. B: At. Mol. Opt. Phys. **45**, 074014 (2012).
21. “Dynamics of D_3^+ slow dissociation induced by intense ultrashort laser pulses”, B. Gaire, J. McKenna, M. Zohrabi, K.D. Carnes, B.D. Esry, and I. Ben-Itzhak, Phys. Rev. A **85**, 023419 (2012).
20. “Controlling strong-field fragmentation of H_2^+ by temporal effects with few-cycle laser pulses”, J. McKenna, F. Anis, A.M. Sayler, B. Gaire, Nora G. Johnson, E. Parke, K.D. Carnes, B.D. Esry, and I. Ben-Itzhak, Phys. Rev. A **85**, 023405 (2012).
19. “Frustrated tunneling ionization during laser-induced D_2 fragmentation: Detection of excited metastable D^* atoms”, J. McKenna, S. Zeng, J.J. Hua, A.M. Sayler, M. Zohrabi, Nora G. Johnson, B. Gaire, K.D. Carnes, B.D. Esry, and I. Ben-Itzhak, Phys. Rev. A **84**, 043425 (2011).

18. “Dynamic modification of the fragmentation of autoionizing states of O_2^+ ”, W. Cao, G. Laurent, S. De, M. Schöffler, T. Jahnke, A.S. Alnaser, I.A. Bocharova, C. Stuck, D. Ray, M.F. Kling, I. Ben-Itzhak, Th. Weber, A.L. Landers, A. Belkacem, R. Dörner, A.E. Orel, T.N. Rescigno, and C.L. Cocke, *Phys. Rev. A* **84**, 053406 (2011).
17. “Effect of linear chirp on strong field photodissociation of H_2^{2+} ”, Vaibhav S. Prabhudesai, Uri Lev, Oded Heber, Daniel Strasser, Dirk Schwalm, Daniel Zajfman, Adi Natan, Barry D. Bruner, Yaron Silberberg, and Itzik Ben-Itzhak, *Journal of Korean Physical Society* **59**, 2890 (2011).
16. “Following dynamic nuclear wave packets in N_2 , O_2 and CO with few-cycle infrared pulses”, S. De, M. Magrakvelidze, I.A. Bocharova, D. Ray, W. Cao, I. Znakovskaya, H. Li, Z. Wang, G. Laurent, U. Thumm, M.F. Kling, I.V. Litvinyuk, I. Ben-Itzhak, and C.L. Cocke, *Phys. Rev. A* **84**, 043410 (2011).
15. “Vibrationally resolved structure in O_2^+ dissociation induced by intense ultrashort laser pulses”, M. Zohrabi, J. McKenna, B. Gaire, Nora G. Johnson, K.D. Carnes, S. De, I.A. Bocharova, M. Magrakvelidze, D. Ray, I.V. Litvinyuk, C.L. Cocke, and I. Ben-Itzhak, *Phys. Rev. A* **83**, 053405 (2011).
14. “Velocity map imaging as a tool for gaining mechanistic insight from closed-loop control studies of molecular fragmentation”, Bethany Jochim, R. Averin, Neal Gregerson, J. McKenna, S. De, D. Ray, M. Zohrabi, B. Bergues, K.D. Carnes, M.F. Kling, I. Ben-Itzhak, and E. Wells, *Phys. Rev. A* **83**, 043417 (2011).
13. “Single-shot carrier-envelope-phase-tagged ion-momentum imaging of nonsequential double ionization of argon in intense 4-fs laser fields”, Nora G. Johnson, O. Herrwerth, A. Wirth, S. De, I. Ben-Itzhak, M. Lezius, B. Bergues, M.F. Kling, A. Senftleben, C.D. Schröter, R. Moshhammer, J. Ullrich, K.J. Betsch, R.R. Jones, A.M. Saylor, T. Rathje, K. Rühle, W. Müller, and G.G. Paulus, *Phys. Rev. A* **83**, 013412 (2011).
12. “Three-dimensional energy profile measurement of a molecular ion beam by coincidence momentum imaging compared to a retarding field analyzer”, W. Wolff, J. McKenna, R. Vácha, M. Zohrabi, B. Gaire, K.D. Carnes, and I. Ben-Itzhak, *Journal of Instrumentation* **5**, 10006 (2010).
11. “Dynamic control of the fragmentation of CO^{q+} excited states generated using high-order harmonics”, W. Cao, S. De, K.P. Singh, S. Chen, M. Schöffler, A. Alnaser, I. Bocharova, G. Laurent, D. Ray, M.F. Kling, I. Ben-Itzhak, I. Litvinyuk, A. Belkacem, T. Osipov, T. Rescigno, and C.L. Cocke, *Phys. Rev. A* **82**, 043410 (2010).
10. “Time-dependent dynamics in intense laser-induced above threshold Coulomb explosion”, B.D. Esry and I. Ben-Itzhak, *Phys. Rev. A* **82**, 043409 (2010).
9. “Resonances in electron-capture total cross sections for C^{4+} and B^{5+} collisions with $H(1s)$ ”, P. Barragán, L.F. Errea, F. Guzmán, L. Mández, I. Rabadán, and I. Ben-Itzhak, *Phys. Rev. A* **81**, 062712 (2010).
8. “Vibrationally cold CO^{2+} in intense ultrashort laser pulses”, J. McKenna, A.M. Saylor, F. Anis, N.G. Johnson, B. Gaire, Uri Lev, M.A. Zohrabi, K.D. Carnes, B.D. Esry, and I. Ben-Itzhak, *Phys. Rev. A* **81**, 061401(R) (2010).
7. “Tracing the photodissociation probability of H_2^+ in intense fields using chirped laser pulses”, Vaibhav S. Prabhudesai, Uri Lev, Adi Natan, Barry D. Bruner, Adi Diner, O. Heber, D. Strasser, D. Schwalm, I. Ben-Itzhak, J.J. Hua, B.D. Esry, Y. Silberberg, and D. Zajfman, *Phys. Rev. A* **81**, 023401 (2010).
6. “Closed-loop control of vibrational population in CO^{2+} ”, E. Wells, J. McKenna, A.M. Saylor, Bethany Jochim, Neal Gregerson, R. Averin, M. Zohrabi, K.D. Carnes, and I. Ben-Itzhak, *J. Phys. B* **43**, 015101 (2009).
5. “Examining the feedback signals used in closed-loop control of intense laser fragmentation of CO^+ ”, E. Wells, Michael Todt, Bethany Jochim, Neal Gregerson, R. Averin, Nathan G. Wells, N.L. Smolnisky, Nathan Jastram, J. McKenna, A.M. Saylor, Nora G. Johnson, M. Zohrabi, B. Gaire, K.D. Carnes, and I. Ben-Itzhak, *Phys. Rev. A* **80**, 063402 (2009).
4. “Controlling two-electron dynamics in double photoionization of lithium by initial state preparation”, G. Zhu, M. Schuricke, J. Steinmann, J. Albrecht, J. Ullrich, I. Ben-Itzhak, T.J.M. Zourus, J. Colgan, M. Pindzola, and A. Dorn, *Phys. Rev. Lett.* **103**, 103008 (2009).
3. “Suppressed dissociation of H_2^+ vibrational states by reduced dipole coupling”, J. McKenna, F. Anis, B. Gaire, Nora G. Johnson, M. Zohrabi, K.D. Carnes, B.D. Esry, and I. Ben-Itzhak, *Phys. Rev. Lett.* **103**, 103006 (2009).
2. “Benchmark measurements of H_3^+ nonlinear dynamics in intense ultrashort laser pulses”, J. McKenna, A.M. Saylor, B. Gaire, Nora G. Johnson, K.D. Carnes, B.D. Esry, and I. Ben-Itzhak, *Phys. Rev. Lett.* **103**, 103004 (2009).
1. “Dissociation and ionization of an HD^+ beam induced by intense 395-nm ultrashort laser pulses”, J. McKenna, A.M. Saylor, B. Gaire, Nora G. Johnson, E. Parke, K.D. Carnes, B.D. Esry, and I. Ben-Itzhak, *Phys. Rev. A* **80**, 023421 (2009).

ⁱ In addition to the close collaboration with the theory group of *Brett Esry*, some of our studies are done in collaboration with *Lew Cocke*’s group, *Matthias Kling*’s group, *C.W. Fehrenbach*, and others

Structure and Dynamics of Atoms, Ions, Molecules and Surfaces: Atomic Physics with Ion Beams, Lasers and Synchrotron Radiation

C.L.Cocke, Physics Department, J.R Laboratory, Kansas State University,
Manhattan, KS 66506, cocke@phys.ksu.edu

During the past year we have studied the structure of attosecond pulse trains generated by two-color (800 nm/400nm) driving fields and determined that the even harmonics brought in by the second color may be out of phase with the usual odd harmonics; we have completed our EUV/IR pump/probe studies of the dissociation dynamics of autoionizing states of O_2^+ ; we observed spectral bifurcation of the harmonics generated in a semi-infinite gas cell and have used a RABITT technique to identify the electron trajectories responsible of each branch; and we have initiated a velocity-map-imaging study of the electron spectra from C_{60} .

1. Attosecond control of orbital parity mix interferences and the relative phase of even and odd harmonics in an attosecond pulse train. *G. Laurent, W. Cao, H. Li, Z. Wang, I. Ben-Itzhak, and C. L. Cocke.* The real-time dynamics of an atom or molecule can be studied through the exposure of the target to both an optical IR field and an attosecond pulse train of extreme-ultraviolet (EUV) pulses, with a variable time delay between the two. Of particular interest are APTs formed using a two-color driving field (the IR plus its first harmonic). Such APTs have a recurrence time of a full (rather than half, when a single-color driving field is used) optical cycle of the infrared. These pulses offer the possibility to “strobe” [1] an atom or molecule with an attosecond pulse occurring at a unique time during the IR optical cycle. Ultimately the usefulness of such pulses will be limited by the degree to which the relative phases of the frequency components can be measured and controlled. A recent theoretical study suggested combining an APT and its fundamental field as an efficient means for generating strong asymmetric emission of continuum electrons along the direction of the laser polarization[2]. In this work, we demonstrate that the asymmetric photoelectron emission from atomic targets induced by APTs in the presence of a weak IR field can be controlled on an attosecond time scale by varying the time delay between APTs and IR pulses. We show that such asymmetric emission is also related to the relative phases of the harmonics in the comb, allowing, for the first time, the measurement of the phase difference between consecutive odd and even order harmonics. We find the previously unreported result that the relative phase shift between consecutive odd and even order harmonics in the plateau region appears to be near $\pi/2$. The basic principle of our experiment is presented in fig. 1. Argon atoms are ionized using an APT comprised of a comb of odd and even high-order, in the presence of a weak IR field. Starting from the $3p^6$ ground state, absorption of one XUV photon of frequency ω_q leads to an electron wave-packet in s and d orbital states. By absorption of one XUV photon of frequency ω_{q-1} (ω_{q+1}) plus absorption (emission) of one IR photon of frequency ω_0 , p and f orbital states are populated. Consequently, a mix of energy degenerate even (s , d) and odd (p , f) parity states is fed in the continuum. The opposite parity amplitudes interfere, producing an Up-Down asymmetry which oscillates as the time delay is varied. We refer to this process as First order/Second order Interference (FSI).

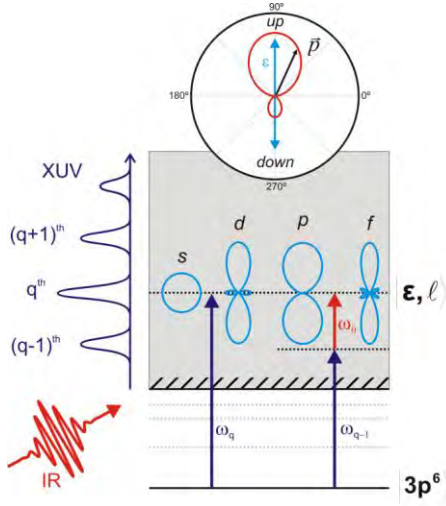


Fig.1: Principle of the measurement. A mix of energy-degenerate even and odd parity states are fed in the continuum by using a comb of even and odd high-order harmonics in THE presence of a weak IR field. Interferences between those states lead to a strong asymmetry in the angular emission of the photoelectrons respect to the polarization vector. The schematic is drawn for an azimuthal quantum number $m=0$ for the initial (and final), electron.

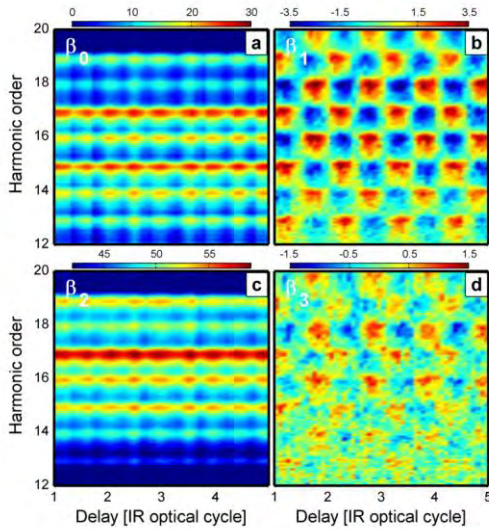


Fig 2. The angular distributions of the photoelectrons are expanded in Legendre polynomials. The usual RABBIT terms are seen in the even-order coefficients (a,c) which oscillate at $2\omega\tau$, while the FSI terms are the odd-order coefficients (b,d) which oscillate at $\omega\tau$.

Sample results are shown in fig. 2. The striking “checkerboard” pattern seen for the FSI term in panel b leads to the interpretation that the even harmonics are generated, in this case, with a phase of approximately $\pi/2$ relative to the even harmonics. Such an APT does not represent a single “strobe” pulse once per IR cycle, as is often assumed, in spite of the nearly equal intensity of even and odd harmonics. Details are provided in publication 7.

2. Dynamic modification of the fragmentation of autoionizing excited states of O_2^+ .

W. Cao, G. Laurent, S. De, M. S. Schöffler, T. Jahnke, A. Alnaser, I.A. Bocharova, C. Stuck, D. Ray, M. F. Kling, I. Ben-Itzhak, T. Weber, A. Landers, A. Belkacem, R. Dorner, A. Orel, T. Rescigno and C. L. Cocke. The tracking of the dynamics of wave packet motion in small molecules using pump/probe timing, with infrared pump and infrared probe, is now a mature subject. The use of EUV as the pump has the advantage over the IR pump that the EUV can populate, via a single photon process, a range of excited states of various ionization states of the molecule. When High Harmonic Generation (HHG) is used to generate the EUV, the resulting radiation is in the form of a short attosecond pulse train (APT) which can be made short enough (below tens of fs) to track vibrational motion in even light molecules. Such an APT still retains

some spectral resolution, allowing the experimentalist some degree of control over the range of excitation generated by the pump. In this work we fragment the oxygen molecule with an APT. It is well known that the fragmentation of any oxygen-bearing diatomic molecule can produce autoionizing excited states of neutral atomic oxygen fragments. Since the autoionization usually occurs on a time scale longer than that for fragmentation, the population of cation states of the molecule which dissociate to a charged ion plus autoionizing atomic oxygen atoms ultimately results in the observation of ion pairs in the dication channel. This study involves two parts: first, the dissociation of the dication of O_2 into O^+ ions is observed in a COLTRIMS experiment carried out by a multi-institutional collaboration (LBNL, UC Davis, KSU, Frankfurt, Auburn, Sharjah) with a monochromatic 41.6 eV photons from the ALS. From the kinetic energy release spectra and the electron energy spectra was determined that the population of this channel is mainly due to the population of highly excited states of the cation of O_2 which dissociate first and the autoionize into the dication final channel. Second, the dynamics of this dissociation is followed at KSU using a short (10-20fs) EUV APT to populate these states and initiate the dissociation, followed by an intense IR pulse to interrupt the process. The IR pumps the dissociating cation states to dication potential curves. Theoretical calculations are used to identify the specific potential curves involved. A model based on these curves agrees well with the observed dependence of the KER on the time delay between APT and IR. Details are provided in publication 1.

3. Spectral Splitting and quantum path study of high harmonic generation from a semi-infinite gas cell. *Wei Cao, Guillaume Laurent, Cheng Jin, Hui Li, Zhenghua Wang, C D Lin, I Ben-Itzhak and C L Cocke* The three-step model conceptually describes the process of harmonics from a classical point of view. Two well-known major quantum paths of the returning electron (short and long trajectory) have been identified in this intuitive classical picture. One phenomenon which can result from the participation of both paths is the spectral splitting of each harmonic into two components. Previous measurements on the spectral splitting have been limited to intensity profiles. In order to gain deeper insight into the harmonics process it is necessary to know the phase as well as the intensity of each harmonic. Here we provide such phase measurements. We do this by performing a EUV-IR cross-correlation experiment. When the harmonics are synchronized with a weak fundamental laser field and both fields interact with atoms, photoelectrons will be produced via a two-photon process with energies sitting between those produced by adjacent harmonic photoelectrons (we will call these side-band photoelectrons hereafter). By performing an EUV-IR cross correlation experiment, we are able to use the phase behavior of the different sub-peaks of each harmonic to identify them with different electronic trajectories. Both microscopic and macroscopic analysis of the spectra effects are made. The identification of a particular trajectory with a particular component of the splitting on the basis of a single-atom model is found to be incorrect, while the full macroscopic treatment is in agreement with the experiment. Details are provided in publication 3.

4. Velocity-map-imaging of electrons extracted from C_{60} by short intense laser pulses. *Z. Wang, H. Li, C.L. Cocke and M. Kling.* Recent velocity-map-imaging spectra of laser-ionized C_{60} have suggested that super-atomic-molecular-orbitals in the C_{60} can be identified by using the energy and angular distributions of low energy electrons (below 4 eV) [3]. An earlier interpretation of similar structures was attributed to Rydberg states in C_{60} [4]. In the latter case, the lifetimes expected for the states is estimated to be sufficiently long (10-100 fs) that the observations made with 120 fs pulses might be expected to be very different if shorter pulses were used. We have pursued this issue using 35 fs (and shorter) pulses at 800 and 400 nm. While the

earlier angular distributions were describable in terms of Legendre polynomials of order no higher than 2, we observe rich angular structure of much higher order, similar to that observed for Freeman resonances in atomic targets. The energy structure is definitely not lost with the shorter pulses. Further documentation and interpretation of these spectra are in progress.

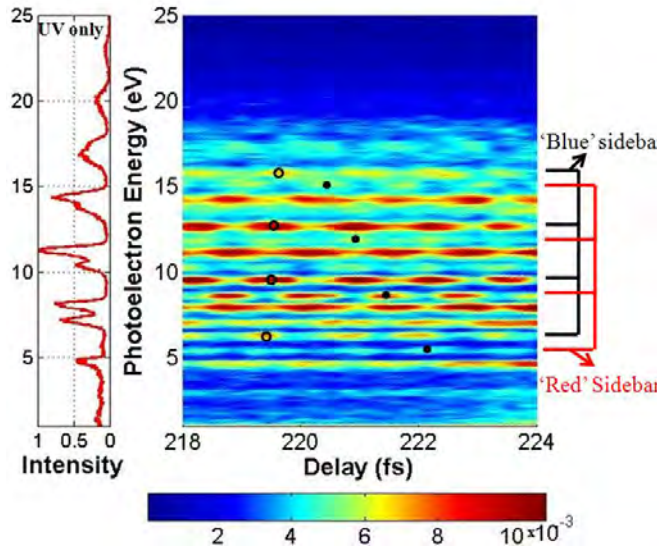


Fig.3. (left panel): Harmonic spectrum as seen from the photoelectron yield with no probe IR present. (right panel) Density plot of yield versus photoelectron energy and IR/APT delay (RABITT scan). The open and filled dots are placed at the maxima of the yields of the two harmonic branches.

References:

1. J. Mauritsson, P. Johnsson, E. Gustafson, A. L'Huillier and M. B. Gaarde, *Phys. Rev. Lett.* 97, 013001 (2006).
2. N. N. Choi, T. F. Jiang, T. Morishita, M.-H. Lee, and C. D. Lin, *Phys. Rev. A* 82, 013409 (2010).
3. J. Olof Johansson, *et al.*, *Phys. Rev. Lett.* 108, 173401 (2012).
4. M. Boyle *et al.*, *Phys. Rev. Lett.*, 87, 273401 (2001).

Publications since 2011:

- 1) Dynamic modification of the fragmentation of autoionizing states of O_2^+ , W. Cao, G. Laurent, S. De, M. Schöffler, T. Jahnke, A. S. Alnaser, I. A. Bocharova, C. Stuck, D. Ray, M. F. Kling, I. Ben-Itzhak, Th. Weber, A. L. Landers, A. Belkacem, R. Dörner, A. E. Orel, T. N. Rescigno, and C. L. Cocke, *Phys. Rev. A* **84**, 053406 (2011).
- 2) Vibrationally resolved structure in O_2^+ dissociation induced by intense ultrashort laser pulses, M. Zohrabi, J. McKenna, B. Gaire, Nora G. Johnson, K. D. Carnes, S. De, I. A. Bocharova, M. Magrakvelidze, D. Ray, I. V. Litvinyuk, C. L. Cocke, and I. Ben-Itzhak, *Phys. Rev. A* **83**, 053405 (2011).
- 3) Spectral splitting and quantum path study of high-harmonic generation from a semi-infinite gas cell, W. Cao, G. Laurent, Cheng Jin, H. Li, Z. Wang, C. D. Lin, I. Ben-Itzhak and C. L. Cocke, *J. Phys. B: At. Mol. Opt. Phys.* 45, 074013 (2012).
- 4) Orientation dependence of the ionization of CO and NO in an intense femtosecond two-color laser field, H. Li, D. Ray, S. De, I. Znakovskaya, W. Cao, G. Laurent, Z. Wang, M. F. Kling, A. T. Le, and C. L. Cocke, *Phys. Rev. A* **84**, 043429 (2011).
- 5) Following dynamic nuclear wave packets in N_2, O_2 , and CO with few-cycle infrared pulses, S. De, M. Magrakvelidze, I. A. Bocharova, D. Ray, W. Cao, I. Znakovskaya, H. Li, Z. Wang, G. Laurent, U. Thumm, M. F. Kling, I. V. Litvinyuk, I. Ben-Itzhak, and C. L. Cocke, *Phys. Rev. A* 84, 043410 (2011).
- 6) Momentum spectra of electrons rescattered from rare-gas targets following their extraction by one- and two-color femtosecond laser pulses, D. Ray, Zhangjin Chen, S. De, W. Cao, I. V. Litvinyuk, A. T. Le, C. D. Lin, M. F. Kling, and C. L. Cocke, *Phys. Rev. A* **83**, 013410 (2011).
- 7) Attosecond control of orbital parity mix interferences and the relative phase of even and odd harmonics in an attosecond pulse train, G. Laurent, W. Cao, H. Li, Z. Wang, I. Ben-Itzhak, and C. L. Cocke, *Phys. Rev. Lett.* (submitted, 2012).

Strong-field coherent control of molecules

B.D. Esry

J. R. Macdonald Laboratory, Kansas State University, Manhattan, KS 66506

esry@phys.ksu.edu

<http://www.phys.ksu.edu/personal/esry>

Program Scope

One main component of my program is to quantitatively understand the behavior of simple benchmark systems in ultrashort, intense laser pulses. As we gain this understanding, we will work to transfer it to other more complicated systems. In this effort, my group works closely with the experimental groups in the J.R. Macdonald Laboratory, including, in particular, the group of I. Ben-Itzhak.

The second main component of my program is to develop novel analytical and numerical tools to (i) more efficiently and more generally treat these systems and (ii) provide rigorous, self-consistent pictures within which their non-perturbative dynamics can be understood. The ultimate goal is to uncover the simplest picture that can explain the most — ideally, without heavy computation being necessary.

1. Theory of multi-color control of ultrafast processes

Recent progress

One of our ongoing efforts shows that carrier-envelope phase (CEP) effects, two-color control, and the physics of overlapping attosecond pulse trains and infrared pulses are all manifestations of multi-color control and can all be treated with exactly the same analytical framework. In particular, our formulation shows that these effects arise from interference between different multiphoton pathways.

For instance, writing a two-color laser field as

$$\begin{aligned} \mathcal{E}(t) = & \mathcal{E}_1(t) \cos(\omega t + \varphi_1) \\ & + \mathcal{E}_N(t) \cos[N\omega(t + \tau) + \varphi_N], \end{aligned} \quad (1)$$

with φ_i the CEPs and τ the relative delay between the two colors, implies that we can expand the total wave function $\Psi(t)$ on a Fourier basis since Ψ must be periodic in φ_1 and in $\varphi'_N = N\omega\tau + \varphi_N$. Explicitly,

$$\Psi(t) = \sum e^{i(n\varphi_1 + m\varphi'_N)} \psi_{nm}(t). \quad (2)$$

The dependence of $\Psi(t)$ on φ_1 and φ'_N has thus been made explicit since the $\psi_{nm}(t)$ do not depend on them. Physically, $\psi_{nm}(t)$ is the amplitude for the exchange of n *net* fundamental and m *net* harmonic photons with the laser field. This representation is exact in the limit that all n and m are included.

Given $\Psi(t)$ from Eq. (2), one can calculate all physical observables. In particular, the momentum distribution is

$$\begin{aligned} \frac{\partial P}{\partial \mathbf{k}} = & |\langle \psi_{\mathbf{k}}^{(+)} | \Psi(t) \rangle|^2 \\ = & \sum e^{i(n-n')\varphi_1} e^{i(m-m')\varphi'_N} \\ & \times \langle \psi_{n'm'} | \psi_{\mathbf{k}}^{(+)} \rangle \langle \psi_{\mathbf{k}}^{(+)} | \psi_{nm} \rangle. \end{aligned} \quad (3)$$

for an energy-normalized outgoing-wave scattering state $\psi_{\mathbf{k}}^{(+)}$ with asymptotic momentum \mathbf{k} .

Equation (3) shows that any CEP or delay dependence results from interference of different photon pathways. For instance, $\omega\tau$ dependence (via φ'_N) only occurs if channels with different m have the same final \mathbf{k} , which requires the net energy $(n+mN)\omega$ along each pathway to be the same. Moreover, the dominant $\omega\tau$ dependence is likely to be a linear combination of $\sin(N\omega\tau)$ and $\cos(N\omega\tau)$ since these result from the interference of pathways with $\Delta m = \pm 1$. For maximal control, $|\langle \psi_{n'm'} | \psi_{\mathbf{k}}^{(+)} \rangle|$ and $|\langle \psi_{\mathbf{k}}^{(+)} | \psi_{nm} \rangle|$ should be comparable which is primarily affected by the intensities of the two colors.

Equation (3) also shows that asymmetrical spatial distributions of the fragments — a common measure of strong-field control — can be achieved only if even and odd parities interfere. That is, the amplitudes $\langle \psi_{n'm'} | \psi_{\mathbf{k}}^{(+)} \rangle$ and $\langle \psi_{\mathbf{k}}^{(+)} | \psi_{nm} \rangle$ should have opposite signs under $\mathbf{k} \rightarrow -\mathbf{k}$. Since n and m count photons, the dipole selection rule thus requires that $n+m$ be even and $n'+m'$ be odd, or vice versa.

It is important to emphasize that no particular system has been specified. The conclusions are thus completely general, applying to all systems from atoms to complex polyatomic molecules. The ψ_{nm} will depend on the details of the system, but — armed only with the time-independent structure of the system, dipole selection rules, and energy conservation — broad, nontrivial statements about the controllability of the system with the laser parameters can be made.

We have been working with I. Ben-Itzhak's group on the two-color control of strong-field dissociation of D_2^+ and HD^+ which serves as a good demonstration of the theory. In particular, we found that the spatial asymmetry can be controlled by the relative phase between the fundamental (ω , 790 nm) and sec-

ond harmonic (2ω , 395 nm) components of a linearly-polarized ultrashort laser pulse — as has been observed in, for example, Refs. [1–3].

Although this spatial asymmetry has often been ascribed to electron localization, the proper demonstration of control over electron localization is the channel asymmetry — that is, the degree to which the dissociation into distinguishable final states can be controlled. This follows from the fact that, by definition, dissociation occurs when the binding electron becomes localized. The spatial asymmetry, on the other hand, indicates control over the interference of nuclear parities as discussed above. Previous experiments found spatial — but not channel — asymmetry.

In Fig. 1, we show the dependence of the spatial asymmetry parameter,

$$\mathcal{A}_s = \frac{P_{\text{up}} - P_{\text{down}}}{P_{\text{up}} + P_{\text{down}}}, \quad (4)$$

on the ω - 2ω delay $\omega\tau$. The spatial asymmetries oscillate with a periodicity of π as predicted by our general theory above, indicating that the two interfering pathways differ by a single harmonic photon ($|\Delta m|=1$) — as expected [1, 3–5]. Moreover, the results are qualitatively reproduced by our numerical solution of the three-dimensional time-dependent Schrödinger equation [6].

Because the experiment could resolve the $v=8$ and 9 states of D_2^+ , we could explore \mathcal{A}_s for each as shown in Figs. 1(a) and 1(b), respectively. Our calculations predict that the relative phase between these neighboring levels is too small to be observed experimentally — a fact confirmed by the data.

In contrast to \mathcal{A}_s , we observed no delay dependence in the channel asymmetry \mathcal{A}_c ,

$$\mathcal{A}_c = \frac{P_{\text{H}^+\text{D}} - P_{\text{H}^+\text{D}^+}}{P_{\text{H}^+\text{D}} + P_{\text{H}^+\text{D}^+}}, \quad (5)$$

in agreement with previous measurements on HD targets [1]. In fact, application of our general theory

2. Enhancing the carrier-envelope phase control of molecular dissociation

Recent Progress

Unfortunately, the CEP-induced asymmetries measured so far for dissociation fragments have been rather small [7–10]. These weak effects — combined with the challenge of producing intense, few-cycle, CEP stabilized pulses — greatly limit experimentalists’ abilities to explore this intriguing means of control. One important recent advance, however, is the

shows that, to a good approximation,

$$\mathcal{A}_c \approx a + b \sin 4\omega\tau + c \cos 4\omega\tau \quad (6)$$

for constants a , b , and c . This 4ω frequency indicates the interference of pathways that differ by the net exchange of 2 harmonic photons. Thus, it can only be observed at high harmonic intensities. In other words, at the intensities of our (and previous) experiments, a dominates in \mathcal{A}_c . Indeed, we observed a constant, non-zero \mathcal{A}_c .

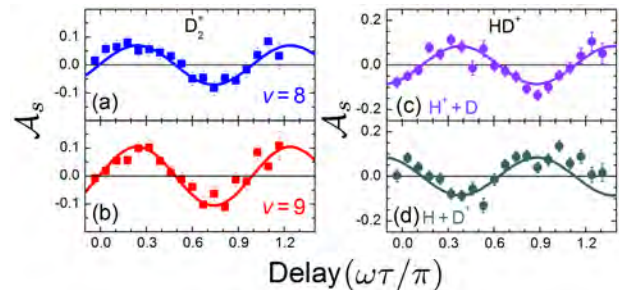


Figure 1: Two-color measurements using 790 nm, 6×10^{14} W/cm² mixed with 395 nm, 4×10^{12} W/cm² pulses: (a)&(b) D_2^+ \mathcal{A}_s for $v=8$ and 9; (c)&(d) HD^+ \mathcal{A}_s for each channel. The curves in are sinusoidal fits with π periodicity.

Future plans

We want to use our general theory to derive similar rules for other physical observables in two-color control and to do the same for a more general second color. We also want to include a third, and possibly more, colors. We know that we can derive rules similar to those for two colors, but we do not know whether they will be similarly simple. The value of enumerating the possible outcomes is substantial, especially given that we can also state how the experimental conditions need to be changed to enhance a chosen outcome. We also want to pursue other generalizations of our multi-color control theory, including applications to attosecond-scale pulses and electron dynamics as well as to controlling the branching ratios in the breakup of more complex systems.

ability to measure the CEP of each pulse [11, 12], alleviating the need for CEP stability during the measurements but not the need to identify larger effects.

Equation (3) shows that CEP-dependent spatial asymmetry results primarily from the interference of n - and $(n+1)$ -photon pathways that end at the same energy [13] since dipole selection rules dictate that they will have opposite parity. In this case, Eq. (3)

predicts that the asymmetry will be a combination of $\sin \varphi$ and $\cos \varphi$. In order for n - and $(n+1)$ -photon processes to contribute at the same final energy, the bandwidth must be large; and thus the pulse, short.

In Pub. [P14], we presented a pump-probe scheme to enhance CEP effects by an order of magnitude and demonstrated its utility for H_2^+ . In fact, we found larger asymmetries — at longer pulse lengths — than have been observed to date in H_2 experiments [7–10]. In making this claim, we also considered the experimentally important effect of focal volume averaging and proposed ways to separate the pump and probe signals. All of the supporting numerical calculations utilized our diatomic molecules code that neglects only ionization [6, 14]. This approach should be very nearly exact at the intensities we considered.

One fundamental problem lies in the fact that H_2^+ typically has a broad rovibrational distribution [15]. Since the asymmetry varies rather dramatically with v , the broad vibrational distribution tends to wash out the overall asymmetry. Even worse, the spatially symmetric $n=1$ dissociation of higher v dominates the total dissociation [6], especially after focal volume averaging [15].

For the probe-only in Fig. 2(a), we can already see reasonable asymmetry. Comparing the pump-probe case in Fig. 2(b) to Fig. 2(a), however, we find a five-fold enhancement of $|\mathcal{A}_s|$. A further two-fold relative enhancement is found after focal volume averaging.

References

- [1] B. Sheehy, B. Walker, and L. DiMauro, “Phase-control in the 2-color photodissociation of HD^+ ,” *Phys. Rev. Lett.* **74**, 4799 (1995).
- [2] M. R. Thompson, M. K. Thomas, P. F. Taday, J. H. Posthumus, A. J. Langley, L. J. Frasinski, and K. Codling, “One and two-colour studies of the dissociative ionization and Coulomb explosion of H_2 with intense Ti:sapphire laser pulses,” *J. Phys. B* **30**, 5755 (1997).
- [3] D. Ray, F. He, S. De, W. Cao, H. Mashiko, P. Rani-tovic, K. P. Singh, I. Znakovskaya, U. Thumm, G. G. Paulus, M. F. Kling, I. V. Litvinyuk, and C. L. Cocke, “Ion-energy dependence of asymmetric dissociation of D_2 by a two-color laser field,” *Phys. Rev. Lett.* **103**, 223201 (2009).
- [4] P. Brumer and M. Shapiro, “Laser control of molecular processes,” *Annu. Rev. of Phys. Chem.* **43**, 257 (1992).
- [5] M. Shapiro and P. Brumer, *Principles of the Quantum Control of Molecular Processes* (Wiley-Interscience, 2003).

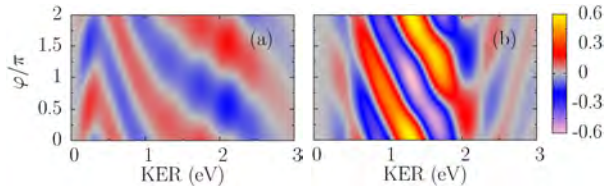


Figure 2: (a) Franck-Condon-averaged asymmetry \mathcal{A}_s for the probe-only case and (b) for the pump-probe case. (Adapted from Pub. [P14].)

Future Plans

This study proves the principle that preparing the system in states that fragment via multiple multi-photon pathways to the same final state produces a large asymmetry. Conversely, any states that fragment with a single n are not controllable via the CEP and should be excluded through, for instance, their depletion. These statements, based on our general theory, are equally applicable to more complex systems.

Moreover, since prediction of the possible pathways and their final energies requires, in principle, only structural information, we believe our general picture and our proposed scheme provide a promising means for identifying CEP-controllable processes in complex molecules not readily available with other methods. We thus want to test this belief.

- [6] F. Anis and B. D. Esry, “Role of nuclear rotation in dissociation of H_2^+ in a short laser pulse,” *Phys. Rev. A* **77**, 033416 (2008).
- [7] M. Kremer, B. Fischer, B. Feuerstein, V. L. B. de Jesus, V. Sharma, C. Hofrichter, A. Rudenko, U. Thumm, C. D. Schröter, R. Moshhammer, and J. Ullrich, “Electron localization in molecular fragmentation of H_2 by carrier-envelope phase stabilized laser pulses,” *Phys. Rev. Lett.* **103**, 213003 (2009).
- [8] B. Fischer, M. Kremer, T. Pfeifer, B. Feuerstein, V. Sharma, U. Thumm, C. D. Schröter, R. Moshhammer, and J. Ullrich, “Steering the electron in H_2^+ by nuclear wave packet dynamics,” *Phys. Rev. Lett.* **105**, 223001 (2010).
- [9] M. Kling, C. Siedschlag, A. Verhoef, J. Kahn, M. Schultze, Y. Ni, T. Uphues, M. Uiberacker, M. Drescher, F. Krausz, and M. Vrakking, “Control of electron localization in molecular dissociation,” *Science* **312**, 246 (2006).
- [10] M. F. Kling, C. Siedschlag, I. Znakovskaya, A. J. Verhoef, S. Zhrebtsov, F. Krausz, M. Lezius, and M. J. J. Vrakking, “Strong-field control of electron localisation during molecular dissociation,” *Mol. Phys.* **106**, 455 (2008).

- [11] N. G. Johnson, O. Herrwerth, A. Wirth, S. De, I. Ben-Itzhak, M. Lezius, B. Bergues, M. F. Kling, A. Senftleben, C. D. Schröter, R. Moshhammer, J. Ullrich, K. J. Betsch, R. R. Jones, A. M. Sayler, T. Rathje, K. Ruehle, W. Mueller, and G. G. Paulus, “Single-shot carrier-envelope-phase tagged ion-momentum imaging of nonsequential double ionization of argon in intense 4-fs laser fields,” *Phys. Rev. A* **83**, 013412 (2011).
- [12] T. Wittmann, B. Horvath, W. Helml, M. G. Schaetzl, X. Gu, A. L. Cavalieri, G. G. Paulus, and R. Kienberger, “Single-shot carrier-envelope phase measurement of few-cycle laser pulses,” *Nature Physics* **5**, 357 (2009).
- [13] J. J. Hua and B. D. Esry, “The role of mass in the carrier-envelope phase effect for H_2^+ dissociation,” *J. Phys. B* **42**, 085601 (2009).
- [14] F. Anis, Ph.D. thesis, Kansas State University, Manhattan, Kansas, U.S.A. (2009).
- [15] P. Q. Wang, A. M. Sayler, K. D. Carnes, J. F. Xia, M. A. Smith, B. D. Esry, and I. Ben-Itzhak, “Dissociation of H_2^+ in intense femtosecond laser field studied by coincidence 3d momentum imaging,” *Phys. Rev. A* **74**, 043411 (2006).

Publications of DOE-sponsored research in the last 3 years

- [P14] “Enhancing the intense field control of molecular fragmentation,” F. Anis and B.D. Esry, *Phys. Rev. Lett.* (accepted).
- [P13] “Multiphoton dissociation of HeH^+ below the $He^+(1s)+H(1s)$ threshold,” D. Ursrey, F. Anis and B.D. Esry, *Phys. Rev. A* **85**, 023429 (2012).
- [P12] “Dynamics of D_2^+ slow dissociation induced by intense ultrashort laser pulses,” B. Gaire, J. McKenna, M. Zohrabi, K.D. Carnes, B.D. Esry, and I. Ben-Itzhak, *Phys. Rev. A* **85**, 023419 (2012).
- [P11] “Controlling strong-field fragmentation of H_2^+ by temporal effects with few-cycle laser pulses,” J. McKenna, F. Anis, A.M. Sayler, B. Gaire, N.G. Johnson, E. Parke, K.D. Carnes, B.D. Esry, and I. Ben-Itzhak, *Phys. Rev. A* **85**, 023405 (2012).
- [P10] “Frustrated tunneling ionization during laser-induced D_2 fragmentation: detection of excited metastable D^* atoms,” J. McKenna, S. Zeng, J.J. Hua, A.M. Sayler, M. Zohrabi, N.G. Johnson, B. Gaire, K.D. Carnes, B.D. Esry, and I. Ben-Itzhak, *Phys. Rev. A* **84**, 043425 (2011).
- [P9] “Protonium formation in collisions of antiprotons with atomic and molecular hydrogen: A semiclassical study,” R. Cabrera-Trujillo and B.D. Esry, *Radiation Effects and Defects in Solids* **166**, 346 (2011).
- [P8] “Time-dependent dynamics of intense laser-induced above threshold Coulomb explosion,” B.D. Esry and I. Ben-Itzhak, *Phys. Rev. A* **82**, 043409 (2010).
- [P7] “Comparison of theoretical analyses of intense-laser-induced molecular dissociation,” B. Abeln, J.V. Hernández, F. Anis, and B.D. Esry, *J. Phys. B* **43**, 155005 (2010).
- [P6] “Vibrationally-cold CO^{2+} in intense ultrashort laser pulses,” J. McKenna, A.M. Sayler, F. Anis, N.G. Johnson, B. Gaire, U. Lev, M.A. Zohrabi, K.D. Carnes, B.D. Esry, and I. Ben-Itzhak, *Phys. Rev. A* **81**, 061401(R) (2010).
- [P5] “Tracing the photodissociation probability of H_2^+ in intense fields using chirped laser pulses,” V.S. Prabhudesai, U. Lev, A. Natan, B.D. Bruner, A. Diner, O. Heber, D. Strasser, D. Schwalm, I. Ben-Itzhak, J.J. Hua, B.D. Esry, Y. Silberberg, and D. Zajfman, *Phys. Rev. A* **81**, 023401 (2010).
- [P4] “Field-free orientation of CO molecules by femtosecond two-color laser fields,” S. De, I. Znakovskaya, D. Ray, F. Anis, N.G. Johnson, I.A. Bocharova, M. Magrakvelidze, B.D. Esry, C.L. Cocke, I.V. Litvinyuk, and M.F. Kling, *Phys. Rev. Lett.* **103**, 153002 (2009).
- [P3] “Enhancement of carrier-envelope phase effects in photoexcitation of alkali atoms,” F. Anis and B.D. Esry, *J. Phys. B* **42**, 191001(FTC) (2009).
- [P2] “Suppressed dissociation of H_2^+ vibrational states by reduced dipole coupling,” J. McKenna, F. Anis, B. Gaire, N.G. Johnson, M. Zohrabi, K.D. Carnes, B.D. Esry, and I. Ben-Itzhak, *Phys. Rev. Lett.* **103**, 103006 (2009).
- [P1] “Benchmark measurements of H_3^+ nonlinear dynamics in intense ultrashort laser pulses,” J. McKenna, A.M. Sayler, B. Gaire, N.G. Johnson, K.D. Carnes, B.D. Esry, and I. Ben-Itzhak, *Phys. Rev. Lett.* **103**, 103004 (2009).

Lightwave control and attosecond tracing of electron dynamics in atoms, molecules and nanosystems

Matthias F. Kling

James R. Macdonald Laboratory, Department of Physics
Kansas State University, Manhattan, KS 66506
Email: kling@phys.ksu.edu

Program Scope

The goal of our research is to gain deeper insight into the lightwave control of electron dynamics in atoms, molecules and nanosystems. Our research is motivated by gaining fundamental insight into the real-time dynamics of many-electron systems and to gain control over more complex, highly-correlated systems. The control and tracing of collective electron motion in molecules and nanoparticles is an important step towards the realization of lightwave molecular and nano-electronics.

Recent progress

Few-cycle laser light pulses with controlled electric field waveform can be utilized to steer electronic motion in a variety of systems. The control over the light waveform can be achieved via a variation of the carrier-envelope phase (CEP) of few-cycle pulses. In order to guide electron motion inside a molecule and thereby achieve efficient laser-driven charge directed reactivity [Weinkauff et al.(1995)], it is necessary to match the timescale of the control over the electronic motion to the timescale of the nuclear motion. As an example, the dissociation time for the molecular hydrogen ion via bond-softening (BS) may be estimated as ca. half of a vibrational period, corresponding to 12 fs [Ergler et al.(2006)]. Another necessary criterion for CEP-control is to keep the number of contributing laser cycles small. Longer wavelengths allow producing pulses with optical periods which are significantly longer in time than their counterparts (with the same numbers of cycles) in the near-infrared. Consequently, few-cycle laser pulses in the mid-infrared are expected to result in efficient CEP-control of charge directed reactivity. We have recently studied the charge-directed reactivity by few-cycle mid-infrared pulses for the prototypical dissociative ionization of D₂ [Znakovskaya et al.(2012)]. The control is achieved by superimposing two electronic states of different parity with a well-defined phase-relationship that depends on the CEP. The demonstration of efficient control of charge-directed reactivity in this proof-of-principle study is relevant to the control of larger molecules and complex molecular processes. As an example, the branching ratio at conical intersections is expected to be strongly dependent on charge localization induced by a mid-infrared few-cycle pulse [von den Hoff et al.(2012)].

Furthermore, within the last year, in collaboration with Gerhard Paulus (University Jena) and others, we have developed and implemented single-shot carrier-envelope phase tagging in conjunction with 3-dimensional imaging techniques as an alternative to the detection of CEP-effects implementing carrier-envelope phase stabilization [Rathje et al.(2012)]. As a result, we were able to significantly improve the signal-to-noise ratio in CEP-dependent measurements and acquire high-quality, long acquisition time measurements using velocity-map imaging (VMI) and cold-target-ion-recoil momentum spectroscopy (COLTRIMS) at kHz repetition rates for the first time. We will highlight the attosecond control of correlated electron emission in non-sequential double ionization, reported recently in Nature Communications [Bergues et al.(2012)], and the CEP-control of the electron emission and acceleration from nanoparticles, reported in [Zherebtsov et al.(2012)]. We have completed our attosecond streaking setup and conducted first VMI measurements on atoms (specifically on the ionization and Auger decay in rare gas atoms), that were selected as a highlight of 2011 in J. Phys. B [Zherebtsov et al.(2011a)].

Sub-cycle control of the dissociative ionization of D_2 in the mid-infrared

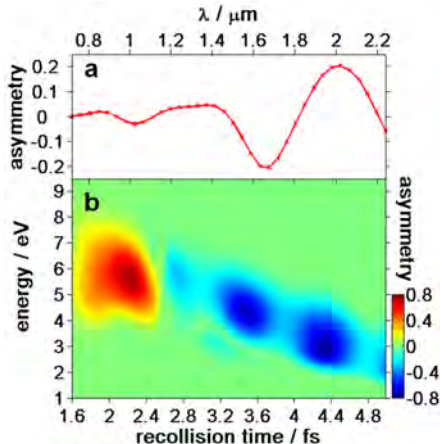


Figure 1: Wavelength dependence of the CEP-control of the dissociative ionization of D_2 : a) Asymmetry amplitude in the bond softening channel for various laser wavelength assuming a 3.5-cycle pulse. b) Asymmetry map as a function of kinetic energy and recollision time (corresponding to the wavelength given on the top axis) for the recollision excitation channel. From [Znakovskaya et al.(2012)].

to less than 3 eV at 2.1 μm . In agreement with this theoretical prediction, we have recently experimentally observed a strong CEP control of both dissociation channels in the mid-infrared employing few-cycle CEP-stable 2.1 μm pulses with pulse durations of 25 fs, that were obtained from a self-CEP stabilized optical parametric chirped pulse amplification (OPCPA) laser system [Znakovskaya et al.(2012)]. These studies open the path towards the control over electronic motion in complex chemical reactions with mid-infrared few-cycle light sources.

Attosecond control of correlated electron emission

Many fundamental processes in nature such as the formation and dissociation of molecules are governed by multiple-electron dynamics (MED). Understanding MED is one of the grand contemporary challenges of quantum physics. While the ground state properties of multi-electron systems are described with reasonable accuracy, the modeling of their dynamics is still in its infancy. Even for rather simple systems involving only a few interacting electrons, such as low- Z atoms beyond helium (Z being the nuclear charge), the exact theoretical treatment of MED is hardly practicable. The identification of suitable approximations which capture the essential features of MED relies on the development of experiments aimed at resolving the electron dynamics on the characteristic attosecond timescale of their motion. Using COLTRIMS in combination with the recently developed single-shot carrier-envelope-phase (CEP) tagging technique [Johnson et al.(2011), Rathje et al.(2012), Kübel et al.(2012)], we investigated the control of the sub-cycle dynamics of the non-sequential double ionization (NSDI) process in rare gas atoms in near single-cycle laser pulses [Bergues et al.(2012)]. Using a near-single-cycle laser pulse with appropriate CEP, the double ionization dynamics of argon could be confined to an isolated recollision event, allowing us to investigate the elementary process responsible for NSDI.

The measured correlated two-electron momentum spectrum (see Fig. 2a)) has a cross shaped structure, which has not been observed in previous experiments [de Morisson and Liu(2011)], all of them using longer laser pulses. This suggests that the transition from the multi-cycle to the near-single-cycle regime substantially modifies the dynamics of NSDI. Resolving the CEP-dependence of the correlated two-electron spectra (see Fig. 2b-e)) provided new insights into the double ionization dynamics. In particular, we have shown that, due to depletion of the excited Ar^+ ions, the second electron is emitted 210 attoseconds before the maximum of the laser electric field, which agrees well with 230 attoseconds obtained from a simple semiclassical model [Bergues et al.(2012)]. More generally, the highly differential data obtained in our experiment provide strong constraints to multi-electron theories and may greatly stimulate their development. While our semi-classical model captures the essential features of the data, electron correlations enter the model only indirectly via the ionic excitation and the scattering angle. More sophisticated models accounting for Coulomb and exchange interaction are certainly needed to fully resolve the correlated electron motion.

The wavelength dependence of the asymmetry amplitude for the directional dissociation of D_2^+ and the sign of the asymmetry are shown in Fig. 1. The asymmetry amplitudes for the BS channel considering ionization at the peak electric field (for CEP = 0) using a 3.5-cycle pulse for different wavelengths are shown in Fig. 1a). The asymmetry oscillates close to zero in the nearinfrared regime, explaining the difficulty to observe the CEP-control in this channel in previous experiments [Kling et al.(2006)]. By increasing the wavelength, the asymmetry amplitude reaches higher values. This behavior is independent of the pulse duration. The wavelength dependence of the dissociation after recollision excitation is shown in Fig. 1b) as a function of the D^+ fragment kinetic energy and the recollision time. With increasing wavelength, the recollision time increases as well. This leads to an excitation to the $2p\sigma_u^+$ state of the molecular ion at larger internuclear distances. As a result the kinetic energy of the D^+ fragments is decreasing from initially around 6 eV at 760 nm

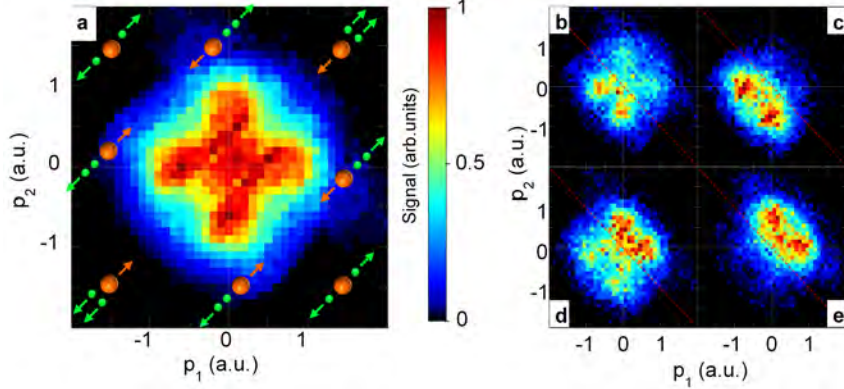


Figure 2: Experimental two-electron momentum distributions for the double ionization of argon with near-single cycle, 4 fs laser pulses at a maximum instantaneous intensity of 3.0×10^{14} W/cm². Here, p_1 and p_2 are the momentum components of the first and the second electron along the laser polarization direction, respectively. The cartoons in panel (a) illustrate the emission direction of the two electrons (green spheres) and the ion (red spheres). The arrows represent the sign of the longitudinal momentum of the fragments. A cross-shaped structure is seen in the phase-integrated plot (a), reflecting the correlated nature of the NSDI process. In images (b)-(e) spectra are shown for different values of the CEP, namely (b) 65°, (c) 155°, (d) 245°, and (e) 335°. Adapted from [Bergues et al.(2012)].

Attosecond control of the electron emission and acceleration from nanoparticles

In our research on nanosystems, we have investigated the electron emission and acceleration from dielectric nanospheres in strong few-cycle laser fields. In our recent studies, intense ($1 - 4.5 \times 10^{13}$ W/cm²) CEP-stabilized laser pulses with a central wavelength of 720 nm and 5 fs pulse duration were focused onto a beam of 90 nm SiO₂ nanospheres [Zherebtsov et al.(2011b)]. The nanoparticles were inserted into the gas phase by aerosol preparation and aerodynamic lens focusing and the momentum distribution of emitted electrons was obtained with a VMI spectrometer [Zherebtsov et al.(2011b)]. By using a beam of isolated nanoparticles we can also explore the regime near, at and beyond the material damage threshold. The extremely short pulse duration of only a few cycles in our studies ensures that the electron dynamics responsible for the observed phenomena occurs before any nuclear dynamics. High kinetic energy electrons up to 100 eV were observed. The asymmetry of the electron emission in the direction of the polarization vector showed a pronounced CEP dependence in the energy range up to the cutoff energy [Zherebtsov et al.(2011b)]. The intensity dependent measurements indicated a nearly linear dependence of the cutoff energy on laser intensity in the investigated intensity range with an average cutoff value of ca. $50 U_p$ (U_p is the ponderomotive potential of an electron in the laser field). This number is about a factor of five over the classical $10 U_p$ cutoff for above-threshold ionization of atoms.

We have recently extended on these first results using our novel combined single-shot phase-tagged VMI approach [Süßmann et al.(2011)]. The phase-tagging approach allows efficient suppression of background contributions in the experimental data and the accurate retrieval of the CEP dependent electron yield amplitudes and phases for each point in the projected 2-dimensional momentum images. The advantage of working with the projected images is the absence of any assumptions on the symmetry of the electron momentum distribution, as imposed in the regular VMI-based photoemission analysis via the Abel inversion procedure. Furthermore, the direct analysis of the CEP dependent signal removes the cross-coupling of forward and backward emission channels in the usual analysis of forward-backward asymmetries.

The CEP dependent electron yields and electron emission asymmetries excellently agree with the results from semi-classical meanfield Monte-Carlo simulations [Zherebtsov et al.(2012)]. The comparison of the momentum-resolved amplitudes and phases of the CEP dependent signal to theory offers unprecedented insights into the underlying electron acceleration mechanisms. The symmetry of the amplitude and phase maps with respect to the direction of laser propagation demonstrates that the nanoparticle response is not affected by field propagation and retardation effects in the investigated size regime. The overall structure and symmetry properties of the amplitude and phase maps in the direction of the polarization axis show the phase-selectivity of the emission from different sides of the nanoparticle and confirm that electron backscattering from the surface is the major process for the CEP dependent generation of energetic electrons.

Work in progress and outlook

We have recently extended our research into correlated electron emission dynamics to the ionization of diatomic molecules in linear [Gzibegovic-Busuladzic et al.(2011), Betsch et al.(2012)] and elliptically polarized pulses. NSDI proceeds via an inelastic recollision process, where the recollision is typically strongly suppressed in laser fields with elliptical polarization due to the transverse drift velocity of the electron. We experimentally investigated the effect of elliptical polarization on NSDI in NO in 4 fs laser fields at 750 nm. The first experiments have been carried out at the Max Planck Institute of Quantum Optics taking advantage of laser capabilities which have now been implemented at JRML. The momentum of the NO dications (see Fig.3) was measured with phase-tagged COLTRIMS. Even for high ellipticities, where NSDI is found to vanish for Ar, significant double ionization was observed for NO and the CEP-resolved dication momenta show clear signatures of the recollision process. These studies are currently being continued and completed at JRML.

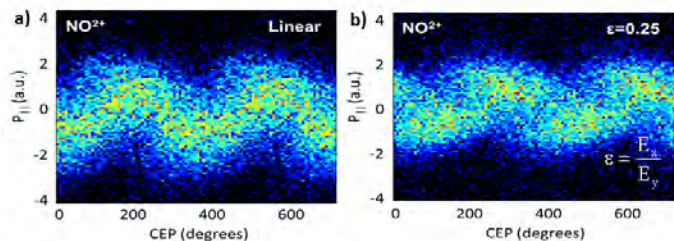


Figure 3: Momentum distribution of NO^{2+} ions parallel to the major axis of the laser polarization measured for the double ionization of NO using linear (a) and elliptical (b) polarized 4 fs laser pulses at an instantaneous intensity (along the major axis E_y) of 1.5×10^{14} W/cm².

fs pulses. We plan to improve on these experiments significantly by operating the setup with the higher, 10-kHz repetition rate PULSAR laser that was recently installed. With PULSAR we expect shorter pulses of about 4 fs duration after hollow-core fiber broadening and chirped mirror compression due to measured 21 fs pulses from the amplifier. First progress in this direction will be reported at the contractors meeting.

Furthermore, we aim at tracing the electron dynamics in nanostructures in real-time using single attosecond XUV light pulses (DOE Early Career Award). We will utilize techniques such as attosecond streaking spectroscopy, which we have theoretically developed for isolated nanospheres [Süßmann and Kling(2011)] and recently applied to measure the photoemission in Ne and Auger decay in Ar [Zherebtsov et al.(2011a)]. The application of this approach to probing the collective electron motion in nanomaterials may reveal completely novel insight into how nanolocalized fields build-up and decay in the presence of ultrashort and intense laser fields. An extension of our experiments towards high laser intensities holds the promise of becoming a fruitful approach for investigating the onset of highly nonlinear processes (see e.g. [Durach et al.(2011), Stebbings et al.(2011)]).

References

- [Weinkauff et al.(1995)] R. Weinkauff et al., J. Phys. Chem. **99**, 11255 (1995).
- [Ergler et al.(2006)] T. Ergler et al., Phys. Rev. Lett. **97**, 193001 (2006).
- [Znakovskaya et al.(2012)] I. Znakovskaya et al., Phys. Rev. Lett. **108**, 063002 (2012).
- [von den Hoff et al.(2012)] P. von den Hoff et al., IEEE J. Select. Top. Quantum. Electron. **18**, 119 (2012).
- [Rathje et al.(2012)] T. Rathje et al., J. Phys. B: At. Mol. Opt. Phys. **45**, 074003 (2012).
- [Bergues et al.(2012)] B. Bergues et al., Nature Commun. **3**, 813 (2012).
- [Zherebtsov et al.(2012)] S. Zherebtsov et al., New J. Phys. **12**, 075010 (2012).
- [Zherebtsov et al.(2011a)] S. Zherebtsov et al., J. Phys. B **44**, 105601 (2011a).
- [Kling et al.(2006)] M. F. Kling et al., Science **312**, 246 (2006).
- [Johnson et al.(2011)] N. G. Johnson et al., Phys. Rev. A **83**, 013412 (2011).
- [Kübel et al.(2012)] M. Kübel et al., New J. Phys. **in press** (2012).
- [de Morisson and Liu(2011)] F. F. de Morisson and X. Liu, J. Mod. Opt. **58**, 1076 (2011).
- [Zherebtsov et al.(2011b)] S. Zherebtsov et al., Nature Phys. **7**, 656 (2011b).
- [Süßmann et al.(2011)] F. Süßmann et al., Rev. Sci. Instrum. **82**, 093109 (2011).
- [Gzibegovic-Busuladzic et al.(2011)] A. Gzibegovic-Busuladzic et al., Phys. Rev. A **84**, 043426 (2011).
- [Betsch et al.(2012)] K. Betsch et al., Phys. Rev. A **submitted** (2012).
- [Süßmann and Kling(2011)] F. Süßmann and M. Kling, Phys. Rev. B **84**, 121406 (2011).
- [Durach et al.(2011)] M. Durach et al., Phys. Rev. Lett. **107**, 086602 (2011).
- [Stebbing et al.(2011)] S. Stebbings et al., New J. Phys. **13**, 073010 (2011).

Controlling rotations of asymmetric top molecules: methods and applications

Vinod Kumarappan

James R. Macdonald Laboratory, Department of Physics
Kansas State University, Manhattan, KS 66506
vinod@phys.ksu.edu

Program Scope

The goal of this program is to improve molecular alignment methods, especially for asymmetric top molecules, and then use well-aligned molecules for further experiments in ultrafast molecular physics. We use multi-pulse sequences for 1D and 3D alignment of molecules.

Recent progress

Multi-pulse 3D alignment of asymmetric top molecules: Theory

(V. Makhija, X. Ren, and V. Kumarappan)

Field-free 3D alignment was first demonstrated with two time-separated, orthogonally-polarized laser pulses [1, 2]. The basic idea was to 1D align the most polarizable axis with one linearly polarized pulse and to spin the molecule around this axis with the second pulse, inevitably degrading the 1D alignment produced by the first pulse in the process. Elliptically polarized pulses [3] suffer from similar limitations; a theoretical optimal control investigation of the two approaches concluded that they yield nearly the same degree of alignment [4]. Multiple elliptical pulses were shown not to produce good 3D alignment [5], although this study only considered identical pulses with the ellipticity chosen according to a criterion suggested in Ref. [3].

To overcome these limitations, we have developed a multi-pulse excitation scheme for field-free 3D alignment. This scheme is based on the structure of the matrix elements of the interaction Hamiltonian and of $\langle \cos^2 \delta \rangle$ — a single measure of 3D alignment we recently proposed [P1] — in the symmetric top basis. We were able to formulate a condition on the ellipticity of the second pulse such that instead of degrading the 1D alignment produced by the first pulse, the second pulse enhances it while also aligning the other two axes. We also found that with such an ellipticity, multiple pulses can be used, allowing the excitation of a very broad wavepacket and to synchronize the alignment of individual axes. With a sequence of four pulses, we were able to obtain $\langle \cos^2 \delta \rangle = 0.72$ (the maximum, isotropic and minimum values of this measure are 1, 0.5 and 0.25, respectively) for 1,3 difluoroiodobenzene (DFIB) in TDSE calculations [P2]. Unlike the two-pulse case for iodobenzene [P1], the 1D alignment of the C-I axis improves after each pulse. The pulse parameters used are not optimal — the first three pulses used in this calculation correspond to those we could produce in the experiment — and we expect an optimization algorithm will be able to find better multi-pulse sequences.

Multi-pulse 3D alignment of asymmetric tops: Experiment

(X. Ren, V. Makhija, and V. Kumarappan)

To demonstrate that such a scheme does, in fact, work in the laboratory, we 3D aligned DFIB using a sequence consisting of one linear pulse followed by two elliptical pulses. The most polarizable axis of the molecule is the C-I axis, the and second most polarizable one lies in the molecular plane (parallel to the F-F axis). According the TDSE calculations, our three-pulse scheme should align the C-I axis with the polarization axis of the first pulse, and the F-F axis should then be aligned along the minor axis of the two elliptically polarized pulses.

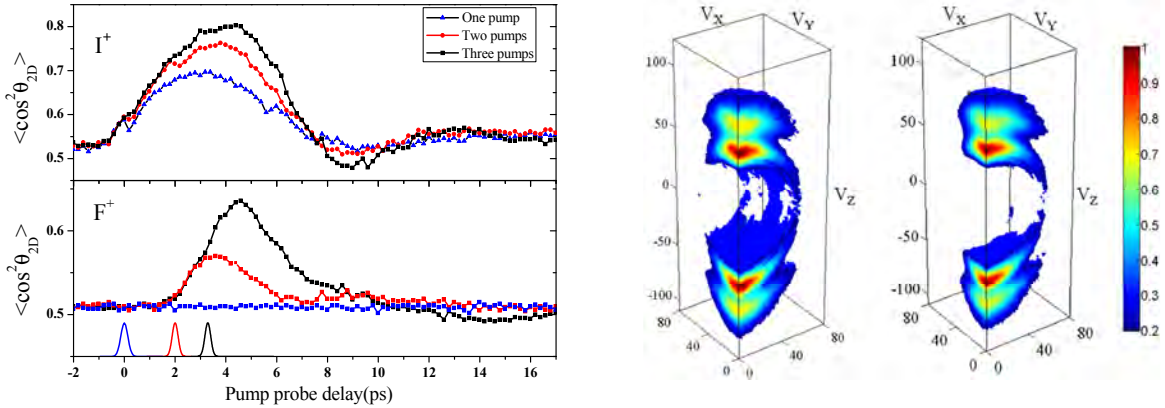


Figure 1: Left panel: The evolution of $\langle \cos^2 \theta_{2D} \rangle$ for I^+ (top) and F^+ (bottom) fragments, indicating the confinement of the C-I axis to the polarization of the first (linearly-polarized, 7.3 TW/cm², 325 fs FWHM) pulse and of the molecular plane to the polarization plane by the two subsequent elliptically polarized pulses. Right panel: 3D velocity distributions of I^+ , at the peaks of 1D (left, at 3.2 ps) and 3D (right, at 4.6 ps) alignment. The distributions were normalized to the peak values, and the velocities are in arbitrary units. Figure adapted from Ref. [P2]

We used velocity map imaging of I^+ and F^+ ions produced by an intense probe for the measurement. Angular distributions of I^+ and F^+ ions were measured in the plane of the detector. For each ion, we measured “side view” (C-I axis aligned parallel to the detector) and “end view” (C-I axis aligned perpendicular to the detector) images. By measuring the time evolution of $\langle \cos^2 \theta_{2D} \rangle$ (shown in Fig. 1 on the left panel, with θ_{2D} defined in the plane of the detector, for both ion fragments we were able to show that the elliptical pulses do all the axes and that the alignment of the three molecular axes peak at the same time.

Since velocity map images are 2D projections of 3D velocity distributions, some information is lost. In this experiment, the most important consequence is that it is difficult to distinguish between a distribution in which the I^+ ions are aligned along one axis and one in which they are smeared over the polarization plane. The experiment does not have cylindrical symmetry when the molecules are 3D aligned and Abel inversion is not possible. Since our biggest challenge is to align the F-F axis while minimizing the spreading of the C-I axis distribution in the polarization plane, we measured the full 3D momentum distribution of I^+ using tomography in the momentum space [6]. For this purpose, the molecular ensemble was rotated in space by simultaneously rotating all the laser polarizations with a single waveplate and 90 projections of the velocity distribution were measured at 2° intervals. The reconstructed distributions are shown in Fig. 1, and show that the C-I does remain confined; in fact the value of $\langle \cos^2 \theta \rangle$ increases from 0.56 for 1D alignment after one pulse to 0.65 after the two elliptical pulses. This clearly shows that our multi-pulse scheme performs as expected, improving the alignment of all the axes simultaneously. This work has been submitted for publication [P2].

The multi-pulse scheme is an important step forward in the quest for molecular frame measurements. It shows that it is not necessary to compromise the alignment of the most polarizable axis to obtain alignment of the the other axes. The scheme as implemented by us is not even optimal — the parameter space is very large and we do not have computational or experimental tools to find an optimal solution. Optimal control theory [4] could be used for the former, but is beyond our capability at this point. A polarization shaper [7] can, in principle, be used, but SLM-based polarization shapers cannot handle the power required due to the low damage threshold on the SLM itself.

High harmonic generation from asymmetric tops

(V. Makhija, X. Ren, J. Tross, S. Mondal, A.T. Le, C. Trallero and V. Kumarappan)

In the last several years, molecular axis alignment and high harmonic generation (HHG) has been show to be potent combination for investigating ultrafast dynamics in molecules. In JRM we have the fortunate combination of expertise in both theoretical and experimental HHG and in the alignment of molecules. We have embarked on a investigation of HHG in well-aligned molecules. In the past few months, we have made

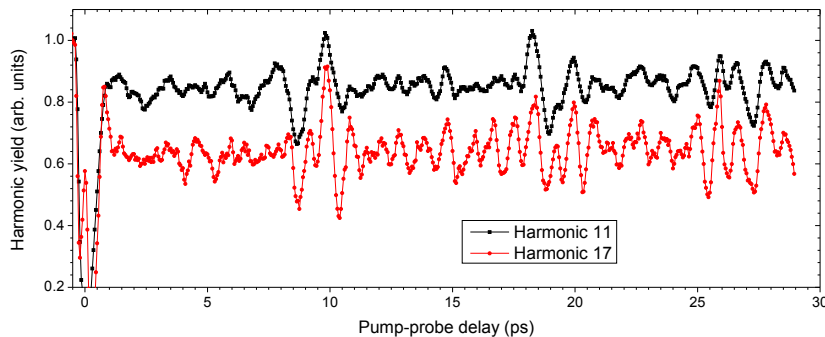


Figure 2: Left: Revivals in the yield of harmonics 11 and 17 from 1D-aligned ethylene molecules. Right: Molecular ion signal as a function of pump-probe delay, with two pump pulse at the location of the large spikes. The probe pulse was polarized parallel (red) or perpendicular to the pumps (black).

detailed measurements of HHG in nitrogen and ethylene, a linear and an asymmetric top, respectively. Some of the results of the N_2 experiments are discussed in Carlos Trallero’s contribution to this document; here we focus on the ethylene experiments.

Ethylene is a light asymmetric top molecule that is not very polarizable, and does not exhibit strong rotational revivals due to the large asymmetry of its moment of inertia tensor. Previous measurements of the alignment of ethylene have obtained $\langle \cos^2 \theta \rangle \leq 0.4$. By using a 10 bar of stagnation pressure in our Even-Lavie valve, we were able to get sufficient density in the front of the nozzle for HHG with a ~ 30 fs, 790 nm pulses. The molecules were aligned with a single pump pulse at an intensity too low to produce significant ionization. Fig. 2(a) shows the 11th and 17th harmonic from ethylene. The so-called J type and C type, with revival periods of 9 and 10 ps, respectively, can clearly be seen in both harmonics. H17 exhibits a considerably more complex structure than H11, indicating that the angle-dependence of tunnel ionization (which would show up as identical features in both harmonics) is not the only angular contribution to the revival structure. Other possibilities are the angle- and energy-dependent photoionization cross section (PICS; see Carlos Trallero’s contribution on N_2), increasing contribution from HOMO-1 at higher harmonic orders, and the evolution of the nuclear wavepacket on the ionic potential surface between the ionization and the recombination steps. We are attempting to disentangle these effects by measuring ionization rates independently and by comparison with QRS calculations. Measurements with deuterated ethylene are also planned.

Optical measurement of alignment:

(V. Makhija, X. Ren, and V. Kumarappan)

We recently developed a pump-DFWM technique for characterizing the degree of alignment of molecules. By using a spatial mask to generate the three DFWM beams, and carefully removing scattered background light and normalizing the signal to the isotropic signal, we were able to characterize rotational revivals with high fidelity. This year we expanded our code for calculating the DFWM signal from the rotational wavepacket, including when the pump pulses do not maintain cylindrical symmetry for 3D alignment. For asymmetric top molecules with large moments of inertia and polarizability, this can be a fairly large calculation. The 1D alignment results were reported in Ref [P3]; the 3D data are still being analysed. Accurate characterization of rotational revivals is essential for the HHG experiments.

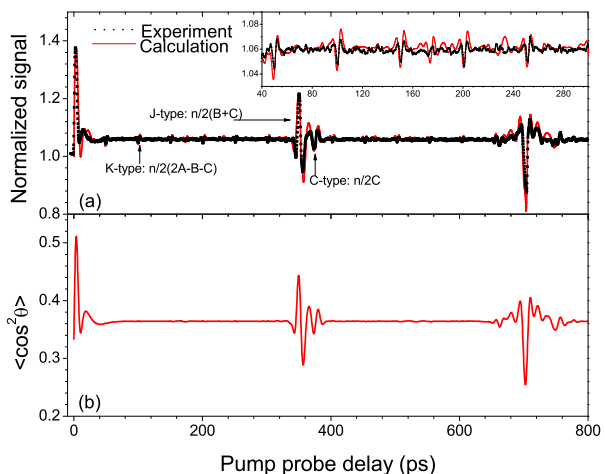


Figure 3: Top: Pump-probe measurement of the DFWM signal from 1D aligned iodobenzene (black squares) and the calculated signal (red line). The inset shows small K-type revivals. Bottom: calculated values of $\langle \cos^2 \theta \rangle$ from rigid-rotor TDSE. Figure reproduced from Ref. [P3].

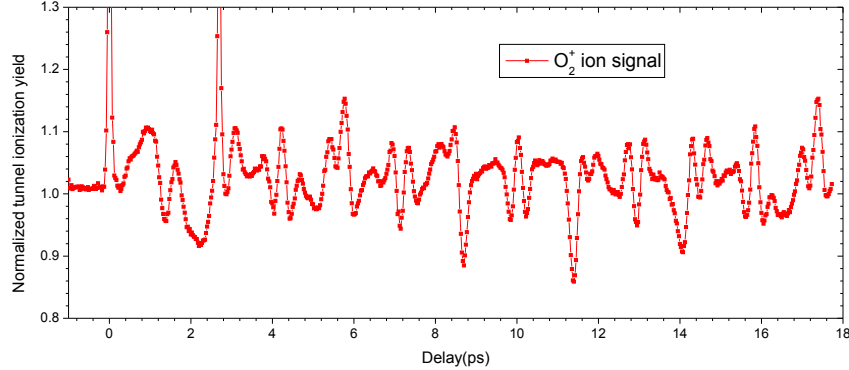


Figure 4: Oxygen molecular ion signal as a function of pump-probe delay, with two pump pulse at the location of the large spikes. The probe pulse was polarized parallel to the pumps. The rotational revival period for O_2 is 11.6 ps; strong $1/8^{\text{th}}$ revivals and hints of smaller fractions can be seen.

Work in progress and outlook

An important consideration in understanding HHG from molecules is the rate of tunnel ionization as a function of angle between the molecular axis and the laser polarization vector. As an example, if the quantitative rescattering theory is to be used in conjunction with HHG to extract field-free photo-ionization cross section of molecules, accurate knowledge of angle-dependent tunnel ionization rates is essential. There are several theoretical approaches available, but it is difficult to pick from among these without access to comparison with experiments. By measuring the molecular ion yield under the same ionization conditions as used in the HHG experiments, either directly as a function of angle, or indirectly in a revival scan, we will provide detailed data to aid the theorists. The first experiments measured the revival spectrum of singly-charged molecular fragments from N_2 , O_2 , CO_2 and C_2H_4 . The data from the O_2 measurement is shown in Fig. 4. We estimate that $\langle \cos^2 \theta \rangle \geq 0.8$. HHG measurements under these conditions have already revealed detailed features not observed before (see Carlos Trallero's contribution). In the case of asymmetric top molecules, we are trying to extract tunnel ionization rates as a function of two Euler angles, θ and χ .

We will continue to study HHG from well-aligned molecules in collaboration with Carlos Trallero, A.T. Le and C. D. Lin. Detailed comparison of the experimental data with theoretical calculations are expected to lead to improved theoretical understanding of HHG from molecules. We expect to acquire a high power phase-stabilized laser and a high energy OPA in near future, which will allow us to use two-cycle mid-IR pulses and extend the spectrum of the harmonics.

Publications from DOE-funded research:

- [P1] V. Makhija, X. Ren and V. Kumarappan, Phys. Rev. A **85**, 033425 (2012).
- [P2] X. Ren, V. Makhija and V. Kumarappan, Phys. Rev. Lett (submitted).
- [P3] X. Ren, V. Makhija and V. Kumarappan, Phys. Rev. A **85**, 033405 (2012).

References

- [1] J. G. Underwood, B. J. Sussman, and A. Stolow, Phys. Rev. Lett. **94**, 143002 (2005).
- [2] K. F. Lee, D. M. Villeneuve, P. B. Corkum, A. Stolow and J. G. Underwood, Phys. Rev. Lett. **97**, 173001 (2006).
- [3] A. Rouzee, S. Guerin, O. Faucher and B. Lavorel, Physical Review A **77** (4), 043412 (2008).
- [4] M. Artamonov and T. Seideman, Phys. Rev. A **82**, 023413 (2010).
- [5] S. Pabst and R. Santra, Phys. Rev. A **81**, 065401 (2010).
- [6] M. Wollenhaupt, M. Krug, J. Köhler *et al.*, Appl. Phys. B **95**, 647 (2009).
- [7] T. Brixner and G. Gerber, Opt. Lett. **26**, 557-559 (2001).

Strong field rescattering physics and attosecond physics

C. D. Lin

J. R. Macdonald Laboratory, Kansas State University
Manhattan, KS 66506
e-mail: cdlin@phys.ksu.edu

Program Scope:

We investigate the interaction of ultrafast intense laser pulses, and of attosecond pulses, with atoms and molecules. Most notable accomplishments in the past year are: (1) Demonstration of femtoseconds temporal and sub-angstroms spatial resolution in bond relaxation following tunneling ionization of O₂ and N₂ by mid-infrared lasers. Result of this collaboration with Ohio State group has been published in Nature. (2) The effect of propagation in the gas medium of high-harmonics has been extensively examined and compared to experiments. (3) Photoelectron and transient absorption spectra in attosecond pulses coupled to intense IR lasers have been examined in a gas medium. (4) Further studies have been carried out on nonsequential double ionization of Ne and Ar. Additional results and plans for the coming year will be summarized.

Introduction

When an atom or molecule is exposed to an intense infrared laser pulse, an electron which was released earlier may be driven back by the laser field to recollide with the parent ion. The collision of electrons with the ion may result in high-order harmonic generation (HHG), the emission of high-energy above-threshold-ionization (HATI) electrons and non-sequential double ionization (NSDI). Based on the quantitative rescattering theory (QRS) established in 2009 we are now capable of studying these processes at the quantitative level to compare with experiments. We also study the control of the dynamics of electrons exposed to attosecond pulses in the presence of strong coupling IR lasers and how the XUV pulses are shaped in the gaseous medium.

1. Study of HHG including propagation effect for atoms and molecules

Recent progress

In the last year, a graduate student Mr. Cheng Jin has put together the QRS theory in combination with the propagation equation to obtain theoretical HHG spectra such that theoretical results can be compared with experimental data. He has carried out a wide-range of studies with the new codes he developed. They include: (i) explaining HHG spectra from atoms and molecules reported in the literature [A11]; (2) effects of multiple orbitals on HHG from molecules [A10]; (3) effects of gas pressure on HHG [A7]; (4) effects of focusing conditions in a long gas cell and the spectral splitting of HHG [A3]; (5) generation of isolated attosecond pulses by mid-infrared laser in the far field by spatial filtering [A8]; (6) comparison of HHG spectra from a Gaussian vs a Bessel laser beam [A2]; and (7) conditions for extracting photoionization cross sections from HHG spectra [A1]. A number of these papers are with experimentalists from JRML and outside laboratories.

Ongoing projects and future plan

In the coming year, several topics will be studied. More accurate HHG spectra are coming out of JRML from better aligned molecules. New features have been seen. We (with Robert Lucchese) will check if more accurate photoionization cross sections will help. This is quite exciting since the latter has never been examined on aligned molecules in photoionization experiments. Another direction is HHG from 1D to 3D oriented polyatomic molecules that can now be carried out experimentally at JRML. This will involve collaboration with Robert Lucchese and his postdoc. The QRS theory for

molecules has been restricted to molecules where the nuclear positions are fixed. One of the important “applications” of HHG is to probe the dynamic systems. We have been able to formulate and carry out accurate calculations by extending the QRS to molecules undergoing large vibrational motions, and reproduced the HHG spectra of N_2O_4 reported by the JILA group. We still need to extend this theory to include more than one electronic surface. This is a very challenging project; every step has to be checked before we proceed to higher complexities.

2. Attosecond Physics and nonlinear quantum optics in the time domain

Recent progress

At present, single attosecond pulses (SAP) and attosecond pulse trains (APT) in the XUV region are generated by the HHG processes. In the last few years, such pulses are becoming more widely available. Most of the experiments have been carried out using an attosecond (AS) pulse in the presence of an intense IR laser. The AS interacts weakly with the target, but the presence of an intense IR modifies the medium, such that the effect of XUV on the target can be controlled nonlinearly in the time domain, by changing the time delay between the two pulses. Most of the existing theoretical studies adopt the “brute-force” method by solving the time-dependent Schrödinger Equation directly. We seek to identify situations where simpler models can be employed where the effect of the IR is most prominent.

Initially we have focused on AS pulses exciting the $2s2p$ (1P) of He in the presence of the IR. Since the IR can couple near-resonantly to the $2p^2$ (1S) state, the autoionization of the $2s2p$ (1P) state is strongly modified, depending on the time delay and the IR intensity. Such change can be seen by measuring photoelectron spectra or by photoabsorption spectra, the former as in Gilberston et al [PRL,105, 263003 (2011)] and the latter as in Loh et al [Chem. Phys. 350, 7 (2008)]. Since the linewidth of a resonance is only a few fractions of one eV, the spectra of Gilberston et al was not able to observe the change of the resonant profile. In Loh et al the change has been observed since better resolution can be achieved with photon spectra.

In our theoretical study, we noticed that the above system is analogous to a three-level atom except that the two upper levels are autoionizing states. If the coupling laser is changed to about 540 nm, then the $2s2p$ (1P) state can be coupled strongly to the lower $2s^2$ (1S) state. The advantage of this system is that nonlinear coupling effect will set in before ionization of these two autoionizing states becomes important. We have studied such model three-level systems, first the photoelectron spectra, then the photoabsorption spectra. The model uses the known resonance parameters of the target, thus it can be used for general atomic and molecular resonances. We also have shown that the two types of measurement reveal equivalent information [A5, A9], but the absorption spectra offer higher resolution such that the control of lineshape vs the time delay or the intensity can be investigated.

Ongoing projects and future plan

To compare our model calculations with experimental transient absorption spectra, the effect of the propagation of the XUV pulses in the gas medium has to be included. Since the absorption spectra depend on the time delay and the IR intensity, the emerged XUV from the gas medium can be manipulated. We have found that with proper tuning, in some spectral region the XUV can emerge even stronger than the input XUV light, and one can use IR to shape the XUV pulses. Such controls are similar to EIT (electromagnetic induced transparency) and other related phenomena studied since 1990's. Using attosecond pulses we can investigate the different possible controls by manipulating the IR lasers. Further extension of such studies to few-level systems will be initiated. We perceive transient absorption spectroscopy to offer a wealth of new possibilities for attosecond physics. The attosecond XUV pulses can easily eject electrons into the driving laser field that can efficiently manipulate the motion of electrons as in strong field physics. This opens up a lot of possibilities for understanding electron dynamics if the optical control of the ejected electrons is understood.

3. Laser induced electron diffraction (LIED) for dynamic imaging of molecules

Recent progress

The LIED idea we introduced in 2010 has been tested experimentally in collaboration with Ohio State University. The first results on N₂ and O₂ were reported in Nature [A4]. It established that spatial resolution of better than 0.05 Å can be achieved if mid-infrared lasers with wavelength around 2 μm or more are used as the driving laser, thus proving that LIED has the potential to be developed into a powerful tool for dynamic imaging of small molecules. This experiment also showed that the bond length of O₂ shrinks by 0.1 Å in 5 fs after the electron is removed by tunnel ionization from the O₂ molecule.

Ongoing projects and future plan

We will continue to collaborate with Ohio State University where more complex molecules are being investigated. From the theoretical side, improved methods for extracting the bond lengths and bond angles from the diffraction images should be further developed. Such tools also should be further extended to diffraction images from aligned and/or oriented molecules. With the recent emphasis of dynamic imaging of molecules in AMO physics, better software should be developed aiming at extracting weak signals that are buried in the experimental spectra since all dynamic imaging experiments will have to face such issues. We intend to tiptoe into this area, starting with familiarizing ourselves with what other tools are being used in different disciplines. A new graduate student will be devoted to this initiative.

Another related area (also important for HHG) is to look into waveform synthesis where a few lasers with wavelength in the range of 500-2000 nm are combined to optimize the yield of the returning wave packet within a pre-selected returning energy range. This investigation is underway, and enhancement of returning wave packets of two orders of magnitude has been shown. The technology of waveform synthesis is on the horizon. Implementation of such technology in the laboratory would greatly enhance signals for all rescattering phenomena without significantly increasing the power of the driving laser. We note that both LIED and HHG can all benefit greatly when synthesized waves are the driving femtosecond pulses.

4. QRS theory for NSDI

Recent progress

This program has not been continued since July 2011 with the departure of Dr. Zhangjin Chen. He is continuing to pursue this topic at his current academic position in China. We will be marginally involved only due to the lack of manpower. For the last work on this topic, see [A6].

Publications

A. Published papers (Total 31 papers since 2010)

A1. Guoli Wang, Cheng Jin, Anh-Thu Le and C. D. Lin, “Conditions for extracting photoionization cross sections from laser-induced high-order-harmonic spectra”, Phys. Rev. A86, 015401 (2012).

A2. Chen Jin and C. D. Lin, “Comparison of high-order harmonic generation of Ar using truncated Bessel and Gaussian beams”, Phys. Rev. A85, 033423 (2012).

A3. Wei Cao, Guillaume Laurent, Cheng Jin, Hui Li, Zhenghua Wang, C D Lin, I Ben-Itzhak and C L Cocke, “Spectral Splitting and quantum path study of high harmonic generation from a semi-infinite gas cell”, J. Phys. B 45, 074013 (2012).

A4. Cosmin I. Blaga, Junliang Xu, Anthony D. DiChiara, Emily Sistrunk, Kaikai Zhang, Pierre Agostini, Terry A. Miller, Louis F. DiMauro, C. D. Lin, “Observation of femtosecond, sub-Angstrom molecular bond relaxation using laser-induced electron diffraction”, **Nature** (Letter) 483, 194-197 (2012).

A5. Wei-Chun Chu and C. D. Lin, Photoabsorption of attosecond XUV light pulses by two strongly laser-coupled autoionizing states”, *Phys. Rev. A* 85, 013409 (2012).

A6. Zhangjin Chen, Y. Liang, D. H. Madison and C. D. Lin, “Strong Field nonsequential double ionization of Ar and Ne”, *Phys. Rev. A* 84, 023414 (2011).

A7. Guoli Wang, Cheng Jin, A. T. Le and C. D. Lin “Influence of gas pressure on high-order-harmonic generation of Ar and Ne”, *Phys. Rev. A* 84, 053404 (2011).

A8. Cheng Jin, A. T. Le, C. Trallero-Herrero and C. D. Lin, “Generation of isolated attosecond pulses in the far field by spatial filtering with an intense few-cycle mid-infrared laser”, *Phys. Rev. A* 84, 043411 (2011).

A9. Wei-Chun Chu, Song-Feng Zhao and C. D. Lin, “Laser-assisted-autoionization dynamics of helium resonances with single attosecond pulses”, *Phys. Rev. A* 84, 033426 (2011).

A10. Cheng Jin, Anh-Thu Le and C. D. Lin, “Analysis of effects of macroscopic propagation and multiple molecular orbitals on the minimum in high-order harmonic generation of aligned CO₂”, *Phys. Rev. A* 83, 053409 (2011).

A11. Cheng Jin, Hans Jakob Wörner, V. Tosa, Anh-Thu Le, Julien B. Bertrand, R. R. Lucchese, P. B. Corkum, D. M. Villeneuve, and C. D. Lin, “Separation of Target Structure and Medium Propagation Effects in High-Harmonic Generation”, *J. Phys. B* 44, 095601 (2011)

Papers submitted for publication

B1. Junliang Xu, Cosmin I Blaga, A. D. DiChiara, E. Sistrunk, K Zhang, Zhangjin Chen, A. T. Le, Toru Morishita, C. D. Lin, P. Agostini and L. F. DiMauro, “Laser-induced electron diffraction for probing rare gas atoms”, submitted to PRL.

B2. A. T. Le, T. Morishita, R. R. Lucchese and C. D. Lin, “Theory of high harmonic generation for probing time-resolved large-amplitude molecular vibrations with few-cycle intense lasers”, submitted to PRL.

B3. Wei-Chun Chu and C. D. Lin, “Spectral compression and enhancement of single attosecond pulses by time-delayed control field”, submitted to *J. Phys. B*.

B4. C. D. Lin, Cheng Jin, Anh-Thu Le, and R. R. Lucchese, “Probing molecular frame photoelectron angular distributions via high-order harmonic generation from aligned molecules”, submitted to *J. Phys. B*.

B5. C. D. Lin and Junliang Xu, “Imaging ultrafast dynamics of molecules with laser-induced electron diffraction”, invited perspective article to appear in PCCP.

Spatio-temporal imaging of light-induced dynamics: *From strong-field physics to ultrafast photochemistry*

Artem Rudenko

*Department of Physics Kansas State University 116 Cardwell Hall
Manhattan, Kansas 66506
rudenko@phys.ksu.edu*

Scope

My anticipated research program at the J.R. Macdonald Laboratory aims at studying basic physics of non-linear light-matter interactions in a broad span of wavelengths, from terahertz and infrared (IR) to XUV and X-ray domains, and applying the knowledge gained for imaging the structure and dynamics of photo-excited systems (atoms, molecules, clusters) with Å spatial and (sub-) femtosecond temporal resolution. The program particularly focuses on two main topic areas. The first one concentrates on real-time imaging of photo-induced reactions triggered by infrared, visible or ultraviolet laser pulses. Here, depending on a particular target, evolution of the created electronic and/or nuclear wave packets will be probed by a variety of multi-dimensional imaging techniques such as Coulomb explosion imaging, photoelectron spectroscopy/diffraction/holography, X-ray scattering or fluorescence, etc. The second major theme deals with electronic relaxation processes, charge and energy transfer, and nuclear rearrangement upon inner-shell ionization of molecules.

The program is expected to be based on a two-fold experimental infrastructure: (i) the lab-based laser and high-harmonic pump-probe setup at JRML and (ii) experiments at the external free-electron laser (FEL) facilities, such as the Linac Coherent Light Source (LCLS) and Free-electron LASer at Hamburg (FLASH). Here, one would define the optimal pump and probe configuration for a particular reaction, realizing at the JRML schemes based on optical pulses, or those employing moderately intense XUV radiation, and going to the LCLS or FLASH facilities for the experiments which need ultraintense high-frequency pulses, or require an X-ray probe beyond the wavelengths available with the high harmonic setup at JRML.

Beyond similar strategic goals, an inherent link between the two pillars (lab-based studies at JRML and experiments at LCLS/FLASH) will be provided by employing similar detection/imaging schemes in both cases. Those are expected to be based on imaging spectrometers for charged particles (coincident photoelectron and cold-target recoil ion momentum spectroscopy (COLTRIMS) or velocity map imaging (VMI)), and in certain cases complemented by simultaneous detection of scattered or fluorescent photons.

Recent progress

The program outlined here is based on vast experimental and theoretical knowledge in three-dimensional momentum imaging of strong-field processes induced by the ultrafast IR lasers acquired at the JRML and at the Max Planck Institute for Nuclear Physics in Heidelberg over the last decade, as well as on unique experience with ultrashort intense X-ray/XUV pulses gained during the first years of LCLS and FLASH operation. The main preparatory work with IR lasers includes basic experimental and theoretical studies on one- and few-electron ionization of atoms and molecules performed employing the COLTRIMS technique [1-4], and imaging of nuclear wave packets in simple molecular systems in all-optical pump-probe experiments [5-9]. In particular, the latter work resulted in the production of a

femtosecond “molecular movie” (i.e., real time sequence of the snapshots of nuclei positions) for the most basic, fastest molecular systems such as hydrogen and deuterium molecules [6,7].

The development of the first XUV/soft X-ray FEL, FLASH, extended the studies of non-linear multiphoton processes into this photon energy range [10-12], and opened up a variety of new possibilities for using short-wavelength radiation to image ultrafast molecular dynamics [13]. Employing an XUV pulse as a pump made highly excited or ionic molecular states accessible for time-domain measurements (which is important for plasma physics or for the chemistry of upper planetary atmospheres) [12-14], whereas short-pulsed soft X-rays enabled time-resolved studies upon inner-shell excitations [15]. Using XUV as a probe also offered a few advantages compared to the optical domain, in particular efficient ionization without strong dependence of the transition probability on the internuclear distance [12,13]. Since the precision of the time synchronization between the FEL beam and any external laser is currently limited to a few hundred femtoseconds by the inherent jitter caused by the stochastic nature of the self-amplified spontaneous emission generating FEL light, an XUV pump/XUV probe scheme based on a split-mirror setup has been developed [12,13] in order to achieve better time resolution. This arrangement has been used to perform a few proof-of-principle experiments on nuclear wave packet imaging in simple diatomic molecules (time resolution better than 20 fs has been demonstrated [16,17]), and then successfully applied to study XUV-induced isomerization reactions [18]. Very recently the same experimental setup enabled studies on internuclear distance-dependent charge exchange in dissociating iodine molecules and was used to define the time scale for interatomic Coulombic decay [19].

Finally, the start-up of the first hard X-ray FEL, LCLS, has allowed one to study for the first time multiphoton multiple inner-shell ionization [20-22] and offered a number of novel probe schemes, such as photoelectron diffraction and holography [23] for small or mid-sized molecules and X-ray diffractive imaging for larger single particles [24], aerosols [25], clusters [26], and nanocrystals [27,28]. Many of these proof-of-principle experiments at LCLS became possible due to the extensive capabilities offered by the newly developed CFEL-ASG MultiPurpose end station (CAMP), a machine aimed at simultaneous detection of ions, electrons, and scattered or fluorescent photons [29]. This multi-coincidence instrument, combining advanced few-particle momentum spectrometers (COLTRIMS or a double-sided velocity-map imaging (VMI) setup) with large-area, energy-resolving, fast-readout pnCCD detectors for X-ray imaging, was developed to ensure the most effective use of very expensive LCLS machine time and has housed more than 20 LCLS experiments in the first 3.5 years of operation. Of particular importance for the planned research are the combined ion and fluorescence measurements revealing the role of resonances in multiple X-ray ionization of heavy atoms [22], Coulomb explosion imaging experiments [31], and photoelectron diffraction studies on aligned molecular ensembles [32]. In addition, a cross-correlator between the LCLS X-ray beam and the external IR laser has been developed, which has enabled IR pump/X-ray probe experiments with the time resolution limited only by the pulse duration [33]. This setup has been successfully used to study the role of the molecular environment in X-ray ionization of heavy atoms in IR-dissociated molecules and to define the spatial range of interatomic relaxation processes [31].

Future plans

Based on the latest results and experimental developments outlined above, I plan to pursue the following research goals:

1) *real-time imaging and control of prototypical photo-induced structural rearrangement reactions*

Here, the first experiments at JRML will focus on constructing 3D “molecular movies” of the isomerization of acetylene and ethylene cations and dications. Following the first proof-of-principle experiments at FLASH [13,18], these reactions will be triggered either by a strong-

field IR ionization or by one XUV high harmonic photon and probed by Coulomb explosion with an intense IR pulse. In particular, differences between IR and XUV excitation and IR-induced modification of the potential surfaces involved in the transition will be studied. Further experiments will include similar 3d momentum imaging of ring closure and ring opening reactions triggered by UV/XUV photons in systems like allene or cyclo-hexadiene. In all cases, the experiments will be based on the COLTRIMS technique combined with the new 10 kHz JRML Pulsar laser and the high-harmonic setup driven with this system. In a broader context an important goal of all these studies is to understand molecular dynamics in the vicinity of conical intersections, where most of the photochemical transitions are likely to occur, to establish common ground between experiment and theory (similar to the earlier work on acetylene [18,33]), and to use the knowledge gained for developing schemes to control these dynamics.

This lab-based component will be complemented by the experiments at LCLS aimed at developing novel X-ray based schemes for imaging ultrafast molecular dynamics. Here, the most promising approach for defining atomic positions (and, thus, taking the snapshots of a “molecular movie”) is site-selective core-shell ionization and subsequent photoelectron diffraction (for low-energy electrons) [34] or holography (for high-energy ones) [13, 23]. This approach relies on measuring photoelectron angular distributions and, thus, requires a knowledge of the molecular orientation for the structure determination. From the two major schemes of defining molecular axes, active laser alignment [35] and “*a posteriori*” orientation determination by coincident ion detection [34], the former appears more suitable for sources with moderate repetition rates and, therefore, has been employed in our previous LCLS experiments (60-120 Hz) [32] and is planned for the upcoming runs. However, having in mind anticipated future developments of multi-kHz X-ray FELs, such as the European XFEL and the Next Generation Light Source (NGLS) at Berkeley, pursuing the coincidence scheme, which is (i) field-free and (ii) potentially capable of providing much more detailed alignment/orientation information, has a similarly high priority.

2) understanding the ultrafast matter response to (multiple) inner-shell photoabsorption, in particular, subsequent electronic relaxation processes, charge and energy transfer mechanisms, and nuclear rearrangement dynamics

This part of the program aims at understanding the electronic response of matter to X-ray absorption on a single atom level and then extending those concepts to larger systems, first to small or mid-sized organic molecules, then to nano-scale particles, and finally to those of biological relevance. This is extremely important in the context of prospective coherent diffractive imaging, since the processes mentioned above define mechanisms of radiation damage. Some of the central issues are (i) the influence of the environment on the inner-shell ionization, (ii) internuclear distance-dependent electronic relaxation dynamics, and (iii) charge and/or energy transfer from the absorbing atom to the environment. A straightforward way to address these issues is to embed a single heavy atom (in which X-ray absorption is enhanced and localized) into an organic molecular system (which can be pre-dissociated by another laser pulse), and then study the charge redistribution and atomic motion induced. Of particular interest are interatomic relaxation processes, which are typically entangled with the contributions of (often dominant) *intraatomic* channels but can be distinguished in some weakly bound Van-der-Waals systems, or in the dissociating molecule.

Part of this topic area dealing with single inner-shell photoabsorption at moderate energies (e.g., by the iodine 4d level, where the absorption cross section is huge because of the giant resonance) can be addressed at JRML employing a high-harmonic setup at photon energies of 60-90 eV. Measurements requiring multiple photoabsorption and those addressing deeply lying shells and triggering Auger cascades will be performed at LCLS. One of the important short-term goals of these experiments is to understand on the microscopic level basic radiation damage mechanisms in terms of both electronic rearrangement and the nuclear

motion, and to establish a link between individual atom responses and our dedicated radiation damage studies on larger systems [36,37].

Some of these experiments, such as, e.g., internuclear-distance resolved Auger spectroscopy or ionization mass spectrometry in the presence of the environment, can be performed at the high-field physics end station of the LCLS AMO beamline. Although the CAMP instrument mentioned above has gone back to Hamburg and will be installed as a permanent user end station at FLASH, there is a realistic hope that its updated version, LAMP (LCLS – ASG – Michigan Project) will come online soon, making multidimensional imaging experiments at LCLS feasible.

References

- [1] A. Rudenko, K. Zrost, C.D. Schröter, et al., *J. Phys. B* **37**, L407 (2004)
- [2] A. Rudenko, K. Zrost, B. Feuerstein, et al., *Phys. Rev. Lett.* **93**, 253001 (2004)
- [3] A. Rudenko, B. Feuerstein, K. Zrost, et al., *J. Phys. B* **38**, 487 (2005)
- [4] A. Rudenko, V.L.B. de Jesus, Th. Ergler et al., *Phys. Rev. Lett.* **99**, 263003 (2007)
- [5] Th. Ergler, A. Rudenko, B. Feuerstein, et al., *Phys. Rev. Lett.* **95**, 093001 (2005)
- [6] Th. Ergler, A. Rudenko, B. Feuerstein, et al., *Phys. Rev. Lett.* **97**, 193001 (2006)
- [7] A. Rudenko, Th. Ergler, B. Feuerstein, et al., *Chem. Phys.* **329**, 193 (2006)
- [8] B. Feuerstein, Th. Ergler, A. Rudenko, et al., *Phys. Rev. Lett.* **99**, 153002(2007)
- [9] M. Kremer, B. Fischer, B. Feuerstein, et al., *Phys. Rev. Lett.* **103**, 213003 (2009)
- [10] A. Rudenko, L. Foucar, M. Kurka, et al., *Phys. Rev. Lett.* **101**, 073003 (2008)
- [11] M. Kurka, A. Rudenko, L. Foucar, et al., *J. Phys. B* **42**, 141002 (2009)
- [12] A Rudenko, Y H Jiang, M Kurka, et al., *J. Phys. B* **43**, 194004 (2010)
- [13] J. Ullrich, A. Rudenko and R. Moshhammer, *Annual Rev. of Phys. Chem.* **63**, 635 (2012)
- [14] Y. H. Jiang, A. Rudenko, K.U. Kühnel, et al., *Phys. Rev. Lett.* **102**, 123002 (2009)
- [15] M. Krikunova, T. Maltezopoulos, P. Wessels, et al., *J. Chem. Phys.* **134**, 024313 (2011)
- [16] Y. H. Jiang, A. Rudenko, J. F. Perez-Torres, et al., *Phys. Rev. A* **81**, 051402(R) (2010)
- [17] Y. H. Jiang, T. Pfeiffer, A. Rudenko, et al., *Phys. Rev. A* **82**, 041403(R) (2010)
- [18] Y. H. Jiang, A. Rudenko, O. Herrwerth, et al., *Phys. Rev. Lett.* **105**, 263002 (2010)
- [19] K. Schnor, A. Rudenko, A. Senftleben et al., in preparation
- [20] L. Young, E.P. Kanter, B. Krässig, et al., *Nature* **466**, 56 (2010)
- [21] M. Höner, L. Fang, O. Kornilov, et al., *Phys. Rev. Lett.* **104**, 253002 (2010)
- [22] B. Rudek, S.-K. Son, L. M. Foucar, et al., *Nature Photonics*, accepted (2012)
- [23] F. Krasniqi, B. Najjari, L. Strüder, et al., *Phys. Rev. A* **81**, 033411 (2010)
- [24] M. M. Seibert, T. Ekeberg, F. R. N. C. Maia, et al., *Nature* **470**, 78 (2011)
- [25] N. D. Loh, C.Y. Hampton, A.V. Martin, et al., *Nature* **486**, 513 (2012)
- [26] T. Gorkhover, M. Adolph, D. Rupp, et al., *Phys. Rev. Lett.* **108**, 245005 (2012)
- [27] H. N. Chapman, P. Fromme, A. Barty, et al., *Nature* **470**, 73 (2011)
- [28] A. Aquila, M. S. Hunter, R. B. Doak, et al., *Optics Express* **20**, 2706 (2012)
- [29] L. Strüder, S.W. Epp, D. Rolles, et al., *Nucl. Inst. Meth. A* **614**, 483 (2010)
- [30] S. Schorb, T. Gorkhover, J.P. Cryan, et al., *Appl. Phys. Lett.* **100**, 121107 (2012)
- [31] B. Erk, D. Rolles, A. Rudenko et al., in preparation
- [32] R. Boll, A. Rudenko, D. Rolles et al., in preparation
- [33] M.E.-A. Madjet, O. Vendrell, R. Santra, *Phys. Rev. Lett.* **107**, 263002 (2011)
- [34] A. Landers, Th. Weber, I. Ali, *Phys. Rev. Lett.* **87**, 013002 (2001)
- [35] H. Stapelfeldt, T. Seidemann, *Rev. Mod. Phys.* **75**, 543 (2003)
- [36] L. Lomb, T. R. M. Barends, S. Kassemeyer, et al., *Phys. Rev. B* **84**, 214111 (2011)
- [37] A. Barty, C. Carleman, A. Aquila, et al., *Nature Photonics* **6**, 35 (2012)

Structure and Dynamics of Atoms, Ions, Molecules and Surfaces: Atomic Physics with Ion Beams, Lasers and Synchrotron Radiation

Uwe Thumm

J.R. Macdonald Laboratory, Kansas State University, Manhattan, KS 66506, thumm@phys.ksu.edu

Theoretical analysis of dissociation pathways in heavy diatomic molecules

Project scope: To develop numerical and analytical tools to (i) efficiently predict the effects of strong IR-laser and XUV fields on the bound and free electronic and nuclear dynamics in small molecules and (ii) fully image the laser-controlled nuclear and electronic dynamics.

Recent progress: Extending our investigations of the dissociative ionization dynamics of H_2 (and D_2), and in close collaboration with experimental groups, we modeled the nuclear dynamics of heavy diatomic molecules (N_2 , O_2 , CO , and Ar_2) in short IR laser and XUV pulses. We calculated *ab-initio* adiabatic molecular potential curves (and their light-induced dipole-coupling matrix elements) and designed an iterative scheme for identifying dissociation pathways that is based on the comparison of several distinct features (including vibrational periods, revival times, beat frequencies, and light-induced coupling effects) of measured and calculated kinetic-energy-release (KER) spectra in both, the time and energy domain.

Example 1: Time-resolved IR-light-induced fragmentation dynamics in N_2 , O_2 , CO (with M. Magrakvelidze, S. De, C. Aikens, I. Ben-Itzhak, L. Cocke, and M. Kling). We performed classical and quantum-mechanical calculations to investigate the bound and dissociative nuclear dynamics of electronically and vibrationally excited heavy diatomic molecular ions that are generated by a few-cycle IR-pump-laser pulse and probed by a second, delayed few-cycle IR pulse [1-4]. These calculations were based on the molecular potential curves available in the literature or on potential curves and dipole coupling matrix elements between pairs of molecular electronic states that we calculated using the quantum chemistry code GAMESS [4]. Our main interest in this project was to understand the nuclear dynamics as seen in measured delay-dependent IR-pump - IR-probe KER spectra [1-3,5]. We proceeded as follows. First, in order to identify relevant transiently populated electronic states of the molecular ions, we modeled the pump step in Franck-Condon approximation and calculated the time evolution of initial vibrational wave packets *separately* for selected potential curves of the molecular ions. The comparison of calculated KER spectra as a function of time delay, quantum-beat frequency, and vibrational revival times for one adiabatic curve at a time with experimental spectra served us as a guide for selecting relevant electronic states of the molecular ions. Next, we included probe-laser-induced dipole couplings between the relevant molecular potential curves and compared the improved calculated KER spectra with experimental data (Fig. 1), in an attempt to reveal light-induced non-adiabatic effects in measured KER spectra [3,4].

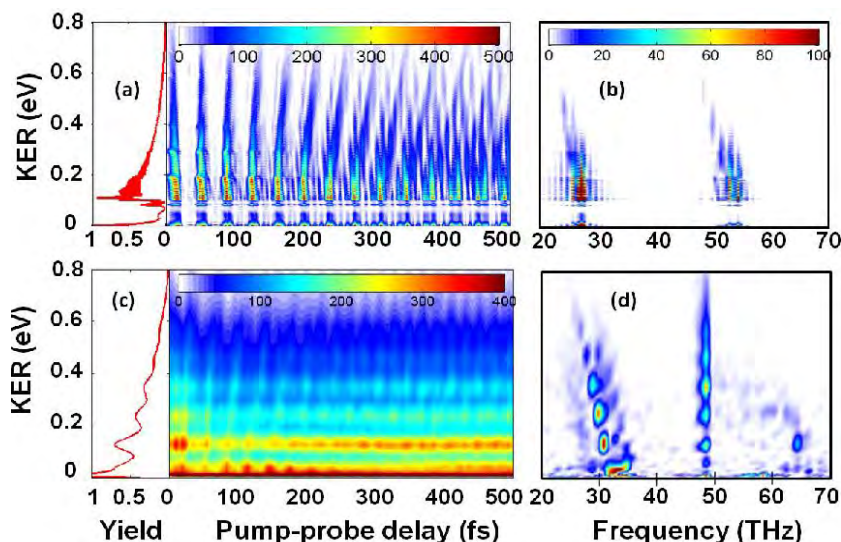


Fig. 1: (a,b) Calculated [4] and (c,d) measured [3] KER spectra for O_2^+ as a function of (a,c) pump-probe delay and (b,d) frequency. Calculated KER spectra include dipole-coupling of the $a^4\Pi_u$ and $f^4\Pi_g$ states by the 10 fs, 3×10^{14} W/cm² probe-laser pulse that has a 100 fs, 5×10^{11} W/cm² pedestal. (b,d) Power spectra obtained for a sampling time of 2 ps.

For O₂ and CO cations a distinctive vibrational structure is resolved (below 2 eV) in both, energy- and frequent-dependent KER spectra, with a characteristic spacing in energy E and oscillation period T, respectively. The product of E and T is found to be \hbar , indicating that we are observing the same physical process in the energy and the time domain. Furthermore, the power spectra (Fourier transform of the delay-versus-KER plot) show that the wave packets are chirped: higher KER is accompanied by smaller oscillation frequencies because the vibrational spacing is smaller. Our two-state numerical simulations reproduce this chirp for both O₂ and CO in good qualitative agreement with the experiment, but at lower oscillation frequencies than those observed [3].

Future plans: We believe that the simultaneous study of measured and simulated KER spectra in both, time and energy domains provides a powerful tool [6,7,8] that we intend to refine in order to better understand the complicated ro-vibrational [9,10] nuclear dynamics of laser-excited (and ionized) diatomic molecules.

Example 2: Steering the nuclear motion in Ar₂⁺ with mutually detuned laser pulses (with M. Magrakvelidze, J. Wu, and R. Dörner). We started to model how ultrashort pump and probe laser pulses of *different* central wavelengths can be employed to steer the slow nuclear motion in Ar₂⁺ and how this control can be traced in delay-dependent fragment KER spectra [5]. Our model consists in launching a nuclear wave packet on the I(1/2)_u potential curve of Ar₂⁺ at the equilibrium internuclear distance R₀ of Ar₂ (point A in Fig. 2). This wave packet subsequently starts to move inwards on the I(1/2)_u curve of Ar₂⁺. Depending on the central wavelength of the laser pulse, here 780 or 1450 nm, the wave packet may undergo a dipole-allowed one-photon transition to the II(1/2)_g curve at points B or C, respectively, followed by dissociation. The final fragment KERs are given by the difference of the nuclear potential energies in the I(1/2)_u and II(1/2)_g states at distances R₀ and ∞, respectively, and the photon energies in the 780 or 1450 nm pulses.

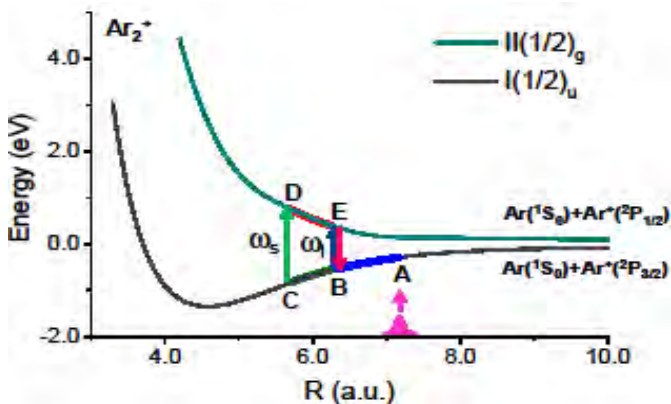


Fig. 2: Sketch of the Ar₂⁺ dissociation dynamics in two mutually delayed and detuned ultrashort laser pulses with central frequencies of ω_s (780 nm) and ω_1 (1450 nm).

The experimental data show a striking “gap” in the pump-probe-delay-dependent KER spectrum *only* if the probe-pulse wavelength exceeds the pump-pulse wavelength. This “frustrated dissociation effect” is reproduced by our two-state quantum-mechanical model, validating the interpretation as a pump-pulse-induced population transfer between dipole-coupled adiabatic electronic states of the dissociating Ar₂⁺ molecular ion [5]. Our numerical results also reproduce the measured collapse and fractional revivals of the oscillating Ar₂⁺ nuclear wave packet, as well as the decrease of the KER with increasing laser wavelength.

Future plans: We intend to further investigate the bound and dissociation dynamics of Ar₂⁺ first for different combinations of pump and probe laser wavelengths and later by including one (and more) additional “control” laser pulse(s) that is (are) detuned relative to the pump and probe pulse. We also plan to apply this model to other noble-gas dimers. This will allow us to extend our previous studies on the controlled vibrational heating and cooling of vibrational wave packets in oriented H₂⁺ molecules [11,12] by adding one (or more) “control knob(s)”, given by the frequency (-ies) of the control-laser pulse(s).

Example 3: Tracing the nuclear dynamics in diatomic molecular ions with XUV-pump and XUV-probe pulses (with M. Magrakvelidze, M. Kling, I. Ben-Itzhak, A. Rudenko, R. Moshhammer, J. Ullrich) In collaboration with experimental colleagues at JRML and in Germany, we started to model the KER from N₂ and O₂ targets in 38 eV

XUV-pump - XUV-probe experiments at the Free Electron Laser in Hamburg (FLASH) and performed first classical and quantum-mechanical calculations (Fig. 3) [13]. Our classical calculations reproduce some features of the measured KER spectra and indicate that following the classical nuclear dynamics on quantum-mechanical adiabatic potential curves can be a valid scheme for deriving fragment KERs (with limited accuracy). In our quantum-mechanical nuclear-wave-packet-propagation simulations, we investigated various dissociation paths by calculating KER spectra separately for different (bound and dissociating) intermediate adiabatic electronic states of $O_2^{+,2+}$ and $N_2^{+,2+}$ with partial success. While some of these trial dissociation paths generated signatures in the calculated spectra that can be related to structures in the measured KER spectra, our identification of these measured structures is neither complete nor unique.

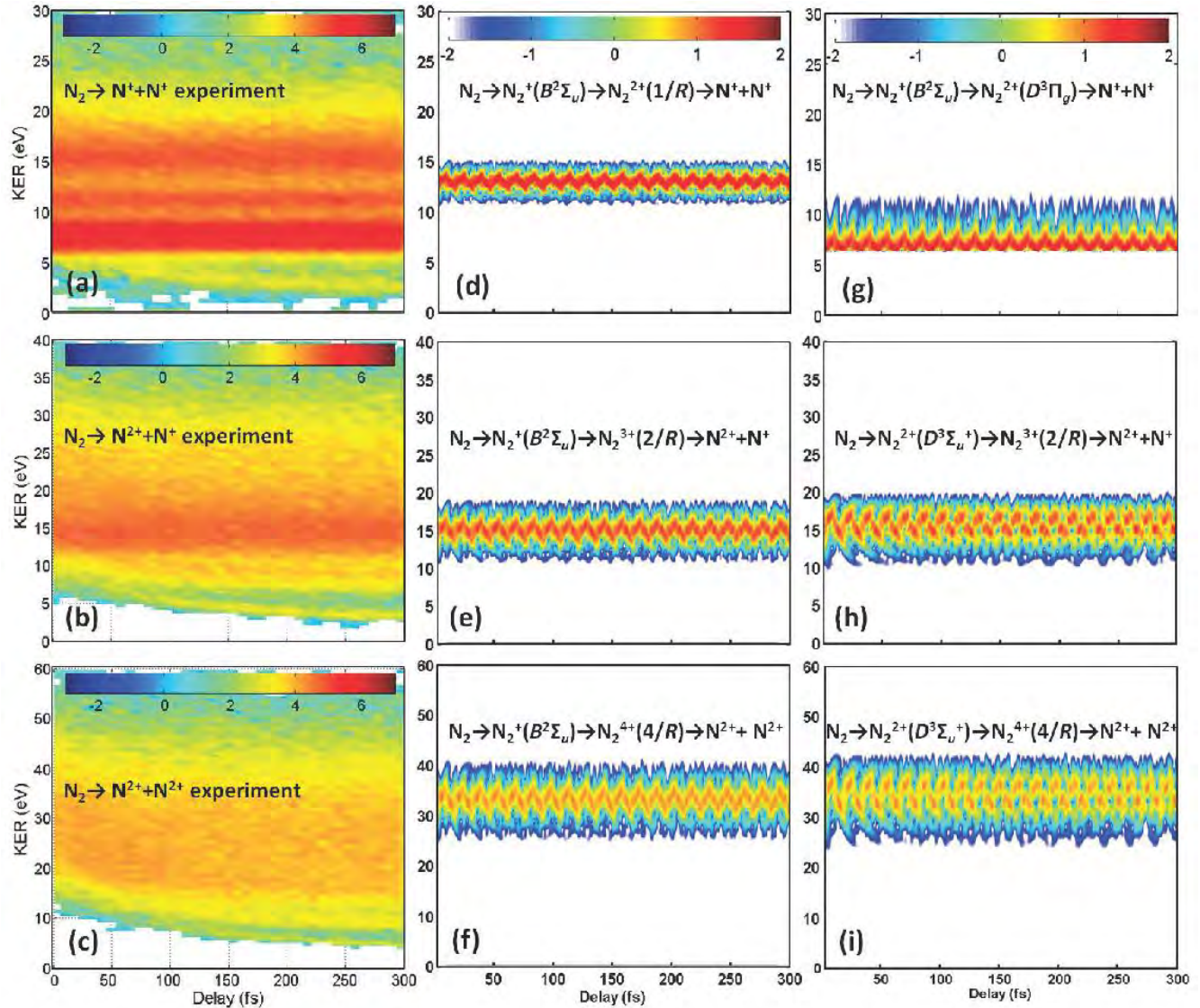


Fig. 3: (a,b,c) Measured KER spectra as a function of XUV-pump - XUV probe-delay for the dissociation of N_2 into different fragment-charge channels. (d-i) Corresponding quantum-mechanical calculations.

Future plans: We plan to improve and extend these investigations in various ways. First, we intend to examine the relevance of intermediate and final electronic states of singly to quadruply charged N_2 and O_2 ions that we have not yet been able to include. For this purpose we will refer to published adiabatic molecular potential curves and, where not available, preform *ab-initio* calculations using the GAMESS molecular structure program package [4]. Next, we plan to include dipole couplings between two (later more) selected adiabatic states. We will compute these couplings using GAMESS and attempt to match the existing measured KER spectra as closely as possible in order to improve our assignment of likely dissociation pathways.

Publications and manuscripts addressed in this abstract

- [1] *Tracking dynamic wave packets in the O₂ dication using a pump-probe approach*, S. De, I. Bocharova, M. Magrakvelidze, D. Ray, W. Cao, B. Bergues, U. Thumm, M. F. Kling, I. V. Litvinyuk, and C. L. Cocke, *Phys. Rev. A* **82**, 013408 (2010).
- [2] *Time-resolved Coulomb explosion imaging of nuclear wave-packet dynamics induced in atomic molecules by intense few-cycle laser pulses*, I.A. Bocharova, A. S. Alnaser, U. Thumm, T. Niederhausen, D. Ray, C.L. Cocke, and I.V. Litvinyuk, *Phys. Rev. A* **83**, 013417 (2011).
- [3] *Following dynamic nuclear wave packets in N₂, O₂ and CO with few-cycle infrared pulses*, S. De, M. Magrakvelidze, I. Bocharova, D. Ray, W. Cao, I. Znakovskaya, H. Li, Z. Wang, G. Laurent, U. Thumm, M. F. Kling, I. V. Litvinyuk, I. Ben-Itzhak, and C. L. Cocke, *Phys. Rev. A* **83**, 013417 (2011).
- [4] *Dissociation dynamics of diatomic molecules in intense laser fields: a scheme for the selection of relevant molecular potential curves*, M. Magrakvelidze, C.M. Aikens, and U. Thumm, *Phys. Rev. A* **86**, 023402 (2012).
- [5] *Steering the nuclear motion in singly ionized argon dimers with mutually detuned laser pulses*, J. Wu, M. Magrakvelidze, A. Vredenburg, L. Ph. H. Schmidt, T. Jahnke, A. Czasch, R. Dörner, and U. Thumm, *Phys. Rev. Lett.*, submitted.
- [6] *Towards a complete characterization of molecular dynamics in ultra-short laser fields*, B. Feuerstein, T. Ergler, A. Rudenko, K. Zrost, C.D. Schroeder, R. Moshhammer, J. Ullrich, T. Niederhausen, and U. Thumm, *Phys. Rev. Lett.* **99**, 153002 (2007).
- [7] *Time-series analysis of vibrational nuclear wave packet dynamics in D₂⁺*, U. Thumm, T. Niederhausen, and B. Feuerstein, *Phys. Rev. A* **77**, 063401 (2008).
- [8] *Quantum-beat imaging of the nuclear dynamics in D₂⁺: Dependence of bond softening and bond hardening on laser intensity, wavelength, and pulse duration*, M. Magrakvelidze, F. He, T. Niederhausen, I. V. Litvinyuk, and U. Thumm, *Phys. Rev. A* **79**, 033410 (2009).
- [9] *Multidimensional quantum-beat spectroscopy: Towards the complete temporal and spatial resolution of the nuclear dynamics in small molecules*, M. Winter, R. Schmidt, and U. Thumm, *Phys. Rev. A* **80**, 031401(R) (2009).
- [10] *Quantum-beat analyses of the rotational-vibrational dynamics in D₂⁺*, M. Winter, R. Schmidt, and U. Thumm, *New Journal of Physics*, *New J. of Phys.* **12**, 023023 (2010).
- [11] *Controlled vibrational quenching of nuclear wave packets in D₂⁺*, T. Niederhausen and U. Thumm, *Phys. Rev. A* **77**, 013407 (2008).
- [12] *Laser-controlled vibrational heating and cooling of oriented H₂⁺ molecules*, T. Niederhausen, U. Thumm, and F. Martin, in *J. Phys. B: At. Mol. Opt. Phys.* **45**, 105602 (2012).
- [13] *Tracing nuclear wave packet dynamics in singly and doubly charge states of N₂ and O₂ with XUV pump – XUV probe experiments*, M. Magrakvelidze, O. Herrwerth, Y.H. Jiang, A. Rudenko, M. Kurka, L. Foucar, K.U. Kühnel, M. Kübel, Nora G. Johnson, C.D. Schröter, S. Düsterer, R. Treusch, M. Lezius, C.L. Cocke, I. Ben-Itzhak, R. Moshhammer, J. Ullrich, M. F. Kling, and U. Thumm, *Phys. Rev. A* **86**, 013415 (2012).

Other recent publications and manuscripts (2011-12)

- *Attosecond timing of asymmetric chemical bond breaking*, J. Wu, M. Magrakvelidze, L. Ph. H. Schmidt, M. Kunitski, T. Pfeifer, M. Schöffler, M. Pitzer, M. Richter, S. Voss, H. Sann, H. Kim, T. Jahnke, A. Czasch, U. Thumm, and R. Dörner, *Nature*, submitted.
- *Attosecond time-resolved photoelectron spectroscopy of surfaces*, U. Thumm and C.-H. Zhang, invited paper, *Light at extreme intensities* (Szeged, HU 2011), *AIP Conf. Proc* **1462**, 57 (2012).
- *Effects of wave-function localization on the time delay in photoemission from surfaces*, C.-H. Zhang and U. Thumm, *Phys. Rev. A* **84**, 065403 (2011).
- *Probing dielectric response effects with attosecond time-resolved streaked photoelectron spectroscopy of metal surfaces*, C.-H. Zhang and U. Thumm, *Phys. Rev. A* **84**, 063403 (2011).
- *Attosecond probing of instantaneous AC Stark shifts in helium atoms*, F. He, C. Ruiz, A. Becker, and U. Thumm, *J. Phys. B: At. Mol. Opt. Phys.* **44**, 211001 (2011).
- *Hydrogen-anion formation near (2x1) reconstructed Si (100) surfaces: Substrate-electronic-structure and trajectory dependence*, B. Obreshkov and U. Thumm, *Phys. Rev. A* **83**, 062902 (2011).

Strong-Field Time-Dependent Spectroscopy

Carlos A. Trallero

J. R. Macdonald Laboratory, Kansas State University, Manhattan, KS 66506

carlos@phys.ksu.edu

Scope

The main scope of my program is to measure and control the state of molecular systems. In particular, I'm interested in observing molecules evolve with attosecond and/or femtosecond time resolution.

1 Coherent spectroscopy of large molecular systems

in collaboration with A.-T Le, R. Lucchese and E. Poliakoff

As mentioned in the introduction, one of our main research objectives under this grant is to create a solid frame for the utilization of HHG as a new tool for molecular spectroscopy. We have established a collaboration between JRML, Erwin Poliakoff from Louisiana State University and Robert Lucchese from Texas A& M University to extend such studies to larger molecules. In addition, while spectroscopic studies with HHG have been done already [1, 2], there is a large controversy on whereas the observed structure is stable or not to phase matching conditions [3] [4]. Therefore, one question we also intend to answer is how robust the HHG method is to macroscopic conditions. In this section we focus on extracting PCIS from large molecules whose electron spatial distribution is close to isotropic and the role of the induced macroscopic wavepacket to the extracted cross sections. In Section 2 we focus on molecules with electronic density on the HOMO that is far from isotropic.

For the first studies of our collaboration we generated harmonics from SF₆, CF₄ and SiCl₄ in all cases we changed the driving laser energy and focus position. These are the main parameters influencing the macroscopic behavior of HHG. In particular, we are interested in studying shape resonances, which are present in highly symmetric molecules like the ones proposed.

The preliminary results for the high harmonic spectroscopy of SF₆ confirm effects of a shape resonance on the harmonic signal. The experiment was conducted by moving the lens on an automated stage in order to position the focal point at different locations in the molecular beam. As is expected due to phase matching conditions, spectra taken from lens positions on the front side of the molecular beam have a higher harmonic cutoff and greater harmonic intensity. The higher intensity results in increased sensitivity relative to the observation of effects previously studied in photoionization cross sections. This trend is further shown in Fig. 1 In this figure, the envelope from the near side of the gas jet has a much higher harmonic cutoff and overall intensity. It is in this envelope that the effect of a shape resonance is easy to observe. A shape resonance has been reported at 27.1 eV in the ground state of SF₆ corresponding to a location between the 17th and 19th harmonic. A dip is clearly visible in each envelope but is more pronounced in the data with a higher cutoff. A low energy shape resonance is also present in the ground state of CF₄ at 30 eV. Though there is some evidence of a dip at the 21st harmonic of CF₄ similar to the dip found in the SF₆ spectra, more analysis is needed before a conclusion can be reached.

SiCl₄ also shows some indication of the presence of an expected shape resonance around 23eV. The data for this molecule is however not as clean. Since SiCl₄ is a liquid, we bubble He gas through SiCl₄ to have enough molecular density at target. Given the low I_p of the gas and the low density, our measurements are still inconclusive. We expect that by using the new HITS laser and few cycle pulses in the mid-IR we will be able to generate HHG with a longer cutoff and higher resolution.

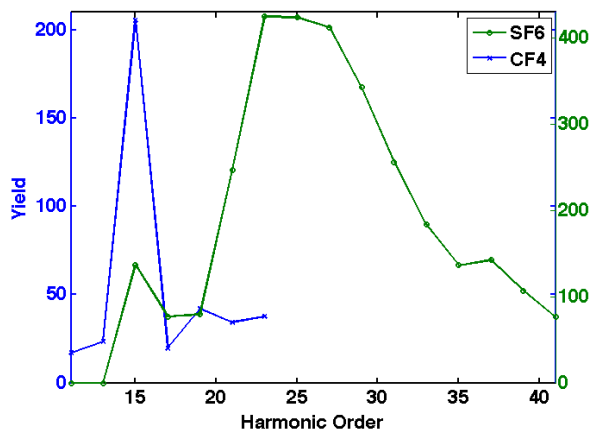


Figure 1: Lineouts of the total HHG yield in SF₆ (green) and CF₄ (blue) generated with 30fs, 800nm pulses.

2 High harmonic generation from well-aligned molecules

in collaboration with V. Kumarappan, A.-T Le and R. Lucchese

For these experiments, we coupled the Trallero group’s flat-field XUV spectrometer with Vinod’s group source chamber containing the Even-Lavie valve. Together, the entire system is very stable, and allows us to measure fine details in the rotational revival scans of HHG. Since the system was put together for the first time in March 2012, we have studied HHG from nitrogen with the goal of extracting the angle and energy dependent photo-ionization cross section of nitrogen using QRS, and the unexpected revival structure and angular distribution of the near-threshold harmonics in N_2 .

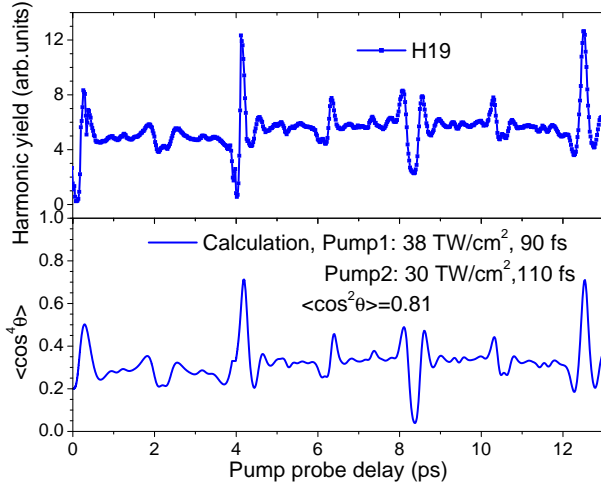


Figure 2: Harmonics H19 from N_2 as a function of pump-probe delay. Two pump pulses, centered at -3.9 ps and 0 ps, were used to align the molecules. Also shown are $\langle \cos^2 \theta \rangle$ and $\langle \cos^4 \theta \rangle$ calculated from the rotational wavepacket. Note that the HHG revivals are similar but not identical to the $\langle \cos^4 \theta \rangle$, especially for H37. The revival structure calculated with QRS for these harmonics are also shown.

obtained $\langle \cos^2 \theta \rangle = 0.82$, which is considerably better than the typical values of ~ 0.6 that other groups have reported. With the alignment so good, the revival spectrum shows high-order fractional revivals that reflects not only the rotational wavepacket but also the various partial wave contributions to the HHG spectrum. The revival structure for harmonic H19 together with a theoretical fit are shown in Fig. 2.

We also measured the angular distribution of the harmonics at the full rotational revival of N_2 , at 8.3 ps after the second pump pulse. The HHG driver polarization was kept fixed, and the molecules were rotated by means of a zero-order half-wave plate. Just like the revival scans, the angular distributions are expected to reflect the molecular PICS as a function of XUV energy. In Fig. 3, we show the angular distributions of many harmonics from threshold to well past the cutoff. In our data a distinct minimum appears at 0° and 180° , and the maximum is shifted to near 40° . This is the first time, to the best of our knowledge, that this Cooper minimum has been observed directly in the HHG angular distribution. While our results show a clear minima at 0° , the energy range is shifted by 10eV from the predicted minimum (see Fig. 4),

Another important feature that is apparent in our data is the ~ 30 eV $3\sigma_g \rightarrow k\sigma_u$ shape resonance that lies near 0° . This resonance enhances the contribution the contribution of harmonics M to N relative to the isotropic value, but only when the angel between the molecular axis and the driver polarization is $\leq 30^\circ$. As a comparison, we also show in Fig. 4 the theoretical photorecombination cross section in N_2 from [5]. We believe that the reason why the measured resonance is narrower than predicted theoretically is interference with lower order harmonics which in turn are affected by threshold and resonant effects.

We employ the kHz Even-Lavie valve to produce rotationally cold molecular targets. The cooling of diatomic molecules like N_2 is not as effective, but is still quite good compared to lower pressure jets. In order to strongly align molecules, multi-pulse sequences are used. This scheme together with the cold jet enables us to carry out HHG experiments with substantially better aligned molecules than are available anywhere else.

QRS, which has been very successful in modelling the HHG process in atoms and molecules, relies on a separation of a target-independent electron wavepacket and the field-free photoionization cross-section of the target. Our goal is to extract fully-differential PICS using our ability to align molecules and to characterize the rotational wavepacket quite well. N_2 is a well studied system in which to attempt this reconstruction. Theoretically, an angle- and energy-dependent shape resonance has been predicted near 30 eV that extends from 0° to $\sim 40^\circ$ in angle. Also predicted is a Cooper minimum near 50 eV between 0° to $\sim 15^\circ$. Neither of these structures has been directly observed by synchrotron or HHG experiments.

We aligned N_2 using two pump pulses and obtained

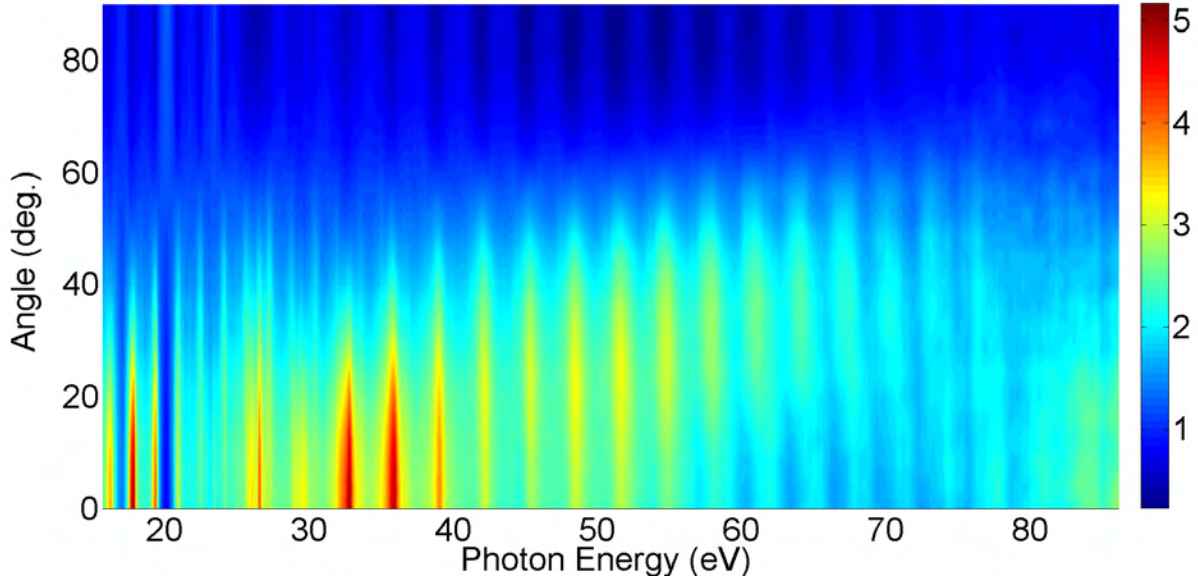


Figure 3: Angular distribution of H11 to H47 from N_2 normalized to the isotropic harmonics.

3 Phase matching studies of HHG

in collaboration with A.-T Le

HHG is intrinsically a collective process. Therefore, to use this process as a spectroscopic tool, we need to understand the influence of macroscopic parameters in HHG spectra. Our goal in this topic is to find the ideal (and practical) experimental conditions to perform spectroscopic experiments with HHG.

Phase matching plays an important role in the generation of IAPs and the HHG process in general. Since phase matching is a macroscopic effect, the mode of the laser beam will play an important role. Empirically, this is observed in labs when the beam profile is slightly changed to improve the quality of the harmonics profile. In addition, few cycle pulses are generated using hollow core fibers whose spatial modes are Bessel instead of the mainly assumed Gaussian. In this section we explore the effect of truncated Gaussian modes and few cycle Bessel modes in the phase matching of HHG. To guarantee that the focusing conditions remain consistent for all modes we also measure the ionization yield in parallel. As ions are only intensity dependent they will reveal if additional distortions are occurring at the focus. Our position and intensity measurements for all beam profiles show a smooth intensity distribution through the focus.

The experimental setup has a source chamber with a piezo driven pulsed coupled to a flat-field spectrometer. Our spectrometer has been designed to operate without any filters (the driver light is spatially filtered out using baffles), and uses a holographically-ruled flat-field grating to minimize ghosts and other artifacts in the spectrum. As a result high-contrast HHG spectra can be recorded starting from the 11th harmonic of the fundamental at 800nm (18eV).

Fig. 6 a) to c) show the total HHG yield in Kr with 800nm, 30fs pulses as a function of energy and

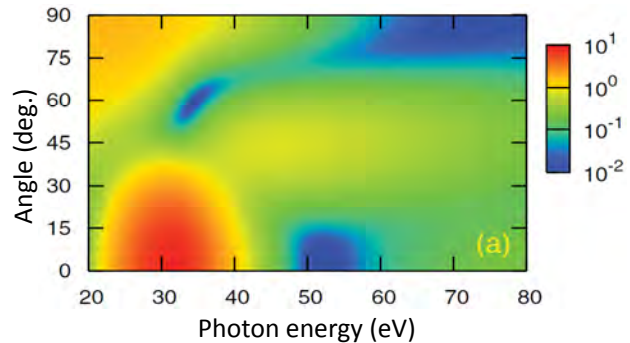
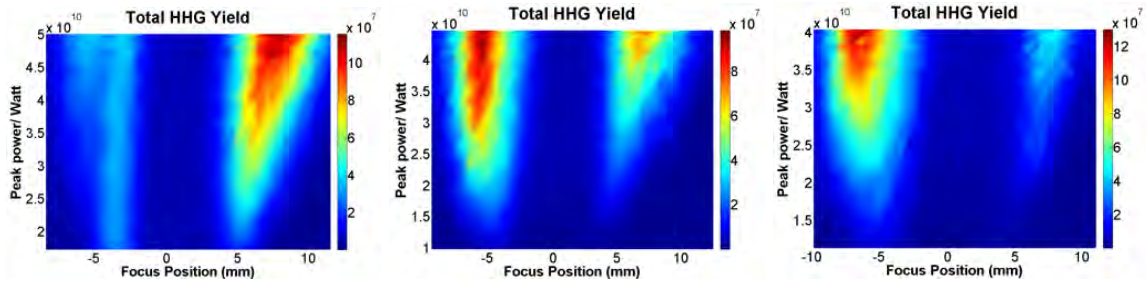


Figure 4: Theoretical calculation PICS for N_2 from [5].

Figure 5: Comparison between theoretical calculations for the PICS and the angular distribution of harmonics in aligned N_2 . In the experiment, $\langle \cos^2\theta \rangle = 0.82$ obtained with a sequence of pulses (see text)



(a) Un-clipped beam (gaussian). (b) 10% of the energy clipped. (c) 20% of the energy clipped beam

Figure 6: Total HHG yield as a function of pulse power, and focus position for three beam profiles.

focus position. To guarantee the same conditions for all experiments, the energy is controlled using a half wave plate and a cube polarizer. Position is changed using an automated translation stage for the lens, after double checking that the focus does not change its perpendicular position. In all the figures, the 0 focus corresponds to the focus obtained in the ionization signal, done in correlation with each HHG measurement. Each panel in Fig. 6 corresponds to different mode profiles. Mode profiles were modified with an iris in front of the focusing lens ($f=40\text{cm}$) by closing the iris until a given percentage of the energy is lost. With this method we can modify the beam profile in a controlled and repeatable manner. Fig. 6 a) shows the total HHG yield, integrated over the entire spectrum for an unmodified beam (assumed Gaussian) out of our KLS amplifier. As expected for Gaussian and Gaussian-like beam profiles, the HHG yield has two maxima, one corresponding to short trajectories and the other one corresponding to long trajectories. It should be noted that neither maxima is not at the focus. Panel b) of the same figure shows the harmonic yield as function of energy and focus position for a beam that has been clipped by 10% of the energy. In this case, the global maximum in the harmonic yield is reversed. That is, while a Gaussian profile shows a maximum yield when the focus is behind the gas jet, a truncated Gaussian mode shows a global maximum when the focus is in front of the jet. We repeated the same experiments with Ar and for a wide variety of pressures, in all cases we observed the same behavior. We are also currently investigating few cycle pulses and changes in the XUV profile. In addition, we are analyzing the difference in brightness for individual harmonics as a function of energy and focus position.

DOE Supported Publications

- C. Jin, and A.-T. Le, C. A. Trallero-Herrero, and C. D. Lin. Generation of isolated attosecond pulses by far field spatial filtering high-order harmonic generation of Xe in an intense mid-infrared laser. *Phys. Rev. A*, 84:043411, 2011
- C. A. Trallero-Herrero, C. Jin, B. Schmidt, A. Shiner, D. M. Villeneuve, P. B. Corkum, C. D. Lin, F. Légaré and A. T. Le, Generation of broad XUV continuous high harmonic spectra with intense mid-infrared lasers. *J. Phys. B.*, 45:011001, 2011.

References

- [1] A. D. Shiner, B. E. Schmidt, C. Trallero-Herrero, *et. al. Nat. Phys.*, 7(6):464–467, 2011.
- [2] H. J. Wörner, H. Niikura, J. B. Bertrand, *et. al. Phys. Rev. Lett.*, 102:103901, 2009.
- [3] J. P. Farrell, L. S. Spector, B. K. McFarland, *et. al. Phys. Rev. A*, 83:023420, 2011.
- [4] Cheng Jin, Anh-Thu Le, and C. D. Lin. *Phys. Rev. A*, 83:023411, Feb 2011.
- [5] Cheng Jin, Julien B. Bertrand, R. R. Lucchese, *et. al Phys. Rev. A*, 85:013405, 2012.

Engineered Electronic and Magnetic Interactions in Nanocrystal Quantum Dots

Victor I. Klimov

*Chemistry Division, C-PCS, MS-J567, Los Alamos National Laboratory
Los Alamos, New Mexico 87545, klimov@lanl.gov, <http://quantumdot.lanl.gov>*

1. Program Scope

Using nanocrystal (NC) quantum dots one can produce extremely strong spatial confinement of electronic excitations not accessible with other types of nanostructures. Because of this confinement, electronic energies in nanocrystals are directly dependent upon their dimensions, which is known as the quantum-size effect. This effect has been a powerful tool for controlling spectral responses of NCs, enabling potential applications such as multicolor labeling, optical amplification and low-cost lighting. In addition to spectral tunability, strong spatial confinement results in a significant enhancement of carrier-carrier interactions that lead to a number of novel physical phenomena including large splitting of electronic states induced by electron-hole exchange coupling, ultrafast multiexciton decay via Auger recombination, and direct generation of multiple excitons by single photons via carrier multiplication. Confinement-induced mixing between the conduction and the valence band can also lead to interesting peculiarities in magnetic interactions such as switching of the sign of the g-factor in magnetically doped NCs. The major thrust of this project is to understand the physics of electronic and magnetic interactions under conditions of extreme quantum confinement, and to develop methods for controlling these interactions. Research topics explored here include: control of Auger recombination via engineered exciton-exciton interactions in heterostructured and alloyed NCs with a goal of realizing the regime of continuous-wave lasing; new functional behaviors via NC doping with optically active ions such as copper; control of single-exciton dynamics via tunable fine-structure excitonic splitting; and controlled exchanged interactions in magnetically doped NCs probed by steady state and time-resolved magneto-optical spectroscopies.

2. Recent Progress

Overview. During the past year, we continued the studies of the role of interfacial properties of core/shell CdSe/CdS NCs on multi-carrier dynamics and Auger recombination and practical applications of these nanostructures in light-emitting diodes (LEDs). We have also developed a novel technique for probing multiexciton emission quantum yields (QYs) in individual NCs via two-photon correlation measurements. Using this method, we have observed a significant spread in biexciton QYs across an ensemble of nominally identical NCs. These results indicated the importance of subtle structural differences (such as the “smoothness” of the confinement potential) in Auger recombination. We have also continued our studies of Mn-doped NCs and observed an unusual effect of strong Zeeman splitting of emission originating from the internal Mn transition. These data highlighted the influence of strong quantum confinement on both the excitation and the emission mechanisms of magnetic ions in nano-materials. An exciting new direction explored during the past year has been associated with studies of NCs doped with Cu impurities. This work was enabled by our recent success in incorporation of Cu-ions into core-shell ZnSe/CdSe NCs. In the next sub-section, we provide a brief overview of our studies of these NCs with emphasis on their unusual spectroscopic properties arising from strong electronic and optical coupling between the impurity and intrinsic NC states.

During 2010-12, this project produced 13 papers published in top quality journals (1 Nature Comm., 3 Phys. Rev. Lett., 5 Nano Lett., 2 ASC Nano, and 2 JACS). These papers have been referenced in the literature ~180 times, which corresponds to ca. 14 citations per paper on average. Various aspects of this work were presented in 30 invited/keynote talks at major research forums such as APS March meetings, Gordon Research Conferences, Spring and Fall MRS meetings, and ACS National meetings.

P-type, copper-doped nanocrystals with “permanent” optically active holes. At present, practical applicability of colloidal NCs is greatly limited by the difficulty of controlled introduction of *permanent* electrically and/or optically active charges. The resolution of this problem would greatly benefit applications of NCs in areas such as photovoltaics, and LEDs, and lasing. So far, most successful NC doping efforts have focused on magnetically active Mn ions. Temporary introduction of active charge carriers using strongly reducing chemical agents has also been demonstrated previously. *Permanent* incorporation of charges into NCs, however, would require placement of active impurities into the lattice. Doping of NCs with transition-metal ions that exhibit variable valence is a promising strategy to achieve this goal, and an increasing number of efforts have been devoted to incorporation of ions such as Cu, Ag, and Au into various NCs.

The concept of NC doping with optically and electrically active impurities is illustrated in Fig. 1. In the example in panel ‘a’, the deep acceptor impurity creates an optically active intra-gap hole state, which can capture an electron from the conduction band via a radiative transition and thus produce optical emission without injection of a hole. An interesting feature of this transition is that it has an “emission-only”, one-directional

character that does not produce competing optical absorption. This property can be utilized to realize a highly efficient four-level optical gain scheme (Fig. 1a, right), which so far has not been demonstrated for semiconductors. Such a scheme would be especially beneficial for NC materials, as it would allow for optical amplification in the regime of a vanishingly small concentration of excitons (hence, the concept of “zero-threshold” gain) before the onset of multiexciton Auger recombination. This would help to overcome a major problem in NC lasing associated with ultrafast optical gain decay via the Auger process.

In Fig. 1b, we show a different example of doping when an acceptor impurity state is located in close proximity to the valence band and thus can thermally inject holes into the extended states of the host semiconductor. In the case of colloidal nanostructures, such doping with electrically active charges would facilitate charge transport (Fig. 1b, right) and could help to resolve the problem of extremely low intrinsic conductivity of NC assemblies. It will also benefit practical applications of NCs in electronic and optoelectronic devices by allowing for a facile engineering of built-in electric fields via controlled placement of *p-n* junctions.

Intra-gap luminescence centers associated with Cu defects in bulk II-VI semiconductors have been known since the early 1960s. These earlier studies have demonstrated that in II-VI materials such as ZnSe and ZnS, Cu replaces cations and introduces two levels within the forbidden gap. These levels, typically labeled as *t* (higher energy) and *e* (lower energy), reside near the valence band edge and can be described by the superposition of 3*d*, 3*p*, and 4*s* states. They are optically and electronically active and can exchange electrons with conduction and valence bands via radiative and nonradiative transitions. When the Fermi level is above the *t*-state, both impurity levels are occupied. This corresponds to the +1 oxidation state of Cu with the completely filled 3*d* shell [electronic configuration (Ar)3*d*¹⁰]. When the Fermi level is below the *t*-state, this state can be considered as having a hole, which corresponds to electronic configuration (Ar)3*d*⁹ and the +2 oxidation state of Cu. In principle, the second electron can be removed from the 3*d* shell, which will produce a hole in the *e*-state and result in the (Ar)3*d*⁸ configuration of the Cu ion.

Recently, several publications reported the development of a characteristic intra-gap Cu-related emission feature in copper-doped II-VI NCs. Several studies have also attempted to characterize the oxidation state of Cu upon incorporation into NCs. The results of these investigations, however, have been controversial as both +1 and +2 oxidation states have been ascribed to copper dopants. Distinguishing between these two possibilities is important for understanding the electronic, optical, and magnetic properties of Cu impurities. Specifically, the +1 state is diamagnetic (has a filled 3*d*¹⁰ shell) and does not

Figure 1. Concepts of NC doping with optically- and electrically-active charges. (a) A pre-existing “permanent” hole associated with a deep impurity acceptor state (left), which is not thermally accessible by valence-band electrons, is optically active and can participate in radiative transitions involving conduction-band electrons. (b) A hole residing in a shallow acceptor state (left) is electrically active as it can be thermally excited into the valence band and can then participate in charge transport through delocalized quantized states of the NCs (right). (c) The difference in optical behaviors of Cu¹⁺ and Cu²⁺ impurities. The Cu¹⁺ state is optically passive (left) and can participate in radiative transitions only after capturing a hole from the valence band. On the other hand, the Cu²⁺ state is optically active as it contains a hole which can radiatively capture a conduction band electron.

contribute to emission without capturing an external hole. On the other hand, the +2 state is paramagnetic (3*d*⁹) and can be considered as a state with a *permanent* optically-active hole, which can participate in emission without the injection of a hole. Furthermore, if the Cu ions are preferentially in the +2 state, this implies that the Fermi level is below the Cu impurity *t*-level and hence is located near the valence-band edge, which is an unambiguous signature of *p*-doped materials.

In this project, we have addressed the nature of the state associated with Cu impurities in II-VI NCs by conducting comprehensive spectroscopic and magneto-optical studies of nanostructures composed of Cu-doped ZnSe cores overcoated with CdSe shells. The use of core/shell architectures served two critical purposes: (1) It helped to retain the dopants in the core during the chemical synthesis and thus overcome the problem of “self purification”; (2) Further, it allowed for the extension of the range of spectral tunability into the near-infrared region through control of the spatial distribution of the electronic wave functions between the core and the shell regions. Via spectroscopic and magneto-optical studies, we have conclusively demonstrated that Cu impurities represent paramagnetic 2+ species, and hence, can serve as a source of optically active permanent holes. This implies that activation of optical emission due to the Cu level requires injection of only an electron without a need

for a valence-band hole. This peculiar *electron-only* emission mechanism has been confirmed by experiments in which the titration of the NCs with hole-withdrawing molecules resulted in enhancement of Cu-related photoluminescence (PL) while simultaneously suppressing the intrinsic, band-edge emission (Fig. 2).

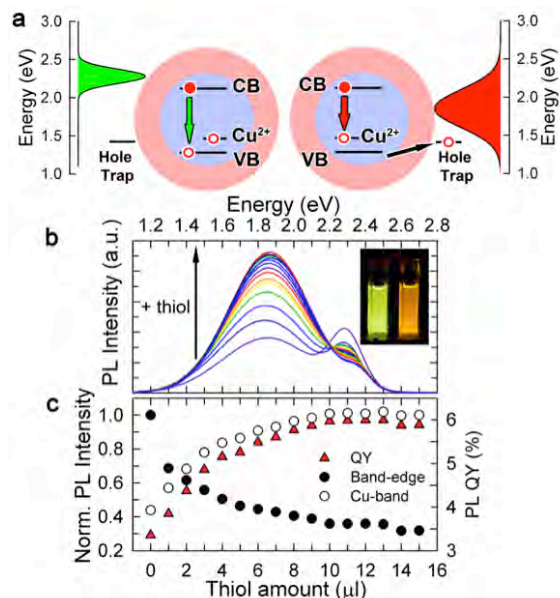


Figure 2. Interplay between band-edge and Cu-related recombination channels during titration of Cu-doped NCs with hole-withdrawing molecules. (a) If a photogenerated hole is present in the NC for sufficiently long time, radiative recombination is primarily due to a band-edge transition as it is much faster than the band-to-Cu transition (left). If a photogenerated hole is instead quickly removed from the NC emission becomes dominated by the Cu-impurity band (right). (b,c) Titration of Cu:ZnSe/CdSe NCs ($R_0 + H = 1.6$ nm) with an increasing amount of hole accepting molecules of dodecane thiol (DDT) leads to a progressive increase of the Cu-related band accompanied by the suppression of band-edge emission; this results in a pronounced change of the emission color as shown in the inset.

occupancy of electron traps, which results in the overall PL “brightening” under negative potential (leads to deactivation of electron traps) and “dimming” under positive potential. While these measurements do not exclude the possibility that some of the NCs might contain +1 copper ions, they strongly suggest that PL from our samples is primarily due to Cu^{2+} ions.

These newly developed Cu-doped nanomaterials show unprecedented emission tunability from near infrared (1.2 eV) to the blue (3.1 eV) and reduced losses from re-absorption due to a large Stokes shift (up to 0.7 eV). These properties make them very attractive for applications in light-emission and lasing technologies and especially for the realization of novel device concepts such as “zero-threshold” optical gain and “electron-only” light emitting diodes.

3. Future Plans

In our future work in this project, we will develop and study a new type of nanostructures where we will combine both quantum- and bulk-like (that is, classical) regions in a single colloidal nanoparticle. This effort will be built upon our previous studies of “giant” CdSe/CdS NCs. Using recently developed synthetic strategies, we will take these structures to a new extreme by increasing the thickness of the outer CdS shell to a bulk-like limit. Preliminary synthetic work shows that we can synthesize an exceptionally thick CdS shell while preserving high quality of the resulting material (Fig. 3). An important advantage of the new method over a traditional synthetic protocol based on the “successive ionic layer adsorption and reaction” (SILAR) is that it is much faster and less prone to errors. For example, using SILAR it would require up to 40 deposition steps performed consecutively over more than 50 hours for growing a 6 nm shell and the composition error at each of these steps could jeopardize the entire synthesis. On the other hand, by our new method, the entire synthesis of a bigger 20-nm CdSe/CdS NCs can be accomplished through only three injection steps over a total time of less than 6 hours. As a result, we can explore a much greater range of core radii and shell thickness than with a SILAR method thereby

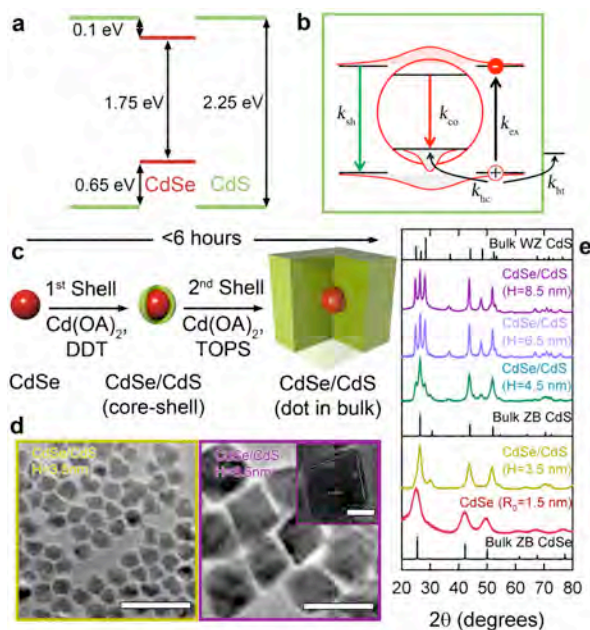


Figure 3. Synthesis, electronic structure and transmission electron microscopy images of “dot-in-bulk” CdSe/CdS NCs. (a) A band alignment diagram of bulk CdSe and CdS. (b) Schematic of a “dot-in-bulk” NC showing the different carrier relaxation and recombination pathways. (c) Schematic diagram illustrating the synthesis of core/shell CdSe/CdS NCs. (d) Transmission electron microscopy images of CdSe/CdS NCs with core radius, $R_0 = 1.5$ nm, and increasing shell thickness ($H = 0$, $H = 2.5$, $H = 3.5$ and $H = 8.5$ nm). Size bars in main panels correspond to 40 nm and 10 nm in the inset of top right panel. (e) X-ray diffraction patterns of NCs with $R_0 = 1.5$ nm and increasing thickness ($H = 0$, $H = 2.5$, $H = 3.5$, $H = 4.5$, $H = 6.5$ and $H = 8.5$ nm) compared to bulk materials.

achieving a much wider range of color tunability compared to giant CdSe/CdS NCs. Importantly, we can also produce not yet realized NCs with exceptionally thick CdS shells (more than 25 CdS monolayers) that are larger than the Bohr exciton radius in CdS (~ 3 nm). In this size regime, the core/shell CdSe/CdS NCs become effectively “dot-in-bulk” systems where the electronic structure of the core is quantized while the shell can be described in bulk-like terms. In conjunction with the quasi type II nature of the interface, this structure can be pictured as a bulk-like colloidal particle with an *engineered* hole trap represented by the quantum-confined CdSe core (Fig. 3). In this project, we will study the coupling between quantum confined and bulk-like excitations by applying both single-NC and ensemble spectroscopic techniques. We will also investigate the behavior of these structures in the regime of electrical charge injection.

4. Publications (2010 - 2012)

1. S. Brovelli, C. Galland, R. Viswanatha, V. I. Klimov, Tuning Radiative Recombination in Cu-Doped Nanocrystals via Electrochemical Control of Surface Trapping, *Nano Lett.* **12**, 4327 (2012).
2. B. N. Pal, Y. Ghosh, S. Brovelli, R. Laocharoensuk, V. I. Klimov, Jennifer Hollingsworth, H. Htoon, “Giant” CdSe/CdS core/shell nanocrystal quantum dots as efficient electroluminescent materials: Strong influence of shell thickness on light-emitting diode performance, *Nano Lett.* **12**, 331 (2012).
3. R. Viswanatha, S. Brovelli, A. Pandey, S. A. Crooker, V. I. Klimov, Copper-Doped Inverted Core/Shell Nanocrystals with “Permanent” Optically Active Holes, *Nano Lett.* **11**, 4753 (2011).
4. R. Viswanatha, J. M. Pietryga, V. I. Klimov, and S. A. Crooker, Circularly-polarized Mn^{2+} emission from Mn-doped colloidal nanocrystals, *Phys. Rev. Lett.* **107**, 067402 (2011).
5. S. Brovelli, R. D. Schaller, S. A. Crooker, F. Garcia-Santamaria, Y. Chen, R. Viswanatha, J. A. Hollingsworth, H. Htoon, V. I. Klimov, Nano-engineered electron-hole exchange interaction controls exciton dynamics in core-shell semiconductor nanocrystals, *Nature Comm.* **2**, 280 (2011)
6. Y.-S. Park, A. V. Malko, J. Vela, Y. Chen, Y. Ghosh, F. Garcia-Santamaria, J. A. Hollingsworth, V. I. Klimov, H. Htoon, Near-unity quantum yields of biexciton emission from CdSe/CdS nanocrystals measured using single-particle spectroscopy, *Phys. Rev. Lett.* **106**, 187401 (2011).
7. L. Li, A. Pandey, D. J. Werder, B. P. Khanal, J. M. Pietryga, V. I. Klimov, Efficient synthesis of highly luminescent indium sulfide based core/shell nanocrystals with surprisingly long-lived emission, *J. Am. Chem. Soc.* **133**, 1176 (2011).
8. Garcia-Santamaria, F., S. Brovelli, R. Viswanatha, J. A. Hollingsworth, H. Htoon, S. Crooker, V. I. Klimov, Breakdown of volume scaling in Auger recombination in CdSe/CdS heteronanocrystals: The role of the core-shell interface, *Nano Lett.* **11**, 687 (2011).
9. McGuire, J. A., M. Sykora, I. Robel, L. A. Padilha, J. Joo, J. M. Pietryga, V. I. Klimov, Spectroscopic signatures of photocharging due to hot-carrier transfer in solutions of semiconductor nanocrystals under low-intensity ultraviolet excitation, *ACS Nano* **4**, 6087 - 6097 (2010).
10. Schaller, R. D., S. A. Crooker, D. A. Bussian, J. M. Pietryga, J. Joo, V. I. Klimov, Revealing the exciton fine structure in PbSe nanocrystal quantum dots, *Phys. Rev. Lett.* **105**, 067403 (2010).
11. Htoon, H., A. V. Malko, D. Bussian, J. Vela-Becerra, Y. Chen, J. A. Hollingsworth, V. I. Klimov, Highly emissive multiexcitons in steady-state photoluminescence of individual “giant” CdSe/CdS core/shell nanocrystals, *Nano Lett.* **10**, 2401 (2010).
12. Lee, D. C., I. Robel, J. M. Pietryga, V. I. Klimov, Infrared-active heterostructured nanocrystals with ultralong carrier lifetimes. *J. Am. Chem. Soc.* **132**, 9960 (2010).
13. Sykora, M., A. Y. Kopusov, J. A. McGuire, O. Tretiak, J. M. Pietryga, V. I. Klimov, Effect of air exposure on surface properties, electronic structure and carrier relaxation in PbSe nanocrystals, *ACS Nano* **4**, 2021 (2010).

Atomic, Molecular and Optical Sciences at LBNL

Ali Belkacem, Daniel J. Haxton, Clyde W. McCurdy, Thomas N. Rescigno and Thorsten Weber

Chemical Sciences Division, Lawrence Berkeley National Laboratory, Berkeley, CA 94720

Email: abelkacem@lbl.gov, djhaxton@lbl.gov, cwmcurdy@lbl.gov, tnrescigno@lbl.gov, tweber@lbl.gov

Objective and Scope

The AMOS program at LBNL is aimed at understanding the structure and dynamics of atoms and molecules using photons and electrons as probes. The experimental and theoretical efforts are strongly linked and are designed to work together to break new ground and provide basic knowledge that is central to the programmatic goals of the Department of Energy as formulated in the “*Grand Challenges*”. The current emphasis of the program is in three major areas with important connections and overlap: inner-shell photo-ionization and multiple-ionization of atoms and small molecules; low-energy electron impact and dissociative electron attachment of molecules; and time-resolved studies of atomic processes using a combination of femtosecond X-rays and femtosecond laser pulses. This latter part of the program is folded in the overall research program in the Ultrafast X-ray Science Laboratory (UXSL).

The experimental component at the Advanced Light Source makes use of the Cold Target Recoil Ion Momentum Spectrometer (COLTRIMS) to advance the description of the final states and mechanisms of the production of these final states in collisions among photons, electrons and molecules. Parallel to this experimental effort, the theory component of the program focuses on the development of new methods for solving multiple photo-ionization of atoms and molecules. This dual approach is key to break new ground and provide a new understanding how electronic energy channels into nuclear motion and chemical energy in polyatomic molecules as well as unravel unambiguously electron correlation effects in multi-electron processes.

Inner-Shell Photoionization and Dissociative Electron Attachment to Small Molecules

Ali Belkacem and Thorsten Weber

Chemical Sciences Division, Lawrence Berkeley National Laboratory, Berkeley, CA 94720

Email: abelkacem@lbl.gov, tweber@lbl.gov

Objective and Scope

This program is focused on studying photon and electron impact ionization, excitation and dissociation of small molecules and atoms. The first part of this project deals with the interaction of X-rays with atoms and simple molecules by seeking new insight into atomic and molecular dynamics and electron correlation effects. These studies are designed to test advanced theoretical treatments by achieving a new level of completeness in the distribution of the momenta and/or internal states of the products and their correlations. The second part of this project deals with the interaction of low-energy electrons with small molecules with particular emphasis on Dissociative Electron Attachment (DEA). Both studies are strongly linked to our AMO theoretical studies led by C.W. McCurdy and T.N. Rescigno and are designed to break new ground and provide basic knowledge that is central to the programmatic goals of BES in electron-driven chemistry. Both experimental studies (photon and electron impact) make use of the powerful COLd Target Ion Momentum Spectroscopy (COLTRIMS) method to achieve a high level of completeness in the measurements.

K-shell photoionization and Auger decay of N₂.

We studied the differences and analogies between a quantum optical and light-matter interaction approach in a study of K-shell photoionization of N₂ in which the photoelectron and the subsequently emitted Auger electron are both measured in coincidence in the body fixed frame of the molecule. We found that the Auger electron and the photoelectron form an entangled state in the ionization process. The single-particle basis from which this entangled state is generated is gerade and ungerade (rather than spin-up and -down). Analogous to spin-type Bell states the measurement of the spin component of one particle fixes the spin of the second; in our case a measurement of the parity of one of the electrons fixed the parity of the second one. We selected Auger electrons of one parity by choosing a certain photoelectron emission angle with respect to the molecular axis where the contribution of this parity maximizes and the opposing parity state emission pattern has a node (see fig. 1). We were also

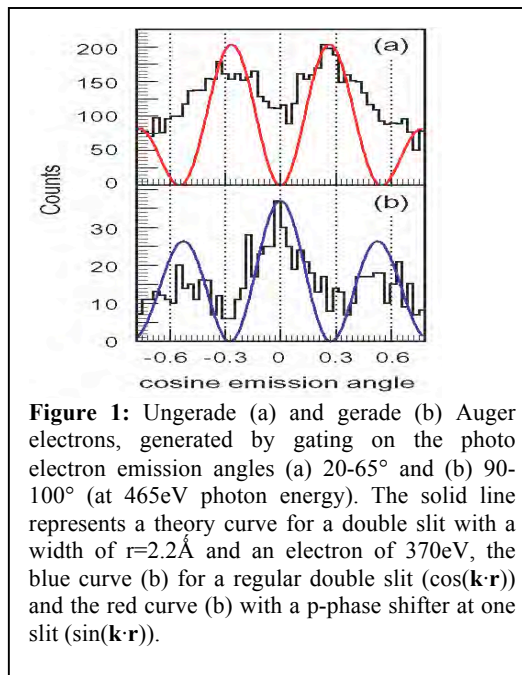


Figure 1: Ungerade (a) and gerade (b) Auger electrons, generated by gating on the photo electron emission angles (a) 20-65° and (b) 90-100° (at 465eV photon energy). The solid line represents a theory curve for a double slit with a width of $r=2.2\text{\AA}$ and an electron of 370eV, the blue curve (b) for a regular double slit ($\cos(\mathbf{k}\cdot\mathbf{r})$) and the red curve (b) with a p-phase shifter at one slit ($\sin(\mathbf{k}\cdot\mathbf{r})$).

able to investigate the interference term between the photoelectron waves of gerade and ungerade parities by selecting Auger electrons at angles where the states of both parities contribute equally. This demonstrated that the angular distribution of the photoelectron is a result of an interfering gerade or ungerade wave that is multiple scattered in the molecular potential. By changing the photon energy we created different types of interference in the photoelectron and the Auger electron wave. The optical Gedanken experiment analogue to this molecular investigation would be a classical double slit with a wavelength depending on a phase shift at one of the slits.

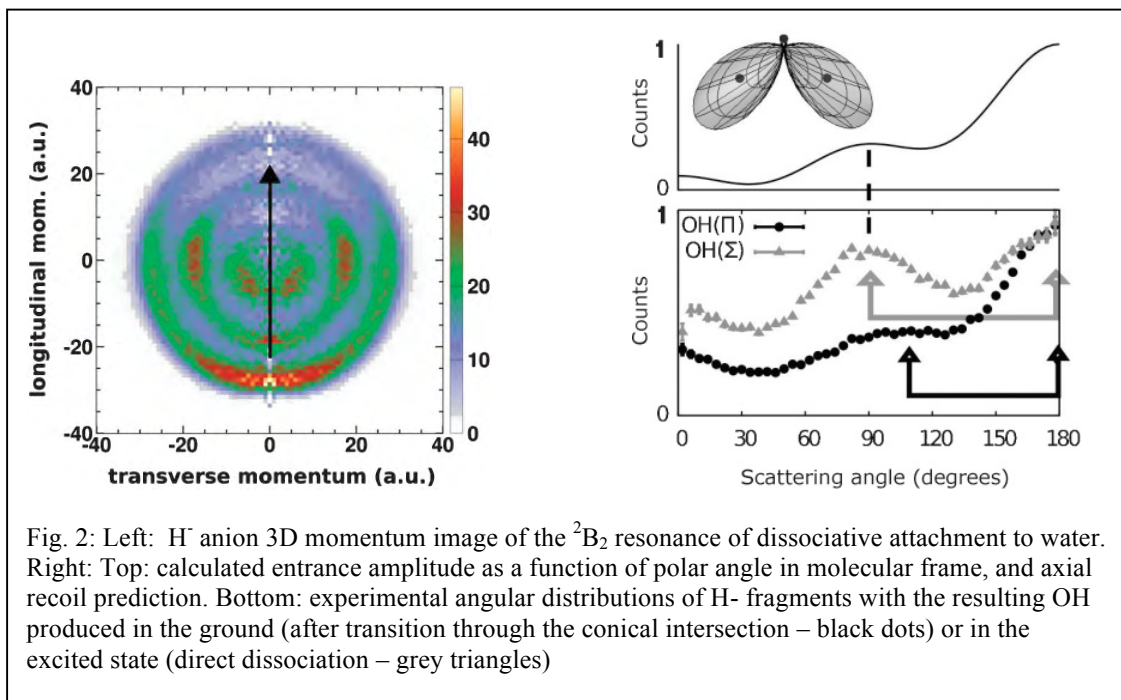
Autoionization of small molecules (O_2 , C_2H_4 and C_2H_2) after inner-valence photoionization.

In this ongoing research project we targeted the photo double ionization of small molecules (30 to 45eV, linear polarized light) and pursued the following goals: We identified the fragmentation pathways after inner valence ionization and the subsequent dissociation in PhotoIon-PhotoIon Coincidence (PIPICO) measurements and investigated the dissociation pathways in so called Energy CORrelation Maps (ECOMs); i.e. we measured the kinetic electron energy and electron sum energy as a function of the Kinetic Energy Release (KER). With this we traced the transitions from a relaxation of small molecular ions to the atomic autoionization while measuring the bond length via the KER of the ionic fragments. Subsequently we analyzed the emission patterns of the two outgoing electrons, i.e. the photo electron and the Auger electron, in the body fixed frame (MFPADs and MFAADs) to track down correlation effects and molecular dynamics. This work was partly inspired to complement time resolved KER measurements on O_2 molecules by our KSU partner (L. Cocke et al.) in the spectral domain. Single photon double ionization of O_2 at photon energies below and above the adiabatic double ionization threshold is dominated by single ionization followed by the dissociation and autoionization of atomic oxygen. About a dozen of different intermediate states could be identified in the ECOMs and their MFPADs and MFAADs could be followed as a function of the photon energy and the KER revealing their symmetry. A clear connection between MFPADs and MFAADs could be found indicating the correlation between the photo electron and excited electron of the intermediate state mediated by shape resonances. For small hydrocarbons like C_2H_4 the analysis could then be extended beyond the symmetric breakup towards fragmentation channels like deprotonation and hydrogen elimination and isomerization channels in C_2H_2 ; producing a stable $C_2H_4^{++}$ dication was found to be unlikely (~5.5%) in contrast to the photo double ionization of C_2H_2 (~65%). Exploiting the power of the ECOMs and the close connection with theory (D. Haxton, T. Rescigno and A. Ore) the contributions of singlet and triplet states could be identified for each reaction pathway and compared to core shell ionization followed by Auger decay where triplet states are suppressed.

Dissociative electron attachment to water molecules and dynamics through conical intersections.

Dissociative electron attachment (DEA) to the deceptively simple H_2O molecule involves complex electronic and nuclear dynamics. In the gas phase, it proceeds via three transient anion states of 2B_1 , 2A_1 and 2B_2 symmetries which are responsible for three distinct broad peaks in the DEA cross section at electron energies of 6.5, 9 and 12 eV. The negative ion states subsequently fragment to produce H^- , O^- and possibly OH^- , in various two-body as well as three-body breakup channels. The most intriguing results for DEA to water are found in the H^- (D^-) channel of the 2B_2 . For this resonance the electron attaches to the molecule along the OH bond, impinging from the hydrogen side. We applied techniques of momentum imaging and *ab initio* scattering calculations to the process of dissociative electron attachment to water via the highest-energy 2B_2 resonance. We focus on the H^- anion fragment, which is produced via dynamics passing through and avoiding the conical intersection with the lower A_1 state, leading to OH ($^2\Pi$) and OH ($^2\Sigma$),

respectively. The momentum imaging technique, when combined with theoretical calculations on



the attachment amplitude and dissociation dynamics, demonstrate that the angular distributions provide a signature of the location of the conical intersection at H-O-H angle of $\sim 80^\circ$ in the space of nuclear configurations. Our theory group predicted the presence of this conical intersection. One remarkable aspect of this measurement is that we are able to control with high precision the fraction of the wave-packet that funnels through the conical intersection and dissociate on the lower 2A_1 state by tuning the energy of the electron around the 2B_2 .

Future Plans

We plan to continue application of the COLTRIMS approach to achieve complete descriptions of the single photon double ionization of CO, O₂ and their analogs. Of particular interest is an in-depth study of the “photoelectron and autoionization-electron” correlation and entanglement. We will also study double Auger decay of small molecules after photo excitation and photo ionization of inner shell electrons. The main scientific goals are to investigate the dissociation pathways and ionization mechanism during the double Auger decay. We plan to continue using our Dissociative Electron Attachment modified-COLTRIMS to study DEA to methanol and ethanol to unravel the OH functional group effects as well as some relevant molecules such as CO₂ or DNA bases such as uracil. This latter work will be done in collaboration and theoretical support from Vincent McKoy.

Recent Publications (2010-2012)

1. S.K. Semenov, M.S. Schoeffler, J. Titze, N. Petridis, T. Jahnke, K. Cole, L.P.H. Schmidt, A. Czasch, D. Akoury, O. Jagutzki, J.B. Williams, T. Osipov, S. Lee, M.H. Prior, A. Belkacem, A.L. Landers, H. Schmidt-Bocking, Th. Weber, N.A. Cherepkov, R. Doerner, “Auger decay $1\sigma_g$ and $1\sigma_u$ hole states of the N_2 molecule: Disentangling decay routes from coincidence measurements”, Phys. Rev. A **81**, 043426 (2010).
2. T. Osipov, M. Stener, A. Belkacem, M. Schoeffler, Th. Weber, L. Schmidt, A. Landers, M.H. Prior, R. Doerner and C.L.Cocke, “Carbon K-shell photoionization of fixed-in-space C_2H_4 ”, Phys. Rev. A **81**, 033429 (2010).

3. T. Osipov, Th. Weber, T.N. Rescigno, S.Y. Lee, A.E. Orel, M. Schoeffler, F.P. Sturm, S. Schoessler, U. Lenz, T. Havermeier, M. Kuhnel, T. Jahnke, J.B. Williams, D. Ray, A. Landers, R. Doerner and A. Belkacem, “*Formation of inner-shell autoionizing CO⁺ states below the CO²⁺ threshold*”, *Phys. Rev. A* **81**, 011402 (2010).
4. N.A. Cherepkov, S.K. Semenov, M.S. Schoffler, J. Titze, N. Petridis, T. Jahnke, K. Cole, L. Ph. H. Schmidt, A. Czasch, D. Akoury, O. Jagutzki, J.B. Williams, T. Osipov, S. Lee, M.H. Prior, A. Belkacem, A.L. Landers, H. Schmidt-Böcking, R. Dorner, and T. Weber, “*Auger decay of 1σ_g and 1σ_u hole states of the N₂ molecule. II. Young-type interference of Auger electrons and its dependence on internuclear distance*”, *Phys. Rev. A* **82**, 023420 (2010).
5. T. Jahnke, H. Sann, T. Havermeier, K. Kreidi, C. Stuck, M. Meckel, M. Schoeffler, N. Neumann, R. Wallauer, S. Voss, A. Czasch, O. Jagutzki, A. Malakzadeh, F. Afaneh, T. Weber, H. Schmidt-Böcking, and R. Doerner, “*Ultrafast energy transfer between water molecules*”, *Nature Physics* **6**, 139 (2010).
6. H. Sann, T. Jahnke, T. Havermeier, K. Kreidi, C. Stuck, M. Meckel, M. Schöffler, N. Neumann, R. Wallauer, S. Voss, A. Czasch, O. Jagutzki, Th. Weber, H. Schmidt-Böcking, S. Miyabe, D.J. Haxton, A.E. Orel, T. N. Rescigno, and R. Dörner, “*Electron diffraction self imaging of molecular fragmentation in two step double ionization of water*”, *Phys. Rev. Lett.* **106**, 133001 (2011).
7. D.S. Slaughter, H. Adaniya, T.T. Rescigno, D.J. Haxton, A.E. Orel, C.W. McCurdy, A. Belkacem, “*Dissociative electron attachment to carbon dioxide via 8.2 eV Feshbach resonance*”, *J. Phys. B: At. Mol. Opt. Phys.* **44** (2011) 205203.
8. D.J. Haxton, H. Adaniya, D.S. Slaughter, B. Rudek, T. Osipov, T. Weber, T.N. Rescigno, C.W. McCurdy, A. Belkacem, “*Observation of the dynamics leading to a conical intersection in dissociative electron attachment to water*”, *Phys. Rev. A* **84** (2011) 030701.
9. H. Adaniya, B. Rudek, T. Osipov, D.J. Haxton, T. Weber, T.N. Rescigno, C.W. McCurdy, and A. Belkacem, “*Comment on “Imaging the molecular dynamics of dissociative electron attachment to water”*”, *Phys. Rev. Lett.* **106**, (2011) 049302.
10. Schoffler M.S., Jahnke T., Titze J., Petridis N., Cole K., Schmidt L.P.H., Czasch A., Jagutzki O., Willams J.B., Cocks C.L., Osipov T., Lee S., Prior M.H., Belkacem A., Landers A.L., Schmidt-Böcking H., Dorner R., Weber T., “*Matter wave optics perspective at molecular photoionization: K-shell photoionization and Auger decay of N₂*”, *New J. Phys.* **13** (2011) 095013.
11. T. Jahnke, J. Titze, L. Foucar, R. Wallauer, T. Osipov, E.P. Benis, O. Jagutzki, W. Arnold, A. Czasch, A. Staudte, M. Schöffler, A. Alnaser, T. Weber, M.H. Prior, H. Schmidt-Böcking, R. Dörner, “*Carbon K-shell Photo Ionization of CO: Molecular frame angular Distributions of normal and conjugate shakeup Satellites*”, *J. Electron Spectroscopy and Related Phenomena*, **183**, (2011), 48-52.
12. Adaniya H., Slaughter D.S., Osipov T. Weber T., Belkacem A., “*A momentum imaging microscope for dissociative electron attachment*”, *Rev. Scient. Inst.* **83** (2012) 023106.
13. J.B. Williams, C.S. Trevisan, M.S. Schoffler, T. Jahnke, I. Bocharova, H. Kim, B. Ulrich, R. Wallauer, F. Sturm, T. N. Rescigno, A. Belkacem, R. Dorner, Th. Weber, C.W. McCurdy, A. L. Landers, “*Imaging polyatomic molecules in three dimensions using molecular frame photoelectron angular distributions*”, *Phys. Rev. Lett.* **108** (2012) 233002.
14. F. Robicheaux, M.P. Jones, M. Schoeffler, T. Jahnke, K. Kreidi, J. Titze, C. Stuck, R. Doerner, A. Belkacem, Th. Weber and A.L. Landers, “*Calculated and measured angular correlation between photoelectrons and Auger electrons from K-shell ionization*”, *J. Phys. B: At. Mol. Opt. Phys.*, **45**, (2012), 175001.
15. F. Trinter, L.Ph.H. Schmidt, T. Jahnke, M.S. Schöffler, O. Jagutzki, A. Czasch, J. Lower, T. A. Isaev, R. Berger, A.L. Landers, Th. Weber, R. Dörner, H. Schmidt-Böcking, “*Multi fragment vector correlation imaging: A search for hidden dynamical symmetries in many-particle molecular fragmentation processes*”, *Molecular Physics: An International Journal at the Interface Between Chemistry and Physics: A Festschrift for Dudley Herschbach*”, Editor: B. Friedrich, Publisher: Taylor & Francis, DOI:10.1080/00268976.2012.686642, (2012).
16. J.B. Williams, C.S. Trevisan, M.S. Schoeffler, T. Jahnke, I. Bocharova, H. Kim, B. Ulrich, R. Wallauer, F. Sturm, T.N. Rescigno, A. Belkacem, R. Doerner, Th. Weber, C.W. McCurdy, and A.L. Landers, “*Probing the Dynamics of Dissociation of Methane Following Core Ionization Using Three-Dimensional Molecular Frame Photoelectron Angular Distributions*”, *Accepted for publication in J. Phys. B: At. Mol. Opt. Phys.*, (2012).

Electron-Atom and Electron-Molecule Collision Processes

T. N. Rescigno, C. W. McCurdy and D. Haxton

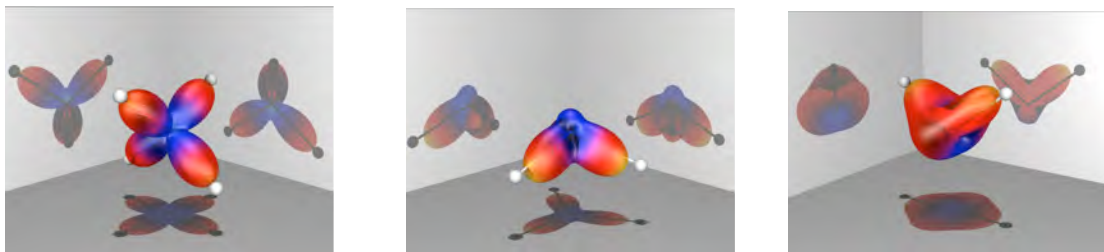
Chemical Sciences, Lawrence Berkeley National Laboratory, Berkeley, CA 94720

tnrescigno@lbl.gov, cwmccurdy@lbl.gov

Program Scope: This project seeks to develop theoretical and computational methods for treating electron processes that are important in electron-driven chemistry and physics and that are currently beyond the grasp of first principles methods, either because of the complexity of the targets or the intrinsic complexity of the processes themselves. A major focus is the development of new methods for solving multiple photoionization and electron-impact ionization of atoms and molecules. New methods are also being developed and applied for treating low-energy electron collisions with polyatomic molecules and clusters. A state-of-the-art approach is used to treat multidimensional nuclear dynamics in polyatomic systems during resonant electron collisions and predict channeling of electronic energy into vibrational excitation and dissociation.

Recent Progress and Future Plans:

Coincident measurement of K-shell photoelectrons and fragment ion momenta from molecular dissociation following Auger decay allows one to study photoelectron angular distributions in the molecular-frame (MFPAD). These distributions are generally far richer than conventionally measured laboratory-frame angular distributions. This fact was dramatically illustrated in a joint experimental (COLTRIMS)/ theoretical study using methane as a probe. The K-shell MFPADs were calculated using the fixed-nuclei, complex Kohn variational method. A striking, an unexpected, result of this study was the fact that at low photoelectron energies the photoelectron tends to be focused along the bond directions, and that the MFPAD, averaged over all polarization directions, effectively images the geometry of the molecule. This study was published in Phys. Rev. Letters (ref. 15). To see whether the MFPAD imaging we found for methane was specific to that molecule or whether similar imaging takes place in the case of other target molecules that contain a single heavy atom, we carried out theoretical calculations on water and ammonia and found similar results (ref.17).

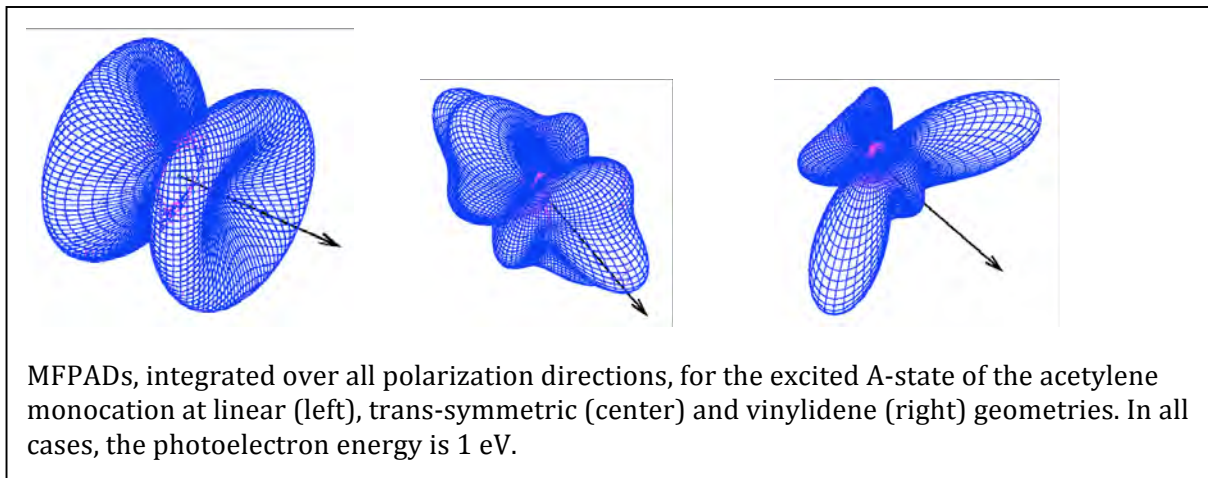


Molecular-frame photoelectron angular distributions (MFPADs), integrated over all polarization directions, for methane (left), ammonia (center) and water (right). In all cases, the photoelectron energy is 1 eV.

The fact that K-shell MFPADs are sensitive to nuclear geometry suggests that this technique of photoelectron diffraction might be taken into the time domain to image chemical reactions on their natural timescales. To demonstrate this idea, we carried out a theoretical study of the isomerization of the electronically excited acetylene cation (ref.18) in which we demonstrated that the MFPADs can be used to image the cation in 3D as it progress along a reaction path from

its initial linear geometry through a trans-symmetric conical intersection to a final vinylidene geometry.

It is well known that the vertical double ionization thresholds of small molecules generally lie above the dissociation limits corresponding to formation of singly charged fragments because of



the long-range repulsive interaction between singly charged ions. This leads to a phenomenon known as indirect double ionization where inner-valence photoionization can create an excited monocation that emits a second electron by autoionization, but only at large internuclear separations where the ionic state crosses into the electron+dication continuum. This process was examined for molecular oxygen in a time-resolved EUV pump/ IR probe experiment, where the probe can be triggered to destroy the excited monocation before it autoionizes. Since the autoionization usually occurs on a time scale longer than that for fragmentation, the population of cation states of the molecule which dissociate to a charged ion plus autoionizing atomic oxygen atoms ultimately results in the observation of ion pairs in the dication channel. To assist in the interpretation of the experimental observations, we carried out electronic structure calculations to identify the relevant mono- and dication oxygen states. Using [the autoionizing cation states obtained from CI calculations and](#) reasonable assumptions concerning the form of the dication state(s) involved, a model for the fragmentation process was evaluated which showed good agreement with the experiment (ref. 12).

Dissociative electron attachment (DEA) is fundamentally important in electron-driven chemistry because it can induce chemical reactions with electrons whose energies lie below the threshold for ionization. With polyatomic targets, conical intersections can play a key role in the dissociation dynamics following resonant electron attachment. In the case of water, a conical intersection between the 2B_2 and 2A_1 metastable states of the water anion was predicted and demonstrated to be central to the dynamics following attachment to the 2B_2 state. In a collaborative experimental/theoretical study, which has been published in Phys. Rev. A (ref. 11), we focused on the H⁻ anion fragment, which is produced via dynamics either passing through and avoiding the conical intersection with the lower A_1 state, leading to OH (${}^2\Pi$) and OH (${}^2\Sigma$), respectively. This study clearly demonstrated how the angular distributions of the dissociating fragments give a signature of the location of the conical intersection in the space of nuclear configurations.

We have continued our investigation of dissociative electron attachment to CO₂. Our first efforts had targeted the main DEA peak at 8.2 eV, which our ab initio studies showed to

involve attachment through a doubly excited (Feshbach) resonance of ${}^2\Pi_g$ symmetry followed by dissociation through a conical intersection with a lower energy shape resonance. This result was confirmed by COLTRIMS measurements and our joint experimental/theoretical study was published in *J. Phys. B* (ref. 10). Our more recent efforts have turned to the 4 eV resonance, which evidently feeds both vibrational excitation and dissociative electron attachment, the latter involving a symmetry (C_{2v}) conical intersection, different from the conical intersection relevant to the 8.2 eV resonance that occurs near linear geometry. The topology of the CO_2 anion surfaces is quite complicated and the extant literature on the subject is riddled with misconceptions. Our goal is to fully characterize the relevant portions of the anion surfaces and to provide a consistent picture of the resonant vibrational excitation and dissociative attachment dynamics.

Publications (2010-2012):

1. T. Osipov, Th. Weber, T. N. Rescigno, S. Y. Lee, A. E. Orel, M. Schöffler, F. P. Sturm, S. Schössler, U. Lenz, T. Havermeier, M. Kuehnel, T. Jahnke, J. B. Williams, D. Ray, A. Landers, R. Dörner and A. Belkacem, "Formation of inner-shell autoionizing CO^+ states below the CO^{++} threshold", *Phys. Rev. A* **81**, 011402(R) (2010).
2. F. L. Yip, C. W. McCurdy and T. N. Rescigno "Hybrid Orbital and Numerical Grid Representation for Electronic Continuum Processes: Double Photoionization of Atomic Beryllium", *Phys. Rev. A* **81**, 053407 (2010).
3. F. L. Yip, C. W. McCurdy and T. N. Rescigno, "Double Photoionization of excited Lithium and Beryllium", *Phys. Rev. A* **81**, 063419 (2010).
4. L. Tao, C. W. McCurdy and T. N. Rescigno, "Grid-based methods for diatomic quantum scattering problems. III. Double photoionization of molecular hydrogen in prolate spheroidal coordinates", *Phys. Rev. A* **82**, 023423 (2010).
5. W. Cao, S. De, K.P. Singh, S. Chen, M.S. Schöffle, A. Alnaser, I.A. Bocharov, G. Laurent, D. Ray, M. F. Kling, S. Zherebtso, I. Ben-Itzhak, I.V. Litvinyuk, T. N. Rescigno, A. Belkacem, T. Osipov and C. L. Cocke, "Dynamic modification of the fragmentation of CO^{qt} excited states generated with high-order harmonics", *Phys. Rev. A* **82**, 043410 (2010).
6. S. Miyabe, D. J. Haxton, T. N. Rescigno and C. W. McCurdy, "Role of nuclear dynamics in the Asymmetric molecular-frame photoelectron angular distributions for C 1s photoejection from CO_2 ", *Phys. Rev. A* **83**, 023404 (2011).
7. S. Miyabe, D. J. Haxton, K. V. Lawler, A. E. Orel, C. W. McCurdy and T. N. Rescigno, "Vibrational Feshbach resonances in near threshold HOCO^- photodetachment; a theoretical study", *Phys. Rev. A* **83**, 043401 (2011).
8. H. Adaniya, B. Rudek, T. Osipov, D. J. Haxton, T. Weber, T. N. Rescigno, C. W. McCurdy, and A. Belkacem, "Reply to Comment on "Imaging the dynamics of dissociative electron attachment to water", *Phys. Rev. Lett.* **106**, 049302 (2011).
9. H. Sann, T. Jahnke, T. Havermeier, K. Kreidi, C. Stuck, M. Meckel, M. Schöffler, N. Neumann, R. Wallauer, S. Voss, A. Czasch, O. Jagutzki, Th. Weber, H. Schmidt-Böcking, S. Miyabe, D.J. Haxton, A.E. Orel, T. N. Rescigno and R. Dörner, "Electron diffraction self-imaging of molecular fragmentation in two-step double ionization of water", *Phys. Rev. Lett.* **106**, 133001 (2011).
10. D. S. Slaughter, H. Adaniya, T. N. Rescigno, D. J. Haxton, A. E. Orel, C. W. McCurdy and A. Belkacem, "Dissociative Electron Attachment to Carbon Dioxide via the 8.2eV Feshbach resonance", *Phys. Rev. A* **44**, 205203 (2011).
11. D. J. Haxton, H. Adaniya, D. S. Slaughter, B. Rudek, T. Osipov, T. Weber, T. N. Rescigno, C. W. McCurdy and A. Belkacem, "Observation of the dynamics leading to a conical intersection in dissociative electron attachment to water", *Phys. Rev. A* **84**, 030701(R) (2011).
12. W. Cao, G. Laurent, S. De, M. Schöffler, T. Jahnke, A. Alnaser, I. A. Bocharova, C. Stuck, D. Ray, M. F. Kling, I. Ben-Itzhak, Th. Weber, A. Landers, A. Belkacem, R. Dörner, A. E. Orel, T. N. Rescigno and C. L. Cocke, "Dynamic modification of the fragmentation of autoionizing states of O_2^{+} ", *Phys. Rev. A* **84**, 053406 (2011).
13. F. L. Yip, F. Martín, T. N. Rescigno and C. W. McCurdy, "Double K -shell photoionization of atomic

- beryllium”, *Phys. Rev. A* **84**, 053417 (2011).
14. F. L. Yip, A. Palacios, C. W. McCurdy, T. N. Rescigno and F. Martín, “Time-depedent formalism of double ionization of multielectron atomic targets”, *Chem. Phys.* (in press).
 15. J. B. Williams, C. S. Trevisan, M. S. Schöffler, T. Jahnke, I. Bocharova, H. Kim, B. Ulrich, R. Wallauer, F. Sturm, T. N. Rescigno, A. Belkacem, R. Dörner, Th. Weber, C. W. McCurdy and A. L. Landers, “Imaging Polyatomic Molecules in Three Dimensions using Molecular Frame Photoelectron Angular Distributions”, *Phys. Rev. Lett.* **108**, 233002 (2012).
 16. J. B. Williams, C. S. Trevisan, M. S. Schöffler, T. Jahnke, I. Bocharova, H. Kim, B. Ulrich, R. Wallauer, F. Sturm, T. N. Rescigno, A. Belkacem, R. Dörner, Th. Weber, C. W. McCurdy and A. L. Landers, “Probing the Dynamics of Dissociation of Methane Following Core Ionization Using Three-Dimensional Molecular Frame Photoelectron Angular Distributions”, *J. Phys. B* (in press).
 17. C. S. Trevisan, C. W. McCurdy and T. N. Rescigno, “Imaging Molecular Shapes with Molecular Frame Photoelectron Angular Distributions from Core Hole Ionization”, *J. Phys. B* (in press).
 18. T. N. Rescigno, N. Douguet and A. E. Orel, “Imaging Molecular Isomerization Using Molecular-Frame Photoelectron Angular Distributions”, *J. Phys. B* (in press).
 19. N. Douguet, T. N. Rescigno and A. E. Orel, “Time-resolved molecular-frame photoelectron angular distributions: Snapshots of acetylene-vinylidene cationic isomerisation”, *Phys. Rev. A* (in press).

Ultrafast X-ray Science Laboratory

C. William McCurdy (Director), Ali Belkacem, Oliver Gessner, Dan Haxton, Martin Head-Gordon, Stephen Leone, Daniel Neumark, Robert W. Schoenlein, Thorsten Weber

Chemical Sciences, Lawrence Berkeley National Laboratory, Berkeley, CA 94720

CWMcCurdy@lbl.gov, ABelkacem@lbl.gov, OGessner@lbl.gov, DJHaxton@lbl.gov, MHead-Gordon@lbl.gov, SRLeone@lbl.gov, DMNeumark@lbl.gov, RWSchoenlein@lbl.gov, TWeber@lbl.gov

Program Scope: This program exploits short pulses of X-rays to provide basic knowledge of ultrafast dynamics of photo-excited molecules in the gas phase and condensed phase from the natural time scale of electron motion to the time scale of the chemical transformations. There five subtasks in the UXSL effort, outlined below.

Recent Progress and Future Plans:

1. Soft X-ray high harmonic generation and applications in chemical physics

This part of the laboratory is focused on the study of ultrafast chemical dynamics by means of novel femtosecond XUV and soft x-ray light sources. Laboratory based experiments using high-order harmonic generation light sources are complemented by studies at the Linac Coherent Light Source (LCLS) free electron laser. Experimental techniques include photoelectron spectroscopy, electron- and ion-imaging, transient absorption spectroscopy, and, most recently, coherent diffractive imaging.

Strong-field induced electronic dynamics in xenon atoms and electronic and nuclear dynamics in vinyl bromide have been studied by transient XUV absorption spectroscopy using photon energies in the range 50 eV - 73 eV. For vinyl bromide, a distinct difference between the strong-field ionization induced dynamics after removal of an electron from the HOMO and the HOMO-1 orbitals is observed. The creation of an electronically excited ion induces intramolecular relaxation dynamics that are traced with element-specificity by a time-dependent shift of the Br 3d - (HOMO-1) transition energy shown in

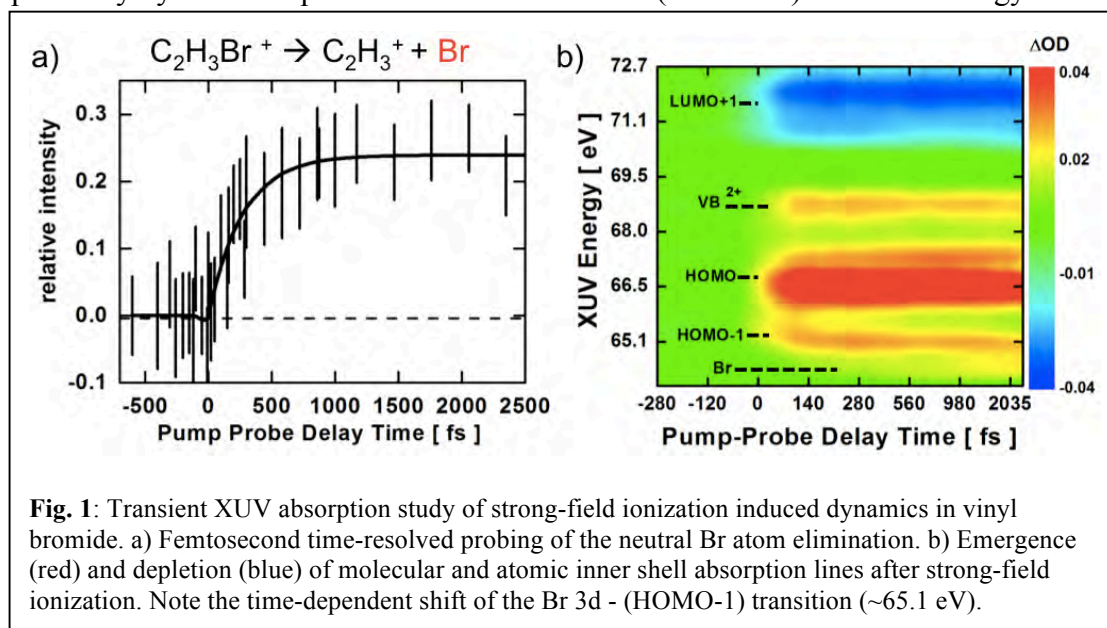
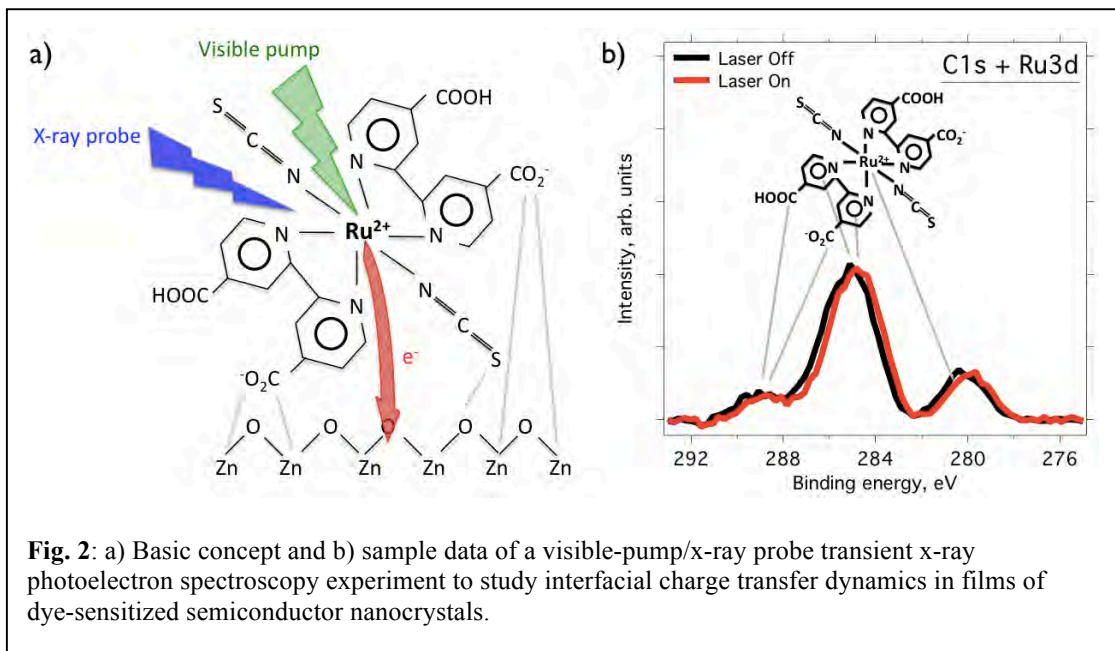


Fig. 1. The results suggest a correlation between intramolecular vibrational energy redistribution (IVR) in electronically excited ions and the elimination of neutral Br atoms.

For xenon atoms, a strong-field induced threefold enhancement of the XUV transmission at photon energies corresponding to Xe 4d-6p inner-shell excitations at 65.1 eV and 67.0 eV is observed. The results are modeled within a picture of Autler-Townes splitting due to coupling of the field-free resonances to neighboring core-excited states by an intense infrared pulse. A broad, strong-field induced absorption feature between 60 eV and 65 eV is interpreted as the result of Autler-Townes multiplet splitting corresponding to a breakdown of the rotating-wave approximation at the highest field strengths used in the experiment.

Two experimental campaigns at the LCLS emerged from the chemical physics subtask of the UXSL. A femtosecond time-resolved x-ray photoelectron spectroscopy (TRXPS) experiment was performed at the LCLS SXR instrument. The study aimed for a better understanding of the charge-transfer dynamics between molecular dyes and metal oxide semiconductor nanocrystals, which form the critical interface in dye-sensitized solar cells. Preliminary results indicate the observation of a transient oxidation state of the molecular dye by a visible laser-induced chemical shift in the Ru 3d⁻¹ inner shell photoline emerging from the transition metal center of the dye.

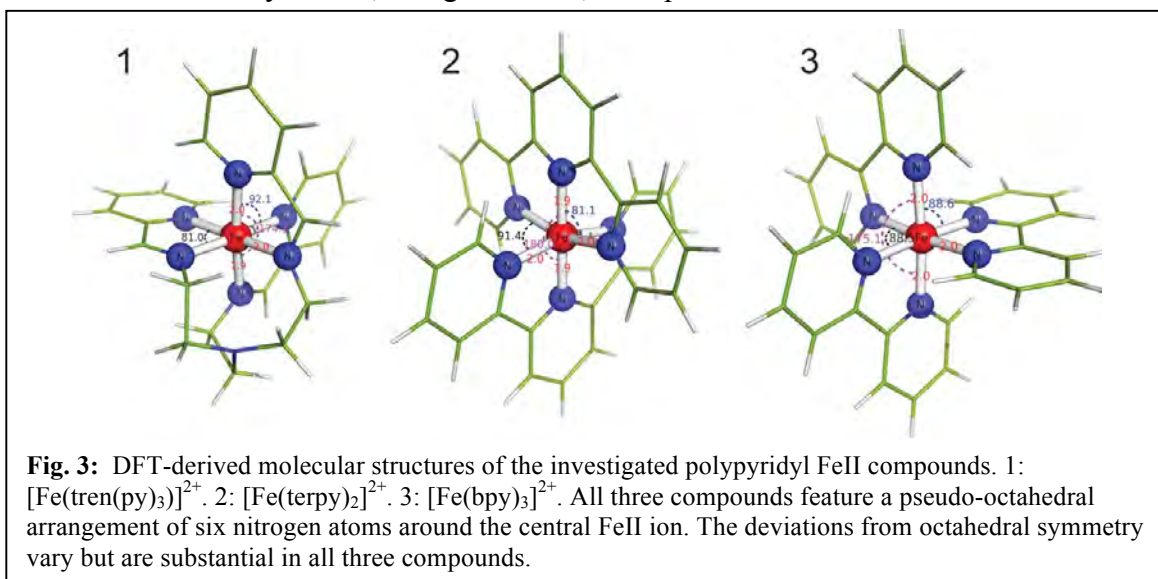


A second LCLS experiment was performed at the AMO instrument using the CAMP chamber of the Max-Planck Society and a helium cluster source from the University of Southern California. The goal of this study was the first unambiguous detection of quantum vortices in superfluid helium nanodroplets by coherent diffractive imaging. The experiment produced a wealth of images from pure and doped helium nanodroplets with an unexpected large variety of shapes and features. The transformation of the diffraction images into real-space information, which is a prerequisite for a physical interpretation, is ongoing.

2. Ultrafast X-ray Studies of Condensed Phase Molecular Dynamics

The objective of this part of the program is to advance our understanding of solution-phase molecular dynamics using ultrafast X-rays as time-resolved probes of the evolving electronic and atomic structure of solvated molecules. Two beamlines have been developed at the Advanced Light Source, with the capability for generating ~ 200 fs x-ray pulses from 200 eV to 10 keV. We have also developed a new capability for transmission XAS studies of thin liquid samples in the soft x-ray range, based on a novel Si_3N_4 cell design with controllable thickness $< 1 \mu\text{m}$.

Present research is focused on charge-transfer processes in solvated transition-metal complexes, which are of fundamental interest due to the strong interaction between electronic and molecular structure. In particular, Fe^{II} complexes exhibit strong coupling between structural dynamics, charge-transfer, and spin-state interconversions.



This year we have focused on understanding changes of valence charge density in polypyridyl Fe^{II} complexes upon spin-crossover for different coordination environments of the metal center. Specifically, we studied the three compounds displayed in Fig. 3 to examine the extent to which soft X-ray absorption spectroscopy techniques could provide information concerning small variations in the local ligand field of Fe^{II} ion. The compounds in Fig. 3 are often approximated as possessing O_h symmetry; in reality, the three pyridine and three imine nitrogen donors of compound 1 effectively reduce this to C_3 symmetry. And while compounds 2 and 3 all present pyridine nitrogen donors to the metal center, distortions due to the geometric constraints of the ligands result in symmetry reductions to C_2 and D_3 symmetry, respectively. In principle, even a slight reduction of molecular symmetry formally lifts some of the orbital degeneracies, which may in turn noticeably affect electronic interactions between the metal center and the ligands and give rise to detectable perturbations in the X-ray absorption properties of both the ground- and photo-induced excited states of these compounds.

Picosecond and femtosecond XANES studies of compound 1, at the Fe L-edge show a clear 1.7 eV dynamic shift in the Fe- L_3 absorption edge with the ultrafast formation of the high-spin state on a 200 fs time scale. This reflects the evolution of the ligand-field

splitting, and comparison with charge-transfer multiplet calculations reveals a reduction in ligand field splitting of ~ 1 eV in the high-spin state. A significant reduction in orbital overlap between the central Fe-3d and the ligand N-2p orbitals is directly observed, consistent with the expected 0.2 Å increase in Fe-N bond length upon formation of the high-spin state. The overall occupancy of the Fe-3d orbitals remains constant upon spin crossover, suggesting that the reduction in σ -donation is compensated by significant attenuation of π -back-bonding in the metal-ligand interactions. Similar studies of compounds 2 and 3 are underway.

More detailed information about metal–ligand interactions in coordination compounds is provided via X-ray spectroscopy of the ligand atoms bound to the metal center(s). These lighter elements such as carbon, nitrogen, and oxygen reveal the ‘ligand perspective’ by probing their 1s \rightarrow 2p (and higher energy) core-level transitions. Initial N K-edge studies of compounds 1-3 reveal X-ray lineshapes corresponding to the chemically distinct nitrogen species. X-ray studies of the charge-transfer dynamics are now in progress.

An important goal is to apply time-resolved X-ray techniques to understand the structural dynamics of more complicated reactions in a solvent environment. Future research will focus on charge-transfer, and ligand dynamics in bi-transition-metal complexes and porphyrins. Solvated metal carbonyls represent a model system where photo-induced ligand dissociation is strongly solvent dependent. In these complexes, the molecular intermediates and solvent exchange mechanisms are poorly understood. Time-resolved XAS will provide important new insight to the molecular dynamics.

3. Time-resolved studies and non-linear interaction of femtosecond x-rays with atoms and molecules:

This subtask of the UXSL is focused on using two-color Extreme Ultraviolet (XUV) pump and XUV probe to study non-Born-Oppenheimer dynamics in polyatomic molecules as well as non-linear x-ray processes. Higher-order harmonic generation has reached intensities high enough as to induce multiphoton ionization processes. The design and construction of our intense XUV source is based on scaling-up in energy of the loose focusing high harmonic generation scheme. Pump/probe delay is achieved with a newly constructed split mirror interferometer (SMI). VUV and XUV wavelength selection in each arm of the SMI is achieved through a combination of transmission filters and coatings on the two D-shaped mirrors. We applied our two-color VUV/XUV pump-probe system to the study non-Born-Oppenheimer dynamics in excited-state molecules. Through a combined experimental and theoretical approach, we investigated the nonadiabatic dynamics of the prototypical ethylene C₂H₄ molecule upon $\pi\rightarrow\pi^*$ excitation with 161 nm light. We combine femtosecond pulses of vacuum ultraviolet (VUV) and extreme ultraviolet (XUV) radiation with variable delay to perform time resolved photo-ion fragment spectroscopy. The XUV (17 eV < $h\nu$ < 23 eV) probe pulses are sufficiently energetic to break the C-C bond in photoionization, or photoionize the dissociation products of the vibrationally hot ground state. The experimental data is directly compared to excited state *ab initio* molecular dynamics simulations explicitly accounting for the probe step in Fig. 4. Enhancements of the CH₂⁺ and CH₃⁺ photo-ion fragment yields, corresponding to molecules photoionized in ethylene (CH₂CH₂) and

ethylidene (CH_3CH) like geometries are observed within 100 fs after $\pi \rightarrow \pi^*$ excitation. Quantitative agreement between theory and experiment on the relative CH_2^+ and CH_3^+ yields provides experimental confirmation of the theoretical prediction of two distinct conical intersections and their branching ratio (Tao, et al. *J. Phys. Chem. A.* **113**, 13656 (2009)). Fast, non-statistical, elimination of H_2 molecules and H atoms is observed in the time resolved H_2^+ and H^+ signals.

The 10 Hz HHG system was successfully upgraded to higher repetition rate to enable the application of our successful COLTRIMS technique to time-resolved investigations. The assembly of a dedicated new endstation for Momentum Imaging Spectroscopy for Time Resolved Studies (MISTERS) is almost complete. A reaction microscope

was fabricated and designed and equipped with two position and time sensitive multihit detectors that are currently in the testing and debugging phase. Moreover, a dedicated and improved Split Mirror Interferometer as well as a dispersive spectrometer for diagnosing the high harmonics light next to the interaction region, spawned by the back focused light and the supersonic gas jet, were constructed and tested. The latter components will improve the interface between the high harmonics beamline and the experimental endstation. In the next fiscal year we will combine the MISTERS apparatus, the interferometer, a collimation section, and the HH diagnostics to one beamline that will be set up downstream from the high harmonics generation chamber in the laser lab. In an initial phase these instruments will be optimized for a startup program on two-color two-photon single ionization of rare gas atoms like He, Ne and Ar followed by the investigation of small molecules like H_2 and O_2 .

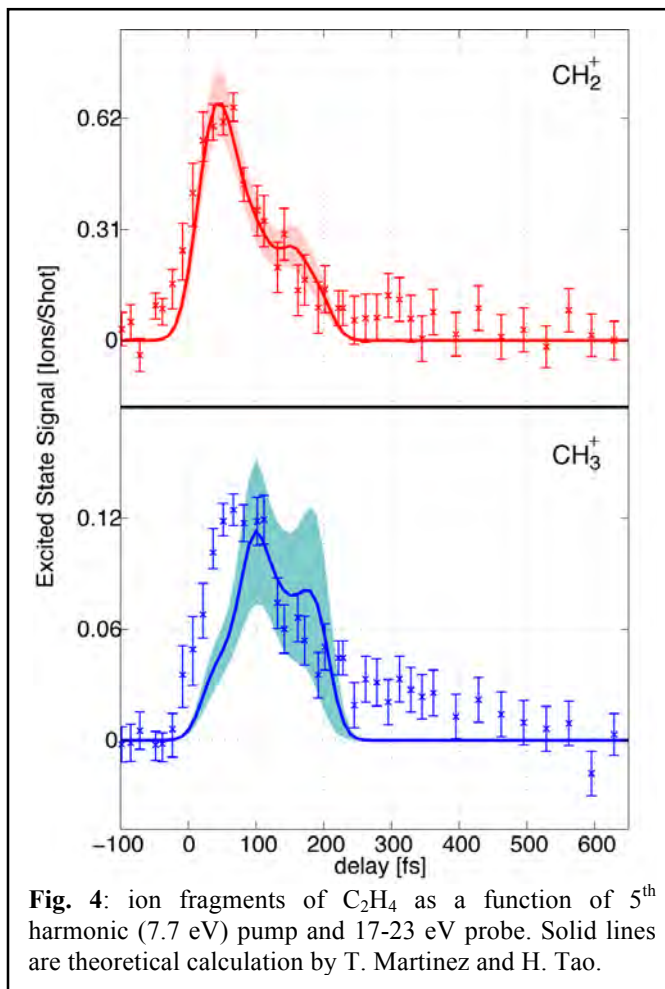
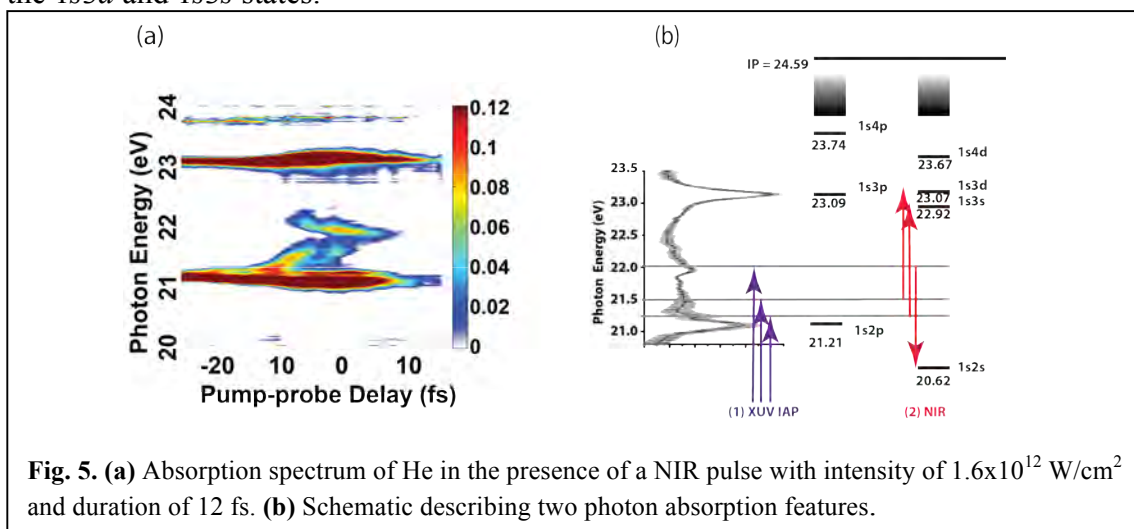


Fig. 4: ion fragments of C_2H_4 as a function of 5th harmonic (7.7 eV) pump and 17-23 eV probe. Solid lines are theoretical calculation by T. Martinez and H. Tao.

4. Attosecond atomic and molecular science

Attosecond dynamics are explored experimentally in this part of the program, focusing on direct measurements of time scales for processes that are driven by electron-electron interactions, such as autoionization and Auger decay. Isolated attosecond pulses are generated over the spectral range of 15 eV to 80 eV via high harmonic generation and Double Optical Gating (DOG) for use in time-resolved photoelectron or mass spectroscopy measurements. Recent work utilizes isolated attosecond pulses spectrally limited to 15-24 eV (by 200 nm or 300 nm thick Sn filters) with pulse durations of approximately 400 as. Additionally, the new experimental capability of transient absorption allows direct measurement of changes to an atom or molecule's absorption probability on the sub-femtosecond timescale.

Changes to an atomic or molecular species' ability to absorb photons in the presence of a strong field ("laser-dressed absorption") are of importance because such modifications can be used to excite selected atomic and molecular states and dark states that can affect experimental outcomes. For the first time, the transmitted spectra of isolated attosecond pulses (20-24 eV; 400 as) are measured following the simultaneous interaction of the attosecond pulse and a strong NIR pulse with atomic helium, as shown in Fig. 6. Alone, the attosecond pulse accesses the $1s2p$ (21.21 eV) and $1s3p$ (23.08 eV) Rydberg states of He, but when the attosecond pulse is overlapped in time with the NIR pulse new features appear in the absorption spectra corresponding to a resonant two photon transition. Theoretical calculations by Prof. Ken Schafer's research group at LSU explain, for example, a new light induced structure (LIS) at 22 eV as the absorption of one XUV photon from the isolated attosecond pulse and emission of one NIR photon to reach the $1s2s$ state of He. Similar LISs are observed connecting the ground state of He to the $1s3d$ and $1s3s$ states.



Transient absorption spectroscopy has been used to directly measure the autoionization lifetimes for the $5s5p^56p$ and $5s5p^57p$ states of atomic xenon. Isolated attosecond pulses excite the $5s5p^56p$ and $5s5p^57p$ states (at 20.95 and 22.23 eV, respectively) which appear as Fano resonances in the absorption spectra due to interference between an autoionization pathway and a direct pathway to reach continuum states. If the NIR pulse interacts with the excited state before it decays, absorption of

additional photons from the NIR pulse promote the autoionizing states to other nearby $5s5p^5ns$ and $5s5p^5nd$ states or continuum states and, as a result, suppress the Fano resonance. The resonance is unmodified if the NIR pulse arrives at the Xe after the states have decayed. In this way lifetimes of the $5s5p^56p$ and $5s5p^57p$ states (consistent with lifetimes calculated from linewidths reported in literature) are measured to be 19.6 ± 1.1 and 52 ± 24 fs, respectively.

Experiments are underway to investigate the competition between autoionization and predissociation in superexcited states of molecular nitrogen. Theoretical calculations predict lifetimes ranging from 10s of fs to <1 fs. Isolated attosecond pulses (spectrally limited to 15-24 eV by a 200 nm thick Sn filter) access a superexcited state of N_2 with an energy around 23 eV, which decays via autoionization to N_2^+ or predissociates to N and excited N atoms, N^* . An optical (800 nm) few-fs pulse ionizes N^* to N^+ , which is then detected in the mass spectrometer. Preliminary pump-probe measurements of predissociation products suggest the lifetime of the superexcited state is less than 10 fs. In a collaborative effort, the AMO theory group (Orel and Rescigno) has estimated the timescale of autoionization as 17 fs.

Future experimental plans include XUV photoionization of spin-orbit wave packets and alignment created by strong field ionization of atomic krypton to investigate alignment, coherence, and phase information about the atomic superposition. Polarization control of optical fields will be critical for these experiments. The timescale of Auger decay of molecular species such as HBr will be measured with transient absorption and compared to the analogous atomic case, krypton.

4. Theory and computation

This part of the program focuses on the theoretical description of the next generation of ultrafast XUV and X-ray experiments. To that end, we have completed an entirely new implementation of the Multiconfiguration Time-dependent Hartree Fock (MCTDHF) method with “all electrons active” based on finite-element grids in prolate spheroidal coordinates to represent the time-dependent orbitals.

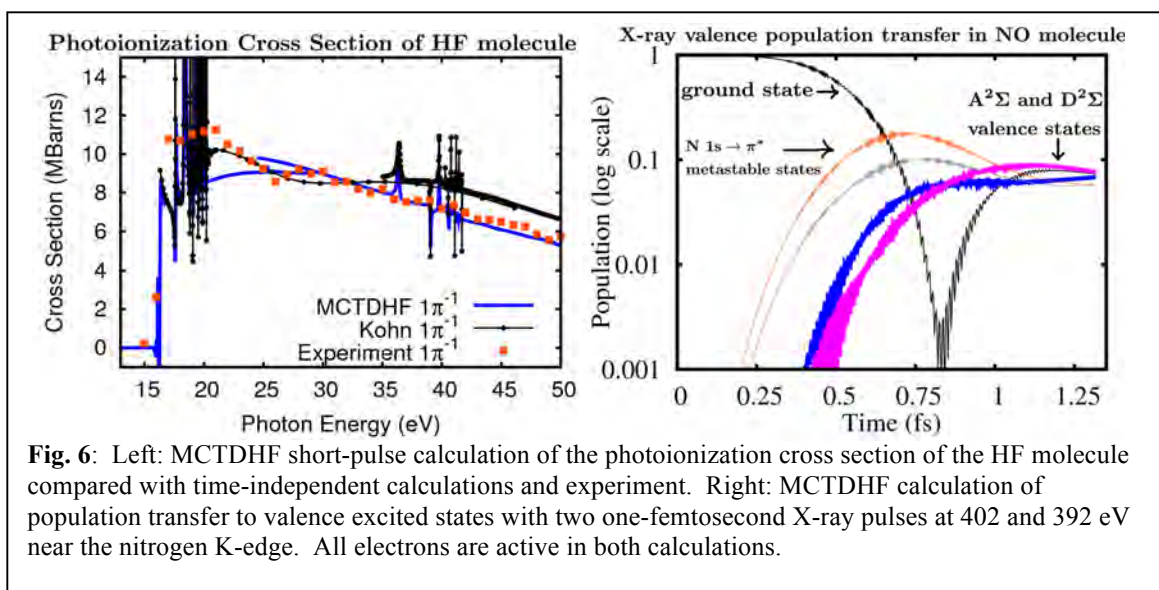
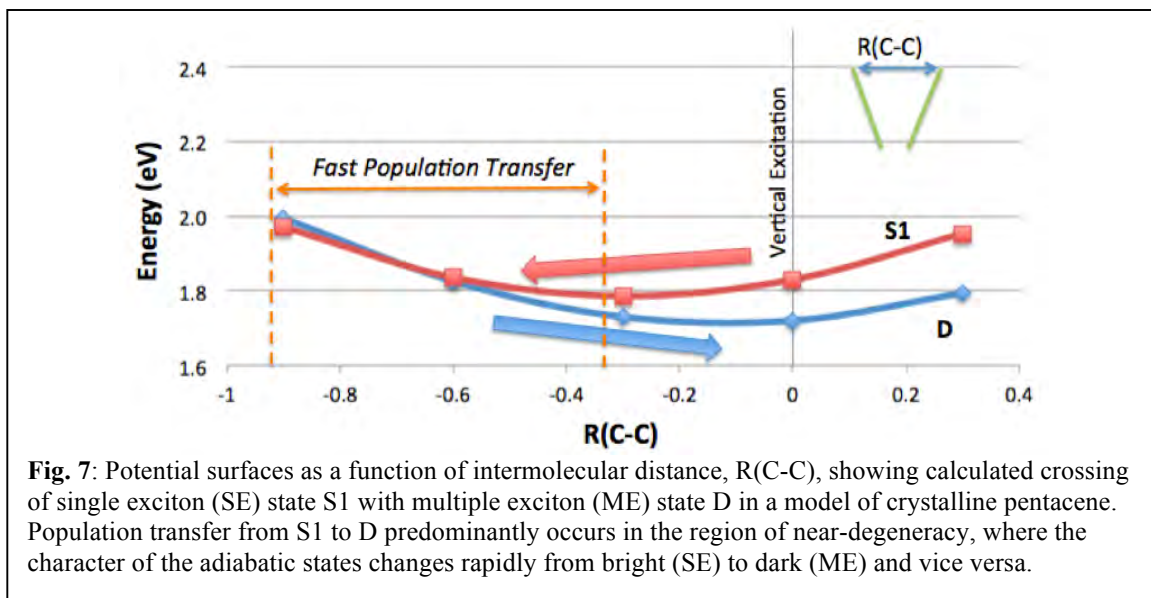


Fig. 6: Left: MCTDHF short-pulse calculation of the photoionization cross section of the HF molecule compared with time-independent calculations and experiment. Right: MCTDHF calculation of population transfer to valence excited states with two one-femtosecond X-ray pulses at 402 and 392 eV near the nitrogen K-edge. All electrons are active in both calculations.

The method treats general diatomics including for the first time the combination of (1) a rigorous representation of the ionization continuum via the method of exterior complex coordinate scaling, (2) an all-electrons-active treatment in which excitations are allowed from all orbitals and all orbitals are time dependent, and (3) the possibility of treating nuclear motion in diatomics on the same footing as electronic motion. This capability has opened the door to the *ab initio* simulation of both many-electron atoms and many-electron diatomic molecules in short, intense XUV and X-ray pulses.

In Fig. 6 we show two recent results from this newly developed capability. With a 500 as pulse in the XUV a diatomic molecule can be photoionized into a broad energy range of the ionization continuum. The calculated electron flux correlation function can be Fourier transformed to give the photoionization cross section within the bandwidth of that single pulse. Highly excited autoionizing states and the inclusion of all open ionization channels in the hydrogen fluoride molecule emerge naturally in this test of the new MCTDHF capability. Also shown in Fig. 6 are the results of a stimulated X-ray Raman transfer of population from the ground state of nitric oxide to a wave packet of valence excited states using two 1 femtosecond pulses near the nitrogen K-edge. This calculation demonstrates the feasibility of controlled population transfer among valence states using ultrafast X-ray pulses, and thus allows us to explore the possibility of site-selective nonlinear X-ray spectroscopy with new free electron laser facilities.

Calculations on short pulse transfer of population and other direct probes of correlated electron dynamics in the Li, Be and Ne atoms are currently underway using the version of this capability specialized for atoms with using grid methods in spherical polar coordinates. Initial calculations on short pulse ionization of H₂ including nuclear motion without the Born Oppenheimer approximation were also completed this year.



The crucial photochemical events in processes ranging from vision to light-harvesting to light emission involve ultrafast processes that involve multiple excited states. Experiments provide one window on the relevant states while first principles computations offers another, complementary view. Recent work has relied on our

development of spin-flipping methods to enable new calculations that provide fresh insight into the excited states relevant to the process of singlet fission in pentacene crystals. Our calculations on this process, where a single photon can yield two electron-hole pairs (via two triplets), suggest a crucial role for a conical intersection, as illustrated in Fig. 7.

We have also recently reported calculations of high harmonic generation spectra for the H₂ and N₂ molecules, using quantum chemistry methods, to illustrate their applicability to this time-domain problem. Our work on calculating excited states of helium clusters has moved from statics to dynamics with the use of *ab initio* trajectories to explore the ejection of He atoms and pairs of atoms. Additionally, the development of local excited state methods that are capable of treating much larger cluster sizes than standard algorithms is approaching production capability.

UXSL Publications, by Subtask (2010-2012)

1. Oleg Kornilov, Chia C. Wang, Oliver Bünemann, Andrew T. Healy, Mathew Leonard, Chunte Peng, Stephen R. Leone, Daniel M. Neumark, and Oliver Gessner, "Ultrafast Dynamics in Helium Nanodroplets Probed by Femtosecond Time-Resolved EUV Photoelectron Imaging", *J. Phys. Chem. A* **114**, 1437 (2010).
2. Oleg Kornilov, Russell Wilcox, and Oliver Gessner, "Nanograting-based compact VUV spectrometer and beam profiler for in-situ characterization of high-order harmonic generation light sources", *Rev. Sci. Instrum.* **81**, 063109 (2010).
3. M. Hoener, L. Fang, O. Kornilov, O. Gessner, S. T. Pratt, M. Gühr, E. P. Kanter, C. Blaga, C. Bostedt, J. D. Bozek, P. H. Bucksbaum, C. Buth, M. Chen, R. Coffee, J. Cryan, L. DiMauro, M. Glowonia, E. Hosler, E. Kukk, S. R. Leone, B. McFarland, M. Messerschmidt, B. Murphy, V. Petrovic, D. Rolles, and N. Berrah, "Ultra-intense X-ray Induced Ionization, Dissociation, and Frustrated Absorption in Molecular Nitrogen", *Phys. Rev. Lett.* **104**, 253002 (2010).
4. James M. Glowonia, J. Cryan, J. Andreasson, A. Belkacem, N. Berrah, C. I. Blaga, C. Bostedt, J. Bozek, L. F. DiMauro, L. Fang, J. Frisch, O. Gessner, M. Gühr, J. Hajdu, M. P. Hertlein, M. Hoener, G. Huang, O. Kornilov, J. P. Marangos, A. M. March, B. K. McFarland, H. Merdji, V. S. Petrovic, C. Raman, D. Ray, D. A. Reis, M. Trigo, J. L. White, W. White, R. Wilcox, L. Young, R. N. Coffee, and P. H. Bucksbaum, "Time-resolved pump-probe experiments at the LCLS", *Opt. Express* **18**, 17620 (2010).
5. L. Fang, M. Hoener, O. Gessner, F. Tarantelli, S. T. Pratt, O. Kornilov, C. Buth, M. Gühr, E. P. Kanter, C. Bostedt, J. D. Bozek, P. H. Bucksbaum, M. Chen, R. Coffee, J. Cryan, M. Glowonia, E. Kukk, S. R. Leone, and N. Berrah, "Double core hole production in N₂: Beating the Auger clock", *Phys. Rev. Lett.* **105**, 083005 (2010).
6. James P. Cryan, J. M. Glowonia, J. Andreasson, A. Belkacem, N. Berrah, C. I. Blaga, C. Bostedt, J. Bozek, C. Buth, L. F. DiMauro, L. Fang, O. Gessner, M. Guehr, J. Hajdu, M. P. Hertlein, M. Hoener, O. Kornilov, J. P. Marangos, A. M. March, B. K. McFarland, H. Merdji, V. Petrovic, C. Raman, D. Ray, D. Reis, F. Tarantelli, M. Trigo, J. White, W. White, L. Young, P. H. Bucksbaum, and R. N. Coffee, "Auger electron angular distribution of double core hole states in the molecular reference frame", *Phys. Rev. Lett.* **105**, 083004 (2010).
7. O. Gessner, O. Kornilov, M. Hoener, L. Fang, and N. Berrah, "Intense Femtosecond X-ray Photoionization Studies of Nitrogen - How Molecules interact with Light from the LCLS" in *Ultrafast Phenomena XVII*, M. Chergui, D. M. Jonas, E. Riedle, R. W. Schoenlein, A. J. Taylor, Eds., Oxford University Press (2011).

8. Oleg Kornilov, Oliver Bünermann, Daniel J. Haxton, Stephen R. Leone, Daniel M. Neumark, and Oliver Gessner, "Femtosecond photoelectron imaging of transient electronic states and Rydberg atom emission from electronically excited He droplets", *J. Phys. Chem. A* **115**, 7891 (2011).
9. Oliver Bünermann, Oleg Kornilov, Stephen R. Leone, Daniel M. Neumark, and Oliver Gessner, "Femtosecond Extreme Ultraviolet Ion Imaging of Ultrafast Dynamics in Electronically Excited Helium Nanodroplets", *IEEE J. Sel. Top. Quantum Electron.* **18**, 308 (2012).
10. J. P. Cryan, J. M. Glowina, J. Andreasson, A. Belkacem, N. Berrah, C. I. Blaga, C. Bostedt, J. Bozek, N. A. Cherepkov, L. F. DiMauro, L. Fang, O. Gessner, M. Gühr, J. Hajdu, M. P. Hertlein, M. Hoener, O. Kornilov, J. P. Marangos, A. M. March, B. K. McFarland, H. Merdji, M. Messerschmidt, V. Petrovic, C. Raman, D. Ray, D. Reis, S. K. Semenov, M. Trigo, J. White, W. White, L. Young, P. H. Bucksbaum, and R. N. Coffee, "Molecular Frame Auger Electron Energy Spectrum from N₂", *J. Phys. B: At. Mol. Opt. Phys.* **45**, 055601 (2012).
11. Oliver Bünermann, Oleg Kornilov, Daniel J. Haxton, Stephen R. Leone, Daniel M. Neumark, and Oliver Gessner, "Ultrafast Probing of Ejection Dynamics of Rydberg Atoms and Molecular Fragments from Electronically Excited Helium Nanodroplets", *J. Chem. Phys.*, *submitted* (2012).
12. Andrey Shavorskiy, Amy Cordones, Josh Vura-Weis, Katrin Siefertmann, Daniel Slaughter, Felix Sturm, Fabian Weise, Matthew Strader, Hana Cho, Ming-Fu Lin, Camila Bacellar, Champak Khurmi, Marcus Hertlein, Jinghua Guo, Hendrik Bluhm, Tolek Tyliczszak, David Prendergast, Giacomo Coslovich, Joseph Robinson, Robert Kaindl, Robert W. Schoenlein, Ali Belkacem, Thorsten Weber, Daniel M. Neumark, Stephen R. Leone, Dennis Nordlund, Hirohito Ogasawara, Anders R. Nilsson, Oleg Krupin, Joshua J. Turner, William F. Schlotter, Michael R. Holmes, Philip A. Heimann, Marc Messerschmidt, Michael P. Minitti, Martin Beye, Sheraz Gul, Jin Zhang, Nils Huse, and Oliver Gessner, "Time-Resolved X-Ray Photoelectron Spectroscopy Techniques for Real-Time Studies of Interfacial Charge Transfer Dynamics", *Application of Accelerators in Research and Industry*, AIP Conf. Proc., *submitted* (2012).
13. Fabian Weise, Daniel M. Neumark, Stephen R. Leone, and Oliver Gessner, "Differential Near-Edge Coherent Diffractive Imaging for Element-Specific Contrast Enhancement in Ultrafast Imaging Applications", *Opt. Express*, *submitted* (2012).
14. Ming-Fu Lin, Adrian N. Pfeiffer, Daniel M. Neumark, Stephen R. Leone, and Oliver Gessner, "Strong-Field induced XUV Transmission and Autler-Townes Multiplet Splitting in $4d^{1}6p$ Core-excited Xe studied by Femtosecond XUV Transient Absorption Spectroscopy", *J. Chem. Phys.*, *submitted* (2012).
15. N. Huse, T.-K. Kim, L. Jamula, J.K. McCusker, F.M.F. de Groot, and R.W. Schoenlein, "Photo-Induced Spin-State Conversion in Solvated Transition Metal Complexes Probed via Time-Resolved Soft X-ray Spectroscopy," *J. Am. Chem. Soc.*, **132**, 6809-6816 (2010).
16. N. Huse, H. Cho, T.K. Kim, L. Jamula, J.K. McCusker, F.M.F. de Groot, and R.W. Schoenlein, "Ultrafast spin-state conversion in solvated transition metal complexes probed with femtosecond soft x-ray spectroscopy," in **Ultrafast Phenomena XVII**, M. Chergui, D.M. Jonas, E.Riedle, R.W. Schoenlein, A.J. Taylor, Eds., Oxford University Press, New York, p. 370-372, (2011)
17. N. Huse, H. Wen, H. Cho, T.K. Kim, R.W. Schoenlein, and A.M. Lindenberg, "Ultrafast conversions of hydrogen-bonded structures in liquid water observed via femtosecond soft x-ray spectroscopy," in **Ultrafast Phenomena XVII**, M. Chergui, D.M. Jonas, E.Riedle, R.W. Schoenlein, A.J. Taylor, Eds., Oxford University Press, New York, p. 460-462, (2011)
18. N. Huse, H. Cho, K. Hong, L. Jamula, F.M.F. de Groot, T.K. Kim, J.K. McCusker, and R.W. Schoenlein, "Femtosecond soft x-ray spectroscopy of solvated transition metal complexes: Deciphering the interplay of electronic and structural dynamics," *J. Phys. Chem. Lett.* **2**, 880-884 (2011).
19. H. Cho, M.L. Strader, K. Hong, L. Jamula, J.K. McCusker, T.K. Kim, R.W. Schoenlein, and N. Huse, "Transient X-ray absorption spectroscopy of polypyridyl Fe(II) spin-crossover compounds," *Faraday Discuss.* in press (2012).

20. B.E. Van Kuiken, N. Huse, H. Cho, M.L. Strader, M.S. Lynch, R.W. Schoenlein, and M. Khalil, "Probing the electronic structure of a photoexcited solar cell dye with transient X-ray absorption spectroscopy," *J. Phys. Chem. Lett.*, in press (2012).
21. James M. Glowonia, J. Cryan, J. Andreasson, A. Belkacem, N. Berrah, C. I. Blaga, C. Bostedt, J. Bozek, L. F. DiMauro, L. Fang, J. Frisch, O. Gessner, M. Gühr, J. Hajdu, M. P. Hertlein, M. Hoener, G. Huang, O. Kornilov, J. P. Marangos, A. M. March, B. K. McFarland, H. Merdji, V. S. Petrovic, C. Raman, D. Ray, D. A. Reis, M. Trigo, J. L. White, W. White, R. Wilcox, L. Young, R. N. Coffee, and P. H. Bucksbaum, "Time-resolved pump-probe experiments at the LCLS", *Opt. Express* **18**, 17620 (2010).
22. James P. Cryan, J. M. Glowonia, J. Andreasson, A. Belkacem, N. Berrah, C. I. Blaga, C. Bostedt, J. Bozek, C. Buth, L. F. DiMauro, L. Fang, O. Gessner, M. Guehr, J. Hajdu, M. P. Hertlein, M. Hoener, O. Kornilov, J. P. Marangos, A. M. March, B. K. McFarland, H. Merdji, V. Petrovic, C. Raman, D. Ray, D. Reis, F. Tarantelli, M. Trigo, J. White, W. White, L. Young, P. H. Bucksbaum, and R. N. Coffee, "Auger electron angular distribution of double core hole states in the molecular reference frame", *Phys. Rev. Lett.* **105**, 083004 (2010).
23. T.E. Glover, M.P. Hertlein, S.H. Southworth, T.K. Allison, J. van Tilborg, E.P. Kanter, B. Krassig, H.R. Varma, B. Rude, R. Santra, A. Belkacem and L. Young, "Controlling X-rays with light", *Nature Physics* **6**, 69 (2010)
24. Y.H. Jiang, A. Rudenko, J.F. Perez-Torres, O. Herrwerth, L. Foucar, M. Kurka, K. U. Kuhnel, M. Toppin, E. Plesiat, F. Morales, F. Martin, M. Lezius, M.F. Kling, T. Jahnke, R. Doerner, J.L. Sanz-Vicario, J. van Tilborg, A. Belkacem, M. Schultz, K. Ueda, T.J.M. Zouros, S. Dusterer, R. Treusch, C.D. Schroter, R. Moshhammer, and J. Ullrich, "Investigating two-photon double ionization of D2 by XUV-pump-XUV-probe experiments", *Phys. Rev. A* **81**, 05140(R) (2010).
25. Y.H. Jiang, A. Rudenko, E. Plesiat, L. Foucar, M. Kurka, K. U. Kuhnel, Th. Ergler, J.F. Perz-Torres, F. Martin, O. Herrwerth, M. lezius, M.F. Kling, J. Titze, T. jahnke, R. Doerner, J.L. Sanz-Vicario, M. Schoffler, J. van Tilborg, A. Belkacem, K. Ueda, T.J.M. Zouros, S. Dusterer, R. Treusch, C.D. Schroter, R. Moshhammer, and J. Ullrich, "Tracing direct and sequential two-photon double ionization of D2 in femtosecond extreme-ultraviolet laser pulses", *Phys. Rev. A* **81**, 021401 (R) (2010).
26. Y.H. Jiang, A. Rudenko, O. Herrwert, L. Foucar, M. Kurka, K.U. Kuhnel, M. Lezius, M. F. Kling, J. van Tilborg, A. Belkacem, K. Ueda, S. Dusterer, R. Treusch, C.D. Schroter, R. Moshhammer, and J. Ullrich, "Ultrafast extreme untraviolet induced isomerization of acetylene cations:", *Phys. Rev. Lett.* **105**, 263002 (2010)
27. T.K. Allison, T.W. Wright, A.M. Stooke, C. Khurmi, J. van Tilborg, Y. Liu, R.W. Falcone, and A. Belkacem, "Femtosecond spectroscopy with vacuum ultraviolet pulse pairs", *Optics Lett.* **35**, 3664 (2010)
28. W. Cao, S. De, K.P. Singh, S. Chen, M.S. Schoffler, A.S. Alnaser, I.A. Bocharova, G. Laurent, D. Ray, S. Zherebtsov, M.F. Kling, I. Ben-Itzak, I.V. Litvinyuk, A. Belkacem, T. Osipov, T. Rescigno, and C.L. Cocke, "dynamics modification of the fragmentation of CO(q+) excited states generated with high-order harmonics", *Phys. Rev. A* **82**, 043410 (2010)
29. H. Tao, T.K. Allison, T.W. Wright, A.M. Stooke, C. Khurmi, J. van Tilborg, Y. Liu, R.W. Falcone, A. Belkacem, and T.J. Martinez, "ultrafast internal conversion in ethylene. I. The excited state lifetime", *J. Chem. Phys.* **134**, 244306 (2011).
30. Cao W., Laurent G., De S., Schoffler M., Jahnke T., Alnaser A.S., Bocharova I.A., Stuck C., Ray D., Kling M.F., Ben-Itzhak I., Weber T., Landers A.L., Belkacem A., Dorner R., Orel A.E., Rescigno T.N., Cocke C.L., "Dynamics modification of the fragmentation of autoionizing states of O2+", *Phys. Rev. A* **84**, 053406 (2011).
31. R. Moshhammer, Th. Pfeifer, A. Rudenko, Y.H. Jiang, L. Foucar, M. Kurka, K.U. Kuhnel, C.D. Schroter, J. Ullrich, O. Herrwerth, M.F. Kling, X.J. Liu, K. Motomura, H. Fukuzawa, A. Yamada, K. Ueda, K.L. Ishikawa, K. Nagaya, H. Iwayama, A. Sugishima, Y. Mizoguchi, S. Yase, M. Yao, N. Saito, A. Belkacem, M. Nagasono, A. Higashiya, M. Yabashi, T. Ishikawa, H. Ohashi, H. Kimura, T.

- Togashi, “second-order autocorrelation of XUV FEL pulses via time resolved two-photon single ionization of He”, *Optics Express* **19**, 21698 (2011).
32. Allison T.K., Tao H., Glover W.J., Wright T., Stooke A.M., Khurmi C., van Tilborg J., Liu Y., Falcone R.W., Martinez T.J., Belkacem A., “Ultrafast internal conversion in ethylene. II. Mechanisms and pathways for quenching and hydrogen elimination”, *Jour. Chem. Phys.* **136**, 124317 (2012).
 33. Cryan, J.P., Glowia J.M., Andreasson J., Belkacem A., Berrah N., Blaga C.I., Bostedt C., Bozek J., Cherepkov N.A., Dimauro L.F., Fang L., Gessner O., Guhr M., Hajdu J., Hertlein M.P., Hoener M., Korlinov O., Marangos J.P., March A.M., McFarland B.K., Merdji H., Messerschmidt M., Petrovic V.S., Raman C., Ray D., Reis D.A., Semenov S.K., Trigo M., White J.L., White W., Young L., Bucksbaum P.H., Coffee R.N., “Molecular frame Auger electron spectrum from N₂”, *Jour. Phys. B – At. Mol. Opt. Phys.* **45**, 055601 (2012).
 34. M Kurka , J Feist , D A Horner , A Rudenko , Y H Jiang , K U Kühnel , L Foucar , T N Rescigno, C W McCurdy , R Pazourek , S Nagele , M Schulz , O Herrwerth , M Lezius , M F Kling , M Schöffler , A Belkacem , S Düsterer , R Treusch , B I Schneider , L A Collins , J Burgdörfer , C D Schröter , R Moshhammer and J Ullrich, “Differential cross sections for non-sequential double ionization of He by 52 eV photons from the Free Electron Laser in Hamburg, FLASH” *New J. Phys.* **12**, 073035 (2010).
 35. E. Goulielmakis, Z.-H. Loh, A. Wirth, R. Santra, N. Rohringer, V. S. Yakovlev, S. Zherebtsov, T. Pfeifer, A. M. Azzeer, M. F. Kling, S. R. Leone, and F. Krausz, “Real-time observation of valence electron motion,” *Nature* **466**, 739 (2010).
 36. H. Mashiko, M. J. Bell, A. R. Beck, M. J. Abel, P. M. Nagel, C. P. Steiner, J. Robinson, D. M. Neumark, and S. R. Leone, “Tunable frequency-controlled isolated attosecond pulses characterized by either 750 nm or 400 nm wavelength streak fields,” *Opt. Exp.* **18**, 25887 (2010).
 37. M. J. Abel, D. M. Neumark, S. R. Leone, and T. Pfeifer, “Classical and Quantum Control of Electrons using the Carrier-Envelope Phase of a Strong Field.” *Laser Photonics Rev.* **25**, 1 (2011).
 38. H. Mashiko, M. J. Bell, A. R. Beck, D. M. Neumark, and S. R. Leone, “Frequency tunable attosecond apparatus,” *Progress in Ultrafast Intense Laser Science X*, K. Yamanouchi, G. Paulus, D. Mathur, eds., Springer Science+Business Media, inc. , *in press*.
 39. D. J. Haxton, K. Lawler and C. W. McCurdy, “Multiconfiguration Time-dependent Hartree-Fock Treatment of Electronic and Nuclear Dynamics in Diatomic Molecules,” *Phys. Rev. A* **83**, 063416 (2011).
 40. D. J. Haxton, K. V. Lawler and C. W. McCurdy, “Single photoionization of Be and HF using the multiconfiguration time-dependent Hartree-Fock method,” *Phys. Rev. A* **86**, 013406 (2012).
 41. K.D. Closser and M. Head-Gordon, “Ab initio calculations on the electronically excited states of small helium clusters,” *J. Phys. Chem. A* **114**, 8023-8032 (2010).
 42. F. Bell, D. Casanova and M. Head-Gordon, “Theoretical study of substituted PBPB dimers: Structural analysis, tetra-radical character and excited states,” *J. Am. Chem. Soc.* **132**, 11314–11322 (2010).
 43. F.-L. Liu, Z. Gan, Y. Shao, C.-P. Hsu, A. Dreuw, M. Head-Gordon, B.T. Miller, B.R. Brooks, J.-G. Yu, T.R. Furlani and J. Kong, “A parallel implementation of the analytic nuclear gradient for time-dependent density functional theory within the Tamm-Dancoff approximation,” *Mol. Phys.* **108**, 2791-2800 (2010).
 44. J. Azar , W. Kurlancheek, and M. Head-Gordon, “Characterization of electronically excited states in anionic acetonitrile clusters,” *Phys. Chem. Chem. Phys.* **13**, 9147-9154 (2011).
 45. P.M. Zimmerman, F. Bell, D. Casanova, and M. Head-Gordon, “Mechanism for Singlet Fission in Pentaene and Tetracene: From Single Exciton to Two Triplets,” *J. Am. Chem. Soc* **133**, 19944-19952 (2011).
 46. E. Luppi and M. Head-Gordon, “Computation of high harmonic generation spectra of H₂ and N₂ due to intense laser pulses using quantum chemistry methods and time-dependent density functional theory,” *Mol. Phys.* **110**, 909-923 (2012).

Early Career: Ultrafast X-ray Studies of Intramolecular and Interfacial Charge Migration

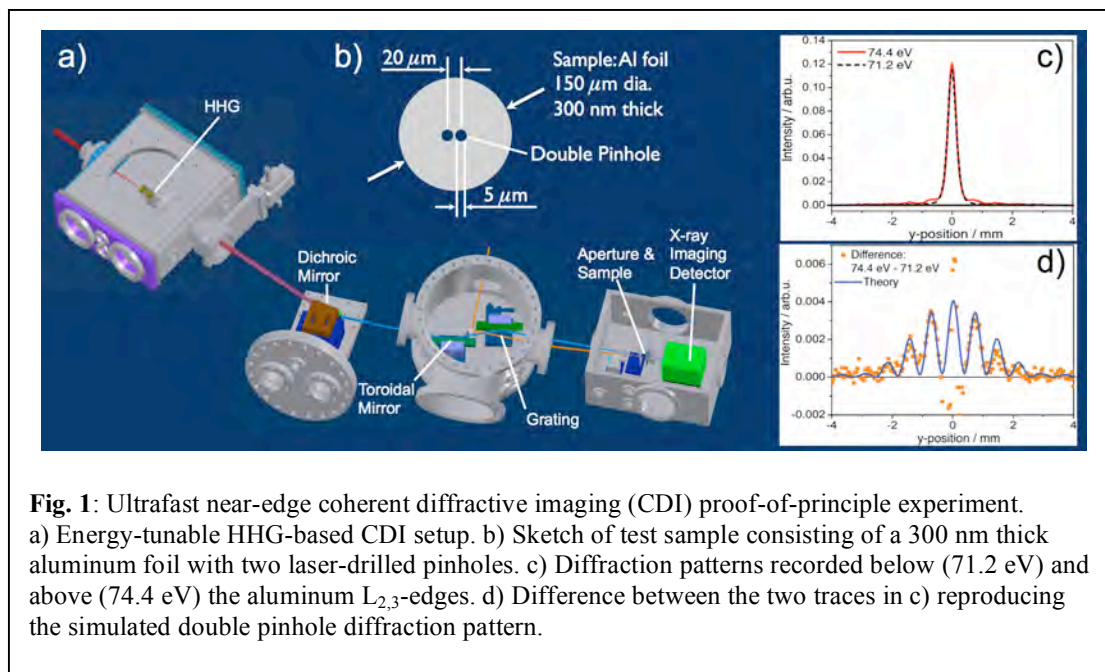
Oliver Gessner

Chemical Sciences, Lawrence Berkeley National Laboratory, Berkeley, CA 94720

OGessner@lbl.gov

Program Scope: Intramolecular and interfacial charge-transport mechanisms in novel molecular devices for sustainable energy solutions will be studied on their natural timescales and with atomic specificity by means of a new class of ultrafast x-ray experiments. The central motivation is to derive an accurate description not only of the complex electronic structure that emerges from extended molecular and interfacial assemblies, but in particular of the dramatic changes in these electronic structures that, by definition, have to occur in order to enable, for example, long-range charge transfer and/or catalytic function. The combination of different x-ray techniques will provide the capability to test molecular level models of intramolecular and interfacial charge migration by a new set of molecular level probes.

This new initiative has been enabled by an Early Career Research Program Award of the DOE Office of Science. Time-resolved inner shell photoelectron spectroscopy, time-resolved Auger-electron spectroscopy, and time-resolved near-edge coherent diffractive imaging (CDI) techniques will be developed to study charge-transfer processes in complex systems in real-time and with sub-micron spatial resolution. Laboratory-based experiments driven by femtosecond high harmonic generation (HHG) light sources will be complemented by accelerator-based experiments at the Linac Coherent Light Source (LCLS) and the Advanced Light Source (ALS).



Recent Progress and Future Plans: Key concepts of the proposed experimental methods have been tested in a series of proof-of-principle experiments at the SXR instrument of the LCLS, at the Molecular Environmental Science beamline of the ALS, and with a newly constructed HHG-based near-edge CDI setup (Fig. 1).

The experiments at the LCLS and at the ALS support the potential of time-resolved x-ray photoelectron spectroscopy (TRXPS) to trace electronic dynamics in films of dye-sensitized nanocrystals. In particular, the LCLS results show strong indications for a transient chemical shift of the Ru-3d¹ inner-shell photoelectron line emitted by the transition metal center of a molecular dye (N3) attached to ZnO nanocrystals. In the next step, the experimental results will be interpreted by means of an ab-initio description of the transient electronic structure of the molecule-semiconductor interface. Preliminary findings indicate a significant influence of the semiconductor substrate on the photoinduced changes in the molecular inner shell photoelectron spectrum.

An experimental scheme has been implemented at the ALS that enables visible-pump/x-ray-probe TRXPS measurements during multi-bunch operation and without the need to control the relative time delay between the exciting visible laser pulse and the probing x-ray pulse from the ALS. The scheme is based on measuring the relative delay of the pulses by means of a time- and position-sensitive electron detector interfaced to a commercial hemispherical electron energy analyzer. The time-resolution of the setup is currently limited by the nanosecond pump-pulses from a Q-switched ND:YLF laser. Efforts are underway to replace this system by a high repetition-rate fiber-laser system with pulse durations below the ALS bunch length (~40 ps - 70 ps). The combination of the ALS- and LCLS-based experiments will provide complementary information on the complex interfacial electron dynamics, which are marked by a variety of rates that span several orders of magnitude.

Ultrafast x-ray microscopy techniques have the potential to provide direct access to the relationship between the mesoscopic structure and the microscopic electronic function of molecular electronic devices. A key quest is to translate the chemical sensitivity of energy-domain x-ray microscopy techniques into the time-domain in order to be able to monitor valence electron dynamics in time and space. An important milestone of the project will be the implementation of a laboratory-based sub-picosecond time-resolved imaging setup. This activity will greatly benefit from a proof-of-principle experiment that was recently enabled by Laboratory Directed Research and Development (LDRD) funds from Lawrence Berkeley National Laboratory (LBNL). A HHG light source has been interfaced with a monochromator and an XUV imaging setup, facilitating energy-resolved CDI experiments in a laboratory setting (Fig. 1). Experiments at the Al L_{2,3} edges (~73 eV) demonstrated that the fringe visibility in the XUV diffraction pattern from a double pinhole in a 300 nm thick Al foil is increased from 0 below the absorption edges to 0.73±0.08 in the differential image that combines two measurements below and above the edges. The next stage of the project will focus on the extension of the near-edge CDI experiments into the time-domain by implementing a two-color pump-probe scheme.

SLAC Ultrafast Chemical Science Program

Philip Bucksbaum (spokesperson), David Reis, Michael Bogan, Kelly Gaffney, Markus Guehr, and Todd Martinez

Overarching science goal: The Ultrafast Chemical Science Program at SLAC focuses on ultrafast chemical physics research enabled by LCLS, the world's first hard x-ray free-electron laser. Our overarching goal is to establish research at SLAC that makes optimal use of this new SLAC tool for fundamental discoveries and new insights in ultrafast science. The on-site presence of LCLS with its facilitating connections to our research is one of two distinguishing advantages of this program within the AMOS portfolio. Our other distinguishing advantage is our close connection to Stanford University maintained through our task leaders' affiliations with the **Stanford PULSE Institute**. These help to keep us competitive on a national and international level.

Major themes: There are three major themes in the current program:

- **Imaging on the nanoscale in space and the femtoscale in time.** Microscopy at its most essential level in both space and time is paramount to the BES mission to control matter. Non-periodic nano-structures and ultrafast timescales dominate the workings of biology and chemistry. To understand and control function we therefore must first observe structure and motion on these scales.

LCLS is a revolutionary x-ray source for investigations on the nanoscale, and our largest subtask is devoted to developing science using coherent x-ray imaging techniques at this and other x-ray free electron lasers. This work includes nanocrystal imaging on the few-Angstrom scale; nonperiodic imaging of single biomolecules; cell imaging; and imaging of aerosols.

Imaging of still smaller structures such as small molecules use other techniques, such as particle fragment velocity maps, and electron holography. Here we are exploring fundamental energy-relevant processes such as photo-induced isomerization, dissociation, and x-ray damage, using optical and x-ray probes, and a combination of linear and nonlinear spectroscopic methods.

Time scale measurements are a particular challenge at the femtosecond scale, but this is where chemistry happens and therefore we devote much of our effort to this range. Simple- "pump-probe" spectroscopy at visible and infrared wavelengths must be extended to the soft and hard x-ray range, and to new sources such as FELs.

- **Light conversion chemistry.** Light from the sun is the primary source of energy on earth, and so we are exploring its conversion to electron motion and then to chemical bonds. Some molecules are particularly adept at this conversion and we would like to understand how they work. For example, we are especially interested in the process of photocatalysis within coordination complexes and similar materials.

Energy conversion is initiated by charge separation, and we know that the charge distribution of the electron and hole, as well as the presence of low energy ligand field excited states greatly influence the lifetime of optically generated charge transfer excited states. Still, the detailed mechanism for the excited state quenching remains unclear. New methods of linear and nonlinear spectroscopy, and especially x-ray spectroscopy involving short-pulse FEL's, can help provide the answer.

An equally important problem is the protection of some chemical bonds, particularly in biology, from destruction in the presence of ultraviolet sunlight. Photoprotection is also an ultrafast process involving charge transfer, and so these new techniques such as ultrafast x-ray absorption and Auger emission can show how critical bonds are protected.

The incorporation of theory within this program is critical for rapid progress in light conversion chemistry. The theory group helps us to focus our efforts in areas of greatest impact.

• **The eV scale in time, space, and field strength.** This is the fundamental scale that determines structure and dynamics of electrons in molecules, and motivates advances in sub-femtosecond time-resolution and Angstrom spatial resolution in theory and experiments. To achieve an adequate view of the molecular realm with at this level, we must interrogate atoms with fields comparable to Coulomb binding fields, and on time scales set by the electronic energy splittings in atoms.

One method to reach this scale is through high harmonic generation. We plan to extend our use of this technique to higher energies and with greater control over the target molecule, to interrogate the detailed motion of the electrons. We are particularly interested in coupled motion of multiple electrons, that goes beyond the “single active electron” approximation that has dominated thinking about strong field laser-atom physics. New theoretical approaches are also required for this, and we are tackling these as well.

LCLS is a source which is also capable of sub-femtosecond or few femtosecond pulses, and these have the unique property of wavelengths short enough to reach the most deeply bound electrons in first and second row atoms. Through the use of novel methods such as low bunch charge, double-slotted spoilers, strong laser fields, and novel data sorting methods, as well as future methods such as self-seeding, we will incorporate LCLS fully as a tool for sub-femtosecond spectroscopy.

Management structure: The research program is managed by the Director of the Chemical Sciences Division, SLAC Photon Sciences Directorate. The current acting Director is Chi-Chang Kao, who also serves currently as the Photon Science Directorate’s acting Associate Laboratory Director.

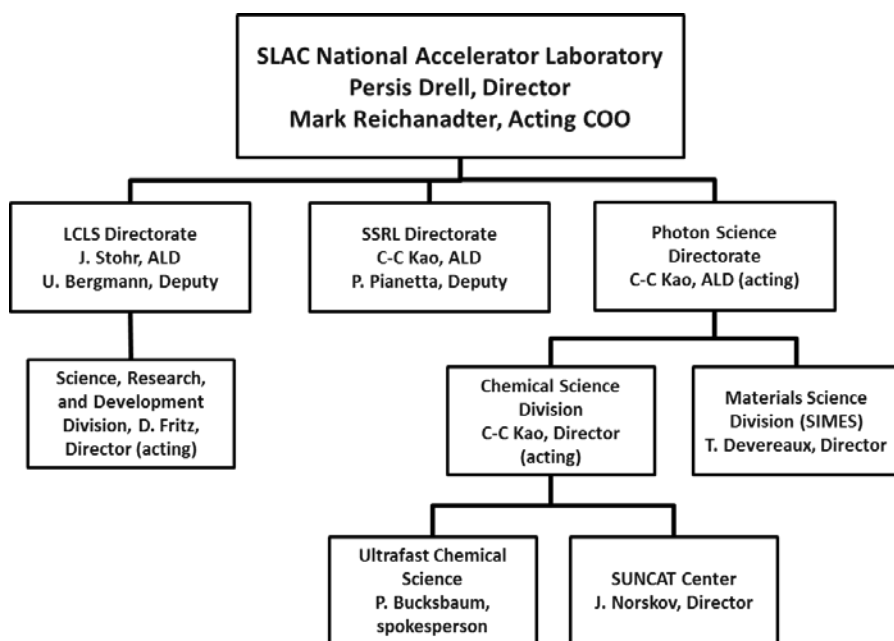


Figure 1: Partial organization chart for SLAC, showing the relation of the Ultrafast Chemical Science Program to other units with close research ties.

The Ultrafast Chemical Science program is the primary source of research funds and SLAC salary for six Principal Investigators, who are responsible for proposing and carrying out this science:

- Professor Philip Bucksbaum, AMO Physics, Program Spokesperson;
- Associate Professor David Reis, Nonlinear x-ray science, Deputy Spokesperson;
- Assistant Professor Kelly Gaffney, Physical Chemistry;
- Professor Todd Martinez, theory;
- Research Scientist Dr. Mike Bogan, biochemistry;
- Senior Research Scientist Dr. Markus Guehr, AMO science.

Four of our six PIs perform all of their SLAC effort in this program. Dr. Guehr splits his effort with his Early Career FWP, which is also managed within the Chemical Sciences Division. Prof. Reis splits his SLAC effort with a SIMES program, located in the Directorate's Materials Science Division. (His total SLAC effort is three-quarters time because of his one-quarter calendar year appointment with Stanford).

Subtasks: These six key personnel are responsible for six subtasks, which represent six different areas of expertise:

1. UTS: Ultrafast Theory and Simulation (Martinez)
2. ATO: Attoscience (Bucksbaum, Guehr)
3. SPC: Ultrafast Chemistry (Gaffney)
4. NPI: Non-periodic X-ray Imaging (Bogan)
5. SFA: Strong Field AMO Physics (Bucksbaum)
6. NLX: Strong Field and Nonlinear X-ray Optical Science (Reis)

The broad backgrounds of our PIs provide needed synergy for effective collaborations in cross-disciplinary projects.

Support operations (finance, HR, safety, purchasing, travel) are directed by the Photon Science Associate Laboratory Director and the Chemical Sciences Director and their staff. They provide oversight and delegate the work to appropriate offices in the SLAC Operations Directorate or to the staff of the Stanford PULSE Institute.

Connections to other units within the SLAC organizational structure: Close collaborations are maintained with the Science R&D Division within the LCLS Directorate; the Materials Science Division (SIMES) within the Photon Science Directorate; SSRL; and the SUNCAT Center within our own Chemical Sciences Division, as shown in figure 1. Our colocation with these facilities and research organizations at SLAC greatly aids collaboration.

Other important connections: The PIs have many separate affiliations with other Stanford University research and academic units: Most especially, all members of this program are members of the Stanford PULSE Institute. In addition, several are affiliated with the SIMES Institute, Bio-X, the Ginzton Laboratory, and the Departments of Chemistry, Physics, and Applied Physics.

We also have collaborative connections to other outside research labs, including DESY, the Lawrence Berkeley Laboratory, the Center for Free Electron Lasers (CFEL) in Hamburg, and BES funded groups at the University of Michigan, the Ohio State University, Western Michigan University, LSU, Northwestern, and the University of Wisconsin Milwaukee.

Knowledge transfer to LCLS: We stress that *LCLS does not grant any preferred status to research proposals from this program, nor for any research program at SLAC!* This is considered an important principle to maintain fairness in the international research community. Nonetheless, the transfer of knowledge to and from LCLS is extremely fluid and critical to our success. Much of our research creates benefits for LCLS by providing new research methods and research results, and in addition there are several more direct transfers of our research product to help LCLS:

- We helped commission the original AMO instrument and continue to assist in commissioning and setup space, particularly for the AMO beam line (AMO), soft x-ray beam line (SXR), the hard x-ray pump probe beam line (XPP), and the coherent x-ray imaging beam line (CXI).
- Some of our graduate students provide user support through the LCLS laser group, and receive salary supplements for this work. This activity was recently endorsed by a "White Hat" review of laser operations at SLAC.
- We have assisted in the development of timing tools currently in use at LCLS.
- Some of our postdocs and students have transferred to permanent staff positions at LCLS.

- We connect LCLS to the Stanford PULSE Institute, since all of our staff are members of PULSE, and LCLS Director Jo Stohr is a member of PULSE as well. PULSE assists LCLS in several direct ways:
 - PULSE has helped LCLS to institute a Graduate Fellowship program, and PULSE manages LCLS graduate student campus appointments.
 - PULSE conducts an annual Ultrafast X-ray Summer School to train students and postdocs about LCLS science opportunities.

Advisory committee. The Ultrafast Chemical Science program receives valuable external advice from the External Advisory Board of the Stanford PULSE Institute. This board of advisors serves the PULSE Institute Director and meets annually. It reports to the PULSE Director and to the Stanford Dean of Research. The reports have also been forwarded to the SLAC Director, the ALD for Photon Science, and to the SLAC Science Policy Committee at their request.

Educational programs and outreach activities. We have an extremely active outreach and visitors program through our affiliation with the Stanford PULSE Institute. PULSE maintains a Stanford-funded visitors program, a website (ultrafast.stanford.edu) as well as an annual Ultrafast X-ray Summer School. This school, which was founded by the PIs of this program in 2006, continues to be a main mechanism for expanding the research community interested in using x-ray free electron lasers for their research. In 2011 we teamed up with CFEL in Hamburg and began to rotate the school between DESY and SLAC in alternate years. The school has received continued strong support from BES, Stanford, and from CFEL. The school will be held at SLAC in 2014 and 2016.



LCLS Director Jo Stohr lectured at the 2012 Ultrafast X-ray Summer School, organized by the PULSE Institute at SLAC in June 2012.

ATO: High harmonic generation and electronic structure

Philip H. Bucksbaum, Markus Gühr

Ultrafast Chemical Science, SLAC National Accelerator Laboratory, Menlo Park, CA 94025

phb@slac.stanford.edu, mguehr@slac.stanford.edu

Scope: The goal of this task is to investigate non-adiabatic molecular processes and electronic dynamics using high harmonic spectroscopy (HHS) as a probe. Having explored aspects of multiple orbital contributions and attosecond dynamics in high harmonics, we are also now investigating the complex harmonic structure of asymmetric top molecules. We will extend this research to monitor electronically excited states in this system that undergo complex electronic-nuclear coupling. Apart from our table top based activities we also have invested a considerable effort into the nucleobase photoprotection experiment at LCLS.

Recent Progress P. H. Bucksbaum, J. P. Farrell, M. Guehr, T. Martinez, B. McFarland, S. Miyabe, L. Spector

Quantified angular contributions for high harmonic emission of molecules in three dimensions (in collaboration with M. Artamonov and T. Seideman, Northwestern University): We quantify the high harmonic dependence on molecular orientation for laser polarizations aligned with each of the three principal axes in sulfur dioxide (SO₂). We do this by using a signal sensitive to all five prolate top revival types and to fractional and multiple revivals [1].

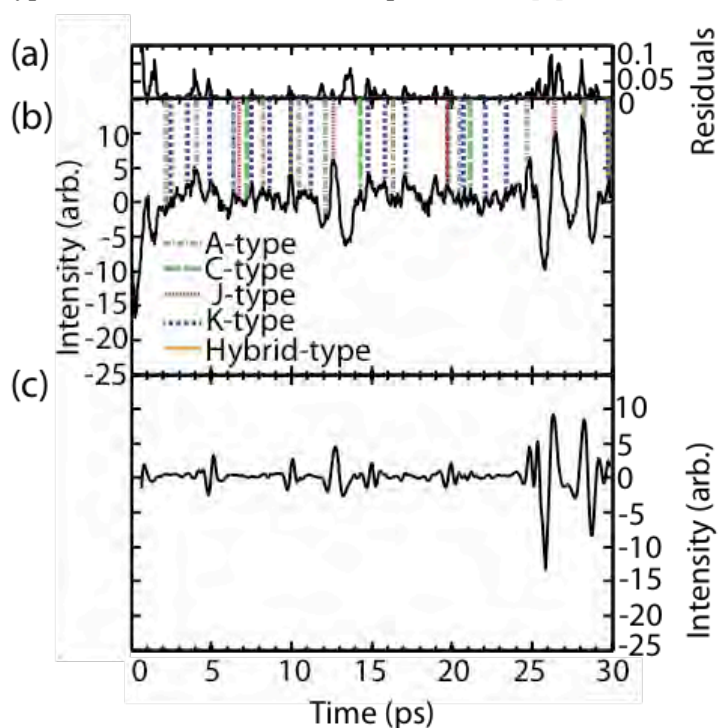


Fig. 1: a) Comparison between experiment and a best-fit theory curve. (a) Residuals between experiment and best-fit theory. (b) Data for high harmonic 19 (29.5 eV) for the first 30 ps following alignment. Harmonic intensity is arbitrary. Several revivals are shown with vertical lines, and identification of these revivals is done in Table I. The high harmonic data is very sensitive to SO₂ revivals, with order up to 1/16 revivals visible. (c) Best-fit theory curve fits all 3 single-axis revival patterns to the data, yielding quantitative information about the angles from which HHG emission originated.

Figure 1(b) shows our data of the 19th harmonic of sulfur dioxide. The revival structure is complex since the molecules shows revivals about all axes. As a near-prolate asymmetric top molecule, SO₂ is expected to exhibit J-type and K-type revivals corresponding to quasi-symmetric-top-like rotations. However, since SO₂ is an asymmetric top, it can also exhibit A-type, C-type and Hybrid-type revivals. Each rotation in the asymmetric top has a unique revival signature. All revival types are identified in the figure with colored vertical lines representing each type of revival. This experiment shows a very high level of sensitivity to rotational revivals. In the pioneering work of Lee et al., SO₂ was aligned along two of its three axes, but alignment was inferred using only the initial alignments with no revivals reported. Each axis of the molecule will exhibit a different revival curve, which depends on the sensitivity of that axis to different types of rotations. Once we have a set of three perpendicular alignment curves, we can

extract the harmonic signal along each of the principal axes of the molecule by combining these to form a best fit to the data. We used a 3-parameter Nelder-Mead procedure to optimize the fit. The result is shown in Fig. 1(c) and the residuals are shown in Fig. 1(a). The coefficients from the fit show the relative amount of high harmonic emission originating from each molecular direction to obtain the single-molecule angular contributions of SO₂ to HHG. We conclude that emission comes primarily from molecules aligned with the polarization along the symmetry (C_{2v}) axis. Our data further indicate that the harmonic emission is suppressed by more than two orders of magnitude at the orientations along the O-O axis, where the polarizability is largest.

We extracted quantitative three-dimensional information about the geometric dependence of HHG in an asymmetric top by exploiting the rich information available in the quantum rotational revivals. We find that HHG is extremely sensitive to molecular alignment and therefore is a powerful probe of molecular geometry. Using HHG, we were able to detect multiple full revivals in SO₂. We have observed rotations about different axes and can identify all possible revival types in our high harmonic spectra and were able to see partial and multiple revivals in the data, as predicted by theory. We see a strong dependence of the recombination dipole on the HHG signal for SO₂. We present a method that uses only a single impulse to extract information about all three axes. This removes the necessity to align a polyatomic molecule along all three dimensions and points the way towards HHG-based tomography in asymmetric tops.

Attosecond dynamics in water (collaboration with M. Negro, Politecnico Milan): We observed nuclear and electronic motion of the water molecule on the attosecond time scale by comparing high harmonic spectra of water (H₂O) and heavy water (D₂O). Both the highest energy occupied orbital (HOMO) and also lower orbitals can participate in HHG. In water, the more deeply bound HOMO-1 ionization launches a wave packet that straightens the bend angle (Fig. ATO1a,b). The ionization from the lone pair HOMO orbital does not launch a motion in the molecule. The efficiency of HHG emission from HOMO-1 is then governed by the spatial overlap of the ionic state nuclear wave packet and the neutral vibrational ground state following recombination. This decreases as the bent molecule straightens out. The loss of overlap is less pronounced for the slower moving heavier isotope, so the harmonic ratio of H₂O and D₂O maps the bond motion. This observation shows how HHG can record rapid motion, and also reinforces growing evidence that HHG from multiple orbitals is not unusual [2,5].

Currently we are working on extending the technique of HHG to different isotopes. The first excited state and the ionic ground state merge in a Renner Teller crossing at 180 deg. bond angle. Eventhough we cannot currently follow the wavepacket for a long enough time, we are working on extending the current observation time window. We use the long trajectories to follow the nuclear dynamics on the excited ionic electronic surface for longer time intervals. Future studies combining longer driver wavelengths with measurements of the long trajectories will allow us to observe the wavepacket at this interesting molecular geometry.

As the name implies, the long electron trajectories sample a longer time interval between ionization and recombination. Upon recombination, the long trajectories will access a more extended molecular nuclear wavefunction leading to a stronger reduction in the harmonic amplitude of the light isotope with respect to the heavier isotope.

Figure 2 shows the D₂O/H₂O harmonics ratio for short and long trajectories (red – with beam profile in bottom image), and exclusively for the long trajectories (blue, with beam profile showing only the long trajectory ring in the top). The red curve is dominated by short trajectory harmonics and confirms our expectations: the low harmonics result from relatively short travel times (therefore small D₂O/H₂O), and ratio increases with the travel time (harmonic number). For the long trajectories we would expect that the highest harmonics coincide with the short trajectory ratio, while the ratio should monotonically increase towards lower harmonics. While this is the case from harmonic 17 to 15, the range between harmonics 19 and 23 does not show this trend. We are currently performing more experiments to understand this trend.

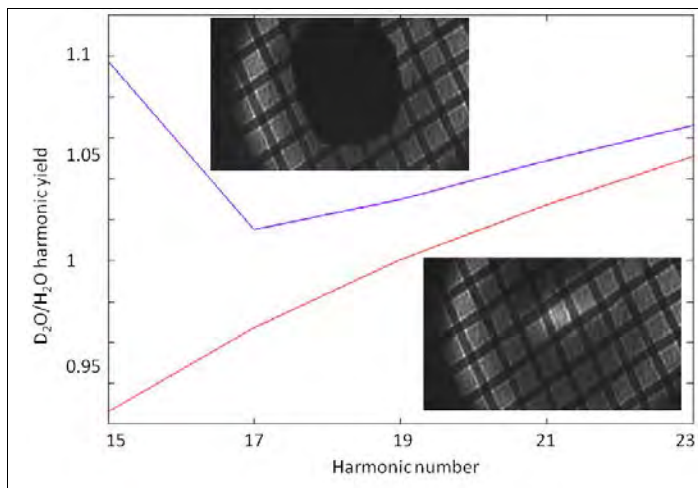


Fig. 2: Ratio of heavy to light water harmonic yield with respect to harmonic number. The inserts show the beam profile with the typical short trajectory maximum in the center of the lower image accompanied by a ring formed by long trajectories (spectrally integrated over all harmonics). The short trajectory harmonics are blocked in the upper image. The red line reflects the ratio of all (long and short) trajectories. It confirms our published results [5]. The blue curve shows the ratio when blocking the short trajectory center.

High repetition rate high harmonic spectroscopy: We have recently installed a fiber laser system for producing high repetition rate vacuum ultraviolet (VUV) laser pulses. The fiber laser produces 100 uJ pulses of 300 fs duration at a repetition rate of 200 kHz. It is tunable up to 2 MHz at lower pulse energies. The pulses from the fiber laser are currently spectrally broadened in gas filled hollow fiber and we aim for subsequently compressing them to below 100 fs. These pulses will be used to generate high harmonics from a gas source to reach photon energies up to ~ 60 eV with a maximal flux of 10^{11} photons per harmonic per second.

A hollow fiber pressure cell has been constructed and the broadened pulses will be characterized within the next few weeks, after which a prism compressor will be constructed to compensate for the group velocity dispersion from the hollow fiber. A high harmonic generator and sample chamber have been commissioned for a previous experiment and will be installed at the fiber laser setup.

Nucleobase photoprotection studies at LCLS: Although nucleobases absorb strongly in the near ultraviolet region transmitted by the Earth's atmosphere, the UV excitation surprisingly does not lead to photoinduced chemistry or damage of the base molecules. Theory and previous experiments indicate that the photoprotection of the nucleobases proceeds via fast (femtoseconds to picoseconds) non-adiabatic transitions. Even for isolated nucleobases the understanding of the non-Born-Oppenheimer approximation (non-BOA) dynamics is currently controversial. Theory and previous experiments indicate that the photoprotection of the nucleobases proceeds via fast (femtoseconds to picoseconds) non-adiabatic transitions, but understanding of the energy transfer mechanisms and the detailed relaxation pathways is currently a matter of debate. In particular it is not understood if the relaxation occurs through a reaction barrier. For thymine, models assuming the barrier predict a non-adiabatic transition to the optically dark n^* state within a few picoseconds after photoexcitation whereas the models without barrier predict ~ 100 femtoseconds for this process. We proposed to directly determine the transient electronic occupation during photoprotection by a UV-pump – LCLS probe experiment on thymine. The UV light starts the photoprotection mechanism, whereas the soft x-ray LCLS pulse leads to photo- and Auger electrons. Auger electrons emitted from the oxygen atoms in the photoexcited base sensitively display the n^* state occupation. Measuring the time constants of the Auger channel associated with the n^* state will therefore allow a direct experimental statement about the reaction barrier in the photoprotection pathway.

We have combined LCLS and ALS measurements to determine the relaxation path and time scale in UV-excited Thymine. A UV pulse excited the molecule, a time delayed soft x-ray pulse generates Auger electrons which reflect the changing electronic structure as the molecule undergoes non-Born Oppenheimer dynamics. The transient Auger data are still under analysis, but clearly show electron dynamics with 100 fsec decay constant. M. Guehr was the spokesperson and leader of this experiment, which is a large collaboration between SLAC photon science, LCLS, Western Michigan and other international institutions.

Future Progress

In the next three years we will advance our knowledge of ultrafast multielectron phenomena in small molecules, and take this knowledge of attoscience to the LCLS. Three specific projects are proposed within the ATO subtask. All use the expertise and infrastructure that we have already developed to explore new science.

1. Excited state transient dynamics in small molecules probed by HHG that examine physics beyond the Born-Oppenheimer (BO) approximation.
2. Coherent multielectron effects in atoms and small molecules that go beyond the Single Active Electron (SAE) approximation
3. Dynamics initiated by femtosecond or sub-femtosecond x-rays at LCLS

High rep. rate VUV spectroscopy: The VUV pulses will be used for photoelectron spectroscopy of gas phase and we plan to start collaborations with colleagues in condensed phase systems. A high repetition rate VUV source is desirable for photoelectron spectroscopy to limit space charge effects and for measurements of coincidences and correlation effects.

High harmonic spectroscopy – SO₂: In conjunction with alignment, we expect that the electronically excited state harmonic spectroscopy will deliver details on the non-Born Oppenheimer dynamics.

High harmonic spectroscopy – water: We will align water and single out the harmonic emission amplitude and also the phase of the HOMO-1 channel. We will use the above threshold ionization yield of water, a non-phase matched signal, as a possible probe of attosecond nuclear and electronic dynamics.

Nucleobase photoprotection studies at LCLS: The nucleobase collaboration has put forward a follow up proposal and the ATO task will actively support all future activities. Furthermore, we plan to import the electron recombination science of harmonic generation to LCLS by use of infrared – x-ray nonlinear mixing.

Publications over the past 3 years

1. L. S. Spector, M. Artamonov, *et al.*, Quantified angular contributions for high harmonic emission of molecules in three dimensions, arXiv, arXiv:1207.2517v1 (2012)
2. M. Gühr, Getting molecular electrons into motion, *Science* **335**, 1314 (2012)
3. V. S. Petrovic, M. Siano, *et al.*, Transient X-Ray Fragmentation: Probing a Prototypical Photoinduced Ring Opening, *Phys. Rev. Lett.* **108**, 253006 (2012)
4. J. P. Cryan, J. M. Glowonia, *et al.*, Molecular frame Auger electron energy spectrum from N-2, *J. Phys. B* **45**, 055601 (2012)
5. J. P. Farrell, S. Petretti, *et al.*, Strong field ionization to multiple ionic states of water, *Phys. Rev. Lett.* **107**, 083001 (2011)
6. J. P. Farrell, L. S. Spector, B. K. McFarland, *et al.*, Influence of Phase Matching on the Cooper Minimum in Ar High Harmonic Spectra, *Phys. Rev. A*, **83**, 023420 (2011)
7. J. P. Cryan, J. M. Glowonia, *et al.*, Auger electron angular distribution of double core hole states in the molecular reference frame, *Phys. Rev. Lett.*, **105**, 083004 (2010)
8. L. Fang, M. Hoener, *et al.*, Double core hole production in N₂: Beating the Auger clock, *Phys. Rev. Lett.*, **105**, 083005 (2010)
9. J. M. Glowonia, J. Cryan, *et al.*, Time resolved pump-probe experiments at the LCLS, *Optics Express*, **18**, 17620 (2010)
10. M. Hoener, L. Fang, *et al.*, Ultraintense X-Ray Induced Ionization, Dissociation, and Frustrated Absorption in Molecular Nitrogen, *Phys. Rev. Lett.*, **104**, 253002 (2010)
11. J. P. Farrell, L. S. Spector, M. B. Gaarde, B. K. McFarland, P. H. Bucksbaum and M. Gühr, Strongly Dispersive Transient Bragg Grating for High Harmonics, *Optics Letters*, **35**, 2028 (2010)
12. J. P. Farrell, B. K. McFarland, P. H. Bucksbaum, and M. Gühr, Calibration of a high harmonic spectrometer by laser induced plasma emission, *Optics Express* **17**, 15134-15144 (2009)
13. B. K. McFarland, J.P. Farrell, P. H. Bucksbaum and M. Gühr, High harmonic phase of nitrogen, *Phys. Rev. A*, **80**, 033412 (2009)
14. J.P. Farrell, B. K. McFarland, M. Gühr, and P. H. Bucksbaum, Relation of high harmonic spectra to electronic structure in N₂, *Chem. Phys.*, **366**, 15-21 (2009)

NLX: Ultrafast X-ray Optical Science and Strong Field Control

David A. Reis, Shambhu Ghimire

*Ultrafast Chemical Science, SLAC National Accelerator Laboratory, Menlo Park, CA 94025
dries@slac.stanford.edu*

Program Scope:

The goal of this subtask in the Ultrafast Chemical Sciences FWP at SLAC is to understand and control the fundamental processes that occur during the interaction of ultrafast and ultra-strong electromagnetic fields with matter, in these two important extreme and relatively unexplored regions of the electromagnetic spectrum. We are particularly interested in the discovery and development of fundamental ultrafast optical, coherent and nonlinear phenomena in the x-ray regime and investigation of the attosecond electronic response in dense optical media and its scaling with wavelength from THz to x-ray. We are focused on two major areas: (1) long-wavelength strong-field interactions in periodic media, including a detailed comparison of both the above and below threshold harmonics in gas and solid phase argon, excited state electronic structure, and the measurement and control of temporal coherence of high-order harmonics and (2) fundamental x-ray nonlinear optics including the measurement of two-photon inner-shell absorption cross-sections and non-resonant third harmonic generation that is expected to show an enhanced nonlinearity due to periodicity.

Progress Report

Under DOE Chemical Sciences support, we explored several fundamental strong-field effects in periodic optical media over the past three years. Notably, we observed the first nonperturbative high-order harmonics in crystals (Ghimire Nat. Phys 2011). The harmonics were generated by a strong mid-infrared laser field that drives coherent Bragg scattering of electrons from the lattice potential. The crystalline HHG differs from nonperiodic atomic and molecular HHG in several key ways, including linear scaling of the cutoff with field, relative insensitivity to elliptical polarization, odd only or odd and even harmonics depending on symmetry. We also predict that the energy of the high harmonic cutoff will be insensitivity to wavelength (Ghimire PRA 2012). The process occurs in a regime of tunnel ionization where the field competes with the interatomic bonding, and the electron wavepacket becomes increasingly localized. Here we have also shown that the electronic properties are altered dramatically but only transiently in the presence of the field—as evidenced by strong photon assisted tunneling of near band gap light (Ghimire PRL, 2011)—all with no permanent damage. This has implications for both understanding the high-field electronic structure of solids and the possibility of extending the cutoff and efficiency of high harmonics.

We also collaborated on many of the first experiments on LCLS including the creation of hollow atoms (Young Nature, 2010), inner shell Rabi flopping and the discovery of hidden resonances (Kanter PRL 2011) as well as the first observation of coherent two-photon inner shell absorption (Doumy PRL 2011) as well as collaborated on several LCLS experiments on the SFA subtask described elsewhere in the SLAC Ultrafast Chemical Science Abstract.

The next three years: In a recent Continuation, we proposed to further develop our understanding and ability to control the strong-field interactions with optical media. The proposal is divided into two areas: (1) long-wavelength strong-field interactions in periodic media,

including a detailed comparison of both the above and below threshold harmonics in gas and solid phase argon, excited state electronic structure, and the measurement and control of temporal coherence of high-order harmonics and (2) fundamental x-ray nonlinear optics including the measurement of two-photon inner-shell absorption cross-sections and non-resonant third harmonic generation that is expected to show an enhanced nonlinearity due to periodicity.

First or lead author publications and reports supported by NLX subtask

- [1] S. Ghimire, A. D. DiChiara, E. Sistrunk, P. Agostini, L. F. DiMauro, and D. A. Reis. Observation of high-order harmonic generation in a bulk crystal. *Nature Physics*, 7(2):138–141, 2011.
- [2] S. Ghimire, A. D. DiChiara, E. Sistrunk, L. F. DiMauro, P. Agostini, and D. A. Reis. High-harmonic generation in strongly driven bulk periodic solid. In *Lasers and Electro-Optics (CLEO) and Quantum Electronics and Laser Science Conference (QELS), 2010 Conference on*, pages 1–2, May 2010.
- [3] S. Ghimire, A. D. DiChiara, E. Sistrunk, G. Ndabashimiye, U. B. Szafruga, A. Mohammad, P. Agostini, L. F. DiMauro, and D. A. Reis. Generation and propagation of high-order harmonics in crystals. *Physical Review A*, 85:043836, 2012.
- [4] S. Ghimire, A. D. DiChiara, E. Sistrunk, U. B. Szafruga, P. Agostini, L. F. DiMauro, and D. A. Reis. Redshift in the optical absorption of ZnO single crystals in the presence of an intense midinfrared laser field. *Physical Review Letters*, 107:167407, 2011.
- [5] S. Ghimire, G. Ndabashimiye, and D. A. Reis. High-order harmonic generation in solid argon. In *CLEO: QELS-Fundamental Science*, page QW1F.1. Optical Society of America, 2012.
- [6] S. Ghimire, D. Reis, A. DiChiara, E. Sistrunk, L. F. DiMauro, and P. Agostini. Strong-field induced optical absorption in zno crystal. In *Quantum Electronics and Laser Science Conference*, page QMF6. Optical Society of America, 2011.
- [7] D. Reis. Strong-field nonperturbative effects in solids. In *42nd Annual Meeting of the APS Division of Atomic, Molecular and Optical Physics*, volume 56, page T4.00001, 2012.

Contributing author publications and reports supported by the NLX subtask:

- [1] J. P. Cryan, J. M. Glowonia, J. Andreasson, A. Belkacem, N. Berrah, C. I. Blaga, C. Bostedt, J. Bozek, C. Buth, L. F. DiMauro, L. Fang, O. Gessner, M. Guehr, J. Hajdu, M. P. Hertlein, M. Hoener, O. Kornilov, J. P. Marangos, A. M. March, B. K. McFarland, H. Merdji, V. S. Petrović, C. Raman, D. Ray, D. Reis, F. Tarantelli, M. Trigo, J. L. White, W. White, L. Young, P. H. Bucksbaum, and R. N. Coffee. Auger electron angular distribution of double core-hole states in the molecular reference frame. *Phys. Rev. Lett.*, 105(8):083004, 2010.
- [2] J. P. Cryan, J. M. Glowonia, J. Andreasson, A. Belkacem, N. Berrah, C. I. Blaga, C. Bostedt, J. Bozek, N. A. Cherepkov, L. F. DiMauro, L. Fang, O. Gessner, M. Gühr, J. Hajdu, M. P. Hertlein, M. Hoener, O. Kornilov, J. P. Marangos, A. M. March, B. K. McFarland, H. Merdji, M. Messerschmidt, V. S. Petrović, C. Raman, D. Ray, D. A. Reis, S. K. Semenov, M. Trigo, J. L. White, W. White, L. Young, P. H. Bucksbaum, and R. N. Coffee. Molecular frame auger electron energy spectrum from n 2. *Journal of Physics B: Atomic, Molecular and Optical Physics*, 45(5):055601, 2012.
- [3] D. Daranciang, J. Goodfellow, M. Fuchs, H. Wen, S. Ghimire, D. A. Reis, H. Loos, A. S. Fisher, and A. M. Lindenberg. Single-cycle terahertz pulses with $>0.2\text{V}/\text{\AA}$ field amplitudes via coherent transition radiation. *Appl. Phys. Lett.*, 99(14):141117, 2011.
- [4] D. Daranciang, J. Goodfellow, S. Ghimire, H. Loos, D. Reis, A. S. Fisher, and A. M. Lindenberg. Generation of $>100\text{ fJ}$ Broadband THz Transients with $>10\text{ MV/cm}$ Fields via Coherent Transition Radiation at the Linac Coherent Light Source. In *CLEO:2011 - Laser Applications to Photonic Applications*, page CMW7. Optical Society of America, 2011.

- [5] A. DiChiara, S. Ghimire, C. Blaga, E. Sistrunk, E. Power, A. March, T. Miller, D. Reis, P. Agostini, and L. DiMauro. Scaling of high-order harmonic generation in the long wavelength limit of a strong laser field. *Selected Topics in Quantum Electronics, IEEE Journal of*, PP(99), 2011.
- [6] G. Doumy, C. Roedig, S.-K. Son, C. I. Blaga, A. D. DiChiara, R. Santra, N. Berrah, C. Bostedt, J. D. Bozek, P. H. Bucksbaum, J. P. Cryan, L. Fang, S. Ghimire, J. M. Glowonia, M. Hoener, E. P. Kanter, B. Krässig, M. Kuebel, M. Messerschmidt, G. G. Paulus, D. A. Reis, N. Rohringer, L. Young, P. Agostini, and L. F. DiMauro. Nonlinear atomic response to intense ultrashort x rays. *Phys. Rev. Lett.*, 106(8):083002, 2011.
- [7] G. Doumy, S.-K. Son, C. Roedig, C. I. Blaga, A. D. DiChiara, R. Santra, C. Bostedt, J. Bozek, P. Bucksbaum, J. Cryan, J. M. Glowonia, S. Ghimire, L. Fang, M. Hoener, N. Berrah, E. Kanter, B. Krässig, D. Reis, N. Rohringer, L. Young, P. Agostini, and L. DiMauro. Nonlinear atomic response to intense, ultrashort x rays. In *42nd Annual Meeting of the APS Division of Atomic, Molecular and Optical Physics*, volume 56, page L1.00060, 2011.
- [8] T. E. Glover, D. M. Fritz, M. Cammarata, T. K. Allison, S. Coh, J. M. Feldkamp, H. Lemke, D. Zhu, R. N. Coffee, M. Fuchs, S. Ghimire, J. Chen, S. Schwartz, D. A. Reis, S. E. Harris, and J. B. Hastings. X-ray and optical wave mixing. *Nature (in press)*, 2012.
- [9] J. M. Glowonia, J. Cryan, J. Andreasson, A. Belkacem, N. Berrah, C. I. Blaga, C. Bostedt, J. Bozek, L. F. DiMauro, L. Fang, J. Frisch, O. Gessner, M. Gühr, J. Hajdu, M. P. Hertlein, M. Hoener, G. Huang, O. Kornilov, J. P. Marangos, A. M. March, B. K. McFarland, H. Merdji, V. S. Petrovic, C. Raman, D. Ray, D. A. Reis, M. Trigo, J. L. White, W. White, R. Wilcox, L. Young, R. N. Coffee, and P. H. Bucksbaum. Time-resolved pump-probe experiments at the lcls. *Opt. Express*, 18(17):17620–17630, 2010.
- [10] E. P. Kanter, B. Krässig, Y. Li, A. M. March, P. Ho, N. Rohringer, R. Santra, S. H. Southworth, L. F. DiMauro, G. Doumy, C. A. Roedig, N. Berrah, L. Fang, M. Hoener, P. H. Bucksbaum, S. Ghimire, D. A. Reis, J. D. Bozek, C. Bostedt, M. Messerschmidt, and L. Young. Unveiling and driving hidden resonances with high-fluence, high-intensity x-ray pulses. *Phys. Rev. Lett.*, 107:233001, 2011.
- [11] A. M. March, L. Young, S. H. Southworth, E. P. Kanter, B. Krässig, R. Santra, Y. Li, N. Berrah, M. Hoener, L. Fang, J. P. Cryan, J. M. Glowonia, D. A. Reis, S. Ghimire, P. Bucksbaum, L. DiMauro, G. Doumy, C. Roedig, J. D. Bozek, C. Bostedt, and M. Messerschmidt. Characterization of lcls x-ray pulses using atomic spectroscopy. In *41st Annual Meeting of the APS Division of Atomic, Molecular and Optical Physics*, volume 55, page M1.00104, 2010.
- [12] C. Roedig, G. Doumy, S.-K. Son, C. I. Blaga, A. DiChiara, R. Santra, N. Berrah, C. Bostedt, J. D. Bozek, P. H. Bucksbaum, J. P. Cryan, L. Fang, S. Ghimire, J. M. Glowonia, M. Hoener, E. P. Kanter, B. Krässig, M. Kuebel, M. Messerschmidt, G. Paulus, D. A. Reis, N. Rohringer, L. Young, P. Agostini, and L. DiMauro. Multi photon physics at the lcls. In *Laser Science*, page LThE1. Optical Society of America, 2011.
- [13] L. Young, E. P. Kanter, B. Krässig, Y. Li, A. M. March, S. T. Pratt, R. Santra, S. H. Southworth, N. Rohringer, L. F. DiMauro, G. Doumy, C. A. Roedig, N. Berrah, L. Fang, M. Hoener, P. H. Bucksbaum, J. P. Cryan, S. Ghimire, J. M. Glowonia, D. A. Reis, J. D. Bozek, C. Bostedt, and M. Messerschmidt. Femtosecond electronic response of atoms to ultra-intense x-rays. *Nature*, 466(7302):56–61, 2010.

NPI: Non-Periodic Imaging

Michael J. Bogan

Ultrafast Chemical Science, SLAC National Accelerator Laboratory, Menlo Park, CA 94025

Email: mbogan@slac.stanford.edu

PROGRAM SCOPE The Non-Periodic Imaging task of the Ultrafast Chemical Science FWP is focused on the goal of extending x-ray microscopy to the atomic level and femtosecond timescale. These efforts are paramount to the DOE mission of understanding and controlling matter. Non-periodic structure dominates nature and biology is nature's version of nanotechnology. To master energy and information on the nanoscale and create new technologies with capabilities rivaling those of living things we need revolutionary new approaches to characterizing non-periodic structure. The development of x-ray free electron lasers (FELs) is such a revolutionary driving force.

One of the great scientific opportunities enabled by x-ray FELs is study of matter currently inaccessible to high-resolution structural examination. A prominent goal is the study of inherently non-crystalline biological materials such as cells or biomolecules that are difficult to crystallize. These experiments were key motivators for the development of hard x-ray FELs. We helped pioneer single pulse coherent x-ray diffractive imaging (CXDI), which utilizes the ultrafast and ultrabright x-ray pulses to help overcome current resolution limitations due to x-ray induced damage to the object. The electron density of the object is reconstructed from the scattered intensity data in the coherent diffraction pattern using lensless imaging techniques based on iterative phase retrieval techniques. The principles of CXDI, and solutions to phase retrieval problem in particular, are well established and single-shot diffraction patterns are representative of the original structure before the manifestation of damage.

The Non-periodic imaging program has fully shifted from early demonstration experiments at the FLASH free electron laser facility in Hamburg, where we experimentally verified "diffract and destroy" science and pioneered the experimental XDI methods, to the first hard x-ray FEL XDI experiments at the Linac Coherent Light Source (LCLS) at the SLAC National Accelerator Laboratory. The program's near-term goals include continued analysis of LCLS data collected from 2009-2012, development of new algorithms for interpreting structure from single-shot diffraction patterns, solving time-resolved protein structures at atomic resolution using LCLS serial crystallography, and extension of our studies of dynamics of airborne particulate matter.

RECENT PROGRESS

During the past three years our program has shifted from experiments at the FLASH free electron laser facility in Hamburg to the Linac Coherent Light Source (LCLS) at SLAC. Overall we have demonstrated that ultrafast soft and hard x-ray FELs, combined with coherent lensless imaging offer unprecedented new opportunities to characterize non-periodic structure. From FLASH we reported the first aerosol imaging with an FEL (Bogan 2008; Bogan 2010b) and the first experiment and algorithm to recover 3D structure from snapshots of identical particles in unknown orientations (Bogan 2010a; Loh 2010). We also predicted the power of FELs to uncover structural information from complex non-periodic matter such as soot (Bogan 2010c).

At LCLS we are progressing from analysis of strong scattering periodic objects like protein crystals (Barty 2011; Chapman 2011; Lomb 2011; Aquila 2012; Boutet 2012; Johansson 2012; Kern 2012; Koopmann 2012) to large strong scattering non-periodic objects (soot, viruses) (Martin 2011; Yoon 2011; Loh 2012a; Martin 2012a; Martin 2012b) to smaller and smaller non-periodic objects (small viruses, protein complexes, nanoparticles) (Kassemeyer 2012; Loh 2012b; Starodub 2012). During FY10-12 we led 2 and contributed to 20 other LCLS

experiments. In 2012 we have an additional 5 beamtimes scheduled. We have 14 LCLS-related publications in print, including a Nature paper from a beamtime we led, and 6 more currently under review. A review of all of this collaborative research is beyond the scope of this brief section so selected work led by our group will remain the sole focus.

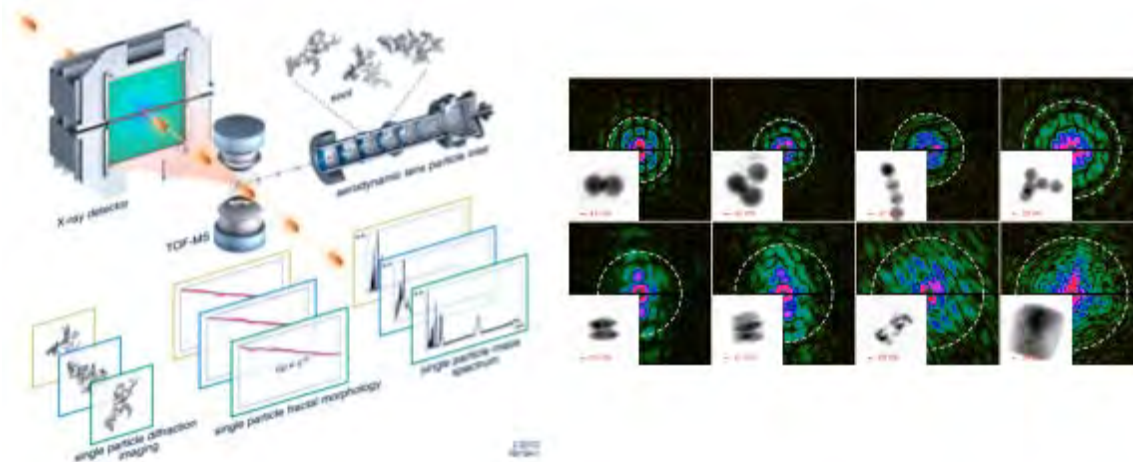


Figure 1: (left) Schematic of our diffractive imaging experiment. 60 Hz X-ray FEL pulses are crossed with a particle stream, producing a diffraction pattern whenever a pulse and particle coincide; the particle explodes and a mass spectrometer captures its ion fragments. (right) Diffraction patterns of evaporative self-assemblies of particles in flight, and reconstructions of their electron densities: (right top) polystyrene spheres of 70 nm and 44 nm radii, (right bottom) ellipsoidal nanoparticles, a spark-generated soot particle, and a salt-soot mixture. Electron density contrast (identical scales) were averaged from ten independent phase retrieval reconstructions, each beginning from a different random contrast. The diameters of the black circles in these insets are scaled to the full-period resolutions (white circles in the diffraction patterns).

We have pioneered the use of x-ray FELs to extract structural information from airborne particulate matter (PM)(Loh 2012a) such as soot, a class of matter never before susceptible to nanoscale microscopy (Fig 1). We found that an unbiased selection of the largest fractals within a controlled preparation had the unmistakable fractal fingerprint, and even determined the range of length scales within each soot particle where this fingerprint was most apparent. We also noticed significant fluctuations in the fractal dimensions of individual soot particles. Our direct observation now raises a number of questions: if these fluctuations exist in soot that were produced in a controlled manner, then what of soot particles produced in messy environments like a car's combustion engine? If the general soot particle inherently has such large fluctuations in fractal dimension, then what is the significance of specifying an average fractal dimension? The importance of PM_{2.5} provides motivation to extend the ability of CXDI to large isolated objects to cover this size range. The current limit is about 500 nm. We have developed a new darkfield imaging approach to extend CXDI to 2 micron objects for the first time(Martin 2012a). We also developed several new algorithms to extract non-periodic structural information from single-shot x-ray diffraction data, including an algorithm to extract fractal dimension from single-shot diffraction patterns(Bogan 2010c; Loh 2012a) and the first use of speckle correlations to solve a structure from identical particles in random orientations (Starodub 2012).

We have helped pioneer serial femtosecond crystallography (SFX). SFX crystallography permits the collection of data at near-physiological temperatures and requires only nanocrystals with small mosaic spread, thus broadening the range of possible complexes and conformational states that can be examined at high resolution. We have invented and received a provisional patent(Bogan 2012) for a new nanoflow micron-sized liquid jet in vacuo for serial femtosecond

crystallography that consumes 60-100 times less sample than existing methods (Fig 6.4.1N) (Sierra 2012). We applied our liquid microjet to SFX of a large membrane protein, Photosystem II (Kern 2012)

FUTURE PLANS Despite the rapid progress made in CXDI, many basic questions remain regarding the optimum acquisition of single-shot diffraction data, in particularly for the assembly of 3D structures, from aerosols, biomolecules, viruses, or clusters. In CXDI experiments at LCLS, hard x-ray pulses reaching peak powers up to 40 GW are focused onto an area that is several micron-squared or smaller. Knowing how a pulse's intensity distribution changes longitudinally would help determine where samples should be injected to maximize its diffraction signal. For holography, characterizing the wavefront shape and its fluctuations is essential to interpreting the collected diffraction data. However, profiling such pulses are challenging because of their high peak intensities and small sizes. Sustained efforts to characterize and shape the focused FEL pulses is necessary because the fine structure of the FEL pulses has measureable impact on the recorded diffraction patterns from randomly positioned samples.

Improvements in the methods for delivery of sample material to x-ray lasers can be made. Nanoflow liquid microjets with sub-micron diameters are necessary to accommodate sample delivery into the submicron x-ray focus now achievable (<300 nm at the LCLS Coherent X-ray Imaging endstation CXI). To best take advantage of the time structure of LCLS pulses to probe dynamic biomolecular structure, improved photoactivation and chemical mixing schemes are necessary for time-resolved diffraction experiments of crystallography and fluctuation scattering.

At the core of non-periodic structural studies with x-ray lasers are the algorithms necessary for simulations of experimental design and for the recovery of structural information. To date, no 3D structure has been published from single shot diffraction patterns of non-crystalline material collected at LCLS. Our recently published demonstration is still the only 3D structure reported from FEL single shots of identical particles in random orientations. A further limitation lies in the size of object amenable to iterative phase retrieval. Overcoming the missing data problem present in CXDI would enable single-shot imaging of objects larger than 500 nm, such as cells or airborne particulate matter. Taking advantage of correlated x-ray scattering for single particle structure remains intensively studied theoretically. The Non-Periodic Imaging team is devoted to tackling these and other unforeseen challenges by developing the basic theoretical and experimental science necessary to open entirely new fields of non-periodic structural study with x-ray lasers.

Our experimental campaign at LCLS continues with hard x-ray XDI experiments at the CXI endstation focusing on time-resolved nanocrystallography with the simultaneous spectroscopy, the structure of water and airborne particulate matter. Data analysis efforts will include new algorithm developments for 3D and 2D structures. We will continue to develop the particle beam generation and diagnostics instrumentation necessary to perform any experiments utilizing laser interactions with single particles.

COLLABORATIONS: This work is done with colleagues from SLAC, Stanford, LLNL, Uppsala, LBNL, Arizona State University, Max Planck Biomedical Heidelberg, CFEL@DESY and others.

Publications and reports in which the NPI task was primary author

Bogan, M. J., et al. (2010a). *Physical Review Special Topics - Accelerators and Beams* **13**: 094791.
Bogan, M. J., et al. (2010b). *Aerosol Science and Technology* **44**(3): 1-6.

Bogan, M. J., D. Starodub, C. Y. Hampton and R. G. Sierra (2010c). *Journal of Physics B: Atomic, Molecular and Optical Physics* **43**: 194013.
 Bogan, M. J. (2011) *MRS Proceedings*, mrss11-1349-dd1307-1305
 Bogan, M. J., R. G. Sierra and H. Laksmono (2012). provisional patent.
 Loh, N. D., et al. (2012a). *SPIE Optics and Photonics Proceedings* **in press**.
 Loh, N. T. D., et al. (2010). *Physical Review Letters* **104**: 225501.
 Loh, N. T. D., et al. (2012b). *Nature* **486**: 513-517.
 Loh, N. T. D., et al. (2012c). *Physical Review Letters*: submitted.
 Sierra, R. G., et al. (2012). *Acta Crystallographica D*: in revision.
 Starodub, D., et al. (2012). *Nature Communications*: in revision.
 Starodub, D., J. C. H. Spence and D. K. Saldin (2011). *Proc. SPIE* **7800**: 78000O78001-78009.

Selected publications and reports in which the NPI task was a major collaborator

Alonso-Mori, R., et al. (2012). *Proceedings of the National Academy of Sciences*: in review.
 Aquila, A., et al. (2012). *Optics Express* **20**(3): 2706-2716.
 Barty, A., et al. (2011). *Nature Photonics* **6**: 35-40.
 Boutet, S., et al. (2012). *Science* **337**, 362-364.
 Chapman, H., et al. (2011). *Nature* **470**: 73-77.
 Davis, C. E., et al. (2010). *IEEE Sensors Journal* **10**(1): 114-122.
 Frank, M., et al. (2011). Rapid Characterization of Microorganisms by Mass Spectrometry. Demirev, American Chemical Society: 161-196.
 Hau-Riege, S. P., et al. (2010). *Physical Review Letters* **104**: 064801.
 Huang, C., et al. (2012). *Nature*: in revision.
 Johansson, L. C., et al. (2012). *Nature Methods* **9**(3): 263-265.
 Kassemeyer, S., et al. (2012). *Optics Express* **20**(4): 4149-4158.
 Kern, J., et al. (2012). *Proceedings of the National Academy of Sciences* **109**(25): 9721-9726.
 Koopmann, R., et al. (2012). *Nature Methods* **9**(3): 259-262.
 Lomb, L., et al. (2011). *Physical Review B* **84**: 214111.
 Martin, A. V., et al. (2011). *Proceedings of SPIE: Advances in x-ray free electron lasers* **8078**(807809).
 Martin, A. V., et al. (2012a). *Optics Express* **20**(12): 13501-13512.
 Martin, A. V et al. (2012b). *Optics Express* **20**(15): 16650-16661.
 Pedersoli, E., et al. (2011). *Review of Scientific Instruments* **82**(4): 043711.
 Saldin, D. K., et al. (2011). *Physical Review Letters* **106**: 115501.
 Saldin, D. K., et al. (2010a). *New Journal of Physics* **12**: 035014.
 Saldin, D. K., et al. (2010b). *Acta Crystallographica Section A* **66**(1): 32-37.
 Seibert, M. M., et al. (2010). *Journal of Physics B: Atomic, Molecular and Optical Physics* **43**(19): 194015.
 Seibert, M. M., et al. (2011). *Nature* **470**: 78-81.
 Yoon, C. H., et al. (2011). *Optics Express* **19**(17): 16542-16549.

SFA: Strong-field laser mater interactions

P. Bucksbaum, A. Natan
Ultrafast Chemical Science Program
SLAC National Accelerator Laboratory, Menlo Park, CA 94025
Email: phb@slac.stanford.edu

Program Scope: The core issue under investigation in SFA is *the nature of the short wavelength strong field interaction with bound and free electrons*. We explore the fs regime of bound electron dynamics in strongly driven molecules. We study both *core-hole wavepacket dynamics (1-10 fs)* and *driven electron intramolecular dynamics (20-250 fs)* in molecules, utilizing intense laser and x-ray fields and momentum and energy resolved multidimensional detection. Key questions concern the interplay between correlated electron motion and relaxation, nuclear motion, and photabsorption when molecules are subjected to strong infrared, optical or x-ray fields. These are critical issues for strong-field imaging, molecular dynamics, and light source development.

Recent Progress: We have made key contributions to the science and methods used to align molecules so that LCLS angle-resolved spectroscopy can take place in the body-fixed frame of the system. We have also co-lead with LCLS research scientists several LCLS experiments including the first ultrafast pump-probe spectroscopy, first multiple core hole Auger spectroscopy, and the first x-ray-pump, x-ray probe experiments, which commissioned use of the LCLS double-slotted spoiler. We trained two of the first Ph.D.s (James Cryan and Mike Glowonia) on LCLS science.

Quantum control for molecular alignment: A key quantum control technology for investigations using ultrafast light sources is rotational alignment. Transient stimulated impulsive Raman scattering is a popular alignment method utilizing intense coherent ultrafast laser pulses to produce coherent rotational wave packets, which bring the molecule into transient alignment periodically. Impulsive alignment must avoid fields high enough to induce strong field ionization instead of rotational Raman excitation. We have developed a gentler multi-pulse method based on quantum control to achieve a high level of laser-induced transient alignment, even in room temperature and high density diatomic molecules. Our measurements have shown that very high degrees of alignment are possible without ionizing the gas. Under some conditions it is even possible to produce high degrees of non-transient “permanent” field free alignment in this way, because transient Raman scattering can produce high J , low m_J populations. This opens the possibility for field free aligned molecular ensembles at ultrafast laser sources like LCLS.

Strong field quantum control of adiabatic alignment Adiabatic control of the orientational degrees of freedom of molecules has been used in the past for simple alignment tasks. We have begun to explore adiabatic control protocols that can place molecules in more complicated coherent states that do more. One example is the “molecular stopwatch” (1) a strong-field induced non-dispersing rotating ensemble of molecules with a well-defined rotational speed, established through a process of rapid adiabatic passage.

Ultrafast x-ray physics: Our first time-resolved x-ray/optical pump-probe experiments at LCLS used a combination of feedback methods and post-analysis binning techniques to synchronize an ultrafast optical laser to the linac-based x-ray laser. The strong-field dissociation of x-ray generated quasi-bound molecular dications was used to establish the residual timing jitter. This analysis shows that the relative arrival time of the Ti:Sapphire laser and the x-ray pulses had a distribution with a standard deviation of approximately 120 fs. The largest contribution to the jitter noise spectrum was the locking of the laser oscillator to the reference RF of the accelerator, which suggests that simple technical improvements could reduce the jitter to better than 50 fs (2). Later we helped to commission two different timing tool techniques based on ultrafast changes in the optical properties of x-ray-irradiated insulators (3, 4).

Strong field x-ray physics: LCLS can deliver 2×10^{11} photons in a 5 fs pulse, with a focus capable of producing to produce double core vacancies through rapid sequential ionization. This enables double core vacancy Auger electron spectroscopy, an entirely new way to study femtosecond chemical dynamics with Auger electrons that probe the local valence structure of molecules near a specific atomic core. Using 1.1 keV photons for sequential x-ray ionization of impulsively aligned molecular nitrogen, we observed a rich single-site double core vacancy Auger electron spectrum near 413 eV, in good agreement with ab initio calculations, and we measured the corresponding Auger electron angle dependence in the molecular frame (5).

We also performed the first angle-resolved, non-resonant (normal) Auger spectra for impulsively aligned nitrogen molecules. We measured the angular pattern of Auger electron emission following K-shell photoionization by 1.1 keV photons from the LCLS. The competing COLTRIMS method of extracting Auger angular distributions is only effective for states that promptly dissociate, and thereby revealing their orientation post hoc. However, our technique, which uses impulsive molecular alignment to make molecular frame measurements directly in the lab, can collect angular information with equal effectiveness for both promptly dissociating and quasi-bound final states, such as the di-cation states of molecular nitrogen. The capability to resolve Auger emission angular distributions in the molecular frame of reference provides a new tool for spectral assignments in congested Auger electron spectra that takes advantage of the symmetries of the final dication states (6).

Other experiments at LCLS involved femtosecond studies of diatomic molecules under the influence of extremely short x-ray pulses. Here we are looking directly at the competition between Auger relaxation and second ionization in the first 1-10 fs following core ionization. One experiment was performed on ground state oxygen using pairs of femtosecond x-ray pulses with precise and variable temporal spacing. Another involved diatomic oxygen irradiated with a single x-ray pulse of variable duration. Yet another experiment involved exciting nuclear wave packets on excited states in iodine, and then viewing the dynamics with x-ray induced fragmentation. These experiments are still undergoing analysis.

Finally, we have been heavily involved as collaborators with the Young group, the Berrah group, and the DiMauro group in early LCLS experiments. Particularly noteworthy are the early round AMO experiments establishing the physics of hollow atoms (2, 7, 8), multiphoton processes (9), and coherent processes (10).

Future work

We will extend our studies of ultrafast processes to shorter time scales, and to detailed investigations of non-adiabatic processes. Both hardware and analysis improvements are under construction and commissioning.

We have developed and are currently commissioning an electron velocity map imager for strong-field produced (ATI) electrons, to complement our current studies of non-adiabatic ultrafast processes in molecules. Here the idea is that ATI electrons display diffraction interference of systems under the influence of strong laser fields. Both above and below the classical cutoff of $2U_p$, ATI electrons can yield structural information that is similar to high harmonic generation, but with significant advantages. ATI experiments can take place at extremely low densities, and are therefore consistent with experiments in the soft x-ray regime of LCLS in Hutch 1. Also, ATI electrons can be detected with essentially unit efficiency and without any of the masking effects of phase matching that limit HHG to a narrow range of momentum vectors.

Second and complementary to this we will continue to expand our use of *nonlinear effects in pump-probe experiments* in molecules at LCLS, with a goal to achieving single femtosecond resolution.

LCLS is capable of few-femtosecond or even sub-femtosecond pulses, but the SASE process and drifts between the multi-kilometer fel and the optical laser systems in LCLS make jitter noise unavoidable. Full use of the LCLS for femtosecond or attosecond pump-probe experiments is therefore limited by jitter. The state of the art in reducing the inherent residual jitter stands approximately 50 fs, using phenomena such as the ultrafast reflectivity and absorption responses of SiN targets. While these tools are still improving, they cannot yet resolve the intrinsic time structure set by the LCLS coherent spike duration.

We have done previous work on this problem (2, 4, 11) and will continue to help implement several improvements in the next three years. Two of these are directly tied to studies currently underway at LCLS: The double-slotted spoiler and self-seeding for hard x-rays. We are also studying how to implement our molecular stopwatch as a timing tool.

Data sorting. Several important ultrafast x-ray induced processes occur on timescales substantially below pump-probe timing jitter. For example, we would like to trace the evolution of the coherent dynamics excited by fs x-ray photoionization of core vacancies, such as core-hole wavepackets, in the regime before and during Auger decay.

Since LCLS does produce some pulses that are only a few femtoseconds long it might be possible to view femtosecond dynamics by sorting the laser pulses after the experiment, using some sophisticated data analysis. We have developed a number of data sorting techniques and laboratory feedback control methods, including Principal Control analysis, Most Correlated Feature analysis, Learning Feedback analysis and similar methodologies such as Singular Value Decomposition for ultrafast quantum control (12).

Recently we have begun to use Manifold Embedding, in collaboration with the Ourmazd group at the University of Wisconsin – Milwaukee. Preliminary observations show that it is possible to extract high fidelity temporal information on the single femtosecond scale from data collected in short bunch mode at LCLS, despite the presence of jitter greater than 50 fs (FWHM) and noisy pulses due to SASE. Re-analysis of some of the early runs at LCLS from 2009 on nitrogen dissociation suggest that un-mixing methods appear possible in large data sets collected in x-ray-pump, strong-field-probe single-shot detector experiment. We plan to validate and exploit this new capability to overcome both the SASE and jitter constraints at LCLS and achieve full femtosecond resolution.

We can study several linear molecular systems where core-driven dynamics affect dissociation, vibration, and higher order motional modes. Since Auger relaxation in C, N, and O, occur in approximately 5 fs, and fall within a range that should be ideally accessible to this technique. Strong field laser-atom interactions can also be viewed in this way, particularly if the strong field optical period is on the order of 5 fs or longer. Therefore we also plan to study transient processes induced by x-ray ionization followed by strong-field interactions. For example, laser assisted Auger relaxation in molecules will display transient coherent phenomena associated with nuclear and electronic wave packet states that evolve in the interval between the photoelectron emission and Auger emission.

Correlation mapping is another statistical tool which extracts correlated features in multichannel or multidimensional data sets. An example where correlation mapping could be useful to resolve a physics question in an LCLS experiment are the high charge states created in molecules subjected to focused x-rays. Over the past three years the AMO community have established that at LCLS ultraintense x-ray lasers can create high charge states through multiple pathways. The so-called PPAA process leads to a highly charged atom through rapid ionization of both 1s electrons followed by high energy Auger electrons. The PAPA process leads to the same final state through a sequential series of ionization and Auger. The competition between these two channels depends on the Auger lifetime, and has been inferred from data with the same fluence but different pulse

duration. But a more powerful technique would seek to extract this information from multiparticle correlations in the data.

Publications, 2010-2012: The work of the past three years (FY2010-FY2012) have resulted in a number of publications where our group was the primary or sole research team, and therefore the lead authors on the paper: (1, 5, 6, 13-21). In addition, we made collaborative contributions in several research efforts that were led by other groups at PULSE or SLAC or within the BES AMOS program at other laboratories and universities:(2-4, 7-12, 22-29).

1. J. P. Cryan, J. M. Glownia, D. W. Broege, Y. Ma, P. H. Bucksbaum, *Physical Review X* **1**, 011002 (2011).
2. M. Hoener *et al.*, *Physical Review Letters* **104**, 253002 (Jun, 2010).
3. S. Schorb *et al.*, *Applied Physics Letters* **100**, 121107 (Mar, 2012).
4. M. R. Bionta *et al.*, *Optics Express* **19**, 21855 (Oct, 2011).
5. J. P. Cryan *et al.*, *Physical Review Letters* **105**, 083004 (2010).
6. J. P. Cryan *et al.*, *Journal of Physics B: Atomic, Molecular and Optical Physics* **45**, 055601 (2012).
7. L. Young *et al.*, *Nature* **466**, 56 (2010).
8. B. Krässig *et al.*, paper presented at the DAMOP, 2010.
9. G. Doumy *et al.*, *Physical Review Letters* **106**, 083002 (Feb, 2011).
10. E. P. Kanter *et al.*, *Physical Review Letters* **107**, 233001 (2011).
11. M. Beye *et al.*, *Applied Physics Letters* **100**, (Mar, 2012).
12. J. L. White, J. Kim, V. S. Petrovic, P. H. Bucksbaum, *The Journal of Chemical Physics* **136**, 054303 (2012).
13. P. Bucksbaum, paper presented at the DAMOP, 2010.
14. P. H. Bucksbaum, R. Coffee, N. Berrah, in *Advances In Atomic, Molecular, and Optical Physics*, E. Arimondo, P. R. Berman, C. C. Lin, Eds. (Academic Press, 2011), vol. Volume 60, pp. 239-289.
15. J. Cryan, J. Glownia, P. Bucksbaum, R. Coffee, paper presented at the DAMOP, 2010.
16. J. Cryan, J. Glownia, N. A. Cherepkov, P. H. Bucksbaum, R. N. Coffee, paper presented at the DAMOP, Conference Atlanta, GA, 2011.
17. J. Glownia, J. Cryan, P. Bucksbaum, R. Coffee, paper presented at the DAMOP, 2010.
18. J. M. Glownia *et al.*, *Opt. Express* **18**, 17620 (2010).
19. J. M. Glownia *et al.*, paper presented at the CLEO, Conference San Jose, CA, 2012.
20. J. M. Glownia *et al.*, paper presented at the CLEO, 2010.
21. J. P. Cryan *et al.*, paper presented at the CLEO, 2010.
22. G. Doumy *et al.*, paper presented at the DAMOP, 2010.
23. G. Doumy *et al.*, paper presented at the DAMOP, Conference Atlanta, GA, 2011.
24. L. Fang *et al.*, *Physical Review Letters* **105**, 083005 (Aug, 2010).
25. L. Fang *et al.*, paper presented at the CLEO, 2010.
26. A. M. March *et al.*, paper presented at the DAMOP, 2010.
27. J. B. Rosenzweig *et al.*, *Nuclear Instruments and Methods in Physics Research Section A: Accelerators, Spectrometers, Detectors and Associated Equipment* **653**, 98 (2011).
28. C. Buth *et al.*, *The Journal of Chemical Physics* **136**, 214310 (2012).
29. P. Emma *et al.*, *Nat Photonics* **4**, 641 (2010).

SFA: Solution Phase Chemical Dynamics

Kelly Gaffney

*Ultrafast Chemical Science Program, SLAC National Accelerator Laboratory, Menlo Park, CA
email: kgaffney@slac.stanford.edu*

Characterizing and controlling the evolution of the electronic structure and the nuclear configuration during a chemical transformation represents a core objective of the chemical sciences. The direct observation of chemical transformations represents a key experimental approach to understanding chemical reactivity. The unique attributes of the LCLS x-ray laser present new and exciting opportunities for experimental studies of chemical dynamics. For a limited number of molecular systems, ultrafast optical studies have provided a clear characterization of the dynamics during a chemical reaction, but for the majority of chemical systems ultrafast spectroscopy provides an incomplete and often ambiguous account of the reaction mechanism. Distinguishing electronic and nuclear dynamics in optical spectroscopy proves difficult because both directly influence the time evolution of the spectrum. X-ray spectroscopy and scattering provide alternative approaches to characterizing electronic and nuclear structure, with distinct and complementary strengths when compared to optical methods. X-ray scattering far from an absorption edge characterizes the nuclear structure and lacks sensitivity to the valence electronic structure. Hard x-ray emission spectroscopy characterizes the electronic structure with atomic specificity and resolution largely independent of the local nuclear structure. The development of the LCLS, an ultrafast x-ray free electron laser, presents a tremendous opportunity to harness the advantages of x-ray scattering and spectroscopy to investigate chemical dynamics.

Recent Research Highlights

The Solution Phase Chemical Dynamics sub-task has focused on two key research objectives the last three years: electronic excited state dynamics in coordination chemistry (Meyer et al. 2010; Hartsock et al. 2011; Zhang et al. 2012) and hydrogen bond and ligand exchange dynamics in ionic solutions (Park, Odelius and Gaffney 2009; Ji, Odelius and Gaffney 2010; Ji, Park and Gaffney 2010; Park, Ji and Gaffney 2010; Gaffney et al. 2011; Ji and Gaffney 2011; Ji et al. 2011; Ji et al. 2012). We have also pursued a limited number of related seed projects during this time. (Hillyard et al. 2009; Jha et al. 2011; Jha et al. 2012; Zhang et al. 2012). In the next three years we will focus our resources on electronic excited state dynamics in coordination chemistry.

Mechanistic studies of ion recognition and ligand exchange in aqueous ionic solutions: The solvent-ion interaction mediates ion recognition, pairing, and assembly in solution. Gaining a mechanistic understanding of ion recognition and assembly has potential impact on our ability to control nanostructure assembly and understand polyelectrolyte conformational dynamics. We have focused our efforts on the ligand exchange dynamics of Ca^{2+} and Mg^{2+} with thiocyanate (NCS^-) in aqueous solution. Mg^{2+} and Ca^{2+} have similar aqueous chemistry and similar concentrations in natural waters and blood, yet biological systems sustain intracellular Mg^{2+} concentrations orders of magnitude higher than the Ca^{2+} concentrations. The ion recognition mechanism utilized by cells to distinguish Ca^{2+} and Mg^{2+} remains unclear, but the mechanism for ligand exchange into and out of the ion first solvation shell likely plays a key role.

We have used the CN-stretch of thiocyanate (NCS^-) to investigate the mechanism and dynamics of ligand exchange for aqueous Ca^{2+} and Mg^{2+} with 2DIR spectroscopy (Park, Ji and Gaffney 2010; Gaffney et al. 2011). These studies have shown that ligand exchange follows a dissociative exchange mechanism for Mg^{2+} and an associative mechanism for Ca^{2+} . These measurements indicate that the lability of the first solvation shell dictates the ligand exchange mechanism, where a narrow distribution of equilibrium solvation shell structures supports dissociative ligand exchange and a broad distribution of equilibrium structures leads to associative ligand exchange. These mechanistic distinctions could be key to the biological recognition of Mg^{2+} and Ca^{2+} .

Structural dynamics and bond isomerization in photocatalytic coordination compounds: We have utilized femtosecond-resolution optical pump-probe spectroscopy to study the electronic excited state dynamics of bimetallic Ir₂ metal cores held together by four 1,8-diisocyano-menthane (dimen) bridging ligands ([Ir₂(dimen)₄]²⁺) (Hartsock et al. 2011). We complemented these initial optical measurements with ultrafast x-ray scattering studies at the LCLS, with preliminary results shown in Figure 1. The interpretation of these experimental results will be a focal point for our work over the next year.

The [Ir₂(dimen)₄]²⁺ complex has the dual attraction of interesting photo-physical and photo-catalytic properties. The length of the metal-metal bond in the molecular crystal depends sensitively on the steric properties of the alkyl component of the bridge and the nature of the counter ion. For dimen bridging ligands, these molecules can form weak metal-metal bonds with bond lengths as large as 4.5 Å and eclipsed 1,8-diisocyano-menthane ligands. In solution, the electronic absorption spectrum indicates that the Ir(I)₂-dimer forms two bond isomers with Ir-Ir bond lengths of roughly 3.5 Å and 4.5 Å. Upon excitation to the lowest energy electronic excited state, the metal-metal bond length has been proposed to shrink significantly and only result in a single bond conformation since visible excitation promotes an electron from a metal-metal anti-bonding state to a bonding state (Hartsock et al. 2011). These large photo-induced changes in molecular structure make [Ir₂(dimen)₄]²⁺ an ideal molecule for the development of ultrafast x-ray scattering as a probe of excited state dynamics in coordination chemistry.

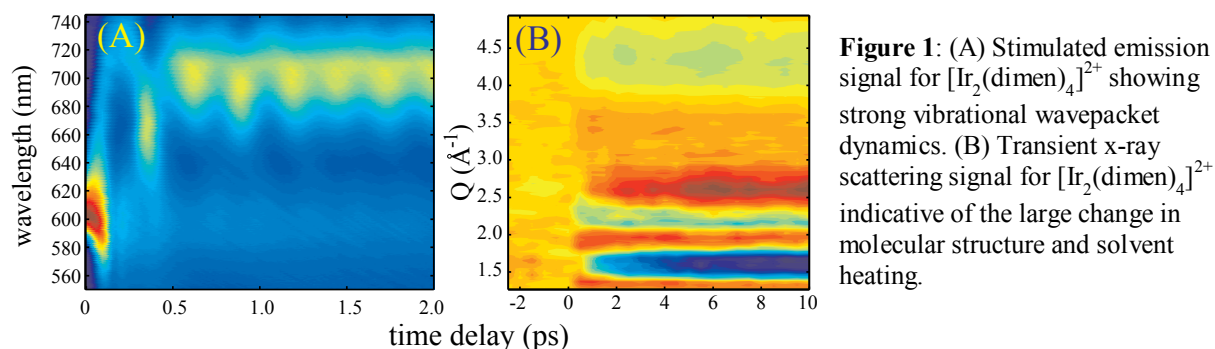


Figure 1: (A) Stimulated emission signal for [Ir₂(dimen)₄]²⁺ showing strong vibrational wavepacket dynamics. (B) Transient x-ray scattering signal for [Ir₂(dimen)₄]²⁺ indicative of the large change in molecular structure and solvent heating.

Solvent mediated electron localization dynamics in charge transfer excited states: Fast and efficient energy migration and charge separation represent essential steps in molecularly based light-harvesting materials. High symmetry and strong intermolecular coupling facilitate fast energy migration, while solvent disorder leads to the symmetry breaking that facilitates charge separation. The interplay of electronic coupling and solvent disorder, both dynamic and static, has a critical impact on the electron mobility in molecular materials. We have investigated the dynamics of electron localization with polarization resolved UV pump mid-IR probe spectroscopy to investigate the dynamics of electron hole localization for excited state ligand-to-metal charge transfer (LMCT) excitation in [Fe(CN)₆]³⁻ (Zhang et al. 2012). Our measurements showed that the initial excited state preserves the octahedral symmetry of the electronic ground state by delocalizing the ligand hole in the LMCT excited state on all six cyanide ligands. This delocalized LMCT excited state decays to a second excited state with two CN-stretch absorption bands. The presence of two CN-stretch absorption bands demonstrates that this secondary excited state has lower symmetry, which we have attributed to localization of the ligand hole on a single cyanide ligand.

Future Research Directions: *Non-adiabatic dynamics of charge transfer excitations in coordination chemistry*

The catalytic properties of coordination compounds derive from the ability of transition metal centers to bind substrates and shuttle electrons to and from the substrate. Numerous transition metal complexes also strongly absorb visible radiation making them targets for the development of photocatalysts. The electron and hole in the excited state can catalyze chemical reactions, but only for the duration of the electronic

excited state. The charge distribution of the electron and hole, as well as the presence of low energy ligand field excited states greatly influence the lifetime of optically generated charge transfer excited states, but the detailed mechanism for the excited state quenching remains unclear in coordination chemistry. The inability of optical spectroscopy to robustly track the charge and spin distribution in coordination complexes limits the effectiveness of ultrafast optical spectroscopy for studying the electron dynamics in coordination complexes. We propose coordinated studies using ultrafast x-ray spectroscopy and scattering to provide a powerful alternative approach capable of measuring these elusive properties and complementing optical spectroscopy studies.

The charge distribution and non-adiabatic interactions between distinct electronic states also influence the electron transfer and catalysis of complexes in their ground electronic state. The presence of nearly degenerate and degenerate electronic states facilitates multiple electron transfers and can be achieved in molecular catalysts with multiple metal centers or redox active ligands. Bond activation requires multiple electron transfers, and non-innocent ligands provide a means of making these multiple electron transfers energetically feasible with earth abundant transition metals, rather than the precious metals traditionally used in catalysis. The catalytic function of such complexes depends critically on the dynamics of the charge distribution. We propose to use soft x-ray resonance Raman scattering to study the charge distribution dynamics of electronic excited states and steady state x-ray spectroscopy and ultrafast vibrational spectroscopy to study the charge distribution dynamics in the electronic ground state.

This experimental program will address two core questions regarding the electronic and nuclear dynamics in coordination chemistry:

How do ligand field excited states influence the relaxation of charge transfer excited states? What nuclear coordinates and geometries lead to intersections and seams between non-adiabatically coupled electronic states?

What is the electron distribution in the ground and excited electronic states of coordination complexes? How does the distribution evolve in response to solvent and nuclear re-arrangement?

These core questions highlight the importance of non-adiabatic nuclear dynamics and correlated electron dynamics in molecular photocatalytic applications.

Publications Supported by AMOS Program

Gaffney, K. J., M. B. Ji, M. Odelius, S. Park, et al. (2011). H-bond switching and ligand exchange dynamics in aqueous ionic solution. *Chem. Phys. Lett.* **504**: 1.

Hartsock, R. W., W. K. Zhang, M. G. Hill, B. Sabat, et al. (2011). Characterizing the Deformational Isomers of Bimetallic Ir-2(dimen)(4)(2+) (dimen=1,8-diisocyno-p-menthane) with Vibrational Wavepacket Dynamics. *J. Phys. Chem. A* **115**: 2920.

Hillyard, P. W., S. Kuchibhatla, T. E. Glover, M. P. Hertlein, et al. (2009). Atomic resolution mapping of the excited-state electronic structure of Cu₂O with time-resolved x-ray absorption spectroscopy. *Phys. Rev. B* **80**: 125210.

Jha, S. K., M. B. Ji, K. J. Gaffney and S. G. Boxer (2011). Direct measurement of the protein response to an electrostatic perturbation that mimics the catalytic cycle in ketosteroid isomerase. *Proc. Nat. Acad. Sci.* **108**: 16612.

Jha, S. K., M. B. Ji, K. J. Gaffney and S. G. Boxer (2012). Site-Specific Measurement of Water Dynamics in the Substrate Pocket of Ketosteroid Isomerase Using Time-Resolved Vibrational Spectroscopy. *J. Phys. Chem. B* **accepted**.

- Ji, M. B. and K. J. Gaffney (2011). Orientational relaxation dynamics in aqueous ionic solution: Polarization-selective two-dimensional infrared study of angular jump-exchange dynamics in aqueous 6M NaClO₄. *J. Chem. Phys.* **134**: 044516.
- Ji, M. B., R. W. Hartsock, Z. Sun and K. J. Gaffney (2011). Interdependence of Conformational and Chemical Reaction Dynamics during Ion Assembly in Polar Solvents. *J. Phys. Chem. B* **115**: 11399.
- Ji, M. B., R. W. Hartsock, Z. Sung and K. J. Gaffney (2012). Influence of solute-solvent coordination on the orientational relaxation of ion assemblies in polar solvents. *J. Chem. Phys.* **136**.
- Ji, M. B., M. Odellius and K. J. Gaffney (2010). Large Angular Jump Mechanism Observed for Hydrogen Bond Exchange in Aqueous Perchlorate Solution. *Science* **328**: 1003.
- Ji, M. B., S. Park and K. J. Gaffney (2010). Dynamics of Ion Assembly in Solution: 2DIR Spectroscopy Study of LiNCS in Benzonitrile. *J. Phys. Chem. Lett.* **1**: 1771.
- Meyer, D. A., X. N. Zhang, U. Bergmann and K. J. Gaffney (2010). Characterization of charge transfer excitations in hexacyanomanganate(III) with Mn K-edge resonant inelastic x-ray scattering. *J. Chem. Phys.* **132**: 134502.
- Park, S., M. B. Ji and K. J. Gaffney (2010). Ligand Exchange Dynamics in Aqueous Solution Studied with 2DIR Spectroscopy. *J. Phys. Chem. B* **114**: 6693.
- Park, S., M. Odellius and K. J. Gaffney (2009). Ultrafast Dynamics of Hydrogen Bond Exchange in Aqueous Ionic Solutions. *J. Phys. Chem. B* **113**: 7825.
- Zhang, W. K., M. B. Ji, Z. Sun and K. J. Gaffney (2012). Dynamics of Solvent-Mediated Electron Localization in Electronically Excited Hexacyanoferrate(III). *J. Amer. Chem. Soc.* **134**: 2581.
- Zhang, W. K., Z. G. Lan, Z. Sun and K. J. Gaffney (2012). Resolving Photo-Induced Twisted Intramolecular Charge Transfer with Vibrational Anisotropy and TDDFT. *J. Phys. Chem. B* **accepted**.

UTS: Ultrafast Theory and Simulation

Todd J. Martínez

Ultrafast Chemical Science Program, SLAC National Accelerator Laboratory, Menlo Park, CA
Email: toddjmartinez@gmail.com

Objective and Scope

The goal of this subtask is to develop and apply the theoretical and computational tools needed to understand energy and charge flow in molecular systems. A first goal in this endeavor is improvement of the efficiency and accuracy of solutions to the electronic structure problem, especially for excited electronic states. We further are developing methods to determine the requisite potential energy surfaces by interpolation and/or direct computation during subsequent simulations of dynamics. These dynamical simulations provide details of the interactions between electrons and moving nuclei including the breakdown of the Born-Oppenheimer approximation (for example due to conical intersections).

Recent Progress

We developed a new method for describing electronic excited states, incorporating a correlation factor that depends explicitly on interelectronic distance in a multiconfigurational wavefunction ansatz.¹ This “geminal-augmented multiconfigurational self-consistent field” or GA-MCSCF approach was shown to describe dynamic and static electron correlation simultaneously and we are currently pursuing extensions to this approach which will allow the treatment of multiple electrons. We have also developed a new method to allow interpolation of potential energy surfaces and nonadiabatic coupling vectors.³ Importantly, this avoids the need for a global diabaticization – as has been shown in the past, such global diabaticization requirements lead to major difficulties when developing a model that incorporates a finite number of electronic states.

We have also begun the development of a method for modeling electron dynamics based on an expansion in traveling Gaussian wavepackets. We showed that the accuracy of such an approach can be considerably improved by including *both* static and dynamic basis functions, i.e. by combining the approaches typically used in quantum chemistry with those typically used for time-dependent wave packet dynamics. We are exploring the extension of this approach to systems with more than two electrons and their application in the context of high harmonic generation spectra.

We have expanded our ability to combine ab initio multiple spawning (AIMS) treatments of nonadiabatic dynamics with photoionization probe pulses. We incorporated a description of the continuum ejected electron, going beyond previous descriptions in terms of Franck-Condon-like matrix elements. This will

allow us to go beyond the prediction of energy-resolved photoelectron ejection intensities to also describe photoelectron angular distributions. We used these new methods to help interpret recent experiments on the ultrafast dynamics of ethylene (a paradigmatic molecule for photoinduced isomerization).^{5,7,8,9} We carried out the first “on the fly” simulations of excited state dynamics using the multireference perturbation theory approach which is able to model both static and dynamic electron correlation effects. This allowed us to incorporate the Rydberg states in the dynamical simulations, resolving a long-standing question about the role of Rydberg states in the dynamics. We found that the Rydberg states were largely “bystanders” and that previous calculations focusing on valence states capture much of the observed dynamics.

Future Plans

Work planned over the next funding period focuses on 1) extending the range of probes that can be modeled in ultrafast experiments, 2) developing methods to describe the detailed attosecond electron and nuclear dynamics in strong fields for high harmonic generation, 3) developing new methods to describe excited state dynamics initiated by complex shaped pulses, and 4) investigating the excited state dynamics of Fe- and Ru-based organometallic complexes which have promising uses in solar energy applications.

Publications (2009-2011):

1. S. A. Varganov and T. J. Martínez, *Variational Geminal Augmented Multireference Self-Consistent Field Theory: Two Electron Systems*, J. Chem. Phys. **132**, 054103 (2010).
2. T. J. Martínez, *Seaming is Believing*, Nature **467**, 412-413 (2010).
3. C. R. Evenhuis and T. J. Martínez, *A Scheme to Interpolate Potential Energy Surfaces and Derivative Coupling Vectors Without Performing a Global Diabatization*, J. Chem. Phys. **135**, 224110 (2011).
4. H. Tao, L. Shen, M. H. Kim, A. G. Suits and T. J. Martínez, *Conformationally Selective Photodissociation Dynamics of Propanal Cation*, J. Chem. Phys. **134**, 054313 (2011).
5. A. L. Thompson and T. J. Martínez, *Time-resolved Photoelectron Spectroscopy from First Principles*, Faraday Disc. **150**, 293-311 (2011).
6. S. Yang and T. J. Martínez, *Ab Initio Multiple Spawning: First Principles Dynamics Around Conical Intersections* in Conical Intersections: Theory, Computation and Experiment, Eds. W. Domcke and H. Koppel, World Scientific, Singapore, 2011.
7. H. Tao, T. K. Allison, T. W. Wright, A. M. Stooke, C. Khurmi, J. van Tilborg, Y. Liu, R. W. Falcone, A. Belkacem and T. J. Martínez, *Ultrafast Internal Conversion in Ethylene. I. The Excited State Lifetime*, J. Chem. Phys. **134**, 244306 (2011).
8. T. K. Allison, H. Tao, W. J. Glover, T. W. Wright, A. M. Stooke, C. Khurmi, J. Van Tilborg, Y. Liu, R. W. Falcone, T. J. Martínez and A. Belkacem, *Ultrafast Internal Conversion in Ethylene. II. Mechanisms and Pathways for Quenching and Hydrogen Elimination*, J. Chem. Phys. **136**, 124317 (2012).

9. T. Mori, W. J. Glover, M. S. Schuurman and T. J. Martínez, *Role of Rydberg States in the Photochemical Dynamics of Ethylene*, J. Phys. Chem. A **116**, 2808-2818 (2012).
10. V. S. Petrovic, M. Siano, J. L. White, N. Berrah, C. Bostedt, J. D. Bozek, D. Broege, M. Chalfin, R. N. Coffee, J. Cryan, L. Fang, J. P. Farrell, L. J. Frasinski, J. M. Glowacka, M. Guehr, M. Hoener, D. M. P. Holland, J. Kim, J. P. Marangos, T. J. Martínez, B. K. McFarland, R. S. Minns, S. Miyabe, S. Schorb, R. J. Sension, L. S. Spector, R. Squibb, H. Tao, J. G. Underwood and P. H. Bucksbaum, *Transient X-Ray Fragmentation: Probing a Prototypical Ring-Opening*, Phys. Rev. Lett. **108**, 253006 (2012).
11. J. Kim, H. Tao, J. L. White, V. S. Petrovic, T. J. Martínez and P. H. Bucksbaum, *Control of 1,3-Cyclohexadiene Photoisomerization Using Light-Induced Conical Intersections*, J. Phys. Chem. A **116**, 2758-2763 (2012).

Understanding Photochemistry using Extreme Ultraviolet and Soft X-ray Time Resolved Spectroscopy

Emily Sistrunk, Jakob Grilj, Markus Gühr, SLAC National Accelerator Laboratory, Menlo Park, CA 94025
mguehr@slac.stanford.edu

Scope of the program

The scientific scope of this early career program is the site specific probing of chemical processes. For this purpose, we use light in the extreme ultraviolet (EUV) and soft x-ray (SXR) spectral range providing the site specificity due to the distinct absorption and emission features of core electrons. We are especially interested in non-Born-Oppenheimer approximation (non-BOA) dynamics, because of its importance for light harvesting [1], atmospheric chemistry [2] and DNA nucleobases photoprotection [3]. We use three different technical approaches for our studies: Laboratory based high harmonic generation (HHG) sources in the range of 20-100 eV delivering pulses with a few femtoseconds duration, synchrotrons with a wide spectral range from the EUV to the high SXR and the Linac Coherent Light Source (LCLS) providing high pulse energy femtoseconds pulses in the soft and hard x-ray range.

Progress in 2011/2012

Setup of new laser lab at SLAC

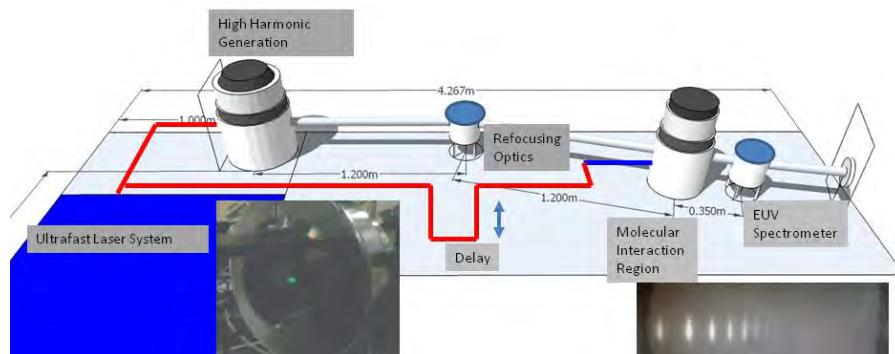


Fig. 1: Setup for site specific probing of chemistry using EUV pulses from HHG. A pump beam excites the molecular target; a delayed EUV probe pulse generated from HHG is refocused on the interaction region and analyzed in the EUV spectrometer. The first EUV light from the high efficiency HHG source is visible in the left insert – a simple phosphor screen without amplification shows the high brightness of the source. The right insert shows the spectrally resolved low harmonics #15-27.

We are currently setting up a new laser laboratory in Room 101, Bldg. 40 of the SLAC campus. This lab will host a setup to observe photochemistry with high spatial resolution and in a site specific way using EUV femtoseconds pulses from a HHG source. We will use pulses in the near ultraviolet range to excite molecular valence electrons which results in a coupled electron-nuclear dynamics. We are especially interested in the non-BOA dynamics and have identified first interesting molecules. In this lab, we are especially interested in compounds containing transition metals.

The 3d transition metal M-edges are located in the EUV spectral region and allow us to probe the metal center view of the valence electron and nuclear dynamics via transient absorption spectroscopy. We start out with simple metal carbonyls. Based on the outcomes and expertise we gain on these molecules, we will be able to extend our studies to larger and more complicated metal containing molecules.

The setup for the experiments is shown in Figure 1. We start with the generation and amplification of infrared pulses in a commercial laser system. The pulses are then split to produce near UV pump light and the EUV probe light via HHG. The EUV continuum between 20-100eV is then imaged by a grazing incidence mirror onto the molecular sample being optically pumped by the near UV pulses. The transmitted EUV light is spectrally analyzed as a function of delay between the UV and EUV pulse.

First light is shown in the inserts in Fig. 1. From simple estimates we expect a flux of 10^{12} - 10^{13} photons/sec within a single harmonic of ~ 300 meV bandwidth with a duration below 20 fs. The flux parameters start to become comparable to third generation synchrotron EUV beamlines, however at ultrashort pulse duration. In addition to the absorption spectroscopy setup we will also construct a time resolved photoelectron apparatus for use with with narrow bandwidth EUV probe pulses (not shown in Fig. 1).

First Experiments

We have performed first experiments for this task using synchrotron and free electron laser light sources. Two very different types of molecules have been in the focus of our studies up to now: the metal carbonyls and nucleobases.

Metal carbonyl non-BOA dynamics

Metal carbonyls show a strong ultraviolet absorption leading to the dissociation of one or more CO ligands, exposing the catalytically active metal center. Although the photoactivation of these molecules is used in organic synthesis [4], the electronic mechanism behind the dissociation is poorly understood. The ultraviolet excitation provides an excitation from the electronic ground state to bound metal to ligand charge transfer (MLCT) states, which in a few femtoseconds undergo non-BOA transitions to dissociating ligand field (LF) states. We want to understand the details of the mechanism and in particular understand if there is any time delay in the dissociation of multiple CO fragments, as debated in the literature (see ref. [5] and references therein). We currently concentrate on iron pentacarbonyl ($\text{Fe}(\text{CO})_5$) and chromium hexacarbonyl ($\text{Cr}(\text{CO})_6$). We have already performed first explorative electron photoemission studies in the range of 40-120 eV at BL 10 of the Advanced Light Source at LBNL and will have more beamtime coming up soon. We have first indications for resonant photoemission and follow this path to possibly gain insight into molecular dynamics under EUV excitation.

Future plans: We will investigate metal carbonyls in the gas phase with time resolved absorption and photoelectron spectroscopy

Nucleobase photoprotection studies Nucleobase photoprotection collaboration [10], Spokesperson M. Gühr

The second class of molecules we are concentrating on are nucleobases, the carrier of genetic information in DNA. Although nucleobases absorb strongly in the near ultraviolet region transmitted by the Earth's atmosphere, the UV excitation surprisingly does not lead to photoinduced chemistry or damage of the base molecules. Theory and previous experiments indicate that the photoprotection of the nucleobases proceeds via fast (femtoseconds to picoseconds) non-adiabatic transitions [3,6]. Even for isolated nucleobases the understanding of the non-Born-Oppenheimer approximation (non-BOA) dynamics is currently controversial. Past experiments rely heavily on simulations to interpret the observed timescales and depending on the level of *ab-initio* approximations, different timescales are predicted.

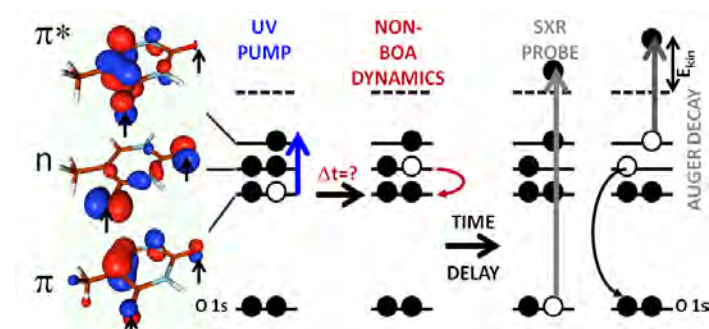


Fig. 2: Valence orbitals of thymine – oxygen marked by arrows. A UV fs pulse excites from the π to a π^* orbital. Non-Born-Oppenheimer dynamics funnels a lone pair electron (n orbital) into the π orbital (leading to the $n\pi^*$ state), the timescale for this process is currently a matter of debate. The x-ray probe pulse ionizes the K shells. We observe Auger electrons from the oxygen K-edge decay (site specific probe). The Auger spectrum with UV excitation contains transient features. Their peak strength and position as a function of delay contains all the information on the photoprotection path.

The UV light excites an electron from the π orbital (see Fig. 2) to the initially unoccupied π^* orbital. This $\pi\pi^*$ (one electron in π one in π^*) state is highly reactive. To avoid photoinduced reactions, non-Born-Oppenheimer dynamics funnels the electronic population down to the ground state on a fast timescale. The first step is a radiationless transition in which the hole in the π orbital is filled by the electron from the n orbital, leading to the $n\pi^*$ state. For thymine, theoretical models predict either a few picoseconds [7] or 100 fs

[8,9] for this process, depending on the *ab-initio* approximations made. Current experiments contain both timescales and an unambiguous interpretation is not possible at the moment.

To shed new light on the photoprotection mechanism, we conducted an experiment at the Linac Coherent Light Source (LCLS) free electron laser to get a more direct insight into the transient valence occupation during photoprotection via element sensitive Auger spectroscopy. Using soft x-ray transitions for probing molecular electronic processes has the advantage of element sensitivity and increased electronic sensitivity to certain valence orbitals.

Independent of our LCLS measurement, we measured the molecular Auger decays at the carbon, nitrogen and oxygen edges of Thymine at BL 8 at the Advanced Light Source at LBNL. We measured rich participant and spectator Auger features and are currently working on an interpretation with F. Tarantelli (Perugia).

Figure 3 shows the experimental Auger spectra of thymine at the carbon, nitrogen and oxygen edges (thick lines). The theoretical values (thin lines) show good agreement and most importantly reveal the decay channels of the Auger process. The oxygen 1s decay is dominated by the n lone pair valence orbital, which is most critically involved in the $\pi\pi^*$ - $n\pi^*$ conical intersection. Thus this oxygen Auger spectra are especially sensitive on thymine's non-BOA dynamics. We have also measured resonant Auger spectra and absorption spectra at all three edges. These results have given the bases for new proposals at LCLS and ALS and are currently prepared for publication.

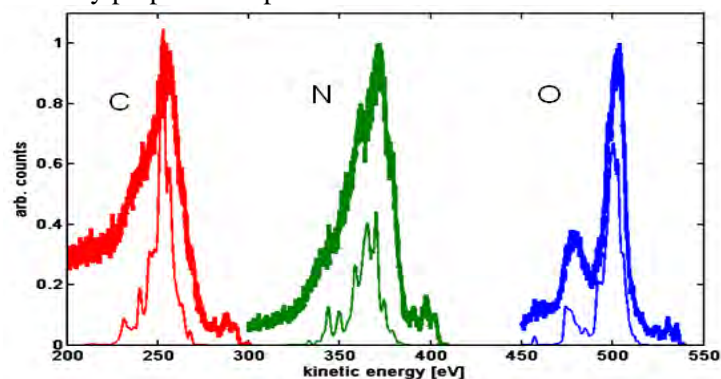


Fig. 3: Auger spectra of isolated thymine excited at the carbon, nitrogen and oxygen edges. The thick lines display the experimental results gained at beamline 8 of the Advanced Light Source at LBNL. The simulations (thin lines) have been done by F. Tarantelli using an algebraic-diagrammatic construction. The simulation exhibits that the oxygen Auger decay is dominated by the lone pair n valence orbital. This warrants for the high sensitivity of Auger spectra on thymine non-BOA dynamics in the excited state. Special acknowledgement: A. Aguilar, W. Yang and D. Hardy, ALS, LBNL.

At the LCLS, we used an ultrashort UV laser pulse to initiate the photoprotection mechanism in thymine (see Fig 2). The soft x-ray pulse from LCLS acted as a probe by generating photo- and Auger electrons. We tuned the LCLS to 565 eV photon energy, which is about 25 eV above the oxygen K edge. Calculations of Auger rates confirmed that Auger electrons emitted from the oxygen atoms in the photoexcited base are very sensitive to the population of the lone pair orbital (n in Fig. 2), which is strongly localized at the oxygen atoms. The jitter between the UV laser pump and SXR probe pulse was measured for every shot via a transient reflection. We then resorted our data according to this jitter leading to relative delay accuracy below 100 fs.

The Auger spectrum of Thymine in its ground state is given in Fig. 4A. The occupied valence states contribute to a broad band around a kinetic energy of 500 eV. Figure 4B shows the effects of UV excitation on a transient Auger spectrum. We plot the difference of Auger spectra with UV on and off normalized on the sum of Auger spectra with UV on and off for each time delay. Depending on spectral region and time delay, we observe either a loss in Auger signal (blue) or newly created signal due to UV irradiation (red). The main Auger band at 500 eV bleaches in its upper half from about 500 eV on. We attribute this to UV induced depopulation of the π orbital, which weakens the main Auger band. Furthermore, we observe a UV induced transient increase in the Auger decay. For early delays around 0-100 fs, new Auger features appear between 505 and 515 eV kinetic energy. At later delays the features shift to the interval between 510 to 520 eV. We measured the Auger spectra for delays up to 20 ps (not shown) and do not observe any more major shifts in the features for times outside the shown scale. We attribute the UV created Auger decay to initially unoccupied orbitals that get filled by the UV pulse. In particular, this channel is due to the excited π^* electrons. We have evidence from resonant Auger spectroscopy at the synchrotron (ALS Berkeley Natl. Lab) that these kinetic energies display the π^* orbital.

Members of our collaboration (S. Miyabe, SLAC and F. Tarantelli, Perugia) are currently working on a more detailed attribution of Auger channels to valence states which will open the chance to shed new light onto the UV photoprotection mechanism. In particular we are simulating the kinetic energy and strength of the Auger decay for the $\pi\pi^*$, $n\pi^*$ and vibrationally hot ground state geometries. While it is too early to draw definite conclusions on the exact electronic dynamics, we can already state that the blue shifted Auger features are reproduced by excited electronic state molecular geometries.

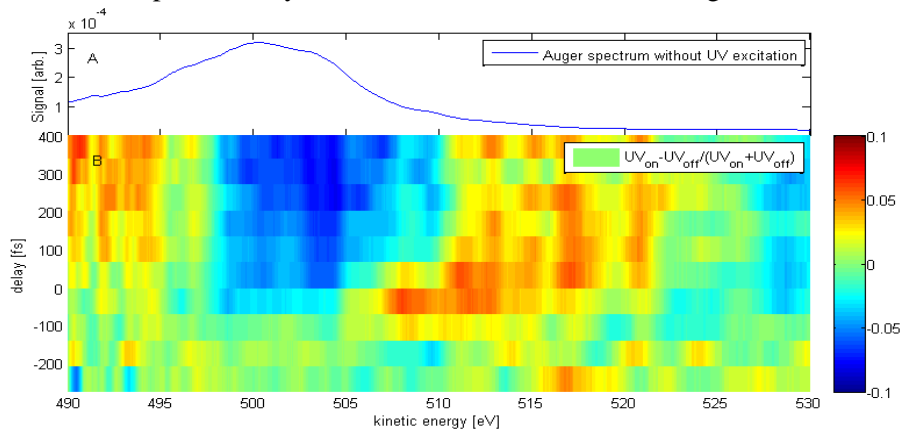


Fig. 4: A) Oxygen Auger spectrum of the electronic ground state of thymine. B) Difference between Auger electron spectra with UV on and Auger electron spectra with UV off divided by the sum. The horizontal axis is electron kinetic energy and the vertical axis is delay between the UV and x-ray pulses. Red color is positive and blue is negative. Data taken at LCLS.

Future plans: We submitted a proposal on time resolved soft x-ray absorption spectroscopy on thymine and uracil that we will lead. We will also participate in time resolved soft x-ray photoelectron studies on uracil.

This work was funded by the Office of Science Early Career Research Program through the Office of Basic Energy Sciences, U.S. Department of Energy. Portions of this research were carried out at the Linac Coherent Light Source (LCLS) at the SLAC National Accelerator Laboratory. LCLS is an Office of Science User Facility operated for the U.S. Department of Energy Office of Science by Stanford University. The Advanced Light Source (ALS) is supported by the Director, Office of Science, Office of Basic Energy Sciences, of the U.S. Department of Energy under Contract No. DE-AC02-05CH11231.

Publications of this task:

- A. B. K. McFarland, J. P. Farrell, N. Berrah, C. Bostedt, J. Bozek, P.H. Bucksbaum, R. N. Coffee, J. Cryan, L. Fang, R. Feifel, K. Gaffney, J. Glowia, T. Martinez, M. Mucke, B. Murphy, S. Miyabe, A. Natan, T. Osipov, V. Petrovic, S. Schorb, Th. Schultz, L. Spector, F. Tarantelli, I. Tenney, S. Wang, W. White, J. White, M. Gühr, Probing Nucleobase Photoprotection with soft x-rays, *Ultrafast Phenomena 2012*, EDP Sciences **submitted**
- B. J. P. Farrell, B. K. McFarland, N. Berrah, C. Bostedt, J. Bozek, P.H. Bucksbaum, R. N. Coffee, J. Cryan, L. Fang, R. Feifel, K. Gaffney, J. Glowia, T. Martinez, M. Mucke, B. Murphy, S. Miyabe, A. Natan, T. Osipov, V. Petrovic, S. Schorb, Th. Schultz, L. Spector, F. Tarantelli, I. Tenney, S. Wang, W. White, J. White, M. Gühr : Ultrafast x-ray probe of nucleobase photoprotection, *CLEO/QELS San Jose, QW1F4* (2012)
- C. M. Gühr, Getting molecular electrons into motion, *Science* **335**, 1314 (2012)

References:

- [1] C. C. Hu, and K. Schulten, *Physics Today* **50**, 28 (1997).
- [2] Dermota T. E., A. P. Hydustry, N. J. Bianco, et al., *J. Phys. Chem. A* **109**, 8259 (2005).
- [3] C. E. Crespo-Hernandes *et al.*, *Chem Rev* **104**, 1977 (2004).
- [4] T. E. Bitterwolf, *J. Organomet. Chem.* **689**, 3939 (2004).
- [5] S. A. Trushin, K. Kosma, W. Fuss, and W. E. Schmid, *Chem. Phys.* **347**, 309 (2008).
- [6] S. Ullrich, T. Schultz, M. Z. Zgierski, A. Stolow, *Phys. Chem. Chem. Phys.* **6**, 2796 (2004).
- [7] H. R. Hudock, B. G. Levine, A. L. Thompson, *et al.*, *J. Phys. Chem. A* **111**, 8500 (2007).
- [8] M. Merchan, R. Gonzalez-Luque, T. Climent, L. Serrano-Andres *et al.*, *J. Phys. Chem. B* **110**, 26471 (2006).
- [9] S. Perun, A. L. Sobolewski, and W. Domcke, *J. Phys. Chem. A* **110**, 13238 (2006).
- [10] LCLS Nucleobase photoprotection collaboration: J. P. Farrell^{1,2}, B. K. McFarland¹, N. Berrah³, C. Bostedt⁴, J. Bozek⁴, P.H. Bucksbaum^{1,2}, R. Coffee⁴, J. Cryan^{1,2}, L. Fang³, R. Feifel⁵, K. Gaffney¹, J. Glowia^{1,2}, T. Martinez^{1,6}, M. Mucke⁵, B. Murphy³, S. Miyabe^{1,6}, A. Natan¹, T. Osipov³, V. Petrovic^{1,2}, S. Schorb⁴, Th. Schultz⁷, L. Spector^{1,2}, F. Tarantelli⁸, I. Tenney^{1,2}, S. Wang^{1,2}, W. White⁴, J. White^{1,2}, M. Gühr¹¹ *PULSE, SLAC National Accelerator Lab, Menlo Park, CA 94025*, ²*Dpts. Physics and Applied Physics, Stanford University, Stanford, CA 94305*, ³*Physics Department, Western Michigan University, Kalamazoo, MI 49008*, ⁴*LCLS, SLAC National Accelerator Lab, Menlo Park, CA 94025*, ⁵*Department of Physics, Uppsala University, Uppsala, Sweden*, ⁶*Department of Chemistry, Stanford University, Stanford, CA 94305*, ⁷*Max-Born-Institut, 12489 Berlin, Germany*, ⁸*Dipartimento di Chimica, Universita di Perugia, and ISTM-CNR, 06123 Perugia, Italy*

University Research Summaries
(by PI)

DOE-SISGR: Coherent Control of Electron Dynamics

Principal Investigator: Andreas Becker

JILA and Department of Physics, University of Colorado at Boulder,
440 UCB, Boulder, CO 80309-0440

andreas.becker@colorado.edu

Introduction

Current advances in laser technology and computing power are allowing us to enter a fundamentally new regime, where the coupled electron-nuclei dynamics in a molecule can be captured and manipulated in real time. In recent years different ultrashort intense laser sources have been developed, which generate pulses over a broad wavelength regime (from the ultraviolet over the optical/near-infrared to the X-ray regime) and as short as a few tens of attoseconds. This opens the perspective to tackle questions how the motions of electrons and nuclei in molecules are coupled with each other during chemical reactions, or how light can be used to control chemical reactions at the level of electrons. We have recently provided a review of the experimental and theoretical progress in the observation and control of electron dynamics on the attosecond time scale [DOE5]. In this project we provide theoretical support for ongoing and future experimental studies to analyze electron dynamics as well as the energy exchange between electronic and nuclear degrees of freedom on the natural time scale of the constituents of atoms and molecule using the whole variety of laser light sources which are now available.

Recent Progress and Future Goals

Our activities in the project can be summarized in the following sub-projects.

A. Time-dependent analysis of few-photon coherent control schemes and application to X-ray laser technology

In recent years we provided a complementary view in the temporal domain on coherent control schemes for certain sets of spectral modulated pulses. Our results for the atomic and the molecular case showed that at intermediate times during the interaction the population in the target state can exceed the final state population and, in particular, is nonzero for so-called dark (or transparent) pulses [DOE1,DOE4]. The temporal analysis provided also new insights into the control of ionization processes via an intermediate excited state. Models based on the single-active-electron approximation for the interaction of atoms and molecules with intense light have been developed.

We plan to apply the single-active-electron models and our experiences in few-photon control schemes to the new regime of keV laser pulse technology [1]. In particular, we want to develop and analyze techniques (involving inner-shell processes) which can be used to observe the so far unknown temporal structure of these keV X-ray pulses.

B. Attosecond laser-driven intramolecular electron dynamics

Ionization of atoms and molecules by a laser field is the doorway state to many phenomena in strong-field science, e.g. the generation of higher-order harmonics and attosecond pulses, molecular dissociation and its control and ultrafast molecular imaging. Widely used ionization pictures and theories make use of quasistatic or cycle-averaged approximations for the interaction of the electrons with the laser electric field [2-4]. In case of molecules the process is therefore usually viewed on the femtosecond time scale of nuclear dynamics. Up to now, little attention has been given to the sub-cycle dynamics of the electron driven by the oscillating laser electric field inside the atom or molecule before or during the ionization process.

In collaboration with the experimental group of Dr. Reinhard Dörner (Frankfurt, Germany) we reexamined the ionization of hydrogen molecular ion by a circularly polarized laser pulse. The experimental observations, in agreement with our results from numerical solutions of the time-dependent Schrödinger equation, showed an electron momentum distribution tilted in the same direction as the rotation of the laser electric field [DOE3]. This is in contrast to the expectations from the standard quasistatic (charge-resonance-enhanced) ionization picture for the hydrogen molecular ion [3,4], which would give rise to a momentum distribution peaked perpendicular to the molecular axis.

Our theoretical analysis of the process showed that the tilted momentum distribution occurs due to delayed emission of the electron wave packet from the ion [DOE3]. The late emission of the electron wave packet is induced by the strong coupling between the ground and first excited state of the molecular ion, as predicted by us previously for linear polarization of the field [5]. This induces a complex electron dynamics in the molecule, which leads to the attosecond time lag and the initial momentum in the electron emission. The ionization process maps these features of the electron dynamics onto the tilt angle and the magnitude of the observed electron momentum distribution.

Although the detailed theoretical analysis has been previously performed for the specific case of the hydrogen molecular ion [6], we expect that the general features of the electron dynamics found for H_2^+ hold for other molecules with pair(s) of quasi-degenerate charge resonant states as well. Indeed, results of numerical simulations for the electron dynamics in linear H_3^{2+} [7] and H_4^{3+} model system, in which the electron dynamics is restricted along the molecular axis, are in qualitative agreement with these expectations.

In view of the recent development of ultrashort (phase stabilized) laser systems over a wide range of wavelengths in the near- and mid-infrared, we plan to systematically analyze the dependence of the phenomenon on the wavelength, carrier-to-envelope phase as well as polarization of the applied laser light. Further goals include studies of the attosecond electron dynamics on the basis of different molecular model systems and single-active-electron models to determine if and how the phenomenon depends on e.g. the structure of the molecule (linear vs. cyclic), the number of states coupled or the symmetry of the pair of states involved.

C. Multiphoton coherent control of vibrational excitation and dissociation of molecules at infrared laser wavelengths

In the report of last year we presented our results and interpretation of a new coherent control scheme of the vibrational state distribution in the (non-polar) hydrogen molecular ion at mid-infrared laser wavelengths. The control mechanism is based on a selective two-photon transition between the (Stark-shifted) vibrational states [DOE2].

In view of the resurgence of strong laser systems at infrared wavelengths we reexamined excitation, dissociation and ionization of the molecular hydrogen ion with unchirped laser pulses over a broad wavelength regime systematically. Our results of numerical simulations supported by model calculations revealed a many order-of-magnitude enhancement of vibrational excitation and dissociation (over ionization) of the molecular ion at infrared wavelengths [8]. For example, at wavelengths of about 12 μm the dissociation probability at infrared wavelengths can be up to 10% and may exceed both the dissociation probability at near-infrared wavelengths as well as the ionization probability at infrared wavelengths by a few *orders* of magnitude. The origin of the enhancement is related to the strong-field two- (and higher-order) photon transitions between different vibrational levels of the molecular ion, which we studied previously in the above mentioned control scheme [DOE2]. Our results show that, in contrast to earlier assumptions [9,10], a strong vibrational excitation of a diatomic molecule leading to its dissociation without ionization at infrared wavelengths appears to be possible without chirping the laser pulse and taking account of the anharmonicity of the molecular vibrations.

D. Numerical simulation and theoretical analysis of time delays in light induced ionization

We started to theoretically investigate the recently observed time delay in ultrashort photoionization of electrons from different subshells of an atom [11]. Previous theoretical analysis typically made use of the concept of the so-called Wigner-Smith time delay, which is however expected to fail in case of a Coulombic problem (i.e., e.g. in the case of the experiment). We use an alternative but more fundamental definition of the time delay, based on the quantum mechanical definition of the time a particle spends in a certain region in space, and applied it to numerical simulations based on test systems in 1D (Yukawa and Coulomb potential). Our preliminary results show, as expected, the inapplicability of the Wigner-Smith time delay concept for photoionization in a Coulomb potential, but also provide new insights into the role and the influence of an external streaking field (as used in the experiment) on the observed time delay. Indeed, we have found that there is a negligible effect of the streaking field on the time delay over a wide range of intensities, which is in qualitative agreement with the experimental observations [11].

In future, we plan to continue our theoretical studies, based on 1D systems, to clarify under which conditions a time delay for a Coulombic system can be theoretically well-defined. We also intend to simulate the streaking process and compare the corresponding measured time delay with the results based on our theory in order to provide further insights into the streaking method itself. Finally, we will extend our

studies to the 3D atomic and the diatomic molecular case as well as to two-photon and multiphoton processes.

Publications of DOE sponsored research

[DOE1] S. Chen, A. Jaroń-Becker, and A. Becker, *Time-dependent analysis of few-photon coherent control schemes*, Physical Review A **82**, 013414 (2010).

[DOE2] A. Picon, J. Biegert, A. Jaroń-Becker, and A. Becker, *Coherent control of the vibrational state population in a nonpolar molecule*, Physical Review A **83**, 023412 (2011).

[DOE3] M. Odenweller, N. Takemoto, A. Vredenburg, K. Cole, K. Pahl, J. Titze, L.Ph.H. Schmidt, T. Jahnke, R. Dörner and A. Becker, *Strong-field electron emission from fixed in space H_2^+* , Physical Review Letters **107**, 143004 (2011).

[DOE4] J. Su, S. Chen, A. Jaroń-Becker and A. Becker, *Temporal analysis of nonresonant two-photon coherent control involving bound and dissociative molecular states*, Physical Review A **84**, 065402 (2011).

[DOE5] A. Becker, F. He, A. Picon, C. Ruiz, N. Takemoto and A. Jaroń-Becker, *Observation and control of electron dynamics in molecules* (invited), in *New trends in Attophysics*, ed. by A. Zair, R. Torres, and L. Plaja (Springer, accepted for publication)

References

- [1] T. Popmintchev et al., Science **91**, 1287 (2012).
- [2] L.V. Keldysh, Zh. Eksp. Teoret. Fiz. **47**, 1945 (1964) [Sov. Phys. JETP **20**, 1307 (1965)]
- [3] T. Zuo and A.D. Bandrauk, Phys. Rev. A **52**, R2511 (1995)
- [4] T. Seideman, M.Yu. Ivanov and P.B. Corkum, Phys. Rev. Lett. **75**, 2819 (1995)
- [5] N. Takemoto and A. Becker, Phys. Rev. Lett. **105**, 203004 (2010)
- [6] N. Takemoto and A. Becker, Phys. Rev. A **84**, 023401 (2011)
- [7] A. Becker, N. Takemoto, A. Picon and A. Jaron-Becker, submitted for publication
- [8] A. Picon, A. Jaron-Becker and A. Becker, submitted for publication
- [9] N. Bloembergen and A.H. Zewail, J. Phys. Chem. **88**, 5459 (1988).
- [10] S. Chelkowski, A.D. Bandrauk, and P.B. Corkum, Phys. Rev. Lett. **65**, 2355 (1990).
- [11] M. Schultze et al., Science **328**, 1658 (2010).

Probing Complexity using the LCLS and the ALS

Nora Berrah

Physics Department, Western Michigan University, Kalamazoo, MI 49008
e-mail:nora.berrah@wmich.edu

Program Scope

The research program objective is to investigate *fundamental interactions between photons and gas-phase systems* to advance our understanding of correlated and many body phenomena. Our research investigations focus on probing multi-electron interactions in order to understand and ultimately control energy transfer processes from electromagnetic radiation. Most of our work is carried out in a strong partnership with theorists.

Our current interests include: 1) The study of non linear and strong field phenomena in the x-ray regime using the linac coherent light source (LCLS), the most powerful ultra-fast x-ray free electron laser (FEL) facility at the SLAC National Laboratory. Our investigations focus on probing physical and chemical processes that happen on ultrafast time scales. This is achieved by examining both electronic and nuclear dynamics subsequent to the interaction of molecules and clusters with LCLS pulses of various intensity and pulse duration. 2) The study of correlated processes in select anions with vuv-soft x-rays from the Advanced Light Source (ALS) at Lawrence Berkeley Laboratory. We present here results completed and in progress this past year and plans for the immediate future.

Recent Progress

1) Double Core-Hole Spectroscopy for Chemical Analysis with an Intense X-Ray Femtosecond Laser.

Theory predicted that double-core hole (DCH) spectroscopy can provide a new powerful means of differentiating between similar chemical systems with a sensitivity not hitherto possible [a,b]. Although double core-hole ionization on a single site (ssDCH) in molecules was recently measured with double and single photon absorption, double core holes with single vacancies on two different sites (tsDCH), allowing unambiguous chemical analysis, had remained elusive. We were able however to report for the first time the direct observation of tsDCH, produced via sequential two-photon absorption, using short, intense x-ray pulses from the Linac Coherent Light Source (LCLS) Free-Electron Laser (FEL) and compare it with theoretical modeling in the case of CO [1]. The observation of DCH states, which exhibit a unique signature, and agreement with theory proved the feasibility of the method [1]. We also carried out experiments on N₂O and CO₂ to compare our previous results in N₂ [19] with N₂O and compare our findings in CO with CO₂ to assess the validity of the method; ie, even though single core hole ionization can not differentiate between CO and CO₂ or between N₂ and N₂O, could tsDCH, measured via two photon photoelectron spectroscopy, allow the differentiation between similar chemical environment? Our results demonstrated that this methodology is indeed successful [1,2]. Our findings exploited the ultrashort pulse duration of the FEL to eject two core electrons on a time scale comparable to that of Auger decay and demonstrate possible future x-ray control of physical inner-shell processes [1,2].

2) Absolute Photodetachment Cross Section of H^-

We have measured the absolute photodetachment cross section of H^- at both the ALS and also at the SOLEIL facility in France to test the calculations by Yip et al. [c] which cover a photon energy range between 12-45 eV. This experiment is very important from a fundamental point of view since it represents the three-body Coulomb breakup problem. It is “unique” because of the greater importance of the electron repulsion relative to the Coulomb attraction of the electrons to the nucleus when $Z=1$. Thus the atomic properties of H^- are more sensitive to electron correlation effects when compared to Helium for example [c]. Furthermore, there is no experimental data available to test published calculations [c]. Measuring the absolute photodetachment cross section of H^- is important because H^- is responsible for a large part for the opacity of stellar atmospheres, including our own sun. Thus it is relevant to understand fundamentally the interaction of the H^- ions with the vuv/x-rays produced by our sun by simulating this experiment in the laboratory. We used the SOLEIL facility in France in order to access the low photon energy (12-20 eV, not easily accessible at the ALS). We have however used the ALS BL 10 undulator at zero order in combination with filters to access the low photon energy range. The data are presently being analyzed to determine if the latter experiment is not contaminated with higher order effects.

Future Plans.

The principal areas of investigation planned for the coming year are:

1) Prepare and carry out the approved LCLS 2012 October and November experiments consisting of ionizing molecules with ultra-short and intense x-rays. 2) Analyze the data from our May 2012 experiment that consisted of creating and probing a nanoplasma by ionizing C_{60} molecules with intense x-rays of pulse duration that varied between 5-180 fs. 3) Analyze the photodetachment experiment on H^- using single photon ionization from the ALS. 4) Finish writing the manuscript on the K-shell photodetachment experiment on C_{60}^- using the ALS (conducted in collaboration with the UNR, DU, ALS and Giessen groups).

References:

- [a] L. S. Cederbaum, et al., J. Chem. phys. 85, 6513-6523 (1986).
- [b] R. Santra et.al, . Phys. Rev. Lett. 103, 013002-013005 (2009).
- [c] F. L. Yip, D. A. Horner, C. W. McCurdy, and T. N. Rescigno, Phys. Rev. A 75, 042715 (2007).

Publications from DOE Sponsored Research

1. N. Berrah, L. Fang, T. Osipov, B. Murphy, E. Kukk, K. Ueda, R. Feifel, P. van der Meulen, P. Salen, H. Schmidt, R. Thomas, M. Larsson, R. Richter, K. C. Prince, J. D. Bozek, C. Bostedt, S. Wada, M. Piancastelli, M. Tashiro, M. Ehara, “Double Core-Hole Spectroscopy for Chemical Analysis with an Intense X-Ray Femtosecond Laser” Proc. Natl. Acad. Sci., PNAS **108**, issue 41, 16912 (2011).
2. P. Salen, P. van der Meulen, H.T. Schmidt, R.D. Thomas, M. Larsson, R. Feifel, M.N. Piancastelli, L. Fang, B. Murphy, T. Osipov, N. Berrah, E. Kukk, K. Ueda, J.D. Bozek, C. Bostedt, S. Wada, R. Richter, V. Feyer and K.C. Prince, “X-ray FEL-induced Two-Site Double Core-Hole Formation for Chemical Analysis”, Phys. Rev. Lett. PRL 108, 153003 (2012)
3. James P. Cryan, J. M. Glowonia, Andreasson, A. Belkacem, N. Berrah, C. I. Blaga, C. Bostedt, J. Bozek, N. A. Cherepkov, L. F. DiMauro, L. Fang, O. Gessner, M. Guehr, J.

- Hajdu, M. P. Hertlein, M. Hoener, O. Kornilov, J. P. Marangos, A. M. March, B. K. McFarland, H. Merdji, M. Messerschmidt, V. Petrovic, C. Raman, D. Ray, D. Reis, S. K. Semenov, M. Trigo, J. L. White, W. White, L. Young, P. H. Bucksbaum, and R. N. Coffee, "Molecular frame Auger electron energy spectrum from N₂" *J. Phys. B: At. Mol. Opt. Phys.* **45**, 055601 (2012).
4. H. Thomas, A. Helal, K. Hoffmann, N. Kandadai, J. Keto, J. Andreasson, B. Iwan, M. Seibert, N. Timneanu, J. Hajdu, M. Adolph, T. Gorkhover, D. Rupp, S. Schorb, T. Möller, G. Doumy, L.F. DiMauro, M. Hoener, B. Murphy, N. Berrah, M. Messerschmidt, J. Bozek, C. Bostedt and T. Ditmire, "Explosions of Xe-clusters in ultra-intense femtosecond x-ray pulses from the LCLS Free Electron Laser", *Phys. Rev. Lett.* **108**, 133401 (2012).
 5. Christian Buth, Ji-Cai Liu, Mau Hsiung Chen, L. Fang, M. Hoener, N. Berrah, "Ultrafast absorption of intense x rays by nitrogen molecules", *J. Chem. Phys. J. Chem. Phys.* **136**, 214310 (2012)
 6. V. S. Petrović, M. Siano, J.L. White, N. Berrah, C. Bostedt, J. D. Bozek, D. Broege, M. Chalfin, R. N. Coffee, J. Cryan, L. Fang, J. P. Farrell, L. J. Frasinski, J. M. Glowina, M. Gühr, M. Hoener, D.M. P. Holland, J. Kim, J. P. Marangos³, T. Martinez, B. K. McFarland, R. S. Minns, S. Miyabe, S. Schorb, R. J. Sension, L. S. Spector, R. Squibb, H. Tao, J. G. Underwood, and P. H. Bucksbaum "Transient X-ray fragmentation: Probing a prototypical photoinduced ring opening", *Phys. Rev. Lett.* **108**, 253006, (2012).
 7. N. Berrah, R.C. Bilodeau, I. Dumitriu, D. Toffoli, and R. R. Lucchese, "Shape and Feshbach Resonances in Inner-Shell Photodetachment of Negative Ions, *J. Elect. Spectr. and Relat. Phen. Kai Siegbahn Memorial Volume* **183**, 64 (2011)
 8. G. Doumy, C. Roedig, S.-K. Son, C. I. Blaga, A. D. DiChiara, R. Santra, N. Berrah, C. Bostedt, J. D. Bozek, P. H. Bucksbaum, J. P. Cryan, L. Fang, S. Ghimire, J. M. Glowina, M. Hoener, E. P. Kanter, B. Krässig, M. Kuebel, M. Messerschmidt, G. G. Paulus, D. A. Reis, N. Rohringer, L. Young, P. Agostini, and L. F. DiMauro, *Phys. Rev. Lett.* **106**, 083002 (2011).
 9. O. Gessner, O. Kornilov, M. Hoener, L. Fang, and N. Berrah, "Intense Femtosecond X-ray Photoionization Studies of Nitrogen - How Molecules interact with Light from the LCLS" in *Ultrafast Phenomena XVII*, M. Chergui, D. M. Jonas, E. Riedle, R. W. Schoenlein, A. J. Taylor, Eds., Oxford University Press, 47 (2011).
 10. E. P. Kanter, B. Krässig, Y. Li, A. M. March, N. Rohringer, R. Santra, S. H. Southworth, L. F. DiMauro, G. Doumy, C. A. Roedig, N. Berrah, L. Fang, M. Hoener, P. H. Bucksbaum, S. Ghimire, D. A. Reis, J. D. Bozek, C. Bostedt, M. Messerschmidt, L. Young, "Modifying Auger Decay with Femtosecond X-ray Pulses" *Phys. Rev. Lett.* **107**, 233001 (2011).
 11. L. Fang, M. Hoener, N. Berrah, "Ultra intense x-ray induced non-linear processes in Molecular nitrogen", *J. of Physics*, **288**, 012019 (2011)
 12. N. Berrah, R.C. Bilodeau, I. Dumitriu, D. Toffoli, and R. R. Lucchese, "Shape and Feshbach Resonances in Inner-Shell Photodetachment of Negative Ions, *J. Elect. Spectr. and Relat. Phen., Kai Siegbahn Memorial Volume* **183** pp 64-69. (2011)
 13. D.A. Esteves, R.C. Bilodeau, N.C. Sterling, R.A. Phaneuf, A.L D. Kilcoyne, E.C. Red, and A. Aguilar, "Absolute high-resolution Se⁺ photoionization cross-section measurements with Rydberg-series analysis," *Physical Review A*, **84**(1), 013406-1 (2011).
 14. N.C. Sterling, M.C. Witthoef, D.A. Esteves, R.C. Bilodeau, A.L. Kilcoyne, E.C. Red, R.A. Phaneuf, G. Alna'Washi, and A. Aguilar, "New atomic data for trans-iron elements and their application to abundance determinations in planetary nebulae," *Canadian Journal of Physics* **89**(4), 379-385 (2011).
 15. N.C. Sterling, D.A. Esteves, R.C. Bilodeau, A.L D. Kilcoyne, E.C. Red, R.A. Phaneuf, and A. Aguilar, "Experimental photoionization cross-section measurements in the ground and metastable state threshold region of Se⁺," *Journal of Physics B: Atomic, Molecular and Optical Physics* **44**(2), 025701 (2011).

16. Philip H. Bucksbaum, Ryan Coffee, and Nora Berrah, “The First Atomic and Molecular Experiments at the Linac Coherent Light Source X-Ray Free Electron Laser” Book Chapter, *Advances in Atomic, Molecular, and Optical Physics*, Volume 60, p. 240, (2011).
17. B.F. Murphy, L. Fang, T.Y. Osipov, M. Hoener, and N. Berrah, “Intense X-ray FEL-Molecule Physics: Highly Charged Ions”, the American Institute of Physics (AIP) Conference Proceedings of ICAPiP, **1438**, 249 (2012).
18. T.Y. Osipov, L. Fang, B.F. Murphy, M. Hoener, and N. Berrah, “X-Ray FEL Induced Double Core-Hole and High Charge State Production”, *Journal of Physics: Conference Series (JPCS)*, published by IOP Publishing (in press).
19. L. Fang, M. Hoener, O. Gessner, F. Tarantelli, S.T. Pratt, O. Kornilov, C. Buth, M. Guehr, E.P. Kanter, C. Bostedt, J.D. Bozek, P.H. Bucksbaum, M.Chen, R. Coffee, J. Cryan, M. Glowonia, E. Kukk, S.R. Leone, and N. Berrah, “Double core hole production in N₂: Beating the Auger clock”, *Phys. Rev. Lett.* **105**, 083005 (2010).
20. J. P. Cryan, J. M. Glowonia, J. Andreasson, A. Belkacem, N. Berrah, C. I. Blaga, C. Bostedt, J. Bozek, C. Buth, L. F. DiMauro, L. Fang, O. Gessner, M. Guehr, J. Hajdu, M. P. Hertlein, M. Hoener, 10 O.Kornilov, J. P. Marangos, 11 A. M. March, 12, B. K. McFarland, H. Merdji, V. Petrovic, C. Raman, D. Ray, 15 D. Reis, F. Tarantelli, M. Trigo, J. White, W. White, L. Young, P. H. Bucksbaum, and R. N. Coffee, “Auger electron angular distribution of double core hole states in the molecular reference frame”, *Phys. Rev. Lett.* **105**, 083004 (2010),
21. J. M. Glowonia, J. Cryan, J. Andreasson, A. Belkacem, N. Berrah, C. I. Blaga, C. Bostedt, J. Bozek, L. F. DiMauro, L. Fang, J. Frisch, O. Gessner, M. Gühr, J. Hajdu, M. P. Hertlein, M. Hoener, G. Huang, O. Kornilov, J. P. Marangos, A. M. March, B. K. McFarland, H. Merdji, V. S. Petrovic, C. Raman, D. Ray, D. A. Reis, M. Trigo, J. L. White, W. White, R. Wilcox, L. Young, R. N. Coffee, and P. H. Bucksbaum, “Time-Resolved Pump-Probe Experiments at the LCLS” *Optics Express*, **18**, Issue 17, 17620 (2010).
22. M. Hoener, L. Fang, O. Kornilov, O. Gessner, S.T. Pratt, M. Guehr, E.P. Kanter, C. Blaga, C. Bostedt, J.D. Bozek, P.H. Bucksbaum, C. Buth, M. Chen, R.Coffee, J. Cryan, L. DiMauro, M. Glowonia, E. Hosler, E. Kukk, S.R. Leone, B.McFarland, M. Messerschmidt, B. Murphy, V. Petrovic, D. Rolles, and N. Berrah, “Ultra-intense X-ray Induced Ionization, Dissociation and Frustrated Absorption in Molecular Nitrogen” *Phys. Rev. Lett.* **104**, 253002 (Published June 23, 2010). First published work from LCLS.
23. I. Dumitriu, R. Bilodeau, D. Gibson, W. Walter, A. Aguilar E. Reed and N. Berrah “Photoionization of Fe⁻”, *Phys. Rev. A*, **81**, 053404 (2010).
24. I. Dumitriu, R. C. Bilodeau, T. W. Gorczyca, C. W. Walter, N. D. Gibson, Z. D. Pesic, D. Rolles and N. Berrah, “Inner-shell photodetachment from Ru⁻”, *Phys. Rev. A*. **82**, 043434 (2010).
25. N. Berrah, J. Bozek, J. T. Costello, S. Düstererd, L. Fanga, J. Feldhausd, H. Fukuzawae, M. Hoenera, Y. H. Jiang; P. Johnsson, E. T. Kennedy, M. Meyer,; R. Moshammer, P. Radcliffed, M. Richtera, A. Rouzée; A. Rudenko, . A. Sorokind, K. Tiedtke, K. Ueda, . Ullrich, M. J. J. Vrakking “Non-linear processes in the interaction of atoms and molecules with intense EUV and X-ray fields from SASE free electron lasers (FELs)” *Journal of Modern Optics, Topical Review*, **57**, Issue 12, 1015 (2010).
26. L. Young, E. P. Kanter, B. Krässig, Y. Li, A. M. March, S. T. Pratt, R. Santra, S. H. Southworth, N. Rohringer, L. F. DiMauro, G. Doumy, C. A. Roedig, N. Berrah, L. Fang, M. Hoener, P. H. Bucksbaum, J. P. Cryan, S. Ghimire, J. M. Glowonia, D. A. Reis, J. D. Bozek, C. Bostedt, M. Messerschmidt, “Femtosecond electronic response of atoms to ultraintense x-rays” *Nature* **466**, 56-61 (2010).
27. M. Hoener, D. Rolles, A. Aguilar, R. C. Bilodeau, D. Esteves, P. Olalde Velasco, Z. D. Pesic, E. Red, and N. Berrah, “Site-selective ionization and relaxation dynamics in heterogeneous nanosystems”, *Phys. Rev. A*, **81**, 021201(R) (2010).

Reactive Scattering of Ultracold Molecules

Principal Investigator

John Bohn
JILA, UCB 440
University of Colorado
Boulder, CO 80309
Phone (303) 492-5426
Email bohn@murphy.colorado.edu

Program Scope

In an effort to probe ever deeper into the fundamental dynamics of chemical reactions, one is faced these days with two options. One may either increase resolution in the time domain and deliberately push around molecular constituents, as in the rapidly maturing field of ultrafast dynamics; or increase resolution in the energy domain by effectively slowing the beams, as is done in the nascent field of cold and ultracold molecules. This program is concerned with the latter approach. It seeks to address what new information may be afforded by molecular gases cooled to sub-milliKelvin temperatures. In these experiments, the incident channel of the reactants can be completely specified in terms of the internal state, as well as an extremely low relative translational energy that, in favorable cases, allows probing the reactivity of a single partial wave in the incident channel.

We are constructing a theoretical framework for exploring chemistry from within these novel experiments. To do so it is crucial to distinguish the long-range physics, when reactant molecules are far from one another, from the short-range physics of the reaction itself. The long-range physics is dominated by slowly-moving molecules whose detailed motion is highly susceptible to the controllable actions of electromagnetic fields. Manipulating the molecules on their approach can alter the “gateway” by which they enter into the reaction region, thus filtering the information gleaned from the experiment.

Recent Progress

In the past year we have considered problems relevant to both the long-range and short-range physics. For the long-range, we seek to exploit the value of multichannel quantum defect theory (MQDT) for not only calculating accurate results, but also parametrizing complex scattering observables such as resonances in a compact way. MQDT is known to be a powerful method when applied to ultracold collisions of atoms, thanks to previous work by Mies, Julienne, Gao, Greene, and others. It has always been problematic, however, when applied to molecules, where rotational excitation and intrinsically anisotropic potentials can make high partial waves relevant. In collaboration with C. Greene, we have recently perfected a method for generating numerically accurate, linearly

independent QDT basis functions for this purpose, opening up MQDT as a powerful tool for molecular cold collisions. A manuscript on this work is in preparation.

In a second project, we have explored the role of scattering resonances in realistic molecules. Here we have focused on ground-state alkali dimers, which have been successfully created at ultracold temperatures in several labs (although so far only one has observed them colliding). We have estimated the density of ro-vibrational resonant states for these systems, finding them to be huge, e.g., hundreds of resonances per Gauss of magnetic field for p -wave collisions of Rb atoms with KRb molecules. In such a situation, it is probably hopeless to identify each resonance explicitly. Rather, it is more reasonable to understand the *statistical* consequences of these many resonances. To this end, we have constructed a hybrid theory, which combines random matrix theory from nuclear physics to assess the distribution of resonant states and their width, with the MQDT that provides complete detail of such matters as field and energy dependence near threshold. Sample collision data from this model are shown below.

In a recent publication, we have employed this model to lay out concrete predictions for ultracold atom-molecule scattering of alkali dimers. We suggest specific experiments to probe the unique dynamics of this system, including the ergodicity of the resonant state, the likelihood of nuclear-spin-changing collisions, and trends across different molecules. We also predict the onset of Ericson fluctuations in spectra for molecules that are in excited hyperfine states. This implies a transition from a regime where individual resonances may in principle be resolved, to a regime where resonances broaden so that only broad fluctuations are seen. Such a transition has been observed in nuclear scattering, as the collision energy spans hundreds of MeV of energy. In ultracold collisions, it requires only the change of a nuclear spin state, to completely alter character of the observed spectrum.

In more recent work, being written up now, we consider molecule-molecule scattering from the same perspective. Naturally, the density of ro-vibrational states is even higher here. We find, in fact, that this density of states corresponds to lifetimes of the molecule-molecule resonant complex that can be of the order of milliseconds for RbCs-RbCs collisions. During this time, which is typically a good fraction of the duration of an experimental shot, these complexes can be hit by other molecules, leading to trap loss. This new mechanism puts limits on experimental lifetimes and needs to be characterized if degenerate quantum gas experiments are to proceed.

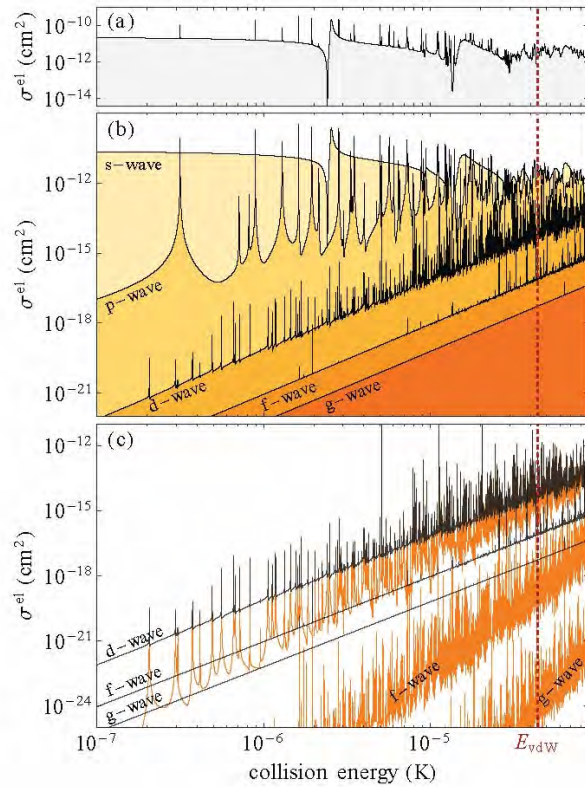


Figure. Sample collision spectrum within the statistical model of Rb+KRb ultracold collisions, with both collision partners in their absolute ground state (including nuclear spin). In panel (a) is shown the total elastic cross section, which is decomposed into partial wave contributions in panel (b). Panel (c) removes long-range contributions to the phase shifts, to better bring out the resonances in higher partial waves. $E_{\text{vdW}} \sim 40 \mu\text{K}$ is the characteristic van der Waals energy of the collision.

Future Plans

Buoyed by the success of the higher partial wave MQDT theory for non-polar species, we will advance to the case of strongly anisotropic dipolar interactions. This will lead us to realistic scattering of such molecules as dysprosium and erbium, both of which have recently been Bose condensed. In the case of erbium, dozens of Fano-Feshbach resonances have already been observed, but even the beginnings of their classification have not been accomplished. We believe that the MQDT will be both sufficiently numerically powerful and transparent enough in form, to enable the interpretation of such complex spectra. These complex atoms, where all resonances are in principle resolved, will be an important stepping stone toward the interpretation of complex

molecular collision data in the cold and ultracold regime. At the same time, the dense spectra of erbium resonances gives us also the opportunity to explore in more quantitative detail the statistical models.

DOE-supported publication in the past three years

Remark: prior to the first year of this funding cycle, the grant focused primarily on many-body physics of ultracold dipoles. This is reflected in the bibliography below.

Critical Superfluid Velocity in a Trapped Dipolar Gas

R. M. Wilson, S. Ronen, and J. L. Bohn, Phys. Rev. Lett. **104**, 094501 (2010).

Zero Sound in Dipolar Fermi Gases

S. Ronen and J. L. Bohn, Phys. Rev. A **81**, 033601 (2010).

Anisotropic Superfluidity in a Dipolar Bose Gas

C. Ticknor, R. M. Wilson, and J. L. Bohn, Phys. Rev. Lett. **106**, 065301 (2011).

Emergent Structure in a Dipolar Bose Gas in a One-Dimensional Lattice

R. M. Wilson and J. L. Bohn, Phys. Rev. A **83**, 023623(2011).

Statistical Aspects of Ultracold Resonant Scattering

M. Mayle, B. P. Ruzic, and J. L. Bohn, Phys. Rev. A **85**, 062712 (2012).

Ultrafast Electron Diffraction from Aligned Molecules

Martin Centurion

Department of Physics and Astronomy, University of Nebraska, Lincoln, NE 68588-0299
mcenturion2@unl.edu

Program Scope

The aim of this project is to record time-resolved electron diffraction patterns of aligned molecules and to reconstruct the 3D molecular structure. The molecules will be aligned non-adiabatically using a femtosecond laser pulse. A femtosecond electron pulse will then be used to record a diffraction pattern while the molecules are aligned. The experiment consists of a laser system, a pulsed electron gun, a gas jet that contains the target molecules and a detector to capture the diffraction patterns. The diffraction patterns will then be processed to obtain the molecular structure.

Introduction

The majority of known molecular structures have been determined using either x-ray diffraction for crystallized molecules or Nuclear Magnetic Resonance (NMR) spectroscopy for molecules in solution. However, for isolated molecules there has been no method demonstrated to measure the three dimensional structure. Electron diffraction has been the main tool to determine the structure of molecules in the gas phase[1] and also to investigate ultrafast changes in structure[2-4]. In this method the diffraction pattern is compared with a calculated structure iteratively until an appropriate match between experiment and theory is found. Diffraction patterns from randomly oriented molecules contain only one-dimensional information, and thus input from theoretical models is needed to recover the structure. We propose to use pulsed electron diffraction from aligned molecules to recover the three dimensional structure, and to investigate molecular dynamics.

In previous experiments, electron diffraction patterns of aligned molecules have been recorded using adiabatic alignment with long laser pulses (in this case the laser is longer than the rotational period and is present during the alignment)[5], and by selective alignment in a photo-dissociation reaction[6]. However, in both cases the degree of alignment was found to be too weak to extract structural information. Additionally, in adiabatic alignment the presence of a strong laser field can distort the molecular structure, while selective alignment relies on a change in the structure. In our experiments, the molecules are impulsively aligned with a femtosecond laser pulse and probed with femtosecond electron pulses in a field-free environment at the peak alignment. This ensures that the molecules are not distorted by the laser field when the structure is probed by the electron pulse.

Recent Progress

We have recently demonstrated, for the first time, three dimensional imaging of isolated molecules. The molecular structure is recovered without any prior knowledge of the structure. We assume only that the constituent atoms are known, but not their spatial distribution. These results were achieved using femtosecond electron pulses diffracting from a sample of laser-aligned trifluoroiodomethane (CF_3I) molecules. CF_3I is a symmetric top molecule, which we have aligned using a linearly polarized laser pulse. The laser impulsively aligns the long axis (along the C-I bond) of the molecule along the direction of laser polarization. The molecule rotates freely about the perpendicular axis, so an average over many molecules results in a cylindrically symmetric structure. The peak of the alignment was found to occur 2 ps after the arrival of the laser pulse.

The experimental setup is shown schematically in Figure 1. The direction of the alignment laser, electron pulse and gas jet are all mutually orthogonal. A supersonic gas jet is produced by flowing a mixture of CF_3I and helium through a convergent-divergent nozzle. The laser pulses are split in two for alignment and triggering the electron pulse. The alignment laser pulse has a duration of 300 fs and is focused to an intensity of $2.2 \times 10^{13} \text{ W/cm}^2$ on the molecular target. A small fraction of the laser pulse energy is frequency tripled and focused on a photocathode to trigger the emission of electrons. The electrons are accelerated to 25 keV using a static electric field and collimated by a magnetic lens. Each electron pulse contains approximately two thousand electrons and has a duration of 500 fs at the target. The electron pulse duration is kept short by using a short distance from the source to the target and keeping the charge low. The overall resolution of the experiment is 850 fs, considering velocity mismatch in the finite size interaction volume and the duration of the pulses. After traversing the sample, the unscattered electron beam is stopped by a copper beam block, and the diffraction pattern is captured using a

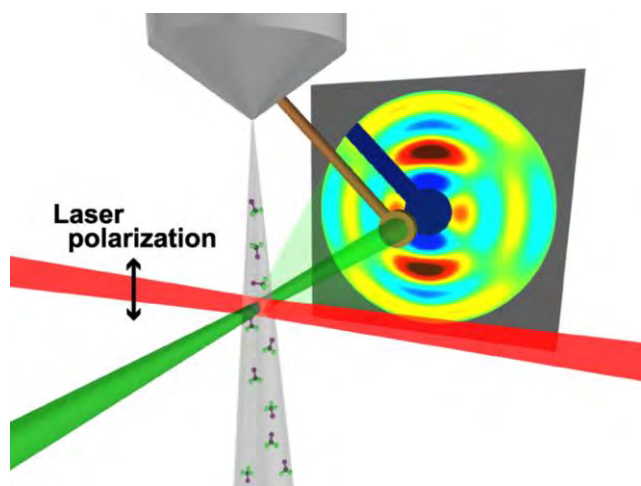


Figure 1. Experimental Setup

2D detector comprising a phosphor screen, image intensifier and CCD camera.

If the molecules are perfectly aligned (or if the diffraction were from a single molecule), then a single diffraction pattern could be sufficient to recover the structure. However, a high degree of alignment is very difficult to achieve experimentally. We have found that there were no phase retrieval methods that could successfully reconstruct the structure for experimentally accessible degrees of alignment. Thus, we developed a genetic algorithm that can

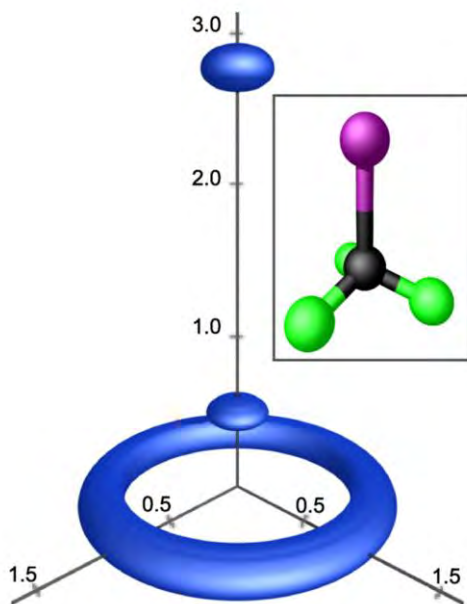


Figure 2. Experimental reconstruction of the CF_3I molecule. The CF_3I molecules rotate freely about the C-I axis, which results in a cylindrically symmetric structure. The units are in angstroms. See Methods section for details on the reconstruction. The inset shows a theoretical model of the CF_3I molecule for comparison. The fluorine atoms are colored green, carbon is black and the iodine atoms is purple.

combine several diffraction patterns with a low degree of alignment to reconstruct the diffraction pattern of a single molecule. We recorded several diffraction patterns corresponding to different orientations of the alignment axis (different projections of the molecule). The direction of the alignment axis can be changed continuously by rotating the direction of the linear polarization of the alignment laser. In our experiments, the degree of alignment was $\langle \cos^2 \alpha \rangle = 0.5$, where α is the angle between the long axis of the molecule and the laser polarization. Once the single-molecule diffraction pattern is constructed, we use the holographic algorithm of Ho et al. [21] to retrieve an image of the molecule. Figure 2 shows the retrieved molecular structure. The inset is a model of the molecule using the known interatomic distances. The three fluorine atoms appear as a band on the experimental reconstruction because the molecule rotates freely along the long axis. Additional knowledge, such as the number of fluorine atoms would be sufficient to fully determine the structure. Table 1 shows the distances and the main molecular angle retrieved from our measurements are in good agreement with known values.

	Experimental results	Previous results
r_{CI}	$2.19 \pm 0.07 \text{ \AA}$	2.14 \AA
r_{FI}	$2.92 \pm 0.09 \text{ \AA}$	2.89 \AA
I-C-F Angle	$120 \pm 9^\circ$	111°

Table 1. CF_3I interatomic distances and angles

Future Plans

After this first demonstration of three-dimensional imaging we plan to apply the method to more complex molecules. This will most likely require three-dimensional alignment, i.e. fixing two rotation axes of the molecule, having shorter electron pulses, and developing a phase retrieval

algorithm that can deal with the additional complexity. We are currently investigating methods for delivering shorter electron pulses on the target (see list of publications). For the alignment, a pulse with elliptical polarization can be used or two linearly polarized pulses with orthogonal polarization. We also plan to use our imaging method to investigate time-resolved dynamics in molecules. We will use two laser pulses, one for alignment and a second pulse to trigger the dynamics, followed by the electron pulse to probe the structure at a specific time. An additional improvement to the setup will be a new method to deliver the target molecules. The new device will include a heater to create a molecular beam with molecules with a low vapor pressure.

References

- [1] P. W. Allen and L. E. Sutton, *Acta Crystallogr.* 3, 46 (1950).
- [2] H. Ihee, V. A. Lobastov, U. M. Gomez, B. M. Goodson, R. Srinivasan, C. Y. Ruan, and A. H. Zewail, *Science* 291, 458 (2001).
- [3] C. I. Blaga, J. Xu, A. D. DiChiara, E. Sistrunk, K. Zhang, P. Agostini, T. A. Miller, L. F. DiMauro, and C. D. Lin, *Nature* 483, 194 (2012).
- [4] R. Srinivasan, J. Feenstra, S. Park, S. Xu, and A. Zewail, *Science* 307, 558 (2005).
- [5] K. Hoshina, K. Yamanouchi, T. Ohshima, Y. Ose, and H. Todokoro, *J. Chem. Phys.* 118, 6211 (2003).
- [6] P. Reckenthaeler, M. Centurion, W. Fuss, S. A. Trushin, F. Krausz, and E. E. Fill, *Phys. Rev. Lett.* 102, 213001 (2009).

Publications of DOE sponsored research in the past 3 years

1. “Imaging of Isolated Molecules with Ultrafast Electron Pulses”, Christopher J. Hensley, Jie Yang, and Martin Centurion, *Physical Review Letters* (Accepted)
2. “Dispersion Compensation for Attosecond Electron Pulses”, Peter Hansen, Cory Baumgarten, Herman Batelaan, Martin Centurion, *Applied Physics Letters* (Accepted)

Atomic and Molecular Physics in Strong Fields

Shih-I Chu
Department of Chemistry, University of Kansas
Lawrence, Kansas 66045
E-mail: sichu@ku.edu

Program Scope

In this research program, we address the fundamental physics of the interaction of atoms and molecules with intense ultrashort laser fields. The main objectives are to develop new theoretical formalisms and accurate computational methods for *ab initio* nonperturbative investigations of multiphoton quantum dynamics and very high-order nonlinear optical processes of one-, two-, and many-electron quantum systems in intense laser fields, taking into account detailed electronic structure information and many-body electron-correlated effects. Particular attention will be paid to the exploration of the effects of electron correlation on high-harmonic generation (HHG) and multiphoton ionization (MPI) processes, multi-electron response and underlying mechanisms responsible for the strong-field ionization of diatomic and small polyatomic molecules, time-frequency spectrum, coherent control of HHG processes for the development of tabletop x-ray laser light sources, and for the exploration of attosecond AMO processes, etc.

Recent Progress

1. Low-Energy Structure of Above-Threshold-Ionization Electron Spectra: Role of the Coulomb Threshold Effect

Recent experimental observations of above-threshold ionization of rare gas atoms and diatomic molecules by mid-infrared laser fields [1,2] revealed a prominent maximum in the electron energy spectrum very close to the ionization threshold which cannot be reproduced by the widely used Keldysh-Faisal-Reiss theories. We have recently performed the first fully *ab initio* theoretical analysis and precision calculations [3] to explore the quantum origin of the low-energy structure (LES) observed in the experiments. Our study shows that an important role in shaping of LES is played by the effect of Coulomb attraction in the final electron state and the Coulomb threshold effect. We demonstrated that the exact amplitude, in contrast with the KFR approximation, does not vanish at the threshold provided the interaction of the ejected electron with the residual is represented by the attractive Coulomb potential. In the attractive Coulomb field, the density of slow electrons is condensed in the core region favoring the ionization process. We also have performed numerical calculations on the hydrogen atom subject to intense mid-infrared laser fields with the wavelengths 0.8 to 2 μm . In accordance with the theoretical predictions, the numerical data show a maximum close to the threshold in the energy spectra of the electrons emitted in the polarization direction of the laser field, similar to the low-energy structure revealed by recent experiments on noble gas atoms and diatomic molecules [1,2]. While the Coulomb threshold effect alone may not explain the whole picture of the low-energy ATI electron spectra, it plays an important role in shaping such spectra, including the emergence of LES. More detailed study will be continued in the future.

2. Probing the Origin of Elliptical High-order Harmonic Generation from Aligned Molecules in Linearly Polarized Laser Field

For ensembles of atoms or unaligned molecules, the polarization of the harmonics is expected to be the same as the polarization of the driving laser field. For aligned molecules, however, the harmonic radiation has two components: one parallel and another perpendicular to the laser polarization direction. Experiments showed that the linear polarization state of HHG driven by linearly polarized laser fields is tilted due to the nonvanishing perpendicular component of HHG. A recent experiment [4] has demonstrated that elliptically polarized high-order harmonic generation (HHG) can be produced from linearly polarized driving fields for aligned molecular systems. In order to reveal the underlying physical mechanisms of elliptical harmonics, we

present fully *ab initio* and high-precision calculations and analyses of the amplitude, phase, and polarization state of the harmonic radiation from molecular hydrogen ions with arbitrary orientation [5]. We find that high ellipticity arises from molecular orbital symmetry and two-center interference effects. Our *ab initio* exploration and findings lead to a general rule that the ellipticity becomes high for molecular orbitals represented by a symmetric combination of atomic orbitals, whereas it becomes low for molecular orbitals represented by an antisymmetric combination. This finding also applies to the general case of aligned linear molecules [5]. We note that in order to attain high ellipticity, both of the following conditions must be satisfied: (i) the amplitudes of the parallel (\parallel) and perpendicular (\perp) components are of the same order and (ii) their phase difference is around $\pm\pi/2$.

3. High Precision Study of the Orientation Effects in MPI/HHG of H_2^+ in Intense Laser Fields

Recently we have developed a time-dependent generalized pseudospectral (TDGPS) method for accurate and efficient treatment of the time-dependent Schrödinger equation (TDSE) of two-center diatomic molecules systems in prolate spheroidal coordinates [6,7]. This method naturally accounts for the symmetry of diatomic molecules and provides accurate description of Coulomb singularities due to non-uniform distribution of the grid points. The GPS method delivers high accuracy while using only moderate computer resources; it is easy to implement since no calculation of potential matrix elements is required, and kinetic energy matrices have simple analytical expressions. The method is applied to a fully *ab initio* 3D study of the orientation effects in MPI and HHG of H_2^+ subject to intense laser pulses. We discuss the multiphoton resonance and two-center interference effects in the HHG spectra which can lead both to enhancement and suppression of the harmonic generation [6,7].

4. Exploration of Strong-Field Multiphoton Double Ionization, Rescattering, and Electron Angular Distribution of He Atoms in Intense Long-Wavelength Laser Fields: The Coupled Coherent-State Approach

We extend the coupled coherent-state (CCS) approach to simulate the strong-field ionization of helium atoms at long wavelengths [8]. This approach uses a basis of trajectories guided by frozen Gaussian coherent states, sampled from a Monte Carlo distribution, as the initial states of the quantum time-dependent Schrödinger equations. The CCS trajectories move over averaged potentials, which can remove the Coulomb singularities exactly. The low-energy structure is predicted by our CCS calculation and a “rescattering” event is clearly identified in the higher-energy regime. In addition, the nonsequential double ionization is also explored and the rescattering event can be identified as the major mechanism. Finally, we also study the electron angular distribution of helium. It is found that the maximum angle between the electron and electric field directions becomes smaller with increase in the laser intensity and wavelength [8].

5. High-order-harmonic Generation in Homonuclear and Heteronuclear Diatomic Molecules: Exploration of Multiple Orbital Contributions

We present a time-dependent density functional theory (TDDFT) approach with proper asymptotic long-range potential for accurate nonperturbative treatment of MPI/HHG of diatomic molecules with arbitrary orientation [9-11]. A time-dependent two-center generalized pseudospectral method in prolate spheroidal coordinate system is used for accurate and efficient treatment of the TDDFT equations in space and time. The theory is applied to a detailed *all-electron* nonperturbative investigation of HHG processes of homonuclear (N_2 and F_2) [9-11] and heteronuclear (CO, BF, and HF) molecules [11] in intense ultrashort laser pulses with the emphasis on the role of multiple molecular orbitals (MOs). The results reveal intriguing and substantially different nonlinear optical response behaviors for homonuclear and heteronuclear molecules. Our analysis of the HHG spectra shows that homonuclear molecules have destructive interference between the orbital contributions to the total harmonic signal. This happens because the induced dipole moments of different orbitals oscillate in time with opposite phases, so their contributions are canceled out in the total dipole moment. The destructive interference in the HHG spectrum accounts for the unexpected observation that some of the individual orbital harmonic power spectra have greater intensity than that of the total HHG. The HHG process by the heteronuclear diatomic molecules, on the other hand, has a quite different characteristic. First, heteronuclear molecules can generate even and odd harmonics since they lack the inversion symmetry. Second,

for all the heteronuclear molecules studied so far, the individual MO contribution to the total HHG spectrum is dominated by the highest occupied molecular orbital (HOMO) only. Also, the interference between the different orbitals in the total HHG spectrum is found to be mostly constructive [11].

6. Precision Calculation of Above-threshold Multiphoton Ionization in Intense Short-wavelength Laser Fields: The Time-dependent Generalized Pseudospectral Method in Momentum-space.

We develop a new approach in momentum (P) space for the accurate study of multiphoton and above-threshold ionization (ATI) dynamics of atomic systems driven by intense laser fields [12]. In this approach, the electron wave function is calculated by solving the P -space time-dependent Schrödinger equation (TDSE) in a finite P -space volume under a simple zero asymptotic boundary condition. The P -space TDSE is propagated accurately and efficiently by means of the time-dependent generalized pseudospectral method (TDGPS) with optimal momentum grid discretization and a split-operator time propagator in the *energy* representation. The differential ionization probabilities are calculated directly from the continuum-state wave function obtained by projecting the total electron wave function onto the continuum-state subspace using the projection operator constructed by the continuum eigenfunctions of the unperturbed Hamiltonian. As a case study, we apply this approach to the nonperturbative study of the multiphoton and ATI dynamics of a hydrogen atom exposed to intense ultrashort wavelength laser fields. High-resolution photoelectron energy-angular distribution and ATI spectra have been obtained. We find that with the increase of the laser intensity, the photoelectron energy-angular distribution changes from circular to dumbbell shaped and is squeezed along the laser field direction. We also explore the change of the maximum photoelectron energy with laser intensity and strong-field atomic stabilization phenomenon in detail [12].

7. Coherent Control of the Electron Quantum Paths for the Optimal Generation of Single Ultrashort Attosecond Laser Pulse

We report a new mechanism and experimentally realizable approach for the coherent control of the generation of an isolated and ultrashort attosecond (*as*) laser pulse from atoms by means of the optimization of the two-color laser fields with a proper time delay [13]. Optimizing the laser pulse shape allows the control of the electron quantum paths and enables high-harmonic generation from the long- and short-trajectory electrons to be enhanced and split near the cutoff region. In addition, it delays the long-trajectory electron emission time and allows the production of extremely short attosecond pulses in a relatively narrow time duration. As a case study, we show that an isolated 30 *as* pulse with a bandwidth of 127 eV can be generated directly from the contribution of long-trajectory electrons alone.

We have then explored the optimization of three-color laser field for the generation of single ultrashort attosecond pulse [14]. We show that the plateau of high-order harmonic generation is extended dramatically and a broadband supercontinuum spectra is produced. As a result, an isolated 23 *as* pulse with a bandwidth of 163 eV can be obtained directly by superposing the supercontinuum harmonics near the cutoff region. We show that such a metrology can be realized experimentally.

More recently, we have further investigated the effect of macroscopic propagation on the supercontinuum harmonic spectra and the subsequent attosecond-pulse generation [15]. The effects of macroscopic propagation are investigated in near and far field by solving Maxwell's equation. The results show that the contribution of short-trajectory electron emission is increased when the macroscopic propagation is considered. However, the characteristics of the dominant long-trajectory electron emission (in the single-atom response case) are not changed, and an isolated and shorter *as* pulse can be generated in the near field. Moreover, in the far field, the contribution of long-trajectory electron emission is still dominant for both on-axis and off-axis cases. As a result, an isolated and shorter *as* pulse can be generated directly. Similar results are obtained when the atomic target position is changed.

8. Fast-kick-off Monotonically Convergent Algorithm for Searching Optimal Control Fields

We have recently developed a new search algorithm for quickly finding optimal control fields in the state-to-state transition probability control problems, especially those with poorly chosen initial control fields [16]. The algorithm is based on the extension of a recently formulated monotonically convergent scheme [17,18].

Specifically, the local temporal refinement of the control field at each iteration is weighted by a fractional inverse power of the instantaneous overlap of the backward-propagating wave function, associated with the target state and the control field from the previous iteration, and the forward-propagating wave function, associated with the initial state and the concurrently refining control field. Extensive numerical simulations for controls of vibrational transitions and ultrafast electron tunneling show that the new algorithm not only greatly improves the search efficiency but also is able to attain good monotonic convergence quality when further frequency constraints are required. The algorithm is particularly effective when the corresponding control dynamics involves a large number of energy levels or ultrashort control pulses [16].

9. We have completed an invited book chapter on the recent development of *self-interaction-free* time dependent density functional theory (TDDFT) for the nonperturbative treatment of atomic and molecular multiphoton processes in intense ultrashort laser fields [19].

Future Research Plans

In addition to continuing the ongoing researches discussed above, we plan to initiate the following several new project directions: (a) Development of time-dependent (TD)- Voronoi-cell finite difference (VFD) method for the study of MPI/HHG processes in triatomic and small polyatomic molecular systems. (b) Extension of the TDGPS method in momentum space to the study of HHG/ATI processes in intense ultrashort laser fields. (c) Development of the coherent-state Ehrenfest trajectory (CSET) approach [20] for probing atomic and molecular processes in intense long-wavelength laser fields. (d) Development of *self-interaction-free* TDDFT with proper *derivative discontinuity* for the treatment of double ionization of complex atoms in intense laser fields [21]. (e) Development of nonperturbative methods for the accurate treatment of transient absorption and subcycle dynamics in MIR+ attosecond pulses.

References Cited (* Publications supported by the DOE program in the period of 2010-2012).

- [1] C. I. Blaga *et al.*, Nat. Phys. **5**, 335 (2009).
- [2] W. Quan *et al.*, Phys. Rev. Lett. **103**, 093001 (2009).
- *[3] D. A. Telnov and S.I. Chu, Phys. Rev. A **83**, 063406 (2011).
- [4] X. Zhou *et al.*, Phys. Rev. Lett. **102**, 073902 (2009).
- *[5] S. K. Son, D. A. Telnov, and S. I. Chu, Phys. Rev. A **82**, 043829 (2010).
- [6] D. A. Telnov and S. I. Chu, Phys. Rev. A **76**, 043412 (2007).
- *[7] D. A. Telnov and S. I. Chu, Computer Phys. Comm. **182**, 18 (2011).
- *[8] J. Guo, X.-S. Liu, and S. I. Chu, Phys. Rev. A **82**, 023402 (2010).
- [9] D. A. Telnov and S. I. Chu, Phys. Rev. A **79**, 041401(R) (2009).
- [10] D. A. Telnov and S. I. Chu, Phys. Rev. A **80**, 043412 (2009).
- *[11] J. Heslar, D. A. Telnov, and S. I. Chu, Phys. Rev. A **83**, 043414 (2011).
- *[12] Z. Y. Zhou and S.I. Chu, Phys. Rev. A **83**, 013405 (2011).
- *[13] I. L. Liu, P.-C. Li, and S.I. Chu, Phys. Rev. A **84**, 033414 (2011).
- *[14] P. C. Li, I. L. Liu, and S.I. Chu, Opt. Express **19**, 23857 (2011).
- *[15] P. C. Li and S.I. Chu, Phys. Rev. A **86**, 013411 (2012).
- *[16] S.L. Liao, T.S. Ho, S.I. Chu, and H. Rabitz, Phys. Rev. A **84**, 031401 (2011).
- *[17] T. S. Ho, H. Rabitz, and S. I. Chu, Comput. Phys. Comm. **182**, 14 (2011).
- [18] T. S. Ho and H. Rabitz, Phys. Rev. E **82**, 026703 (2010).
- *[19] S.I. Chu and D.A. Telnov, in *Computational Studies of New Materials II: From Ultrafast Processes and Nanostructures to Optoelectronics, Energy Storage and Nanomedicine*, edited by T.F. George, D. Jelski, R.R. Letfullin, and G. Zhang (World Scientific, 2011), p. 75–101.
- *[20] Z. Y. Zhou and S. I. Chu, Phys. Rev. A **83**, 033406 (2011).
- *[21] D. A. Telnov, J. Heslar, and S.I. Chu, Chem. Phys. **391**, 88 (2011).

Formation of Ultracold Molecules

Robin Côté

Department of Physics, U-3046
University of Connecticut
2152 Hillside Road
Storrs, Connecticut 06269

Phone: (860) 486-4912
Fax: (860) 486-3346
e-mail: rcote@phys.uconn.edu
URL: <http://www.physics.uconn.edu/~rcote>

Program Scope

Current experimental efforts to obtain ultracold molecules (*e.g.*, photoassociation (PA), buffer gas cooling, or Stark deceleration) raise a number of important issues that require theoretical investigations and explicit calculations.

The main aims of this Research Program are to identify efficient approaches to obtain ultracold molecules, and to understand their properties. To that end, we often need to calculate the electronic properties (energy surfaces, dipole and transition moments, ro-vibrational states, etc.), as well as the interaction of the molecules with their environment (surrounding atoms, molecules, or external fields).

Recent Progress

Since the start of this Program (August 1st 2005), we have worked on several projects. During FY 2012, we have made progress on 4 main axes of research: 1) Rydberg-Rydberg interactions, 2) Energy surfaces and reactions, 3) Long-range interaction between diatomic (homonuclear and heteronuclear) molecules, and 4) Formation of dimers and tetramers. Below, we refer to DOE supported articles during the last three years only; new articles published since the last annual report filling (August 2011) are listed as [N...], while those of the prior years since 2009 by [P...].

1) Rydberg-Rydberg interactions

We extended our previous work on Rydberg-Rydberg interactions explaining spectral features observed in ^{85}Rb experiments, namely resonances correlated to the $69p_{3/2} + 71p_{3/2}$ asymptote [J. Stanojevic *et al.*, *Eur. Phys. J. D* **40**, 3 (2006)], and to $69d + 70s$ asymptote [J. Stanojevic *et al.*, *Phys. Rev. A* **78**, 052709 (2008)], to investigate the existence of potential wells of doubly-excited atoms due to ℓ -mixing. In our previous work [P1], we showed the existence of potential wells for 0_g^+ symmetry of doubly-excited atoms, and that these wells are robust against small electric fields, and support many bound states.

In [N1], we continued and extended our calculations of potential wells for other molecular symmetries (0_u^- and 1_u) of Rb_2 Rydberg macrodimers, and obtained their n -scaling of the equilibrium depth and separation. We also computed bound levels, and showed that their lifetimes are limited by the lifetime of the Rydberg atoms themselves. We study how these vibrational levels could be populated via photoassociation, and how the signature of the ad-mixing of various ℓ -character producing the potential wells becomes apparent in photoassociation spectra. Finally, we have started to explore the possibility of forming metastable long-range *macrotrimers* made of three Rydberg [N2]. Our preliminary results show the existence of shallow (roughly 20 MHz deep) long-range wells for three Rydberg atoms forming a linear molecule.

2) Energy surfaces and reactions

A recent effort in my group towards reactive scattering involving cold molecules and molecular ions has started with the calculation of potential energy surfaces (PES). In our previous work, we

studied PES for trimers, such as the lowest doublet electronic state of Li_3 ($1^2A'$) [P2], or the lowest $^2A''$ surface arising from the $\text{Li}_2[X^1\Sigma_g^+]+\text{Li}^*[^2P]$ interaction [P3]. In [N3], we extended this work to obtain accurate long-range *ab initio* PES for the ground state X^2A' of Li_3 in the frozen diatom approximation using all electron RCCSD (T). We also obtained molecular van der Waals dispersion coefficients and three-body dispersion damping terms for the atom-diatom dissociation limit and showed them to be an essentially exact representation of the *ab initio* surface at long range.

Together with my collaborators, we have studied the collisions of trapped molecules with slow beams, particularly of $\text{OH}(J = \frac{3}{2}, M_J = \frac{3}{2})$ molecules with ^4He atoms [P4], and demonstrated the importance of including the effects of non-uniform trapping fields. More recently, we computed rate coefficients for reaction and vibrational quenching of the ultracold collision $\text{D} + \text{H}_2(v, j = 0)$ for a wide range of initial vibrationally excited states v [N4]. The v -dependence of the zero-temperature limit shows two distinct regimes: a barrier dominated regime for $0 \leq v \leq 4$, and a barrierless regime for $v \geq 5$. We found an approximate conservation of the internal vibrational energy, which should allow us to obtain approximate expressions for reactive scattering problems.

We extended our previous work on the structure of K_2Rb_2 tetramers and thermochemistry relevant to $\text{KRb}+\text{KRb}$ collisions and reactions [P5] to all possible alkali tetramers formed from $\text{X}_2+\text{X}_2 \rightarrow \text{X}_4$, $\text{X}_2+\text{Y}_2 \rightarrow \text{X}_2\text{Y}_2$, and $\text{XY}+\text{XY} \rightarrow \text{X}_2\text{Y}_2$ association reactions [N5]. For all alkali metals, we also found two stable structures for the tetramers, rhombic (D_{2h}) and planar (C_s), and that there are barrier-less pathways for the formation of tetramers from dimer association reactions.

Finally, we have continued our new effort on molecular ions, carefully calculating their energy surface and transition dipole moments. We started with alkaline-earth elements, since they can be cool to very low temperatures. In [P6], we reported *ab initio* calculations of the $X^2\Sigma_u^+$ and $B^2\Sigma_g^+$ states of Be_2^+ , and found two local minima, separated by a large barrier, for the $B^2\Sigma_g^+$. We extended this work to Ca_2^+ in [N6], computing the PES of the $X^2\Sigma_u^+$, $B^2\Sigma_g^+$, and $^2\Pi_u$ states. Again, we found a double well for $B^2\Sigma_g^+$ (its barrier is however below threshold). We also computed the spectroscopic constants, bound vibrational levels, transition moments and lifetimes in this state.

3) Long-range interaction between diatomic molecules

In our previous work on K_2Rb_2 [P5], we calculated the minimum energy path for the reaction $\text{KRb}+\text{KRb} \rightarrow \text{K}_2+\text{Rb}_2$ and found it to be barrierless. However, we recently showed that long-range barriers originating from the anisotropic interaction due to higher electrostatic, induction, and dispersion contributions could exist and stabilize a molecular sample [N7]. In addition, we showed that by changing the orientation of the molecules using an external DC electric field, and by varying its strength, one could control the effective inter-molecular interaction, switching it from attractive to repulsive (and vice-versa). Recently, we generalized our treatment to the long-range interaction between homonuclear alkali dimers [N8], where there are still anisotropic interactions (e.g. due to quadrupolar terms). Finally, we extended this work to the case of heteronuclear diatomic alkali molecules [N9]; in addition to the multipole expansion and van der Waals terms, we also give an analytic expression for molecules in an external (weak) DC electric field.

4) Formation of dimers and tetramers

In previous papers sponsored by DOE [E. Juarros *et al.*, PRA **73**, 041403(R) (2006), E. Juarros *et al.*, JPB **39**, S965 (2006), N. Martinez de Escobar *et al.*, PRA **78**, 062708 (2008)], we explored the formation of homo- and hetero-nuclear diatomic molecules in their ground electronic state from one- and two-photon photoassociative processes [P6]. We also worked on using many coherent laser pulses [E. Kuznetsova *et al.*, PRA **78**, 021402(R) (2008)], and Feshbach resonances [P. Pellegrini

et al., PRL **101**, 053201 (2008)] to increase the formation rate of ultracold diatomic molecules [P7, P8, P9]. We recently started to explore how Feshbach resonances could enhance the pump-dump scheme to produce ground state molecules [N10], and we are using the same approach to investigate the possible formation of tetramers [N11]. In fact, by controlling the long-range interaction between polar diatomic molecules using external DC electric field [N9], we could increase the shorter-range overlap of the continuum and excited states (as in FOPA [P8, P9]), and thus the formation rate of tetramers.

Future Plans

In the coming year, we expect to carry more calculations on Rydberg-Rydberg interactions, especially the possibility of forming metastable long-range *macrotrimers* made of three Rydberg. We will continue and extend our work on computing electronic properties of molecules (PES and moments), especially for the molecular ions, where not much is available. We plan to extend our work on the long-range interaction between molecules to more complex systems (e.g. diatomic + triatomic molecules, etc.). Finally, we will investigate in detail paths to form larger ultracold molecules by controlling the inter-molecular interactions in order to enhance formation rate.

New DOE sponsored publications since August 2011

- N1. Nolan Samboy and Robin Côté, *Rubidium Rydberg macrodimers*, J. Phys. B **44**, 184006 (2011).
- N2. Nolan Samboy and Robin Côté, *Rydberg macrotrimers: long-range linear triatomic molecules*. In preparation: to be submitted to Phys. Rev. Lett.
- N3. Jason N. Byrd, H. Harvey Michels, John A. Montgomery, Jr., and Robin Côté, *Long-range three-body atom-diatom potential for doublet Li_3* , Chem. Phys. Lett. **529**, 23 (2012).
- N4. Ion Simbotin, Subhas Ghosal, and Robin Côté, *A case study in ultracold reactive scattering: $D + H_2$* , Phys. Chem. Chem. Phys. **13**, pp. 19148-19155 (2011).
- N5. Jason N. Byrd, H. Harvey Michels, John A. Montgomery, Robin Côté, and William C. Stwalley, *Structure, energetics, and reactions of alkali tetramers*, J. Chem. Phys. **136**, 014306 (2012).
- N6. Sandipan Banerjee, John A. Montgomery, Jr., Jason N. Byrd, H. Harvey Michels, and Robin Côté, *Ab initio potential curves for the $X\ ^2\Sigma_u^+$, $A\ ^2\Pi_u$, and $B\ ^2\Sigma_g^+$ states of Ca_2^+* , Chem. Phys. Lett. **542**, 138-142 (2012).
- N7. Jason N. Byrd, John A. Montgomery, and Robin Côté, *Controllable Binding of Polar Molecules and Metastability of One-Dimensional Gases with Attractive Dipole Forces*, Phys. Rev. Lett. **109**, 083003 (2012).
- N8. Jason N. Byrd, Robin Côté, and John A. Montgomery, *Long-range interactions between like homonuclear alkali metal diatoms*, J. Chem. Phys. **135**, 244307 (2011).
- N9. Jason N. Byrd, John A. Montgomery, and Robin Côté, *Long range forces between polar alkali diatoms aligned by external electric fields*. Submitted to Phys. Rev. A. See also [arXiv:1207.3546](https://arxiv.org/abs/1207.3546).
- N10. M. Gacesa, I. Simbotin, J.N. Byrd, S. Ghosal, and R. Côté, *Enhanced formation of alkali dimers using a pump-dump scheme near a Feshbach resonance: the case of $LiRb$* . In preparation (to be submitted to Phys. Rev. A).
- N11. J.N. Byrd, S. Ghosal, and R. Côté, *The formation of tetramers of alkali metals by controlling inter-molecular interactions*. In preparation (to be submitted to Phys. Rev. Lett.).

Prior DOE sponsored publications since 2009

- P1. N. Samboy, J. Stanojevic, and R. Côté, *Formation and properties of Rydberg macrodimers*, Phys. Rev. A **83**, 050501(R) (2011).
- P2. J.N. Byrd, J.A. Montgomery (Jr.), H.H. Michels, and R. Côté, *Potential energy surface of the $1^2A'$ Li_2+Li doublet ground state*, Int. J. of Quantum Chem., **109**, Issue 13, pp. 3112-3119, 5 November (2009).
- P3. J.N. Byrd, J.A. Montgomery (Jr.), H.H. Michels, and R. Côté, *Electronic Structure of the Li_2 [$X^1\Sigma_g^+$] + $LI^*[P_2]$ Excited A'' Surface*, Int. J. of Quantum Chem **109**, 3626 (2009).
- P4. T. V. Tscherbul, Z. Pavlovic, H. R. Sadeghpour, R. Côté, and A. Dalgarno, *Collisions of trapped molecules with slow beams*, Phys. Rev. A **82**, 022704 (2010).
- P5. J.N. Byrd, J.A. Montgomery (Jr.), and R. Côté, *Structure and thermochemistry of K_2Rb , KRb_2 and K_2Rb_2* , Phys. Rev. A **82**, 010502 (2010).
- P6. S. Banerjee, J. N. Byrd, R. Côté, H. H. Michels, J. A. Montgomery, Jr. *Ab initio potential curves for the $X^2\Sigma_u^+$ and $B^2\Sigma_g^+$ states of the Be_2^+ : Existence of a double minimum*, Chem. Phys. Lett. **496**, 208 (2010).
- P7. E. Juarros, K. Kirby, and R. Côté, *Formation of ultracold molecules in a single pure state: LiH in $a^3\Sigma^+$* . Phys. Rev. A **81**, 060704 (2010).
- P8. P. Pellegrini, and R. Côté, *Probing the unitarity limit at low laser intensities*. New J. Phys. **11**, 055047 (2009).
- P9. E. Kuznetsova, M. Gacesa, P. Pellegrini, S.F. Yelin, and R. Côté, *Efficient formation of ground state ultracold molecules via STIRAP from the continuum at a Feshbach resonance*. New J. Phys. **11**, 055028 (2009).
- P.10 J. Deiglmayr, A. Grochola, M. Repp, R. Wester, M. Weidemüller, O. Dulieu, P. Pellegrini, and R. Côté, *Influence of a Feshbach resonance on the photoassociation of $LiCs$* . New J. Phys. **11**, 055034 (2009).

Optical Two-Dimensional Spectroscopy of Disordered Semiconductor Quantum Wells and Quantum Dots

Steven T. Cundiff

JILA, University of Colorado and NIST, Boulder, CO 80309-0440

cundiff@jila.colorado.edu

August 24, 2012

Program Scope: The goal of this program is to implement optical 2-dimensional Fourier transform spectroscopy and apply it to electronic excitations, including excitons, in semiconductors. Specifically of interest are quantum wells that exhibit disorder due to well width fluctuations and quantum dots. In both cases, 2-D spectroscopy will provide information regarding coupling among excitonic localization sites.

Progress: Semiconductor quantum dots (QDs) are promising candidates for applications in quantum information technologies and devices relying on coherent nonlinear light-matter interactions. A current limitation to the scalability of devices beyond the single or few QD limit is the strong influence of the three-dimensional confinement potential on the emission and dephasing properties of multi-particle states including excitons, biexcitons and trions. The experimental workhorse for measuring these properties for single QDs has been spectrally- and time-resolved photoluminescence. Single QD studies show variation of the biexciton binding energy with exciton emission energy, and perhaps more importantly, a large scatter of binding energies. These aspects impose challenges for utilizing QD ensembles in applications that rely on coherent exciton-biexciton interactions.

Theory has established that the biexciton binding energy depends on the relative strength of pair-wise direct Coulomb interactions, analogous to a mean-field approximation, and Coulomb correlations beyond mean-field [1, 2, 3, 4]. Nonlinear techniques such as transient absorption spectroscopy [5] and time-integrated four-wave mixing [6] provided insight into the influence of the confinement potential – and therefore Coulomb interactions – on the biexciton nonlinear response in QD ensembles, however these techniques cannot reliably distinguish between the effects of dephasing, inhomogeneity, and correlations between exciton and biexciton transition energies [7].

These ambiguities are eliminated by using optical two-dimensional Fourier-transform spectroscopy (2DFTS) [L]. Our measurements on an annealed InAs QD ensemble reveal that the biexciton energy is constant and essentially perfectly correlated with the exciton emission energy within the ground state inhomogeneous distribution. Values in the literature typically show a decrease in the biexciton binding energy with increasing emission energy at a rate ranging from 0.025 to 0.1 [3], with significant dot-to-dot scatter. Despite significant experimental and theoretical progress towards understanding the influence of confinement on Coulomb interactions in QDs, the effects of confinement on the biexciton binding energy and exciton-biexciton correlated broadening have been difficult to establish.

2DFTS has not previously been used to study InAs QDs, which exhibit stronger confinement and longer dephasing times than GaAs QDs [H] but have a weaker nonlinear response because of smaller dipole moments. 2DFTS has advantages over other nonlinear experiments because it simultaneously measures the inhomogeneous and homogeneous line widths within the ensemble, reveals coherent coupling between transitions [8] and clearly separates biexciton and exciton contributions to the nonlinear response [B]. We measured the $\chi^{(3)}$ and $\chi^{(5)}$ nonlinear response of excitons, biexcitons, and trions using a combination of co- and cross-linear polarizations for various excitation intensities. The sample consisted of 10 quantum-mechanically isolated self-assembled InAs/GaAs QD layers epitaxially grown on a GaAs (100) substrate. The sample is thermally annealed post-growth at 900 °C for 30 seconds. Electron-hole exchange couples the exciton spin states, forming two linear orthogonally-polarized states split by the fine-structure splitting (Δ_{FSS}) for an asymmetric confinement potential [9]. Exciton states are excited by linearly polarized pulses, whereas two-exciton states can be excited by two co-linearly polarized pulses, which form a four-particle state that is red-shifted (blue-shifted) from the two-exciton state by a positive (negative) biexciton binding energy, Δ_{XX} .

2D spectra are shown for the highest excitation power in Figs. 1(a) and 1(b) for co-linearly (HHHH) and cross-linearly (HV VH) polarized excitation and detection. The spectra are normalized to the strongest peak. The maximum amplitude for HHHH polarization is approximately two orders of magnitude larger than for HV VH polarization. In a strongly inhomogeneously broadened system, the line width of a slice taken along the diagonal provides the inhomogeneous line width but is limited by the excitation spectrum in these experiments, whereas a slice perpendicular to the diagonal, shown in the inset of Fig. 1(a), measures the homogeneous line shape [F]. For HV VH polarization, additional peaks appear shifted above and below the diagonal line by equal energy.

The states contributing to the features in Fig. 1 are identified by exploiting the dipole selection rules and comparing the 2D spectra to simulations. For HHHH polarization, excitons and biexcitons are optically accessible in neutral QDs, whereas only positively charged trions are optically excited in QDs with resident holes due to Pauli blocking. Because of inhomogeneity, the exciton and trion distributions overlap on the diagonal and are spectrally indistinguishable. The excitonic contribution is eliminated by using HV VH polarization for which no quantum mechanical pathways exist for the exciton. Local field effects, two-photon coherences and excitation-induced effects previously measured and calculated to generate a nonlinear response at the exciton energy in quantum wells for HV VH polarization are not present, verified through auxiliary measurements similar to negative delay two-pulse FWM experiments [E]. Therefore, the remaining spectral amplitude on the diagonal in Fig. 1(b) isolates the trion response. In charged QDs, optical excitation creates a single electron-hole pair, and the three-particle state forms a singlet trion. Identification of this feature as a trion resonance is further supported by a narrower line width for HV VH polarization by a factor of ≈ 1.5 consistent with time-resolved photoluminescence measurements of annealed InGaAs QDs showing positive trions having a longer radiative lifetime than excitons.

Suppression of the exciton for HV VH polarization enhances the biexciton relative amplitude, which is three orders of magnitude weaker than that of the exciton in the HHHH spectrum. Observed as beats in time-integrated FWM signals, the $\chi^{(3)}$ response of the bound biexciton has appeared in 2D rephasing spectra of GaAs quantum wells as a peak red-shifted from the diagonal along the emission energy axis $\hbar\omega_t$ by the biexciton binding energy Δ_{XX} [B], similar to peak XX_L observed in Fig. 1(b). An additional peak, XX_U in Fig. 1(b), appears above the diagonal red-shifted by Δ_{XX} along the *absorption* energy axis, $\hbar\omega_\tau$, for excitation intensities greater than 65 W cm^{-2} . A power dependence of the peak amplitudes for HV VH polarization indicates that XX_U increases quintically with power and thus is due to the $\chi^{(5)}$ biexciton nonlinear response, verified by simulations. For excitation intensities below 65 W cm^{-2} , $X+$ and XX_L increase cubically, confirming that the experiment is performed in the $\chi^{(3)}$ regime at low power. For both polarization schemes, the homogeneous line widths do not vary with the incident power. The exciton (γ_X), trion (γ_{X+}) and biexciton (γ_{XX_L}) cross-diagonal line widths are nearly constant within the ground state inhomogeneous distribution and are equal to 12, 8, and $35 \mu\text{eV}$, respectively, after deconvolving the spectrometer resolution. Interestingly, Δ_{XX} is equal to 2.3 meV for all emission energies within the ground state inhomogeneous distribution, with a statistical uncertainty of less than 1%.

Insight into the mechanisms responsible for the biexciton nonlinear response is attained by perturbatively expanding the equations of motion for the density matrix up to fifth-order in the applied field following a similar approach used in Ref. [7]. The calculations are performed using delta function pulses in time. Inhomogeneity is included as a two-dimensional Gaussian distribution for the exciton and biexciton energies with inhomogeneous line widths Γ_X and Γ_{XX} , respectively. We allow for uncorrelated broadening between the exciton \rightarrow ground and biexciton \rightarrow exciton

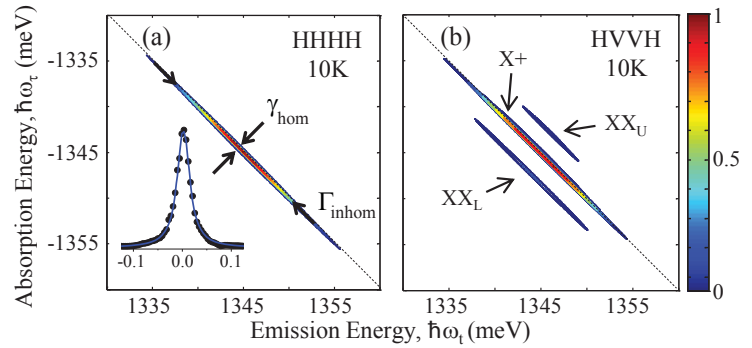


Figure 1: Rephasing spectra for co- and cross-linearly polarized excitation and detection for an excitation intensity of 200 W cm^{-2} are shown in (a) and (b), respectively. A cross-diagonal slice (points) at the peak and a $\sqrt{\text{Lorentzian}}$ fit (line) are shown in the inset to (a).

transitions. Perfect correlation (correlation coefficient $R = 1$) implies that for a specific exciton energy, the biexciton energy can be uniquely determined, whereas a fluctuating Δ_{XX} would result in $R < 1$. A positive Δ_{XX} is used for both $\chi^{(3)}$ and $\chi^{(5)}$ contributions to the simulated nonlinear response. For HVVH polarization, the trion peak X+ is modeled assuming only a single circularly polarized transition in a charged QD is optically accessible. Consequently we only consider quantum mechanical pathways for an exciton excited along this single transition.

The simulated spectra accurately reproduce the measured spectra for $R \geq 0.9999$, $\Gamma_{XX} = \Gamma_X$ and $\gamma_{XX} \leq 3 \cdot \gamma_X$. Both X+ and XX_L arise from the $\chi^{(3)}$ nonlinear response, whereas XX_U is only present when extending the simulation to fifth-order. The fraction of charged QDs is estimated by noting that the third-order polarization and the homogeneous line width are proportional to the fourth and second power of the dipole moment, respectively. We assume that a single dipole moment can characterize the quantum mechanical pathways leading to each multi-particle state. By measuring the peak amplitudes and line widths for both HHHH and HVVH polarization and relating them through the dipole moments, we estimate that 52% of the QDs are charged.

Perfectly correlated broadening and equal exciton-biexciton inhomogeneity presented here indicate that Coulomb effects dictating the biexciton renormalization energy are independent of the details of confinement in this system. Calculations using configuration interactions methods [1, 3, 4] established that the biexciton binding energy is positive only when Coulomb correlations beyond the mean-field limit are considered. Schliwa *et al.* calculate that direct pair-wise Coulomb interactions depend on the relative shape and position of wave functions in the QDs, whereas the strength of correlations are determined by the number of bound states and their relative energy level separation within the QDs. For a significant decrease in QD size (increase in emission energy), the number of confined states in the QDs and the influence of correlations are predicted to decrease, resulting in a transition from positive to negative binding energy. More importantly, if the fractional change in the number of bound states is small or zero with changing QD size, then the degree of correlation is unchanged and the biexciton binding energy is essentially unaffected.

The results presented here are consistent with this model, and we suggest that post-growth annealing of the sample is responsible. High-temperature annealing causes In/Ga intermixing and leads to an In gradient across the QD, which results in a more uniform QD distribution with a similar number of confined states and wave function distribution for all QDs in the ensemble. Consequently, the strength of Coulomb correlations is unaffected by changes in the exciton emission energy and the biexciton binding energy is constant.

Future Plans: We plan to continue to study ensembles of InGaAs quantum dots in the near future. Our initial results, discussed above, provide some interesting contrasts to prior single-dot work. To try to understand these differences, we will investigate samples that have not been annealed, which requires working at longer wavelengths. We have a new spectrometer that uses an optical parametric amplifier as a light source that will allow us to do this. In addition, we plan to study samples grown with both high densities of quantum dots, and low densities. The single dot studies all require the low density dots, so it will be interesting to see if our measurements can discern any differences.

Publication during the last 3 years from this project:

- A. I. Kuznetsova, P. Thomas, T. Meier, T. Zhang, and S. T. Cundiff, "Determination of homogeneous and inhomogeneous broadenings of quantum-well excitons by 2DFTS: An experiment-theory comparison," to appear in *Physica Status Solidi (c)* **6**, 445 (2009).
- B. A.D. Bristow, D. Karaiskaj, X. Dai, R.P. Mirin and S.T. Cundiff, "Polarization dependence of semiconductor exciton and biexciton contributions to phase-resolved optical two-dimensional Fourier-transform spectra," *Phys. Rev. B* **79**, 161305(R) (2009).
- C. S.T. Cundiff, T. Zhang, A.D. Bristow, Denis Karaiskaj and X.Dai, "Optical Two-Dimensional Fourier Transform Spectroscopy of Semiconductor Quantum Wells, *Acct. Chem. Res.* **42**, 1423 (2009).
- D. A.D. Bristow, D. Karaiskaj, X. Dai, T. Zhang, C Carlsson, K.R. Hagen, R. Jimenez and S.T. Cundiff, "A Versatile Ultra-Stable Platform for Optical Multidimensional Fourier-Transform Spectroscopy," *Rev. Sci. Instr.* **80**, 073108 (2009).
- E. D. Karaiskaj, A.D. Bristow, L. Yang, X. Dai, R.P. Mirin, S. Mukamel and S.T. Cundiff, "Two-Quantum Many-Body Coherences in Two-Dimensional Fourier-Transform Spectra of Exciton Resonances in Semiconductor Quantum Wells," *Phys. Rev. Lett.* **104**, 117401 (2010).

- F. M.E. Siemens, G. Moody, H. Li, A.D. Bristow and S.T. Cundiff, "Resonance lineshapes in two-dimensional Fourier transform spectroscopy," *Opt. Express* **18**, 17699 (2010).
- G. G. Moody, M. E. Siemens, A. D. Bristow, X. Dai, D. Karaiskaj, A. S. Bracker, D. Gammon, and S.T. Cundiff, "Spectral broadening and population relaxation in a GaAs interfacial quantum dot ensemble and quantum well nanostructure," *Phys. Stat. Sol. (b)* **248**, 829-832 (2011).
- H. G. Moody, M. E. Siemens, A. D. Bristow, X. Dai, D. Karaiskaj, A. S. Bracker, D. Gammon, and S. T. Cundiff, "Exciton-exciton and exciton-phonon interactions in an interfacial GaAs quantum dot ensemble," *Phys. Rev. B* **83**, 115324 (2011). [This paper was selected as an "Editors Suggestion" in Physical Review B]
- I. A.D. Bristow, T. Zhang, M.E. Siemens, S.T. Cundiff and R.P. Mirin, "Separating homogeneous and inhomogeneous line widths of heavy- and light-hole excitons in weaklydisordered semiconductor quantum wells," *J. Phys. Chem. B* **115**, 5365-5371 (2011).
- J. G. Moody, M. E. Siemens, A. D. Bristow, X. Dai, A. S. Bracker, D. Gammon, and S. T. Cundiff, "Exciton relaxation and coupling dynamics in a GaAs/AlGaAs quantum well and quantum dot ensemble," *Phys. Rev. B* **83** 245316 (2011).
- K. S.T. Cundiff, "Optical two-dimensional Fourier transform spectroscopy of semiconductor nanostructures," *J. Opt. Soc. Am. B* **29**, A69-A81 (2012).
- L. S.T. Cundiff, A.D. Bristow, M. Siemens, H. Li, G. Moody, D. Karaiskaj, X. Dai and T. Zhang, "Optical Two-Dimensional Fourier Transform Spectroscopy of Excitons in Semiconductor Nanostructures (Invited)," *IEEE J. Spec. Topics Quantum Electr.* **18**, 318-328 (2012).
- M. D. B. Turner, P. Wen, D. H. Arias, K. A. Nelson, H. Li, G. Moody, M. E. Siemens, and S. T. Cundiff, "Measuring many-body interaction dynamics in GaAs quantum wells using two-dimensional electronic correlation spectroscopy," *Phys. Rev. B* **85**, 201303(R) (2012).

References

- [1] M. Braskén, M. Lindberg, D. Sundholm, and J. Olsen, "Full configuration interaction calculations of electron-hole correlation effects in strain-induced quantum dots," *Phys. Rev. B* **61**(11), 7652–7655 (2000).
- [2] M. Wimmer, S. V. Nair, and J. Shumway, "Biexciton recombination rates in self-assembled quantum dots," *Phys. Rev. B* **73**, 165305 (2006).
- [3] A. Schliwa, M. Winkelkemper, and D. Bimberg, "Few-particle energies versus geometry and composition of $\text{In}_x\text{Ga}_{1-x}\text{As}/\text{GaAs}$ self-organized quantum dots," *Phys. Rev. B* **79**(7), 075443 (2009).
- [4] M. Abbarchi, T. Kuroda, T. Mano, K. Sakoda, C. A. Mastrandrea, A. Vinattieri, M. Gurioli, and T. Tsuchiya, "Energy renormalization of exciton complexes in GaAs quantum dots," *Phys. Rev. B* **82**(20), 201301 (2010).
- [5] A. S. Lenihan, M. V. G. Dutt, D. G. Steel, S. Ghosh, and P. Bhattacharya, "Biexcitonic resonance in the nonlinear optical response of an InAs quantum dot ensemble," *Phys. Rev. B* **69**(4), 045306 (2004).
- [6] W. Langbein, P. Borri, U. Woggon, V. Stavarache, D. Reuter, and A. D. Wieck, "Control of fine-structure splitting and biexciton binding in $\text{In}_x\text{Ga}_{1-x}\text{As}$ quantum dots by annealing," *Phys. Rev. B* **69**(16), 161301 (2004).
- [7] S. T. Cundiff, "Effects of correlation between inhomogeneously broadened transitions on quantum beats in transient 4-wave-mixing," *Phys. Rev. A* **49**, 3114–3118 (1994).
- [8] S. T. Cundiff, "Coherent Spectroscopy of Semiconductors," *Opt. Express* **16**, 4639–4664 (2008).
- [9] M. Bayer, G. Ortner, O. Stern, A. Kuther, A. A. Gorbunov, A. Forchel, P. Hawrylak, S. Fafard, K. Hinzer, T. L. Reinecke, S. N. Walck, J. P. Reithmaier, F. Klopff, and F. Schäfer, "Fine structure of neutral and charged excitons in self-assembled $\text{In}(\text{Ga})\text{As}/(\text{Al})\text{GaAs}$ quantum dots," *Phys. Rev. B* **65**(19), 195315 (2002).

SISGR: Understanding and Controlling Strong-Field Laser Interactions with Polyatomic Molecules

DOE Grant No. DE-SC0002325

Marcos Dantus, dantus@msu.edu

Department of Chemistry and Department of Physics and Astronomy, Michigan State University, East Lansing MI 48824

We formally request continued funding for this project.

1. Program Scope

When intense laser fields interact with polyatomic molecules, the energy deposited leads to fragmentation, ionization and electromagnetic emission. The objective of this project is to determine to what extent these processes can be controlled by modifying the phase and amplitude characteristics of the laser field according to the timescales for electronic, vibrational, and rotational energy transfer. Controlling these processes will lead to order-of-magnitude changes in the outcome from laser-matter interactions, which may be both of fundamental and technical interest.

The proposed work involves experiments in which intense shaped laser pulses as short as 5fs in duration interact with a series of polyatomic molecules. Products of these interactions such as electrons, ions and photons, will be detected in order to provide valuable detailed information relevant to the electronic (<50 fs), vibrational (10-1000 fs) and rotational (1-100 ps) coherence time scales, as well as for intramolecular vibrational redistribution process (1-100 ps). The proposed work is unique because it seeks to combine knowledge from the field of atomic-molecular-optical physics with knowledge from the field of analytical chemistry, in particular ion chemistry. This multidisciplinary approach is required to understand to what extent the shape of the field affects the outcome of the laser-molecule interaction and to which extent the products depend on ion stability. The information resulting from the systematic studies will be used to construct a theoretical model that tracks the energy flow in polyatomic molecules following interaction with an ultrafast pulse.

2. Recent Progress

In the field of Coherent Control, there has always been some uncertainty and ambiguity as to what is coherent and to what extent coherence or decoherence plays a role in the various laser control experiments. When a laser pulse interacts with a molecule, the coherent response of the molecule may include rotational, vibrational and electronic quantum state coherence. Determining if electronic coherence plays a role in Coherent Control experiments has been very difficult because of the short timescales for electronic coherence, and because it is difficult to unravel the interference between the electric fields of the pump and probe laser pulses. For example, when two ultrashort pulses are scanned collinearly, they interfere, and this linear optical interference dominates the short time response of the molecule with the laser field in the timescale of the pulse duration.

Recently we introduced a novel method for creating replica pulses that have no frequencies in common and therefore exhibit no first-order linear optical interference. The method is known as Multiple Independent Comb Shaping, and it is based on the selection of independent sets of comb lines in the spectrum of the original laser pulse, and introducing a phase that delays one set of comb lines with respect to the other. With proper selection of the subset of comb lines, two pulses are created that have the same carrier frequency and bandwidth, but have no comb lines in common. The method is illustrated in Figure 1 (left). In the right hand, the interferometric signal is collected at the fundamental frequency (red) and at the frequency doubled signal (blue). Note that the fundamental frequency does not show sign of interference in this unique measurement.³ This allows us to untangle the contribution of the optical interference inherent in other time-resolved methods, with the true electronic coherence which involves molecular quantum mechanical states.

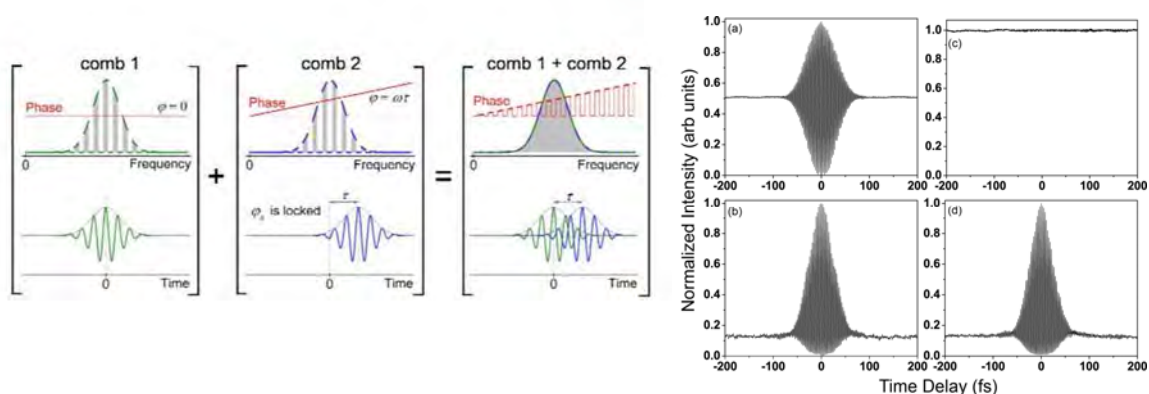


Figure 1: Left: Pulse shaping scheme for interferometric multiple independent comb shaping. Right: interferometric autocorrelation of the (a) fundamental, (b) SHG for a Michelson interferometer, and the interferometric autocorrelation of the (c) fundamental and (d) SHG using MICS. Note that there is no linear optical interference in trace (c) but the SHG autocorrelation is identical in both cases.

In order to simplify the physics and gain a better perspective of the physical processes that can be studied by MICS, we turned our attention first to cesium, a two-level atomic system, and then to an organic dye molecule, IR144, which has a well-known single photon excitation that is resonant with the central frequency of the laser pulses. Results from these simpler systems are shown in figure 2, and are much simpler to interpret.

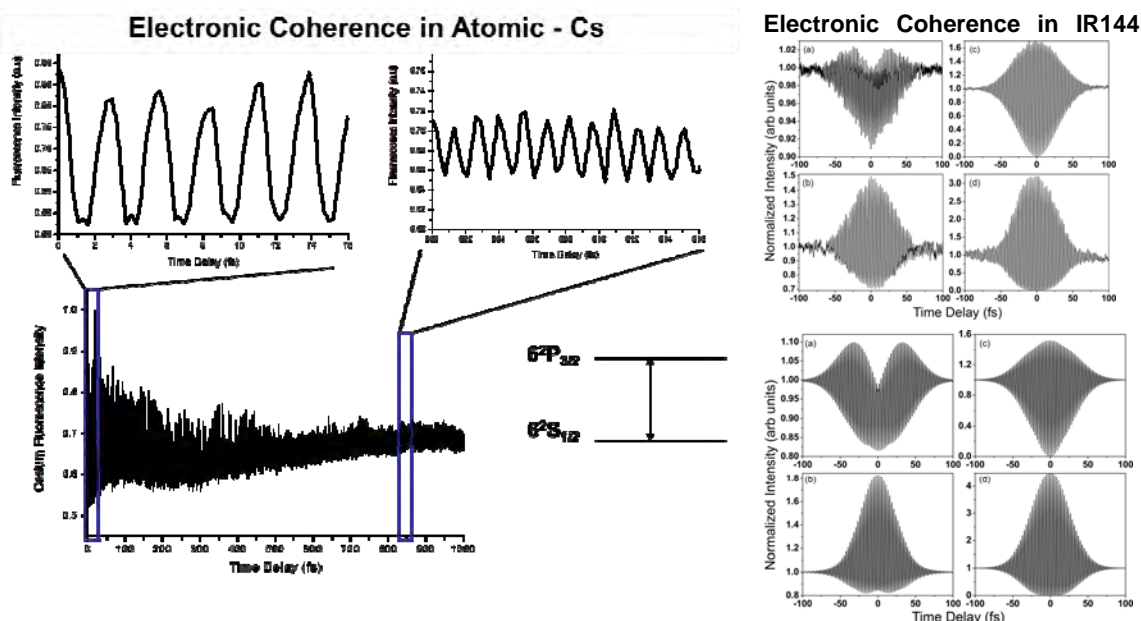


Figure 2: Left: Interferometric data obtained with two 800 nm pulses created using MICS as they interrogate atomic Cs at 50 °C, showing the expected long-lived electronic coherence between the ground and excited states. Right: Experimental results on IR144 in solution using two 800 nm pulses (left column MICS, and right column obtained with interfering pulses), given that this is a large molecule in condensed phase, the electronic coherence between the ground and excited states is short lived. Notice that fluorescence (panel c) is dominated by optical interference, but not for MICS (panel a). The stimulated emission transients are very similar because this is a nonlinear optical process. The results are modeled successfully by a two level system with fast relaxation.

Having confirmed that MICS allows us to prove electronic coherence, we turned our attention back to strong-field molecular fragmentation. Our initial studies found that most of the organic molecules that we had studied such as the nitrotoluenes and substituted acetophenones showed very short lived electronic coherence; on a time scale of the 35 fs pulses being used. We then turned our attention to a dicyclo-pentadiene a molecule that shows the clearest

evidence for formation of a long-lived (~ 400 fs) electronic coherence in the ion state. Results for DCPD are shown in Figure 3.

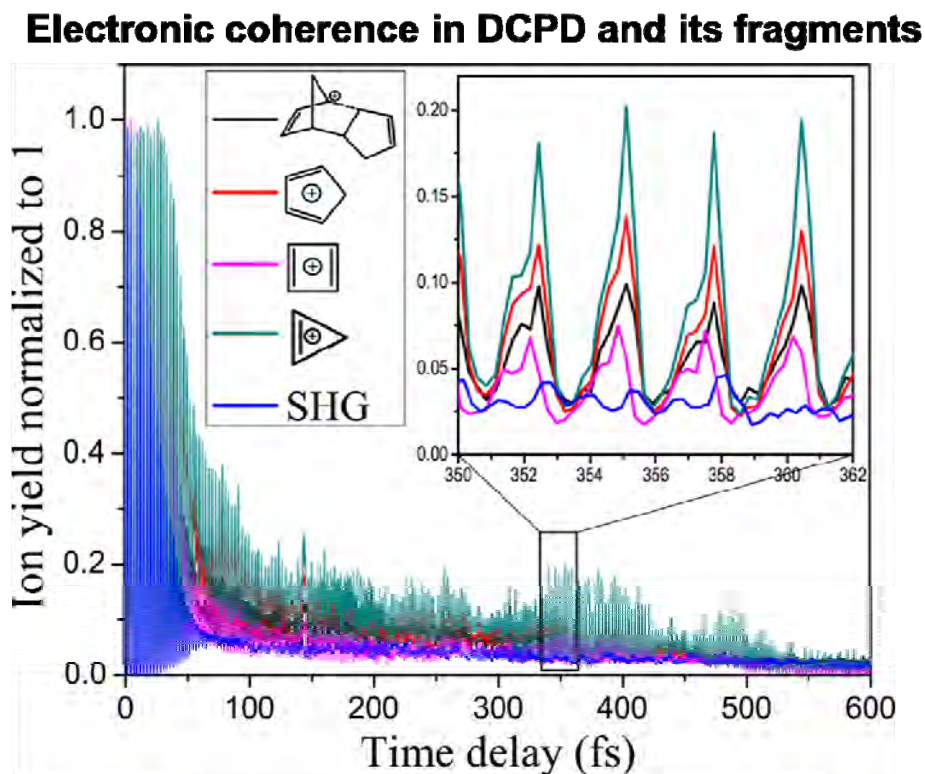


Figure 3: Experimental measurement using a pair of 800nm pulses created by MICS on gas phase dicyclopentadiene (DCPD) detected by time of flight mass spectrometry. The SHG shows that the laser pulses used for these experiments were ~ 35 fs in duration and the pulses show no pulse-pulse interaction beyond 75 fs. The zoomed-in area near 350 fs, shows the high-amplitude oscillations observed, in particular for the cyclo-pentadiene, cyclobutadiene, and cyclopropyl ions. The oscillations do not agree with any residual oscillation observed in the SHG signal (shown here as a reference) and are slightly different than the carrier frequency of the laser pulses.

We are in the process of completing the study on DCPD and hydroxy-substituted DCPD, where we discuss the observed electronic coherence and the fact that each of the different chemical photodissociation pathways observed show a different vibrational coherence signature within the first two-picoseconds. These results will be published soon, and will include results on coherent control of the reaction processes, with experimental demonstration that the control mechanism involves electronic coherence.

Summary:

- (a) We have developed a new method to explore electronic coherence that involves pairs of replica ultrafast pulses. The method can be used with ultrashort pulses at any wavelength and can be applied to study dynamics in gas, liquid, solid and plasma states of matter.
- (b) We have found a way to measure resonance-structure dynamics in substituted benzene compounds. This is a very significant observation that represents the first direct measurement of resonance structures as have been postulated by chemists for over 100 years. Resonance structures involve flow of electron density that is schematically shown as changes in the electronic structure of molecules. One paper has been published and a second will be published once we complete the DCPD and IR-144 manuscripts.
- (c) We have made direct measurements of the extent of electronic coherence during strong-field excitation of polyatomic molecules. Measurements on DCPD have uncovered the first evidence of long-lived electronic coherence during strong field laser-polyatomic molecule interactions. This will lead to two publications, one on the observation and a second one exclusively on coherent control.
- (d) Our experiments on IR-144 have led to detailed understanding of the early optical response of large organic molecules in solution, including the solvation Stokes shift. Our results have been confirmed through additional experiments as a function of temperature and molecular structure. Further studies on IR 144 by

exploiting the Phase and Amplitude Shaping have also been carried out to study the mechanism of decoherence in solution and a manuscript reporting the results is currently in preparation. Additional experiments using chirped pulses have led to a new theoretical model to interpret the early solvation dynamics. These results complete some of the earliest results in the field of laser control using chirped pulses. In particular we found that the magnitude of the chirp effect on fluorescence intensity and stimulated emission is a second order process on laser intensity but the shape of the chirp dependence is independent of laser intensity.

- (e) We are building a PEPICO instrument that will give us additional information about the electronic states involved in the strong field experiments.

3. Future Plans

- (a) We plan to complete the studies of IR144, IR125 and HDITCP in solution, these studies should provide an independent method to measure electronic coherence, dephasing and solvation effects using shaped pulses.
- (b) We plan to report on the electronic coherence involved in laser control of chemical reactions, in particular intense non-resonant fields. We have measured this for small molecules like oxygen and nitrogen, and for large molecules like DCPD. Our findings indicate that small molecules without resonant states (one-, two- or three-photon) show very short coherence time, but some large molecules with closely spaced electronic ion states show longer coherence times.
- (c) We plan to complete a set of measurements for a number of substituted acetophenones with electron withdrawing and electron donating groups in order to ascertain the observation of resonance structure dynamics as observed by pump-probe measurements.

One of the important goals of our proposed work was to upgrade our molecular beam in order to be able to carry out experiments in which photoelectron and photoions are detected in coincidence (PEPICO). The advantage of PEPICO will be that we will be able to determine how much energy was deposited in the molecule by the laser field to produce each of the different fragment ions. We will also be able to correlate the origin of the ejected electron with a specific fragment. All parts for that instrument have arrived, machining is almost complete and we have started the construction of the system.

Publications Resulting from this Grant

1. A. Konar, V. V. Lozovoy and M. Dantus, "Solvation Stokes-Shift Dynamics Studied by Chirped Femtosecond Laser Pulses", *J. Phys. Chem. Lett.* **3**, 2458-2464 (2012).
2. A. Konar, J. D. Shah, V. V. Lozovoy and M. Dantus, "Optical Response of Fluorescent Molecules Studied by Synthetic Femtosecond Laser Pulses", *J. Phys. Chem. Lett.* **3**, 1329-1335 (2012).
3. X. Zhu, V. V. Lozovoy, J. D. Shah and M. Dantus, "Photodissociation dynamics of acetophenone and its derivatives with intense nonresonant femtosecond pulses," *J. Phys. Chem. A* **115**, 1305-1312 (2011).

Picosecond x-ray diagnostics for third and fourth generation synchrotron sources

Matthew F. DeCamp
Department of Physics and Astronomy
University of Delaware, Newark, DE 19716
mdecamp@udel.edu
DOE Grant No: DE-FG02-11ER46816

1 Program Scope

The objective of this research program is to design and implement a series of experiments utilizing, or improving upon, existing time-domain hard x-ray diagnostics at a third generation synchrotron source. Specifically, the research program aims at three experimental projects to be explored in the grant cycle: 1) implementing a picosecond x-ray Bragg switch using a laser excited nano-structured metallic film, 2) designing a robust x-ray optical delay stage for x-ray pump-probe studies at a hard x-ray synchrotron source, and 3) building/installing a laser based x-ray source at the Advanced Photon Source for two-color x-ray pump-probe studies.

2 Recent Progress

During this first year of this three year grant, we have studied the laser induced dynamics in metallic thin films using both optical and hard x-ray probes. In particular, we have studied the generation of picosecond acoustic pulses with a gold photo-acoustic transducer as well as the ultrafast dynamics of optical phonons in a 20nm bismuth film.

Time-resolved x-ray diffraction of acoustic pulses

The first goal of this research plan is the use of an ultrafast photo-acoustic transducer to efficiently switch x-ray radiation on a picosecond timescale. In particular, we are trying to implement the phonon “Bragg switch” using a lithographically printed metallic grating on a crystalline substrate. This method has the potential of producing sub-picosecond x-ray bursts from a third generation synchrotron sources or it could be used to measure the hard x-ray pulse length of fourth generation x-ray synchrotron sources. While we have been waiting for access to the Advanced Photon Source (APS) at Argonne National Laboratories, we have begun preliminary experiments using a table-top laser-based picosecond x-ray source. In particular, we have recently published work in *Applied Physics Letters* [1], studying the generation and structure of a coherent acoustic pulse generated by a laser excited metallic film on a germanium substrate.

Upon ultrafast optical excitation, photo-electrons are generated in a layer consistent with the optical penetration depth ($\sim 15\text{nm}$) and then rapidly diffuse through out the entire 100nm thick film. Almost immediately, the hot-electrons cause the gold film to expand, causing a coherent acoustic pulse to propagate into the crystalline substrate. To probe the picosecond lattice dynamics, a time-resolved x-ray diffraction experiment was performed on the substrate crystal. The gold film is sufficiently thin to effectively be transparent

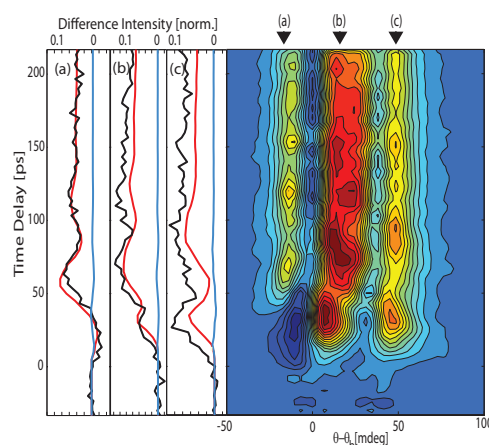


Figure 1: Differential time-resolved x-ray diffraction of a gold coated Germanium crystal. Experiment: black. Simulation: 100 nm (15 nm) strain pulse red (blue).

to the incoming x-ray radiation, making it possible to directly probe the propagating acoustic pulse in the substrate.

In figure 1, we show the results of the time-resolved x-ray diffraction experiment. Upon the generation of the acoustic pulse, we see significant sidebands on the x-ray diffraction peak, corresponding to the generation of acoustic wavevectors in crystalline substrate. In addition, we see no evidence of crystalline heating (i.e. peak shift), indicating that the diffraction sidebands are solely due to the generation and transmission of an isolated acoustic pulse from the laser excited gold film. This was confirmed by directly comparing the experimental results with x-ray diffraction simulations. The resulting diffraction sidebands have significant amplitude, indicating that the proposed “picosecond Bragg switch” could have efficiencies as large as 10%, sufficient for picosecond x-ray experiments at the APS.

Optical pump-probe studies of bismuth thin films

While an acoustic phonon Bragg switch has the potential of producing a picosecond x-ray pulse at a conventional third generation synchrotron source, the time-scale of the switch will be limited to the acoustic velocity in the substrate. To overcome this physical limitation, one can use a coherent optical phonon. These transitions can have vibrational periods in the 10s of femtoseconds, providing the potential of generating femtosecond x-ray pulses through the Bragg switch. We are investigating the possibility of using a nano-structured bismuth film as an optical phonon Bragg switch.

Prior experiments performed by the PI have demonstrated the possibility of generating high-wavevector optical phonons in Bismuth using a photolithographic engineered structure. To efficiently utilize the bismuth for an x-ray switch, because the optical penetration depth of the semi-metal is so small ($\sim 20\text{nm}$), it will be necessary to excite the large amplitude optical phonon in a thin film. In work recently published in the *Journal of Applied Physics* [2], we studied the dynamics of optical phonon generation in thin Bismuth films. In particular, although the we excited a “fully symmetric” optical phonon mode, we reported results indicating the phase and amplitude of the phonon is highly sensitive to the polarization states and incident angle of the pump-probe pulses (see figure 2). This is due to the presence of a surface plasmon resonance within the bismuth thin film, which significantly changes the dielectric properties and therefore the excitation mechanism of the optical phonon mode. These result may have implications on the use of metallic crystals in the use of the Bragg switch.

3 Work in Progress

Currently we are working on several parallel tracks towards the development of ultrafast x-ray tools at the APS. This includes designing a photolithographic mask for the acoustic phonon Bragg switch and construction of an x-ray delay line and pulsed x-ray source for x-ray pump/x-ray probe experiments. In addition, we are currently measuring the phonon generation in a variety of metallic thin films, paving a way to optimizing the Bragg switch.

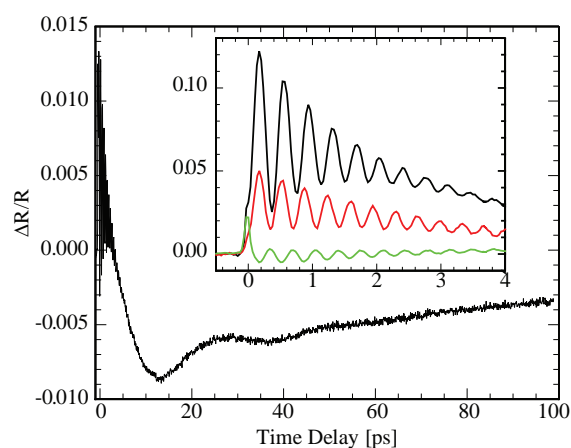


Figure 2: Optical pump-probe spectra of a 20nm thick bismuth thin film near a surface plasmon resonance. Femtosecond (picosecond) oscillations are due to a coherent optical (acoustic) phonon in the film. Polarization states: S-pump/S-probe (black), P-pump/S-probe (red), and P-pump/P-probe (green).

Time-resolved x-ray diffraction of a photo-acoustic transducer

In an effort to better understand the dynamics of the generated acoustic pulses for use in the photo-acoustic Bragg switch, we are currently studying the acoustic phonon generation process from a series of transducer geometries. In particular, we are utilizing differing thickness gold films to generate acoustic phonons with a distinct spatio-temporal structure, as well as measuring the absolute efficiency of the process by directly measuring the dynamics generated by the metallic films.

To directly measure the gold film dynamics, we have grown a quasi-single crystal 200nm gold film on a Germanium substrate. A time-resolved x-ray diffraction experiment of the gold (111) peak demonstrates that the optical excitation increases the temperature of the film by 100 degrees in under 10ps (see figure 3). This rapid increase is consistent with the diffusion of the hot-electrons at speed at least 6 times that of the sound velocity in the gold film.

Performing time-resolved x-ray experiments on the Germanium substrate, we determine the shape of the generated acoustic pulse that propagates into the substrate (see figure 4). These experiments confirm that the acoustic pulse shape is primarily determined by the film thickness, in particular, the generated wavevectors are directly proportional to the film thickness. When compared directly with a time-resolved x-ray diffraction of a bare Ge (111) substrate, the lattice dynamics are clearly different. In addition, it appears as though the electron dynamics in the gold film also play a role in the evolution time of the acoustic pulse.

We have recently had photolithographic time granted to us by the Center for Nanoscale Materials at Argonne National Lab to construct the prototype photoacoustic Bragg switch. The generated mask will allow us to generate a series of metallic gratings with differing wavevectors on a crystalline substrate, making it possible to have a tunable acoustic phonon switch. In addition, we anticipate that we will have beamtime at the APS within the next 6 months, providing a venue for testing the engineered acoustic phonon Bragg switch.

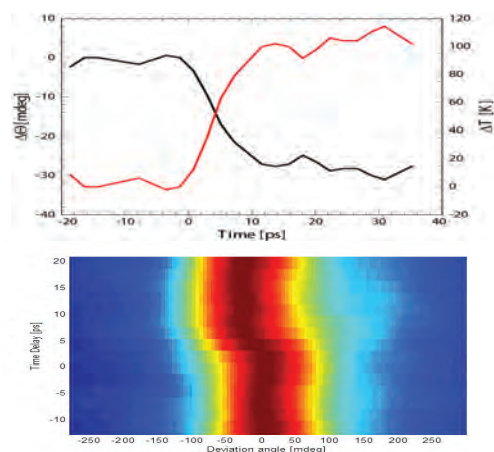


Figure 3: Bottom: Time-resolved x-ray diffraction of a 200nm quasi-single crystal gold film. Top: inferred lattice (black)/temperature (red) change as a function of time.

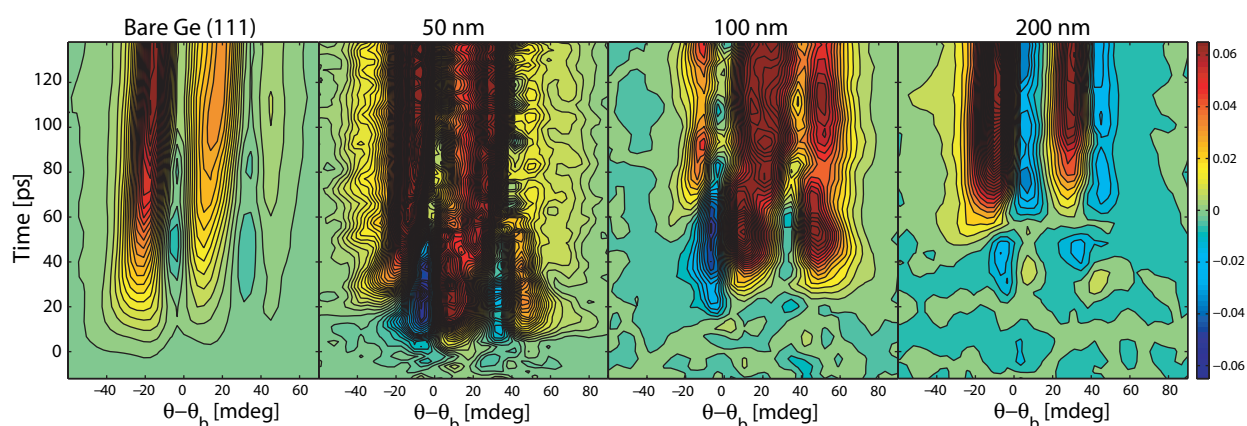


Figure 4: From left to right, the differential time-resolved x-ray diffraction of a bare germanium crystal, 50nm gold film on Ge, 100nm gold film on Ge, and 200nm gold film on Ge.

Construction of a pulsed x-ray source for Argonne National Labs

In addition to the construction of the x-ray Bragg switch, we are currently developing a series of pulsed x-ray tools for the APS for x-ray pump/x-ray probe spectroscopy. This includes the design and testing of a delay line for an x-ray pump-probe spectrometer and the construction of a laser-driven x-ray diode. The laser-driven diode is currently being constructed and tested at the University of Delaware. This diode will generate sufficient hard x-ray flux to have a viable x-ray probe of picosecond crystalline dynamics at the APS. When completed, we plan on installing this device at the APS for testing of an x-ray pump/x-ray probe experiment. In particular, the tunable x-ray pump pulse will be generated by the APS. Any x-ray dynamics will be probed using the picosecond x-ray diode and a conventional x-ray CCD camera.

Publications related to DOE funding

1. "Generation of acoustic pulses from a photo-acoustic transducer measured by time-resolved x-ray diffraction," Y. Gao and **M.F. DeCamp** *Applied Physics Letters* **100** 191903 (2012).
2. "Measurement of optical phonon dynamics in a bismuth thin film through a surface plasmon resonance" Z. Chen and **M.F. DeCamp**, *Journal of Applied Physics* **112** 013527 (2012).

Production and trapping of ultracold polar molecules

D. DeMille

Physics Department, Yale University, P.O. Box 208120, New Haven, CT 06520

e-mail: david.demille@yale.edu

Program scope: The goal of our project is to produce and trap polar molecules in the ultracold regime. Once achieved, a variety of novel physical effects associated with the low temperatures and/or the polar nature of the molecules should be observable. We have previously formed vibrationally excited RbCs molecules in an optical lattice trap. Recently, we have discovered an efficient method to produce and accumulate ultracold RbCs in its absolute rovibronic ground state, and are studying this as a means to produce large trapped samples. Molecules in such a sample will be stable against inelastic collisions and hence suitable for further study and manipulation. Once in place, we will study chemical reactions at ultracold temperatures, dipolar effects in collisions, etc.

Our group earlier pioneered techniques to produce and state-selectively detect ultracold heteronuclear molecules. These methods yielded RbCs molecules at translational temperatures $T < 100 \mu\text{K}$, in any of several desired rovibronic states—including the absolute ground state, where RbCs has a substantial electric dipole moment. Our previous method for producing ultracold, ground state RbCs consisted of several steps. In the first step, laser-cooled and trapped Rb and Cs atoms were bound into an electronically excited state via photoassociation (PA).¹ These states decayed rapidly into a few, weakly bound vibrational levels in the ground electronic state manifold.² We demonstrated the ability to transfer population from these high vibrational levels, into the lowest vibronic states $X^1\Sigma^+(v=0,1)$ of RbCs³ using a laser “pump-dump” scheme.⁴ We detect ground-state molecules with vibrational-state selectivity with a two-step, resonantly-enhanced multiphoton ionization process (1+1 REMPI) followed by time-of-flight mass spectroscopy. Subsequently, we incorporated a CO₂-laser based 1D optical lattice into our experiments. This made it possible to trap vibrationally-excited RbCs molecules as they were formed. The precursor Rb and Cs atoms could also be trapped with long lifetimes (>5 s). We

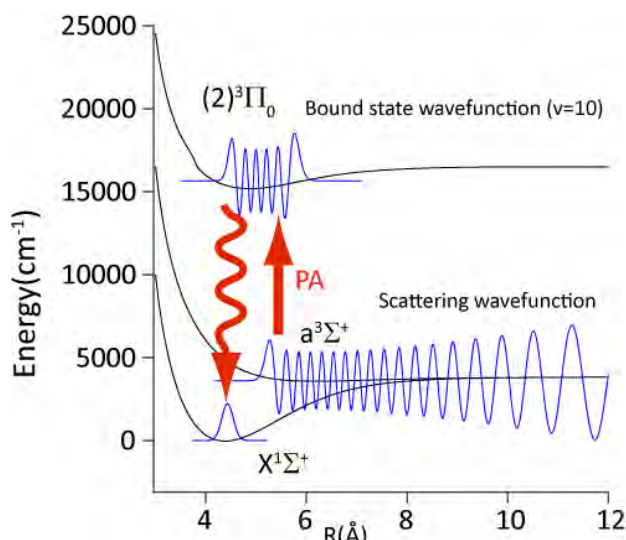


Fig. 1: Scheme for ground state molecule formation via direct short-range photoassociation.

used this capability to measure inelastic (trap loss) cross-sections for individual RbCs vibrational levels on both Rb and Cs atoms in the ultracold regime, and also developed a simple theoretical model for these collisions.⁵

We recently have focused on a new method to directly create rovibronic ground-state $X^1\Sigma^+(v=0, J=0)$ RbCs molecules (Fig. 1). The basic idea is to drive PA transitions into tightly-bound states of excited electronic potentials. Such states can in principle decay with high probability to the $X^1\Sigma^+(v=0, J=0)$ absolute ground state, which also has small internuclear separation. PA to short-range states was previously believed to be impractical, since in the WKB approximation

the scattering-state wavefunction of two colliding atoms has negligible amplitude at distances comparable to the separation of atoms in the molecular ground state.⁶ Hence, Franck-Condon factors (FCFs) for the free-to-bound PA transition were expected to be too small to drive efficiently.

Despite these expectations, recent observations from groups working on similar heteronuclear bi-alkali systems has shown that it is sometimes possible to drive PA transitions into tightly-bound states of excited electronic potentials. These include observations of short-range PA transitions in LiCs,⁷ NaCs,⁸ and RbCs.^{9,10} In all cases the PA rate was often found to be much larger than the naïve expectation, although the underlying mechanisms were sometimes unclear. For LiCs and NaCs it was found that PA to $J = 1$ levels was strongly suppressed; hence production of the rovibronic $X^1\Sigma^+(v=0, J=0)$ ground state via decay of a PA level could not be performed efficiently. In RbCs, the $J=1$ PA resonance was not suppressed; however, the state assignment of the short-range PA level was unclear, and thus so was the question of whether it could decay to the $X^1\Sigma^+(v=0)$ vibronic ground state.

In our recent work, we have found that formation of rovibronic ground-state RbCs via short-range PA is indeed viable, and in fact more favorable than any previously found case in other species. We first used our REMPI detection method to show that the short-range PA level of Ref. [9] indeed results in population of the $X^1\Sigma^+(v=0)$ state. Using existing spectroscopic data on RbCs,¹¹ we were able to assign the PA level definitively to the $2^3\Pi(0^-)$ state, which can decay to $X^1\Sigma^+$ only via a two-photon cascade. This led us to speculate that more efficient routes for population of $X^1\Sigma^+(v=0)$ could be found by using PA through the neighboring $2^3\Pi(0^+)$ state, which can decay to $X^1\Sigma^+$ directly via single photon emission. Again using existing spectroscopic data for state identification, we demonstrated PA into several vibrational levels of $2^3\Pi(0^+)$ state, with dramatically larger rates of $X^1\Sigma^+(v=0)$ formation than using the previously known resonance (Fig. 2).

We subsequently compared the rates of formation of $X^1\Sigma^+(v=0)$, via PA through different $2^3\Pi(0^+)[v']$ sublevels, to expectations based on FCFs for the free-bound and bound-bound transitions. We found excellent qualitative agreement, indicating that our description of

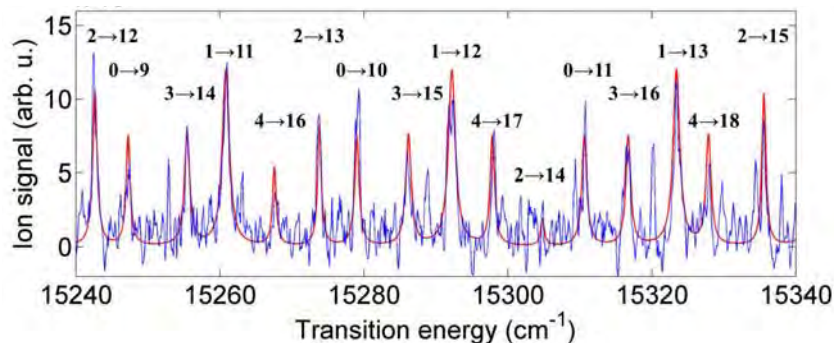


Fig. 2: Population of $X^1\Sigma^+(v=0)$ via short-range PA. The plot shows signal (blue) vs. detection laser frequency, with the PA laser tuned to the short-range $2^3\Pi(0^+)[v=10]$ state. The red curve is a simulated spectrum, based on known energies of the $X^1\Sigma^+(v'')$ and $2^3\Pi[v']$ states and FCFs for these transitions. Labels indicate the $(v'' \rightarrow v')$ quantum numbers of each transition. The only free parameters in the fit are an overall scale for the linewidth, and the relative populations of the $X^1\Sigma^+(v'')$ levels.

excitation and decay processes in terms of simple FCFs is valid. This model relies on no unusual circumstances such as resonant coupling between bound states or scattering resonances. Rather, it simply takes advantage of the fact that the triplet-state scattering wavefunction is considerably larger than would be expected based on the WKB approximation; and that (non-resonant) spin orbit coupling is strong in bi-alkali molecules containing Cs. We also demonstrated that the PA

transition could be fully saturated under typical experimental conditions, in agreement with calculated PA rates based on the FCFs. This means that formation of rovibronic ground state molecules can proceed at a rate given by the unitarity-limited scattering rate (i.e., the theoretical maximum PA rate), times the branching ratio $b \sim 0.3\%$ for decay of the $J = 1$ PA resonance into the $X^1\Sigma^+(v=0, J=0)$ state. We are now undertaking high-resolution “depletion spectroscopy” measurements¹² to explicitly verify that the $X^1\Sigma^+(v=0, J=0)$ is populated by the decay of the $J = 1$ PA resonance; we have already seen preliminary signals from $X^1\Sigma^+(v=0, J=1)$ levels populated by decay of the $J = 0$ PA resonance.

This method should make it possible to continuously produce and accumulate $X^1\Sigma^+(v=0, J=0)$ RbCs molecules into an optical trap. This is fundamentally different from existing approaches to form similar molecular samples, which use Feshbach-resonance association followed by stimulated optical transitions to the ground state.¹³ Here the dissipation associated with decay of the PA resonance allows irreversible accumulation. Key to this approach is that, unlike many heteronuclear alkali species, RbCs is immune to inelastic, chemically-reactive collisions with itself, and with Cs atoms. Hence, molecule production in the presence of a dense Cs vapor (and less dense Rb) can allow the accumulation of large molecular samples. In addition, the Cs atoms can act as a “scrubber” to remove residual rovibrationally-excited RbCs molecules that would otherwise accumulate in the trap, via inelastic collisions. We plan to explore the dynamics of the accumulation and scrubbing processes in an optical trap next.

Along with this main focus of our work, we recently completed an analysis of the full set of Cs₂ two-color PA data (previously described in part in Ref. [14]), with the goal to provide a more complete description of the coupled $^3\Sigma_u^+$ and $X^1\Sigma_g^+$ ground state potentials in Cs₂.¹⁵

References

- ¹A.J. Kerman *et al.*, Phys. Rev. Lett. **92**, 033004 (2004).
- ²T. Bergeman *et al.*, Eur. Phys. J. D **31**, 179 (2004).
- ³J.M. Sage, S. Sainis, T. Bergeman, and D. DeMille, Phys. Rev. Lett. **94**, 203001 (2005).
- ⁴A.J. Kerman *et al.*, Phys. Rev. Lett **92**, 153001 (2004).
- ⁵E. R. Hudson, N.B. Gilfoy, S. Kotochigova, J.M. Sage, and D. DeMille, Phys. Rev. Lett. **100**, 203201 (2008). [DOE SUPPORTED]
- ⁶W.C. Stwalley and H.J. Wang, J. Mol. Spectrosc. **195**, 194 (1999)
- ⁷J. Deiglmayr *et al.*, Phys. Rev. Lett. **101**, 133004 (2008)
- ⁸P. Zabawa, A. Wakim, M. Haruza, and N. P. Bigelow, Phys. Rev. A **84**, 061401(R) (2011).
- ⁹C. Gabbanini and O. Dulieu, Phys. Chem. Chem. Phys. **13**, 18905 (2011).
- ¹⁰Z. Ji *et al.*, Phys. Rev. A **85**, 013401 (2012).
- ¹¹Y. Lee, Y. Yoon, S. Lee, J.-T. Kim, and B. Kim, J. Phys. Chem. A **112**, 7214 (2008).
- ¹²D. Wang *et al.*, Phys. Rev. A **75**, 032511 (2007).
- ¹³S. Ospelkaus *et al.*, Science **327**, 853 (2010).
- ¹⁴D. DeMille *et al.*, Phys. Rev. Lett. **100**, 043202 (2008). [DOE SUPPORTED]
- ¹⁵S. Sainis, J. Sage, E. Tiesinga, S. Kotochigova, T. Bergeman, and D. DeMille. [DOE SUPPORTED]

SPATIAL-TEMPORAL IMAGING DURING CHEMICAL REACTIONS

Louis F. DiMauro
Co-PI: Pierre Agostini
Department of Physics
The Ohio State University
Columbus, OH 43210
dimauro@mps.ohio-state.edu
agostini@mps.ohio-state.edu

1.1 PROJECT DESCRIPTION

This document describes the BES funded project (grant #: DE-xx) entitled “Spatial-temporal imaging during chemical reactions” at The Ohio State University (OSU). Imaging, or the determination of the atomic positions in molecules is of central importance in physical, chemical and biological sciences. X-ray and electron diffraction are well-established method to obtain static images with sub-Angstrom spatial resolution. However their temporal resolution is limited to picoseconds. This proposal builds on the “molecule self-imaging” approach, based on bursts of coherent electron wave packets emitted by the molecule under interrogation itself when irradiated by an intense laser. We will investigate two complementary self-imaging methods: Laser-Induced Electron Diffraction (LIED) [1] and high harmonic tomography [2, 3]. In both, the scaling of strong-field interactions at long wavelengths is used to improve the fundamental imaging principles.. Concurrently, high harmonic molecular tomography providing spatio-temporal imaging of the electronic molecular orbitals will be investigated.

Progress over the past year include: (1) a demonstration that LIED at long wavelength enables femtosecond resolution together with atomic precision [4]. (2) The development of experimental techniques to achieve a complete measurement of the harmonics amplitude and phase which are required for the tomographic reconstruction of the Dyson orbital.

1.2 PROGRESS IN FY12: THE LASER INDUCED ELECTRON DIFFRACTION

The LIED approach is one of the molecules self-probing technique which can be compared to the conventional electron diffraction (CED). In CED, an external multi-kilovolt electron beam elastically scatters from a molecular gas sample and the resulting small-angle, forward-scattering, diffraction pattern contains information on the molecular structure. The bond-length information can be retrieved from the pattern, provided some approximations. One key-point is that the high-energy electrons penetrate the core and thus, the short range atomic-like potential dominates the electron-molecule, while the bonding valence electrons look transparent. This situation enables the independent atom model scattering can be described by the contribution from individual atoms, and an interference term between atoms (molecular term).

In LIED, one simply records the photoelectron momentum distribution produced by the molecule irradiated by a strong mid-infrared laser. Electron energies much lower than in CED (100 eV under typical conditions) are used, but very large angle scattering can be detected and furthermore the scattering cross-section can be retrieved for different energies by recording the photoelectron momentum distribution. Since the spatial resolution is directly dependent on the momentum transfer at rescattering, it can be high even at the electron energies allowed by the laser interaction. Besides, LIED contains information on the time difference between the instant when the electron is extracted and the instant when it is scattered by the molecule. These two times are separated by an interval, which is easily obtained from the classical equation of motion of the photoelectron driven from and back to the molecule by the laser field. There lies the principle of time-resolved imaging built into LIED since this time can be acted upon by tuning the laser wavelength.

The QRS model [5] postulates that the differential scattering cross-section is the product of the field-free differential cross-section, which contains the angular dependence, and an angle-independent factor, which contains all the effects of the field. The model provides the connection between the photoelectron momentum distribution and the scattering cross-section. The differential cross-section versus scattering angle and energy can be retrieved from the momentum distribution using the standard methods of the conventional electron diffraction. The laser acts, first, as a source of photoelectrons and second, as a clock which controls the emission and scattering times.

LIED on atoms. The LIED experiments on atoms are discussed first, followed by the results on molecules, and, especially the important aspect of the time information or, in other words, our first vibrating molecule movie.

It is important to test the core-penetrating properties of the photoelectrons driven back to the interrogated object by the strong laser field. Argon atoms have been chosen as the target for such a test. From the high-resolution experimental momentum distributions (energies up to 300 eV) obtained with a mid-infrared laser ($\lambda=2 \mu\text{m}$) we extract the differential cross-sections using the QRS model, show that above 100 eV at large angles they are nearly the same for neutral atoms and singly-charged ions, and that the returning electron wave packets, when scaled in field units, obey a simple universal scaling law, displaying no target dependence. This demonstrates the close collision nature of the LIED process in the long wavelength limit, an essential property for studying the molecular structures (Fig.1).

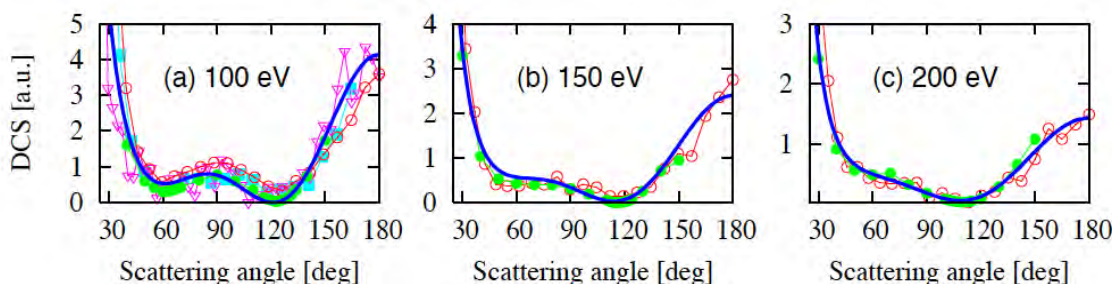


Fig. 1 Comparison of retrieved, theoretical, and conventional electron diffraction scattering differential cross-sections versus scattering angle and three different electron energies extracted from momentum distributions of photoelectrons emitted by argon atoms at different laser wavelengths and intensities (unpublished).

LIED on molecules: Time-dependent imaging.

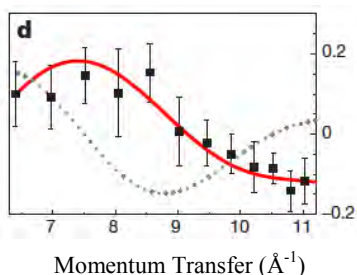


Fig.2 Experimental (dots), fit (red line) and calculated molecular contrast factor for equilibrium bond length (grey dotted line) versus momentum transfer.

Applying the same method on oxygen and nitrogen molecules for several laser wavelengths and intensities allows extracting the bond lengths under different irradiation conditions. An utmost interesting case is that of O_2 for which the molecular contrast factor extracted from the photoelectron momentum distribution and which, according to the well-established methods of CED contains the bond-length information [4], shows a severe discrepancy with the theoretical calculation assuming the equilibrium bond-length (Fig.2). This appears to suggest that the molecule was caught in an excited vibration state at the moment of scattering. Measurements carried out with different laser wavelengths indeed support this interpretation. The red curves depict the

evolution of the nuclear wave packet's center, computed in the Frank–Condon approximation (Fig.3) [1].

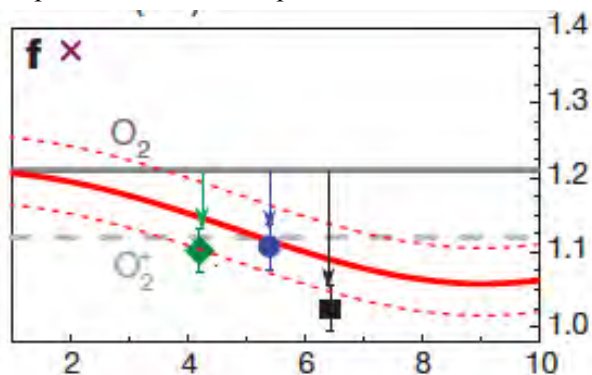


Fig.3 Oxygen bond length versus time extracted from the measurement at three mid-infrared wavelengths (symbols) compared to the equilibrium distances of O_2 and O_2^+ and the Frank-Condon prediction (red).

In this experiment the time resolution is provided by the laser optical period (and therefore by the wavelength). Several assumptions underline this conclusion, to be systematically investigated in the next period of the grant: in particular the nature of the laser-driven electron trajectory and the neglect of the multiple returns.

1.3 PROGRESS IN FY12: TOMOGRAPHIC APPROACH

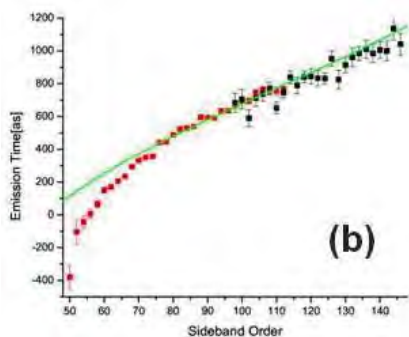


Fig.4 Emission times versus order compared to the classical prediction (unpublished).

The first spectral phase measurements of high harmonics at long wavelength, over a large number of harmonic orders, when compared to the classical predictions, show a clear discrepancy at low orders, which is still under investigation. This effect appears, at this time, to be connected to the Gouy phase of the focusing optics and is still under investigation. (See the Attosecond and Ultrafast X-ray report for more details). Since the tomographic retrieval of the molecular Dyson orbital depends on the harmonic amplitude and phase [3], it is crucial to thoroughly understand and control the measurement.

1.5 FUTURE PLANS

LIED: We will focus on fundamental studies and applications of the LIED: 1) the limits of spatial precision, the influence of multiple trajectories (long versus short and higher-order returns) on temporal precision, the dependence of the ionization rate on molecular alignment and the applicability of theoretical tools developed for CED analysis to LIED. 2) Applications of LIED to determining or observing structure changes in simple or complex systems; studies on isomeric systems and pump-probe interrogations.

Larger molecules pose new challenges on experimental precision and theoretical methods. The inverse Fourier transform of the LIED image will be explored as an alternate structural retrieval method along with coordinated efforts to improve the data statistics using a VMI spectrometer under development.

Tomography: Tomography with long wavelength drivers is a very interesting approach of the fundamentals of strong-field-molecule interaction with, in principle, improved performances. We plan 1) bench-marking the long wavelength tomography of N₂ and CO₂. 2) Experiments on the rather different, open-shell NO molecule which has a permanent dipole and a 2p_xπ or 2p_yπ HOMO (or a linear combination) ground state.

Imaging chemical dynamics using LIED and Tomography: It may now be possible to image the changing nuclear position or molecular orbits of electrons that define a chemical bond, as it breaks either with LIED or tomography. We will try to follow unimolecular dissociation using pump-probe schemes implemented in LIED and tomography: possibly but not only, the breaking of the I-C bond in aligned ICN (I_p = 10.8 eV) by exciting from its ground state to its lowest excited, repulsive A state. The molecules will be first aligned and the A-X transition excited by a 25 fs UV pulse at the first revival. LIED will use the VMI while for tomography, a series of harmonic spectra will be recorded. In both, the process is repeated by delaying the probe pulse until the 200 fs dissociation time-scale is mapped.

1.6 REFERENCES CITED

- [1] M. Meckel et al., "Laser-induced electron tunneling and diffraction", *Science* **320**, 1478-1482 (2008).
- [2] J. Itatani et al., "Tomographic imaging of molecular orbitals", *Nature* **432**, 867-871 (2004).
- [3] S. Haessler et al., "Attosecond imaging of molecular electronic wavepackets", *Nat. Phys.* **6**, 200-206 (2010).
- [4] C. I. Blaga et al. "Imaging ultrafast molecular dynamics with laser-induced electron diffraction", *Nature* **483**, 194 (2012).
- [5] C. D. Lin et al., "Strong-field rescattering physics—self-imaging of a molecule by its own electrons", *J. Phys. B* **43**, 122001 (2010).

1.7 PUBLICATION RESULTING FROM THIS GRANT IN 2010

1. "An investigation of harmonic generation in liquid media with a mid-infrared laser", A. D. DiChiara et al., *Opt. Express* **17**, 20959 (2009).
2. "Observation of high-order harmonic generation in a bulk crystal", S. Ghimire et al., *Nat. Phys.* **7**, 138 (2011).
3. "Redshift in the optical absorption of ZnO single crystals in the presence of an intense midinfrared field", S. Ghimire et al., *Phys. Rev. Lett.* **107**, 167407 (2011).
4. "Imaging ultrafast molecular dynamics with laser-induced electron diffraction", C. I. Blaga et al., *Nature* **483**, 194 (2012).
5. "Generation and propagation of high-order harmonics in crystals", S. Ghimire et al., *Phys. Rev. A* **85**, 043836 (2012).

REVIEW ARTICLES ACKNOWLEDGING DOE AWARD

1. "Scaling of high-order harmonic generation in the long wavelength limit of a strong laser field", A. D. DiChiara et al., *IEEE J. Select. Topics Quan. Electro.* **18**, 419-433 (2012).
2. "Atomic and molecular ionization dynamics in strong laser-fields: from optical to X-rays", P. Agostini and L. F. DiMauro, in *Atomic, Molecular, and Optical Physics*, v.61, eds. P. Berman, E. Arimondo and Chun Lin (Elsevier, Maryland Heights, 2012) pp. 117-158.

ATTOSECOND AND ULTRA-FAST X-RAY SCIENCE

Louis F. DiMauro
Co-PI: Pierre Agostini
Department of Physics
The Ohio State University
Columbus, OH 43210
dimauro@mps.ohio-state.edu
agostini@mps.ohio-state.edu

1.1 PROJECT DESCRIPTION

This document describes the BES funded project (grant #: DE-FG02-04ER15614) entitled “Attosecond & Ultra-Fast X-ray Science” at The Ohio State University (OSU). Attosecond light pulses from gases offer a transition to a new time-scale and open new avenues of science while complementing and directly contributing to the efforts at the LCLS. The main objectives of this grant is the development of competency in generation and metrology of attosecond pulses using mid-infrared drivers and a strategy of employing these pulses for studying multi-electron dynamics in atomic systems. It focuses on applications in which attosecond pulses are produced and transported to a different region of space and applied to a different target, thus providing the greatest degree of spectroscopic flexibility. The proposal has also a strong thrust at the LCLS XFEL for studying the scaling of strong-field interactions into a new regime of x-ray science and the metrology of ultra-fast x-ray pulses.

Progress over the past year includes (1) measurement of the wavelength dependence of the attochirp using a RABBITT method, (2) studies on phase-dependent atomic structural effects, (3) improvement of our ultra-fast 2 μm laser system, (4) investigation of nonlinear excitation with intense x-rays and (5) preliminary measurement of time-resolved Auger decay using a two-color streaking method at the LCLS XFEL.

1.2 PROGRESS IN FY12: THE ATTOSECOND PROGRAM

The technical approach of the Ohio State University (OSU) group is the use of long wavelength ($\lambda > 0.8 \mu\text{m}$) driving lasers for harmonic generation. The objective is to create sufficiently short wavelength attosecond pulses to allow access to core level transitions. This is accomplished by exploiting the favorable scaling of the harmonic cutoff energy $\propto \lambda^2$, which results in attosecond pulses with higher central frequency. An additional benefit is the scaling of the attochirp $\propto \lambda^{-1}$, which leads to inherently shorter attosecond pulses at longer wavelength. Conversely, it has been shown that the single atom harmonic efficiency decreases with longer wavelength [1] but recent work [2] has demonstrated that effective phase-matching conditions can be realized. Using this approach, the OSU group has the ability to produce ~ 100 as pulses spanning 20-200 eV photon energies.

RABBITT measurements using driving laser wavelengths of 0.8 μm , 1.3 μm , and 2.0 μm . We have measured the Group Delay (GD) of high-order harmonics generated with long-wavelength driving lasers using the RABBITT technique. The general trend of our results confirms the expected λ^{-1} scaling of the group delay dispersion (attochirp). However for argon in the energy range from 30-60 eV we have observed a strong variation in the GD that deviates from the simple semi-classical model. This variation is the result of two effects: (1) a single-atom effect caused by the Cooper minimum and (2) a macroscopic propagation effect caused by the neutral-atom dispersion of argon. Working in collaboration with theory group of Prof. Mette Gaarde (Louisiana State University) we have modeled the experiments using a calculations based on 3D-time dependent Schrödinger equation (TDSE) single atom response and macroscopic propagation.

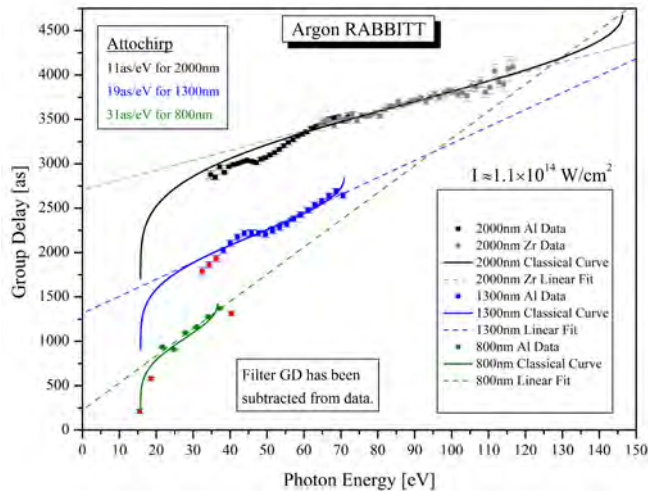


Figure 1: RABBITT measurements of argon at constant intensity and varying wavelength.

Using long wavelength ($\lambda > 1 \mu\text{m}$) laser sources, we have measured the attochirp of harmonics generated in argon gas with $0.8 \mu\text{m}$, $1.3 \mu\text{m}$, and $2 \mu\text{m}$ wavelengths. Figure 1 shows the experimental data points along with the classical single-atom GD calculation for each wavelength. The slope of the GD of the plateau harmonics, indicated by dashed lines in Fig. 1, gives the attochirp. In order to disentangle the intensity dependence of the attochirp, the laser peak intensity is kept constant for all three wavelength studies. In the figure, the GD introduced by the aluminum or zirconium filters has been removed. The results of the wavelength study for the particular intensity of $110 \text{ TW}/\text{cm}^2$, which is well below the saturation intensity of argon, give attochirp measurements of $31 \text{ as}/\text{eV}$, $19 \text{ as}/\text{eV}$, and $11 \text{ as}/\text{eV}$ for the respective wavelengths of $0.8 \mu\text{m}$, $1.3 \mu\text{m}$, and $2 \mu\text{m}$. Within the uncertainty of our experimental intensity, this confirms the expected λ^{-1} scaling of the attochirp.

It is already apparent in Fig. 1 that there is a significant variation of the experimental GD of argon in the region of 30-60 eV that deviates from the classical single-atom expectation. The variation consists of a bump near 43 eV and a dip near 50 eV. In collaboration with Prof. Gaarde we are beginning to gain insight into this phase behavior using modeling of the single-atom response using the TDSE plus the full Maxwell's macroscopic propagation calculations. Our theoretical analysis shows that the single-atom Cooper interference of the "s" and "d" continuum electron wave packets contributes to the structure at 50 eV and thus is not sensitive to macroscopic conditions, consistent with the experiment. In addition, our analysis also shows that the GD variation near 43 eV is a macroscopic effect caused by the neutral atom dispersion. Since the GD of the neutral atom dispersion is proportional to the density-length product of the gas medium, we expect similar behavior whenever high pressures or long gas cells are used. In our experiment, the GD bump is a consequence of the fact that higher pressures are needed to phase-match long wavelength fundamental fields.

Using long wavelength ($\lambda > 1 \mu\text{m}$) laser sources, we have measured the attochirp of harmonics generated in argon gas with $0.8 \mu\text{m}$, $1.3 \mu\text{m}$, and $2 \mu\text{m}$ wavelengths. Figure 1 shows the experimental data points along with the classical single-atom GD calculation for each wavelength. The slope of the GD of the plateau harmonics, indicated by dashed lines in Fig. 1, gives the attochirp. In order to disentangle the intensity dependence of the attochirp, the laser peak intensity is kept constant for all three wavelength studies. In the figure, the GD introduced by the aluminum or zirconium filters has been removed. The results of the wavelength study for the particular intensity of $110 \text{ TW}/\text{cm}^2$, which is well below the saturation intensity of argon, give attochirp measurements of $31 \text{ as}/\text{eV}$, $19 \text{ as}/\text{eV}$, and $11 \text{ as}/\text{eV}$ for the respective wavelengths of $0.8 \mu\text{m}$, $1.3 \mu\text{m}$, and $2 \mu\text{m}$. Within the uncertainty of our experimental intensity, this confirms the expected λ^{-1} scaling of the attochirp.

1.3 PROGRESS IN FY12: NONLINEAR INVESTIGATIONS AT THE LCLS XFEL

Since late 2009, the OSU group has been involved in several experimental campaigns at the LCLS XFEL at SLAC National Laboratory. The OSU group was involved in the early commissioning, the design and construction of the magnetic bottle photoelectron spectrometer for the initial LCLS AMOS end-station and direct involvement in various experimental runs. All the experiments reported here were

The Resolution of Attosecond Beating By Interference of Two-photon Transitions (RABBITT) technique allows us to measure the relative spectral phase difference between successive odd harmonics. This phase difference is then proportional to the GD of the harmonic comb, allowing us to extract the Group Delay Dispersion GDD. A non-zero GDD indicates that attosecond pulses synthesized using the harmonics within a certain bandwidth will have a longer duration than the minimum possible Fourier Transform limit for that bandwidth.

Single-atom models of HHG predict that the harmonics have an intrinsic non-zero GDD called the attochirp. In attosecond science, the attochirp is often divided by to give more convenient units of as/eV . Single-atom models also predict that the attochirp scales as the

conducted on the LCLS AMOS end-station in collaboration with other groups. The following highlights only some of these efforts.

Two-photon nonlinear ionization of Ne^{8+} with intense 1 keV pulses. The nonlinear response to high intensity x-ray pulses were explored at the LCLS XFEL by studying neon and helium atoms in the focused LCLS beam. The ability for the LCLS to produce highly charged states was observed and explained in Ref. [3]. For the nonlinear study, 2-photon ionization of Ne^{8+} , $1s^2$ ground state (1196 eV binding energy) was an excellent candidate. A quadratic response of the Ne^{9+} yield at photon energies below 1196eV provided the first evidence of a two-photon absorption in the hard x-ray regime. Model calculations performed by our collaborator, Dr. Robin Santra, supported the interpretation as direct 2-photon absorption. The results from this experiment, together with the supporting theory, were published in Physical Review Letters.

Time resolved streaking measurement of the KLL Auger decay in neon. The concept of this investigation is to combine the high-energy X-Ray pulses of the XFEL with methods in attosecond science to measure Auger decays in a direct time resolved fashion. The short FEL pulse would promote a neon $1s$ electron (K-shell) to the continuum. A mid-infrared field ($2.3 \mu\text{m}$) from a conventional laser system would provide a phase dependent momentum kick to the resulting photoelectron and Auger electron. The problem is that the XFEL and MIR pulses cannot be synchronized on a few-femtosecond time scale. Thus, an approach is needed to measure the timing for each shot. This can be accomplished by recognizing that an electron ionized in the presence of the MIR field receives a momentum kick which depends on the relative phase between the MIR and X-ray pulses. The momentum shift of the *prompt* photoelectron provides the start time to the decay measurement, while the momentum shift of the Auger electron provides information on the decay itself.

The data is currently undergoing analysis. Some preliminary results show simultaneous observation of the $1s$ and Auger electron with MIR laser driven momentum shifts. The overall signal rate was lower than expected and analysis as well as simulation is ongoing to develop the data extraction techniques for this type of measurement. Monte Carlo simulations suggest that even with the observed signal rates, extraction with the time resolved data should be possible.

Angle-resolved electron spectroscopy of laser-assisted Auger decay. Two-color (x-ray + infrared) electron spectroscopy was used for investigating laser-assisted KLL Auger decay following $1s$ photoionization of atomic Ne with few-femtosecond x-ray pulses from the LCLS. In an angle-resolved experiment, the overall width of the laser-modified Auger electron spectrum and its structure change significantly as a function of the emission angle. The spectra are characterized by a strong intensity variation of the sidebands revealing a gross structure. This variation is caused, as predicted by theory, by the interference of electrons emitted at different times within the duration of one optical cycle of the infrared dressing laser, which almost coincides with the lifetime of the Ne $1s$ vacancy. This work was reported in Physical Review Letters.

1.5 FUTURE PLANS

The long wavelength driver strategy has established itself as the enabling technology for the proposed research. We envision both applications of the existing source for fundamental tests of attosecond control and metrology and developments towards atomic length and time scales, pushing high harmonic generation into soft x-ray regime for core excitation while defining new limits on attosecond pulse durations. Over the final year period of this current grant we will pursue the following.

Attosecond probing of below-threshold harmonics. The lowest energy harmonics probed by a typical RABBITT or streaking experiment is determined by the ionization potential of the detector atom which is satisfactory for obtaining phase information in the HHG plateau region. The plateau region is usually explained using the semi-classical, as discussed in Section 1.2. However, the classical model is not applicable to low-order harmonics produced below the ionization potential of the generation

atom/molecule. A solution to this problem is to use a detector atom with a lower ionization potential than the generation atom. We are currently using our RABBITT apparatus to measure the phase near threshold in order to gain some insight into the classical/quantum correspondence.

Auger decay and x-ray pulse measurements. We are trying to improve our earlier measurements on the time-resolved Auger decay and x-ray metrology by using the Streaking method described above, with THz pulses instead of 2.3 μm . The advantage is that the long period of the THz reference field will be less sensitive to the jitter of the LCLS timing system. Our collaboration has allotted time for December 2012. We have also submitted a proposal requesting LCLS beam time in the first half of 2013.

1.6 REFERENCES CITED

- [1] J. Tate *et al.*, Phys. Rev. Lett. **98**, 013901 (2007).
- [2] T. Popmintchev *et al.*, PNAS **106**, 10516 (2009).
- [3] L. Young *et al.*, Nature **466**, 56 (2010).

1.7 PUBLICATION RESULTING FROM THIS GRANT IN 2010

1. E. Power *et al.*, “XFROG phase measurement of threshold harmonics in a Keldysh scaled system”, Nature Photonics, **4**, 352-356 (2010).
2. L. Young *et al.*, “Femtosecond electronic response of atoms to ultraintense x-rays”, Nature **466**, 56-61 (2010).
3. M. Hoener *et al.*, “Ultra-intense x-ray induced ionization, dissociation and frustrated absorption in molecular nitrogen”, Phys. Rev. Lett. **104**, 253002 (2010).
4. J. M. Glowia *et al.*, “Time-resolved pump-probe experiments at the LCLS”, Opt. Exp. **18**, 17620 (2010).
5. J. P. Cryan *et al.*, “Auger electron angular distribution of double core-hole states in the molecular reference frame”, Phys. Rev. Lett. **105**, 083004 (2010).
6. S. Ghimire *et al.*, “Observation of high-order harmonic generation in a bulk crystal”, Nat. Phys. **7**, 138 (2011).
7. G. Doumy *et al.*, “Nonlinear atomic response to intense ultrashort x-rays”, Phys. Rev. Lett. **106**, 083002 (2011).
8. E. P. Kanter *et al.*, “Unveiling and driving hidden resonances with high-fluence, high-intensity x-ray pulses”, Phys. Rev. Lett. **107**, 233001 (2011).
9. M. Meyer *et al.*, “Angle-resolved electron spectroscopy of laser-assisted Auger decay induced by a few-femtosecond X-ray pulse”, Phys. Rev. Lett. **108**, 063007 (2012).
10. A. D. DiChiara *et al.*, “Scaling of high-order harmonic generation in the long wavelength limit of a strong laser field”, IEEE J. Select. Topics Quan. Electro. **18**, 419-433 (2012).

Ultracold Molecules: Physics in the Quantum Regime

Senior Investigator: John Doyle
Harvard University
17 Oxford Street
Cambridge MA 02138
doyle@physics.harvard.edu
Research Project Abstract 2012

1. Overview of Project

Our research encompasses a unified approach to the trapping of diverse chemical species of both atoms and molecules and study of their collisions. We have developed lasers and apparatus for trapping both CaH and CaF molecules. This includes high power lasers at all the necessary wavelengths. Our current goal is to magnetically trap CaH or CaF. This will be done by taking molecules from our newly developed slow beam source, with velocity of about 50 m/s, and optically pumping them into a deep magnetic trap. All the apparatus is now in place and we are planning our first cool down for October 2012. We have also constructed and tested a smaller, auxiliary apparatus for production of CaF beams and optical pumping tests. We are also, in tandem, working on cooling and spectroscopy of large molecules. We have now demonstrated a full method for trace detection with high specificity of small organic molecules in a mixture.

Publications from this period are:

- [1] *Buffer Gas Cooling and Intense, Cold, Slow Molecular Beams*, N.R. Hutzler, Hsin-I Lu, J.M. Doyle, Chemical Reviews Special Issue on Ultracold Molecules **accepted** published electronically 9May2012 10.1021/cr200362u (2012)
- [2] *Cooling molecules in a cell for FTMW spectroscopy*, D. Patterson and J.M. Doyle, Molecular Physics **accepted** (2012)

2. Future Plans

Our immediate plans are to cool the apparatus down and measure molecules in the trapping region. We are also now performing CaF beam and optical pumping studies in our smaller, auxiliary apparatus. We are also planning on introducing realistic mixtures into our large molecule cooling apparatus for demonstration of trace detection.

3. Other information

There are 2 graduate students working at least 50% of the time on these experiments.

Atomic Electrons in Strong Radiation Fields

J. H. Eberly
University of Rochester, Rochester, NY 14627
eberly@pas.rochester.edu

Scope: Atomic Electron Correlation under Strong Laser Fields

We are interested to understand how very intense laser light couples to atoms and molecules. Theoretical study faces substantial challenges in this domain. These arise from the combination of high intensity, fully phase-coherent character and short-time nature of the laser pulses in use, where the laser's electric-field force roughly matches the Coulomb forces among electrons and the nucleus. An important additional challenge arises when there is a need to account for more than one dynamically active electron.

Our work builds on earlier results obtained from numerical experiments [1, 2]. These were studies of two, three and four active atomic electrons in strong time-dependent and phase-coherent fields, using very large ensembles of classical multi-electron trajectories. Although classical, the technique is completely *ab initio* in the sense that it proceeds from a specific Hamiltonian description of a multi-electron model atom with empirically accurate ionization potentials matching those of familiar experimental target atoms (helium, neon, argon, xenon, magnesium) without perturbative or other simplifying dynamical approximations. The technique, using its ensembles of multi-electron trajectories, is capable of unique theoretical exploration. For example, in the domain of laser intensities in the region near to and above 10^{15} W/cm² it has allowed the first theoretical study of effects arising under elliptical polarization [4, 5, 6]. The field is rich with new phenomena, and fascinating high-field experimental data is emerging [7, 8, 9, 10]. We expect to advance the examination of the possible breakdown of the single-active electron approximation, with new evidence from momentum distribution “twists” [11].

NSDI/SDI Theoretical Methods Overview

Since 1992 we have benefited from two decades of experimental advances and theoretical developments. This has been a period when recognition spread widely among AMO scientists that substantial and surprising challenges to clear understanding are presented by two-electron response to irradiation of atoms and molecules with intensities above and well above 10^{13} W/cm². We have recorded the emergence of different theoretical approaches to these challenges with an overview in Reviews of Modern Physics [12] containing more than 250 citations to both theoretical and experimental works. The conclusion at this intermediate stage is that two theoretical approaches remain active and useful, although strongly distinct in foundation and implementation. These two can be called “all at once” and “step by step”.

One remarkable consequence is that both approaches are about equally productive in explaining experimental results. Another one is that the generic all-at-once classical approach reinforces the

quantum mechanical step-by-step approach in various ways, most strikingly by showing that those classical ensemble trajectories leading to the well-known NSDI “knee” are those that exhibit a recollision event, even though no such condition was imposed. Experimental data, of course, always comes in an all-at-once fashion.

Tunneling Under Test

Theories have been proposed to predict the tunneling rate of an atom exposed to a laser field [13]. These theories are based explicitly on an assumption that the laser electric field is weaker than the over-barrier field of the ionizing electron. The theories continue to be used for guidance even though the errors of these theories are difficult to estimate, and certainly grow substantially as the laser field becomes stronger. Their applicability is now beginning to be open to quantitative test using some of the advantages provided by elliptical polarization of the laser field (for an overview, see [14]).

Under the tunneling scenario an electron’s release time is not really open to question because of the exponential dependence of the emission rate on laser field strength. The electron is almost certainly released at the peak of the laser pulse. With fields that are strong enough to ionize multiple electrons, the fields can be much higher than the over-barrier field of the first electron, so it can be emitted earlier than the peak of the pulse, and thus emission times provide a viable route for testing the formalism. To extend the applicability of the tunneling theories and at the same time keep the simplicity and convenience of the well-known Ammosov-Delone-Krainov tunneling formula [13], an augmented quantum tunneling (AQT) formula has been proposed by Tong and Lin [15] and used successfully for intensities somewhat higher than the saturation level.

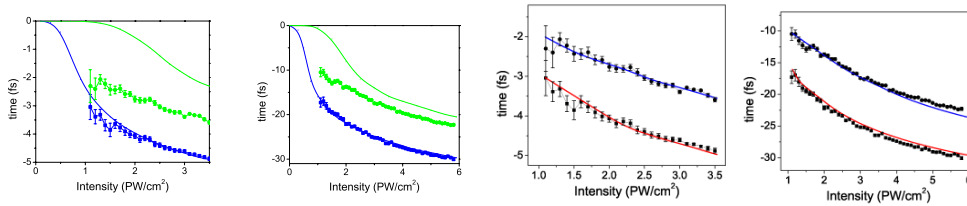


Figure 1: Comparison of experimental data (adapted from [8]) on emission times vs. laser intensity (curves containing error bars) with both the AQT predictions (solid lines, two panels on left) and our subsequent calculations (solid lines, two panels on right). The 1st and 3rd panels are for 7 fs pulses and the 2nd and 4th panels are for 33 fs pulses. In each panel the lower curves are for the first electron released and the upper curves are for the second. Comparison of calculations is discussed in the text.

In Fig. 1 we show release-time comparisons. The results of two different theories are plotted along with the data reported by Pfeiffer *et al.* [8] for double ionization of Ar, using elliptical polarization. The first two panels show that the AQT theory yields good agreement with first release timing, but not with the second release time. The second two panels show that newer calculations, described below, produce good agreement with both first and second release times.

Comparison of Theories and Conjectures

The AQT theory uses a single-active-electron (SAE) approximation, which assumes that only one electron is active at each time, with other electrons playing no role but screening the nucleus. Only after the first electron is ionized does a second electron become active. The release time data shown in Fig. 1 appears to support conjectures that the SAE (or independent-electron) approximation of

tunneling theory breaks down, at least for the release of the second electron, meaning that electron-electron correlations play a role. However the specific role that correlations may play has not been explained.

The same conjecture, that e-e correlation plays a central role has also been advanced for another experiment [16]. In that case, the tunneling theory fails to explain an oscillation feature of the measured ratio between parallel and anti-parallel SDI emissions (i.e., between sequential double ionization with the two electrons released in the same or opposite directions). Interestingly, a fully correlated classical ensemble simulation based on solution of the relevant time-dependent Newton equations (TDNE) qualitatively reproduces the oscillation feature [6]. The physical role of the e-e correlations was again not clearly identified.

New calculations from Zhou, et al., [17] recently used a classical ensemble approach and reported calculations showing the first agreement with the measured two-electron release times, essentially the same as our results shown in Fig. 1. These support the correlation conjecture because Zhou, et al., modelled each atom in their ensemble as containing two fully correlated electrons able to interact constantly with each other, as well as with the laser field and the ion. However, if the e-e correlations were essential in leading to the experimental agreement, the mechanism was not identified.

From this short summary of the current status, one sees that conjectures have been advanced that e-e correlations *must necessarily be present* on either of two different grounds: because (1) the independent-electron SAE-tunneling AQT approach does not agree with the experiments, and/or (2) the fully-correlated classical simulation of Zhou, et al., does agree with the experiments.

Remaining Open Question

Of course, making explanatory conjectures such as the need for e-e correlation should be encouraged. But the lack of any description of the role for such correlations is a weakness of the conjecture. We have recently found that there is a reason for this. Our systematic calculations show [18], surprisingly, that in the present context the need for e-e correlation on the one hand, or quantum tunneling on the other hand, can both be discarded.

To reach this conclusion we have proceeded as follows. Without difficulty, the Newtonian equations of motion can be integrated numerically under an artificially imposed SAE constraint by which the two electrons are allowed to be fully active but only one at a time and in sequence, similar to the dicta of the SAE regime adopted in two-electron quantum tunneling theories, including AQT. Under this SAE regime, the results of our calculated ionization times as a function of intensity are already shown in Fig. 1. Quantitative agreement is obviously satisfactory over the full experimental intensity range.

It is obvious that our classical SAE simulation matches experimental results, as shown in the right-side panels of Fig. 1, while the AQT quantum SAE theory does not, as shown in the left-side panels. The reason for this remains an important open question. Since both calculations are based on the SAE approximation, their key difference appears to be simply rejection or adoption of initiation by tunneling.

We need to emphasize that the above argument by no means proves that the classical model is correct while the AQT theory is wrong. One may equally argue that the AQT theory may be correct, while the disagreement between the argon experiments and the AQT prediction may originate from e-e correlations or multielectron effects excluded from the AQT theory. We cannot deny this possibility but we do not like it. One always prefers simpler theories without complications. More particularly, the conjectured e-e correlations or multielectron effects are too difficult to identify. The

results of the fully correlated theory of Zhou, et al., are entirely in accord with our completely uncorrelated results. The physical reason for the difference between the two SAE theories, our classical simulation and the AQT result, is yet an open question.

The other interesting open issue is in the agreement of our results not only with the experiments, but also with the calculations of Zhou, et al. Those fully include e-e correlation, which our results suggest are surprisingly non-important.

Publications supported by DOE Grant DE-FG02-05ER15713 are marked with * in the listing below.**

References

- [1] R. Panfili, S.L. Haan and J.H. Eberly, *Phys. Rev. Lett.* **89**, 113001 (2002).
- [2] Phay J. Ho, R. Panfili, S. L. Haan and J. H. Eberly, *Phys. Rev. Lett.* **94**, 093002 (2005). See also Phay J. Ho, *Phys. Rev. A* **74**, 045401 (2005), ***Phay J. Ho and J.H. Eberly, *Phys. Rev. Lett.* **95**, 193002 (2005), ***Phay J. Ho and J.H. Eberly, *Phys. Rev. Lett.* **97**, 083001 (2006), and ***S.L. Haan, L. Breen, A. Karim, and J. H. Eberly, *Phys. Rev. Lett.* **97**, 103008 (2006).
- [3] ***P.J. Ho and J. H. Eberly, *Optics Expr.* **15**, 1845 (2007).
- [4] ***Xu Wang and J.H. Eberly, *Phys. Rev. Lett.* **103**, 103007 (2009). See also Xu Wang and J.H. Eberly, *Laser Phys.* **19**, 1518 (2009).
- [5] ***Xu Wang and J.H. Eberly, *Phys. Rev. Lett.* **105**, 083001 (2010). See also, ***Xu Wang and J.H. Eberly, *New J. Phys.* **12**, 093047 (2010).
- [6] ***Xu Wang and J.H. Eberly, arXiv:1102.0221 (2011).
- [7] C.M. Maharjan, A. S. Alnaser, X. M. Tong, et al., *Phys. Rev. A* **72**, 041403(R) (2005).
- [8] A.N. Pfeiffer, C. Cirelli, M. Smolarski, R. Dörner, and U. Keller, *Nat. Phys.* **7**, 428 (2011).
- [9] See commentary in K. Ueda and K. Ishikawa, *Nat. Phys.* **7**, 371 (2011).
- [10] L. Arrissian, et al. *Phys. Rev. Lett.* **105**, 133002 (2010).
- [11] P. Eckle, et al. *Science* **322**, 1525 (2008).
- [12] ***W. Becker, X.J. Liu, P.J. Ho and J.H. Eberly, *Rev. Mod. Phys.* **84**, 1011-1043 (2012).
- [13] L.V. Keldysh, *Sov. Phys. JETP* **20**, 1307 (1965);
A.M. Perelomov, V.S. Popov, and M.V. Terent'ev, *Sov. Phys. JETP* **23**, 924 (1966); and
M.V. Ammosov, N.B. Delone, and V.P. Krainov, *Sov. Phys. JETP* **64**, 1191 (1986).
- [14] ***X. Wang and J.H. Eberly, *Phys. Rev. A* , in press; arXiv:1203.4824 (2012).
- [15] X.M. Tong and C.D. Lin, *J. Phys. B* **38**, 2593 (2005).
- [16] ***A.N. Pfeiffer, C. Cirelli, M. Smolarski, X. Wang, J.H. Eberly, R. Dörner, and U Keller, *New J. Phys.* **13**, 093008 (2011).
- [17] Y. Zhou, C. Huang, Q. Liao, and P. Lu, *Phys. Rev. Lett.* , in press; arXiv:1204.3956 (2012).
- [18] ***X. Wang, et al., arXiv:1208.1516 (2012).
- [19] P. Wang, A. M. Sayler, K.D. Carnes, B.D. Esry, and I. Ben-Itzhak, *Opt. Lett.* **30**, 664 (2005).

Algorithms for X-ray Imaging of Single Particles

Office of Basic Energy Sciences
Division of Chemical Sciences, Geosciences, and Biosciences
Program in Atomic, Molecular, and Optical Sciences

Veit Elser, Department of Physics
PSB 426, Cornell University
Ithaca, NY 14853
(607) 255-2340
ve10@cornell.edu

Program Scope

The many-orders-of-magnitude gains in X-ray brightness achieved by free-electron laser sources such as the LCLS are driving a fundamental review of the data analysis methods in X-ray science. It is not just a question of doing the old things faster and with greater precision, but doing things that previously would have been considered impossible. My group at Cornell is working closely with experimental groups at LCLS and FLASH to develop data analysis tools that exploit the full range of opportunities made possible by the new light sources. More recently we have begun collaborations with David Mueller's electron microscopy group and Sol Gruner's detector group, both at Cornell.

Recent Progress

The work that has attracted the most attention in the past year is the demonstration of algorithmic image reconstruction from ultra-low flux X-ray data[1]. Motivated by the urgent need to check the high quantum efficiency of Cornell's Pixel Array Detector (PAD) for the LCLS, the design of the experiment is surprisingly simple: A table-top X-ray source, highly attenuated by a lead sheet, is directed at a single module (194×185 pixels) of the PAD. In front of the detector there is a mask, a complex shape cut out of another lead sheet, that is mounted on a stage that can be rotated about the beam axis. The beam attenuation went as far as giving an average of only 2.5 photons recorded on the detector per exposure (Figure 1).

The quantum efficiency of the PAD could have been demonstrated by collecting statistics in these ultra-low flux conditions. However, to bring the experiment closer to the single-particle imaging setting, we gave the mask a random rotation between each exposure (mimicking the randomness of particle orientations). We collected nearly a half-million exposures, each recording very few photons and without knowledge of the mask rotation at the time of the exposure. Despite these adverse experimental conditions, our expectation maximization algorithm[2] had no trouble reconstructing the shape of the mask (Figure 2).

Graduate student Kartik Ayyer is currently working with the Gruner team to demonstrate tomographic reconstruction of a 3D object with ultra-low flux X-rays in a setting not unlike cryo-EM studies of small biological particles. He has also further developed the EMC algorithm[3], for the LCLS single particle experiments, to be able to tolerate high levels of background scattering.

Former graduate student Duane Loh, now a postdoc with Mike Bogan at LCLS, recently published a paper[4] that featured soot particle reconstructions. Some of the more challenging data collected in these

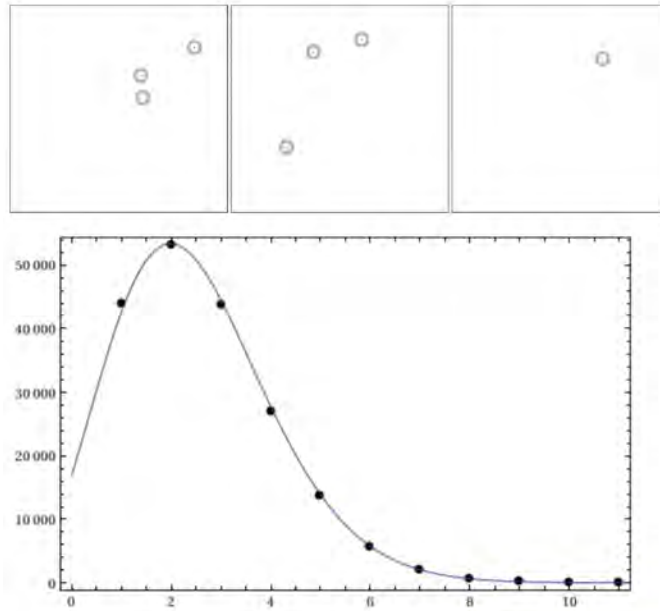


Figure 1: *Top*: Three frames of data from the ultra-low flux X-ray experiment (recorded photons are circled). *Bottom*: Distribution of photon number per frame in a data set with 450,000 frames.

experiments resisted reconstruction in the original publication and have now been successfully reconstructed by current graduate student Hyung Joo Park (Figure 3).

A new direction for us has been the application of our algorithms to reconstructions from electron microscope data. David Mueller (Applied Physics, Cornell) was wondering if our algorithms could deal with the issue of missing data in tomographic reconstructions. Annular dark-field scanning transmission electron microscopes (ADF-STEMs) typically miss a significant range of viewing angles, as shown in Figure 4. By using a support constraint on the Cu_3Pt nano-particle in the field of view, graduate student Yi Jiang was able to reconstruct the missing diffraction speckles in the missing wedge of the particle's Fourier transform. The



Figure 2: *Left*: Mask reconstruction in the ultra-low flux experiment with 11.5 photons per frame. *Right*: Reconstruction with 2.5 photons per frame.

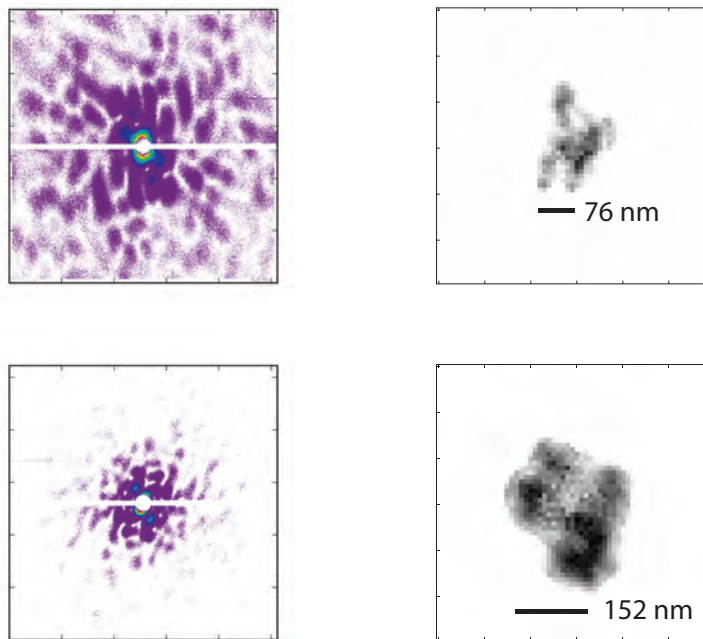


Figure 3: Soot particle reconstructions from single-shot LCLS data[4]. Raw diffraction patterns are on the left, corresponding soot particles on the right.

resulting particle reconstruction is compared with the widely used SIRT method in Figure 4.

At last year's AMOS meeting I had discussions with Martin Centurion and Tony Starace on the possibility of using our algorithms for reconstructing small molecules from their electron diffraction patterns. In these experiments it is possible to partially align the particles (molecules) with a laser, thereby reducing the complexity of the reconstruction problem. This seemed like an excellent opportunity to try a new reconstruction scheme I had developed[5] based on an old idea of Kam[6] where cross-correlations in the fluctuations of many diffraction patterns provide the structural information. Graduate student Zhen Wah Tan has taken charge of this project and is performing simulations for the molecule CH_3I . Since the rotations of the molecules about their symmetry axes cannot be controlled in the experiment, the relatively weak 3-fold modulation must be determined from fluctuations in the intensity.

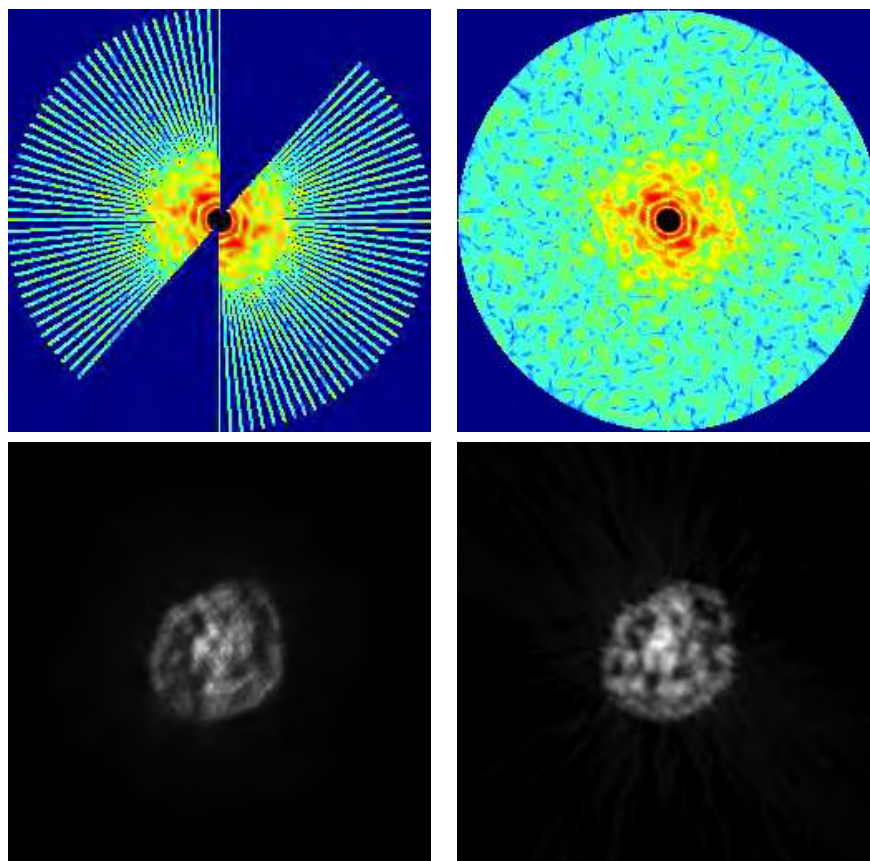


Figure 4: *Top*: Fourier transform ADF-STEM data of a Cu₃Pt nano-particle: raw data on the left and algorithmic missing data reconstruction on the right. *Bottom*: Particle reconstructions: new method on the right contrasted with the SIRT method on the left. The gray scale represents the electrostatic potential sampled on a plane that slices through the center of the particle.

References

- [1] H.T. Philipp, K. Ayer, M.W. Tate, V. Elser & S.M. Gruner, *Solving structure with sparse, randomly-oriented x-ray data*, Opt. Express **12**, 13129-37 (2012).
- [2] V. Elser, *Noise limits on reconstructing diffraction signals from random tomographs*, IEEE Trans. Information Theory **55**, 4715-4722 (2009).
- [3] N.-T. D. Loh & V. Elser, *Reconstruction algorithm for single-particle diffraction imaging experiments*, Phys. Rev. E **80**, 026705 (2009).
- [4] N.D. Loh *et al.*, *Fractal morphology, imaging and mass spectrometry of single aerosol particles in flight*, Nature **486**, 5137 (2012).
- [5] V. Elser, *Three-dimensional structure from intensity correlations*, New J. Phys. **13**, 123014 (2011).
- [6] Z. Kam, *Determination of macromolecular structure in solution by spatial correlation of scattering fluctuations*, Macromolecules **10**, 927-934 (1977).

Collective Coulomb Excitations and Reaction Imaging

Department of Energy 2012-2013

James M Feagin

Department of Physics

California State University–Fullerton

Fullerton CA 92834

jfeagin@fullerton.edu

Innovations in few-body science at molecular nano levels will be a critical component of ongoing international efforts to establish sustainable environmental and energy resources. The varied research paths to be taken will require the development of basic science on broad fronts with increasingly flexible views to crossover technologies. Although the work described in this report is theoretical, our interest in these topics remains motivated by the recent surge in and success of experiments involving few-body atomic and molecular fragmentation and the collection of all the fragments. We accordingly continue two parallel efforts with (i) emphasis on *reaction imaging* while (ii) pursuing longtime work on *collective Coulomb excitations*. As in the past, we continue to place priority on research relevant to experiment.

Tracking Transverse Coherence in Proton-Molecule Scattering

Schulz and coworkers have considered the transverse coherence length of a nearly monochromatic beam of protons, deBroglie wavelength λ , passing through a collimator aperture and scattered by a crossed beam of molecular hydrogen.¹ The two-center nature of the molecular scattering gives rise to a well-established ‘double-slit interference’ effect, which these investigators were able to suppress by reducing the distance L of the target volume to the collimator aperture. A decrease in L increases the angular width $\alpha \simeq a/L$ the collimator aperture subtends at the target, where $a \ll L$ is the aperture width in the scattering plane. They demonstrated that the corresponding decrease in the transverse coherence length λ/α of the scattered protons relative to the two-center molecular bond length suppresses as expected the observed interference effects in the scattering cross section.²

While we feel these experiments have provided a convincing demonstration of the role of transverse coherence in establishing interference effects, we disagree with the conclusions of Schulz and coworkers that individual proton wave packets have been altered by the variable collimation and thus the cross section of individual protons.³ Their experiment involved 75 keV incident protons, monochromatic to less than 1 eV. With a corresponding mean deBroglie wavelength $\lambda = 0.10$ pm and aperture width $a = 0.15$ mm, the protons pass through the collimator with negligible diffraction and thus well represented by sharply peaked free particle wave packets moving essentially without change of shape along classical trajectories, $\psi_i(\mathbf{r}, t) \simeq \psi_i(\mathbf{r} - \mathbf{v}_i t, 0)$. Here, $\mathbf{v}_i = (\hbar \mathbf{k}_i / m) \hat{\mathbf{v}}_i$ is the velocity of the i th incident proton with wavenumber $k = 2\pi/\lambda$ and mass m . Although $\psi_i(\mathbf{r}, t)$ is extremely sharply peaked relative to the collimator aperture, it is nevertheless long and broad relative to the target molecules and therefore well approximated in their vicinity by plane waves, albeit ones incident along \mathbf{v}_i . Thus, contrary to the conclusions of Schulz and coworkers, it is not apparent to us why standard scattering theory should not apply.

¹ K. N. Egodapitiya, S. Sharma, A. Hasan, A. C. Laforge, D. H. Madison, R. Moshhammer, and M. Schulz, *Phys. Rev. Lett.* **106**, 153202 (2011).

² See for example C. Keller, J. Schmiedmayer, and A. Zeilinger, *Opt. Commun.* **179**, 129 (2000), and also J. M. Feagin, *Phys. Rev.* **A73**, 022108 (R) (2006).

³ J. M. Feagin and L. Hargreaves, *Phys. Rev. Lett.*, in preparation (2012).

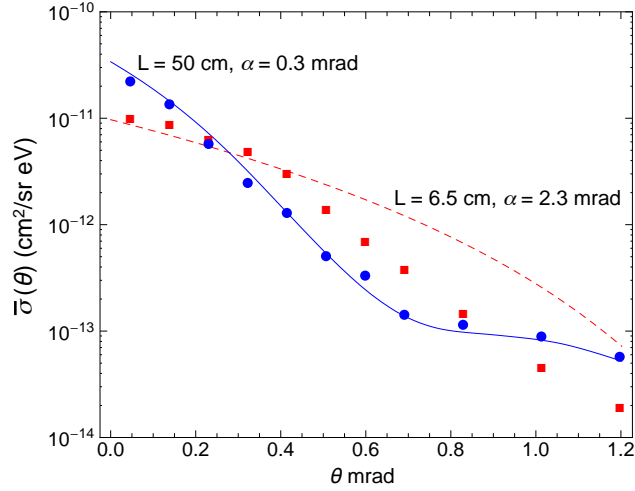


FIG. 1: The proton scattering cross section for ionization of H_2 as a function of scattering angle as in Fig. 1 of Schulz et al.³ Here, the cross section has been averaged according to Eq. (1) over a subensemble of incident protons passing through the collimator aperture and incident on the target volume a distance L away. The round (blue) and square (red) points are the $L = 50$ cm and $L = 6.5$ cm data of Schulz et al., while the solid (blue) and dashed (red) curves show the calculated cross section of Madison and coworkers⁶ but averaged according to Eq. (1).

A projectile proton incident along \mathbf{v}_i simply shifts the scattering cross section⁴ according to $\sigma(\theta) \rightarrow \sigma(\theta + \alpha_i)$, where α_i is a proton angle of incidence and θ the usual angle of scatter both relative to the incident beam axis. The finite collimation is accounted for by averaging $\sigma(\theta + \alpha_i)$ over the subensemble of collimated protons heading towards a small target volume at L . Assuming a uniform distribution of protons over the collimator aperture, this average can be approximated by

$$\bar{\sigma}(\theta) \equiv \frac{1}{\alpha} \int_{-\alpha/2}^{\alpha/2} d\alpha' \sigma(\theta + \alpha'), \quad (1)$$

where $\alpha \simeq a/L$ is the angular width of the aperture, as before. Fig. 1 compares this collimator-averaged cross section with the data of Schulz et al. for two target-volume distances L . At $L = 50$ cm, the aperture angular width $\alpha = 0.3$ mrad, and $\bar{\sigma}(\theta)$ is virtually indistinguishable from $\sigma(\theta)$, the $L \rightarrow \infty$ limit. At $L = 6.5$ cm, $\alpha = 2.3$ mrad and the average in Eq. (1) is over a range roughly double the entire plot range of interest, and it's not surprising the interference dip around 0.8 mrad is fully washed out. Better fits to the $L = 6.5$ cm data will likely require a better representation of the distribution of classical trajectories in the projectile-beam optics than our assumption in Eq. (1) of a uniform distribution across the collimator aperture. We conclude that the changes here in aperture angular width have little effect on the structure of individual proton wave packets.

Electron-Pair Vortex Kinematics

Murray and Read⁵ pioneered the detection of electron pairs scattered by incident electrons fired obliquely to the detection plane. At various energies and for certain electron gun angles and relative angular separation of the scattered electron pair, they observed pronounced minima

⁴ U. Chowdhury, M. Schulz, and D. H. Madison, Phys. Rev. A 83, 032712 (2011).

⁵ A. J. Murray and F. H. Read, Phys. Rev. A 47, 3724 (1993).

in the cross section, which over the years have stubbornly resisted a consistent theoretical interpretation, although modern close-coupling calculations can accurately describe their structure and pinpoint their location.⁶ Very recently, however, Macek and Ovchinnikov⁷ have traced these observed ($e, 2e$) deep minima to the occurrence of vortices in the wavefunction of the continuum electron pair. They have thus demonstrated the existence of nonzero electron-pair angular momentum about a line through the singularity and out of the detection plane.

We have worked to establish an accurate analytic form of the cross section near a vortex in the electron-pair continuum by connecting with the angular momentum of the electron-pair center of mass (CM) about the vortex singularity. Following closely our electron-pair excitation work described above, we thus introduce the relative momentum wavevectors $\mathbf{k}_- = (\mathbf{k}_1 - \mathbf{k}_2)/2$ and $\mathbf{k}_+ = \mathbf{k}_1 + \mathbf{k}_2$ to describe the relative and center of mass (CM) motion, respectively, of the outgoing electron pair. Here, \mathbf{k}_1 and \mathbf{k}_2 are the electron wavevectors relative to the ion. We do not predict where a vortex is, or why, but given that it exists provide instead a compact description of its *kinematics*. In the equal-energy sharing experiments of Murray and Read, one has that $\mathbf{k}_+ \cdot \mathbf{k}_- = E_1 - E_2 = 0$, and the vortex line establishes itself along the relative momentum axis \mathbf{k}_- through a point \mathbf{k}_{+v} . Accordingly, we also introduce the projection $\hbar \lambda = \mathbf{L} \cdot \hat{\mathbf{k}}_-$ of the electron-pair total angular momentum $\mathbf{L} = \mathbf{l}_1 + \mathbf{l}_2$ along \mathbf{k}_- and use $\mathbf{k}'_+ \equiv \mathbf{k}_+ - \mathbf{k}_{+v}$ to describe the momentum of the electron-pair CM relative to the vortex singularity.

Our key notion is to move the angular-momentum origin from the helium ion to the vortex singularity with a momentum boost. Since the scattering amplitude is a momentum-space function, the boost is trivially introduced by the replacement $\mathbf{k}_+ \rightarrow \mathbf{k}'_+ \equiv \mathbf{k}_+ - \mathbf{k}_{+v}$. However, a shift of angular-momentum origin changes $\mathbf{L} \rightarrow \mathbf{L}'$ and moves the centrifugal barrier along with it, and the centrifugal barrier dominates the analytic form of the amplitude near the new origin. We thus derive⁸ a threshold-like analytic expansion of the scattering amplitude in cylindrical partial waves $\lambda = 0, 1, 2, \dots$ of the electron-pair about the vortex

$$f \sim c_0 + c_1 k'_+ \cos \psi' + c_2 k'^2_+ \cos 2\psi' + \dots, \quad (2)$$

where ψ' is the angle \mathbf{k}'_+ makes with incident electron beam and the coefficients c_λ are undetermined but otherwise independent of the momenta. We thus demonstrate good fits to the ($e, 2e$) cross section near the vortex can be obtained with just the lowest two partial waves about the vortex.

Electron-Pair Excitations

Photo double ionization of molecular hydrogen shows a close similarity with the corresponding electron-pair angular distributions well established in helium, especially for relatively low-energy electron pairs.⁹ However, Gisselbrecht et al. identified equal-energy-sharing electron-pair configurations in the molecular fragmentation¹⁰ for which the helium-like description categorically fails. Their observations were a follow-on to somewhat earlier experiments at the ALS by Th. Weber, R. Dörner, A. Belkacem, and coworkers.¹¹ These anomalous angular distributions are noncoplanar and occur when one electron is observed perpendicular to the plane of the other and the polarization direction with the ion-pair direction \mathbf{K}_- either parallel or perpendicular to

⁶ J. Colgan, O. Al-Hagan, D. H. Madison, A. J. Murray, and M. S. Pindzola, J. Phys. B: At. Mol. Opt. Phys. **42**, 171001 (2009).

⁷ J. H. Macek, J. B. Sternberg, S. Y. Ovchinnikov, and J. S. Briggs, Phys. Rev. Lett. **104**, 033201 (2010).

⁸ J. M. Feagin, J. Phys. B: At. Mol. Opt. Phys. **44**, 011001 (2011).

⁹ T. J. Reddish and J. M. Feagin, J. Phys. B: At. Mol. Opt. Phys. **32**, 2473 (1999); J. M. Feagin, J. Phys. B: At. Mol. Opt. Phys. **31**, L729 (1998).

¹⁰ M. Gisselbrecht et al., Phys. Rev. Lett. **96**, 153001 (2006).

¹¹ Th. Weber et al., Nature (London) **431**, 437 (2004).

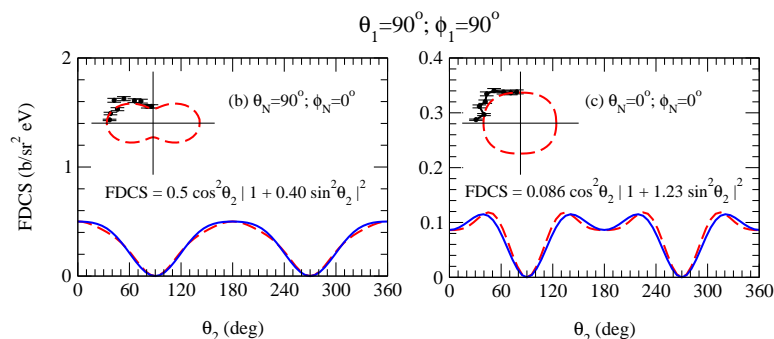


FIG. 2: Fits (solid curves) based on a three-state superposition ${}^1P_{\lambda=1} + {}^1D_{\lambda=1} + {}^1F_{\lambda=1}$ to the H_2 photo double ionization cross sections measured by Gisselbrecht et al. Here, the dashed curves show the TDCC results from J. Colgan.

the polarization. Gisselbrecht et al. termed these and related configurations *frozen-correlation*, since the electron-pair angular separation $\hat{\mathbf{k}}_1 \cdot \hat{\mathbf{k}}_2$ is held fixed in all three cases.

Analysis of the close-coupling results, albeit as expansions in individual electronic angular momenta, show evidence for contributions to the fragmentation from higher electron-pair angular momenta. We thus continue collaboration with J. Colgan, A. Huetz, and T. Reddish to generalize the helium-like molecular description to higher *total* angular momentum of the electron-pair.¹² In the molecular ground state, the electron-pair total angular momentum $\mathbf{L} = \mathbf{l}_1 + \mathbf{l}_2$ is not a good quantum number, so the helium-like dipole selection rule ${}^1S^e \rightarrow {}^1P^o$ generalizes to ${}^1S^e, {}^1P^e, {}^1D^e, \dots \rightarrow {}^1P^o, {}^1D^o, {}^1F^o, \dots$. As depicted in Fig. 2, we have thus found that superpositions of just three molecule symmetrized electron-pair states, ${}^1P^o + {}^1D^o + {}^1F^o$, give a remarkably robust description of the molecular fragmentation distributions including the anomalous out-of-plane *frozen-correlation* configurations. We also find that molecules require special axial-vector geometries in the momenta of the outgoing electron-pair, which are not seen in atoms, and we presented evidence for them in the fragmentation cross section.

Recent Publications and Invited Talks

Comment on "Manipulating Atomic Fragmentation Processes by Controlling the Projectile Coherence," J. M. Feagin and L. Hargreaves, Phys. Rev. Lett., in preparation (2012).

Vortex Kinematics of a Continuum Electron Pair, J. M. Feagin, J. Phys. B: At. Mol. Opt. Phys. **44**, 011001 (2011).

Vortices in the Electron-Pair Continuum or Deep Bubbles in My Guinness?, J. M. Feagin, Invited Talk to the International Symposium on $(e, 2e)$, Double Photoionization, and Related Topics, Dublin, Ireland, July (2011).

Electron-Pair Excitations and the Molecular Coulomb Continuum, J. M. Feagin, J. Colgan, A. Huetz, and T. J. Reddish, Phys. Rev. Lett. **103**, 033002 (2009).

Electron Pairs in the Molecular Coulomb Continuum, J. M. Feagin, Invited Talk to the International Symposium on $(e, 2e)$, Double Photoionization, and Related Topics, Lexington, KY, July (2009).

¹² J. M. Feagin, J. Colgan, A. Huetz, and T. J. Reddish, Phys. Rev. Lett. **103**, 033002 (2009).

Studies of Autoionizing States Relevant to Dielectronic Recombination

T.F. Gallagher
Department of Physics
University of Virginia
P.O. Box 400714
Charlottesville, VA 22904-4714
tfg@virginia.edu

In this research program we have studied doubly excited autoionizing atomic states and the effects of intense low frequency radiation on atomic photoionization. A systematic study of autoionization allows us to understand the reverse process, dielectronic recombination (DR), the recombination of ions and electrons via intermediate autoionizing states. DR provides an efficient recombination mechanism for ions and electrons in astrophysical and laboratory plasmas.¹⁻⁴ In fusion plasmas impurity ions from the wall of the containment vessel capture electrons and radiate power from the plasma, negating efforts to heat the plasma. The most important pathway for DR is through the autoionizing Rydberg states converging to the lowest lying excited states of the parent ion. Because Rydberg states are involved, DR rates are profoundly influenced by other charged particle collision processes and any small electric and magnetic fields in the plasma.^{5,6} Consequently, a major thrust of this program has been understanding how autoionization rates, and thus DR, are affected by external fields. This understanding is broadly useful since DR exhibits similar physics to that found in other contexts, notably zero kinetic energy electron (ZEKE) spectroscopy,⁷ dissociative recombination,⁸ and fluorescence yield spectroscopy.⁹ The use of a microwave field to mimic the rapidly varying fields which occur in electron collisions has led quite naturally to laser photoionization of atoms in stronger microwave fields, and we are exploring this problem to understand it more fully. An atom in a strong microwave field exposed to visible radiation is very similar to an atom in an intense infrared field exposed to a train of attosecond xuv pulses, a problem currently under investigation by many research groups.¹⁰⁻¹³

During the past year we have worked on several projects. First, we describe experiments on autoionization in very weak electric fields. We have examined the spectroscopy of the Ba $6p_{1/2}17k$ Stark states in very low electric fields, <20 V/cm, in which only the $\ell > 4$ states need be considered. In zero field the $6p_{1/2}17h$ state has a width of 10 GHz, and the higher ℓ $6p_{1/2}17\ell$ states of $\ell > 5$ fall within the 10 GHz width of the $6p_{1/2}17h$ state. The widths are less than 1 GHz for $\ell > 7$. The narrow widths of the high ℓ $6p_{1/2}17\ell$ states require the use of a pulse amplified single frequency continuous wave laser to drive the isolated core excitation (ICE) transitions. In these low electric fields the bound $6s17k$ states are composed of all the $6sn\ell$ states of $\ell > 4$. In contrast, the autoionizing $6p_{1/2}17k$ states appear to be a set of discrete Stark states composed of $6p_{1/2}17\ell$ states of $\ell > 5$ and a broad quasi continuum, the $6p_{1/2}17h$ state. Since the initial $6s17k$ state includes the $6s17h$ state, the ICE has an excitation amplitude to the $6p_{1/2}17h$ continuum as well as to the discrete $6p_{1/2}17k$ Stark states, and we have treated the excitation using Fano's configuration interaction theory.¹⁵ A most interesting result of the measurements is that the $6s17k$ - $6p_{1/2}17k$ excitation spectrum appears to be entirely to the discrete states as k approaches 17, but almost entirely to the quasicontinuum as k approaches 5. For $k \sim 17$ maxima appear in the

spectra at the locations of the $6p_{1/2}17k$ states, but for $k \sim 5$ minima appear. This behavior is reproduced by our model. An additional feature is that shake up satellites are only observed on the blue side of the $\Delta k=0$ transition. Our calculations indicate that this satellite pattern occurs when the $6snk$ and $6p_{1/2}nk$ Stark manifolds have different numbers of states and the quantum defects of the bound states are larger than those of the autoionizing states. If the bound quantum defects are smaller, the shake up satellites are only observed to the red of the $\Delta k=0$ transition. We have published a report of this work.¹⁶

We have completed work on bound wavepackets excited in the presence of a microwave field. Earlier we showed that a wavepacket excited by a ps laser tuned above the ionization limit in the presence of a microwave field resulted in a bound atom if the ps laser excitation occurred at the correct phase of the microwave field.¹⁷ This observation is consistent with a classical model based on an extension of the “Simpleman’s Model” in which we take into account the fact that the photoelectron is produced in a coulomb potential, not in a flat potential.¹⁸⁻²⁰ According to the model, just as excitation at the correct phase of the microwave field leads to removal energy from the photoelectron, at the opposite phase energy is given to the photoelectron. Excitation of a bound wavepacket has allowed us to see the phase dependent population transfer to both higher and lower energy. It also demonstrates that there is nothing special about energy transfer across the ionization limit. A report of this work has been published recently.²¹

Microwave spectroscopy of the bound high ℓ Rydberg states allows the determination of the polarizabilities and transition matrix elements of the ionic core.²² These quantities are important for both frequency standards and fundamental measurements. We are exploring a novel method of detecting these transitions. The idea is straightforward, and we use Ba as an example to explain it. The doubly excited high ℓ $6pn\ell$ states have autoionization rates which fall exponentially with ℓ , and the width of the $6sn\ell$ - $6pn\ell$ isolated core excitation (ICE) transition decreases in the same way. Correspondingly, the peak ICE cross section thus increases exponentially with ℓ . If a narrow band laser is tuned to the $6sn\ell$ - $6pn\ell$ transition, atoms driven by a microwave pulse from the $6sng$ state to the $6sn\ell$ state undergo the ICE transition and are detected. Since we already have the narrow band laser required to drive the 493 nm Ba $6sn\ell$ - $6p_{1/2}n\ell$ transition we have started an experiment with Ba to see how well this method works in practice.

Our plans for the coming year are to complete a set of measurements of the Ba $6sng$ - $6sn\ell$ transitions for $\ell=5, 6$, and 7 . These measurements should give improved values for the dipole and quadrupole polarizabilities of the Ba^+ $6s$ state, as well as values for the dipole and quadrupole radial matrix elements connecting the Ba^+ $6s$ state to the $6p$ and $5d$ states. Subsequently we plan to investigate Ca or Yb. Both Ca^+ and Yb^+ ions are of great interest for frequency standards. In the process of analyzing the spectra in weak electric fields we realized the equivalence of Fano's configuration interaction theory and the treatment Lamb used to describe his Lamb shift measurements.^{15,23} We plan to prepare a report showing this connection. Finally, we plan to start experiments in which we excite atoms in the presence of a microwave field using a laser beam which is amplitude modulated synchronously with the microwave field. This approach, when compared to laser excitation by a single ps pulse phase locked to the microwave field will probe the importance of coherence of the wave packet produced by the optical excitation.¹²

References

1. A. Burgess, *Astrophys. J.* **139**, 776 (1964).
2. A.L. Merts, R.D. Cowan, and N.H. Magee, Jr., Los Alamos Report No. LA-62200-MS (1976).
3. S. B. Kraemer, G. J. Ferland, and J. R. Gabel, *Astrophys. J.* **604** 556 (2004).
4. N. R. Badnell, M. G. O'Mullane, H. P. Summers, Z. Altun, M. A. Bautista, J. Colgan, T. W. Gorczyca, D. M. Mitnik, M. S. Pindzola, and O. Zatsarinny, *Astronomy and Astrophysics*, **406**, 1151 (2003).
5. A. Burgess and H. P. Summers, *Astrophysical Journal* **157**, 1007 (1969).
6. V. L. Jacobs, J. L. Davis, and P. C. Kepple, *Phys. Rev. Lett.* **37**, 1390 (1976).
7. E. W. Schlag, *ZEKE Spectroscopy* (Cambridge University Press, Cambridge, 1998).
8. V. Kokoouline and C. H. Greene, *Phys. Rev. A* **68**, 012703 (2003).
9. C. Sathe, M. Strom, M. Agaker, J. Soderstrom, J. E. Rubenson, R. Richter, M. Alagia, S. Stranges, T. W. Gorczyca, and F. Robicheaux, *Phys. Rev. Lett.* **96**, 043002 (2006).
10. P. Johnsson, R. Lopez-Martens, S. Kazamias, J. Mauritsson, C. Valentin, T. Remetter, K. Varju, M. B. Gaarde, Y. Mairesse, H. Wabnitz, P. Salieres, Ph. Balcou, K. J. Shafer, and A. L'Huillier, *Phys. Rev. Lett.* **95**, 013001 (2005).
11. P. Ranitovic, X. M. Tong, B. Gramkow, S. De, B. DePaola, K. P. Singh, W. Cao, M. Magrakelidze, D. Ray, I. Bocharova, H. Mashiko, A. Sandhu, E. Gagnon, M. M. Murnane, H. C. Kapteyn, I. Litvinyuk, and C. L. Cocke, *New J. Phys.* **12**, 013008 (2010).
12. P. Johnsson, J. Mauritsson, T. Remetter, A. L'Huillier, and K. J. Schafer, *Phys. Rev. Lett.* **99**, 233001 (2007).
13. X. M. Tong, P. Ranitovic, C. L. Cocke, and N. Toshima, *Phys. Rev. A* **81**, 021404 (2010).
14. P. Riviere, O. Uhden, U. Saalman, and J. M. Rost, *New J. Phys.* **11**, 053011 (2009).
15. U. Fano, *Phys. Rev.* **124**, 1866 (1961).
16. J. Nunkaew and T. F. Gallagher, "Spectroscopy of barium 6p1/2nk autoionizing states in a weak electric field," *Phys. Rev. A* **86**, 013401 (2012).
17. K. R. Overstreet, R. R. Jones, and T. F. Gallagher, *Phys. Rev. Lett.* **106**, 033002 (2011).
18. E. S. Shuman, R. R. Jones, and T. F. Gallagher, *Phys. Rev. Lett.* **101**, 263001 (2008).
19. H. B. van Linden van den Heuvell and H. G. Muller, in *Multiphoton Processes*, edited by S. J. Smith and P. L. Knight (Cambridge University Press, Cambridge, 1988).
20. T. F. Gallagher, *Phys. Rev. Lett.* **61**, 2304 (1988).
21. K. R. Overstreet, R. R. Jones, and T. F. Gallagher, "Phase-dependent energy transfer in a microwave field," *Phys. Rev. A* **85**, 055401 (2012).
22. S. R. Lundeen, in *Advances in Atomic, Molecular, and Optical Physics*, edited by C. C. Lin and P. Berman (academic Press, New York, 2005).
23. W. E. Lamb, Jr., *Phys. Rev.* **85**, 259 (1952).

Publications 2010-2012

1. J. Nunkaew and T. F. Gallagher, "Up-down asymmetry of the electrons ejected from barium $6p_{1/2}nk$ autoionizing states," Phys. Rev. A **82**, 033413 (2010).
2. K. R. Overstreet, R. R. Jones, and T. F. Gallagher, "Phase-Dependent Electron-Ion Recombination in a microwave field," Phys. Rev. Lett. **106**, 033002 (2011).
3. J. Nunkaew and T. F. Gallagher, "Spectroscopy of barium $6p_{1/2}nk$ autoionizing states in a weak electric field," Phys. Rev. A **86**, 013401 (2012).
4. K. R. Overstreet, R. R. Jones, and T. F. Gallagher, "Phase-dependent energy transfer in a microwave field," Phys. Rev. A **85**, 055401 (2012).

Experiments in Ultracold Collisions and Ultracold Molecules

Phillip L. Gould
Department of Physics U-3046
University of Connecticut
2152 Hillside Road
Storrs, CT 06269-3046
<phillip.gould@uconn.edu>

Program Scope:

Recent progress in the production and manipulation of ultracold atoms and molecules has not only benefited atomic, molecular and optical (AMO) physics, but also impacted a variety of other fields, including quantum information, condensed-matter physics, fundamental symmetries, and chemistry. Although their complex level structure can complicate their manipulation, molecules have attracted increasing interest. They have multiple internal degrees of freedom, including electronic, vibrational, rotational, spin, and hyperfine, which span a wide range of energy scales, allowing interactions with a variety of other systems. Furthermore, heteronuclear molecules can have permanent electric dipole moments, whose long-range and anisotropic potentials lead to strong and controllable interactions. Molecules have been cooled “directly” using buffer gas cooling, electrostatic slowing, and laser cooling. They have also been produced “indirectly” by binding together cold atoms via the processes of photoassociation and Feshbach-resonance magnetoassociation. The resulting cold molecules have been trapped using optical, magnetic, and electrostatic techniques. Interesting applications of ultracold molecules are numerous and include: quantum computation; simulations of condensed-matter systems; quantum degenerate gases; novel quantum phases of dipolar gases; tests of fundamental symmetries and fundamental constants; ultracold chemistry; and ultracold collisions. The main thrust of our experimental program is to coherently control the collision dynamics of ultracold atoms using nanosecond-time-scale pulses of frequency-chirped light. Of particular interest is controlling the photoassociative formation of ultracold molecules.

Our experiments utilize Rb atoms which are cooled and confined in a magneto-optical trap (MOT). Rb has a number of attractive features: 1) its resonance lines at 780 nm and 795 nm are conveniently matched to commercially available diodes lasers; 2) the existence of two abundant and stable isotopes, ^{85}Rb and ^{87}Rb , provides some flexibility in the experiments; 3) ^{87}Rb is widely used in BEC studies; and 4) the photoassociative formation, as well as the state-selective ionization detection of the resulting Rb_2 , have been extensively investigated here at UConn and elsewhere. Our experiments utilize a separate “source” MOT to load a phase-stable MOT. The resulting cold trapped atoms are then illuminated with a sequence of pulses of frequency-chirped light. These pulses are typically 40 ns FWHM and the chirps typically cover 1 GHz in 100 ns. Inelastic excited-state collisions, including photoassociation, are measured via the resulting loss of atoms from the trap. The ground-state Rb_2 molecules formed by photoassociation are directly detected by ionization with a tunable pulsed dye laser. The resulting molecular ions are distinguished from atomic ions by their time-of-flight to the detector.

Recent Progress:

We have recently made progress in a number of areas: quantum dynamical calculations of trap-loss collisions induced by nonlinearly-chirped light and comparison with experiment; formation of ultracold ground-state molecules by photoassociation with both positively- and negatively-chirped light; quantum simulations of this chirped photoassociation; and production of faster chirps using a high-speed (4 GHz) arbitrary waveform generator to drive an electro-optic phase modulator.

The use of frequency-chirped light to induce a collision between a pair of atoms is interesting because it causes the excitation radius to change with time. This Condon radius, R_C , is the atomic separation R at which the light resonantly excites the ground-state atom pair to the long-range attractive molecular potential. Larger detunings below the atomic resonance lead to smaller values of R_C . If the laser frequency changes on the nanosecond time scale, and the excitation is occurring at long range, the resonance condition and the motion of the colliding atoms can evolve on similar time scales. This presents the opportunity to control the collisional dynamics via the frequency chirp. We have seen in the experiments that under certain conditions, the direction of the chirp is very important: the positive (red-to-blue) chirp yields a significantly larger collision rate than the negative (blue-to-red) chirp. This is because the excited atom pair always accelerates inward (towards smaller R) on the attractive potential, while the Condon radius R_C can either increase (positive chirp) or decrease (negative chirp) with time. For the positive chirp, the atom pair can only undergo a single excitation because subsequently, the atom separation R and the Condon radius R_C move in opposite directions. For the negative chirp, however, the Condon radius and the trajectory of the excited atom pair both proceed inward and further interactions, returning the atom pair to the ground state, can occur. This results in less excited-state collisional flux reaching short range, and therefore a reduced trap-loss collisional rate.

Furthermore, we have seen in the experiments that the temporal shape of the chirp can affect the trap-loss collisional rate. We vary this shape by superimposing either positive curvature (concave-up) or negative curvature (concave-down) on the linear variation of the laser frequency. In collaboration with Shimshon Kallush at ORT Braude and Ronnie Kosloff at Hebrew University (both in Israel), we have developed quantum dynamical calculations of these collisions, including the chirp nonlinearities. We find general agreement, in terms of the trends with respect to nonlinearity, between these simulations and the experiment. For negative chirps, we see that the chirp shape does indeed matter, while for positive chirps, it does not. This is consistent with the multiple interactions that can occur for negative chirps.

Trap-loss collisions involve excitation to attractive potentials very near the atomic asymptote, e.g., within 1 GHz, and can thus be considered a version of photoassociation where the vibrational levels are not resolved. We have also used chirped light in more conventional photoassociation, where the chirp range covers a small number of resolved vibrational lines. In this case, we directly detect the resulting ground-state Rb_2 molecules using resonance-enhanced multiphoton ionization (REMPI) with a pulsed dye laser at ~ 600 nm. As with trap-loss collisions, we see a significant dependence of the molecule formation rate on chirp direction. With the chirps centered on a photoassociation

resonance detuned 7.8 GHz below the atomic asymptote, the positive chirp forms more ground-state molecules than the negative chirp.

In an effort to understand this dependence on chirp direction, we have extended our quantum simulations to include the bound vibrational levels in both the ground- and excited-state molecular potentials. In our case, the 0_g^- and 1_u excited states are relevant, and these can populate high vibrational levels of the triplet ground state, $a^3\Sigma_g^+$. In general, the simulations reproduce the trends of the experiment. Examining the time evolution of the various state populations, we find that the positive chirp first passes through a photoassociation resonance, which produces excited molecules, and then through a bound-bound resonance, which drives the excited-state population down to the ground state. For the negative chirp, this sequence occurs in reverse, reducing the efficiency of producing ground-state molecules.

We continue to make progress in producing fast and arbitrarily shaped chirped pulses. We use a 4 GHz arbitrary waveform generator (AWG) to drive an electro-optic phase modulator, yielding chirps of 1 GHz in 2 ns. We have also demonstrated <1 ns pulses by driving an electro-optic intensity modulator with the AWG.

Future Plans:

We will perform chirped molecule formation experiments on time scales faster by a factor of 10 to 100, allowing us to better match the dynamics of more deeply bound molecular levels. For these faster chirps and shorter pulses, we will use a tapered amplifier to realize the higher intensities required. In general, we will take advantage of our ability to control laser frequency and amplitude on the nanosecond time scale in order to manipulate the dynamics of ultracold molecule formation. For example, with guidance from our simulations, we will optimize the production of ground-state molecules in a target vibrational level using our arbitrary waveform generator to vary parameters of the chirped pulses.

Recent Publications:

“Characterization and Compensation of the Residual Chirp in a Mach-Zehnder-Type Electro-Optical Intensity Modulator”, C.E. Rogers III, J.L. Carini, J.A. Pechkis, and P.L. Gould, *Opt. Express* **18**, 1166 (2010).

“Coherent Control of Ultracold ^{85}Rb Trap-Loss Collisions with Nonlinearly Frequency-Chirped Light”, J.A. Pechkis, J.L. Carini, C.E. Rogers III, P.L. Gould, S. Kallush, and R. Kosloff, *Phys. Rev. A* **83**, 063403 (2011).

“Creation of Arbitrary Time-Sequenced Line Spectra with an Electro-Optic Phase Modulator”, C.E. Rogers III, J.L. Carini, J.A. Pechkis, and P.L. Gould, *Rev. Sci. Instrum.* **82**, 073107 (2011).

“Quantum Dynamical Calculations of Ultracold Collisions Induced by Nonlinearly Chirped Light”, J.L. Carini, J.A. Pechkis, C.E. Rogers III, P.L. Gould, S. Kallush, and R. Kosloff, *Phys. Rev. A* **85**, 013424 (2012).

Physics of Correlated Systems

Chris H. Greene

Department of Physics and JILA, University of Colorado, Boulder, CO 80309-0440

and since August 13, 2012 at

Department of Physics, Purdue University, West Lafayette, IN 47907-2036

chgreene@purdue.edu

Program Scope

This theoretical research effort tackles problems at the cusp of the field's current abilities to describe correlated system governed by quantum mechanics, primarily in the context of atoms and molecules, in some cases interacting with external static or time-dependent fields. A standard approach in atomic and molecular physics is to treat the electrons approximately, as though they are moving independently of one another, or independently of other degrees of freedom such as the internuclear vibrations and rotations or an external field. While such uncorrelated approximations are effective in a number of situations, there are many phenomena that require more sophisticated treatments of the quantum behavior. It has been a longstanding goal of the research community to develop theoretical techniques capable of describing such nonperturbative correlations, and this project has been engaged in this class of endeavors. The current research group has been studying the effects of a dressing laser field on electron collisions and half-collisions, the latter representing photoionization processes. In addition, studies have continued in the area of electron collisions with a molecular ion that triggers dissociation and vibrational excitation, especially the process of dissociative recombination (DR), which is one of the most fundamental reactive chemical processes yet one of the most difficult for theory to handle. This overview will focus primarily on work performed and papers published during the past year[1-3], with some discussion of future directions.

Recent Progress and Immediate Plans

(i) Strong-field physics that ensues when an intense light pulse from a laser strikes an atom, molecule, or cluster.

A novel direction in atomic, molecular, and optical physics was triggered by the ability to combine an ultrafast infrared laser pulse with XUV light spawned by a high harmonic generation process. A particularly noteworthy experiment, published a few years ago by the group of Stephen Leone [Chem. Phys. **350**, 7 (2008)], demonstrated how a transient absorption experiment could yield control to some extent over the absorption of XUV light by helium in the photon energy range near 60 eV. While a phenomenological treatment did a reasonable job of accounting for those experimental results in the language of few-level quantum optics, we felt that it would be an important test for theory to develop techniques that could directly solve the time-dependent Schroedinger equation for this simplest two-electron atom. This project was able to build on our previous extensive solutions of the time-independent Schroedinger equation for two-electron atoms, but implementing time-dependent propagators on top of that machinery required extensive retooling and experimentation with alternative algorithms. The most effective algorithm we found for this calculation that was ultimately adopted for production computations was a split-operator treatment in an eigenbasis set of the field-free Hamiltonian constructed from our previously developed R-matrix approach. A complex absorbing potential was added to absorb the ionized electron flux without requiring an extremely large computational volume.

In the 2008 experiment of Loh and Leone, the infrared dressing laser wavelength was 800 nm, which could be viewed as primarily coupling the $2s2p\ ^1P^o$ and $2p^2\ ^1S^e$ autoionizing states of helium. Our calculations published this year [1] have successfully described the complicated transient absorption spectra observed experimentally for pump-probe time delays of 0, 20 fs, 40 fs, 60 fs, and 80 fs. This experimental IR laser wavelength is rather far detuned from being in resonance with the doubly-excited state energy difference, which makes it difficult to identify true quantum optics phenomena such as electromagnetically-induced transparency (EIT) and the Autler-Townes doublet. This is already an important milestone, the demonstration that the first experiment in this key regime can be reproduced through direct solution of the two-electron Schroedinger equation, and it should allow a realistic exploration of the broader parameter space for such processes. As an example of this, we have also changed the detuning to essentially zero in our calculations by repeating them with an IR laser wavelength of 600 nm. Now the expected Autler-Townes doublet emerges far more clearly, especially when the driving IR laser intensity is decreased in order to minimize the additional field-stripped decay channel of the doubly-excited state that was correctly identified by Loh *et al.* as an important aspect of the dynamics in this system.

In another study of laser-dressed electron-atom interactions by this project, calculations are underway for the system of an argon atom that is struck by an electron in the presence of a cw CO_2 laser field. Since the laser light in this case is monochromatic, we have tackled this problem using a mixed-gauge R-matrix formulation in the Floquet representation. This allows the calculation to be mapped onto a time-independent multichannel Schroedinger scattering problem of the type that is effectively handled using R-matrix methods. One reason for investigating this problem has been to test the hypothesis published elsewhere that perhaps the long range polarizability potential in the electron-argon Hamiltonian can cause one or more photons to be absorbed out to surprisingly large distances of order 50-100 Bohr radii. Our preliminary results suggest that this is not in fact the relevant physics for this system, as photon absorption and emission during the collision is almost negligible once the electron is beyond 10 to 15 Bohr radii from the atomic nucleus. Our conclusions, based on calculations that will be finalized and published fairly soon, provide confirmation of previous work carried out on this problem by Francis Robicheaux's group. Moreover, we now see further reason to doubt that the experimental measurements on this system dating back to the late 1980s are consistent with the assumption that electron collisions were occurring with single atoms in those experiments.

(ii) Low energy electron collisions with a molecule, ionized or neutral.

One goal of this project, dating back to our early studies of H_3^+ dissociative recombination over the past 13 years, has always been that lessons gleaned from the study of this simplest prototype polyatomic would carry over and yield insights that might help to theoretically treat more complex species. Often in physics, such hopes turn out to be overoptimistic, because there are frequently fundamental differences between the prototypes and the complex species. In the past year, however, a collaboration with Ann Orel, her postdoc Nicolas Douguet, and Viatcheslav Kokoouline has been able to show that the lessons learned from H_3^+ were decisive in the development of solid theoretical treatments of this challenging process of dissociative recombination for complex polyatomics that are highly symmetric. This collaboration has shown [2] that for closed-shell ionic target molecules CH_3^+ and H_3O^+ , our "simplified DR

treatment" developed originally for the Jahn-Teller-induced dissociation of H_3^+ also yields excellent agreement with experiment for these tetra-atomic target molecules.[2] This confirms as well that the Jahn-Teller mechanism of DR for H_3^+ has a much broader importance for other species. Parenthetically, I should also mention that a further impressive extension carried out by Orel and collaborators without this project's participation [see J. Phys. B 45, 051001 (2012)], obtained excellent results using this same basic method for an even more complicated system, the dissociative recombination of NH_4^+ , which further supports the aforementioned conclusions. These studies confirm that Rydberg pathways appear to usually provide the dominant route to DR at low energy for many and perhaps even most polyatomics that contain multiple hydrogen atoms.

This year has seen a rejuvenation of this project's work on describing dissociative recombination of the chemically-interesting and atmospherically-relevant molecule NO_2^+ . This molecule is challenging and quite different from other species considered so far, in part because there are tight chemical bonds and numerous electronic potential surfaces that are coupled strongly. Because there has been no previous theory or experiment on the DR rate of NO_2^+ , the theoretically predicted rate from this project will provide the first known information about this process in this ion. Our preliminary results, obtained in collaboration with Dan Haxton at LBNL, suggest that indirect Rydberg state pathways play a comparatively small role. Our first study of this richly complicated molecule will be finalized and published in late 2012 or else in 2013.

Another project underway with current postdoc Michal Tarana that is nearing maturity and will hopefully be completed during the coming few months is an extension of the UK electron-molecule R-matrix suite maintained by Jonathan Tennyson to make it capable of handling much larger basis sets. This is being achieved by directly solving for the R-matrix as an inhomogeneous linear system at each energy, as opposed to the usual route which requires a full diagonalization that obtains all eigenvalues and eigenvectors of the Hamiltonian matrix. The method has been known for some years but rarely applied to problems with many-electron molecules that require complicated multiconfiguration basis sets. This method has a disadvantage in requiring a new full linear solve at each desired scattering energy, but it has the advantage of being able to treat far larger basis sets in principle. A first demonstration calculation for electron scattering from the O_2 molecule is encouraging in this regard and will be completed soon. Another problem of interest in this same system is the photodetachment of the negative ion O_2^- , in particular the photoelectron angular distribution which has been studied in recent experiments. Because the experiments resolve the electron energies corresponding to different vibrational channels of the neutral O_2 fragment, we are carrying out a parallel investigation of the photoelectron angular distributions by implementing a vibrational frame transformation treatment. While such frame transformations are well known to be effective for describing electron interactions with positive molecular ions, very few studies exist for electron interactions with neutral species, so this is expected to be an important test case that will hopefully shed light on the strengths and limitations of the theoretical technique. Also while supported by this project, Michal Tarana has finished a major collaborative study of electron collisions with the complicated molecular target CF_3Cl .

It is not anticipated that there will remain unexpended funds at the end of this year of the funding cycle. There have been one postdoc and two part-time graduate students supported during the past year by this grant.

Papers published since 2010 that were supported at least in part by this grant.

- [1] *Femtosecond transparency in the extreme-ultraviolet region*, M Tarana and C H Greene, Phys. Rev. A **85**, 013411-1 to -11 (2012).
- [2] *Dissociative recombination of highly symmetric polyatomic ions*, N Douguet, A E Orel, C H Greene, and V Kokoouline, Phys. Rev. Lett. **108**, 023202-1 to -5 (2012).
- [3] *Dissociative electron attachment and vibrational excitation of CF₃Cl: Effect of two vibrational modes revisited*, M Tarana, K Houfek, Jiri Horacek, and I I Fabrikant, Phys. Rev. A **84**, 052717-1 to -9 (2011).
- [4] *Resonant structure of low-energy H₃⁺ dissociative recombination*, A Petrigani, S Altevogt, M H Berg, D Bing, M Grieser, J Hoffmann, B Jordon-Thaden, C Krantz, M B Mendes, O Novotny, S Novotny, D A Orlov, R Repnow, T Sorg, J Stuetzel, A Wolf, H Buhr, H Kreckel, V Kokoouline, C H Greene, Phys. Rev. A **83**, 032711-1 to -10 (2011). See also the Publisher's Note, Phys. Rev. A **83**, 049906 (2011).
- [5] *Breaking bonds with electrons: Dissociative recombination of molecular ions*, V Kokoouline, N Douguet, and C H Greene, Chem. Phys. Lett. (Frontiers Article) **507**, 1-10 (2011).
- [6] *The role of the Jahn-Teller coupling in dissociative recombination of H₃O⁺ and H₃⁺ ions*, N. Douguet, A. Orel, I. Mikhailov, I. F. Schneider, C. H. Greene, and V. Kokoouline, J. Phys. Conf. Ser. **300**, 012015-1 to -13 (2011).
- [7] *Recombination-pumped triatomic hydrogen infrared lasers*, R J Saykally, E A Michael, J Wang, and C H Greene, J. Chem. Phys. **133**, 234302-1 to -9 (2010).
- [8] *Quantum-defect analysis of 3p and 3d H₃ Rydberg energy levels*, J Wang, C H Greene, Phys. Rev. A **82**, 022506-1 to -8 (2010).
- [9] *Temperature dependence of binary and ternary recombination of D₃⁺ ions with electrons*, T Kotrik, P Dohnal, I Korolov, R Plasil, S Roucka, J Glosik, C H Greene, V Kokoouline, J. Chem. Phys. **133**, 034305-1 to -8 (2010).
- [10] *Calculation of rate constants for vibrational and rotational excitation of the H₃⁺ ion by electron impact*, V Kokoouline, A Faure, J Tennyson, and C H Greene, Mon. Not. R. Astron. Soc. **405**, 1195-1202 (2010).

Using Strong Optical Fields to Manipulate and Probe Coherent Molecular Dynamics

Robert R. Jones, Physics Department, University of Virginia
382 McCormick Road, P.O. Box 400714, Charlottesville, VA 22904-4714
bjones@virginia.edu

I. Program Scope

This project focuses on the exploration and control of non-perturbative dynamics in small molecules driven by strong laser fields. Our goal is to exploit strong-field processes to implement novel ultrafast techniques for manipulating and probing coherent electronic and nuclear motion within molecules. Through the application of these methods, we are working to obtain a more complete picture of the non-perturbative response of molecules to strong fields.

II. Recent Progress

During the past year we: (i) upgraded our laser system with the addition of a hollow-core fiber (HCF) compressor to enable the generation of <10 fs pulses for use in our continuing multi-electron dissociative ionization experiments and for future attosecond pulse generation; (ii) upgraded our supersonic molecular beam apparatus, including the installation of an Even-Lavie pulsed valve, to obtain substantially lower rotational temperatures (~ 1 K) for our continuing molecular orientation experiments; (iii) characterized a source of intense, single-cycle THz pulses based on optical rectification of high-energy, 100 fs, 800nm laser pulses in MgO-doped LiNbO₃ for use in experiments seeking to produce samples of well-oriented gas-phase molecules and for time-resolved manipulation of continuum electron wavepackets; (iv) began an exploration of intense ionization of atoms in the extreme low frequency regime using intense single-cycle THz pulses; (v) began experiments exploring the use of combined optical and THz fields to induce high-contrast field-free molecular orientation. Motivation for, and brief summaries of, our work in (iii)-(v) are provided below.

Intense THz pulses can serve as useful tools for exploring strong field processes and enabling optical control in atoms and molecules. For example, half-cycle THz pulses have been used for two decades to control and probe the dynamics of bound wavepackets as well as continuum electrons. However, in the context of AMO physics, the maximum available field strengths (~ 100 kV/cm) that are routinely available from large aperture photo-conductive switches limited the effectiveness of such sources to Rydberg systems. The availability of more intense single- and/or half-cycle THz pulses opens up a variety of applications in strong field atomic and molecular physics, even if the fields are too weak to influence ground state dynamics. These applications include high-energy electron-core scattering from field-driven Rydberg electrons, modification of electron rescattering dynamics in a laser-dressed continuum, and transient orientation of polar molecules [1-3].

a) Intense Single-Cycle THz Generation and Characterization

During the past year, we have adopted a non-linear optical method [4,5] for producing THz pulses with substantially higher field strength without the large, electrical transients that plague experiments performed with large aperture photoconductive switches. Specifically, optical rectification of tilted pulse-front, 150 fs, 790nm laser pulses in MgO doped stoichiometric Li:NbO₃ is used to produce the intense THz pulses [4]. We have used electro-optic sampling in ZnTe to measure the time-dependent THz field amplitude and characterize its spectral content.

Our measurements show that the THz field has the form of a single-cycle "sine" pulse with a frequency spectrum peaked near 0.3 THz and a FWHM of ~ 0.5 THz.

In preparation for experiments employing THz pulses to produce rotational wavepackets in molecules and to explore strong-field electron dynamics in atoms, we utilized momentum streaking of photoelectrons to measure the peak THz field and confirm that the waveform does indeed resemble a single-cycle sine pulse at its focus in a vacuum TOF spectrometer. For the measurement, Na atoms were ionized by a 150 fs, 390nm laser pulse and the electron energy was measured as the delay between the ionizing pulse and the THz field was varied. The delay-dependent momentum transfer shows a single peak, reflecting the time integral of the electric field (i.e the change in the vector potential) in a single-cycle sine pulse. From the magnitude of the momentum transfer, we infer a peak field exceeding 500kV/cm. This is roughly half the highest reported THz field strength for single-cycle pulses produced via the tilted-pulse front method (1.2 MV/cm as determined through direct energy measurements without transport into a vacuum chamber [5]).

b) Strong-field Ionization of Atoms Using Intense Single-Cycle THz Pulses

We have measured the THz ionization probability for Na *nd* atoms as a function of principal quantum number n ($5 < n < 16$) and field strength. For the measurements, the THz radiation is focused by an off-axis parabolic mirror into a thermal beam of laser-excited Rydberg atoms in a standard time-of-flight (TOF) spectrometer. Before entering the chamber, the THz beam passes through a wire grid polarizer pair which served as a variable attenuator that preserves the polarization and temporal shape of the THz field. Using the field calibration from the THz streaking measurements, we find that the measured ionization probabilities vs. field strength curves are in good agreement with the predictions of a classical Monte Carlo simulation.

We have also measured the electron energy distributions resulting from THz ionization. Interestingly, for a fixed THz field strength, the highest energy electrons (~ 100 eV) are produced during the ionization of the most *tightly* bound electrons. Apparently this is due to the variation in the most probable ionization times for different n -states and the fact that the single-cycle sine waveform does not satisfy the conditions of the slowly varying envelope approximation (SVEA). According to the simpleman's model, in the SVEA, an electron liberated from an atom at the peak of an oscillating field receives no net momentum from the field because the vector potential at the instant of its birth is the same as that at the end of the pulse. However, for a single-cycle sine waveform this is not the case. As a result, ionization near the peak of the field results in an energy transfer of $2U_p$ to the electron, where U_p is the pondermotive energy. In our experiment, most of the electrons from higher n -states are liberated via over-the-barrier ionization earlier in the pulse. These electrons receive a smaller net momentum transfer than electrons originating from more tightly bound states, as these are introduced into the field near the peak of the first half-cycle or are transferred to higher lying states in during the first half-cycle of the field and may then ionize near its zero crossing. Interestingly, due to the breakdown of the SVEA, electrons ionized at the central zero-crossing of a single-cycle sine pulse may obtain a maximum energy transfer of $8U_p$, without rescattering. This differs substantially from the $2U_p$ prediction of the simpleman's model for ionization in multi-cycle fields. Importantly, in the single-cycle case, electrons with energies exceeding $2U_p$ are not necessarily the result of rescattering. Indeed, we observe electrons with energies of at least $4U_p$ which, due to the spatial extent of the Rydberg wavefunctions, are likely not the result of rescattering. The breakdown in the simpleman's model

will be important for interpreting our continuing THz experiments and will impact other work employing single-cycle optical pulses for strong field experiments.

c. Towards Efficient Field Free Molecular Orientation

When a molecule is exposed to an intense laser field, its alignment and orientation relative to the laser polarization are critical parameters in determining the effect of the field. In addition, information on the molecular response to the field, as encoded in photo-fragment distributions, may only be interpretable if the molecule has a well-defined direction in the laboratory frame. Clearly, the establishment of optical methods to orient molecules in free space is an important application of molecular control. Many techniques for adiabatic and transient molecular orientation have been proposed, and several have been demonstrated. Each of these has various advantages and disadvantages. In general, achieving a high degree of molecular orientation is considerably more difficult than obtaining very good alignment.

We are pursuing an all optical, transient orientation method that can be applied to achieve field-free orientation in high-density targets and is readily scalable to kHz repetition rates. The method relies on the preparation of mixed-parity rotational wavepackets through direct THz excitation of a coherent superposition of states in a rotational ladder. Obtaining the highest degree of orientation requires that the coherent excitation proceeds from a single state. If, instead, one starts from an incoherent ensemble, the degree of orientation can be substantially smaller. Hence, significantly greater orientation can be achieved through state-selection and/or rotational pre-cooling of the gas.

We recently began experiments exploring orientation of OCS by combined optical and THz fields. Several other groups have used OCS in their orientation experiments making it a useful benchmark [3,6,7]. The molecules in the skimmed supersonic expansion enter a high vacuum detection chamber where they are exposed to a linearly polarized, 800 nm, ~100 fs pre-alignment pulse and the single-cycle THz field. We use Coulomb explosion, induced by a time-delayed, 800 nm, 30 fsec laser pulse, as a time-resolved probe of molecular alignment and orientation. To date we have observed strong transient alignment due to the optical pulse, but have yet to achieve sufficient spatial overlap and appropriate timing of the optical and THz pulses to confirm orientation.

III. Future Plans

We are continuing our efforts to observe transient, field-free orientation of OCS. Once we are successful we intend to explore strong field ionization and HHG from aligned samples. We will continue our experiments on atoms in strong THz fields. In particular, we will look for evidence of core electron excitation and ionization due to inelastic electron rescattering. We are also adding an optical pulse shaper to our kHz amplifier system in an attempt to improve the contrast and reduce the minimum duration of the pulses from our HCF compressor. We plan to use 2-color asymmetric field pulses as short as <6 fs to better understand why the strong asymmetric MEDI we recently observed in 40 fs, 2-color fields is not induced by asymmetric few-cycle pulses.

IV. Publications from Last 3 Years of DOE Sponsored Research (since September 1, 2009)

- i) K.R. Overstreet, R.R. Jones, and T.F. Gallagher, "Phase dependent energy transfer in a microwave field," *Physical Review A* 85, 055401 (2012).
- ii) Boris Bergues, Matthias Kübel, Nora G. Johnson, Bettina Fischer, Nicolas Camus, Kelsie J. Betsch, Oliver Herrwerth, Arne Senfleben, A. Max Saylor, Tim Rathje, Itzik Ben-Itzhak, Robert R.

Jones, Gerhard G. Paulus, Ferenc Krausz, Robert Moshhammer, Joachim Ullrich, and Matthias F. Kling, “Attosecond Control and Real-Time Observation of Electron Correlations,” *Nature Communications* **3**, 813 (2012).

iii) K.R. Overstreet, R.R. Jones, and T.F. Gallagher, “Phase-dependent Electron-Ion Recombination in a Microwave Field,” *Phys. Rev. Lett.* **106**, 033002 (2011).

iv) Nora G. Johnson, O. Herrwerth, A. Wirth, S. De, I. Ben-Itzhak, M. Lezius, B. Bergues, M.F. Kling, A. Senftleben, C.D. Schröter, R. Moshhammer, J. Ullrich, K.J. Betsch, R.R. Jones, A.M. Saylor, T. Rathje, Klaus Rühle, Walter Müller, and G. G. Paulus, “Single-shot Carrier-Envelope-Phase Tagged Ion-momentum Imaging of Non-sequential Double Ionization of Argon in Intense 4-fs Laser Fields,” *Phys. Rev. A* **83**, 013412 (2011).

v) K.J. Betsch, D.W. Pinkham, and R.R. Jones, “Directional Emission of Multiply-Charged Ions During Dissociative Ionization in Asymmetric Two-Color Laser Fields,” *Phys. Rev. Lett.* **105**, 223002 (2010).

vi) Brett A. Sickmiller and R.R. Jones, “Effects of Phase-Matching on High Harmonic Generation from Aligned N₂,” *Phys. Rev. A* **80**, 031802(R) (2009).

References

[1] M. Machholm and N.E. Henriksen, “Field-Free Orientation of Molecules,” *Phys. Rev. Lett.* **87**, 193001 (2001).

[2] E. Gershnel, I. Sh. Averbukh, and Robert J. Gordon, “Enhanced molecular orientation induced by molecular antialignment,” *Phys. Rev. A* **74**, 053414 (2006).

[3] Sharly Fleischer, Yan Zhou, Robert W. Field, and Keith A. Nelson, “Molecular Orientation and Alignment by Intense Single-Cycle THz Pulses,” *Phys. Rev. Lett.* **107**, 163603 (2011).

[4] For a recent review see: Janos Hebling, Ka-Lo Yeh, Matthias C. Hoffman, Balazs Bartal, and Keith A. Nelson, “Generation of High-Power Terahertz Pulses by Tilted-Pulse-Front Excitation and Their Application Possibilities,” *J. Opt. Soc. Am. B* **25**, B6 (2008).

[5] H. Hirori, A. Doi, F. Blanchard, and K. Tanaka, “Single-cycle Terahertz Pulses with Amplitudes Exceeding 1MV/cm Generated by Optical Rectification in LiNbO₃,” *Appl. Phys. Lett.* **98**, 091106 (2011).

[6] Akihisa Goban, Shinichirou Minemoto, and Hirofumi Sakai, “Laser-Field-Free Molecular Orientation,” *Phys. Rev. Lett.* **101**, 013001 (2008).

[7] Jens H. Nielsen, Henrik Stapelfeldt, Jochen Küpper, Bretislav Friedrich, Juan J. Omiste, and Rosario González-Férez, “Making the Best of Mixed-Field Orientation of Polar Molecules: A Recipe for Achieving Adiabatic Dynamics in an Electrostatic Field Combined with Laser Pulses,” *Phys. Rev. Lett.* **108**, 193001 (2012).

Molecular Dynamics Probed by Coherent Soft X-Rays

Henry C. Kapteyn and Margaret M. Murnane

University of Colorado at Boulder, Boulder, CO 80309-0440

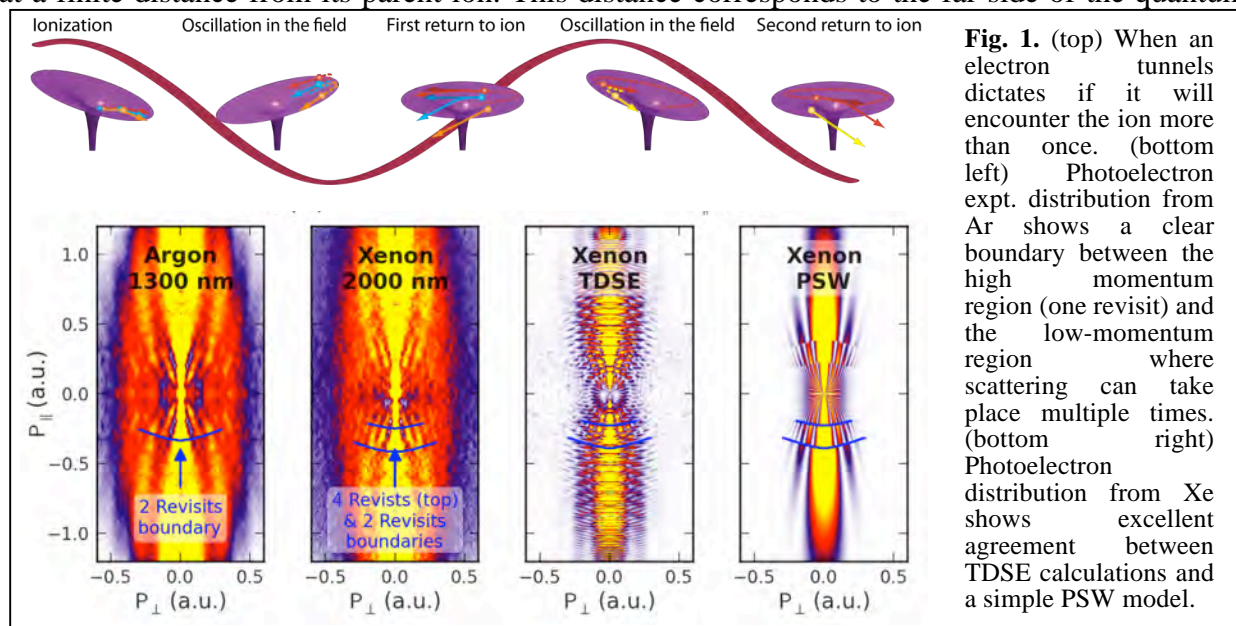
Phone: (303) 492-8198; E-mail: kapteyn@jila.colorado.edu

The goal of this work is to develop novel short wavelength probes of molecules and to understand the response of atoms to strong laser fields, in particular mid-infrared (mid-IR) laser fields. We made exciting advances in several experiments.

1. Strong field ionization using mid-IR driving lasers: beyond the 3-step model

The favorable λ^2 scaling of the ponderomotive energy and resulting cutoff photon energy in high harmonic emission has motivated studies of strong field ionization of atoms and molecules with mid-IR driving pulses. However, until recently, the very different physics associated with mid-IR strong field ionization was not well understood. One reason for this is that the advanced (and very computationally intensive) numerical models required to model strong field ionization in the mid-IR make it challenging to develop a good physical insight.

In work just published in PRL, we showed that when an atom is irradiated by an intense mid-IR femtosecond laser pulse, the simple semi-classical 3-step model often used to describe how an atom ionizes needs to be extended to include the fact that the electron can re-encounter the ion many times before finally ionizing. We first developed an intuitive model for understanding strong-field ionization as a simple superposition of plane and spherical photoelectron waves, corresponding to the directly ionized and rescattering electrons. This approach generalizes the standard 3-step model of strong field ionization that has provided crucial physical insight into strong field ionization and high-harmonic generation. We then used this model to show that new interference structures, which we observe in the experimental photoelectron angular distributions generated by mid-IR lasers, are created by electron trajectories that scatter from the parent ion after passing by the ion several times. The quantum phase accumulated by the electrons during their oscillatory path between ionization and rescattering is directly imprinted onto the photoelectron angular distribution. Thus, the shape and spacing of the interference structures directly correspond to the specific number of times the electron re-encounters its parent ion before scattering strongly. Through an analysis of the energy cutoff of these newly observed structures, we show that when an atom is ionized by an intense laser field, the electron emerges at a finite distance from its parent ion. This distance corresponds to the far side of the quantum



tunneling barrier, and is the first time to our knowledge that this distance has been experimentally measured. Our simple model allows us to uncover valuable physical insight into strong-field electron dynamics and provides an explanation for many of the features previously seen in experimental photoelectron distributions. This work also has implications for further efforts to extract atomic and molecular dynamics from strong-field physics.

2. X-ray driven dynamics in triatomic molecules: radiation femtochemistry

In past work, we combined HHG with a COLTRIMS momentum imaging apparatus to observe directly the chemical dynamics initiated by ionizing radiation i.e. *radiation femtochemistry*. This work immediately yielded new and unanticipated findings - exploring which shake-up states are responsible for dissociation of N_2 , and explaining why autoionization is delayed in O_2 .

In more recent work just published in Nature Physics, we explored how to use laser pulses to control non-Born-Oppenheimer dynamics in x-ray driven triatomic molecules. N_2O is a simple linear triatomic molecule with an asymmetric bond. Using a few-femtosecond 43 eV XUV pulse,

we can create an exotic excited-state target where a simple Born-Oppenheimer picture breaks down. The resultant decay dynamics involves a competition between two decay channels that occur on very fast, 20 fs, timescales, as illustrated in Fig. 2: molecular autoionization by ejecting a second electron ($N_2O^{+*} \rightarrow N_2O^{2+} + e^-$), or dissociation without electron emission - including two-body dissociation to one singly charged atomic (molecular) ion plus another molecular (atomic) neutral fragment, or three-body dissociation to one singly charged atomic ion and two atomic neutral fragments. For the Coulomb explosion channel that involves the emission of a second electron, the transient intermediate doubly charged state then decays by breaking either the N-N or N-O bond:



In the presence of an intense infrared (IR) field, we can interrupt the neutral-ion dissociation channel and strongly enhance the double-ion channel yield, because the excited N_2O^{+*} is very fragile in the laser field and can easily lose a second electron. Moreover, with the addition of an IR field, breaking the N-O bond can be enhanced more than breaking the N-N bond (Fig. 2), indicating the presence of laser-induced non-adiabatic electron motion.

3. Understanding high harmonic generation from molecules

High harmonic generation (HHG) from atoms has been studied for about 25 years, and this area of research continues to yield surprising new physics. In contrast, high harmonic generation from molecules has been studied only in the past 10 years, and the richer nature of the molecular

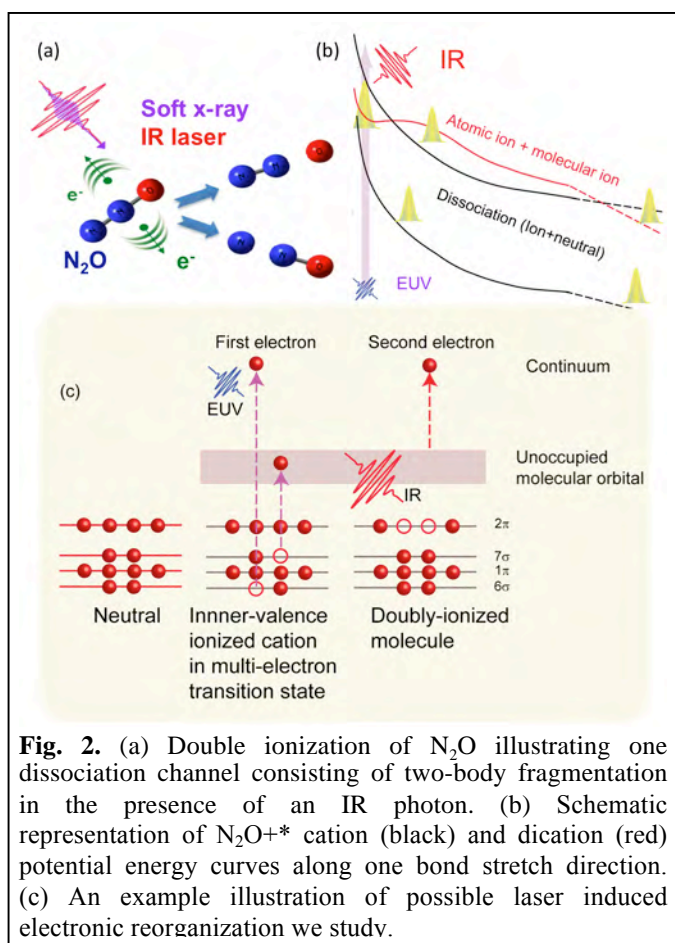


Fig. 2. (a) Double ionization of N_2O illustrating one dissociation channel consisting of two-body fragmentation in the presence of an IR photon. (b) Schematic representation of N_2O^{+*} cation (black) and dication (red) potential energy curves along one bond stretch direction. (c) An example illustration of possible laser induced electronic reorganization we study.

orbital structure provides both challenges and opportunities. We reported several new findings about HHG from molecules, many in collaboration with Tamar Seideman's group -

Extracting continuum electron dynamics from high harmonic emission from molecules: In this work, through high-fidelity measurements of HHG from molecules, we observed and analyzed higher order fractional rotational revivals in molecules (up to the 1/16) for the first time. These observations demonstrate that HHG is the most sensitive probe of rotational wave packet dynamics, allowing us to uncover new insights not observable using conventional probes. Using a two-center model of HHG from molecules, we intuitively explained how the observed HHG is related to the alignment distribution, and extracted the pump laser intensity and the rotational temperature of the medium. More remarkably, by comparing a rigorous theory of HHG from aligned molecules with high signal-to-noise experimental data, we can extract the underlying electronic dipole elements of the HHG signal, as well as information on the continuum electron dynamics. Specifically, we uncover that the continuum electron gains angular momentum from the photon field while propagating in the continuum, and that only a small number of electron partial waves strongly dominate the HHG dynamics. For molecules with antisymmetric ground state orbitals, electrons liberated with low electronic angular momentum $l=1$ recombine from a higher angular momentum state with $l=3$. Such electronic angular momentum non-conserving events dominate over angular momentum conserving events, increasingly so as the harmonic order increases, for both CO_2 and N_2O . Thus, attosecond electron dynamics manifests itself in the experimental observable of higher-order rotational revivals - and is crucial for their observation.

Ultrafast elliptical dichroism in high-order harmonics as a probe of molecular structure and electron dynamics: In our work studying HHG from molecules, again with Tamar Seideman's group, we made a surprising new finding - that the maximum in HHG emission from a molecule does not occur when the molecule is driven by linear polarized laser beams (as is the case for atoms), but rather for a non-zero value of the ellipticity of the driving laser. Moreover, the two polarization states that contribute to the elliptically polarized HHG beam behave very differently. To put this finding in context: for a long time it was known that HHG from atoms is brightest when driven by linearly polarized fields. As the driving laser becomes more elliptically polarized, the electron will simply not recollide with the ion. Thus, any ellipticity in the driving laser reduces the HHG emission in atoms. Clearly this is not the case for molecules.

At first we thought that an advanced and complex model would be needed to explain these surprising results. However, fortunately, we are able to fully interpret them using a simple and intuitive two charge-center model that gives great insight into the physics of HHG from molecules. Our work clearly demonstrates how to use molecular structure and alignment to manipulate the polarization state of high-order harmonics, and also presents a potential new attosecond probe of the underlying molecular dynamics. Specifically, information about molecular orbital structure is contained both in the value of the HHG dichroism as a function of laser ellipticity and laser-molecule angle, and in the variations with harmonic order. The use of an elliptically polarized laser field also provides new insights into the journey of the continuum electron and the underlying bound states of the molecular ion. In the future, our findings will provide useful insights into fundamental coupled electron-ion-structural dynamics in molecules. Moreover, the ability to control the polarization properties of HHG using an elliptical driving field is unique and provides a very valuable tool for the production and tuning of attosecond pulses that are recently finding broad applications in nanoscience.

4. Highlights in related DOE collaborations

In exciting recent work in collaboration with Andrius Baltuska in Vienna, we demonstrated full phase matching of high harmonic generation at photon energies $> 1.6\text{keV}$ for the first time (Science, June 2012). This work extends bright attosecond pulses into the soft x-ray region. We will use this light source for x-ray absorption studies in the gas and liquid phase. Early results that demonstrated full phase matching up to 1.6keV were highlighted on the cover of Nature Photonics, (Dec 2010) with DOE acknowledgement. In work done with Keith Nelson, we observed quasi-ballistic thermal transport through nanostructured interfaces for the first time,

using spatially coherent HHG beams (Nature Materials (2010), NanoLetters (2011)). Finally, in work in collaboration with John Miao (UCLA), we demonstrated 3D imaging from a single view using coherent diffractive imaging (Nature in 2010).

Publications as a result of DOE support since 2009

1. P. Sherratt, R. Lock, X. Zhou, H. Kapteyn, M. Murnane, T. Seideman, "Ultrafast elliptical dichroism in high-order harmonics as a dynamic probe of molecular and electronic structure", submitted (2012).
2. X. Zhou, P. Ranitovic, C. Hogle, H.C. Kapteyn and M.M. Murnane, "Probing and Controlling non-Born-Oppenheimer Dynamics in Super-Excited Triatomic Molecules", Nature Physics **8**, 232 (2012).
3. R. Lock, X. Zhou, H. Kapteyn, M. Murnane, S. Ramakrishna, T. Seideman, "Extracting continuum electron dynamics from high harmonic emission from molecules," Physical Review Letters **108**, 133901 (2012).
4. D. Hickstein, P. Ranitovic, S. Witte, X. Tong, Y. Huismans, P. Arpin, X. Zhou, B. Zhang, C. Ding, K. Keister, P. Johnsson, N. Tushima, M. Vrakking, H. Kapteyn, M. Murnane, "Direct visualization of laser-driven electron multiple-scattering and tunneling distance using velocity-map imaging," Phys. Rev. Lett. **109**, 073004 (2012).
5. M. Spanner, J. Mikosch, A. Boguslavskiy, M. Murnane, A. Stolow, S. Patchkovskii, "Strong Field Ionization and High Harmonic Generation during Polyatomic Molecular Dynamics," Phys. Rev. A **85**, 033426 (2012).
6. Qing Li et al., "Generation and Control of Ultrashort-Wavelength 2D Surface Acoustic Waves at Nano-interfaces", Phys. Rev. B **85**, 195431 (2012).
7. P. Ranitovic, X. M. Tong, C. W. Hogle, X. Zhou, Y. Liu, N. Tushima, M. M. Murnane, and H. C. Kapteyn, "Laser-Enabled Auger Decay in Rare-Gas Atoms," Physical Review Letters **106**, 053002 (2011).
8. D. Nardi et al., "Probing Thermomechanics at the Nanoscale: Impulsively Excited Pseudosurface Acoustic Waves in Hypersonic Phononic Crystals", Nano Letters **11**, 4126 (2011).
9. T. Popmintchev, M.C. Chen, P. Arpin, M. M. Murnane, and H. C. Kapteyn, "The attosecond nonlinear optics of bright coherent X-ray generation," Nature Photonics **4**, 822 (2010). *Featured on cover.*
10. W. Li, A. Becker, C. Hogle, V. Sharma, X. Zhou, A. Becker, H. Kapteyn, M. Murnane, "Visualizing electron rearrangement in space and time during the transition from a molecule to atoms," PNAS **107**, 20219 (2010).
11. K. P. Singh et al., "Control of Electron Localization in Deuterium Molecular Ions using an Attosecond Pulse Train and a Many-Cycle Infrared Pulse," Phys. Rev. Lett. **104**, 023001 (2010).
12. P. Ranitovic et al, "IR-Assisted Ionization of Helium by Attosecond XUV Radiation," New J. Phys. **12**, 013008 (2010).
13. K. S. Raines, S. Salha, R. L. Sandberg, H. D. Jiang, J. A. Rodriguez, B. P. Fahimian, H. C. Kapteyn, J. C. Du, and J. W. Miao, "Three-dimensional structure determination from a single view," Nature **463**, 214 (2010).
14. M. Siemens, Q. Li, M. Murnane, H. Kapteyn, R. Yang, E. Anderson, K. Nelson, "High-Frequency Acoustic Waves in Nanostructures Characterized by Coherent EUV Beams", Appl. Phys. Lett. **94**, 093103 (2009).
15. M. Siemens, Q. Li, R. Yang, K. Nelson, E. Anderson, M. Murnane, H. Kapteyn, "Measuring quasi-ballistic heat transport across nanoscale interfaces using ultrafast coherent soft x-rays", Nature Materials **9**, 26 (2010).
16. P. Arpin, T. Popmintchev, N. Wagner, A. Lytle, O. Cohen, H. Kapteyn, M. Murnane, "Enhanced HHG from Multiply Ionized Ar > 500eV through Laser Pulse Self-Compression," Phys. Rev. Lett. **103**, 143901 (2009).
17. R. M. Lock, X. B. Zhou, W. Li, M. M. Murnane, and H. C. Kapteyn, "Measuring the intensity and phase of high-order harmonic emission from aligned molecules," Chemical Physics **366**, 22 (2009).
18. M.C. Chen, M. Gerrity, S. Backus, T. Popmintchev, X. Zhou, P. Arpin, X. Zhang, H. Kapteyn, M. Murnane, "Spatially coherent, phase matched, EUV beams at 50 kHz," Optics Express **17**, 17376 (2009).
19. T. Popmintchev et al., "Phase matching of high harmonic generation in the soft and hard X-ray regions of the spectrum," PNAS **106**, 10516 (2009).

Imaging Multi-particle Atomic and Molecular Dynamics

Allen Landers

landers@physics.auburn.edu

Department of Physics
Auburn University
Auburn, AL 36849

Program Scope

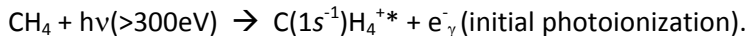
We are investigating phenomena associated with ionization of an atom or molecule by single photons (weak field) with an emphasis on ionization-driven atomic and molecular dynamics. Of particular interest is untangling the complicated electron-correlation effects and molecular decay dynamics that follow an initial photoionization event. We perform these measurements using variations on the well established COLTRIMS technique. The experiments take place at the Advanced Light Source at LBNL as part of the ALS-COLTRIMS collaboration with the groups of Reinhard Dörner at Frankfurt and Ali Belkacem and Thorsten Weber at LBNL. Because the measurements are performed in “list mode” over a few days where each individual event is recorded to a computer, the experiments can be repeated virtually with varying gate conditions on computers at Auburn University over months. We continue to collaborate closely with theoreticians also funded by DOE-AMOS including most recently the groups of F. Robicheaux and C.W. McCurdy.

We highlight below the most exciting result from recent work studying the core photoionization of methane. This research was part of the dissertation project of Joshua Williams and has been published as two separate articles: *Phys. Rev. Lett.* **108** 233002 (2012) and *J. Phys. B: At. Mol. Opt. Phys.*, (special issue, in press).

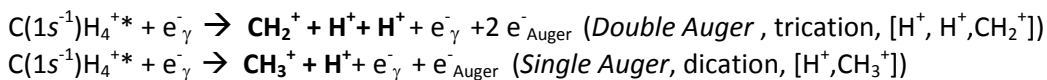
Recent Progress: Core Photoionization of Methane

Methane is one of the simplest polyatomic molecules, and as such provides a useful laboratory to study molecular dynamics. Its complexity is sufficient for exhibiting interesting decay behaviors and for challenging theory, but perhaps just at the boundary so there is great promise for expanding our fundamental understanding of how such complex systems can evolve over short time scales. Methane is a neon analogue with 10 electrons, two of which are deeply bound in the core of the carbon atom. Prompt photoionization of one of these C(1s) electrons leads to a highly excited molecular cation that has valence electronic structure nearly identical to the neutral ground state.

Our experiment uses the standard COLTRIMS approach, where we measure in coincidence up to four particles resulting from the photoionization and subsequent decay (one photoelectron and up to three ions). The initial photoionization reaction is given by



The dipole absorption of the photon promotes the essentially atomic C(1s) electron into a continuum *sp* state that can be strongly influenced by the molecular potential. Following this photoionization, the molecule can decay through multiple pathways, which we organize here into groups corresponding to three of the final fragment states (in bold) that we have measured in the experiment:



There are additional dissociative states, but we will limit the current presentation to the cases above.

1) 3-D Molecule Imaging with Core-Photoionization [*Phys. Rev. Lett.* **108** 233002 (2012)]:

We have confirmed that when double Auger occurs in the molecule, the triply charged molecular ion (trication) is extremely unstable and dissociates rapidly along the bond axes, allowing us to fully orient the molecule in three dimensions. We are then able to observe the electron emission in the molecule frame, in the form of molecular frame photoelectron angular distributions (MFPADs). We show data here for the case of 4.5 eV photoelectron energy.

The most exciting outcome of these measurements is that when we integrate over the polarization axis in the molecule frame, we can fully isolate the influence of the molecular potential on the photoelectron emission. When we do this, we find the striking result that the photoelectrons tend to emerge along the bond axes, effectively imaging the molecule (Fig 1 top left). Although this effect is predicted by complex Kohn variational calculations (McCurdy, Fig 1 bottom left), we still lack a simple model explanation. Furthermore, we find that even in the highly differential case of the molecule oriented relative to a specific polarization axis, we are able to see the complicated emission patterns predicted by the calculation (Fig 1 right).

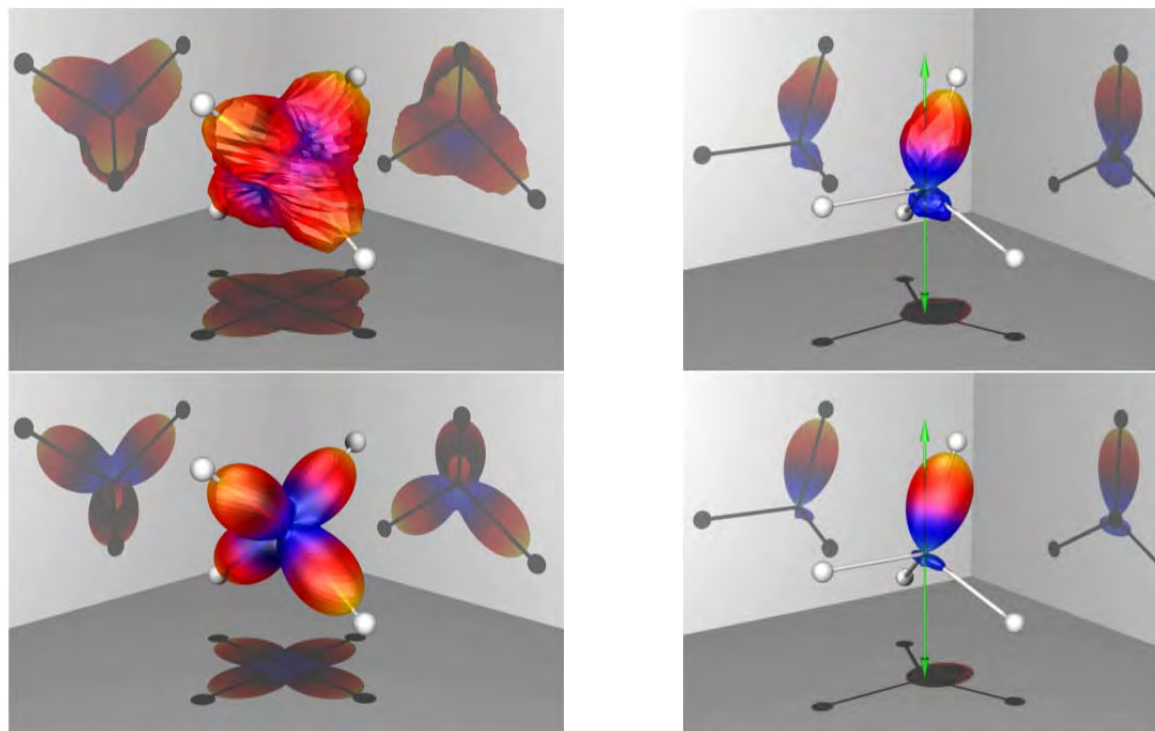


Figure 1: Molecular frame photoelectron angular distributions (MFPADs) following core photoionization of methane. *Top row*: ALS COLTRIMS experiment, *Bottom Row*: Complex Kohn variational calculations. *Left*: MFPAD integrated over polarization axis isolating influence of molecular potential. *Right*: MFPAD for a specific geometry demonstrating level of detailed agreement between experiment and theory.

2) Decay Dynamics [*J. Phys. B: At. Mol. Opt. Phys.*, (special issue, in press)]:

In addition to the imaging measurement shown above, we are also able to gain some understanding of the decay dynamics. For example, in the $[\text{H}^+, \text{CH}_3^+]$ decay channel of the dication, we found that the proton emission angle corresponds to the ground state bond angle only for certain values of the kinetic energy release. In a manuscript recently accepted for publication in *J. Phys. B: At. Mol. Opt. Phys.*, we interpreted this result with theoretical support to be due to the $[\text{H}^+, \text{CH}_3^+]$ decay channel arising through two different mechanisms. Each channel is associated with a different kinetic energy release.

The lower energy decay mode distorts the molecule, and removes the correlation between bond angle and emission angle. The result is simple dipole-shaped distribution where the influence of the molecular potential on electron emission is lost in the measurement. Conversely, the higher energy decay mode ejects the proton along a bond axis, allowing for the measurement of the molecular frame photoelectron distribution.

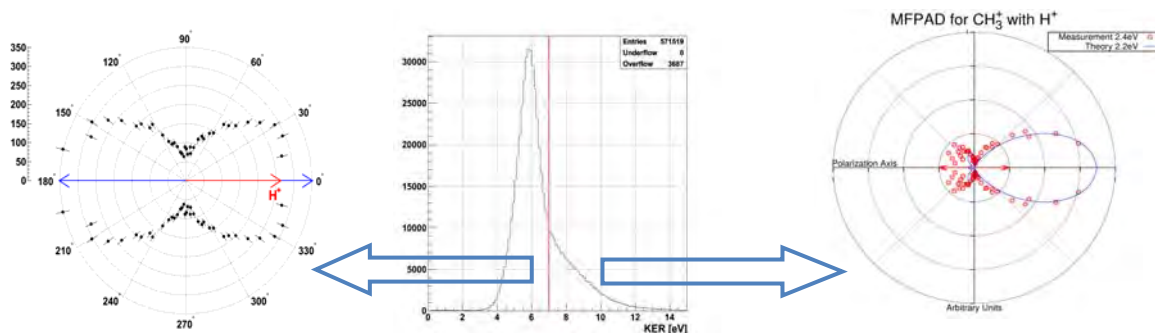


Figure 2: Kinetic energy release for the $[H^+, CH_3^+]$ channel (center) corresponding to axial-recoil breakdown (left) or axial-recoil valid (right) MFPADs. The right panel shows comparison with theory.

Future Plans:

We intend to pursue additional experiments to better understand the effects discussed above and to exploit the above results to study additional phenomena. Here are some examples:

- Study similar systems to explore whether or not the imaging effect observed in methane occurs elsewhere.
- Measure the Auger electrons in coincidence with fragments to produce molecular frame angular distributions for Auger electrons in order to better identify dissociative pathways.
- Measure methane analogues with substitutions for hydrogen (e.g. difluoromethane CH_2F_2) to look at the influence of different electron density distributions along the bond axes.
- Study core-hole localization in C_2H_6 using 3D MFPADS.
- Use larger polyatomic molecules (propane, benzene) to probe the limits of extending these measurements to systems of increasing complexity.

Refereed Publications: Supported by DOE-AMOS (2009-present)

1. **Ejection of quasi free electron pairs from the helium atom ground state by a single photon**, M. S. Schöffler, C. Stuck, M. Waitz, F. Trinter, T. Jahnke, U. Lenz, M. Jones, A. Belkacem, A.L. Landers, C.L. Cocke, J. Colgan, A. Kheifets, I. Bray, H. Schmidt-Böcking, R. Dörner, and Th. Weber *Phys. Rev. Lett.*, (submitted).
2. **Probing the Dynamics of Dissociation of Methane Following Core Ionization Using Three-Dimensional Molecular Frame Photoelectron Angular Distributions**, J. B. Williams, C. S. Trevisan, M. S. Schöffler, T. Jahnke, I. Bocharova, H. Kim, B. Ulrich, R. Wallauer, F. Sturm, T. N. Rescigno, A. Belkacem, R. Dörner, Th. Weber, C. W. McCurdy, and A.L. Landers, *J. Phys. B: At. Mol. Opt. Phys.*, (special issue, in press).
3. **Calculated and measured angular correlation between photoelectrons and Auger electrons from K-shell ionization**, F. Robicheaux, M. P. Jones, M. S. Schöffler, T. Jahnke, K. Kreidi, J. Titze, C. Stuck, R. Dörner, A. Belkacem, Th. Weber, and A.L. Landers *J. Phys. B: At. Mol. Opt. Phys.*, **45** 175001 (2012).

4. **Multi fragment vector correlation imaging - A proposal to search for hidden dynamical symmetries in many-particle molecular fragmentation processes**, F. Trinter, L. Ph. H. Schmidt, T. Jahnke, M. S. Schöffler, O. Jagutzki, A. Czasch, J. Lower, T. A. Isaev, R. Berger, A. L. Landers, Th. Weber, R. Dörner, H. Schmidt-Böcking *Molecular Physics* **110** 1863 (2012).
5. **Imaging polyatomic molecules in three dimensions using molecular frame photoelectron angular distributions**, J. B. Williams, C. S. Trevisan, M. S. Schöffler, T. Jahnke, I. Bocharova, H. Kim, B. Ulrich, R. Wallauer, F. Sturm, T. N. Rescigno, A. Belkacem, R. Dörner, Th. Weber, C. W. McCurdy, and A.L. Landers, *Phys. Rev. Lett.* **108** 233002 (2012).
6. **Dynamic modification of the fragmentation of autoionizing states of O+2**, W. Cao, G. Laurent, S. De, M. Schöffler, T. Jahnke, A. S. Alnaser, I. A. Bocharova, C. Stuck, D. Ray, M. F. Kling, I. Ben-Itzhak, Th. Weber, A. L. Landers, A. Belkacem, R. Dörner, A. E. Orel, T. N. Rescigno, and C. L. Cocke, *Phys. Rev. A* **84** 053406, (2011).
7. **Matter wave optics perspective at molecular photoionization: K-shell photoionization and Auger decay of N₂**, M. Schöffler, T. Jahnke, J. Titze, N. Petridis, K. Cole, L. Ph. H. Schmidt, A. Czasch, O. Jagutzki, J.B. Williams, C.L. Cocke, T. Osipov, S. Lee, M.H. Prior, A. Belkacem, A.L. Landers, H. Schmidt-Böcking, R. Dörner, and Th. Weber, *New Journal of Physics* **13** 095013 (2011).
8. **Production of excited atomic hydrogen and deuterium from H₂, HD and D₂ photodissociation** R Machacek , V M Andrianarijaona , J E Furst , A L D Kilcoyne , A L Landers , E T Litaker , K W McLaughlin and T J Gay *J. Phys. B: At. Mol. Opt. Phys.* **44** 045201 (2011)
9. **Auger decay of 1σ_g and 1σ_u hole states of N₂ molecule: II. Young type interference of Auger electrons and its dependence on internuclear distance** N. A. Cherepkov, S. K. Semenov, M. S. Schöffler, J. Titze, N. Petridis, T. Jahnke, K. Cole, L. Ph. H. Schmidt, A. Czasch, D. Akoury, O. Jagutzki, J. B. Williams, T. Osipov, S. Lee, M. H. Prior, A. Belkacem, A. L. Landers, H. Schmidt-Böcking, R. Dörner and Th. Weber, *Phys. Rev. A* **82**, 023420 (2010).
10. **Auger decay of 1σ_g and 1σ_u hole states of the N₂ molecule: Disentangling decay routes from coincidence measurements** S. K. Semenov, M. S. Schöffler, J. Titze, N. Petridis, T. Jahnke, K. Cole, L. Ph. H. Schmidt, A. Czasch, D. Akoury, O. Jagutzki, J. B. Williams, T. Osipov, S. Lee, M. H. Prior, A. Belkacem, A. L. Landers, H. Schmidt-Böcking, Th. Weber, N. A. Cherepkov, and R. Dörner, *Phys. Rev. A* **81**, 043426 (2010).
11. **Carbon K-shell photoionization of fixed-in-space C₂H₄** T. Osipov, M. Stener, A. Belkacem, M. Schöffler, Th. Weber, L. Schmidt, A. Landers, M. H. Prior, R. Dörner, and C. L. Cocke, *Phys. Rev. A* **81**, 033429 (2010) .
12. **Formation of inner-shell autoionizing CO⁺ states below the CO₂⁺ threshold** T. Osipov, Th. Weber, T. N. Rescigno, S. Y. Lee, A. E. Orel, M. Schöffler, F. P. Sturm, S. Schössler, U. Lenz, T. Havermeier, M. Kühnel, T. Jahnke, J. B. Williams, D. Ray, A. Landers, R. Dörner, and A. Belkacem, *Phys. Rev. A* **81**, 011402 (2010).
13. **Separation of Auger transitions into different repulsive states after K-shell photoionization of N₂ molecules** N. A. Cherepkov, S. K. Semenov, M. S. Schöffler, J. Titze, N. Petridis, T. Jahnke, K. Cole, L. Ph. H. Schmidt, A. Czasch, D. Akoury, O. Jagutzki, J. B. Williams, T. Osipov, S. Lee, M. H. Prior, A. Belkacem, A. L. Landers, H. Schmidt-Böcking, R. Dörner and Th. Weber, *Phys. Rev. A* **80**, 051404(R) (2009).
14. **Photo and Auger Electron Angular Distributions of Fixed-in-Space CO₂** F.P. Sturm, M. Schöffler, S. Lee, T. Osipov, N. Neumann, H.-K. Kim, S. Kirschner, B. Rudek, J.B. Williams, J.D. Daughhetee, C.L. Cocke, K. Ueda, A.L. Landers, Th. Weber, M.H. Prior, A. Belkacem, and R. Dörner, *Phys. Rev. A* **80**, 032506 (2009).
15. **Angular Correlation between Photo- and Auger electrons from K-Shell Ionization of Neon** A.L. Landers, F. Robicheaux, T. Jahnke, M. Schöffler, T. Osipov, J. Titze, S.Y. Lee, H. Adaniya, M. Hertlein, P. Ranitovic, I. Bocharova, D. Akoury, A. Bhandary, Th. Weber, M.H. Prior, C.L. Cocke, R. Dörner, and A. Belkacem, *Phys. Rev. Lett.* **102**, 223001 (2009).

Program Title:

"Properties of actinide ions from measurements of Rydberg ion fine structure"

Principal Investigator:

Stephen R. Lundeen
Dept. of Physics
Colorado State University
Ft. Collins, CO 80523-1875
lundeen@lamar.colostate.edu

Program Scope:

This project determines certain properties of chemically significant Uranium and Thorium ions through measurements of fine structure patterns in high-L Rydberg ions consisting of a single weakly bound electron attached to the actinide ion of interest. The measured properties, such as polarizabilities and permanent moments, control the long-range interactions of the ion with the Rydberg electron or other ligands. The ions selected for initial study in this project, U^{6+} , U^{5+} , U^{4+} , Th^{4+} , and Th^{3+} , all play significant roles in actinide chemistry, and are all sufficiently complex that *a-priori* calculations of their properties are suspect until tested. The measurements planned under this project serve the dual purpose of 1) providing data that may be directly useful to actinide chemists and 2) providing benchmark tests of relativistic atomic structure calculations. In addition to the work with U and Th ions, which takes place at the J.R. Macdonald Laboratory at Kansas State University, a parallel program of studies with stable singly-charged ions takes place at Colorado State University. These studies are aimed at clarifying theoretical questions connecting the Rydberg fine structure patterns to the properties of the free ion cores, thus directly supporting the actinide ion studies. In addition, they provide training for students who can later participate directly in the actinide work.

Recent Progress:

The main goal of our program is measurement of properties of Rn-like and Fr-like U and Th ions. Within the past year, we have very nearly met this goal with regard to the Th ions. Optical RESIS studies of Rydberg ions with Rn-like Th^{4+} and Fr-like Th^{3+} cores have been published, giving preliminary determination of some core properties [4,5]. Much more precise RF studies have now also been completed for both species. A full report of the Th^{4+} results has been published [6,8], giving precise values of both dipole and quadrupole polarizabilities of this ion. A report of the Th^{3+} results is in preparation[9]. The ion properties determined in both cases are listed in Table I. Comparison with theoretical predictions, when available, indicates that only the most advanced relativistic atomic structure methods produce acceptable agreement with these measurements.

Table I. Properties of Thorium ions obtained from Rydberg ion fine structure measurements during the present grant period.

Ion	Property	Measurement
Th ⁴⁺	$\alpha_{D,0}$: dipole polarizability	7.702(6) a.u.
	$\alpha_{Q,0}$: quadrupole polarizability	29(2) a.u.
Th ³⁺	Q : electric quadrupole moment	0.600(3) a.u.
	$\alpha_{D,0}$: scalar dipole polarizability	15.00(25) a.u.
	$\alpha_{D,2}$: tensor dipole polarizability	-5.9(3) a.u.

Studies of the analogous U ions, Rn-like U⁶⁺ and Fr-like U⁵⁺, have been far less successful to date. At least part of the difficulty of these studies is due to significantly higher background rates, which reduces the Signal to Noise ratio and makes observation of smaller resolved RESIS excitation signals much more difficult. One possible source of that background, auto-ionizing Rydberg levels bound to metastable excited levels of the core ion, seems much less likely after studies carried out within the past year that compared background levels with a wide variety of core ions (Th³⁺, Th⁴⁺, U⁵⁺, U⁶⁺, Xe⁵⁺, Xe⁶⁺, Xe⁷⁺, Xe⁸⁺). These studies showed a very strong dependence of the background rate on the net charge of the core ion, with only much weaker dependence on its electron configuration. This strongly suggests a background mechanism that depends only on the dynamics of the Rydberg electron, not on the specific properties of the core ion. One possible mechanism that we are still investigating is ionization of Rydberg ions by black-body radiation in the presence of a strong electric field. At present, our main goal in the U studies is to confirm the source of the background experimentally, as a preliminary to attempting to reduce it.

In parallel with these actinide ion studies, which take place at KSU, we continue studies of neutral Nickel Rydberg levels at CSU. An optical RESIS study of excitation of n=9 Rydberg levels was published in 2010 [1], and a much higher precision RF study of these same levels was completed this year. Since the ground state of Ni⁺ is a ²D_{5/2} level, these Rydberg levels are quite complex, consisting of six energy levels for each value of L. Analysis of this structure to extract core ion properties has been facilitated by the completion of a systematic theoretical derivation of the long-range effective potential model of high-L Rydberg fine structure, published this year [7]. A full report of the Nickel RF study is still in preparation [10], but the preliminary results are shown in Table II. Among the measured Ni⁺ properties are both permanent electric moments, quadrupole and hexadecapole, as well as dipole and quadrupole polarizabilities. The data pattern also shows what appears to be the signature of a permanent magnetic octupole moment of the Ni⁺ ion, although in the absence of any theoretical predictions some alternative explanation cannot be ruled out. This signature is parameterized by the parameter C_{M3}, also shown in Table II.

Table II. Properties of Ni^+ obtained from measurements of $n=9$ Nickel Rydberg fine structure during the present grant period.

Ion	Property	Measurement
Ni^+	Q : electric quadrupole moment	-0.4705(2) a.u.
	Π : electric hexadecapole moment	0.27(9) a.u.
	$\alpha_{D,0}$: scalar dipole polarizability	7.925(10) a.u.
	$\alpha_{D,2}$: tensor dipole polarizability	1.043(33) a.u.
	$\alpha_{Q,0}$: scalar quadrupole polarizability	71(9) a.u.
	C_{M3} : magnetic octupole signature	-0.35(6)

Immediate Future Plans

Except for the Th^{3+} report still in preparation, we consider that the Th ion studies are successfully completed. We are still hoping that the analogous U studies will prove possible, but this will require significant progress in reducing the background levels. Work in that direction is ongoing at KSU.

The current results from the Nickel study are very intriguing since they determine a wider range of ion properties than has ever been extracted from a Rydberg fine structure study. The precision of the extracted properties is currently limited by the range of L 's included in the study ($n=9$, $L=6,7,8$), as well as by uncertainty in one critical core property, the off-diagonal tensor polarizability (Eq. 77 in Ref. [7]) that produces shifts in the Rydberg energy levels. We are exploring the feasibility of a follow-on study that would extend the data pattern to include $n=10$ levels with $L=6-9$, and also determine the off-diagonal tensor polarizability experimentally.

Recent Publications:

1) "Optical spectroscopy of high- L Rydberg states of nickel", Julie A. Keele, Shannon L. Woods, M.E. Hanni, S.R. Lundeen, and W.G. Sturuss, Phys. Rev. A 81, 022506 (2010)

2) "Polarizabilities of Pb^{2+} and Pb^{4+} and Ionization Energies of Pb^+ and Pb^{3+} from spectroscopy of high- L Rydberg states of Pb^+ and Pb^{3+} ". M.E. Hanni, Julie A. Keele, S. R. Lundeen, C.W. Fehrenbach, and W.G. Sturuss, Phys. Rev. A 81, 042512 (2010)

3) "Dipole transition strengths in Ba^+ from Rydberg fine structure measurements in Ba and Ba^+ ", Shannon L. Woods, M.E. Hanni, S.R. Lundeen, and Erica L. Snow, Phys. Rev. A 82, 012506 (2010)

4) "Polarizabilities of Rn-like Th^{4+} from spectroscopy of high- L Rydberg levels of Th^{3+} ", M.E. Hanni, Julie A. Keele, S.R. Lundeen, and C.W. Fehrenbach, Phys. Rev. A 82, 022512 (2010)

5) "Properties of Fr-like Th^{3+} from spectroscopy of high- L Rydberg levels of Th^{2+} ", Julie A. Keele, M.E. Hanni, Shannon L. Woods, S.R. Lundeen, and C.W. Fehrenbach, Phys. Rev. A 83, 062501 (2011)

6) "Polarizabilities of Rn-like Th^{4+} from rf spectroscopy of Th^{3+} Rydberg levels", Julie A. Keele, S.R. Lundeen, and C.W. Fehrenbach, Phys. Rev. A 83, 062509 (2011).

7) "Effective Potential Model for high-L Rydberg atoms and ions", Shannon L. Woods and S.R. Lundeen, Phys. Rev. A 85,042505 (2012)

8) "Measurement of dipole and quadrupole polarizabilities of Rn-like Th⁴⁺", Julie A Keele, Chris S. Smith, S.R. Lundeen, and C.W. Fehrenbach Phys. Rev. A 85, 06452 (2012)

Publications in Preparation

9) "Properties of Fr-like Th³⁺ from RF spectroscopy of high-L n=37 levels of Th²⁺", Julie A Keele, Shannon L. Woods, S.R. Lundeen, and C.W. Fehrenbach (in preparation)

10) "Properties of Ni+ from RF spectroscopy of high-L n=9 levels of Nickel", Shannon L. Woods and S.R. Lundeen (in preparation)

Other Reports

"Rydberg Spectroscopy of Fr-like Thorium and Uranium Ions", Mark E. Hanni, PhD thesis, Colorado State University, Fall 2010

"Ion Properties from high-L Rydberg atom spectroscopy: Applications to Nickel" , Shannon L. Woods, PhD thesis, Colorado State University, Fall 2012

Theory of Atomic Collisions and Dynamics

J. H. Macek

*Department of Physics and Astronomy,
University of Tennessee, Knoxville, Tennessee and
Oak Ridge National Laboratory, Oak Ridge, Tennessee
email:jmacek@utk.edu*

1 Program scope

One can characterize [1-6] atomic dynamics by the exchange of physical quantities such as energy, momentum, and angular momentum between various constituents of atoms, molecules and ions. Our recent projects have concentrated on the exchange of angular momentum. Such exchange has long been studied in connection with bound states excited by photon and charged particle impact.

Recognition that vortices in the time-dependent velocity fields of atomic wave functions are closely connected with angular momentum is a major accomplishment of our research [5]. The discovery of vortices focuses attention onto the field interpretation of atomic wave functions. The velocity field thereby becomes a key quantity for understanding the transfer of angular momentum in atomic processes [1].

Vortices in the velocity field of atomic wave functions cannot be viewed experimentally, but, associated with each vortex there is an isolated zero in the wave function which can be observed. The imaging theorem [1] shows that such zeros appear as zeros in the electron momentum distribution $P(\mathbf{k})$, where k is proportional to the ejected electron momentum. These zeros indicate orientation of continuum states of quantum systems an insight with wide application for essentially all atomic, molecular and optical processes. Up till now vortices in atoms has been of theoretical interest only. Our research has concentrated on experimental aspects of vortex detection and observation [2-6].

The projects listed in this abstract are sponsored by the Department of Energy, Division of Chemical Sciences, through a grant to the University of Tennessee. The research is carried out in cooperation with Oak Ridge National Laboratory under the ORNL-UT Distinguished Scientist program.

2 Recent progress

2.1 Ion-atom collisions: Our Previous work with the Regularized Lattice-Time-Dependent-Schrödinger equation (RLTDSE) method [6] has shown that time dependent wave functions $\psi(\mathbf{r}, t)$ have zeros at isolated points in coordinate space where the real and imaginary parts of the wave function vanish. Using vortex theory, we have shown that if atomic wave functions have non-zero mean angular momentum $\langle \mathbf{J} \rangle$, where the average is taken over a small region of coordinate space, then the velocity fields;

$$\mathbf{v}(\mathbf{r}) = -i\nabla \ln \psi(\mathbf{r}) \quad (1)$$

must diverge at a zeros inside the small volume, *i. e.* the velocity field has a vortex at the wave function zero.

These vortex structures are observable as zeros of electron momentum distributions $P(\mathbf{k})$ since such distributions image *coordinate* space wave functions according to [2]

$$P(\mathbf{k}) = \lim_{t \rightarrow \infty} \left[\left| t^3 \psi(\mathbf{r}, t) \right|^2 \right]_{\mathbf{r}=\mathbf{k}t} \quad (2)$$

where it is understood that $\mathbf{r} \neq \mathbf{r}_Q$ and \mathbf{r}_Q is any potential center. This equation, called the "imaging theorem" allows structure in $P(\mathbf{k})$ to be traced to structure in $\psi(\mathbf{r}, t)$ at earlier times. Using the RLTDSE method and the imaging theorem we have shown that "holes" in highly accurate momentum distributions are due to free vortices [6]. The focus of our research this past year has been to see how these theoretical discoveries can be verified experimentally.

It may be possible to observe the vortices predicted by our time-dependent RLTDSE calculations. It turns out that the COLTRIMS technique is sufficiently sensitive that the zeros in the transfer ionization electron distributions in collisions of alpha particles with He may be observed. To check this possibility we developed a two-electron version of the RLTDSE. Owing to memory requirements of the two-electron code, we are unable to obtain a satisfactory *ab. initio.* electron distribution. In the meantime our experimental colleagues have obtained beautiful and highly resolved spectra which have no clear vortex signatures. To interpret these spectra we have developed a hybrid model where the advanced adiabatic theory is used to model the ion-atom interaction at internuclear separations that are less than 10 au and the

RLTDSE method to propagate the wave functions. These calculations are able to account for all advanced adiabatic theory. For example, the top-of-barrier wave function at large distances is shown in Figure 1.

We also identify interesting super-prominent features associated with

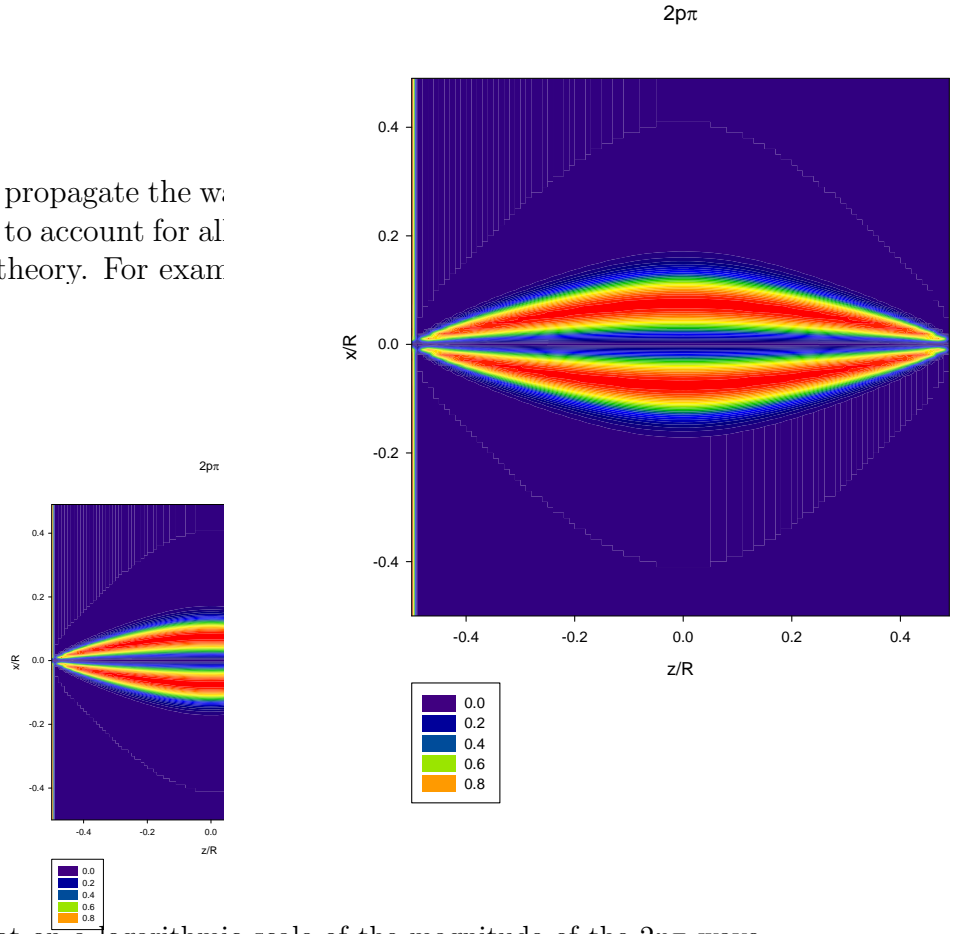


Figure 1. Contour plot on a logarithmic scale of the magnitude of the $2p\pi$ wave function for large R for $He^{2+} + He \rightarrow He^+ + He^{2+}$ collisions with an impact parameter (along x) of 1 a.u. The z -axis is in the direction of the initial velocity of the projectile.

2.2 Electron-atom collisions: Unexplained minima for *electron* impact ionization of He have been identified as zeros associated with vortex structure in $(e,2e)$ wave functions [4]. The angular momentum transfer in this case is to an ejected electron, however, due to the equal momentum of the scattered and ejected electrons, this interpretation is not immediately obvious. Nonetheless, this is the only observation to date that clearly shows vortex structure, therefore we investigate zeros in electron impact ionization amplitudes.

For closely related processes where ejected electrons are much slower than scattered electrons, angular momentum transfer is more readily identified. The $P(\mathbf{k})$ for the ejected electron might show zeros related to vortices. To examine this possibility we use that excitation and ionization by fast electrons scattered through small angles is often modeled using effective photoionization with photons linearly polarized along the momentum transfer axis.

For ionization of K-shells of atoms, we have shown that the effective

photons are actually elliptically polarized indicating that some vector angular momentum is transferred to the ejected electron. The Coulomb Born approximation is used to compute the effective elliptical polarization β for electron impact ionization of carbon K-shells. For the ejection of 7 eV electrons from the carbon K-shell by 1801 eV electrons $\beta = 0.25$ is found for a scattered electron angle of 6° . Since β is non-zero, the electron spectra must have a vortex in the region near $k = 0$. Owing to mixtures of monopole and dipole transitions, the single vortex is at $\mathbf{k} \neq 0$, and zero at this point could be observed. This is to be contrasted with photoionization where there is no admixture of monopole and dipole amplitudes, thus vortices can only appear at $k = 0$.

3 References to DOE sponsored research that appeared in 2009-2011

1. Vortices in Atomic Processes, Joseph H. Macek, in Dynamical Processes in Atomic and Molecular Physics, ed. by Gennadi Ogurtsov and Danielle Dowek, Bentham ebooks, 2012 pp 3-28.
2. Ionization processes in small quasimolecules: $He_2^{2+}(He^{2+} + He)$ G. N. Ogurtsov, S. Yu. Ovchinnikov, J. H. Macek, and V. M. Mikoushkin Phys. Rev. A **84**, 032706 (2011).
3. Creating and Manipulating Vortices in Atomic Wave Functions with Short Electric Field Pulses, Sergey Y. Ovchinnikov, Joseph H. Macek, James B. Sternberg, Teck-Ghee Lee, and David R. Schultz, Phys. Rev. Lett. **105**, 203005 (2010).
4. Theory of Deep Minima in (e,2e) Measurements of Triply Differential Cross Sections, J. H. Macek, J. B. Sternberg, S. Y. Ovchinnikov, and J. S. Briggs, Phys. Rev. Lett., **104**, 033201 (2010).
5. Evolution of Quantum Systems from Microscopic to Macroscopic Scales, Sergey Y. Ovchinnikov, Joseph H. Macek, James S. Sternberg, Teck-Ghee Lee, and David R. Schultz, CAARI 2008 Proceedings AIP Conference Proceedings, **1099**, 164 (2009).
6. Origin, evolution, and imaging of vortices in atomic processes, J.H. Macek J.S. Sternberg and S.Y. Ovchinnikov, T-G. Lee and D.R. Schultz, Phys. Rev. Lett. **102**, 143201(2009).
7. Multiparticle interactions of zero-range potentials, J. H. Macek, Few-Body Syst. **45**,207 (2009).

Photoabsorption by Free and Confined Atoms and Ions

Steven T. Manson, Principal Investigator

Department of Physics and Astronomy, Georgia State University, Atlanta, Georgia 30303
(smanson@gsu.edu)

Program Scope

The goals of this research program are: to provide a theoretical adjunct to, and collaboration with, the various atomic and molecular experimental programs that employ latest generation light sources, particularly ALS, APS and LCLS; to generally enhance our understanding of the photoabsorption process; and to study the properties (especially photoabsorption) of confined atoms and ions. To these ends, calculations are performed employing and enhancing cutting-edge methodologies to provide deeper insight into the physics of the experimental results; to provide guidance for future experimental investigations; and seek out new phenomenology, especially in the realm of confined systems. The main areas of programmatic focus are: manifestations of nondipole effects in photoionization; photodetachment of inner and outer shells of atoms and atomic ions (positive and negative); studies of atoms endohedrally confined in buckyballs, C_{60} , particularly dynamical properties. Flexibility is maintained to respond to opportunities.

Highlights of Recent Progress

1. Confined Atoms

The study of confined atoms is still new. There are a number of theoretical investigations of various atoms endohedrally confined in C_{60} [1,2], but experimental studies are sparse [3-5]. Thus, we are conducting a program of calculations at various levels of approximation, aimed at delineating the properties of such systems, especially photoionization, to guide the experimental community. Among our recent results, we have found that a huge transfer of oscillator strength from the C_{60} shell, in the neighborhood of the giant plasmon resonance, to the encapsulated atom for both $Ar@C_{60}$ [6] and $Mg@C_{60}$ [7]. In addition, confinement resonances [8], oscillations that occur in the photoionization cross section of an endohedral atom owing to the interferences of the photoelectron wave function for direct emission with those scattered from the surrounding carbon shell have been predicted in a broad range of cases; recently, the existence of confinement resonances has been confirmed experimentally [5]. In addition, the photoionization of endohedral atoms within nested fullerenes, called buckyonions, has shown that, as a result of the multi-walled confining structures, the confinement resonances become considerably more complicated [9].

Considering a Xe atom endohedrally confined in C_{60} the formation of a new type of atom-fullerene hybrid state was discovered [10]. These dimer-type states arise from the near-degeneracy of inner levels of the confined atom and the confining shell, in contrast to the known overlap-induced hybrid states around the Fermi level of smaller compounds, and are found to occur in confined noble gas and alkali-earth atoms [11]. The photoionization cross sections of these hybrid states exhibit rich structures and are radically different from the cross sections of free atomic or fullerene states. This also occurs in buckyonions, nested fullerenes. A study of $C_{60}@C_{240}$ reveals strong hybridization between the plasmon excitations of the individual fullerenes leading to a

photoionization cross section of the nested system being dramatically different from the sum of the individual constituents [12]. This result suggests the possibility of creating buckyonions with plasmons of specified character, i.e., *designer resonances*.

Fast charged-particle impact ionization of atoms have been considered, looking at the He@C₆₀ system [13]. The motivation here is that there are experimental results in this area, along with a search for the possible existence of nondipole plasmon resonances. Our first results indicate that confinement resonances appear in the ionization of endohedrals by charged particle impact as well as in photoionization.

These various effects have been calculationally demonstrated in particular cases, their importance is that they are general and will arise in many confined atom systems.

2. Atomic/Ionic Photoionization

The study of photoionization of atoms/ions at high resolution leads to results of great complexity. Our effort is to perform state-of-the-art calculations, in concert with high-resolution synchrotron experiments, to understand this complexity. Using our upgraded relativistic Breit-Pauli R-matrix methodology we have completed a study of the four-electron Be isoelectronic sequence [14-16]. The calculations produce excellent agreement with experiment for five different members of the sequence, and relativistic interactions are crucial for quantitative accuracy, even for the lowest member of the sequence; quite surprising for $Z=4$! Calculations of Ca⁺ [17] and some of the higher members of the K isoelectronic series were performed [18]. It was found that the giant 3p→3d resonances dominated the threshold region for Ti³⁺ (in excellent agreement with experiment) but lay below the ionization threshold for the higher members of the series. The calculation should be even more accurate for higher Z , but a recent experiment on Fe⁷⁺ [19] does not show good agreement with theory. This is not understood as yet.

3. Nondipole Effects in Atoms

Up until relatively recently, the conventional wisdom was that nondipole effects in photoionization were of importance only at photon energies of tens of keV or higher, despite indications to the contrary more than 35 years ago [20]. The last decade has seen an upsurge in experimental and theoretical results [21] showing that nondipole effects in photoelectron angular distributions could be important down to hundreds [22] and even tens [23] of eV. Our recent work included a study of Cl⁻ [24] which revealed that there are strong correlation effects in quadrupole channels, and these effects show up in the nondipole contribution to the photoelectron angular distribution at a level predicted to be measurable at rather low energies. We have also found a case where the quadrupole cross section actually dominates the dipole cross section in the 10 eV range [25], in the Cooper minimum region of Mg 3s. The results also show a dramatic change in the photoelectron angular distribution over a small energy range. This study indicates that laboratory investigations in the neighborhood of dipole Cooper minima (which is now possible owing to high intensity light sources such FEL's) could prove quite fruitful and interesting.

Future Plans

Our future plans are to continue on the paths set out above. In the area of confined atoms, we will look at the possibilities of interatomic Coulomb decay (ICD) of resonances. perform many-body calculations on charged particle impact ionization of endohedral atoms and free fullerene molecules in an effort to elucidate any new insights

inherent in the nondipole channels thus produced. In addition, we shall upgrade our theory to include relativistic interactions to be able to deal with heavy endohedrals with quantitative accuracy. Inner-shell photoabsorption of both the ground 4S and excited 2D states of C^- shall be studied in to understand how the slight excitation of the outer shell affects the inner-shell photoabsorption and to pave the way for experiment, in addition to further study of Na^- and K^- . Additionally, nondipole effects the inner subshells of Hg will be investigated to unravel the combined effects of many-body and relativistic interactions. In addition, the search for cases where nondipole effects are likely to be significant, as a guide for experiment, and quadrupole Cooper minima, will continue.

Publications Citing DOE Support Since 2010

- “Quadrupole matrix element zeros and their effect on photoelectron angular distributions,” L. A. LaJohn, S. T. Manson and R. H. Pratt, *Nuc. Instr. Meth. A* **619**, 7-9 (2010).
- “Photoionization of Xe inside C_{60} : atom-fullerene hybridization, giant enhancement and interchannel oscillation transfer,” M. E. Madjet, D. Hopper, M. A. McCune, H. S. Chakraborty, J.-M. Rost and S. T. Manson, *Phys. Rev. A* **81**, 013202-1-8 (2010).
- “Effects of the fullerene (C_{60}) potential and position of the atom (A) on spectral characteristics of endohedral atoms $A@C_{60}$,” A. S. Baltenkov, U. Becker, S. T. Manson, and A. Z. Msezane, *J. Phys. B* **43**, 115102-1-9 (2010).
- “Satellite Lines in the Photoionization of Ions: The Be Isoelectronic Sequence,” W.-C. Chu, H.-L. Zhou, A. Hibbert and S. T. Manson, *Phys. Rev. A* **81**, 053412-1-5 (2010).
- “Interior static polarization effect in $A@C_{60}$ photoionization,” V. K. Dolmatov and S. T. Manson, *Phys. Rev. A* **82**, 023422-1-3 (2010).
- “Photoionization of the Be-like O^{4+} ion: Total and partial cross sections for the ground $2s^2$ and excited $2s2p^{1,3}P$ states,” D.-S. Kim and S. T. Manson, *J. Phys. B* **43**, 155205-1-12 (2010).
- “Variation of photoelectron angular distributions along Ar and Ca isonuclear sequences,” G. B. Pradhan, J. Jose, P. C. Deshmukh, V. Radojević, and S. T. Manson, *Phys. Rev. A* **81**, 063401-1-4 (2010).
- “Overlapping Resonances in Atomic Ions,” W.-C. Chu, H.-L. Zhou, A. Hibbert and S. T. Manson, *Phys. Rev. A* **82**, 013417-1-4 (2010).
- “Inner Shell Photodetachment of Na^- Using the Multi-Configuration Tamm-Dancoff Approximation,” J. Jose, G. B. Pradhan, V. Radojević, S. T. Manson, and P. C. Deshmukh, *Publ. Astron. Obs. Belgrade* **89**, 29-32 (2010).
- “Photoionization of potassium-like transition metal ions: Ti^{3+} to Fe^{7+} ,” A. M. Sossah, H.-L. Zhou, S. T. Manson, *Phys. Rev. A* **82**, 043416-1-13 (2010).
- “Electron-Impact Ionization of Atoms: Secondary Electron Angular Distributions and Drag Currents,” A. S. Baltenkov, S. T. Manson and A. Z. Msezane, *Cent. Eur. J. Phys.* (in press).
- “Valence photodetachment of Li^- and Na^- using relativistic many-body techniques,” J. Jose, G. B. Pradhan, V. Radojević, S. T. Manson, and P.C. Deshmukh, *Phys. Rev. A* **85**, 053419-1-7 (2011).
- “Cooper Minima: A Window on Nondipole Photoionization at Low Energy,” G. B. Pradhan, J. Jose, P. C. Deshmukh, L. A. LaJohn, R. H. Pratt, and S. T. Manson, *J. Phys. B* **44**, 201001-1-6 (2011).
- “Electron correlation effects near the photoionization threshold: The Ar isoelectronic sequence,” J. Jose, G. B. Pradhan, V. Radojević, S. T. Manson, and P.C. Deshmukh, *J. Phys. B* **44**, 195008-1-8 (2011).
- “Plasmon-plasmon coupling in nested fullerenes: Creation of interlayer plasmonic cross modes,” M. A. McCune, R. De, M. E. Madjet, H. S. Chakraborty, and S.T. Manson, *J. Phys. B* **44**, 241002-1-5 (2011).

- “Magnetic dichroism in K-shell photoemission from laser excited Li atoms,” M. Meyer, A. N. Grum-Grzhimailo, D. Cubaynes, Z. Felfli, E. Heinecke, S. T. Manson, and P. Zimmermann, *Phys. Rev. Letters* **107**, 213001-1-4 (2011).
- “Interference in Molecular Photoionization and Young’s Double-Slit Experiment,” A. S. Baltenkov, U. Becker, S. T. Manson, and A. Z. Msezane, *J. Phys. B* **45**, 035202-1-12 (2012).
- “A Mathematical Model of Negative Molecular Ions,” A. S. Baltenkov, S. T. Manson, and A. Z. Msezane, *Proceedings of Dynamic Systems and Applications 6* (Dynamic Publishers, Atlanta, Georgia, 2012), pp. 53-57.
- “Valence photoionization of small alkaline earth atoms endohedrally confined in C₆₀,” M. H. Javani, M. R. McCreary, A. B. Patel, M. E. Madjet, H. S. Chakraborty and S. T. Manson, *Eur. Phys. J. D* **66**, 189-1-7 (2012).
- “Radiation Damping in the Photoionization of Fe¹⁴⁺,” M. F. Hasoglu, T. W. Gorczyca, M. A. Bautista, Z. Felfli, and S. T. Manson, *Phys. Rev. A* **85**, 040701(R)-1-4 (2012).
- “Photoionization of atomic krypton confined in the fullerene C₆₀,” J. George, H. R. Varma, P. C. Deshmukh and S T Manson, *J. Phys. B* (in press).
- “Photoionization of ground and excited states of Ca⁺ and comparison along the isoelectronic sequence,” A. M. Sossah, H.-L. Zhou, S. T. Manson, *Phys. Rev. A* **86**, 023403-1-10 (2012).

References

- [1] V. K. Dolmatov, A. S. Baltenkov, J.-P. Connerade and S. T. Manson, *Radiation Phys. Chem.* **70**, 417 (2004) and references therein.
- [2] V. K. Dolmatov, *Advances in Quantum Chemistry*, **58**, 13 (2009) and references therein.
- [3] A. Müller *et al*, *Phys. Rev. Lett.* **101**, 133001 (2008).
- [4] R. Phaneuf *et al*, *Bull. Am. Phys. Soc.* **55**(5), 40 (2010) and private communication.
- [5] A. L. D. Kilcoyne, A. Aguilar, A. Müller, S. Schippers, C. Cisneros, G. Alna’Washi, N. B. Aryal, K. K. Baral, D. A. Esteves, C. M. Thomas, and R. A. Phaneuf, *Phys. Rev. Lett.* **105**, 213001 (2010)
- [6] M. E. Madjet, H. S. Chakraborty and S. T. Manson, *Phys. Rev. Letters* **99**, 243003 (2007).
- [7] M. E. Madjet, H. S. Chakraborty, J. M. Rost and S. T. Manson, *Phys. Rev. A* **78**, 013201 (2008).
- [8] V. K. Dolmatov and S. T. Manson, *J. Phys. B* **41**, 165001 (2008).
- [9] V. K. Dolmatov and S. T. Manson, *J. Phys. Rev. A* **78**, 013415 (2008).
- [10] H. S. Chakraborty, M. E. Madjet, T. Renger, J.-M. Rost and S. T. Manson, *Phys. Rev. A* **79**, 061201(R) (2009).
- [11] M. H. Javani, M. R. McCreary, A. B. Patel, M. E. Madjet, H. S. Chakraborty and S. T. Manson, *Eur. Phys. J. D* **66**, 189 (2012).
- [12] M. A. McCune, R. De, M. E. Madjet, H. S. Chakraborty, and S.T. Manson, *J. Phys. B* **44**, 241002-1-5 (2011).
- [13] A. S. Baltenkov, V. K. Dolmatov, S. T. Manson, and A. Z. Msezane, *Phys. Rev. A* **79**, 043201 (2009).
- [14] W.-C. Chu, H.-L. Zhou, A. Hibbert and S. T. Manson, *J. Phys B* **42**, 205003 (2009).
- [15] W.-C. Chu, H.-L. Zhou, A. Hibbert and S. T. Manson, *Phys. Rev. A* **81**, 053412 (2010).
- [16] W.-C. Chu, H.-L. Zhou, A. Hibbert and S. T. Manson, *Phys. Rev. A* **82**, 013417-1-4 (2010).
- [17] A. M. Sossah, H.-L. Zhou, S. T. Manson, *Phys. Rev. A* **86**, 023403 (2012).
- [18] A. M. Sossah, H.-L. Zhou, S. T. Manson, *Phys. Rev. A* **82**, 043416 (2010).
- [19] A. Müller, R. Phaneuf, private communication (2011).
- [20] M. O. Krause, *Phys. Rev.* **177**, 151 (1969).
- [21] O. Hemmers, R. Guillemin and D. W. Lindle, *Rad. Phys. and Chem.* **70**, 123 (2004) and references therein.
- [22] O. Hemmers *et al*, *Phys. Rev. Letters* **91**, 053002 (2003).
- [23] V. K. Dolmatov and S. T. Manson, *Phys. Rev. Letters* **83**, 939 (1999).
- [24] J. Jose, G. B. Pradhan, P. C. Deshmukh, V. Radojević and S. T. Manson, *Phys. Rev. A.* **80**, 023405-1-6 (2009).
- [25] G. B. Pradhan, J. Jose, P. C. Deshmukh, L. A. LaJohn, R. H. Pratt, and S. T. Manson, *J. Phys. B (FTC)* **44**, 201001 (2011).

Combining High Level *Ab Initio* Calculations with Laser Control of Molecular Dynamics

Thomas Weinacht
Department of Physics and Astronomy
Stony Brook University
Stony Brook, NY
thomas.weinacht@stonybrook.edu

Spiridoula Matsika
Department of Chemistry
Temple University
Philadelphia, PA
smatsika@temple.edu

1 Program Scope

We use intense, shaped, ultrafast laser pulses to follow and control molecular dynamics and high level *ab initio* calculations to interpret the dynamics and guide the control. We are applying the techniques and understanding we have developed to dissociative ionization pump-probe spectroscopy and pulse shape spectroscopy.

2 Recent Progress

2.1 Local vs. non-local dynamics

Our pump probe measurements, which follow ultrafast relaxation in DNA bases following excitation in the deep UV, have revealed non-local evolution of the wave function on the excited state surfaces for uracil, cytosine and adenine. We performed quantum dynamics calculations on simple two dimensional model potentials in order to understand the features of the excited state potentials which can lead to the kind of non-local relaxation that we observed in experiments. The dynamics calculations illustrate how barriers on the excited state potential energy surfaces can lead to wave packet spreading while conical intersections (CI) between excited state potentials can lead to bifurcation, both of which can lead to non-local relaxation and the observed spectrum of decay times for different molecular fragments measured in our experiments. Figure 1 shows snapshots of the wave packet at the time it reaches the CI between excited and ground states for five cases studied (varying barrier height, and slope near the Franck Condon region).

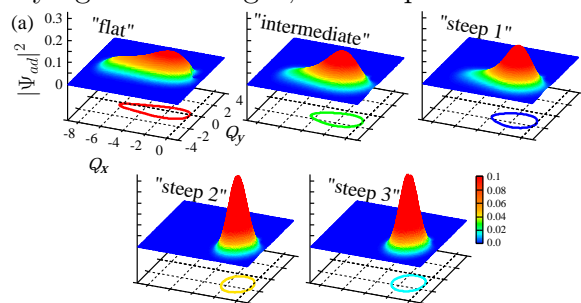


Figure 1: (a) Snapshots of the wave packet at the time it reaches the CI for the five cases studied.

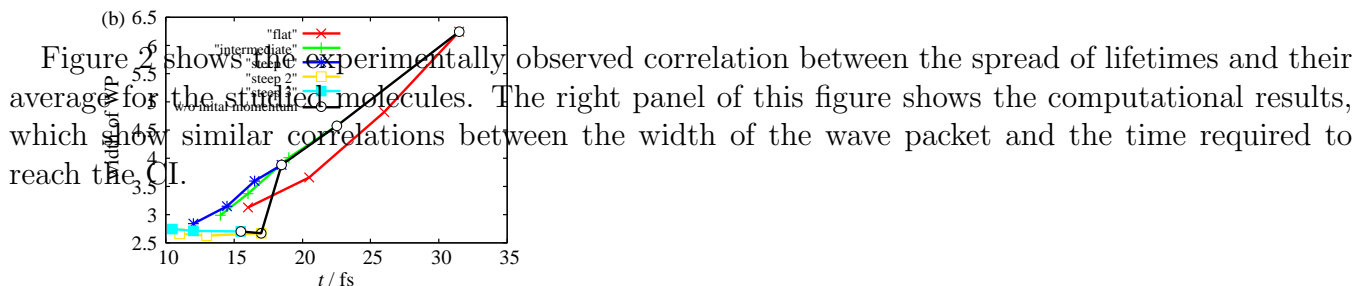


Figure 2 shows the experimentally observed correlation between the spread of lifetimes and their average for the studied molecules. The right panel of this figure shows the computational results, which show similar correlations between the width of the wave packet and the time required to reach the CI.

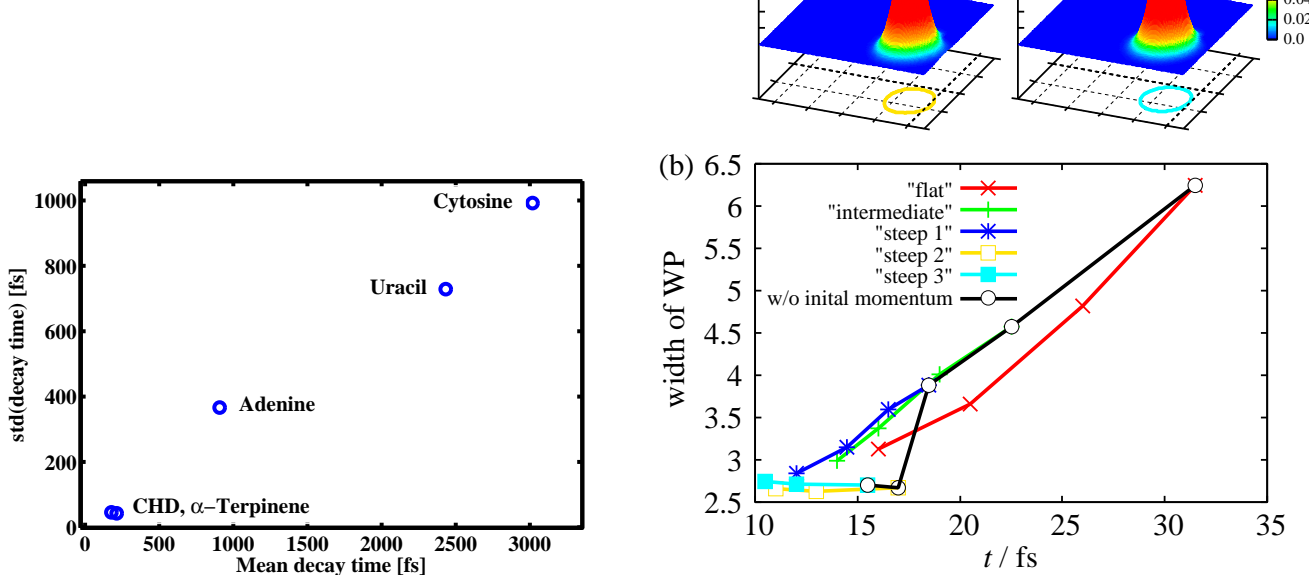
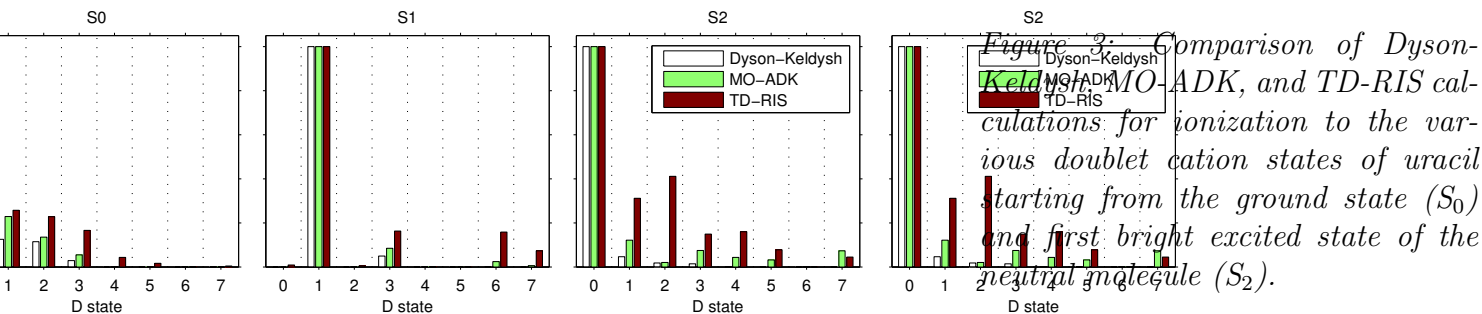


Figure 2: Left: Standard deviation of lifetimes vs. mean lifetime for the fragments produced from 1,3 cyclohexadiene (CHD), α -terpinene, adenine, uracil and cytosine. Right: Width of the wavepacket at the time it reaches the CI as a function of this decay time for the five cases (black line). The colored lines show the width of the wavepacket for each case when varied initial momenta were used

2.2 Dyson orbitals in strong field ionization

Our pump probe measurements described above rely on strong field ionization in order to probe the dynamics on the neutral excited state. The ionization of these excited state molecules is interesting both as a probe of the neutral excited state dynamics and as a fundamental issue in strong field ionization - in particular as a probe of correlations between initial and final states in strong field ionization. While ionization from the molecular ground state is correlated with most of the low lying states of the molecular cation (as they are in many cases dominated by electronic configurations that are ‘single hole’ - with one singly occupied molecular orbital), ionization from a molecular excited state is generally correlated (in the sense of having a large magnitude of the associated Dyson orbital) with only one low lying state of the molecular cation. In collaboration with Michael Spanner and Sergeui Patchovskii at the National Research Council of Canada (who have carried out detailed calculations of strong field ionization for the molecules we are working on), we have studied the role of Dyson orbitals in strong field molecular ionization. Figure 3 shows predicted ionization yields to different ionic states for different levels of theory, including the strong field approximation (Keldysh weighted Dyson orbital magnitudes), molecular ADK theory (MOADK) and the Spanner-Patchkovskii approach (termed Time Dependent Resolution in Ionic States - TD-RIS). The calculations suggest that the Dyson orbital description, which is central to the strong field approximation, is violated substantially in both cytosine and uracil, and our experimental measurements are in qualitative agreement with the Spanner-Patchkovskii calculations.



2.3 Uracil cation fragmentation

A key ingredient in the analysis described above was an understanding of which molecular fragment ions originate from a given ionic state. We calculated the dissociation energies and transition state energies for several fragments from uracil and were able to associate several fragments with specific

states of the molecular cation. *Ab initio* calculations on the ground ionic state of the uracil cation reveal that about 2 eV of energy is needed to produce m/z 69, while an energy of 4 eV will lead to smaller fragments with m/z 28, 41, 42. These energetic requirements enable us to correlate the various observed fragments to the ionic states of uracil. It is assumed in this approach that the ionic states rapidly relax to D_0 and the excess electronic energy is transformed into vibrational energy that leads to fragmentation.

2.4 Two Dimensional Fourier Transform Spectroscopy

Our two dimensional Fourier transform spectroscopy measurements on adenine and uracil showed some differences in the evolution of the spectrum as a function of time delay for the two molecules, which we were able to interpret in terms of the gradient of the excited state surface near the Franck Condon region. They showed that uracil has a much larger gradient than adenine, in agreement with our calculations, gas phase pump probe measurements and resonance Raman measurements. As noted below, we are interested in extending these measurements to systems with coupled chromophores whose excitation spectra lie within our excitation spectrum.

3 Future Plans

We have several goals for the immediate future:

1. We are pursuing our two dimensional Fourier transform spectroscopy measurements on DNA oligomers in an effort to move beyond single chromophore systems. We are currently upgrading our experimental apparatus to work with very small sample volumes and improve our signal to noise to be sensitive to even smaller changes in the two dimensional spectrum.
2. We are currently trying to interpret our time and angle dependent ionization measurements of excited state molecules. There are many puzzling aspects of the measurements that we are trying to understand. One of these is the difference in angle dependent yields for molecules whose transition dipole moments and orbitals are almost identical. Another is the differences between fragment and parent ions. Almost all fragments that we have measured are most efficiently produced for parallel pump and probe polarizations while most parent ions are efficiently produced for perpendicular pump and probe polarizations. We would like to understand the angle dependent yields in detail and determine to what extent the yields are determined by the shape of the molecular orbital(s) from which an electron is removed during ionization.
3. We are interested in how dissociation proceeds from an excited ionic state with a total energy larger than the dissociation energy. For neutral molecules, fluorescence most often originates from the first excited state, even if the molecule has been excited to a higher lying state. A high density of states allows for rapid radiationless decay to the first excited state. This is known as Kasha's rule. We plan on investigating whether a similar phenomenon occurs in ionic states where radiationless decay competes with ultrafast dissociation. We will pursue pump probe experiments in molecular cations, where the pump pulse ionizes the molecule and the probe pulse drives transitions between ionic states, and we will also use velocity map imaging to measure the kinetic energy of fragment ions from the DNA bases with which we have been working.

4 Publications of DOE Sponsored Research

- "Interpreting Ultrafast Molecular Fragmentation Dynamics with *ab initio* Calculations", C. Trallero, B. J. Pearson, T. Weinacht, K. Gilliard and S. Matsika, *J. Chem. Phys.*, **128**, 124107, (2008)

- “Closed-Loop Learning Control of Isomerization using Shaped Ultrafast Laser Pulses in the Deep Ultraviolet”, M. Kotur, T. Weinacht, B. J. Pearson and S. Matsika *J. Chem. Phys.*, **130**, 134311, (2009)
- ”Two Dimensional Ultrafast Fourier Transform Spectroscopy in the Deep Ultraviolet C. Tseng, S. Matsika and T. C. Weinacht, *Optics Express* **17**, 18788 (2009)
- “Distinguishing Between Relaxation Pathways by Combining Dissociative Ionization Pump Probe Spectroscopy and ab initio Calculations: A Case Study of Cytosine ”, M. Kotur, T. Weinacht, C. Zhou, K. A. Kistler, and S. Matsika, *JCP*, **134**, 184309, (2011)
- “Following Ultrafast Radiationless Relaxation Dynamics With Strong Field Dissociative Ionization: A Comparison Between Adenine, Uracil, and Cytosine”, M. Kotur, T. Weinacht, C. Zhou, and S. Matsika, *IEEE Journal of selected topics in Quantum Electronics*, **99**, 1 (2011)
- “Combining dissociative ionization pump probe spectroscopy and ab initio calculations to explore excited state dynamics involving conical intersections”, S. Matsika, C. Zhou, M. Kotur and T. Weinacht, *Faraday Discussions*, **153** 247 (2011)
- “Strong-Field Molecular Ionization from Multiple Orbitals”, M. Kotur, T. C. Weinacht, C. Zhou, S. Matsika *Physical Review X* **1**, 021010, (2011)
- “Nonadiabatic Events and Conical Intersections”, S. Matsika and P. Krause, *Annu. Rev. Phys. Chem.*, **62**, 621 - 643, (2011)
- “Two Dimensional Fourier-Transform Spectroscopy of Adenine and Uracil Using Shaped Ultrafast Laser Pulses in the Deep UV” C. Tseng, P. Sandor, M. Kotur, T. C. Weinacht, S. Matsika *The Journal of Physical Chemistry A* **116** 26542661 (2012)
- “Two Dimensional Fourier-Transform Spectroscopy of Adenine and Uracil Using Shaped Ultrafast Laser Pulses in the Deep UV” C. Tseng, P. Sandor, M. Kotur, T. C. Weinacht, S. Matsika *The Journal of Physical Chemistry A* **116** 26542661 (2012)
- “Fragmentation Pathways in the Uracil Radical Cation” C. Zhou, S. Matsika, M. Kotur, T. C. Weinacht *The Journal of Physical Chemistry* Accepted
- “The influence of excited state topology on wave packet delocalization in the relaxation of photo-excited polyatomic molecules” P. Krause, S. Matsika, M. Kotur, T. C. Weinacht *The Journal of Chemical Physics* Accepted

ABSTRACT

ELECTRON-DRIVEN PROCESSES IN POLYATOMIC MOLECULES

Investigator: Vincent McKoy

A. A. Noyes Laboratory of Chemical Physics

California Institute of Technology

Pasadena, California 91125

email: mckoy@caltech.edu

PROJECT DESCRIPTION

The focus of this project is the development, extension, and application of accurate, scalable methods for computational studies of low-energy electron–molecule collisions, with emphasis on larger polyatomics relevant to electron-driven chemistry in biological and materials-processing systems. Because the required calculations are highly numerically intensive, efficient use of large-scale parallel computers is essential, and the computer codes developed for the project are designed to run both on tightly-coupled parallel supercomputers and on workstation clusters.

HIGHLIGHTS

We have made progress in a number of areas over the past year. Collaborations with leading experimental and computational groups worldwide continue to produce exciting results and are being expanded. Specific accomplishments include:

- A study of low-energy elastic electron collisions with isopropanol, which confirmed a relationship between structure and scattering pattern we had observed in other alcohols
- A computational study of electron-impact vibrational excitation of CO, a prototype system for coupling electron-collision and nuclear dynamics
- A joint experimental/computational study of elastic electron collisions with tetrahydrofuran, a model for the deoxyribose moiety in the DNA backbone
- First results from an ongoing experimental/computational study of inelastic electron collisions with water

ACCOMPLISHMENTS

Biofuels, in particular alcohols, continue to be a major focus for us. Our earlier work on isomers of butanol [1,2] revealed that the angular pattern of resonant elastic scattering at collision energies of 6 to 10 eV is isomer-dependent, with the branched systems having *d*-wave patterns and the straight-chain systems *f*-wave patterns. We followed up this observation with an experimental and computational study of isopropanol [3] and found that, as hypothesized, it displays the *d*-wave pattern of branched systems, in contrast to the *f*-wave pattern seen in the straight-chain form, *n*-propanol [1].

Tetrahydrofuran (THF) is the simplest and perhaps most appropriate model for the furanose ring that links phosphate groups in the backbone of DNA. In support of experiments carried out by the Khakoo group (California State University, Fullerton), we revisited THF [4] using a more extensive treatment of polarization effects than we had used in a previous study of THF [5] and also including a correction for long-range scattering by the electric-dipole potential. Though dipolar scattering only affects the extreme forward cross section at higher energies, it becomes increasingly important as the collision energy decreases. Indeed, we found that the dipole correction changed the differential cross section qualitatively at the lowest energies (0.75, 1, and 1.5 eV), bringing it into close agreement with the measurements. This result is not only encouraging but significant for future studies of strongly polar biomolecules.

We are continuing a collaborative study of electron-impact excitation of the most basic biomolecule, water or H₂O, again in conjunction with Prof. Khakoo's experimental group. Electron collision cross sections for water are critical to understanding radiation chemistry in living systems; in particular, numerical models

of radiation tracks depend on databases of electron-water cross sections. Nonetheless, the low-energy inelastic cross sections have been surprisingly little studied. A paper reporting initial results for the lowest four excited states of H₂O, (^{1,3}B₂ and ^{1,3}A₂), has been submitted for publication, and we are continuing to work on higher-lying states.

As an initial step toward eventual studies of electron-driven nuclear dynamics in biomolecules, we carried out, in collaboration with Prof. Karel Houfek (Charles University, Prague) and one of his students, a study of resonant vibrational excitation of CO by electron impact. Obtaining a good balance between the electronic wavefunctions describing neutral CO and the CO + e⁻ system proved to be the most difficult part of the calculation. However, the final results agree well with recent measurements by Allan [6]. This work is being prepared for publication.

PLANS FOR COMING YEAR

We will continue and expect to complete our studies of electron-impact excitation of H₂O. Our goal is to obtain both widely useful data on a fundamental molecule and insights into how best to carry out inelastic calculations that can be applied to other molecules, in particular methanol, on which we plan to initiate electron-impact excitation studies.

We have been developing collaborations in the area of electron-driven nuclear dynamics, in order to use our computed electron-scattering results to predict cross sections for dissociative attachment and vibrational excitation. As described above, we have been collaborating with the Houfek group on vibrational excitation of CO, and we next plan to move on to a more challenging, higher-dimensional system, CO₂. We are also collaborating with Prof. Márcio Varella (University of São Paulo) on vibrational-excitation and dissociative-attachment dynamics in CH₃Cl.

A third collaboration in this area is with the experimental group of Ali Belkacem at LBL. The Belkacem group has the exciting capability of energy- and angle-resolving anions produced by dissociative attachment, providing much fuller insight into the attachment dynamics than can be obtained from just the total ion yield. We are making modifications to our computer codes to generate the relevant quantities (entrance amplitudes) for comparison with such measurements and are also carrying out electronic-structure calculations on uracil to identify Feshbach resonances that may be responsible for the observed dissociative attachment near 6 eV.

REFERENCES

- [1] M. A. Khakoo, J. Blumer, K. Keane, C. Campbell, H. Silva, M. C. A. Lopes, C. Winstead, V. McKoy, E. M. de Oliveira, R. F. da Costa, M. T. do N. Varella, M. H. F. Bettega, and M. A. P. Lima, *Phys. Rev. A* **78**, 062714 (2008).
- [2] M. H. F. Bettega, C. Winstead, and V. McKoy, *Phys. Rev. A* **82**, 062709 (2010).
- [3] M. H. F. Bettega, C. Winstead, V. McKoy, A. Jo, A. Gauf, J. Tanner, L. R. Hargreaves, and M. A. Khakoo, *Phys. Rev. A* **84**, 042702 (2011).
- [4] A. Gauf, L. R. Hargreaves, A. Jo, J. Tanner, M. A. Khakoo, T. Walls, C. Winstead, and V. McKoy, *Phys. Rev. A* **85**, 052717 (2012).
- [5] C. Winstead and V. McKoy, *J. Chem. Phys.* **125**, 074302 (2006).
- [6] M. Allan, *Phys. Rev. A* **81**, 042706 (2010).

PROJECT PUBLICATIONS AND PRESENTATIONS, 2010–2012

1. “Elastic Electron Scattering by Ethyl Vinyl Ether,” M. A. Khakoo, L. Hong, B. Kim, C. Winstead, and V. McKoy, *Phys. Rev. A* **81**, 022720 (2010).
2. “Electron Scattering in HCl: An Improved Nonlocal Resonance Model,” J. Fedor, C. Winstead, V. McKoy, M. Čížek, K. Houfek, P. Kolorenč, and J. Horáček, *Phys. Rev. A* **81**, 042702 (2010).
3. “Low-Energy Electron Scattering from C₄H₉OH Isomers,” M. H. F. Bettega, C. Winstead, and V. McKoy, *Phys. Rev. A* **82**, 062709 (2010).

4. "Elastic Scattering of Intermediate Energy Electrons from C₆₀ Molecules," L. R. Hargreaves, B. Lohmann, C. Winstead, and V. McKoy, *Phys. Rev. A* **82**, 062716 (2010).
5. "Measurement and Calculation of Absolute Single and Multiple Charge Exchange Cross Sections for Fe^{q+} Ions Impacting H₂O," J. Simcic, D. R. Schultz, R. J. Mawhorter, J. B. Greenwood, C. Winstead, B. V. McKoy, S. J. Smith, and A. Chutjian, *Ap. J.* **722**, 435 (2010).
6. "Absolute Angle-Differential Elastic Cross Sections for Electron Collisions with Diacetylene," M. Allan, C. Winstead, and V. McKoy, *Phys. Rev. A* **83**, 062703 (2011).
7. "Collisions of Low-Energy Electrons with Isopropanol," M. H. F. Bettega, C. Winstead, V. McKoy, A. Jo, A. Gauf, J. Tanner, L. R. Hargreaves, and M. A. Khakoo, *Phys. Rev. A* **84**, 042702 (2011).
8. "Low Energy Elastic Electron Interactions with Pyrimidine," P. Palihawadana, J. Sullivan, M. Brunger, C. Winstead, V. McKoy, G. Garcia, F. Blanco, and S. Buckman, *Phys. Rev. A* **84**, 062702 (2011).
9. "Low-Energy Electron Scattering by Tetrahydrofuran," A. Gauf, L. R. Hargreaves, A. Jo, J. Tanner, M. A. Khakoo, T. Walls, C. Winstead, and V. McKoy, *Phys. Rev. A* **85**, 052717 (2012).
10. "Electron-Biomolecule Collision Studies Using the Schwinger Multichannel Method," C. Winstead and V. McKoy, in *Radiation Damage in Biomolecular Systems*, G. García Gómez-Tejedor and M. C. Fuss, editors (Springer, Dordrecht, 2012), p. 87.
11. "Low-Energy Electron Interactions with Biomolecules," V. McKoy, Physics Department Seminar, Federal University of Amazonas, Manaus, Brazil, June 13, 2011.
12. "Low-Energy Electron Interactions with Biomolecules," C. Winstead, XXVII International Conference on Photonic, Electronic, and Atomic Collisions, Belfast, UK, July 27–August 2, 2011 (*invited talk*).
13. "Anomalously Large Low-Energy Elastic Cross Sections for Electron Scattering from the CF₃ Radical," J. R. Brunton, L. R. Hargreaves, M. J. Brunger, S. J. Buckman, G. Garcia, F. Blanco, O. Zatsarinny, K. Bartschat, C. Winstead, and V. McKoy, XXVII International Conference on Photonic, Electronic, and Atomic Collisions, Belfast, UK, July 27–August 2, 2011.
14. "Cross Sections for Electronic Excitation of Water by Low-Energy Electrons," L. R. Hargreaves, K. Ralphs, M. A. Khakoo, C. Winstead, and V. McKoy, XXVII International Conference on Photonic, Electronic, and Atomic Collisions, Belfast, UK, July 27–August 2, 2011.
15. "Electron and Positron Scattering from Pyrimidine," P. D. Palihawadana, J. R. Machacek, C. Makochekanwa, J. P. Sullivan, M. J. Brunger, C. Winstead, V. McKoy, G. Garcia, F. Blanco, S. J. Buckman, XXVII International Conference on Photonic, Electronic, and Atomic Collisions, Belfast, UK, July 27–August 2, 2011.
16. "Absolute Cross Sections for Electron Collisions with Diacetylene: Elastic Scattering, Vibrational Excitation and Dissociative Attachment," M. Allan, O. May, J. Fedor, B. C. Ibanescu, L. Andric, C. Winstead, and V. McKoy, XXVII International Conference on Photonic, Electronic, and Atomic Collisions, Belfast, UK, July 27–August 2, 2011.
17. "Simulating Quantum Collisions," V. McKoy, School of Computing and Information Sciences, Florida International University, March 23, 2012 (*invited talk, Distinguished Lecture Series*).
18. "Low-Energy Electron Interactions with Biomolecules," C. Winstead, Forty-Third Annual Meeting of the APS Division of Atomic, Molecular and Optical Physics, Orange County, California, June 4–8, 2012 (*invited talk*).

19. “Low-Energy Electron Scattering from Water Vapor,” K. Ralphs, G. Serna, L. Hargreaves, M. A. Khakoo, C. Winstead, and V. McKoy, Forty-Third Annual Meeting of the APS Division of Atomic, Molecular and Optical Physics, Orange County, California, June 4–8, 2012.

ELECTRON/PHOTON INTERACTIONS WITH ATOMS/IONS

Alfred Z. Msezane (email: amsezane@cau.edu)

Clark Atlanta University, Department of Physics and CTSPS
Atlanta, Georgia 30314

PROGRAM SCOPE

The project's primary objective is to gain a fundamental understanding of the near-threshold electron attachment mechanism and determine accurate electron affinities (EAs) of simple and complex atoms. Our elegant Mulholland formula, implemented within the complex angular momentum (CAM) description of scattering, wherein resonances are rigorously defined as singularities of the S-matrix, is used for the investigations [1]. Regge trajectories allow us to probe electron attachment at its most fundamental level near threshold, thereby uncovering new manifestations and possibilities as well as determine the reliable EAs of tenuously bound and complicated atomic and molecular systems [2]. The importance and utility of negative ions in terrestrial and stellar atmospheres as well as in industrially important plasmas for device fabrication are well documented. Laser cooling of atomic anions has been suggested for producing ultra-cold antihydrogens whose scientific importance includes the direct measurement of the gravitational acceleration of antimatter.

The most important accomplishments in this funding cycle of our research are: 1) Linking low-energy electron scattering resonances with chemical reaction dynamics and their application to the oxidation of H_2O to H_2O_2 catalyzed by atomic Au^- and Pd^- ions [3] and 2) Identification of atomic Au^- negative ion catalysis of methane to methanol without CO_2 emission [4]. These demonstrate clearly the great importance of the knowledge of low-energy electron scattering from atoms, resulting in negative ion formation. The electron elastic TCSs of Os^- exhibit a richer structure, leading to a new EA.

Innovative theoretical methods for atoms (ions) with unfilled sub-shells continue to be explored and applied to the photoabsorption spectra for the free Xe atom and C_{60} fullerene as well as to the photoionization of Ce^{3+} @ C_{82} . Methods are developed for calculating the generalized oscillator strength, useful in probing the intricate nature of the valence- and open-shell as well as inner-shell electron transitions. Standard codes such as CIV3 of Hibbert and the Belfast R-matrix are used to generate sophisticated wave functions for investigating configuration interaction (CI) mixing and relativistic effects in atomic ions. The wave functions are also used to explore correlation effects in dipole and non-dipole studies

The newest area of our research involves studies of heavy fermions and strongly correlated systems, a collaboration with our Russian colleagues.

SUMMARY OF RECENT ACCOMPLISHMENTS

A. Complex Angular Momentum Analysis of Low-Energy Electron Scattering by Complex Atoms

The mechanisms of electron-electron correlations and core-polarization interaction are crucial for the existence and stability of most negative ions. In our calculations of the electron elastic scattering total cross sections (TCSs) using the Regge-pole methodology these vital effects are fully embedded in the CAM method. The Mulholland formula converts the infinite discrete sum into a background integral plus the contribution from a few poles to the process under consideration [1]. The power of the method lies in that it extracts the binding energies (BEs) of tenuously bound and complex negative ions from the resonances in the near threshold elastic TCSs, requiring no *a priori* knowledge of the experimental or other theoretical data. Relativistic effects contribute a small percentage in EA calculations [3].

A.1 Multiple excited negative ion formation in slow electron collisions with Tm, Lu and Hf atoms

Recently, the formation of ground and excited negative ions through slow electron collisions with the lanthanide and Hf atoms has been investigated using the CAM method [1]. From the calculated

elastic TCSs the EAs and the BEs of the excited anions were extracted. For Hf the obtained EA was 0.525 eV, in contrast to the value of 0.114 eV obtained using Relativistic configuration interaction calculations. Here we predict, using the CAM method, the formation of multiple excited negative ionic states in low-energy $0 \leq E \leq 1.0$ eV electron elastic scattering from Tm, Lu and Hf atoms. Their BEs are extracted from the calculated elastic total and differential cross sections [5]. Ramsauer-Townsend (R-T) minima and shape resonances are determined as well. We conclude that the recently calculated BE value of 0.114 eV for the Hf⁻ anion actually corresponds to an excited state and not to the EA.

A.2 Low-energy electron scattering from atoms: Search for nanocatalysts

Manipulating the structure and the dynamics of metallic nanoparticles, attractive due to their optical, electronic and magnetic properties, including applications in catalysis, requires a fundamental understanding of the dynamic processes at the atomic level. The fundamental mechanism of catalysis at the atomic scale has already been proposed and demonstrated in the Au, Pd and Au-Pd catalysis of H₂O₂ through the scrutiny of low energy electron elastic TCSs [6]. The use of mixed precious metal catalysts can produce even higher activities compared to Au alone. Here the Au TCSs are used as our benchmark for metal atom catalysts to identify nanoscale catalysts. Calculated, using the recent CAM methodology, electron elastic TCSs for Ag, Pt, Pd, Ru and Y atoms are presented as illustrations [7]. It is concluded that these atoms are suitable candidates for nanocatalysts individually or in combinations. It is now possible to systematically construct effective catalysts for various substances by putting together the catalysts Au, Ag, Pd, Pt, Ru and Y in various combinations; Tl and At are also other possible candidates [8].

A.3 Electron elastic scattering cross sections for Ga, In Tl and At atoms near threshold

The recently measured EA of 383.92(6) meV of In by Walter *et al* {Phys. Rev. A **82**, 032507 (2010)} compared very well with theoretical EAs but differed substantially from a previous measurement. For the Tl atom the calculated and measured EAs differ significantly, while for Ga theory and experiment agree reasonably well. Here we have investigated near-threshold electron scattering from In, Ga, Tl and At to understand the discrepancy between the various calculations and measurements [8]. From the characteristic dramatic resonances in the TCSs, we extract the EAs for these atoms and compare our values with the available data. A dramatically sharp resonance at 0.380 eV in our calculated elastic TCS for In corresponds to the negative ion formed during the collision and defines the EA of In, in excellent agreement with the measurement and the calculation. For Tl the EA value of 0.27 eV compares excellently with our calculated BE of 0.281 eV [8]. However, since our EA for Tl is 2.41 eV, we conclude that the 0.27eV corresponds to the BE of an excited Tl⁻ anion and not to the EA. Our calculated EA for the At atom compared very well with the only calculated value.

A.4 Atomic Gold and Palladium Negative-Ion Catalysis of Light, Intermediate, and Heavy Water to Corresponding Peroxides

Following the identification of the catalytic properties of atomic Au⁻ and atomic Pd⁻ ions, we performed transition state calculations using dispersion-corrected DFT on atomic Au⁻ and atomic Pd⁻ ion catalysis of H₂O, HDO, and D₂O conversion to H₂O₂, HDO₂, and D₂O₂, respectively [3]. The Au⁻ ion is found to be an excellent catalyst; however, the Pd⁻ ion has a higher catalytic effect on the formation of peroxide from light, intermediate, and heavy water. These atomic negative ion catalysts speed up the reactions by lowering the activation energy, with the Pd⁻ ion accomplishing the catalysis by a factor of about three times faster than that by the Au⁻ ion. The fundamental mechanism involves anionic molecular complex formation in the transition state, with the Au⁻ and Pd⁻ ions breaking up the hydrogen bond strength in the water molecules, permitting the formation of the peroxides in the presence of O₂ usually provided by the support. Our theoretical results provide further insight into the mechanism of atomic Au⁻ and Pd⁻ ion catalysis consistent with the recent experimental observations.

A.5 Gold anion catalysis of methane to methanol (A theoretical breakthrough)

The oxidation of CH₄ has been investigated in the presence and absence of the atomic Au⁻ ion catalyst [4]. We have employed the dispersion-corrected DFT calculations for the transition state on the Au⁻ ion and analyzed the thermodynamics properties of the reactions as well. Our results demonstrate that atomic Au⁻ ion could be used to catalyze CH₄ into valuable industrial products without the emission of CO₂, thereby render gold extremely valuable. The fundamental mechanism involves breaking the C-H

bond through the formation of the anionic $\text{Au}^-(\text{CH}_4)$ molecular complex permitting the oxidation of CH_4 to methanol at the lower temperature of 325 K which is below that of CO_2 emission. This proposed catalytic process involving the use of the atomic Au^- ion catalyst promises a first and a giant step toward finding and assembling nanocatalysts atom by atom for various chemical reactions, including the direct partial oxidation of methane to useful products without CO_2 emission.

A.6 Regge trajectories in multi-channel scattering.

A simple direct method for calculating Regge trajectories for a multichannel scattering problem has now been developed [9]. The approach is applied to the case of two coupled Thomas-Fermi type potentials, used as a simple model for electron-atom scattering below the second excitation threshold. It is shown that non-adiabatic interaction may cause the formation of loops in Regge trajectories. The accuracy of the method is tested by evaluating resonance contributions to elastic and inelastic integral cross sections. This development promises a powerful approach to low-energy scattering with the possibility to probe Regge resonances and Feshbach resonances occurring in Bose-Einstein condensates.

B. Confined Atoms

B.1 Photoabsorption spectrum of the $\text{Xe}@C_{60}$ endohedral fullerene

Photoabsorption spectrum of the $\text{Xe}@C_{60}$ endohedral fullerene has been studied using the time-dependent-density-functional-theory (TDDFT), which represents the dynamical polarizability of an interacting electron system by an off-diagonal matrix element of the resolvent of the Liouvillian superoperator and solves the problem with the Lanczos algorithm [10]. The method has been tested with the photoabsorption spectra for the free Xe atom and C_{60} fullerene. The result of the Xe atom encapsulated inside C_{60} confirms the three main peaks observed in the recent measurement in the energy region of the Xe $4d$ giant resonance and indicates the possibility that the Auger decay of the Xe^+ has been greatly suppressed if the ion is encapsulated inside C_{60} . It is suggested to use the current theoretical result around 22 eV to check this possibility.

C. Heavy Fermion Systems (New Area)

C.1 Identification of strongly correlated spin liquid in herbertsmithite

An exotic quantum spin liquid (QSL) is formed with such hypothetical particles as fermionic spinons carrying spin 1/2 and no charge. Here we calculate its thermodynamic and relaxation properties. Our calculations unveil the fundamental properties of QSL, forming a strongly correlated Fermi system located at a fermion condensation quantum phase transition [11]. These are in good agreement with experimental data and allow us to detect the behavior of QSL as that observed in heavy-fermion metals. We predict that the thermal resistivity of QSL under the application of magnetic fields at fixed temperature demonstrates a very specific behavior. The key features of our findings are the presence of spin-charge separation and QSL formed with itinerant heavy spinons in herbertsmithite.

D. Atomic Structure Calculations

D.1 Fine-structure energy levels, radiative rates and lifetimes in Si-like nickel

Large scale CIV3 calculations of excitation energies from ground state as well as of oscillator strengths and radiative decay rates for all electric-dipole-allowed and intercombination transitions among the fine-structure levels of the terms belonging to the $(1s^2 2s^2 2p^6) 3s^2 3p^2$, $3s 3p^3$, $3p^4$, $3s^2 3p 3d$, $3s^2 3p 4s$, $3s^2 3p 4p$, $3s^2 3p 4d$ and $3s^2 3p 4f$ configurations of Ni XV, are performed using extensive configuration-interaction wave functions [12]. The relativistic effects in intermediate coupling are incorporated through the Breit-Pauli Hamiltonian. Our calculated excitation energies, including their ordering, are in excellent agreement with the available NIST results. From our radiative decay rates we have also calculated radiative lifetimes of the fine-structure levels and compared them with the available data. For the high spin level $3s 3p^3(^3S_2)$ our calculated lifetime agrees excellently with the experimental value. We also predict many new and accurate data for various transitions to complete the void in the existing data.

FUTURE PLANS

We continue with the theoretical investigations of low-energy electron scattering from simple and complex atoms, photoionization of endohedral fullerenes, strongly correlated systems and atomic structure calculations as delineated above. New accurate EAs for complex atoms will be obtained and

nanocatalysts will be investigated and identified as well. Our recent CAM method [9] will be employed as well as extended to investigate Feshbach resonances.

REFERENCES AND SOME PUBLICATIONS ACKNOWLEDGING GRANT (2011-2012)

1. D. Sokolovski *et al*, Phys. Rev. A **76**, 012705 (2007).
2. Z. Felfli, A.Z. Msezane and D. Sokolovski, Phys. Rev. A **79**, 012714 (2009); “Complex angular momentum analysis of low-energy electron elastic scattering from lanthanide Atoms”, Z. Felfli, A.Z. Msezane and D. Sokolovski, Phys. Rev. A **81**, 042707 (2010).
3. "Atomic Gold and Palladium Negative-Ion Catalysis of Light, Intermediate, and Heavy Water to Corresponding Peroxides", A. Tesfamichael, K. Suggs, Z. Felfli, X.-Q. Wang, and A.Z. Msezane, Journal of Physical Chemistry C, DOI: 10.1021/jp301861q (2012)
4. “Gold anion catalysis of methane to methanol”, A. Z. Msezane, Z. Felfli, K. Suggs, A. Tesfamichael, X.-Q. Wang, Gold Bull. DOI10.1007/s13404-012-0056-7 (2012)
5. “Low-energy electron elastic collision cross sections for ground and excited Tm, Lu and Hf atoms”, Z. Felfli, A.Z. Msezane and D. Sokolovski, NIMB **269** 1046–1052 (2011)
6. A. Z. Msezane, Z. Felfli and D. Sokolovski, J. Phys. B **43**, 201001 (2010) (FAST TRACK)
7. “Elastic scattering of slow electrons from Y, Ru, Pd, Ag and Pt atoms: Search for nanocatalysts”, Z. Felfli, A.Z. Msezane and D. Sokolovski, J. Phys. B **44**, 135204 (2011)
8. “Slow electron elastic scattering cross sections for In, Tl, Ga and At atoms”, Z. Felfli, A.Z. Msezane and D. Sokolovski, J. Phys. B **45**, 045201 (2012)
9. “Self-intersecting Regge trajectories in multi-channel scattering”, D. Sokolovski, Z. Felfli, A.Z. Msezane, Physics Letters A **376**, 733-736 (2012)
10. “Photoabsorption spectrum of the Xe@ C₆₀ endohedral fullerene”, Zhifan Chen and Alfred Z Msezane, Eur. Phys. J. D **66**, 184 (2012)
11. “Identification of strongly correlated spin liquid in Herbertsmithite”, V.R. Shaginyan, A. Z. Msezane, K. G. Popov, G. S. Japaridze and V. A. Stephanovich, Eur. Phys. Lett. **97**, 56001 (2012)
12. “Fine-Structure energy levels, radiative rates and lifetimes in Si-like Nickel”, G. P. Gupta and A. Z. Msezane, Phys. Scripta **86**, 015303 (2012)
13. “Low-energy electron elastic scattering from Mn, Cu, Zn, Ni, Ag and Cd atoms”, Z. Felfli, A.Z. Msezane and D. Sokolovski, Phys. Rev. A **83**, 052705 (2011)
14. “Photoionization of the Xe atom and Xe@C₆₀ molecule”, Zhifan Chen and A.Z. Msezane, Eur. Phys. J. D **65**, 353 (2011). DOI: <http://dx.doi.org/10.1140/epjd/e2011-20425-4>
15. “Interference in Molecular Photoionization and Young’s Double-Slit Experiment”, A. S. Baltenkov, U. Becker, S. T. Manson and A. Z. Msezane, J. Phys. B **45**, 035202 (2012)
16. “Baryon asymmetry resulting from a quantum phase transition in the early universe”, V. R. Shaginyan, G. S. Japaridze, M. Ya. Amusia, A. Z. Msezane and K. G. Popov, Eur. Phys. Lett. **94**, 69001 (2011)
17. “Thermodynamic Properties of Kagome Lattice in ZnCu₃(OH)₆Cl₂”, V.R. Shaginyan, A.Z. Msezane, and K.G. Popov, Phys. Rev. B **84**, 060401 (R) (2011)
18. “Fine-structure energy levels, oscillator strengths and lifetimes in Cu XVI”, G. P. Gupta and A. Z. Msezane, Phys. Scr. **83**, 055301 (2011)
19. “Atomic Au and Pd Negative Ion-Catalysis of Water to Peroxide: Fundamental Mechanism”, A. Tesfamichael, K. Suggs, Z. Felfli, X.-Q. Wang and A. Z. Msezane, J. Nano. Research, In Press (2012)
20. “Comment on Zeeman-Driven Lifshitz Transition: A Model for the Experimentally Observed Fermi-Surface Reconstruction in YbRh₂Si₂”, V. R. Shaginyan, M. Ya. Amusia, J.W. Clark, A. Z. Msezane, K.G. Popov, M.V. Zverev and V.A. Khodel, Phys. Rev. Lett. **107**, 279701 (2011)
21. “Nondipole Parameters of TDCS for Electron Impact Ionization and Drag Current”, A.K. Baltenkov, S.T. Manson and A.Z. Msezane, Cent. Eur. J. Phys. **9**, 1209-1220 (2011).
22. “A Mathematical Model of Negative Molecular Ion”, A. S. Baltenkov, S. T. Manson, and A. Z. Msezane, Proc. Dynamic Systems and Applications **6** (Dynamic Publishers, Atlanta, Georgia, 2012), pp. 53- 57

Theory and Simulation of Nonlinear X-ray Spectroscopy of Molecules

Shaul Mukamel

University of California, Irvine, CA 92697

Progress Report 2012, August 29, 2012

DOE DE-FG02-04ER15571

Program Scope

This program is aimed at extending nonlinear spectroscopy techniques commonly applied in the visible and infrared regimes to study core-excitations at x-ray frequencies. Theoretical and computational methods are developed to describe coherent resonant nonlinear ultrafast x-ray spectroscopies of molecules. We propose experiments made possible by new X-ray free electron laser (XFEL) and high harmonic generation (HHG) sources. Design principles and tools for multidimensional techniques that make use of sources with broad bandwidths and high frequencies are presented using intuitive loop diagrams. Techniques that either study core excitations or use them as triggers for valence electronic dynamics are proposed and analyzed. Approximate computational tools that can handle large molecules and molecular aggregates, and methods for visualizing the electron correlations revealed by these new measurements are developed. Nonlinear x-ray spectroscopies can characterize atomic interactions in ways previously inaccessible at lower frequency excitations. Basic questions about probing the dynamics of photochemically excited states, charge and energy transport are addressed.

A two-dimensional Stimulated X-ray Raman spectroscopy technique (2D-SXRS) is developed. Both one and two dimensional signals are recast in terms of correlation functions of the x-ray polarizability, highlighting the close similarities between the optical and x-ray stimulated Raman processes. These techniques are applied to N-methyl acetamide (NMA) and to cysteine, an amino acid containing nitrogen, oxygen and sulfur atoms. Transition dipoles and frequencies are calculated using the Restricted Excitation Window Time-dependent Density Functional Theory (REW-TDDFT), a formalism which recasts the core-excitation problem into a form where electron correlations can be easily parametrized by a Coulomb and exchange parts. Novel pulse polarization configurations are examined.

Recent Progress

Restricted window TDDFT protocol for core excitations

We have adapted and used the REW-TDDFT implemented in a development version of NWChem package [M. Valiev, E. Bylaska, N. Govind, et al. *Comput. Phys. Commun.*, vol. 181, p. 1477, 2010.], to calculate the core excited states contributing to X-ray signals. The balance of computational accuracy and cost has made TDDFT the method of choice for excited state calculations. In conventional implementations one must solve all lower-lying states in order to get the very high excited state, an expensive proposition for core excited state calculations. In our approach an orbital energy cutoff set to restrict the excitation window, allows the response equation of TDDFT to be solved in a selected energy-restricted space making highly excited states readily accessible. The method is simple to use and can be applied for deep as well as shallow holes. This approach can handle core hole mixing, partially accounts for correlation, and is computationally faster and more stable compared to the static exchange (STEX) method which was used in our previous studies.

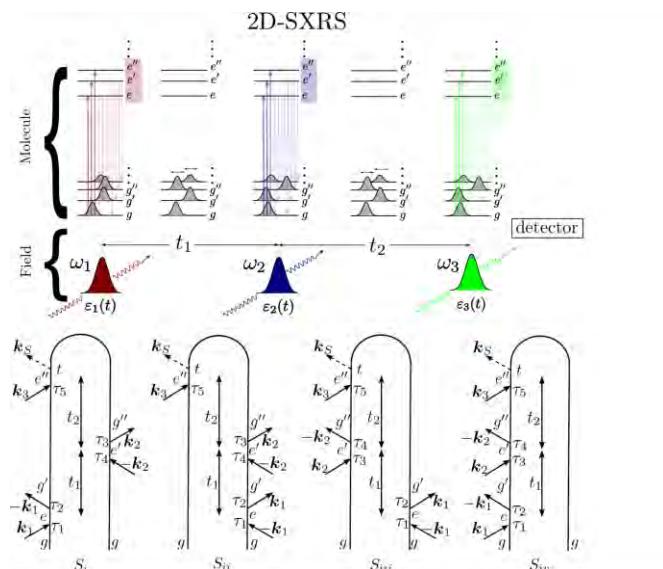


Fig 1: (top) 2D-SXRS experiment: the signal is given by the transmitted intensity of the third pulse as a function of the Fourier transformed delay times t_1 and t_2 . (bottom) Loop diagrams contributing to 2D-SXRS

Stimulated Raman Techniques

2D-SXRS uses three pulses with varying delays (Fig 1), and was proposed and shown to probe molecular valence electronic excitations in greater detail than the one dimensional (two-pulse) signal. Optical resonance Raman spectra can be written as correlation functions of a customized vibrational perturbation operator,

chosen through a choice of a specific intermediate electronic state by tuning the central frequencies of the exciting pulses. The same formalism, in which a fast, switchable subsystem (the core-excitation) creates a custom perturbation operator (the x-ray polarizability), was extended to predict 1D-SXRS and 2D-SXRS measurements. Signals calculated for trans-N-methyl acetamide (NMA) with broad bandwidth pulses tuned to the oxygen and nitrogen K-edges and to the sulfur K-edge in cysteine, revealed crosspeaks in 2D signals sensitive to electronic Franck-Condon overlaps between valence orbitals as well as relaxed orbitals in the presence of the core hole.

The trans-NMA signals at the N and O K-edge were also found to be sensitive to the order in which the atom-specific x-ray excitations were used to perturb and probe the valence electron configuration. Cross-peak intensities are useful for testing various levels of electronic structure theory. 2D-SXRS offers a greater number of pulse combinations, and greater control over the preparation and measurement of electronic wavepackets compared to its 1D counterpart. This is demonstrated in Figure 2 where all pulses are tuned to the oxygen K-edge.

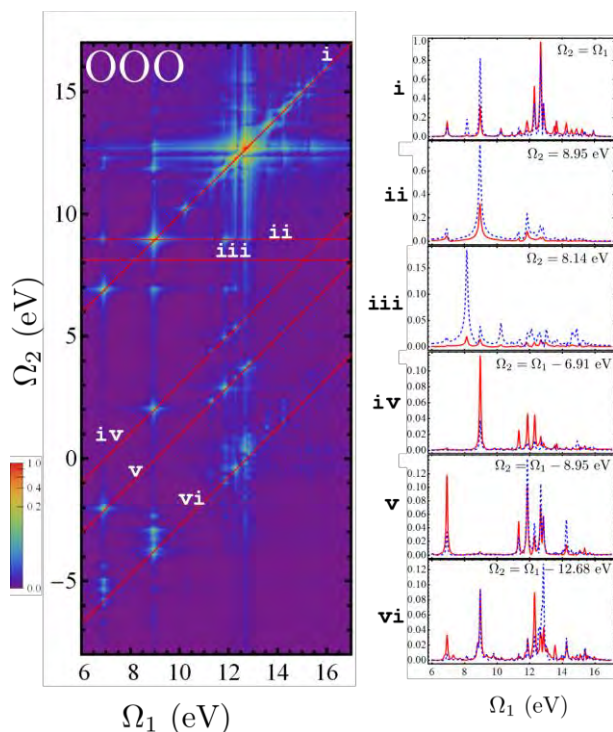


Fig 2: (left) 2D-SXRS signal of NMA with all three pulses tuned to the oxygen k-edge. (right) slices through this spectra sensitive to energy resolved matrix elements of the x-ray polarizability operator.

Novel Pulse Polarization Configurations

Simulating the spontaneous (RIXS) and Stimulated X-ray Raman Scattering (SXRS) signals in isotropic samples requires the rotational averaging of a fourth-rank tensor product of two polarizabilities. Attosecond stimulated x-ray Raman spectroscopy excites multiple valence transitions covered by the pulse bandwidths. These excitations depend on the orientation of the molecule with respect to the pulse polarizations in the lab frame, making the response a high rank tensor operator. The numerous

contributions to the response coming from different tensor components complicate the analysis and interpretation of these measurements. The magic angle between the excitation and detection fields allows to express these signals as correlation functions of the scalar isotropic polarizabilities, aiding their interpretation. We showed that a similar simplification of 2D-SXRS, which depend on a rotationally-averaged sixth-rank tensor, is possible by a Super Magic Angle (SMA) combination of two measurements with specific pulse polarization configurations. Such signals for trans NMA at the nitrogen K-edge reveal

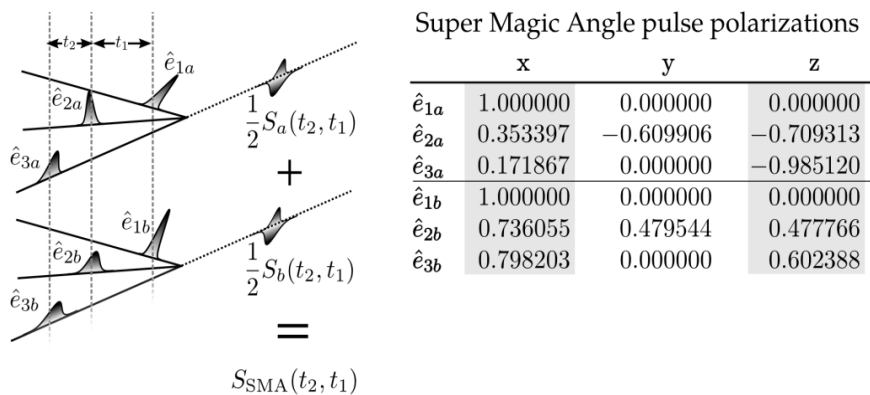


Fig 3

new features compared to the all-parallel polarization configuration. The tensor response function in an ensemble of randomly oriented molecules was decomposed into isotropic and anisotropic parts. We showed that the sum of two signals taken with non-collinear pulses can be used to extract the isotropic part of the 2D-SXRS signal.

Future Plans

Real time visualization of electron correlations: We have demonstrated the capacity of attosecond x-ray pulses to prepare electronic wavepackets with electron and hole densities local to the resonant core atom. These densities were calculated immediately following an excitation at the nitrogen, oxygen and sulfur K-edges of cysteine. Movies of the time-evolving natural orbitals, the reduced electron and hole densities, and their degree of entanglement (natural orbital participation ratio and concurrence) illustrate the correlated many-body dynamics of quasiparticles. The time-dependent participation ratios show a rapid decay of the single particle-hole character of the excitation and the buildup of electron correlations in the valence excited states. Time-dependent particle hole occupations carry additional information on these correlations through both the reduced densities of the electrons and holes themselves, and the cross-correlation between them. Identifying more detailed measures of these correlations, and designing the optimal stimulated Raman, photoelectron or other experimental techniques for measuring this entanglement constitutes an interesting future challenge.

Computing Multiple core states and their Spectroscopic Signatures: Double or multiple core excited states can be studied by X-ray nonlinear spectroscopy. However, the adiabatic approximation, which is common in TDDFT restricts its application to single excitations. To circumvent this limitation we shall combine Δ SCF, which is a well established method for calculating excitation energies, with TDDFT. Δ SCF can be used to get an excited configuration with a core hole. Based on this excited configuration, a TDDFT calculation which targets another core hole would bring us finally to the desired double core excited

state. With this approach, nonlinear x-ray signals could serve as sensitive tests for many-body theory of Fermions.

Electron and Charge Migration in Porphyrin Arrays: Electronic excitations may be described over many length and time-scales using an excitonic picture, where particles and holes interact through a Hamiltonian that controls their correlated time evolution. Multiporphyrin arrays are important structures in photosynthetic light harvesting antenna complexes, with practical applications to molecular conductive wires and optoelectronic devices. Effective core exciton Hamiltonians whose parameters come from Ab-initio quantum chemistry calculations on dimer systems will be constructed. Using such effective Hamiltonians, we plan to simulate X-ray spectroscopy signals of extended arrays and investigate the primary electron and hole motions. The technique has been tested on coherent optical signals of molecular aggregates and semiconductor quantum wells in the visible regime.

Time and Frequency Gated Spontaneous emission of X-ray pumped molecules: The valence particles and holes produced by a stimulated x-ray Raman excitation should be observable through their spontaneous emission in the visible regime. Time- and frequency resolved x-ray induced fluorescence signals should contain signatures of particle and hole overlaps, and provide a powerful experimental window into the valence electronic wavepacket dynamics. Both coherent and incoherent signals will be predicted.

Publications Resulting from the Project

P1 "Simulation and Visualization of Attosecond Stimulated X-ray Raman Spectroscopy(SXRS) Signals in trans-NMA at the Nitrogen & Oxygen K-Edges ", D. Healion, H. Wang and S. Mukamel, J. Chem. Phys. 134, 124101 (2011).

P2 "Multidimensional phase-sensitive Single-Molecule Spectroscopy with Time-and-Frequency-Gated Fluorescence Detection", S. Mukamel and M. Richter, Phys. Rev. A, 83,013815 (2011).

P3 "Quantum Field, Interference, and Entanglement Effects in Nonlinear Optical Spectroscopy", S. Mukamel and Y. Nagata, Procedia. Chem. 3, 132-151 (2011).

P4 "Collective Two-Particle Resonances Induced by Photon Entanglement", M. Richter, S. Mukamel, Phys.Rev. A. 83, 063805(2011).

P5 "Communication: Comment on the Effective Temporal and Spectral Resolution of Impulsive Stimulated Raman Signals". J. Biggs and S. Mukamel. J. Chem. Phys. 134, 161101 (2011).

P6 "Deep UV Resonance Raman Spectroscopy of β -sheet Amyloid Fibrils; A QM/MM Simulation". H. Ren, J. Jiang, and S. Mukamel, J. Phys Chem B, 115, pages 13955-13962 (2011).

P7 "Nonlinear Spectroscopy with Time and Frequency Gated Photon Counting; A Superoperator Diagrammatic Approach", K. Dorfman and S. Mukamel. Phys Rev A, 86, 013810 (2012).

P8 "Reconstruction of the Wavefunctions of Coupled Nanscopic Emitters Using a Coherent Optical Technique". M. Richter, F. Schlosser, M. Schoth S. Burger, F. Schmidt, A. Knorr, and S. Mukamel. Phys Rev B, 86, 085308 (2012).

P9 "Coherent Nonlinear Optical Studies of Elementary Processes in Biological Complexes; Diagrammatic Techniques Based on the Wavefunction vs. the Density Matrix", J. Biggs, J. Voll, and S. Mukamel. Phil Trans Royal Society A, 370, 3709-3727 (2012).

P10 "Weak Exciton Scattering in Molecular Nanotubes Revealed by Double-quantum Two-dimensional Electronic Spectroscopy", D. Abramavicius, A. Nemeth, F. Milota, J. Sperling, S. Mukamel, and H. Kauffmann. Phys Rev Letters. 108, 067401 (2012).

P11 "Trapping Photon-dressed Dirac Electrons in a Quantum Dot Studied by Coherent Two-dimensional Photon Echo Spectroscopy", O. Roslyak, G. Gumbs, and S. Mukamel. J. Chem. Phys. 136, 194106 (2012).

P12 "2D Stimulated Resonance Raman Spectroscopy of Molecules with Broadband X-ray Pulses", J.D. Biggs, Y. Zhang, D. Healion, and S. Mukamel. J. Chem. Phys. 136, 174117 (2012).

P13 "Resolving the Electron Transfer Kinetics in the Bacterial Reaction Center by Pulse Polarized 2-D Photon Echo Spectroscopy", B.P. Fingerhut, and S. Mukamel. J.Phys.Chem. Lett, 1798-1805 (2012)

P14 "Photon Coincidence Counting in Parametric Down Conversion; Interference of Field-Matter Quantum Pathways", K. Dorfman and S. Mukamel. Phys. Rev. A, 86, 023805 (2012).

P15 "Entangled Valence Electron-hole Dynamics Revealed by Stimulated Attosecond X-ray Raman Scattering", D. Healion, Y. Zhang, J.D. Biggs, N. Govind, and S. Mukamel. J. Phys. Chem. Lett. (In Press, 2012)

Nonlinear Photoacoustic Spectroscopies Probed by Ultrafast X-Rays

Keith A. Nelson
Department of Chemistry
Massachusetts Institute of Technology
Cambridge, MA 02139
Email: kanelson@mit.edu

Margaret M. Murnane
JILA
University of Colorado and National Institutes of Technology
Boulder, CO 80309
E-mail: murnane@jila.colorado.edu

Program Scope

In this project, ultrashort electromagnetic pulses in the visible, extreme ultraviolet (EUV), and x-ray spectral ranges are all used in complementary efforts to gain experimental access to elementary material excitations and fundamental condensed matter processes on ultrafast time scales and mesoscopic length scales. Of primary interest are heat transport, whose non-diffusive character at short length scales plays important roles in thermoelectric materials and nanoscale devices, and structural evolution in disordered media, which shows dynamics on wide-ranging time scales that have long eluded first-principles description. Central to these phenomena are acoustic phonons, which mediate both thermal transport and the compressional and shear components of structural relaxation. In addition to direct time-resolved observation of thermal transport, longitudinal, transverse, and surface acoustic wave generation and detection are key elements of our experiments in all spectral ranges.

We develop and use a variety of methods to excite and monitor acoustic waves and thermal transport on a wide range of length and time scales. For length scales in the roughly 1-100 micron range, we use crossed optical pulses to form an interference or "transient grating" (TG) pattern, directly generating thermoelastic responses with the grating period Λ (i.e. with wavevector magnitude $q = 2\pi/\Lambda$). The responses are monitored by time-resolved diffraction of probe laser light, revealing damped acoustic oscillations (from which acoustic speeds and attenuation rates, and elastic and loss moduli, are determined) and showing the kinetics of thermal transport from the heated interference maxima (the transient grating "peaks") to the unheated minima ("nulls"). The acoustic frequencies at these wavelengths are in the MHz or low GHz range. In order to reach higher acoustic frequencies and to monitor heat transport on length scales far less than 1 μm , we are working to extend transient grating methods to EUV wavelengths, taking advantage of ever-increasing EUV pulse energies produced through high harmonic generation (HHG), and to hard x-ray wavelengths using the LCLS facility at Stanford. In parallel with these long-term efforts, we have developed several approaches to provide experimental access to higher wavevectors than those reached through the interference patterns (or the coherent scattering) of visible light. Spatially periodic structures can be deposited onto substrate surfaces so that optical irradiation produces thermoelastic responses at the specified periods which may be as small as a few tens of nanometers. Time-resolved diffraction of variably delayed EUV pulses reveals the corresponding surface acoustic wave oscillations and thermal transport kinetics with extremely high sensitivity. Alternatively, a superlattice structure of alternating layers that have different optical absorption spectra (e.g. absorbing and transparent at an optical excitation pulse wavelength) can be irradiated to generate a thermoelastic response including a bulk compressional acoustic wave with the superlattice period. The acoustic wave may be detected in a variety of ways including measurement of acoustic modulation of the optical absorption strength or interferometric measurement of time-dependent displacements at a sample interface when the acoustic wave arrives there. Alternatively, a thin opaque layer may be irradiated by a sequence of femtosecond optical pulses so that

its periodic thermal expansion launches a multiple-cycle acoustic wave into a substrate. In this case it is not the acoustic wavevector that is specified experimentally but the frequency which is determined by the temporal period of the optical pulse sequence. The wave may be detected by coherent Brillouin scattering within the substrate for moderate acoustic frequencies, or by monitoring motion at the back of the substrate or at an interface.

Recent Progress

Nanoscale thermal transport and acoustics with EUV pulses

Nanoscale thermal transport: Understanding energy flow in nanostructures is very challenging because the basic models describing ballistic and quasi-ballistic transport are still under development, and more sophisticated simulations remain difficult to verify. Thermal energy is carried by phonons that travel ballistically away from a nanoscale heat source for a significant distance before experiencing collisions, leading to non-local (i.e. non-diffusive) thermal energy distributions. In past work published in *Nature Materials*, we used ultrafast coherent high harmonic (HHG) beams to directly measure the ballistic contribution to the transport of thermal energy from a 1D periodic nanoscale heat source into its surroundings. Despite considerable theoretical discussion and direct application to thermal management in nanoelectronics, nano-enabled energy systems, and nanomedicine, this non-Fourier heat dissipation had not been experimentally observed to date. We found a significant (as much as 3 times) decrease in energy transport rates away from the nanoscale heat source compared with Fourier law predictions. This work solved a controversy in the field, because two different theories were proposed, but only one agreed with our measurements.

In more recent experiments, we explored heat flow from 2D nanostructures. Intuitively, confinement of excess energy in a 2D lattice of metal squares is expected to be stronger than for 1D wires of comparable size, which might lead to stronger ballistic effects. We also expect that ballistic effects would appear at larger length scales in 2D than in 1D. We can observe this experimentally - comparing 1D and 2D thermal transport for large (350 nm) and small (80 nm) nanostructures, thermal decay in 2D is much slower than that in 1D on short timescales, corresponding to a stronger ballistic character and confinement for the 2D geometry. On longer timescales, where thermal dissipation into the substrate dominates the signal, thermal decay is identical for 1D and 2D, verifying that the sample substrate properties determine the heat flow kinetics. A three-dimensional thermal transport model is needed to treat heat migration from an array of 2D metallic squares into a bulk substrate, and a finite element simulation framework is under development to fully understand our results.

Nanoscale high-frequency acoustics: Surface acoustic waves (SAWs) are acoustic modes that propagate while confined within a very shallow penetration depth, enabling a broad range of applications in nondestructive material characterization and signal processing. With a penetration depth corresponding to a fraction of the acoustic wavelength, nanometer-scale wavelength SAWs are needed to precisely characterize the mechanical properties of nanostructured materials, multilayers and thin films used in nanoelectronics and nano-bit-patterned data storage devices.

Various approaches have been used for optical generation of SAWs, and most provide access to barely sub-micron acoustic wavelengths if visible light is used. To overcome this limitation, metallic nano-patterned gratings can be deposited onto a substrate surface and optically excited to create shorter wavelength SAWs. The wavelength of the SAW excited with nano-patterned structures is then only limited by the spatial period of the nano-pattern. The SAW response, as well as thermal responses, can be monitored by diffraction if ultrashort probe pulses with sufficiently short wavelengths, comparable to the nano-pattern periods, are available. High harmonic generation provides the EUV pulses that are needed.

In recent work, we showed that we can generate and probe the shortest wavelength surface acoustic waves to date, at 45 nm, with corresponding penetration depths of about 10 nm. This result is significant for nanoscale materials physics because it makes it possible to selectively probe the mechanical properties of very thin films and interfaces, as well as nanostructures deposited on, or embedded within, a surface

for the first time. We also characterized the acoustic dispersion of these nanostructures, which is strongly influenced by the varying penetration depth into the sample. Moreover, to understand and model acoustic dispersion in these 2D phononic crystals, finite element simulations are required, because simple approximations can no longer be used (as in the case for 1D phononic crystals). Finally, we used laser pulse sequences to control SAW generation in 1D nanostructures, to preferentially enhance higher-order SAWs while suppressing lower frequency waves. This allowed us to reduce the generated SAW wavelength, and consequently the SAW penetration depth, by a factor of two with respect to the spatial period set by the sub-optical phononic crystal. This has important implications for the ultimate physical limits that one can probe using photoacoustic metrology.

Optical measurements of GHz-THz acoustics and structural relaxation dynamics

Structural relaxation dynamics: A multiyear, collaborative experimental effort to measure elastic and loss moduli across an unprecedented 13-decade frequency range, from millihertz to hundreds of GHz, was recently concluded. The effort was designed to address the correspondingly wide range of structural relaxation time scales exhibited by viscoelastic materials, which even at a single temperature can show distinct multiexponential relaxation kinetics including relaxation components on disparate time scales. As temperature is varied the range of time scales becomes extraordinary, with lightly viscous behavior (picosecond relaxation dynamics) at high temperatures and glassy behavior at low temperatures. We measured longitudinal and transverse acoustic waves generated at thin absorbing layers (GHz frequencies) and in bulk transient grating measurements (MHz frequencies), while our collaborators conducted dynamic mechanical measurements in the kHz, Hz, and mHz ranges. This is by many decades the most comprehensive study of viscomechanical dynamics ever performed on a single material, and it required development of new measurement methodologies especially in the GHz range. (Among other challenges, 100-GHz acoustic waves only propagate for microns or less through viscous liquids before being fully attenuated.) The full analysis of the data has only recently been completed. Most notably, the results show good agreement with key predictions of mode-coupling theory, the only first-principles description of viscoelastic behavior. The theory is far from universally accepted, and this is the first direct test of some of its predictions. Only dielectric spectroscopy has provided data across comparably broad frequency ranges, and the coupling of structural relaxation to the molecular dipole orientational motion that dielectric spectroscopy measures introduces additional complications in understanding the results. Acoustic measurements directly access structural relaxation dynamics, manifest through compressional and shear fluctuations of local volume elements. The results will be published as a series of three invited papers (subject to review) in a special issue of the *Journal of Chemical Physics*. We are also preparing a short summary paper which will be submitted for letter publication.

High-frequency acoustic wave generation and detection: We have addressed the challenges of GHz and even THz acoustic wave generation and detection in several ways. Using a superlattice formed by a GaN/InGaN multiple quantum well structure (3 nm and 19 nm respective layer thicknesses), we generated bulk longitudinal acoustic waves with frequencies as high as 2.5 THz. The fundamental acoustic frequency corresponding to the superlattice period was 365 GHz, but because the interface quality was excellent, harmonic acoustic frequencies up to the seventh harmonic (with an acoustic wavelength of 3.1 nm) were observed. This is the highest photoacoustic frequency generated to date, to our knowledge.

The detection of high-frequency acoustic waves poses its own set of challenges. Optical detection at an interface can be carried out, but because the probe light has a finite penetration depth even at a metal surface, the measurement integrates over the acoustic response for several picoseconds as the acoustic wave approaches the interface, reflects, and moves back into the bulk. This generally reduces the detection bandwidth to a few hundred GHz. However, we showed that for a high-quality metal layer, even though signal extends over several picoseconds, there is an extremely sharp signal component just as the acoustic wave undergoes reflection. This component preserves THz bandwidth, enabling measurement of even the highest acoustic frequencies.

It is important to generate shear as well as compressional acoustic waves across the broad spectrum of frequencies, since transverse phonons also contribute to thermal transport and since structural relaxation involves both shear and compressional components. We provided a detailed description of GHz shear wave generation and detection and demonstrated good agreement between our experimental and theoretical results.

Finally, practical use of photoacoustic measurements has in many cases been limited to samples with excellent optical quality so that scattered light does not produce excessive noise. We showed that the use of a thin strontium ruthenate metallic layer for both acoustic wave generation and detection largely circumvents this problem. Detection is achieved by the combination of reflection of probe light at the metal layer and coherent scattering of probe light by the acoustic wave underneath the (only partially opaque) metal layer, producing two signal components whose time-dependent interference reveals damped acoustic oscillations despite the strong light scattering within the sample. The measurement was demonstrated on ordinary milk to illustrate its applicability to biological samples.

Future Plans

In addition to continuation of measurements using the methods that generated our recent results, we are planning to try TG measurements with EUV excitation as well as probe pulses. We expect this to be possible based on recent improvements in EUV pulse energy and focusing so that sufficient excitation pulse intensities can be reached at a sample surface. If successful this will enable measurements on samples without deposited structures. Effort is under way to formulate a plan for hard x-ray TG measurements at the LCLS. This will permit study of bulk non-diffusive thermal transport and extremely high-frequency bulk acoustic waves without the need for ultraflat interfaces for acoustic transduction between different materials. Finally, we plan to use recently generated strong THz pulses for direct piezoelectric interconversion to transverse and longitudinal acoustic waves in the GHz-THz frequency range in order to enable versatile tabletop study of bulk acoustic waves in this range.

References

1. Siemens et al., "High-frequency surface acoustic wave propagation in nanostructures characterized by coherent extreme ultraviolet beams," *Appl. Phys. Lett.* **94**, 093103 (2009).
2. M. Siemens et al., "Measurement of quasi-ballistic thermal transport from nanoscale interfaces using ultrafast coherent soft x-ray beams" *Nature Materials* **9**, 26 (2010).
3. D. Nardi et al., "Probing Thermomechanics at the Nanoscale: Impulsively Excited Pseudosurface Acoustic Waves in Hypersonic Phononic Crystals", *Nano Letters* **11**, 4126 (2011).
4. Q. Li et al., "Generation and Detection of Very Short-Wavelength 35nm Surface Acoustic Waves at Nano-interfaces", *Physical Review B* **85**, 195431 (2012).
5. Q. Li et al., "Photoacoustic characterization of ultrathin films using femtosecond coherent extreme-ultraviolet beams", *Proc. SPIE* 8324, doi:10.1117/12.916866 (2012).
6. Q. Li et al., "Ballistic thermal transport from 2D nano-interfaces", in preparation (2012).
7. D. Torchinsky et al., "Mechanical spectra of glass-forming liquids. I. Broadband longitudinal spectra of the silicone oil DC704; II. Gigahertz-frequency longitudinal and shear acoustic dynamics in glycerol and DC704 studied by time-domain Brillouin scattering; III. Low-frequency bulk and shear moduli of DC704 and 5-PPE measured by piezoceramic transducers," (I and II only acknowledge DOE support) invited for submission to *Journal of Chemical Physics*.
8. T. Hecksher et al., "Ultrabroadband mechanical spectroscopy of viscoelastic behavior," in preparation.
9. A.A. Maznev et al., "Broadband terahertz ultrasonic transducer based on a laser-driven piezoelectric semiconductor superlattice," *Ultrasonics* **52**, 1-4 (2012).
10. K.J. Manke et al., "Detection of shorter-than-skin-depth acoustic pulses in a metal film via transient reflectivity," submitted.
11. A.A. Maznev et al., "Coherent Brillouin spectroscopy in a strongly scattering liquid by picosecond ultrasonics," *Optics Letters* **36**, 2925-2927 (2011).

Antenna-Coupled Light-Matter Interactions

Lukas Novotny (novotny@optics.rochester.edu)

University of Rochester, The Institute of Optics, Rochester, NY, 14627.

1. Program Scope

In this project we investigate antenna-coupled light emission on the single quantum emitter level. We tailor the radiative properties of the quantum emitter by means of an optical antenna, - a device that converts localized energy to radiation, and *vice versa*.

2. Recent Progress

In the last project period we studied the optical properties of optical antennas made of self-similar colloidal nanoparticles [16]. The local field enhancement has been probed by single molecule fluorescence using fluorophores with high intrinsic quantum efficiency ($Q^o > 80\%$). Using a self-similar trimer antenna consisting of a 80nm, 40nm and 20nm gold nanoparticle, we demonstrated a fluorescence enhancement of 40 and a spatial confinement of 15 nm. Compared to a single gold nanoparticle, the self-similar trimer antenna improves the enhancement-confinement ratio by more than an order of magnitude.

In general, the smaller a nanoparticle is, the lower the fluorescence enhancement will be. This can be understood by considering the nanoparticle's quasi-static polarizability $\alpha(\omega)$. The energy radiated by the emitter is related to the scattering cross-section

$$\sigma_{\text{scatt}} = \frac{k^4}{6\pi\epsilon_0^2} |\alpha(\omega)|^2, \quad (1)$$

where $k = \sqrt{\epsilon_d}\omega/c$ is the wavevector of the surrounding medium. On the other hand, the energy dissipated by the nanoparticle is derived from the absorption cross-section

$$\sigma_{\text{abs}} = \frac{k}{\epsilon_0} \text{Im}[\alpha(\omega)]. \quad (2)$$

Because $\alpha \propto R^3$, R being the particle radius, the scattering cross-section scales with R^6 whereas the absorption cross-section depends on R^3 . Therefore, absorption dominates over scattering for small particles. Thus, a strong fluorescence enhancement requires a large nanoparticle size which, on the other hand, provides poor localization. Consequently, strong enhancement and high localization appear to be contradictory requirements. We have shown that we can significantly boost the enhancement-localization ratio by using self-similar antennas consisting of coupled gold nanoparticles of decreasing size. For a trimer antenna consisting of 80nm, 40nm and 20nm nanoparticles we achieved a fluorescence enhancement of more than $30\times$ and a localization of ~ 15 nm.

The cascaded field enhancement by a self-similar chain of nanoparticles has been first proposed by Stockman and co-workers (*Phys. Rev. Lett.* **91**, 227402, 2003). In this scheme, the radii of the particles in the chain scale as $R_{n+1} = \kappa R_n$ and the interparticle separations as $d_{n+1,n+2} = \kappa d_{n,n+1}$ with κ denoting a constant scaling factor and n the particle number. This geometry provides a multiplicative cascade effect: the largest particle enhances the incident field by a factor of f , the enhanced field then excites the next smaller particle which in turn enhances the field by another factor of f , and so on. This sequence leads

to a concentration of light at the smallest particle in the chain.

The experimental configuration is illustrated in Fig. 1(a). A radially polarized laser beam ($\lambda = 633 \text{ nm}$) is focused by means of a $\text{NA}=1.4$ objective on the surface of a quartz sample that supports randomly distributed Nile blue molecules ($Q^o > 80\%$) embedded in a $2 - 5 \text{ nm}$ PMMA layer. A self-similar nanoparticle antenna consisting of a chain of gold nanoparticles of decreasing size is supported by a pointed quartz pipette and positioned into the center of the laser focus. The longitudinal field in the focus of the radially polarized beam excites the antenna and the enhanced antenna field locally interacts with individual molecules on the sample surface. The antenna-sample separation can be controlled with Angstrom accuracy by means of a shear-force feedback loop. Fluorescence photons from single molecules are collected with the same objective and recorded with an avalanche photodiode while raster-scanning the sample underneath the optical antenna or varying the antenna-sample distance. Dimer and trimer antennas are fabricated by sequential bottom-up self-assembly. Briefly, gold nanoparticles are dispersed on a clean glass substrate. An amino-silane functionalized quartz tip is first used to map out the distribution of the gold particles on the substrate and is then centered over a selected particle. Upon mechanical contact between gold particle and the functionalized tip, the particle attaches to the tip and can be lifted off the surface. Using 1,6 hexane dithiol linker molecules, the attachment principle can be sequentially repeated to form dimers, trimers, tetramers, or higher multi-particle antennas. Fig. 1(b) depicts a scanning electron micrograph of a typical self-similar trimer antenna fabricated following the procedure described above.

Using an $80 - 40 - 20 \text{ nm}$ gold nanoparticle trimer antenna, we have performed single molecule fluorescence experiments. A fluorescence map of the single molecule sample is shown in Fig. 2(a). Line-cuts through individual fluorescence spots yield a resolution of 15 nm , as seen in Fig. 2(b). This resolution is expected on the basis of the smallest particle size. In general, we observe that the resolution (signal confinement) is slightly better than the true particle size. An 80 nm particle yields a resolution of $\sim 60 \text{ nm}$, a 40 nm particle a resolution of 25 nm , and a 20 nm particle a resolution of 15 nm . Resolution is better than the particle size because of the curvature of the particle surface and the particular field distribution. To

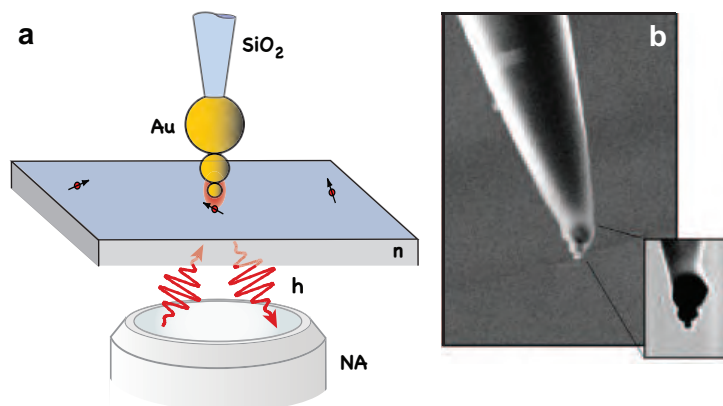


Figure 1: (a) A self-similar optical antenna made of discrete colloidal gold nanoparticles of decreasing size is placed next to a sample with randomly distributed Nile blue molecules. The antenna is irradiated by a tightly focused radially-polarized laser beam with wavelength $\lambda_{\text{exc}} = 633 \text{ nm}$. Fluorescence photons are recorded while the sample is raster scanned at a distance of $\sim 5 \text{ nm}$ underneath the antenna. (b) SEM image of a colloidal trimer antenna.

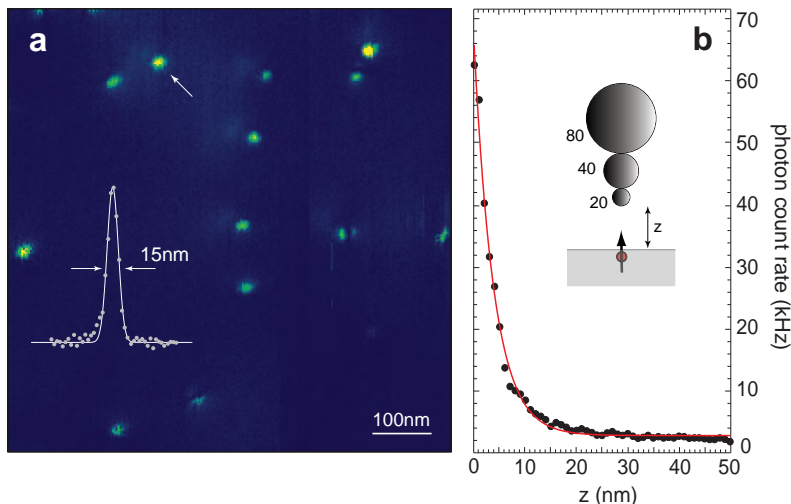


Figure 2: (a) Fluorescence image of the single molecule sample. Inset: Line-cut through the single fluorescence spot marked by the arrow. (b) Fluorescence from a single z -oriented molecule recorded as a function of distance from a trimer antenna. The steep rise of fluorescence counts for separations smaller than 15 nm is due to strong field localization along the z -axis at the apex of the trimer antenna.

demonstrate the strong localization of fields along the z -direction at the apex of the trimer, we recorded a fluorescence approach curve as shown in Fig. 2(c). The sharp increase in signal over the last 15 nm conclusively proves that the localization arises due to the foremost 20 nm diameter particle.

The maximum fluorescence enhancement for the trimer antenna is ~ 40 . Note, however, that the measured fluorescence not only depends on the local field enhancement but also on the quantum yield. Thus, single molecule fluorescence measurements provide a very conservative estimate of the local field enhancement. Compared to a single 80 nm nanoparticle, the trimer antenna improves the enhancement-localization ratio by a factor of 15, and compared to a 20 nm nanoparticle the improvement is almost a factor of 30. Finally, it should be noted that the highest enhancements are seen for vertically oriented molecules, while in-plane oriented molecules yield a factor ~ 3 lower fluorescence enhancement.

3. Future Plans

In the next project period we are particularly interested in exploring the possibility of antenna-coupled electro-optical transduction. To this end, we will combine the self-similar antenna geometry with electron tunneling experiments, similar to our previous work [9].

4. Anticipated Unexpended Funds

None.

5. Number of Students and Postdocs Supported

This grant currently supports one graduate student (Steve Person) and one postdoctoral associate (Hayk Harutyunyan).

6. DOE sponsored publications 2009-2012

- [1] S. Palomba, M. Danckwerts, and L. Novotny, "Nonlinear Plasmonics with Gold Nanoparticle Antennas," *J. Opt. A: Pure and Appl. Opt.* **11**, 114030 (2009).
- [2] P. Bharadwaj, B. Deutsch, and L. Novotny, "Optical antennas," *Adv. Opt. Phot.* **1**, 438 – 483 (2009).
- [3] J. Renger, R. Quidant, N. V. Hulst, S. Palomba, and L. Novotny, "Free-space excitation of propagating surface plasmon polaritons by nonlinear four-wave mixing," *Phys. Rev. Lett.* **103**, 266802 (2009).
- [4] L. Novotny, "Optical antennas: A new technology that can enhance light-matter interactions," *The Bridge* **39**, 14–20 (2009).
- [5] L. Novotny, "Strong coupling, energy splitting, and level crossings: A classical perspective," *Am. J. Phys.* **78**, 1199-1202 (2010).
- [6] P. Bharadwaj and L. Novotny, "Plasmon enhanced photoemission from a single $Y_3N@C_{80}$ fullerene," *J. Phys. Chem. C* **114**, 7444–7447 (2010).
- [7] L. Novotny and N. F. van Hulst, "Antennas for light," *Nature Phot.* **5**, 83-90 (2011).
- [8] J. Renger, R. Quidant and L. Novotny, "Enhanced nonlinear response from metal surfaces," *Opt. Exp.* **19**, 1777-1785 (2011).
- [9] P. Bharadwaj, A. Bouhelier and L. Novotny, "Electrical excitation of surface plasmons," *Phys. Rev. Lett.* **106**, 226802 (2011).
- [10] S. Palomba, H. Harutyunyan, J. Renger, R. Quidant, N. F. van Hulst and L. Novotny, "Nonlinear plasmonics at planar metal surfaces," *Phil. Trans. R. Soc. A* **369**, 3497-3509 (2011).
- [11] P. Bharadwaj and L. Novotny, "Robustness of quantum dot power-law blinking," *Nano. Lett.* **11**, 2137-2141 (2011).
- [12] L. Novotny, "From near-field optics to optical antennas," *Physics Today*, p.47-52, July (2011).
- [13] H. Harutyunyan, G. Volpe and L. Novotny, "Nonlinear optical antennas," in *Optical Antennas* (M. Agio and A. Alu, eds.), Cambridge University Press, in print (2012).
- [14] H. Harutyunyan, G. Volpe, R. Quidant and L. Novotny, "Enhancing the nonlinear optical response using multifrequency-resonant gold-nanowire antennas," *Phys. Rev. Lett.* **108**, 217403 (2012).
- [15] D. A. Bonnell, D. N. Basov, M. Bode, U. Diebold, S. V. Kalinin, V. Madhavan, L. Novotny, M. Salmeron, U. D. Schwarz, and P. S. Weiss, "Imaging physical phenomena with local probes: From electrons to photons," *Rev. Mod. Phys.*, in print (2012).
- [16] C. Höppener, P. Bharadwaj and L. Novotny, "Self-similar gold-nanoparticle antennas for a cascaded enhancement of the optical field," *Phys. Rev. Lett.* **109**, 017402 (2012).
- [17] D. Lopez-Mago and L. Novotny, "Coherence measurements with the two-photon Michelson interferometer," *Phys. Rev. A* **86**, 023820 (2012).
- [18] D. Lopez-Mago and L. Novotny, "Quantum-optical coherence tomography with collinear entangled photons," *Opt. Lett.*, in print (2012).

Electron and Photon Excitation and Dissociation of Molecules

A. E. Orel
Department of Chemical Engineering and Materials Science
University of California, Davis
Davis, CA 95616
aeorel@ucdavis.edu

Program Scope

This program will study how energy is interchanged in electron and photon collisions with molecules leading to excitation and dissociation. Modern *ab initio* techniques, both for the photoionization and electron scattering, and the subsequent nuclear dynamics studies, are used to accurately treat these problems. This work addresses vibrational excitation and dissociative attachment following electron impact, and the dynamics following inner shell photoionization. These problems are ones for which a full multi-dimensional treatment of the nuclear dynamics is essential and where non-adiabatic effects are expected to be important.

Recent Progress

Dissociative Electron Attachment

Momentum imaging experiments on dissociative electron attachment (DEA) to CO₂ were carried out by the experimental AMO group at LBL, using the COLTRIMS method. These results yielded information about partial cross sections into various vibrational states of the final fragments as well as the angular distributions of the fragments. We carried out *ab initio* calculations which combined with the results of momentum imaging spectroscopy clearly showed that the 8.2 eV DEA peak in CO₂ is initiated by electron attachment to a dissociative, doubly excited ²Π state that interacts with a lower ²Π shape resonance through a conical intersection and dissociates to electronic ground-state products. The work resolved a number of several puzzling misconceptions about this system. These results were published in Journal of Physics B (Publication #8). Future calculations will attempt to map out the conical intersection(s). This is complicated since bending breaks the degeneracy of the ²Π states, resulting in a pair of A' and A'' states with different topologies. This topology, and the role it plays in understanding DEA through the 4 eV shape resonance, will be the subject of future calculations.

Formation of autoionizing O* following soft x-ray induced O₂ dissociation

We studied the autoionizing states of O* following soft x-ray induced O₂ dissociation. The experiments used an ultrashort pump beam with a photon energy of 41.6 eV to ionize O₂. For small internuclear separations, autoionization could not occur. At larger separations, >30 au, autoionization occurred. A COLTRIMS apparatus was used to determine the momentum of all charged particles. In order to support the interpretation of the measured data and better characterize the principal autoionizing excited state(s) of the cation involved, we carried out configuration-interaction (CI) calculations on the electronic states of O₂⁺ to identifying inner-valence excited states that can be produced from ground-state (³Σ_g⁻) O₂. States in the energy range of interest (about 39 eV in the Franck-Condon region) involve a 2σ_g vacancy. The calculations show two such states, of symmetry ⁴Σ_g⁻ and ²Δ_g that lie just above the ground-state of the dication in the Franck-Condon with the higher energy state most likely providing the dominant indirect ionization route observed in the COLTRIMS spectra. (Publication #9)

Isomerization of HCCH: Snapshots of a chemical reaction

The Moshhammer group at Heidelberg has begun studies of the dissociative photoionization of HCCH. These are two photon experiments. The first photon ionizes HCCH (below the double ionization limit), and then at a later variable time a second photon ionizes the HCCH⁺. The experiment focused on the (C⁺,CH₂⁺) channel. In order

to reach this channel, the ion must isomerize, with one hydrogen moving into a vinaldyne-type configuration before dissociation. The plan for the experiment is to 'catch' this process by the time-delay for the second photon. We performed calculations on the ion states computing the minimum energy path for the isomerization. We then computed molecular frame photoangular distributions (MFPADs) along this path. We considered both k-shell photoionization (to be published in a special edition of Journal of Physics B, Publication #13) and valence-shell photoionization (published in Physical Review A, Publication #12). We found that the k-shell MFPADs were sensitive to geometry, but insensitive to the electronic state of the target, while the valence-shell MFPADs were sensitive to both.

Future Plans

O 1s ionization in CO₂

Previously we explained a small but measurable asymmetry observed in the measured MFPADs of C 1s in CO₂ photoionization. We plan to return to this system to study O 1s ionization in CO₂. Since after photoionization of one O 1s electron, it would be expected that asymmetric vibrational motion could localize the O k-shell hole, it is plausible that there would exist left/right asymmetry in the MFPAD measured relative to CO⁺ + O⁺ axis. However, this does not seem to exist in the measurements. This may be due to the timescale required for hole localization and the transient nuclear dynamics that takes place between photoionization and Auger decay. We plan carry out calculations, including these dynamics to see if this is indeed the case.

Isomerization of C₂H₄: Snapshots of a chemical reaction continued

Although the results on the MFPADs for the isomerization of acetylene were interesting, experiments on this system may be very difficult to perform. The experiment for this molecule requires two photoionization events; one to first ionize the neutral acetylene in its excited state and another to actually photoionize the monocation. Therefore, they would exist a background noise from the first ionization process affecting the detection of the second photoionization event. In addition, the MFPADs in the vinylidene configuration vary rapidly with photon energy and do not image the molecule. We therefore plan to carry out calculations on C₂H₄, a system which is currently being studied at LBL by the AMO experimental group. For this system, the first step is to an excited state of the neutral. The probe pulse then ionizes this state. We plan to compute molecular frame photoangular distributions (MFPADs) along the isomerization path. Our first calculations will be k-shell photoionization. Our preliminary results indicate that the MFPADs image the molecule. However, we will also consider photoionization from the 2s shell, since this is more accessible for the experiment. The goal is to produce snapshots of the path to products.

Dissociative Electron Attachment

We plan to continue our calculations on the states involved in the dissociative electron attachment of CO₂. In addition we plan to begin studies on formic acid. Considerable attention has been given to the lowest π^* negative ion shape resonance. Virtually nothing is known about the observed higher energy resonances between 7 and 9 eV, which evidently lead to production of O⁻ and OH⁻. At this point it is unclear whether doubly-excited Feshbach resonances or possibly a quasi-bound dipole σ^* state is involved in the DEA dynamics. We plan to study this system in conjunction with planned experimental COLTRIMS studies at Lawrence Berkeley Laboratory. Other systems of interest include methanol and ethanol, which both undergo DEA via Feshbach resonances analogous to water, but evidently show some strikingly different dissociation dynamics which is not presently understood.

Publications

1. Formation of inner-shell autoionizing CO⁺ states below the CO²⁺ threshold (with T. Osipov, Th. Weber, T. N. Rescigno, S. Y. Lee, M. SchŽffler, F. P. Sturm, S. SchŽssler, U. Lenz, T. Havermeier, M. KŠhnel, T. Jahnke, J. B. Williams, D. Ray, A. Landers, R. Dorner, and A. Belkacem) Phys. Rev. A **81** 011402 (2010).

2. Isotope effect in dissociative electron attachment to HCN (with S. T. Chourou) *Phys. Rev. A* **83** 032709 (2011)
3. Dissociative Electron Attachment to HCN, HCCH and HCCCN (with S. T. Chourou) *J. Phys.: Conf. Ser.* **300** 012014 (2011)
4. Electron diffraction self-imaging of molecular fragmentation in two-step double ionization of water (with H. Sann, T. Jahnke, T. Havermeier, K. Kreidi, C. Stuck, M. Meckel, M. Schöffler, N. Neumann, R. Wallauer, S. Voss, A. Czasch, O. Jagutzki, Th. Weber, H. Schmidt-Böcking, S. Miyabe, T. Rescigno and R. Dörner) *Phys. Rev. Lett.* **106** 133001 (2011).
5. Vibrational Feshbach resonances in near threshold HOCO^- photodetachment; a theoretical study (with S. Miyabe, D. J. Haxton, K. V. Lawler, C. W. McCurdy and T. N. Rescigno, *Phys. Rev. A* **83** 043401 (2011).
6. Dissociative Electron Attachment to HCN, HCCH and HCCCN (with S. T. Chourou) *J. Phys.: Conf. Ser.* **300** 012004 (2011).
7. The role of Jahn-Teller couplings in the DR of H_3O^+ and H_3^+ ions (with N. Douguet, I. Mikhailov, I. Schneider, C. H. Greene and V. Kokoouline) *J. Phys.: Conf. Ser.* **300** 012015 (2011).
8. Dissociative electron attachment to carbon dioxide via the 8.2 eV Feshbach resonance D. S. Slaughter, H. Adaniya, T. N. Rescigno, D. J. Haxton, A. E. Orel, C. W. McCurdy and A. Belkacem *J. Phys. B: At. Mol. Opt. Phys.* **44** 205203 (2011)
9. Dynamic modification of the fragmentation of autoionizing states of O_2^+ W. Cao, G. Laurent, S. De, M. Schöffler, T. Jahnke, A. Alnaser, I. A. Bocharova, C. Stuck, D. Ray, M. F. Kling, I. Ben-Itzhak, Th. Weber, A. Landers, A. Belkacem, R. Dörner, A. E. Orel, T. N. Rescigno, and C. L. Cocke *Phys. Rev. A* **84** 053406 (2011)
10. Dissociative Recombination of Highly Symmetric Polyatomic Ions, Nicolas Douguet, Ann E. Orel, Chris H. Greene, and Viatcheslav Kokoouline *Phys. Rev. Lett.* **108** 023202 (2012)
11. Breaking a tetrahedral molecular ion with electrons: study of NH_4^+ , N. Douguet, V. Kokoouline and A. E. Orel, *J. Phys. B: At. Mol. Opt. Phys.* **45** 051001 (2012)
12. Time-resolved molecular-frame photoelectron angular distributions: Snapshots of acetylene-vinylidene cationic isomerization N. Douguet, T. N. Rescigno, and A. E. Orel *Phys. Rev. A* **86**, 013425 (2012)
13. Imaging Molecular Isomerization Using Molecular-Frame Photoelectron Angular Distributions, T. N. Rescigno, Nicolas Douguet and A. E. Orel, *J. Phys. B: At. Mol. Opt. Phys.* **XX** XXXX (2012)
14. Resonant enhanced electron impact dissociation of molecules, D. S. Slaughter, H. Adaniya, T. N. Rescigno, D. J. Haxton, C. W. McCurdy, A. Belkacem, Å. Larson and A. E. Orel, *J. Phys.: Conf. Ser.* **XX** XXXXXX (2012).

“Low-Energy Electron Interactions with Liquid Interfaces and Biological Targets”

Thomas M. Orlando

School of Chemistry and Biochemistry and School of Physics,

Georgia Institute of Technology, Atlanta, GA 30332-0400

Thomas.Orlando@chemistry.gatech.edu, Phone: (404) 894-4012, FAX: (404) 894-7452

Project Scope: The primary objectives of this program are to investigate the fundamental physics and chemistry involved in low-energy (1-250 eV) electron and (25-200 eV) x-ray interactions with complex targets. There is a particular emphasis on understanding correlated electron interactions and energy exchange in the deep valence and shallow core regions of the collision targets. The energy loss channels associated with these types of excitations involve ionization/hole exchange and negative ion resonances. Thus, the energy decay pathways are extremely sensitive to many body interactions and changes in local potentials. Our proposed investigations should help determine the roles of hole exchange via interatomic and intermolecular Coulomb decay and energy exchange via localized shape and Feshbach resonances in the non-thermal damage of biological interfaces. The targets we will examine range in complexity from defined molecular thin films of biologically relevant biomolecules (nucleotides, amino acids, DNA and RNA), aqueous solution interfaces and epitaxial graphene.

Recent Progress:

Project 1. Low-energy electron induced damage of DNA. Low-energy electron

scattering was used as a tool to induce damage to double stranded (DS) DNA and single stranded (SS) DNA films. The films are deposited either on a gold evaporated Si-substrate or on a Chemical Vapor Deposition grown graphene monolayer supported by a gold evaporated Si-substrate. The DNA film damage was analyzed using Raman scattering

micro-spectroscopy. The Raman spectra reveal significant damage at very low-

energies with most single strand breaks (SSBs) occurring below 1eV. Double strain

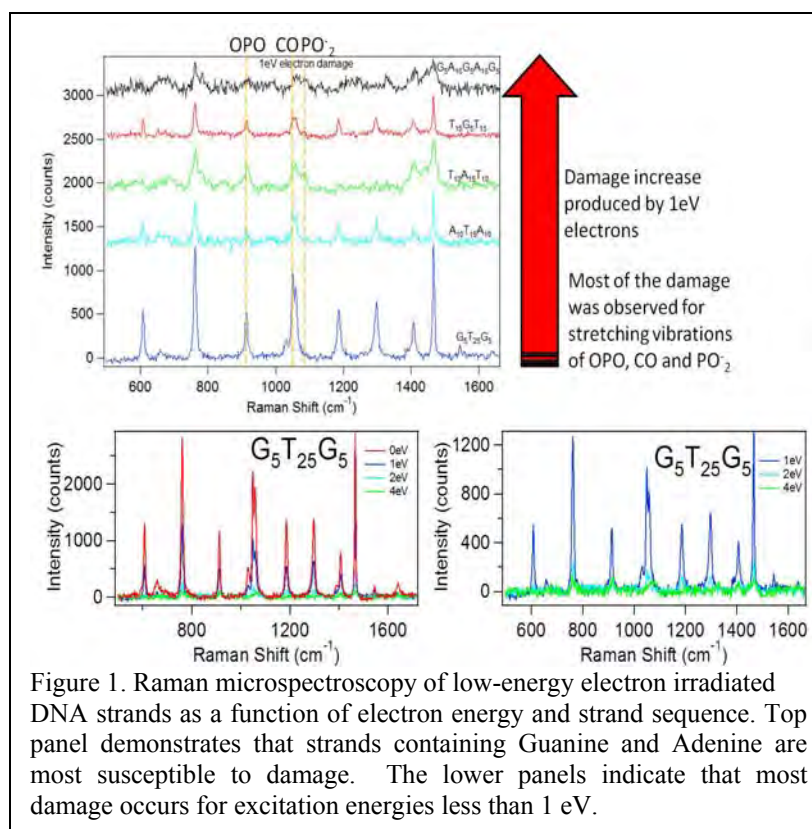
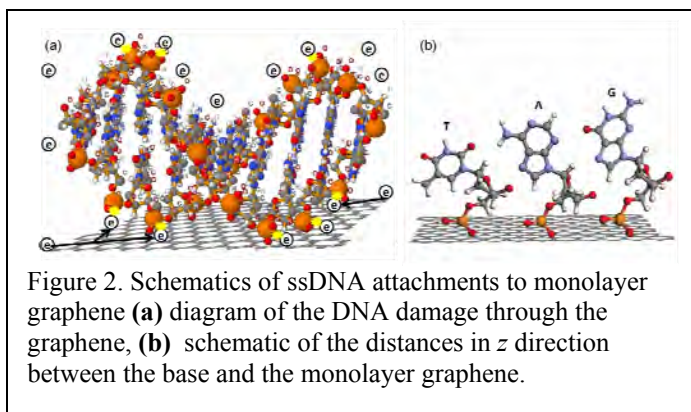


Figure 1. Raman microspectroscopy of low-energy electron irradiated DNA strands as a function of electron energy and strand sequence. Top panel demonstrates that strands containing Guanine and Adenine are most susceptible to damage. The lower panels indicate that most damage occurs for excitation energies less than 1 eV.

breaks (DSBs) do not occur until above 5eV. A new platform such as graphene was used for the enhancement of the DNA signature Raman peaks. This approach has a better signal/noise ratio which allows more accurate molecule specific assessment of the damage. The present results indicate that the damage involves low-lying π^* shape resonances and compound Feshbach resonances initially located on the bases. The electrons can then occupy σ^* sugar-phosphate states and damage occurs primarily via breakage of the C-O-P bonds.

DNA monolayers on gold substrates were also studied using X-ray photoelectron spectroscopy (XPS) and X-ray absorption spectroscopy (XAS) at the University of Wisconsin's Synchrotron Radiation Center light source. The degree of order in the DNA monolayers was controlled by attachment of thiol



groups to the DNA chains, which bind the DNA to the Au substrate. This approach has been shown to form self-assembled monolayers. XPS and XAS experiments probed electron core levels and valence band structure as a function of incident photon energy, fluence, and degree of sample organization. Dose dependent changes were observed in both the core and valence level structure due to reactions induced by secondary electrons produced by the x-rays. Polarization studies also indicate some direct processes.

Project 2. Intermolecular Coulomb decay (ICD) and Coulomb explosions at heterogeneous interfaces. We have begun studying ICD between water clusters adsorbed on simple organic multilayer ices. Specially, we have extended our initial work on graphite containing rare gases and adsorbed water ice clusters to multilayers of ethane with adsorbed water ice clusters. The density of states of the underlying ethane indicates that ICD should be possible. We have also completed studies regarding Coulomb interactions at/on interfaces of aqueous solutions containing either NaCl, NaOH, HCl, or MgCl₂, CaCl₂, SrCl₂, and BaCl₂ using the liquid beam apparatus at Pacific Northwest National Laboratory. Laser excitation at 193 nm produced and removed H₃O⁺, Na⁺, H⁺(H₂O)_n and Na⁺(H₂O)_m from liquid jet surfaces containing either NaCl or NaOH. The bare H₃O⁺ and Na⁺ are the dominant ions and must come directly from the surface. The removal of bare-ions likely results from a localized strong-field emission process initiated by laser-induced photoionization and the formation of a charged sheet at the liquid interface. The H₃O⁺ and protonated water cluster yields dropped with increasing salt concentration, while the Na⁺ and solvated Na⁺ cluster yields increased with concentration. This allows these Coulomb explosion events to serve as very local probes of interfacial ion densities. In the case of multiply charged ions, there is no observable release/desorption of any doubly charged ions. Our initial results are very intriguing since they imply that the singly charged ions may populate the interface. There is no indication of the presence of either Mg²⁺ or Ca²⁺ at the interface. Instead, they undergo a laser-induced charge transfer process that leads to the formation of solvated MgOH⁺ and CaOH⁺.

Project 3. Attosecond angle resolved photoemission studies of epitaxial graphene

We have begun collaborating with H. Kapteyn and M. Murnane and have carried out static and time-resolved angle-resolved resonant photoemission measurements from epitaxial graphene. Our initial experiments have examined few layer graphene grown epitaxially on both the C and Si terminated faces of SiC(0001).

Future Work

- The program will continue to focus on ICD of mixed interfaces containing water and molecules representative of DNA backbones (i.e. sugars, phosphates and nucleosides).
- We will continue to examine low-energy electron induced damage of DNA by examining the sequence dependence of the break probability as well as DNA co-adsorbed with simple amino acids to address the role of protection by proteins. In the near term we are investigating the direct interaction of water with adsorbed phosphates and phosphate containing adenosine monophosphate (AMP).
- We will probe the electronic structure and correlated electron interactions on surfaces by continuing the initial time-resolved ARPES measurements on graphene and adsorbate covered graphene surfaces.

Presentations acknowledging support from this program during 2010-2012

1. T. M. Orlando, "The roles of resonances and diffraction in the electron-beam induced damage of DNA", International Physics Workshop on Dynamical Processes in Irradiated Systems, San Sebastian, Spain, July 26-28, 2010.
2. T. M. Orlando, "Low-energy electron interactions with hydrated DNA and complex biological targets. 240th ACS National Meeting, Boston, MA, United States, August 22-26, 2010.
3. T. M. Orlando, "The roles of resonances and diffraction in the electron-beam induced damage of DNA", International Conference on Ionizing Radiation of Polymers, Univ. of Maryland, Oct. 27-29, 2010.
4. T. M. Orlando, "Photoionization studies of aqueous salt solution interfaces", PacifiChem., Honolulu, HI, Dec. 15-20, 2010.
5. T. M. Orlando, "The role of resonances and low energy electrons in the damage of DNA", Texas Tech., Lubbock, TX, April 20, 2011.
6. T. M. Orlando, "The interaction of low-energy electrons with complex biological targets", Gordon Research Conference on Photoions, Photoionization and Photodetachment, Galveston, TX, Feb. 12-17, 2012.
7. T. M. Orlando, "Stimulated desorption and dynamics at weakly coupled heterogeneous interfaces", International Workshop on Desorption Induced by Electronic Transitions XIII, Stratford-upon Avon, UK, July 2-6, 2012.
8. T. M. Orlando, "Very low-energy electron-induced damage of DNA", University of Rome, LaSapienza, July 10, 2012.

Publications acknowledging support from this program during 2010-2012

1. D. Oh, M. T. Sieger, and T. M. Orlando, "The Theoretical Description and Experimental Demonstration of Diffraction in Electron-stimulated Desorption", *J. of Physics: Condensed Matter*, **22**, 084001 (2010). IOP - Special Recognition Paper

2. G. A. Grieves, J. L. McLain, and T. M. Orlando, “Low-energy Stimulated Reactions in Nanoscale Water Films and Water:DNA interfaces”, Chapter 18, *Charge Particle Interactions with Matter: Recent Advances, Applications and Interfaces*, Taylor, Francis Publishing Co. (2010).
3. B. Olanrewaju, J. Herring-Captain, G. A. Grieves, A. Aleksandrov and T. M. Orlando, “Probing the interaction of Hydrogen Chloride with low-temperature water ice surfaces using thermal and electron-stimulated desorption”, *J. Phys. Chem. A*.dx.doi.org/10.1021/jp110332v (2011).
4. B. Olanrewaju, Ph.D. Thesis, (2011). “Non-thermal processes on ice and liquid microjet surfaces”. Dec. (2011).
5. G. A. Greives and T. M. Orlando, “Intermolecular Coulomb decay at weakly coupled heterogeneous interfaces”, *Phys. Rev. Lett.* 107, 016104 (2011).
6. A. Sidorov and T. M. Orlando, “Sequence specific low-energy electron induced damage of DNA on CVD graphene”, to be submitted to *Phys. Rev. Lett.* in prep. (2012).
7. J. Symonds, R. Rosenberg, R. Naman, and T. M. Orlando, “X-ray induced damaged of DNA films: direct vs. indirect effects”, to be submitted to *Phys. Rev. B.* in prep (2012).

Structure from Fleeting Illumination of Faint Spinning Objects in Flight

Abbas Ourmazd, Russell Fung, and Peter Schwander

Dept. of Physics, University of Wisconsin Milwaukee
1900 E. Kenwood Blvd, Milwaukee, WI 53211
ourmazd@uwm.edu

It is now possible to interrogate molecules and their assemblies “in flight” with intense short pulses of radiation, and record “snapshots” before they are destroyed. We are developing a new generation of powerful algorithms to recover structure *and dynamics* from such ultra-low-signal random sightings. Combining concepts from differential geometry, general relativity, graph theory, and diffraction physics, these techniques promise to revolutionize our understanding of key processes in biological machines, such as enzymes, and ultrafast breaking of bonds in molecules. We report progress in three areas.

1. Spectroscopic movies of bond-breaking in N₂ with 5 femtosecond time resolution in presence of 300fs jitter (with Phillip Bucksbaum et al.)

Time-of-flight (ToF) spectra from pump-probe experiments using femtosecond IR-optical and X-ray pulses from the LCLS X-ray Free Electron Laser were analyzed to investigate the detailed processes underlying the Coulomb explosion of N₂ (Fig. 1). The temporal resolution of these experiments is limited by pump-probe timing jitter, measured to be ~300fs FWHM (1). We have succeeded in revealing the dissociation channels, and determining the dynamics of the Coulomb explosion with 5fs time resolution.

The analysis proceeds as follows. First, we use graph-theoretic manifold-embedding techniques to determine the degrees of freedom open to the system. The resulting manifold is a five-legged spider, with each leg displaying a characteristic time-of-flight (ToF) spectrum (Fig. 2). In order to determine the *dynamics*, i.e., the specific trajectory traversed by the molecule on the manifold during Coulomb explosion, we combine time-lagged embedding (2) with nonlinear singular value decomposition on the manifold (3). The resulting spectra reveal the characteristic (singular) modes of the ToF spectra, and the dynamics followed by each mode. Fig. 3 shows three modes and their time evolution at 5fs resolution.

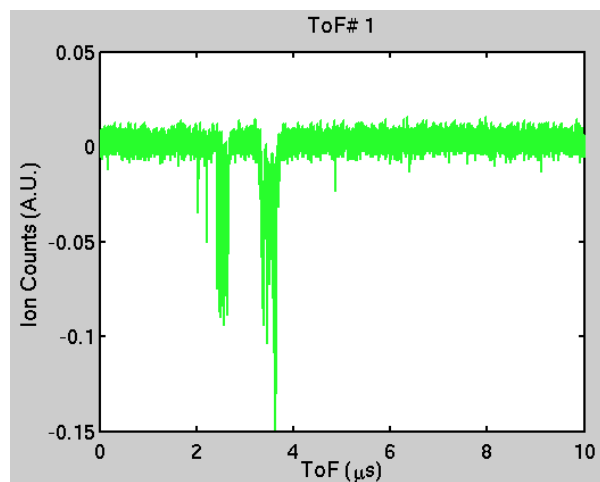


Fig. 1. Typical time-of-flight spectrum obtained from the Coulomb explosion of ~30 nitrogen molecules.

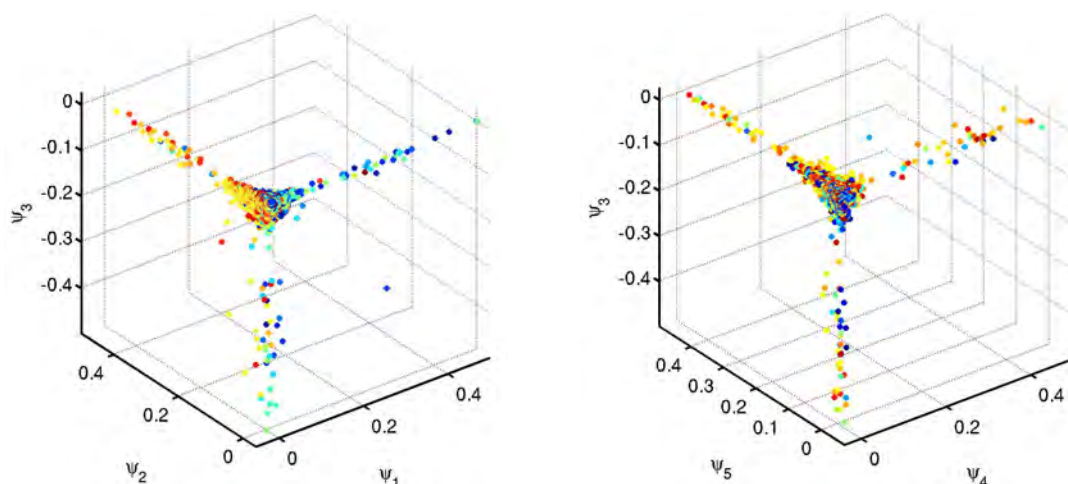


Fig. 2. The five-dimensional manifold defined by the ToF spectra resembles a five-legged spider. Each leg corresponds to a distinct ToF spectrum. This manifold reveals the degrees of freedom open to the system.

Left: Dimensions 1, 2, 3; **Right:** Dimension 3, 4, 5.

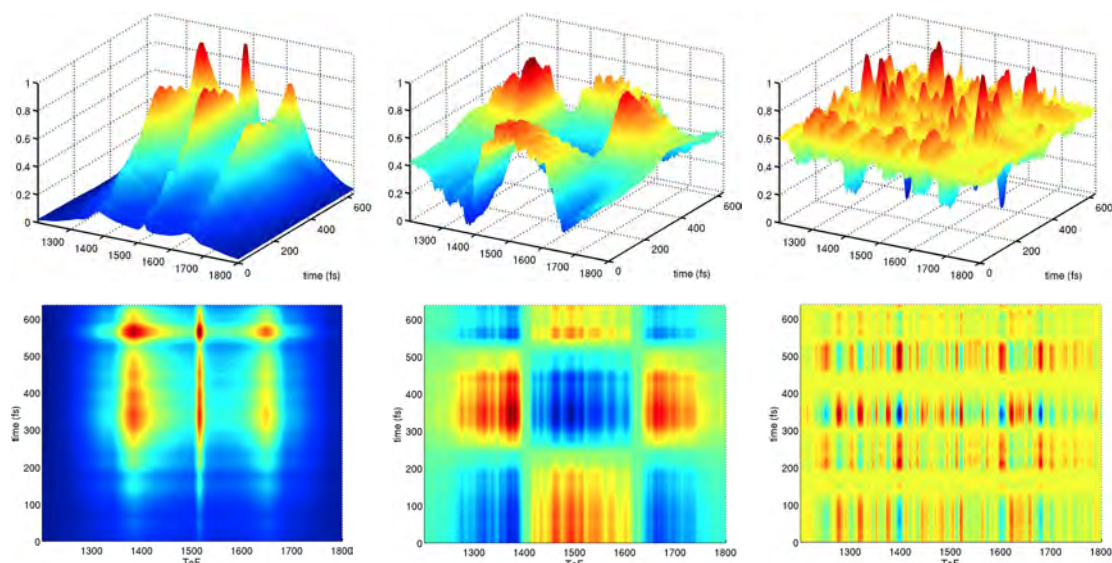


Fig. 3. Time evolution of ToF spectra during the Coulomb explosion of N_2 with 5fs time resolution in the presence of 300fs of pump-probe timing jitter, as revealed by nonlinear Singular Value Decomposition on the manifold of Fig. 2.

Top row: 3D plots (pump-probe delay into the plane of the paper).

Bottom Row: Bird's-eye views (x-axis: time of flight, y-axis: time).

Left: SVD Mode 1; **Center:** SVD Mode 2; **Right:** SVD Mode 4.

In essence Fig. 3 shows spectral movies of the dissociation modes of the exploding molecule at timescales 25 times shorter than the pump-probe timing jitter. As jitter has represented a fundamental limit for pump-probe experiments, particularly impacting the

capability of SASE X-ray Free Electron Lasers for time-resolved work, we believe our approach may have a transformative impact on the study of ultrafast phenomena.

2. Computationally efficient 3D structure recovery from XFEL snapshots (with Ali Dashti et al.)

Extending our demonstration of a computationally efficient approach able to recover structure and conformations at computational complexities 10^4 x higher than previously possible, we have now developed the capability to reconstruct objects from up to 20 million snapshots. This capability is required to map the complex conformational spectrum of biologically flexible systems, such as enzymes, which play a key role in catalysis and energy conversion.

3. Highly accurate unsupervised sorting of conformations of molecular machines (with Joachim Frank et al.)

The ribosome is a key biological molecular machine, the unraveling of whose function has garnered several Nobel prizes. A primary factor limiting our current understanding is extraction of structural information from mixed collections of snapshots showing the molecule in a variety of unknown projections in different stages of its cycle.

To obtain high-resolution structural information on each molecular conformation, highly accurate sorting of such datasets is required at signal-to-noise ratios as low as $6 \cdot 10^{-2}$. We have now succeeded in sorting simulated cryo-EM datasets with 99.96% accuracy, compared with the previously best achieved value of 86%.

Publications from DoE sponsored research

1. C.H. Yoon et al., Unsupervised classification of single-particle X-ray diffraction snapshots by spectral clustering, *Optics Express* **17**, 16542 (2011).
2. D. Giannakis, P. Schwander, and A. Ourmazd, Symmetries of image formation: I. Theoretical framework, *Optics Express* **20**, 12799 (2012).
3. P. Schwander, D. Giannakis, C.H. Yoon, and A. Ourmazd, Symmetries of image formation: II. Applications, *Optics Express* **20**, 12827 (2012).
4. J.M. Glowonia, A. Ourmazd, R. Fung, J. Cryan, A. Natan, R. Coffee, and P.H. Bucksbaum, CLEO Technical Digest, QW1F.3 (2012).

References

1. J. M. Glowonia *et al.*, *Optics Express* **18**, 17620 (Aug 16, 2010).
2. T. Sauer, J. A. Yorke, M. Casdagli, *Journal of Statistical Physics* **65**, 579 (1991).
3. D. Giannakis, A. J. Majda, *PNAS* **109**, (2011).

Energetic Photon and Electron Interactions with Positive Ions

Ronald A. Phaneuf,
Department of Physics
University of Nevada
Reno NV 89557-0220
phaneuf@unr.edu

Program Scope

This experimental program investigates photon and electron initiated processes leading to ionization of positively charged atomic ions, as well as to ionization and fragmentation of molecular ions. The objective is a quantitative understanding of ionization mechanisms, interference effects and of the collective dynamic response of bound electrons in atomic and molecular ions to incident EUV photons and electrons. Monoenergetic beams of photons and electrons are merged or crossed with mass/charge analyzed ion beams to probe their internal electronic structure and the dynamics of their interaction. The primary emphases have been on processes in which the behavior of bound electrons is highly correlated and on associated interference phenomena. These are manifested by giant dipole resonances in the ionization of atomic ions and also of fullerene molecular ions, whose quasi-spherical empty cage structures characterize them as structural intermediates between free molecules and solids. A recent emphasis has been on endohedral fullerenes, in which a noble gas atom trapped inside the fullerene ion cage is photoionized, leading to what have been termed confinement resonances. In addition to precision spectroscopic data for understanding their internal electronic structure, high-resolution measurements of absolute cross sections for photoionization and electron-impact ionization of ions provide critical benchmarks for testing theoretical approximations such as those used to generate photon opacity databases. Their accuracy is critical to modeling and diagnostics of astrophysical, fusion-energy and laboratory plasmas. Of particular relevance to DOE are those produced by the Z pulsed-power facility at Sandia National Laboratories, currently the world's most efficient high-intensity x-ray source, and the National Ignition Facility at Lawrence Livermore National Laboratory, the world's most powerful laser. Both facilities are dedicated to high-energy-density science as well as to the longer-term goal of harnessing thermonuclear fusion as a practical energy source.

Recent Progress

The major research emphasis has been the application of an ion-photon-beam (IPB) research endstation to experimental studies of photoionization of singly and multiply charged positive ions using monochromatized synchrotron radiation at the Advanced Light Source (ALS). Measurements using the IPB endstation on ALS beamline 10.0.1.2 define the state of the art in energy resolution and sensitivity for studies of photon-ion interactions in the 20 – 300 eV energy range. This program developed and retains partial responsibility for operation, maintenance and upgrades of this multi-user research endstation.

Due to their relatively large number of identical atoms, nanometer size and hollow spherical or quasi-spherical cage structures, fullerene molecular ions are of intrinsic interest as structural intermediates between individual molecules and solids, and exhibit

some of the physical properties of each. As is the case for conducting solids, their large numbers of valence electrons may be collectively excited in strong plasmon modes with broad energy signatures in the photoionization cross section. Conversely, the excitation of core electrons is spatially localized and of molecular character with narrower energy signatures characteristic of carbon-carbon bonding.

- An atom confined in a charged spherical shell is an intriguing and fundamental quantum-mechanical system. Unusual phenomena associated with the interaction of EUV light with endohedral fullerene molecules containing caged noble gas atoms have been predicted in numerous theoretical studies by M. Puska, R. Nieminen, M. Amusia, V. Dolmatov, S. Manson, A. Msezane, H. Chakraborty, A. Solov'yev and their collaborators, but remained untested by experiment until recently. In particular, the well-known single, giant 4d dipole resonance in photoionization of atomic Xe is predicted to be significantly distorted by the spherical carbon cage in endohedral $\text{Xe}@C_{60}$, producing distinct maxima and minima that have been termed “confinement resonances”. The predicted interference pattern arises because the outgoing Xe 4d photoelectron waves may either be transmitted or reflected by the C_{60} cage, producing a multi-path interference pattern that depends on both the diameter and thickness of the cage. Exchange of oscillator strength between plasmon modes of the fullerene cage and the trapped atom is also predicted in this single-molecule interferometer. A measurement of photoionization of $\text{Xe}@C_{60}^+$ in the energy range of Xe 4d ionization therefore represents a critical test of the theory of confinement resonances. Such an experiment had not heretofore been possible because of extremely low yields of synthesized noble-gas endohedral fullerenes. At ALS during a period of several months, a 200 eV beam of Xe^+ ions from an ion sputter-gun bombarded the surface of a rotating metal cylinder onto which C_{60} was being continuously deposited in vacuum by evaporation. The powder deposited on the cylinder (several tens of mg) was then scraped from the surface and placed into a small oven for subsequent re-evaporation into a low-power Ar discharge in an ECR ion source. A very small fraction ($\sim 10^{-5}$) of the C_{60} molecules in the accumulated samples containing a Xe atom was sufficient to produce a pure mass/charge analyzed beam of $\text{Xe}@C_{60}^+$ ions with a current of 0.06 – 0.3 pA. Merged-beams measurements of photoionization of $\text{Xe}@C_{60}^+$ at ALS exhibited a clear signature of Xe 4d ionization in this photon energy range as well as structure that was strongly suggestive of confinement resonances. The results of this proof-of-principle experiment were published in Physical Review Letters [1] and have attracted considerable attention from theorists. However, their statistical precision was limited by the extremely small ion beam current that could be achieved, which was in turn limited by the endohedral fullerene yield in the prepared samples.
- A major effort during the past year was devoted to increasing the endohedral yield of the prepared fullerene samples, to facilitate a more definitive measurement of the Xe 4d contribution to photoionization of $\text{Xe}@C_{60}^+$ and of the associated interference structure. In addition to systematically optimizing the parameters for synthesis (e.g. ion current and impact energy, fullerene evaporation rate, drum rotation speed), highly enriched (>99%) ^{136}Xe was obtained for use in the synthesis. These strategies together resulted an order of magnitude increase of the available $\text{Xe}@C_{60}^+$ ion beam current. Fig. 1 presents new ALS measurements for the $\text{Xe}@C_{56}^{3+}$ product ion channel that much more clearly indicate the interference structure. Improved measurements for the $\text{Xe}@C_{60}^{3+}$ and $\text{Xe}@C_{58}^{3+}$ product ion channels show the same

interference structure, and these three product channels together account for more than half of the Xe 4d oscillator strength. Data are still being analyzed and further measurements of $\text{Xe}@C_{54}^{3+}$ products are planned. This systematic investigation of confinement resonances in photoionization/fragmentation of $\text{Xe}@C_{60}^+$ will together constitute the Ph.D. dissertation research of N. Aryal.

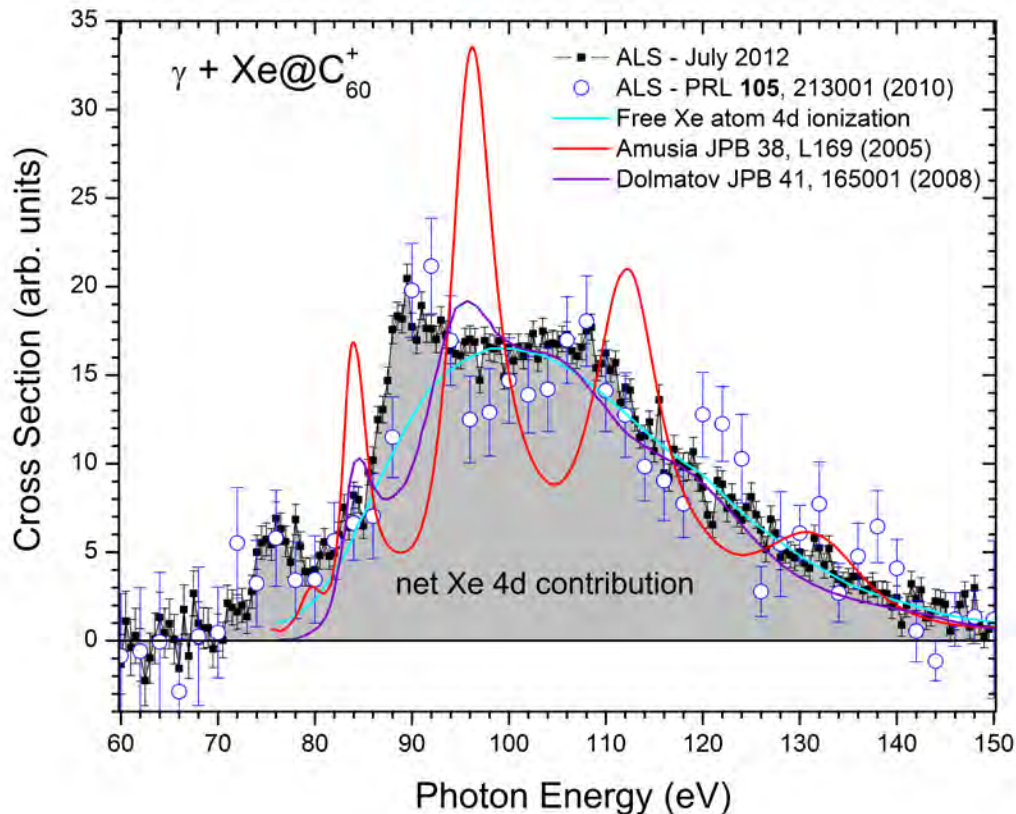


Figure 1. ALS measurements of excess cross section for Xe 4d ionization in double photoionization of endohedral $\text{Xe}@C_{60}^+$, accompanied by the loss of 4 C atoms, yielding $\text{Xe}@C_{56}^{3+}$ products (solid squares). The new measurements are compared with previously published ALS measurements (open circles) [1] and with two theoretical predictions for $\text{Xe}@C_{60}$.

- A series of cross-section measurements for different product ion channels resulting from photoabsorption by C_{60}^+ and C_{70}^+ is in progress at photon energies of 22, 35, 65, 105 and 140 eV. Single photoionization accompanied by the loss of as many as six pairs of C atoms was observed and quantified. These results motivated the measurements of $\text{Xe}@C_{56}^{3+}$ products resulting from photoabsorption by $\text{Xe}@C_{60}^+$ shown in Fig. 1. This systematic investigation of photoionization accompanied by fragmentation of fullerenes will constitute the Ph.D. dissertation research of K. Baral.

Future Plans

The PI retired from his academic position in June, 2012 and will continue working half-time on this project until the current grant ends in early 2013. Priority will be given to completion and publication of the Ph.D. dissertation research of N. Aryal on $\text{Xe}@C_{60}^+$ and K. Baral on C_{60}^+ and C_{70}^+ as described above.

Publications of Research Fully or Partially Funded by DOE Grant (2010-2012)

1. *Confinement Resonances in Photoionization of Xe@C₆₀⁺*, A.L.D. Kilcoyne, A. Aguilar, A. Müller, S. Schippers, C. Cisneros, G. Alna'Washi, N.B. Aryal, K.K. Baral, D.A. Esteves, C.M. Thomas and R.A. Phaneuf, Phys. Rev. Lett. 105, 213001 (2010).
2. *State-resolved valence shell photoionization of Be-like ions: experiment and theory*, A. Müller, S. Schippers, R.A. Phaneuf, A.L.D. Kilcoyne, H. Bräuning, A.S. Schlachter, M. Lu and B.M. McLaughlin, J. Phys. B: At. Mol. Opt. Phys. 43, 225201 (2010)
3. *K-shell photoionization of ground-state Li-like boron ions [B²⁺]: experiment and theory*, A. Müller, S. Schippers, S.W.J. Scully, A. Aguilar, C. Cisneros, M.F. Gharaibeh, A.S. Schlachter and B.M. McLaughlin, J. Phys. B: At. Mol. Opt. Phys. 44, 025701 (2011) J. Phys. B: At. Mol. Opt. Phys. 43, 135602 (2010).
4. *Plasmons in Fullerene Molecules*, R.A. Phaneuf, chapter 35 in "Handbook of Nanophysics," K. Sattler ed. (Taylor & Francis, 2010).
5. *Photoionization of Se ions for the determination of elemental abundances in astrophysical nebulae*, D.A. Esteves, Ph.D. Dissertation, University of Nevada, 2010.
6. *Valence-shell photoionization of the chlorine-like Ca³⁺ ion*, G. Alna'Washi, M. Lu, M. Habibi, R.A. Phaneuf, A.L.D. Kilcoyne, A.S. Schlachter, C. Cisneros and B.M. McLaughlin, Phys. Rev. A 81, 053416 (2010).
7. *Experimental photoionization cross-section measurements in the ground and metastable state threshold region of Se⁺*, N.C. Sterling, D.A. Esteves, R.C. Bilodeau, A.L.D. Kilcoyne, E.C. Red, R.A. Phaneuf and A. Aguilar, J. Phys. B: At. Mol. Opt. Phys. 44, 025701 (2011).
8. *Photoionization measurements for the iron isonuclear sequence: Fe³⁺, Fe⁵⁺ and Fe⁷⁼*, M.F. Gharaibeh, A. Aguilar, A.M. Covington, E.D. Emmons, S.W.J. Scully, R.A. Phaneuf, A.L.D. Kilcoyne, A.S. Schlachter, I. Álvarez, C. Cisneros and G. Hinojosa, Phys. Rev. A 83, 043412 (2011).
9. *Absolute single photoionization cross-section measurements of Se³⁺ and Se⁵⁺*, D.A. Esteves, A. Aguilar, R.C. Bilodeau, R.A. Phaneuf, A.L.D. Kilcoyne and N.C. Sterling, J. Phys. B: At. Mol. Opt. Phys. 45, 115201 (2011).
10. *Valence-shell photoionization of chlorinelike Ar⁺ ions*, A.M. Covington, A. Aguilar, I.R. Covington, G. Hinojosa, C.A. Shirley, R.A. Phaneuf, I. Álvarez, C. Cisneros, I. Dominguez-Lopez, M.M. Sant'Anna, A.S. Schlachter, C.P. Balance and B.M. McLaughlin, Phys. Rev. A 84, 013413 (2011).
11. *Absolute high-resolution Se⁺ photoionization cross-section measurements with Rydberg series analysis*, D.A. Esteves, R.C. Bilodeau, N.C. Sterling, R.A. Phaneuf, A.L.D. Kilcoyne, E.C. Red and A. Aguilar, Phys. Rev. A 84, 013406 (2011).

Molecular photoionization studies of nucleobases and correlated systems

Erwin Poliakoff, Department of Chemistry, Louisiana State University, Baton Rouge, LA 70803, epoliak@lsu.edu

Robert R. Lucchese, Department of Chemistry, Texas A&M University, College Station, TX, 77843, lucchese@mail.chem.tamu.edu

Program Scope

Molecular photoionization is a process that allows one to probe fundamental scattering dynamics of complex systems, and we use powerful experimental and theoretical tools for illuminating the microscopic details of the scattering dynamics. We focus on two primary areas. The first principal focus is to use vibrationally resolved photoelectron spectroscopy to probe the correlated motions of electrons and nuclei, and this allows us to disentangle the geometry and energy dependence of the dipole matrix elements that couple the initial bound state to the continuum scattering state. The experimental approach is to obtain vibrationally resolved photoelectron spectra over a broad range of incident photon energies by exploiting the high brightness capabilities at the Advanced Light Source. On the theory side, we explicitly solve the electron-molecular ion scattering equations to compute the corresponding vibrationally specific matrix elements using the adiabatic approximation. The second major direction is to explore applications of single-photon molecular photoionization to high harmonic generation and related processes. We have made considerable progress, in collaboration with Profs. Trallero and Lin at the McDonald Laboratory. We have initiated studies of high harmonic generation in relatively complex molecules, and this work is progressing very well. All of these research efforts benefit the Department of Energy because the results elucidate structure/spectra correlations that will be indispensable for probing complex and disordered systems of interest to DOE such as clusters, catalysts, reactive intermediates, transient species, and related species.

Recent Progress

Non-Franck-Condon Vibrational Branching Ratios in Acrolein

In the simplest view of molecular photoionization, one assumes that vibrational and photoelectron motion are decoupled, which leads to the Franck-Condon approximation. Nonresonant and resonant processes can result in coupling molecular vibration and photoelectron motion, with the result that vibrational branching ratios become dependent on photon energy, and that forbidden vibrations can be excited. We are working with a wide variety of molecular targets, including nucleobases, substituted thiophenes, and acrolein (C_3H_4O). Experimentally, we have made considerable progress on acrolein. In the analysis of the X^2A' state, seven vibrational transitions are observed, and several of the vibrational branching ratios are varying over extremely wide spectral ranges (e.g., more than 50 eV in the case of ν_{10} , the C=C-C bending mode). We have started Schwinger variational calculations in an effort to understand the mechanism for this broad range behavior.

Non-resonant non-Franck-Condon Effects

We have completed a study of the non-Franck-Condon effects in the valence photoionization of N_2 and CO over an extended range of energies up to 200 eV. The deviation of the vibrational

branching ratio from the Franck-Condon value can be directly related to the logarithmic derivative of the cross section. Defining the electronic factor F as the logarithmic derivative

$$F = \frac{\sigma^{(1)}}{\sigma^{(0)}}$$

where $\sigma^{(0)}$ is the total cross section at the equilibrium geometry and $\sigma^{(1)}$ is the first derivative with respect to bond length, then F can be related to the branching ratios

$$F = \pm \left(2R_{1^-0/0^-0}^{(\text{FC})} \right)^{\frac{1}{2}} \left[\frac{R_{1^-0/0^-0}}{R_{1^-0/0^-0}^{(\text{FC})}} - 1 \right]$$

where the branching ratio is defined as $R_{v_j^+ \leftarrow v / v_i^+ \leftarrow v} = \frac{\sigma_{v_j^+ \leftarrow v}}{\sigma_{v_i^+ \leftarrow v}}$, and $R_{v_j^+ \leftarrow v / v_i^+ \leftarrow v}^{(\text{FC})}$ is the branching ratio in

the Franck-Condon approximation. This analysis allows for the contributions to the breakdown of the Franck-Condon approximation to be identified by partial wave. Consider our measured and computed electronic factors in the case of $\text{CO}^+(X^2\Sigma^+)$, shown in figure 1.

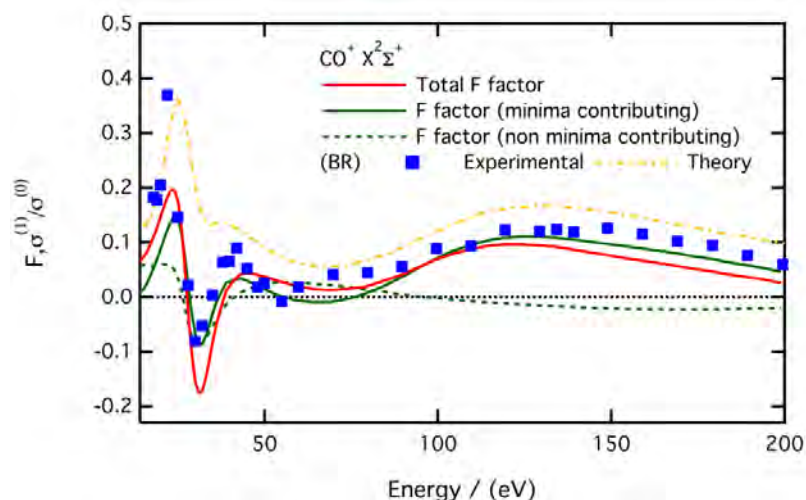


Figure 1. Theoretical and experimental F factors. Experimental values were derived assuming $R^{(\text{FC})} = 0.03713$. The dot-dashed line is a complete adiabatic treatment of the branching ratios. The F factor theoretical lines are derived directly from the derivatives of the fixed-nuclei cross sections.

There are two main sources of the breakdown of the Franck-Condon approximation, geometry dependence of the orbital from which the ionization occurs and geometry dependence in the continuum. In particular, in the partial wave expansion of the photoionization matrix elements one finds energies where certain matrix elements go through zero, leading to what can be described as Cooper minima. In molecular systems where there is no corresponding atomic Cooper minima, the Cooper minima can be identified as coming from Cohen-Fano interference effects. In figure 1, we have separated out the contribution to the non-Franck-Condon deviation of the electronic factor into contributions from partial waves with Cooper minima and contributions from those partial waves without out Cooper minima. In the figure we see that in this channel all of the deviation from the Franck-Condon value is due to partial waves with Cooper minima. The situation is different for other channels in CO , where breakdowns can be attributed to geometry effects in the orbital which is being ionized.

Molecular aspects of HHG: SF₆, SiCl₄, CF₄

A major component of our recent work has been to develop connections between molecular high harmonic generation and photoionization dynamics. The two phenomena are intimately connected, because a central aspect of high harmonic generation involves the high-field driven electron inelastically traversing the molecular framework. This is the conjugate process to photoionization. We have performed experiments on a series of molecules, including SF₆, SiCl₄, and CF₄. This work is done collaboratively with Kansas State researchers, primarily Profs. Carlos Trallero and C.D. Lin. A representative result is shown below for SF₆. Notice the pronounced dip at the 17th harmonic. This energy corresponds closely to a shape resonance in the photoionization continuum. We have seen similar, albeit less dramatic effects, in the other molecules studied. Currently, we are gearing up to do calculations on these systems, and we have already made substantial progress in this area. It is anticipated that this will be a major direction in our future research.

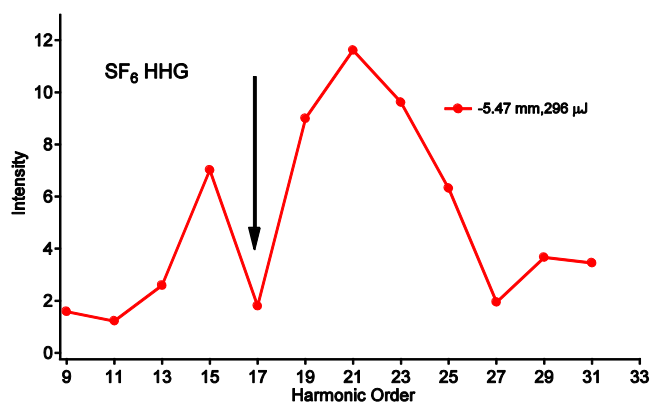


Figure 2. Experimental results on high harmonic generation in SF₆. Note the minimum at the 17th harmonic; this position corresponds closely to a shape resonance in the photoionization of this molecule.

Future Plans

We have a number of systems studied at the ALS where the analysis needs to be completed, and this will be a major activity. These systems include several nucleobases, acrolein, and 2-bromothiophene. We will expand our activities in molecular HHG as the major new experimental and theoretical direction, as described above. New targets are currently being evaluated, and we are planning to incorporate pump-probe capabilities into our HHG work.

Publications in 2010-2012

1. C. Jin, A. T. Le, S. F. Zhao, R. R. Lucchese, and C. D. Lin, Theoretical study of photoelectron angular distributions in single-photon ionization of aligned N₂ and CO₂, *Phys. Rev. A* **81**, 033421:1-12 (2010).
2. R. R. Lucchese, R. Montuoro, K. Kotsis, M. Tashiro, M. Ehara, J. D. Bozek, A. Das, A. Landry, J. Rathbone, and E. D. Poliakoff, The effect of vibrational motion on the dynamics of shape resonant photoionization of BF₃ leading to the E^2A_1' state of BF₃⁺, *Molec. Phys.* **108**, 1055-67 (2010).

3. C. D. Lin, Anh-Thu Le, Zhangjin Chen, Toru Morishita, and Robert Lucchese, Strong-field rescattering physics – self-imaging of a molecule by its own electrons, *J. Phys. B- At. Molec. Opt. Phys.* **43**, 122001:1-33 (2010).
4. Anh-Thu Le, R. R. Lucchese, and C. D. Lin, Polarization and ellipticity of high-order harmonics from aligned molecules generated by linearly polarized intense laser pulses, *Phys. Rev. A* **82**, 023814:1-6 (2010).
5. T. Tanaka, M. Hoshino, R. R. Lucchese, Y. Tamenori, H. Kato, H. Tanaka, K. Ueda, Bending-induced diminution of shape resonances in the core-level absorption region of hot CO₂ and N₂O, *New J. Phys.* **12**, 123017:1-18 (2010).
6. Misaki Okunishi, Hiromichi Niikura, R. R. Lucchese, Toru Morishita, and Kiyoshi Ueda, Extracting electron-ion differential scattering cross sections for partially aligned molecules by laser-induced rescattering photoelectron spectroscopy, *Phys. Rev. Lett.* **106**, 063001:1-14 (2011).
7. N. Berrah, R. C. Bilodeau, I. Dumitriu, D. Toffoli, R. R. Lucchese, Shape and Feshbach Resonances in Inner-Shell Photodetachment of Negative Ions, *J. Electron Spectrosc. Relat. Phenom.* **183**, 64-9 (2011).
8. Song-Feng Zhao, Cheng Jin, R. R. Lucchese, Anh-Thu Le, and C. D. Lin, High-order-harmonic generation using gas-phase H₂O molecules, *Phys. Rev. A* **83**, 033409:1-7 (2011).
9. Cheng Jin, Hans Jakob Wörner, V Tosa, Anh-Thu Le, Julien B. Bertrand, R. R. Lucchese, P. B. Corkum, D. M. Villeneuve, and C. D. Lin, Separation of target structure and medium propagation effects in high-harmonic generation, *J. Phys. B* **44**, 095601:1-5 (2011).
10. Bérenger Gans, Séverine Boyé-Péronne, Michel Broquier, Maxence Delsault, Stéphane Douin, Carlos E. Fellows, Philippe Halvick, Jean-Christophe Loison, Robert R. Lucchese, and Dolores Gauyacq, Photolysis of methane revisited at 121.6 nm and at 118.2 nm: quantum yields of the primary products, measured by mass spectrometry, *Phys. Chem. Chem. Phys.* **13**, 8140-52 (2011).
11. F. Kelkensberg, A. Rouzée, W. Siu, G. Gademann, P. Johnsson, M. Lucchini, R. R. Lucchese, M. J. J. Vrakking, XUV ionization of aligned molecules, *Phys. Rev. A* **84**, 051404(R):1-4 (2011).
12. Cheng Jin, Julien B. Bertrand, R. R. Lucchese, H. J. Wörner, Paul B. Corkum, D. M. Villeneuve, Anh-Thu Le, and C. D. Lin, Intensity dependence of multiple orbital contributions and shape resonance in high-order harmonic generation of aligned N₂ molecules, *Phys. Rev. A* **85**, 013405:1-7 (2012).
13. Hong Xu, U. Jacovella, B. Ruscic, and S. T. Pratt, and R. R. Lucchese, Near-Threshold Shape Resonance In The Photoionization Of 2-Butyne, *J. Chem. Phys.* **136**, 154303:1-10 (2012).
14. Arnaud Rouzée, Freek Kelkensberg, Wing Kiu Siu, Georg Gademann, R. Lucchese, Marc J. J. Vrakking, Photoelectron kinetic and angular distributions for the ionization of aligned molecules using a HHG source, *J. Phys. B* **45**, 074016:1-11 (2012)
15. C. Wang, M. Okunishi, R. R. Lucchese, T. Morishita, O. I. Tolstikhin, L. B. Madsen, K. Shimada, D. Ding, K. Ueda, Extraction of Electron-Ion Differential Scattering Cross Sections for C₂H₄ by Laser-Induced Rescattering Photoelectron Spectroscopy, *J. Phys. B* **45**, 131001:1-5 (2012).
16. J. A. Lopez-Dominguez, D. Hardy, A. Das, E. D. Poliakoff, A. Aguilar, and R. R. Lucchese, Mechanisms of Franck-Condon breakdown over a broad energy range in the valence photoionization of N₂ and CO, *J. Electron Spectrosc. Relat. Phenom.* **185**, 211 (2012).

Control of Molecular Dynamics: Algorithms for Design and Implementation

Herschel Rabitz and Tak-San Ho, Princeton University, Frick Laboratory, Princeton, NJ 08540, hrabitz@princeton.edu, tsho@princeton.edu

A. Program Scope:

This research is concerned with conceptual and algorithmic developments addressing control over quantum dynamics phenomena. The research is theoretical and computational in nature, but its ultimate significance lies in the associated implications and applications in the laboratory. This research program aims at developing a deeper understanding of quantum control and providing new algorithms to extend the laboratory control capabilities.

B. Research Progress:

In the past year, a broad variety of research topics were pursued in the general area of controlling quantum dynamics phenomena. A summary of these activities is provided below.

1. Singularities of quantum control landscapes[1] In this study, we formulated quantum control landscape theory to assess the ease of finding optimal control fields in simulations and in the laboratory. The landscape is the observable as a function of the controls, and a primary goal of the theory is the analysis of landscape features. We analyzed the necessary and sufficient conditions for singular controls to be kinematic or nonkinematic critical solutions and the likelihood of their being encountered while maximizing an observable. An algorithm was introduced to seek singular controls on the landscape in simulations along with an associated Hessian landscape analysis. Simulations were performed for a large number of model finite-level quantum systems, showing that all the numerically identified kinematic and nonkinematic singular critical controls are not traps, in support of the prior empirical observations on the ease of finding high-quality optimal control fields.

2. Critical Points of the Optimal Quantum Control Landscape: A Propagator Approach[2] Numerical and experimental realizations of quantum control are closely connected to the properties of the mapping from the control to the unitary propagator. For bilinear quantum control problems, no general results are available to fully determine when this mapping is singular or not. In this study we gave sufficient conditions, in terms of elements of the evolution semigroup, for a trajectory to be non-singular. We identified two lists of way-points that, when reached, ensure the non-singularity of the control trajectory. It was found that under appropriate hypotheses one of those lists does not depend on the values of the coupling operator matrix.

3. Laser-driven direct quantum control of nuclear excitations[3] We considered the possibility of controlled direct laser-nuclear excitations from a quantum control perspective. The controllability of laser-driven electric dipole and magnetic dipole transitions among pure nuclear states was analyzed. Within a set of realistic and general conditions, atomic nuclei were demonstrated to possess full state controllability. Additionally, an analysis of the nuclear state excitation probability as a function of the laser control field was conducted. We showed that this control landscape possess a generic topology, which has important physical consequences for achieving optimal nuclear state excitation with laser fields. Last, we provided an assessment of the technological challenges that need to be considered when implementing direct nuclear control in the laboratory.

4. Fast-kick-off monotonically convergent algorithm for searching optimal control fields[4] In this work we formulated a fast-kick-off search algorithm for quickly finding optimal control fields in the state-to-state transition probability control problems, especially those with poorly chosen initial control fields. The algorithm is a monotonically convergent scheme that allows for local temporal refinement of the control field at each iteration. We have performed extensive numerical simulations for controls of vibrational transitions and ultrafast electron tunneling and found that the new algorithm not only greatly improves the search efficiency but also is able to attain good monotonic convergence quality when further frequency constraints are required. The algorithm is expected to be particularly effective when the corresponding control dynamics involves a large number of energy levels or ultrashort control pulses.

5. Bounds on the curvature at the top and bottom of the transition probability landscape[5] In this work we analyzed the curvature bounds of the control landscape associated with the transition probability between the states of a controlled quantum system is a function of the applied control field. An initial control likely will produce a transition probability near the bottom of the landscape, while the final goal is to find a field that results in a high transition probability value at the top. For controls producing either of the latter extreme landscape values, the Hessian of the transition probability with respect to the control field characterizes the curvature of the landscape and the ease of leaving either limit. We showed that there exists a lower bound on the number of non-zero Hessian eigenvalues at either the top or bottom of the landscape. In particular, there is at least one non-zero eigenvalue at the top and generally one at the bottom. Under special circumstances, the Hessian may be identically zero at the bottom (i.e. it possesses no non-zero eigenvalues). These results dictate the curvature of the top and bottom of the landscape, which has important physical significance for seeking optimal control fields. At the top, a field that produces a single non-zero Hessian eigenvalue of small magnitude will generally exhibit a high degree of robustness to field noise. In contrast, at the bottom, working with a field producing the maximum number of non-zero eigenvalues will generally assure the most rapid climb towards a high transition probability.

6. Exploring quantum control landscapes: Topology, features, and optimization scaling[6] In this work we analyzed the effort (i.e., the number of algorithmic iterations) required to find an optimal control field appears to be essentially invariant to the complexity of the system. In a series of systematic optimizations on model quantum systems with the number of states N ranging from 5 through 100. Previous theoretical studies on the topology of quantum control landscapes established that they should be free of suboptimal traps under reasonable physical conditions. The simulations in our study included nearly 5000 individual optimization test cases, all of which confirm this prediction by fully achieving optimal population transfer of at least 99.9% on careful attention to numerical procedures to ensure that the controls are free of constraints. Collectively, the simulation results additionally showed invariance of required search effort to system dimension N . This behavior was rationalized in terms of the structural features of the underlying control landscape. The very attractive observed scaling with system complexity may be understood by considering the distance traveled on the control landscape during a search and the magnitude of the control landscape slope. Exceptions to this favorable scaling behavior can arise when the initial control field fluence is too large or when the target final state recedes from the initial state as N increases.

7. Laser-assisted molecular alignment in a strongly dissipative environment[7] In this study we showed that transient alignment of linear molecules in a dense collisional environment can result from the formation of trapped aligned dark states in a laser field constituting either a comb of resonant short pulses or a sinusoidally frequency- modulated wave with a continuous flux. Simulation of the laser-induced dynamics of CO molecules reveals that the latter approach is effective at room temperature and requires three orders of magnitude less laser intensity compared to known alignment

techniques.

C. Future Plans: The research in the coming year will focus on the application of our recently developed monotonically convergent algorithms [3,12,15] and their generalization to allow laboratory constraints, including the fluence constraint on and the removal of dc and high frequency components of the control fields. We also plan to continue our study on various atomic and molecular dynamics control problems, including photo-association processes of atoms and laser induced field-free molecular orientation in thermal gases, and collective excitation of Bose-Einstein condensates. Moreover, we plan to extend the current landscape study on the transition probability [1,2,4,5,8] to investigate the quantum control of arbitrary observables and of ensemble of systems using the density matrix formalism.

D. References:

1. Singularities of quantum control landscapes. Re-Bing Wu, Ruixing Long, Jason Dominy, Tak-San Ho, and Herschel Rabitz, *Phys. Rev. A*, in press (2012).
2. Critical Points of the Optimal Quantum Control Landscape: A Propagator Approach, Tak-San Ho, Herschel Rabitz and Gabriel Turinici, *Acta Appl. Math.*, 118, 4956 (2012).
3. Laser-driven direct quantum control of nuclear excitations, Ian Wong, Andreea Grigoriu, Jonathan Roslund, Tak-San Ho, and Herschel Rabitz, *Phys. Rev. A* 84, 053429 (2011).
4. Fast-kick-off monotonically convergent algorithm for searching optimal control fields, Sheng-Lun Liao, Tak-San Ho, Shih-I Chu, and Herschel Rabitz, *Phys. Rev. A*, 84, 031401(R) (2011)
5. Bounds on the curvature at the top and bottom of the transition probability landscape, Vincent Beltrani, Jason Dominy, Tak-San Ho and Herschel Rabitz, *J. Phys. B: At. Mol. Opt. Phys.* 44, 154009 (2011).
6. Exploring quantum control landscapes: Topology, features, and optimization scaling, Katharine W. Moore and Herschel Rabitz, *Phys. Rev. A* 84, 012109 (2011).
7. Laser-assisted molecular alignment in a strongly dissipative environment, Dmitry Zhdanov and Herschel Rabitz, *Phys. Rev. A* 83, 061402(R) (2011).
8. Control of quantum phenomena, Constantin Brif, Raj Chakrabarti, and Herschel Rabitz, *Adv. Chem. Phys.*, 148, 1-76 (2011).
9. Attaining persistent field-free control of open and closed quantum systems, E. Anson, V. Beltrani, and H. Rabitz, *J. Chem. Phys.*, 134, 124110 (2011).
10. Exploring the top and bottom of the quantum control landscape, V. Beltrani, J. Dominy, T.-S. Ho and H. Rabitz, *J. Chem. Phys.*, 134, 194106 (2011).
11. Volume fractions of the kinematic near-critical sets of the quantum ensemble control landscape, J. Dominy and H. Rabitz, *J. Phys. A*, 44, 255302 (2011).

12. Optimal laser control of molecular photoassociation along with vibrational stabilization, E. F. de Lima, T.-S. Ho, and H. Rabitz, *Chem. Phys. Lett.*, 501, 267 (2011).
13. Why is chemical synthesis and property optimization easier than expected? K. W. Moore, A. Pechen, X.-J. Feng, J. Dominy, V. J. Beltrani, and H. Rabitz, *Phys. Chem. Chem. Phys.*, 13, 10048 (2011).
14. A general formulation of monotonically convergent algorithms in the control of quantum dynamics beyond the linear dipole interaction, T.-S. Ho, H. Rabitz, and S.-I Chu, *Comp. Phys. Comm.*, 182, 14 (2011).
15. Search complexity and resource scaling for the quantum optimal control of unitary transformations, K. W. Moore, R. Chakrabarti, G. Riviello, and H. Rabitz, *Phys. Rev. A*, 83, 012326 (2011).
16. Fidelity between unitary operators and the generation of robust gates against off-resonance perturbations, R. Cabrera, O. M. Shir, R. Wu, and H. Rabitz, *J. Phys. A*, 44, 095302 (2011).
17. Accelerated monotonic convergence of optimal control over quantum dynamics, T.-S. Ho and H. Rabitz, *Phys. Rev E*, 82, 026703 (2010).
18. Features of quantum control in the sudden regime, M. Klein, V. Beltrani, and H. Rabitz, *Chem. Phys. Lett.*, 499, 161 (2010).
19. Control of quantum phenomena: past, present and future, C. Brif, R. Chakrabarti and H. Rabitz, *New J. Phys.*, 12, 075008 (2010).
20. The canonical coset decomposition of unitary matrices through Householder transformations, R. Cabrera, T. Strohecker, and H. Rabitz, *J. Math. Phys.*, 51, 082101 (2010).
21. Environment-invariant measure of distance between evolutions of an open quantum system, M. D. Grace, J. Dominy, R. L. Kosut, C. Brif, and H. Rabitz, *New J. Phys.* 12, 015001 (2010).
22. Multi-polarization quantum control of rotational motion through dipole coupling, G. Turinici and H. Rabitz, *J. Phys. A: Math. Theor.* 43, 105303 (2010).

“Coherent and Incoherent Transitions”

F. Robicieux

*Auburn University, Department of Physics, 206 Allison Lab, Auburn AL 36849
(robicfj@auburn.edu)*

Program Scope

This theory project focuses on the time evolution of systems subjected to either coherent or incoherent interactions. This study is divided into three categories: (1) coherent evolution of highly excited quantum states, (2) incoherent evolution of highly excited quantum states, and (3) the interplay between ultra-cold plasmas and Rydberg atoms. Some of the techniques we developed have been used to study collision processes in ions, atoms and molecules. In particular, we have used these techniques to study the correlation between two (or more) continuum electrons and electron impact ionization of small molecules.

Recent Progress 2011-2012

Extreme two-electron systems: A couple years ago, we collaborated with A. Landers on a project where a photon ejected a slow electron from the Ne 1s-shell. The subsequent Auger electron (~800 eV) interacted with the photo-electron to give a correlated angular distribution. The huge disparity in the energies and the large region over which the electrons interact makes the quantum calculation difficult. Surprisingly, the classical calculation did not agree well with the measured angular distribution. This motivated us to re-express the quantum propagator using discrete variable ideas for the angles. Reference [26] describes the basic idea and applies it to a fully three dimensional model system. The idea is that the $1/r_{12}$ operator is difficult to evaluate when many angular momenta are in the problem because of the large number of multipoles. However, borrowing ideas from discrete variable theory (extensively used in chemistry calculations), we were able to efficiently evaluate the action of the $1/r_{12}$ operator on the wave function. We could propagate the fully three dimensional wave function for two electrons up to the largest number of coupled angular momenta we tested (160). We used this propagator in Ref. [27] as the basis for a method to study the Ne system described above. We found that the quantum calculation could reproduce all aspects of the experiment. We used the quantum wave function to understand why the classical calculations did not give the experimental result. We also performed calculations varying the energies to understand the trends in the angular distributions.

Atomic processes in strong magnetic fields: We performed two studies of atomic processes in strong magnetic fields. These were partially motivated by recent experiments that have demonstrated trapping of anti-matter hydrogen atoms. The first study was a classical and quantum investigation of the ionization of Rydberg H atoms by a slowly ramped electric field.[21] This method of ionization is commonly used to *measure* the energy distribution of Rydberg states (state selective field ionization). This situation is interesting because when there is no magnetic field the quantum states evolve diabatically in the ramped E-field. We performed classical and quantum calculations to gauge the size of quantum effects.

We showed that as the magnetic field is increased the ionization does start for smaller electric fields. However, there exist stable classical trajectories at positive energy that contribute to the possibility of the atom surviving to strong E-fields. In a separate study, we investigated the charge exchange that occurs when positrons scatter from Rydberg atoms.[24] Unlike previous studies, we also investigated the case when the positron kinetic energy was comparable or larger than the binding energy of the atom. We found that the transfer rate scales as $T^{1/2}$ for low temperatures but is substantially below this at higher temperatures. Surprisingly, we found that Ps formed with hotter positrons are more easily destroyed by electric fields if the Ps has center of mass velocity nearly along the B-field contrary to what might be expected from $v \times B$ effective electric fields.

Electron-molecule scattering (ionization): We performed a time dependent close-coupling calculation for electron-impact ionization of Li_2 . [22] Ionization is from the outer $2s\sigma$ subshell. At the peak of the cross section, the non-perturbative cross sections are found to be lower than those calculated using perturbation theory. This reduction is due to electron correlation effects and is in keeping with previous reductions in the peak of the cross section seen in electron-impact ionization of neutral atoms.

Single photon ionization from highly charged ions: We performed calculations of non-perturbative single photoionization of U^{91+} using a time dependent close coupling method for the Dirac equation.[25] In contrast to our previous calculation, we included the full electromagnetic-field potential. A spherical Bessel function expansion was used to go beyond the Lorentz gauge dipole approximation to include higher order radiation field operators in both the Lorentz and Coulomb gauges.

Early times in ultracold neutral plasmas: We performed classical calculations of the early time properties of plasmas formed through near threshold ionization of cold atomic gases.[20] In particular, we study how electrons ejected at very low energies evolve from the strongly coupled to the weakly coupled regime. We studied how the formation of Rydberg atoms leads to heating and how the mass of the ion could enter the dynamics. We also studied how the ion properties evolve by comparing a treatment of the electrons as a fluid to a molecular dynamics simulation. Our study of the ion motion at early times could be used to infer the electron-ion scattering rate in the plasma; we found substantial differences between our results and previous calculations for cold electrons.

High harmonic generation: We were involved in two projects to study high harmonic generation in special circumstances. In Ref. [19], we investigated the enhancement of HHG in the presence of noise by solving the non-perturbative stochastic time-dependent Schrodinger equation. We used the resulting wave function to quantify how varying noise levels affect the frequency components of the high harmonic spectrum. In some cases, a factor of ~ 50 enhancement can be achieved in the yield near the cut-off region. We also observed an effect due to carrier envelope phase for weak noise. In Ref. [23], we investigated the generation of a broad XUV continuum in HHG by spatially inhomogeneous fields. For some cases, we were able to increase the plateau region by roughly a factor of 2. We found that the field inhomogeneity plays a critical role in quantum path selection.

Finally, this program has several projects that are strongly numerical but only require knowledge of classical mechanics. This combination is ideal for starting undergraduates on publication quality research. Since 2004, nineteen undergraduates have participated in this program. Most of these students have completed projects published in peer reviewed journals; three of the papers discussed above[20,21,24] have undergraduates as first author. Two undergraduates, Michael Wall in 2006 and Patrick Donnan in 2012, were one of the 5 undergraduates invited to give a talk on their research at the undergraduate session of the DAMOP meeting. There will be 5 or 6 students doing research during the 2011-12 school year and I expect they will continue the successful tradition of undergraduate research; three of these students are sufficiently advanced to tackle quantum problems.

Future Plans

Global study of multiphoton ionization: T. Topcu recently finished a large scale investigation of the multiphoton ionization of atoms from ground and highly excited states. For many situations, the Keldysh parameter is the only important quantity for characterizing the overall atom-strong laser interaction. The calculations were done for a two dimensional grid of parameters looking for characteristic properties of the ionization rate. The two parameters we varied are the Keldysh parameter and the laser frequency divided by the classical frequency at the binding energy of the atom.

Rydberg Physics Recently published (and some unpublished) measurements from T. F. Gallagher's group show startling behavior of Rydberg atoms in very strong microwave fields. In particular, they find that atoms that are laser excited to near threshold (and above threshold!) energies while the microwaves are on can survive to extremely long times. We will perform quantum and classical calculations for this system to understand the mechanisms that lead to survival. This is a difficult problem because the interesting quantum physics extend to distances of $\sim 10^6 a_0$.

Two electron physics We have recently developed a method for dealing with the quantum mechanics when two electrons extend over very large regions and/or interact for a long time.[26,27] This method will be used for a joint study with R.R. Jones, collaborating on an experimental/theoretical investigation of two weakly bound electrons. In particular, how quickly energy and angular momentum are exchanged between the two electrons is of fundamental interest. There is also the possibility for further collaboration with experiments at the ALS to study the post collision interaction of two outgoing electrons. As a third stream, we are also interested in using our fully quantum method to test the range of validity of some of the approximations that are standard in PCI.

DOE Supported Publications (7/2008-7/2011)

[1] F. Robicheaux, J. Phys. B **42**, 195301 (2009).

[2] A. Denning, S.D. Bergeson, and F. Robicheaux, Phys. Rev. A **80**, 033415 (2009).

- [3] G.B. Andresen et al. (ALPHA collaboration), *Phys. Plasmas* **16**, 100702 (2009).
- [4] S. Jonsell, D. P. van der Werf, M Charlton, and F. Robicheaux, *J. Phys. B* **42**, 215002 (2009).
- [5] M.S. Pindzola, J.A. Ludlow, F. Robicheaux, J. Colgan, and D.C. Griffin, *J. Phys. B* **42**, 215204 (2009).
- [6] J.A. Ludlow, J. Colgan, T.-G. Lee, M.S. Pindzola, and F. Robicheaux, *J. Phys. B* **42**, 225204 (2009).
- [7] M.S. Pindzola, J.A. Ludlow, F. Robicheaux, J. Colgan, and C.J. Fontes, *Phys. Rev. A* **80**, 052706 (2009).
- [8] F. Robicheaux, *J. Phys. B* **43**, 015202 (2010).
- [9] M. Jerkins, J.R. Klein, J.H. Majors, F. Robicheaux, and M.G. Raizen, *New J. Phys.* **12**, 043022 (2010).
- [10] M.S. Pindzola, C.P. Ballance, F. Robicheaux, and J. Colgan, *J. Phys. B* **43**, 105204 (2010).
- [11] T. Topcu and F. Robicheaux, *J. Phys. B* **43**, 115003 (2010).
- [12] T.-G. Lee, M.S. Pindzola, and F. Robicheaux, *J. Phys. B* **43**, 165601 (2010).
- [13] T. Topcu and F. Robicheaux, *J. Phys. B* **43**, 205101 (2010).
- [14] F. Robicheaux, S.D. Loch, M.S. Pindzola, and C.P. Ballance, *Phys. Rev. Lett.* **105**, 233201 (2010).
- [15] S.D. Bergeson, A. Denning, M. Lyon, and F. Robicheaux, *Phys. Rev. A* **83**, 023409 (2011).
- [16] M.S. Pindzola, S.D. Loch, and F. Robicheaux, *Phys. Rev. A* **83**, 042705 (2011).
- [17] M.S. Pindzola, J.A. Ludlow, C.P. Ballance, F. Robicheaux, and J. Colgan, *J. Phys. B* **44**, 105202 (2011).
- [18] T. Topcu and F. Robicheaux, *Phys. Rev. E* **83**, 046607 (2011).
- [19] I. Yavuz, Z. Altun, and T. Topcu, *J. Phys. B* **44**, 135403 (2011).
- [20] K. Niffenegger, K. A. Gilmore, and F. Robicheaux, *J. Phys. B* **44**, 145701 (2011).
- [21] P.H. Donnan, K. Niffenegger, T. Topcu, and F. Robicheaux, *J. Phys. B* **44**, 184003 (2011).
- [22] M.S. Pindzola, Sh. A. Abdel-Naby, J.A. Ludlow, F. Robicheaux, and J. Colgan, *Phys. Rev. A* **85**, 012704 (2012).
- [23] I. Yavuz, E.A. Bleda, Z. Altun, and T. Topcu, *Phys. Rev. A* **85**, 013416 (2012).
- [24] P.H. Donnan and F. Robicheaux, *New. J. Phys.* **14**, 035018 (2012).
- [25] M.S. Pindzola, Sh. A. Abdel-Naby, F. Robicheaux, and J. Colgan, *Phys. Rev. A* **85**, 032701 (2012).
- [26] F. Robicheaux, *J. Phys. B* **45**, 135007 (2012).
- [27] F. Robicheaux, M.P. Jones, M. Schoffler, T. Jahnke, K. Kreidi, J. Titze, C. Stuck, R. Dorner, A. Belkacem, Th. Weber, and A.L. Landers, *J. Phys. B* **45**, 175001 (2012).

Generation of Bright Soft X-ray Laser Beams

Jorge J. Rocca

Department of Electrical and Computer Engineering and Department of Physics

Colorado State University, Fort Collins, CO 80523-1373

rocca@engr.colostate.edu

Program description

This project addresses the challenge of the efficient generation of bright x-ray laser beams. In table-top experiments conducted at Colorado State University in 2011 we succeeded in extending gain-saturated table-top lasers to wavelengths below 10 nm for the first time, demonstrating a $\lambda = 8.8$ nm laser emitting pulses of > 2 μJ energy in a transition of Ni-like La. In addition we observed lasing at wavelengths as short as 7.3 nm by isoelectric scaling to Ni-like Sm. We have also collaborated in an experiment at LCLS that demonstrated an atomic photoionization laser at 1.46 nm in Ne. The atomic laser improves the output characteristics of the pulses generated at the XFEL by providing wavelength stability and greatly increased monochromaticity. Recently we have realized the first measurement of the time it takes the gain to recover in table-top soft x-ray plasma amplifier that is injection seeded with a short high harmonic pulse. A gain-recovery time of ~ 1.5 ps was measured in an $\lambda = 18.9$ nm Ni-like Mo plasma. The results support the possibility to generate ultra-intense fully phase-coherent soft x-ray laser pulses in dense soft x-ray plasma amplifiers. During this past year we have succeeded in increasing the repetition rate of table-top soft x-ray lasers to 100 Hz for the first time, producing a record average power of 0.15 mW at 18.9 nm.

Gain recovery in injection-seeded soft x-ray laser amplifiers

Soft x-ray lasers based on the amplification of spontaneous emission in a dense plasma column are capable to produce laser pulse with energies that match those typically produced by free electron lasers, but with longer pulsewidth. Injection-seeding of plasma amplifiers have been demonstrated to produce fully phase-coherent soft x-ray pulses of ~ 1 ps duration, and has the potential to generate intense coherent femtosecond pulses. However, energy is not efficiently extracted from the amplifier by the seed pulse due to the significant mismatch between the duration of the ultrashort seed pulse and the gain duration that can range from several ps to tens of picoseconds. However, as soon as the seed is amplified the gain can be expected to recover due to re-pumping of the laser upper level, opening the possibility to increase the extracted energy by implementing chirped pulse amplification at soft x-ray wavelengths. A fast recovery of the gain is highly desirable in this case, as it would open the possibility of making use of the re-pumping of the laser upper level to generate ultra-high intensity fully coherent soft x-ray laser pulses from compact devices.

We have realized the first measurement of the gain recovery dynamics in a soft x-ray plasma

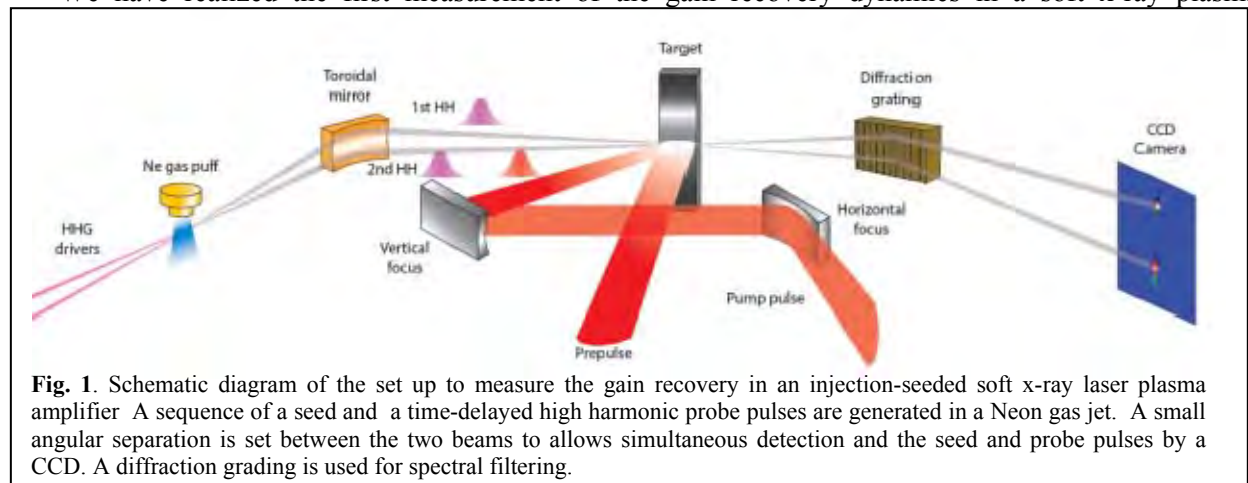


Fig. 1. Schematic diagram of the set up to measure the gain recovery in an injection-seeded soft x-ray laser plasma amplifier. A sequence of a seed and a time-delayed high harmonic probe pulses are generated in a Neon gas jet. A small angular separation is set between the two beams to allow simultaneous detection of the seed and probe pulses by a CCD. A diffraction grating is used for spectral filtering.

amplifier seeded by high harmonic pulses. A sequence of two time-delayed spatially-overlapping high harmonic pulses was injected into an 18.9 nm wavelength nickel-like Mo plasma amplifier to measure the regeneration of the population inversion. Collisional processes were observed to re-establish the population inversion depleted during the amplification of the first seed pulse in about ~ 1.5 ps, in agreement with model simulations. Pulses from the same Ti:Sapphire laser system that pump the soft x-ray laser amplifiers were used to generate two harmonic pulses with controllable time delay that were relay imaged onto the middle point of the plasma amplifier column using a toroidal mirror (Fig. 1). The duration of the gain was measured by seeding the plasma amplifier with a single high harmonic pulse, at different delays respect to the peak of the optical pump pulse that heats the plasma. The gain was measured to rise in about 4 ps to reach its maximum value about 1 ps after the peak of the short pump pulse (Fig. 2(a)). Figure 2 (b) shows the measured recovery of the gain for the situation in which the seed pulse arrives 1 ps prior to the peak of the gain .The first point in the plot corresponds to the arrival of the probe pulse immediately before the seed pulse, a situation in which the probe pulse experiences the full gain. When the probe pulse is injected 0.25 ps after the seed pulse the gain is observed to be completely depleted. However a probe delay of 0.5 ps already shows evidence of a partial gain recovery. At a delay of 1.5 ps the gain recovery is observed to be complete. After the gain is fully recovered the amplification of the delayed probe pulse remains high for about 2 ps, in agreement with the gain duration profile in Fig.2 (a). This shows that a harmonic pulse injected 2 ps after the first pulse should be able to extract a similar amount of energy, doubling the amount of laser pulse energy that could be extracted, supporting the concept of chirped pulse amplification in soft x-ray plasmas amplifiers. Subsequently the amplification of the probe pulse decreases, in accordance to the drop of the gain in Fig.2 (a). This result indicates that an injection-seeding scheme based on the continuous extraction of energy from a soft x-ray plasma-based amplifier by an stretched seed pulse has the potential to generate ultra-intense fully phase-coherent soft x-ray laser pulses.

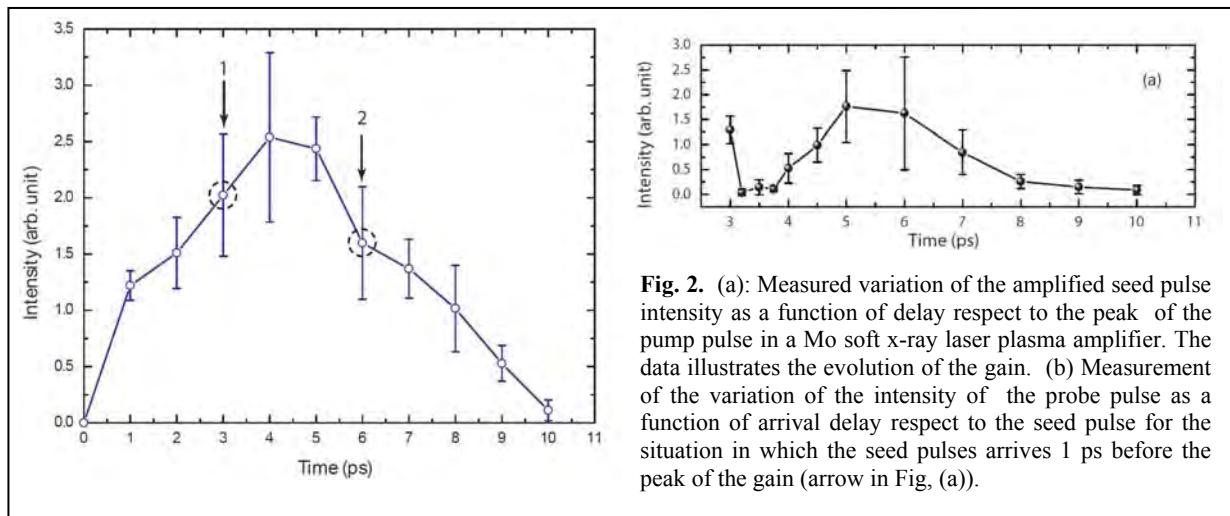
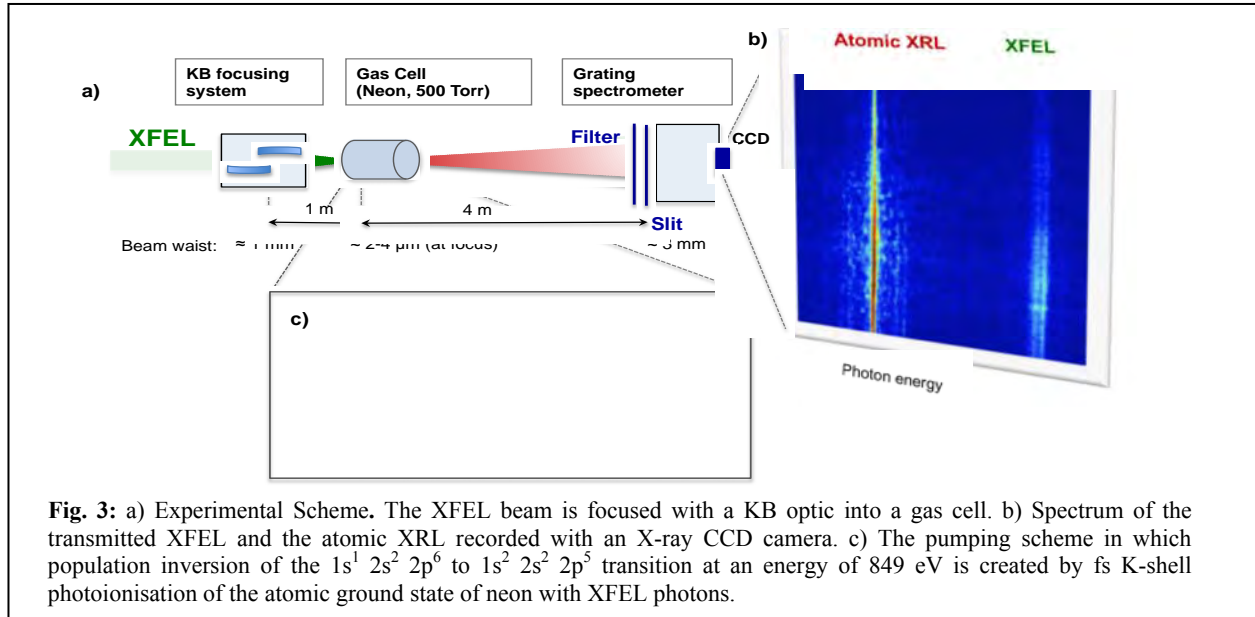


Fig. 2. (a): Measured variation of the amplified seed pulse intensity as a function of delay respect to the peak of the pump pulse in a Mo soft x-ray laser plasma amplifier. The data illustrates the evolution of the gain. (b) Measurement of the variation of the intensity of the probe pulse as a function of arrival delay respect to the seed pulse for the situation in which the seed pulses arrives 1 ps before the peak of the gain (arrow in Fig. (a)).

Demonstration of an atomic inner-shell photoionization laser using LCLS.

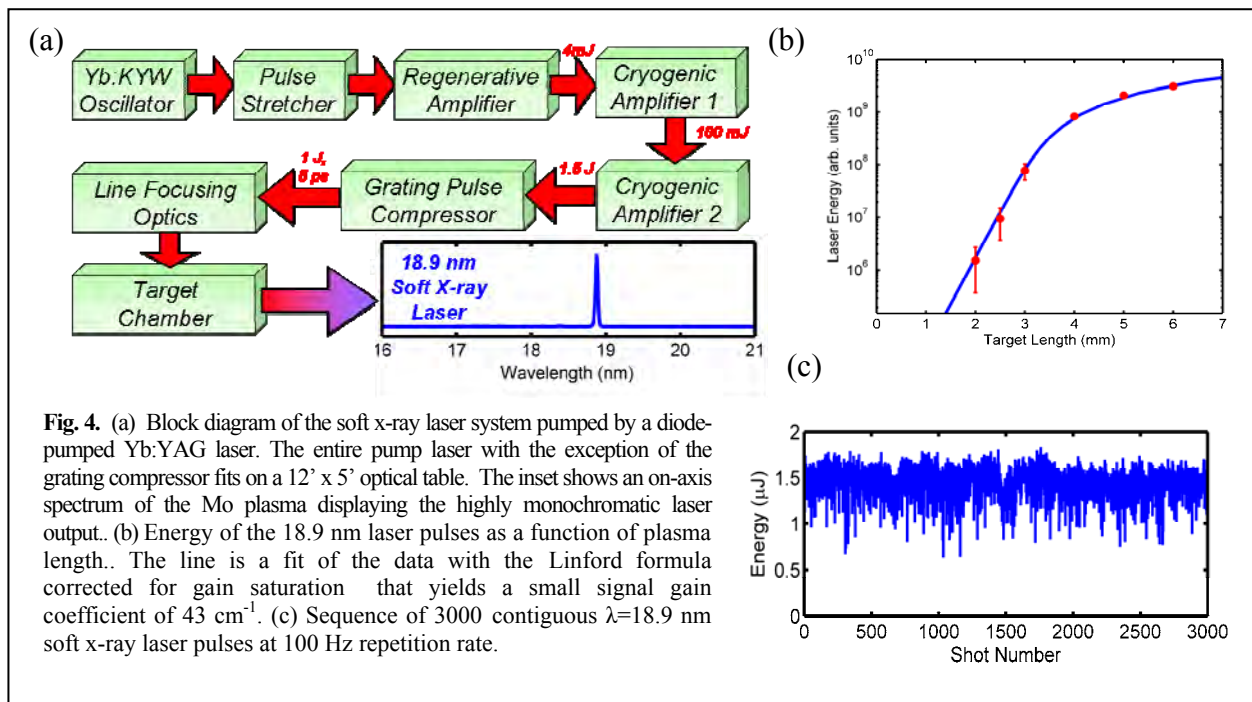
We have also collaborated in an experiment that demonstrated an atomic photoionization laser at 1.46 nm in Ne using pulses from LCLS as the pump. The establishing of a population inversion by rapid photoionisation of an inner-shell electron was first proposed by Duguay and Rentzepis in 1967. A visible inner-shell photoionisation laser in Cd vapor was demonstrated by Silfvast in 1983. Kapteyn proposed and analyzed a Ne K- α laser pumped by laser-produced plasma X rays in 1991, and recently Rohringer and London presented calculations for Ne pumped by XFEL radiation. At intensities achievable at the new XFEL sources rapid inner-shell photoionisation results in short-lived population inversions which can be exploited for lasing from the valence to the core level.



LCLS pulses of 960 eV photons with 40 fs duration were focused to spot sizes of 1-2 μm radius resulting in intensities up to 2×10^{17} W/cm² into a dense volume of neon gas at \approx 500 Torr pressure (Fig.3), yielding an inverse photoionisation rate of \approx 4 fs, i.e. comparable to the Auger lifetime of the 1s core-hole in neon of 2.7 fs. Spontaneously emitted K- α 849 eV photons at the front-end of the plasma column are exponentially amplified along the direction of the propagating XFEL pump pulse. The geometry of the gain medium (\sim 2 cm Rayleigh length and a 1-2 μm radius) is determined by the Kirkpatrick-Baez focusing system. The raw on-axis spectrum shown in the inset of Fig.3 provides strong evidence of lasing. The relatively broad line on the right is the transmitted XFEL pulse. The narrow atomic line radiation is visible at 849 eV with peak intensities one order of magnitude higher than that of the transmitted XFEL. In contrast to the relatively broad (8 eV FWHM) and jittering (14 eV FWHM) spectra of the XFEL pulses, the Ne K- α line has a reproducible spectral shape, narrow width and fixed centroid. To demonstrate exponential amplification on the atomic line transition, the incoming XFEL energy was varied. Doubling the XFEL energy resulted in an average increase in the Ne K- α line intensity by four orders of magnitude. The gain-length product averaged over many shots was estimated to be $GL = 19\text{-}21.3$, that is consistent with the $GL = 19$ resulting from simulations. The highest single-shot energy measured was \sim 1.1 μJ , corresponding to an energy conversion efficiency of 4×10^{-3} . Model simulations predict an average pulse duration of \sim 5 fs at FWHM. The peak brightness of the atomic XRL is estimated to be $\approx 1.3 \times 10^{30}$ (in units of photons/s/mrad²/mm² per 0.1% spectral bandwidth). In comparison, the LCLS has a brilliance of $\approx 3 \times 10^{31}$ at 1 keV photon energy. The demonstrated atomic XRL scheme enhances the capability of present day XFEL sources. Moreover, in contrast to the SASE based XFELs, the atomic XRL is expected to be longitudinally coherent and has a stable wavelength centroid, i.e. a highly reproducible spectrum, and a much narrower bandwidth.

2. Demonstration of a 100 Hz Repetition Rate Table-Top Soft X-Ray Laser.

The average power of plasma-based soft x-ray lasers has been limited by the 10 Hz by the repetition rate of the solid state optical lasers that drive them. To overcome this limitation we have developed a compact, directly diode-pumped CPA laser based on cryogenically-cooled Yb:YAG that produces 1 Joule, 5 ps FWHM duration, $\lambda = 1.03$ μm laser pulses at 100 Hz. This laser was employed to drive a gain-saturated 18.9 nm soft x-ray laser in a nickel-like Mo plasma producing a record high average power of \sim 0.15 mW. Strong lasing at 13.9 nm was also achieved at 100 Hz repetition rate from a Ag plasma.



These results increased the repetition rate and average power of compact sub-20 nm lasers by an order of magnitude, opening new applications in nanoscale surface imaging and nano-scale materials processing.

Fig. 4 shows an schematic diagram of the diode-pumped table-top CPA laser that drives the soft x-ray laser. The system produces 1 Joule, 5 ps laser pulses at 100 Hz repetition rate. In order to achieve lasing at 18.9 nm in the $4d^1S_0 - 4p^1P_1$ transition of Ni-like Mo the pump pulses were focused at a grazing incidence angle of 29° onto a polished Mo target to form a 5.5 mm FWHM long by ~30 μm wide line intensity. Figure 4a shows the resulting soft x-ray laser pulse energy as a function of plasma length. The laser pulse energy is seen to increase exponentially with a gain coefficient of 43 cm⁻¹ until it reaches gain saturation at a plasma column length of ~3.5 mm. Fig. 4b shows consecutive $\lambda=18.9$ nm laser pulses obtained operating the laser at 100. The mean laser pulse energy is 1.5 μJ with a standard deviation of 11.5%. The corresponding laser average power is 0.15 mW, the highest value reported to date for coherent table-top source at a sub-20 nm wavelength.

Journal publications resulting from DOE-BES supported work (2010-2012)

1. L. Urbanski, M.C. Marconi, L.M. Meng, M. Berrill, O. Guilbaud, A. Klisnick, J.J. Rocca, "Spectral linewidth of a capillary discharge Ne-like Ar soft X-ray laser and its dependence on amplification beyond gain saturation", *Physical Review A*, **87**, 033837, (2012).
2. N. Rohringer, D. Ryan, R. London, M. Purvis, F. Albert, J. Dunn, J.D. Bozek, C. Bostedt, A. Graf, R. Hill, S.P. Hau-Ridge, J.J. Rocca, "Inner-shell X-ray laser at 1.46 nm pumped by an X-ray free electron laser", *Nature*, **481**, 488, (2012).
3. S. Carbajo, I.D. Howlett, F. Brizuela, K.S. Buchanan, M.C. Marconi, W. Chao, E.H. Anderson, I. Artiukov, A. Vinogradov, J.J. Rocca and C.S. Menoni, "Sequential single-shot imaging of nano-scale dynamic interactions with a table-top soft x-ray laser", *Optics Letters*, **37**, 2994 (2012).
2. B. Reagan, K. Wernsing, A. Curtis, F. Furch, B. Luther, D. Patel, C.S. Menoni, J.J. Rocca, "Demonstration of a 100 Hz repetition rate gain-saturated diode-pumped soft x-ray laser". *Optics Letters*, (in press, Doc. ID 171866, September 2012).
3. H. Bravo, B.T. Szapiro, P. Wachulak, M.C. Marconi, W. Chao, E.H. Anderson, D.T. Attwood, C.S. Menoni, J.J. Rocca, "Demonstration of nanomachining with focused EUV laser beams", *IEEE J. of Sel. Top. in Quant. Elect.*, **18**, 443, (2012)
4. D. Alessi, Y. Wang, D. Martz, B. Luther, L. Yin, D. Martz, M.R. Woolston, Y. Liu, M. Berrill, J.J. Rocca, "Efficient excitation of gain-saturated sub-9 nm wavelength table-top soft X-ray lasers and lasing down to 7.36 nm", *Physical Review X*, **1**, 021023 (2011)
5. L.M. Meng, D. Alessi, O. Guilbaud, Y. Wang, M. Berrill, B.M. Luther, S.R. Domingue, D.H. Martz, D. Joyeux, S. De Rossi, J.J. Rocca, A. Klisnick, "Temporal coherence and spectral linewidth of an injection-seeded transient collisional soft x-ray laser", *Optics Express*, **19**, 12087, (2011)
6. D. Alessi, D.H. Martz, Y. Wang, M. Berrill, B.M. Luther, J.J. Rocca, "1 Hz Operation of a Gain-Saturated 10.9 nm Table-Top Laser in Nickel-like Te," *Optics Letters*, **35**, 414 (2010).
7. M. Berrill, D. Alessi, Y. Wang, S. Domingue, D.H. Martz, B.M. Luther, Y. Liu, J.J. Rocca, "Improved beam characteristics of solid-state target soft x-ray laser amplifiers by injection seeding with high harmonics", *Optics Letters*, **35**, 2317, (2010)

Spatial Frequency X-ray Heterodyne Imaging of Micro and Nano structured Materials and their Time-resolved Dynamics

Christoph G. Rose-Petruck

Department of Chemistry, Box H, Brown University, Providence, RI 02912
phone: (401) 863-1533, fax: (401) 863-2594, Christoph_Rose-Petruck@brown.edu

Program Scope

A novel x-ray imaging concept named X-ray Spatial Frequency Heterodyne Imaging (XSFHI) is developed. As the name suggests the technique relies on the introduction of a “local oscillator” in the spatial frequency space of an x-ray image. Mathematical cross-terms between the local oscillator and the spatial frequency spectrum of the sample, lead to signal enhancements of selectable spatial frequency components that result in image contrast enhancements by orders of magnitude. In contrast to conventional or phase contrast x-ray imaging, a single exposure can be processed to obtain 1) the traditional x-ray absorption image and 2) an image formed exclusively by deflected or scattered x-rays. The signal in the scattered radiation image is depended on, for instance, the size and orientation of nanostructures or phase interfaces in the sample. We have demonstrated that the image contrast is several orders of magnitude larger than that of phase contrast, which itself typically is 3 orders of magnitude larger than for conventional x-ray absorption imaging. For high emittance x-ray sources or motion blurred samples, the XSFHI makes phase contrast features visible that would otherwise be undetectable. The method does not use any x-ray optics and is well-suited to time resolved imaging studies.

1 Recent Progress

During the last year progress has been made in three research topics funded by this DOE grant.¹⁻⁸

1.1 X-ray Spatial Frequency Heterodyne Imaging theory

The method of in-line X-ray phase contrast imaging^{7,8} provides image contrast that depends on deflections in the X-radiation by index of refraction variations in the object. The salient feature of the method is that it not only records the absorption seen in conventional X-ray imaging, but responds as well to phase variations, so that, in practice, the image appears with highlighted features at the boundaries of objects. Recently, it has been shown that contrast in in-line X-ray phase contrast images can be enhanced by placing a grating in contact with the object, and, following recording an image, viewing harmonics of intensity at the grating frequency.¹⁻³ This year we published¹ the mathematical framework of this imaging concept based on the Kirchhoff-Fresnel integral. We carried out calculations and experiments for X-ray phase contrast imaging showing that the placement of a grating adjacent to the object results in spatial heterodyning of the phase and absorption features of the object. The detected image consists of a conventional absorption and a heterodyned component. The intensity of this heterodyned component is:

$$I_{+2} = \sqrt{\left[1 + 2(\sin(\beta) - \beta \cos(\beta)) \phi(\bar{x}) + \frac{\lambda z}{2\pi} \cos(\beta) \phi''(\bar{x})\right]^2 + \left[\frac{\lambda z}{2\pi} k_g \cos(\beta) \phi'(\bar{x})\right]^2} \quad (1)$$

with

$$\beta = \lambda z k_g^2 / 4\pi = \lambda z \pi / a^2 \quad (2)$$

And the object-detector distance z , the x-ray wavelength λ , the wavenumber k_g of the grid, and the grid period a . For typical experimental setups using hard x-rays, β is small and (1) simplifies to

$$I_{+2} = \sqrt{\left[1 + \frac{\lambda z}{2\pi} \phi''(\bar{x})\right]^2 + \left[\frac{\lambda z}{2\pi} k_g \phi'(\bar{x})\right]^2}, \quad (3)$$

which shows an altogether new dependence of image contrast on the first space derivative of the phase ϕ' with an amplitude enhancement factor of $\lambda z / 2\pi k_g$ arising from heterodyning of the spatial frequencies of the object with that of the grating. The image contrast is expected to be dominated by ϕ' rather than ϕ'' because the latter is multiplied by the factor $\lambda z / 2\pi$ which is small in the X-ray spectral region. Note that the intensity of the 1st derivative can be “amplified” by choosing a finer pitch, i.e., larger k_g , grating. We have tested these equation in ref. ¹.

1.2 XSFH imaging in the soft x-ray water window

For soft x-rays, β may become large and the approximations that lead to (1) are not be valid any more. In that case, the Fresnel-Kirchoff Integral has to be solved rigorously. In order to compare the exact, numerical solution with the experimental data, we performed x-ray imaging experiment in the x-ray water window at a wavelength of

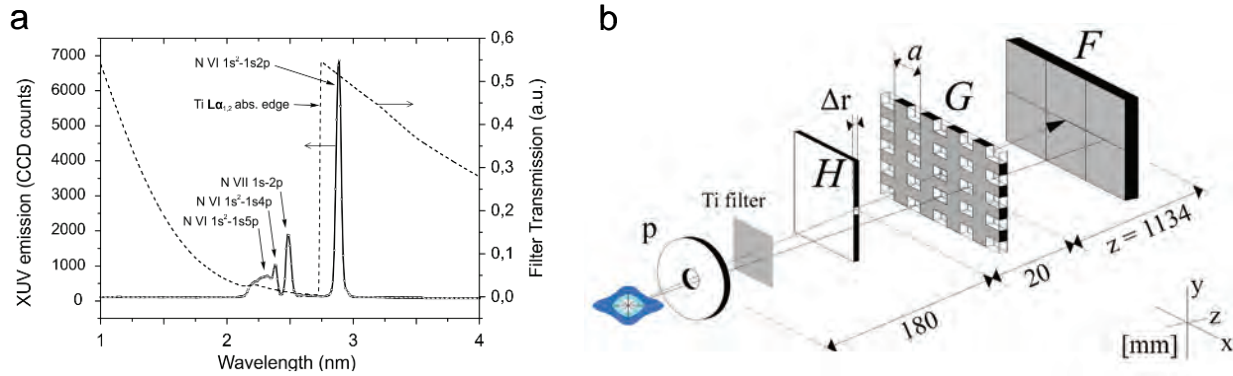


Figure 2: a: Measured soft X-ray emission spectrum of the nitrogen plasma. A calculated 400-nm tick Ti-filter transmission curve is superimposed over the emission spectrum. The filter suppresses all plasma emission except the $N^{6+} 1s2p \rightarrow 1s^2$ line. The temporal coherence was measured as $\Delta E/E = 0.05$.

b: Diagram of the XSFHI setup. The soft x-ray spectrum emitted from the Nitrogen plasma is monochromatized with a Ti filter mounted close to the pinhole p . The sample H , a Kapton foil edge, is mounted between the source and the grid G . The radiation propagates through the grid and it detected by the detector F . The dimensions in z -direction of the setup are indicated in the sketch.

2.88 nm. Furthermore, the effect of the relative spatial phase of the grid and the object was studied. For the verification of the XSFHI theoretical model, we measured and simulated a simple object – an edge of 1- μm thick Mylar foil using a monochromatic, soft x-ray source located at the Czech Technical University. The soft x-radiation is produced by illuminating a N_2 gas jet with a 750-mJ, 7-ns, 1064-nm laser pulses focused to a 60- μm diameter spot. The resulting emission spectrum in the x-ray water window is shown in Figure 2 a. The radiation is transmitted through a 20- μm diameter pinhole and filtered by a 400-nm Ti-foil, which transmits only the $1s2p \rightarrow 1s^2$ emission line at 2.88 nm wavelength from Helium-like Nitrogen. The sample was placed 20 mm downstream from the 1000 lpi nickel grid 02899N-AB (SPI). The rather long x-ray wavelength along with the dimension of the setup shown in Figure 2 b, results in a large $\beta = 4.1$. Thus, equation (3) is not applicable any more.

The spatial phase dependence of the signal has been studied by intentionally positioning the grid and the foil as a small relative angle. This arrangement causes a shift of the relative positions along the vertical direction. Measured intensity profiles of a plain grid and a grid with sample were subject to Fourier transformation analysis resulting in the heterodyned image shown in the Figure 1. Of particular interest is part d of the figure. This XSFH image shows a vertical line that is very “wavy”. This effect is not an artifact or a random variation but its intensity is oscillating as a function of position in vertical direction. This effect is caused by the variation of the differential phase between the grid and the foil’s edge. The experimental

and theoretical data are compared in Figure 3. The phase contrast data in panel a and b are in good agreement, the XSFHI in panel c and d are in approximate agreement. This analysis is ongoing. However, we can already estimate the sensitivity of a position measurement of the foil edge. Figure 4 shows the lineout of the XSFH intensity taken along the direction indicated in Figure 1 d. The intensity oscillates very non-linearly. The slope around 15 μm is 40% /

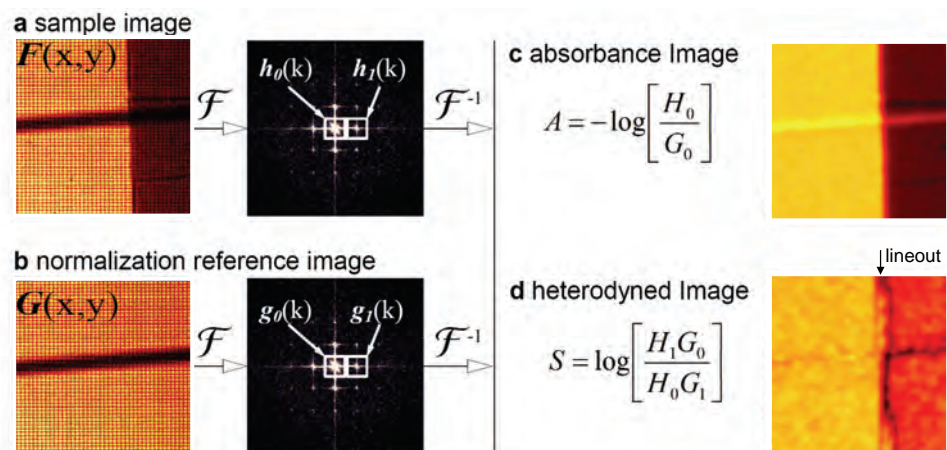


Figure 1: Reconstruction of the absorption and scatter components from a measured sample and reference image. **a:** Measured sample image; the Kapton foil is visible on the right of the image (darker area). The horizontal bar is the support of the Ti-filter and is not related to the image analysis. Fourier transformation yields the spatial frequency spectrum. **b:** image of the grid without foil; **c:** Absorbance image calculated according to the formula; **d:** XSFH image calculated according to the formula.

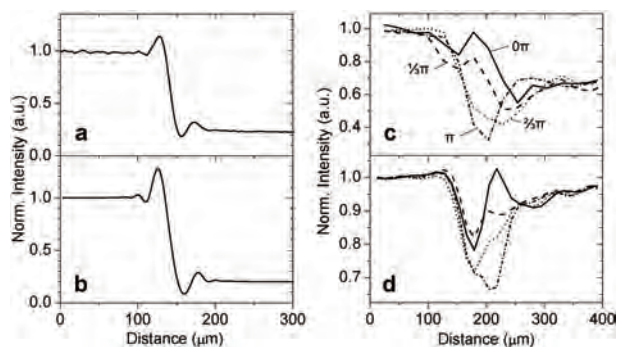


Figure 3: Comparison of measured (a) and simulated (b) phase contrast profiles of a sample (edge of a 1- μm Mylar foil) soft X-ray radiograph. The heterodyned signals from (c) the measured image and (d) the simulated intensity profile oscillate with varying lateral displacement of the grid and the edge.

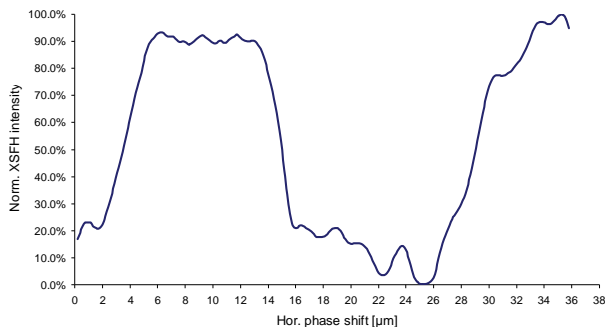


Figure 4: Lineout of the normalized XSFH intensity from panel (d) in Figure 1 as a function of horizontal XSFHift between the foil edge and the grid.

μm . With sufficient flux and resulting high signal-to-noise, an intensity measurement of 1% is certainly possible. This translates into a 25-nm sensitivity for the position measurement of the a samples edge! It is important to note that this sensitivity is possible although the spatial resolution of the imaging system is 5 μm .

1.3 Application of XSFHI to temperature dependent phase transitions of water in carbon nanotubes

Water in confined spaces can show unusual properties that are not observed in the bulk. Carbon Nanotubes (CNTs) are made of hydrophobic graphene sheets. Despite the hydrophobic nature of the grapheme sheets, experimental studies have revealed that water can be confined in CNTs. Transmission Electron Microscopy (TEM) and x-ray diffraction have been used to probe the behavior of water in CNTs. Our objective is to develop SFXHI as an X-ray detection method suitable for studying phase transitions in nanomaterials.

Commercially available CNTs have a large fraction of closed tubes. One of such tubes is shown in Figure 5a. When exposed to water vapor, such tubes may wet on the outside but can not be filled with water. Vacuum annealing of CNT at about 800 K opens the tubes, as shown in Figure 5b, and makes their inside accessible to water.

We prepared samples of treated and untreated CNTs and compared their intensities in XSFH images. Since the untreated CNTs can only wet on the outside while treated CNTs can wet on the inside as well, the difference in signal intensities are a measure of the water filling of the treated CNTs.

The experimental setup is depicted in Figure 6. Heat-treated (open) and un-treated (closed) carbon nanotubes (multiwall, OD 15 ± 5 nm, ID 7 ± 2 nm, length 1-5 micron) were prepared.

Heat-treated and untreated nanotube samples were sealed in quartz vials under vacuum (either dry or with a drop of water) and imaged by XSFHI. The nanotube samples were imaged at room temperature before being heated to 80°C and imaged again. The elevated temperatures causes water to be expelled from the open nanotubes, leading to change in the scattering properties of the nanotubes at different temperatures. Signal intensities for the nanotube samples at 80°C were normalized by the signal in those same samples at room temperature:

The ratios obtained from the absorption images are all smaller than 1; this indicates that there is less material in the viewing field at elevated temperatures than there is at room temperature, suggesting that water has been expelled from the

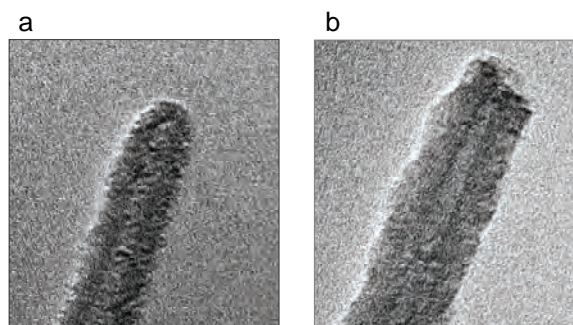


Figure 5: 200-kV TEM images at a magnification of 300,000; **a:** Closed nanotube before heat treatment. **b:** Open nanotube after heat treatment.

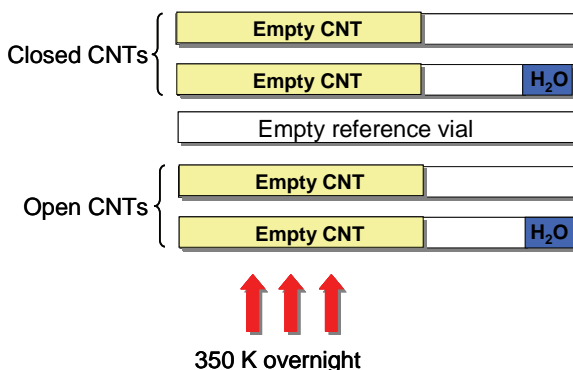


Figure 6: Scheme of the CNT sample setup. A

	Untreated wet CNTs	Untreated dry CNTs	Heat-treated dry CNTs	Heat-treated wet CNTs
Absorption image	0.91 ± 0.001	0.94 ± 0.001	0.94 ± 0.002	0.79 ± 0.007
XSFHI image	4 ± 1.1	7.4 ± 2.024	7.6 ± 2.0	35 ± 9.4

Table 1: Summary of the XSFHI measurements taken on closed and open CNTs.

nanotubes. This effect is most drastic for the heat-treated wet nanotubes, where we expect to have the most open-ended CNTs. The ratios obtained from the x-ray scatter images are all larger than 1; this indicates that there is more scattering at elevated temperatures than there is at room temperature. Again, this effect is most drastic for the heat-treated wet CNTs. The data are summarized in Table 1. Scattering by the heat-treated wet tubes increases by a factor of approximately 35 as the temperature increases. Compared to the untreated CNTs the data show an enhancement of the x-ray scatter intensity by a factor 5, which we attribute exclusively to the accumulation of water inside of the nanotubes.

While the physical effect is obvious, it is not clear yet why water filling of the CNTs causes a reduction of the XSFHI intensity. Several factors contribute to this effect: Filled CNTs have a larger average index of refraction than empty CNTs, which should cause increased small-angle x-ray scatter intensity. On the other hand, the imaging modality is not uniformly sensitive to all diffraction angles. Thus, while the integral of the scattered x-rays from the water-filled tubes is likely higher, the empty tubes may scatter into angles at which the imaging modality is more sensitive. The calibration of the sensitivity of the modality to the particles size is currently being studied using nanoparticles of well-known diameters.

Future plans

The goal of the present funding cycle is to continue the research on Spatial Frequency X-ray Heterodyne Imaging and related techniques using the setups at 7ID-C and at Brown University. Specifically, we will

1. continue the development of the theoretical framework of X-ray Spatial Frequency Heterodyne Imaging,
2. continue XSFHI experiments using the laser-driven plasma x-ray source at Brown University. The goal is to obtain information on the micro-scale structural dynamics during chemical reactions. Primary application: phase transitions in nanoparticle suspensions and in clathrate hydrate slurries.
3. Continue the studies of the phase transitions in CNTs
4. Carry out ultrafast x-ray powder diffraction measurements on melting clathrate hydrates.
5. Implement XSFHI at 7 ID-C in order to carry out phase contrast and XSFH imaging experiments with high spatial resolution and in the anomalous dispersion regime of transition metals in preparation for future ultrafast oxidation state sensitive x-ray heterodyne imaging.

Papers acknowledging this DOE grant

1. "Spatial frequency x-ray heterodyne imaging," B. Wu, Y. Liu, C. Rose-Petruck and G. J. Diebold, *Applied Physics Letters* 100, 061110 (2012).
2. "X-ray spatial harmonic imaging of phase objects," Y. Liu, B. Ahr, A. Linkin, G. J. Diebold and C. Rose-Petruck, *Optics Letters* 36, 2209 (2011).
3. "Nanomaterials for X-ray Imaging: Gold Nanoparticle Enhancement of X-ray Scatter Imaging of Hepatocellular Carcinoma," D. Rand, V. Ortiz, Y. L. Z. Dardak, J. R. Wands, M. Tatiček and C. Rose-Petruck, *Nanoletters* 11 (7), 2678 (2011).
4. "2-ps Hard X-Ray Streak Camera Measurements at Sector 7 Beamline of the Advanced Photon Source (invited)," M. Chollet, B. Ahr, D. A. Walko, C. Rose-Petruck and B. Adams, *Selected Topics in Quantum Electronics, IEEE Journal of* 99, 1 (2011).
5. "Hard X-ray streak camera at the advanced photon source," M. Chollet, B. Ahr, D. A. Walko, C. Rose-Petruck and B. Adams, *Nuclear Instruments and Methods in Physics Research Section A: Accelerators, Spectrometers, Detectors and Associated Equipment* 649 (1), 70 (2011).
6. "Picosecond x-ray absorption measurements of the ligand substitution dynamics of Fe(CO)₅ in ethanol," B. Ahr, M. Chollet, B. Adams, E. M. Lunny, C. M. Laperle and C. Rose-Petruck, *Phys. Chem. Chem. Phys.* 13 (Also PCCP Cover Page, April 2011) (13), 5590 (2011).
7. "X-ray Phase Contrast Imaging: Transmission Functions Separable in Cylindrical Coordinates," G. Cao, T. Hamilton, C. M. Laperle, C. Rose-Petruck and G. J. Diebold, *J. Appl. Phys.* 105, 102002 (2009).
8. "X-ray elastography: Modification of x-ray phase contrast images using ultrasonic radiation pressure," T. J. Hamilton, C. Bailat, S. Gehring, C. M. Laperle, J. Wands, C. Rose-Petruck and G. J. Diebold, *Journal of Applied Physics* 105 (10), 102001 (2009).

Tamar Seideman
Department of Chemistry, Northwestern University
2145 Sheridan Road, Evanston, IL 60208-3113
t-seideman@northwestern.edu

Toward Controlled Electronic Dynamics in Complex Systems

1. Program Scope

Our DOE-supported research during the past year can be broadly categorized into two conceptually and practically related topics: (1) extension of the concept of nonadiabatic alignment from the domain of isolated, rigid diatomic molecules to complex systems; and (2) development and application of theoretical and numerical tools to explore new opportunities in the area of high harmonic generation (HHG) from aligned molecules. Whereas the first topic was the thrust of our original application, the second was motivated by the intense interest of the AMOS Program in attosecond science and rescattering electrons physics, and has been mostly carried out in collaboration with AMOS experimentalists colleagues.

Within the first part, we applied during the past year coherent alignment to chirality control, manipulation of nuclear spin isomers, control of electron transport via molecular junctions, a coherent approach to probe solute-solvent interactions, and a newly discovered field-induced molecular assembly phenomenon. This work is summarized in Secs. 2.1–2.4. Completion of this research, in the next year (Sec. 3.1), will hopefully accomplish our ultimate goal of extending alignment from the domain of physics and optics to make a tool in material science, solution chemistry, and possibly engineering. Within the second part of our DOE-supported research during the past year, we collaborated with the Bucksbaum and Martinez groups on the problem of HHG from aligned asymmetric top molecules (Sec. 2.5) and with the group of Murnane and Kapteyn on two projects in the field of HHG from aligned linear molecules (Secs. 2.6, 2.7). Numerical work on the information content of the ellipticity of high-order harmonics is briefly summarized in Sec. 2.8. In addition, we continued our efforts to develop improved numerical methods to compute the electronic dynamics underlying HHG. Our plans for further research in the area of attosecond physics and HHG during the next funding period is outlined in Sec. 3.2.

2. Recent Progress

2.1 Laser-Induced Ordered Molecular Assembly and Collective Alignment

We explored the physics of alignment and three-dimensional alignment of polyatomic molecular ensembles in moderately-intense laser fields. To that end we developed a purely classical approach to molecular alignment and compared its results with those of quantum mechanical calculations in appropriate limits, finding qualitative agreement. An article was published in a Special Issue of *Mol. Phys.*¹

The method was used to illustrate a new phenomenon in the dynamics of molecular ensembles subjected to moderately intense, far-off-resonance laser fields, namely, field-driven formation of perfectly ordered, defect-free assembly. Interestingly, both the arrangement of the constituting molecules within the individual assembly and the long range order of the assembly with respect to one another are subject to control through choice of the field polarization. Relying on strong induced dipole-induced dipole interactions that are established in dense molecular media, the effect is entirely general. An article was submitted for publication in *Phys. Rev. Lett.*²

2.2 Coherent Torsional Alignment. Chirality Control and Nuclear Spin Dynamics

Our previous DOE-supported research (Ramakrishna and Seideman, *Phys. Rev. Lett.* 99, 103001 (2007)) introduced the concept of torsional alignment and proposed a wide range of applications. A first experimental realization of our approach was reported by Madsen *et al* (*Phys. Rev. Lett.* 102, 073007 (2009)) and two further experiments were published more recently. Our work on torsional alignment this year generalized the approach to fix the torsional angles of polyatomic molecules to an arbitrary value and developed a numerical scheme to simulate the torsional dynamics. By choice of the field parameters, the method can be applied either to drive the torsion angle to an arbitrary configuration or to induce free internal rotation. Transient absorption spectroscopy was suggested as a probe of torsional control and the usefulness of this approach was numerically explored. An article appeared in *J. Chem.*

Phys.³

The approach was extended to control the chirality of molecules exhibiting torsion using a series of laser pulses. Optimal control theory was applied as a tool to maximize the enantiomeric ratio achieved by the control field in two different cases: fixed polarization and variable polarization. Our simulations showed maximum enantiomeric ratios of 24 and 50 for the fixed and variable polarization cases, respectively. An article appeared in a Special Issue of Mol. Phys.⁴

In a second extension of coherent torsional alignment, we illustrated, by means of group theoretical arguments, that this effect depends critically on the nuclear spin of the molecule, hence nuclear spin isomers can be manipulated selectively by a sequence of time-delayed laser pulses. Nuclear spin selective control of the angular momentum distribution was applied to separate the nuclear spin isomers of a polyatomic molecule. An article appeared in J. Chem. Phys.⁵

2.3 Laser Orientation as a Route to Ultrafast Control of Transport in the Nanoscale

Extending our previous DOE-supported research (Phys. Rev. Lett. 101, 208303 (2008); Nature Photonics 3, 4–5 (2009)), where coherent orientation was applied to introduce an ultrafast nanoscale electron switch, we explored the more general problem of the controllability of surface-adsorbed molecules by moderately intense laser fields. Our research introduced the possibility of orientational control of single molecules, and illustrated the new possibilities (and new fundamental questions) arising from plasmonic enhancement of the laser field and substrate enhancement of the molecular polarizability. To that end we developed a 2-dimensional potential energy surface for an organic molecule adsorbed onto a silicon surface and subject to an STM tip, and developed a fast spherical harmonics method to study the corresponding field-driven dynamics. We proposed a molecular system that would make a convenient candidate for experimental realization, and explored the role played by the lateral and vertical positions of the tip. Our results suggest the potential of laser alignment schemes to control electronic processes on surfaces and in junctions.

2.4 Toward Rotational Probes of Exotic Media

In collaborative research with an experimental group, we combined quantum calculations with soft X-ray free-electron laser techniques to introduce a new approach to explore molecular rotations in the time-domain. Near-infrared femtosecond laser pulses were used to excite a coherent superposition of two rotational states of carbon monoxide. The associated wave packet motion was then followed in time by soft X-ray Coulomb explosion. The coupling of the $J = 0$ and $J = 2$ states resulted in an asymmetry of the spatial fragmentation patterns and a time-dependent asymmetry oscillation that prevails for over a ns, covering more than 300 revivals with neither dephasing nor dissipation. This observation can serve as a route to real-time disentangling of intra- and inter-molecular rotational couplings occurring in complex systems and environments, hence a potential probe of interesting media. An article appeared in Phys. Rev. A.⁷

2.5 High Harmonic Generation in Rotating Quantum Asymmetric Tops

In collaborative research with the groups of Bucksbaum and Martinez, we studied HHG in impulsively aligned quantum asymmetric tops. We quantified the angular contributions of HHG emission, making use of the full rotational revival structure. Our results were shown sensitive to all five prolate top revival types and to fractional and multiple revivals, providing a new view of polyatomic rotations. Finally, we illustrated that not only the HOMO orbital shape, but also the orientation dependence of the recombination dipole controls the harmonic efficiency. This finding has implications for HHG-based tomographic imaging. An article was submitted to Phys. Rev. Lett.⁸

2.6 Ultrafast Elliptical Dichroism in High-Order Harmonics

Collaborative research with the group of Murnane and Kapteyn explored the new physics and new opportunities introduced upon illumination of aligned molecules by an elliptically polarized, high intensity laser field, where emission of elliptically polarized high-order harmonics of the driving field ensues. The surprising experimental observations of ultrafast elliptical dichroism in the harmonic emission as the ellipticity of the driving field and the molecular alignment are scanned, were explained within a simple model in which both the collision angle of the continuum electron with the molecule and the interference between recombination at multiple charge centers play a role. Our analysis ties the observed elliptical dichroism to the journey of the continuum electron in the field and the underlying bound state of the molecular ion. These results show how to use molecular structure and alignment to manipulate the polarization state of high-order harmonics, and also present a potential new attosecond probe of the underlying molecular system. Specifically, information about molecular orbital structure is contained

both in the value of the HHG dichroism as a function of laser ellipticity and laser-molecule angle, and in the variations with harmonic order. An article was submitted to Phys. Rev. Lett.⁹

2.7 Extracting Continuum Electron Dynamics from High Harmonic Emission

In a second collaborative project with the group of Murnane and Kapteyn, we illustrated the sensitivity of high harmonic signals to rotational wavepacket revivals, revealing very high order rotational revivals for the first time using any probe. By fitting high-quality experimental data to the exact theory of high harmonic generation from aligned molecules developed in our previous DOE-supported research (Ramakrishna and Seideman, Phys. Rev. Lett. 99 113901 (2007)), we were able to extract the underlying electronic dipole elements for high harmonic emission and uncover that the electron gains angular momentum from the photon field. An article appeared in Phys. Rev. Lett.¹⁰

2.8 Signatures of the Molecular Potential in the Ellipticity of High-Order Harmonics

Building upon our previous DOE-supported research,¹¹ which illustrated that the phase of the continuum electronic wavefunction, and hence the underlying molecular potential, is responsible, at least in part, for the ellipticity observed in harmonic spectra, we conducted a numerical study to explore the information content of the polarization of high-order harmonics emitted from aligned molecules driven by a linearly polarized field. We used a simple model potential and systematically varied the potential parameters to investigate the sense in which, and the degree to which, the shape of the molecular potential is imprinted onto the polarization of the emitted harmonics. Strong ellipticity was observed over a wide range of potential parameters, suggesting that the emission of elliptically polarized harmonics is a general phenomenon, yet qualitatively determined by the molecular properties. The sensitivity of the ellipticity to the model parameters invites the use of ellipticity measurements as a probe of the continuum wavefunction and the underlying molecular potential. An article appeared in Phys. Rev. A.¹²

3. Future Plans

3.1 Alignment, Orientation, and Torsional Alignment in Complex systems. Toward Applications in Material Science

During the next funding period, we will explore three new applications of intense laser alignment in material science. The first study, in collaboration with a Northwestern experimental group, will establish long-range orientational order in an assembly of semiconductor nanorods. The theoretical component will involve a molecular dynamics study using analytical polarizabilities and two-body interactions. The second study will apply torsional alignment of an adsorbed biphenyl derivative to introduce an approach to ultrafast electron spin flipping. Here, use will be made of the recent experimental illustration that chiral molecules adsorbed onto a gold surface can serve as a spin filter for electrons that are photoejected from the metal substrate and are transmitted through the molecules. A third study will establish an approach, based on torsional alignment, to enhance desired forward electron transfer processes while suppressing undesired back transfer processes, which hamper charge separation. One example where such selective torsional control may find important applications is artificial photosynthesis-like solar cells. Another is charge transfer from a semiconducting quantum dot into a bulk semiconductor via a bridge, relevant, for instance, to the problem of designing efficient quantum-dot-sensitized solar cells and to the application of quantum dots in catalysis.

3.2 HHG and Attosecond Science. Method Development and Applications

One goal of our research in the area of HHG and attosecond science during the next funding period is to continue and extend our already fruit bearing collaborative work with the group of Murnane and Kapteyn and with the groups of Bucksbaum and Martinez. Within the first collaboration, we will generalize the theory of Ref. 10 and combine it with measurements of the harmonic phases, currently being initiated, to derive the phases of the electronic dipole elements underlying the HHG process. We hope to introduce a true inversion of the complex dipole elements to extract the continuum electron dynamics. The second collaboration will focus on the problem of HHG from aligned asymmetric top polyatomics.

A second goal of this research is to develop a new numerical method for calculation of HHG signals that will extend our current capabilities, Ref. 11, in a significant way. Our approach will be based on a real time time-dependent density functional theory (TDDFT), currently under development in our group. We will test the new method by application to the case of simple linear molecules, for which we currently have reliable results from solutions of the Schrödinger equation. It will be our main goal, however, to

extend the method to polyatomic molecules. Here we will combine our (already tested) approach to establishing 3D alignment by means of elliptically polarized fields¹³ with a TDDFT solution of the driven electronic dynamics. These studies will be complemented by semiclassical trajectory calculations that will serve both to provide qualitative insights and to simplify aspects of the calculation.

4. Publications from DOE sponsored research(past three years, in citation order)

1. M. Artamonov and T. Seideman, *Three-Dimensional Laser Alignment of Polyatomic Molecular Ensembles*, Special Issue of Molecular Physics **110**, 885 (2012) (**invited**).
2. M. Artamonov and T. Seideman, *Laser-Induced Ordered Molecular Assembly*, submitted for publication in Phys. Rev. Lett.
3. S. M. Parker, M. A. Ratner and T. Seideman, *Coherent Control of Molecular Torsion* J. Chem. Phys. **135**, 224301 (2011).
4. S. M. Parker, M. A. Ratner and T. Seideman, *Coherent Optimal Control of Axial Chirality*, Special Issue of Molecular Physics, in press (**invited**).
5. J. Floss, T. Grohmann, M. Leibscher, and T. Seideman, *Nuclear Spin Selective Torsional Control*, J. Chem. Phys. **136**, 084309 (2012).
6. M. Reuter, M. A. Ratner and T. Seideman, *Laser Alignment as a Route to Ultrafast Control of Electron Transport through Junctions* Phys. Rev. A in press.
7. A. Przystawik, A. Al-Shemmary, S. Dusterer, M. Harmand, A. Kickermann, H.Redlin, L. Schroedter, M. Schulz, N. Stojanovic, S. Toleikis, T. Laarmann, A. M. Ellis, K. von Haeften, F. Tavella, J. Szekeley and T. Seideman, *Generation of the Simplest Rotational Wave Packet in a Diatomic Molecule: Microwave Spectroscopy in the Time Domain without Microwaves*, Phys. Rev. A **85**, 052503 (2012).
8. L. S. Spector, M. Artamonov, S. Miyabe, Todd Martinez, T. Seideman, M. Guehr, and P. H. Bucksbaum, *High Harmonic Generation in Rotating Quantum Asymmetric Tops Reveals New Aspects of Electronic Structure*, submitted for publication in Phys. Rev. Lett.
9. P. A. J. Sherratt, R. M. Lock, X. Zhou, H. C. Kapteyn, M. M. Murnane, and T. Seideman, *Ultrafast Elliptical Dichroism in High-Order Harmonics as a Probe of Molecular Structure and Electron Dynamics*, submitted for publication in Phys. Rev. Lett.
10. R.M. Lock, S. Ramakrishna, X. Zhou, H.C. Kapteyn, M.M. Murnane, and T. Seideman, *Extracting Continuum Electron Dynamics from High Harmonic Emission from Molecules*, Phys. Rev. Lett. **108**, 133901 (2012).
11. S. Ramakrishna, P. Sherratt, A. Dutoi and T. Seideman, *Origin of Ellipticity in High Harmonic Generation from Aligned Molecules*, Phys. Rev. A Rapid Communication **81**, 021802(R) (2010).
12. P. Sherratt, S. Ramakrishna and T. Seideman, *Signatures of the Molecular Potential in the Ellipticity of High-Order Harmonics from Aligned Molecules*, Phys. Rev. A 053425 (2011).
13. M. Artamonov and T. Seideman, *On the Optimal Approach to Field-Free 3D Alignment of Asymmetric Tops*, Phys. Rev. A **82**, 023413 (2010).
14. M. Artamonov and T. Seideman, *Molecular Focusing and Alignment with Plasmon Fields*, Nano Letters, **10** 4908 (2010).
15. G. Pérez-Hernández, A. Pelzer, L. Gonzalez and T. Seideman, *Biologically Inspired Molecular Machines Driven by Coherent Light. A unidirectional Rotor*, Special Issue of New J.Phys. **12** 075007 (2010).
16. C. Marceau, S. Ramakrishna, S. Génier, T.-J. Wang, Y. Chen, F. Théberge, M. Châteauneuf, J. Dubois, T. Seideman, and S. L. Chin, *Femtosecond Filament Induced Birefringence in Argon and in Air: Ultrafast Refractive Index change*, Optics Communications **283**, 2732 (2010).
17. D. Shreenivas, A. Lee, N. Walter, D. Sampayo, S. Bennett and T. Seideman, *Alignment as a Route to Control of Surface Reactions*, J. Phys. Chem. **114**, 5674 (2010)
18. A. Azarm, S. Ramakrishna, A. Talebpour, S. Hosseini, Y. Teranishi, H. L. Xu, Y. Kamali, J. Bernhardt, S. H. Lin T. Seideman, and S. L. Chin, *Population Trapping and Rotational Revival of N₂ Molecules During Filamentation Of A Femtosecond Laser Pulse in Air*, J. Phys. B. **43**, 235602 (2010).
19. S. S. Viftrup, V. Kumarappan, L. Holmegaard, H. Stapelfeldt, M. Artamonov and T. Seideman, *Controlling the Rotation of Asymmetric Top Molecules by the Combination of A Long and A Short Laser Pulse*, Phys. Rev. A, **79**, 023404 (2009).
20. I. Nevo, S. Kapishnikov, A. Birman, M. Dong, S. R. Cohen, K. Kjaer, F. Besenbacher, H. Stapelfeldt, T. Seideman, L. Leiserowitz, *Inducing Alignment in Self-Assembled Molecules on the Water Surface via Linearly Polarized Laser Pulses*, J. Chem. Phys. **140**, 144704 (2009).
21. N. Elghobashi-Meinhardt, L. González, I. Barth, and T. Seideman, *Few-Cycle Laser Pulses to Obtain Spatial Separation of OHF⁻ Dissociation Products*, J. Chem. Phys. **130**, 024310 (2009).

Inelastic X-ray Scattering Under Extreme and Transitional Conditions

Gerald T. Seidler, seidler@uw.edu,
Department of Physics
University of Washington
Seattle, WA 98195-1560

Program Scope

The goal of this program is to expand the scope and scientific potential of time-resolved inelastic x-ray scattering (IXS). First, we are performing combined theoretical and experimental work to critically test, and substantially improve, the use of IXS methods in the study of dense plasmas, such as in the transitional, ‘warm dense matter’ regime. Second, we are using x-ray spectroscopies, soon to include resonant inelastic x-ray scattering, to gain new insight into the energy transfer mechanisms of lanthanide-based phosphors and related luminescent materials and to study the time dynamics of the electronic and structural changes at metal-insulator transitions. Finally, we are continuing several collaborations based on IXS instrumentation and methods developed by the PI, including studies of the time-dynamics of energy transfer in photosynthetic proteins and of the f -electron physics of lanthanide elements and compounds at high pressures.

Recent Progress and Future Directions

I. The electronic structure of warm dense matter

Matter at solid-like and higher densities that is also at temperatures of order a few eV to somewhat past the Fermi energy is frequently referred to as ‘warm dense matter’ (WDM). In this regime, all but the lightest species will still be partially (rather than fully) ionized, resulting in a highly complex admixture of the physics typical of plasmas and that of condensed phases. This regime, whose fundamental interest is seasoned by strong technical relevance for fusion science and direct representation of the thermodynamic conditions of several astrophysical and planetary phenomenon, is seeing emergent interest from both the plasma and condensed phase communities.

However, the highly transient nature of such experiments at large-scale laser facilities and x-ray free electron lasers poses unique challenges for the determination of even the most basic state variables (*e.g.*, pressure, temperature, density, and ionization state). This limitation is critically impeding progress toward understanding of the equation of state or toward any consequent, comprehensive microscopic treatment. As a case in point, WDM thermometry is in a uniquely difficult situation compared to any other regime of quasi-equilibrium matter: no thermometry from other fields of science is applicable to WDM, and the dominant methods used in WDM (specifically, based on inelastic x-ray scattering) are extremely sensitive to models of electronic structure that (to date) have inherently poor applicability outside of the WDM regime.

We are developing improved theoretical tools whose treatment of all atomic and condensed-phase effects can actually be validated against ambient-condition, high-resolution IXS results collected at synchrotron light-sources before being applied to the much poorer-quality IXS spectra that are typical of WDM studies at major laser-plasma facilities and x-ray free electron lasers. Our work includes a real-space Green’s function

treatment of the valence contribution to the IXS spectrum [8], a reinvestigation and gross correction of methods used to treat the core contribution to IXS in WDM experiments,[5] and a comprehensive comparison of methods from solid-state physics and from the plasma community for the treatment of the valence electronic structure in a ‘tepid’ regime, at low, but nonzero, levels of ionization.[1]

II. Time-resolved Studies of Energy Transfer and Electron Correlations

First, lanthanide compounds and coordination complexes are responsible for a wide range of light-gathering and light-emitting applications, including as commercial phosphors in lighting applications, as tools to better match the solar spectrum to the function of photovoltaic devices, and as a critical component in many bioassays. In this lattermost role, an organic ‘antenna’ acts as a strong near-UV photoabsorber before nonradiatively transferring energy to a chelated, trivalent lanthanide ion via a $4f$ - $4f$ intrashell excitation. This dipole-forbidden excitation subsequently decays through the so-called ‘hypersensitive’ pseudo-quadrupolar decay, giving light at delays as long as 1 msec after the initial excitation due to the long lifetime for the $4f$ excitation. This long time-delay allows simplest time-gate filtering of the emission from the luminescent lanthanide complex from that of the host biological system.

The microscopic physics underlying each step in the energy transfer pathway in the luminescent lanthanides, and indeed in all materials used for the applications described above, remain incompletely understood. Our recent work at the Advanced Photon Source on luminescent lanthanide complexes may have high impact in this field by demonstrating an unexpected, but clear expression of the $4f$ intrashell excitation in the time-resolved x-ray absorption near-edge spectrum (XANES) of the lanthanide ion. While a conclusive explanation of this feature will require repeating the experiment with life-time broadening suppression by high-energy resolution fluorescence detection (i.e., resonant IXS, likely requiring the Linac Coherent Light Source), the leading explanations require either an unexpectedly large local structural conformation upon excitation or else a surprisingly dynamic coupling between the $4f$ and $5d$ orbitals of the lanthanide ion. [3]

Second, also at the Advanced Photon Source, we have completed our first beamrun to investigate the time-dynamics of the local structure of unstrained, single-crystal VO_2 nanobeams when forced through the metal-insulator transition by photoabsorption in the valence band. Initial results are promising, requiring one more beamrun to resolve a difficulty with sample ablation. This study follows our completed study of the ambient condition, polarization-dependent XANES of the same samples. [4] Given the uncertain, but possibly influence of strains on the dynamics of the metal-insulator transition, this study may provide the first unbiased perspective on the linkage between electronic and structural degrees of freedom at this purportedly pure Mott-like transition.

III. Instrument development and Instrument-related Collaborations

The PI’s group has a long record in x-ray instrument development and in sharing new experimental technology with facilities and other teams. Under this award, we have further developed the ‘miniXES’ x-ray emission spectrometers [10,11] and started new work on polycapillary-coupled spectrometers for experiments with more modest needs in energy resolution. [6] The miniXES instruments continue to provide a stream of solid

collaborations [*e.g.*, 7, 9]. We have also invested considerable effort to optimize the performance of polycapillary-coupled Bragg spectrometers by enhancing the integral reflectivity of the analyzer crystal by as much as a factor of five through programmed crystallographic damage. [6] The resulting instruments dramatically enhance the options for x-ray emission spectroscopy as a tool to understand the local electronic and magnetic structure of $4f$ species in diamond anvil cells, allowing critical distinction between different theoretical models of $4f$ delocalization at the volume collapse transition. [2]

References

1. B.A. Mattern, C. Fortman, G.T. Seidler, S. Glenzer, "Solid-State Effects in the Electronic Structure of Warm Dense Matter," *in preparation*, Phys. Rev. Lett. (2012).
2. J.A. Bradley, M. Lipp, B.A. Mattern, D. Mortensen, G.T. Seidler, P. Chow, and Y. Xiao, "Toward a general understanding $4f$ delocalization in Rare Earth systems," *in preparation*, Nature Physics (2012).
3. J.I. Pacold, G.T. Seidler, D. Tatum, K. Raymond, X. Zhang, A. Stickrath, D. Mortensen, "New Insights into the Energy Transfer Processes in Luminescent Lanthanide Complexes Probed by Time-Resolved X-ray Absorption Spectroscopy," *in preparation*, Journal of the American Chemical Society (2012).
4. J.I. Pacold, G.T. Seidler, and D. Cobden, "Polarization-dependent X-ray absorption near edge structure across the VO_2 metal-insulator transition," *in preparation*, Phys. Rev. Lett. (2012).
5. B.A. Mattern and G.T. Seidler, "Correct, and Incorrect, Treatments of the Bound-Free Contribution to x-ray Thomson Scattering," *in preparation*, Phys. Rev. B (2012).
6. S.M. Heald, G.T. Seidler, D. Mortensen, B. Mattern, J.A. Bradley, N. Hess, M. Bowden, "Recent Tests of X-ray Spectrometers Using Polycapillary Optics," *submitted*, Proceedings of SPIE (2012).
7. K.M. Davis, B.A. Mattern, J.I. Pacold, T. Zakharova, D. Brewé, I. Kosheleva, R.W. Henning, T.J. Graber, S.M. Heald, G.T. Seidler, Y. Pushkar, "Fast Detection Allowing Analysis of Metalloprotein Electronic Structure by X-ray Emission Spectroscopy at Room Temperature," *accepted*, journal of Physical Chemistry Letters **3**, 1858 (2012).
8. B.A. Mattern, G.T. Seidler, J.J. Kas, J.I. Pacold, J.J. Rehr, "Real-Space Green's Function Calculation of Compton Profiles," Phys. Rev. B **85**, 115135 (2012).
9. J.A. Bradley, K.T. Moore, M. J. Lipp, B.A. Mattern, J.I. Pacold, G. T. Seidler, P. Chow, E. Rod, Y. Xiao, and W. J. Evans, " $4f$ electron delocalization and volume collapse in praseodymium metal," Phys. Rev. B **85**, 100102 (2012).
10. J.I. Pacold, J.A. Bradley, B.A. Mattern, M.J. Lipp, G.T. Seidler, P. Chow, Y. Xiao, E. Rod, B. Rusthoven, and J. Quintana, "A miniature X-ray emission spectrometer (miniXES) for high-pressure studies in a diamond anvil cell," J. Synch. Rad. **19**, 245 (2012).
11. B.A. Mattern, G.T. Seidler, M. Haave, J.I. Pacold, R.A. Gordon, J. Planillo, J. Quintana, B. Rusthoven, "A Plastic Miniature X-ray Emission Spectrometer (miniXES) based on the Cylindrical von Hamos Geometry," Rev. Sci. Instrum. **83**, 023901 (2012).

DYNAMICS OF FEW-BODY ATOMIC PROCESSES

Anthony F. Starace

*The University of Nebraska
Department of Physics and Astronomy
855 North 16th Street, 208 Jorgensen Hall
Lincoln, NE 68588-0299*

Email: astarace1@unl.edu

PROGRAM SCOPE

The goals of this project are to understand, describe, control, and image processes involving energy transfers from intense electromagnetic radiation to matter as well as the time-dependent dynamics of interacting few-body, quantum systems. Investigations of current interest are in the areas of strong field (intense laser) physics, attosecond physics, high energy density physics, and multiphoton ionization processes. Nearly all proposed projects require large-scale numerical computations, involving, e.g., the direct solution of the full-dimensional time-dependent or time-independent Schrödinger equation for two-electron (or multi-electron) systems interacting with electromagnetic radiation. In some cases our studies are supportive of and/or have been stimulated by experimental work carried out by other investigators funded by the DOE AMOS physics program. Principal benefits and outcomes of this research are improved understanding of how to control atomic processes with electromagnetic radiation and how best to transfer energy from electromagnetic radiation to matter.

RECENT PROGRESS

A. Evidence of the $2s2p(^1P)$ Doubly-Excited State in the Harmonic Generation Spectrum of Helium

We have solved the full-dimensional time-dependent Schrödinger equation for a two-active-electron system (helium) in an intense and ultrashort laser field in order to study the role of electron correlation in the resonant enhancement of some harmonics in the HHG spectrum. Our non-perturbative numerical calculations have identified signatures of the well-isolated He $2s2p(^1P)$ autoionizing state on the 9th, 11th, and 13th harmonics for a range of driving laser frequencies ω_L that put these harmonics in resonance with that state (from the ground state). Despite the fact that He is the simplest and most fundamental multi-electron system, our results show that isolating the resonant enhancement of the particular harmonics we investigated is complicated by both low-order multiphoton resonances with singly-excited states and also by resonant coupling between different autoionizing states. Nevertheless, our results show that when resonant coupling between doubly-excited states is absent, the resonant enhancement of the He $2s2p(^1P)$ autoionizing state on the 9th and 13th harmonics is clearly observable when one examines the ratio of the harmonic powers of these two harmonics with those of their lower order neighboring harmonics. These ratios serve to remove the effect of low-order multiphoton resonances with singly-excited states and thus isolate the effect of the resonance with the autoionizing state. Experimental observation of our predicted results seems feasible for experiments employing a spatially-shaped (flat-top) focus. However, even for a Gaussian-shaped driving laser pulse, our results show that resonance behavior as a function of driving laser frequency may be observable. Moreover, the predicted results appear to be reasonably insensitive to variations of intensity. In particular, the energy shifts of the resonance maxima with driving laser intensity appear to be smaller in magnitude than the widths of the resonance profiles. (*See reference [5] in the publication list below.*)

B. Perturbation Theory Analysis of Ionization by a Chirped Few-Cycle Attosecond Pulse

The angular distribution of electrons ionized from an atom by a chirped few-cycle attosecond pulse has been analyzed using the perturbation theory (PT) approach developed in Ref. [3], keeping terms in the transition amplitude up to second order in the pulse electric field. The dependence of the asymmetries in the ionized electron distributions on both the chirp and the carrier-envelope phase (CEP) of the pulse are explained physically using a simple analytical formula that approximates the exactly calculated PT result. This approximate formula (in which the chirp dependence is explicit) reproduces reasonably well the chirp-dependent oscillations of the electron angular distribution asymmetries found numerically by solving the time-dependent Schrödinger equation, as in Ref. [2]. It can also be used to determine the chirp rate of the attosecond pulse from the measured electron angular distribution asymmetry. (*See reference [6] in the publication list below.*)

C. Attosecond Streaking in the Low-Energy Region

We have analyzed few-cycle XUV attosecond pulse carrier-envelope-phase effects on ionized electron momentum and energy distributions in the presence of a few-femtosecond IR laser pulse. Whereas attosecond streaking usually involves high-energy photoelectrons, when photoelectrons have low initial kinetic energies, the IR field can provide a remarkable degree of control of the continuum-electron dynamics. Specifically, a short IR laser pulse can guide some initially ionized electrons back to the parent ion, from which they can rescatter and interfere with directly ionized electrons, thus providing a kind of holographic image of the ionic potential. By increasing the IR laser pulse length, multiple returns of low energy continuum electrons are shown to arise. Using a semiclassical model, we show that the various possible trajectories of the photoelectrons in the continuum can be revealed by the interference patterns exhibited in the low-energy photoelectron spectrum. Our analysis explains the unusual asymmetric structures predicted previously [L.Y. Peng, E.A. Pronin, and A.F. Starace, *New J. Phys.* **10**, 025030 (2008)] by direct solution of the time-dependent Schrödinger equation. (*See reference [7] in the publication list below.*)

D. Two-photon double ionization of helium: Evolution of the joint angular distribution

By directly solving the time-dependent, full-dimensional, two-electron Schrödinger equation for He in the field of a laser pulse, we investigate the two-photon double-ionization (TPDI) process for the case of XUV laser pulses in both the nonsequential and the sequential regimes. We have carried out a systematic analysis of the joint angular distribution (JAD) of the two ionized electrons as a means to elucidate the role of electron correlations in TPDI. In direct (nonsequential) double ionization, the back-to-back emission pattern always dominates, indicating the importance of electron correlations in the intermediate state (i.e., during the interaction of the electrons with the laser pulse). Such a pattern in the JAD is found to be a general one for any energy sharing for photon energies less than 54.4 eV. This distribution pattern thus serves as a hallmark of electron correlation in the intermediate state. In the sequential double-ionization regime, if the two electrons share the excess energy equally, the dominant correlation mechanism is similar to that of the nonsequential double-ionization regime. However, for extremely unequal energy sharing, the Coulomb repulsion between the electrons in the final state (after the end of the laser pulse) becomes the dominant electron correlation effect. Finally, for both the nonsequential and sequential regimes, initial-state electron correlation effects have been identified in the JAD patterns. Namely, an uncorrelated initial state produces only a few angular momentum partial waves in the TPDI process, whereas a correlated ground state produces a richer number of partial waves. The number of partial waves has been shown to greatly affect the pattern of the JAD. These various investigations have

thus demonstrated the value of the JAD as a means of elucidating two-electron dynamics. (*See reference [8] in the publication list below.*)

E. Validity of Factorization of the High-Energy Photoelectron Yield in Above-Threshold Ionization of an Atom by a Short Laser Pulse

We have derived quantum mechanically an analytic result for the above-threshold ionization (ATI) probability that is valid in the high-energy part of the ATI plateau for a short laser pulse of any shape and duration. Factorization of this probability in terms of an electron wave packet function (dependent primarily on laser field parameters) and the field-free cross section for elastic electron scattering (EES) (dependent primarily on the target atom) is shown to occur only for the case of an ultrashort pulse. In general, the probability involves interference of different EES amplitudes involving laser-field-dependent electron momenta. These analytic results allow one to describe very accurately the left-right asymmetry as well as the large-scale (intracycle) and fine-scale (intercycle) oscillations in ATI spectra. In fact, agreement with results of accurate numerical solutions of the time-dependent Schrödinger equation is excellent. To use our results, only the field-free EES amplitude for the target atom and the solutions of certain classical equations describing the active electron motion for a given short laser pulse are needed. Our analytic formulas thus provide an efficient tool for the quantitative description of short-pulse ATI spectra, both elucidating the physics of the process and allowing experimentalists to plan and/or control the processes they investigate. (*See reference [9] in the publication list below.*)

F. Enhanced Asymmetry in Few-Cycle Attosecond Pulse Ionization of He in the Vicinity of Autoionizing Resonances

By solving the two-active-electron, time-dependent Schrödinger equation in its full dimensionality, we investigate the carrier-envelope-phase (CEP) dependence of single ionization of He to the $\text{He}^+(1s)$ state triggered by an intense few-cycle attosecond pulse with carrier frequency ω corresponding to the energy $\hbar\omega = 36$ eV. Effects of electron correlations are probed by comparing projections of the final state of the two-electron wave packet onto (i) field-free highly-correlated Jacobi matrix wave functions with (ii) projections onto uncorrelated Coulomb wave functions. Significant differences are found in the vicinity of autoionizing resonances. Owing to the broad bandwidths of our 115-as and 230-as pulses and their high intensities (1-2 PW/cm²), asymmetries are found in the differential probability for ionization of electrons parallel and antiparallel to the linear polarization axis of the attosecond laser pulse. These asymmetries stem from interference of the one- and two-photon ionization amplitudes for producing electrons with the same momentum along the linear polarization axis. Whereas these asymmetries generally decrease with increasing ionized electron kinetic energy, we find a large enhancement of this asymmetry in the vicinity of two-electron doubly-excited (autoionizing) states on an energy scale comparable to the widths of the autoionizing states. The CEP-dependence of the energy-integrated asymmetry agrees very well with the predictions of time dependent perturbation theory [3]. (*See reference [10] in the publication list below.*)

FUTURE PLANS

Our group is currently carrying out research on the following additional projects:

(1) CEP Effects in Ionization Plus Excitation of He

By solving the two-active-electron, time-dependent Schrödinger equation in its full dimensionality, we are currently investigating XUV few-cycle attosecond pulse ionization plus excitation processes in He. Our results exhibit great sensitivity to the carrier-envelope phase of the attosecond pulse.

(2) *Potential Barrier Features in Three-Photon Ionization Processes in Atoms*

We are currently calculating an extensive set of model potential results on the frequency dependence of three-photon ionization cross sections from inner subshells of rare gas and other closed-shell atoms. These results show that the potential barrier effects we discovered for two-photon ionization processes in the XUV regime [4] persist also for three-photon processes. We have used third order perturbation theory in the X-ray field and sum intermediate states using the well-known Dalgarno-Lewis method (A. Dalgarno and J.T. Lewis, *Proc. R. Soc. A* **233**, 70 (1955)). When one or more photons are above threshold, we employ a complex coordinate rotation method to calculate the three-photon amplitude (B. Gao and A.F. Starace, *Computers in Physics* **1**, 70 (1987)).

PUBLICATIONS STEMMING FROM DOE-SPONSORED RESEARCH (2009 – 2012)

- [1] A. V. Flegel, M. V. Frolov, N. L. Manakov, and Anthony F. Starace, “Plateau Structure in Resonant Laser-Assisted Electron-Atom Scattering,” *Phys. Rev. Lett.* **102**, 103201 (2009).
- [2] L.Y. Peng, F. Tan, Q. Gong, E.A. Pronin, and A.F. Starace, “Few-Cycle Attosecond Pulse Chirp Effects on Asymmetries in Ionized Electron Momentum Distributions,” *Phys. Rev. A* **80**, 013407 (2009).
- [3] E. A. Pronin, A. F. Starace, M. V. Frolov and N. L. Manakov, “Perturbation Theory Analysis of Attosecond Photoionization,” *Phys. Rev. A* **80**, 063403 (2009).
- [4] L.-W. Pi and A.F. Starace, “Potential Barrier Effects in Two-Photon Ionization Processes,” *Phys. Rev. A* **82**, 053414 (2010).
- [5] J.M. Ngoko Djiokap and A.F. Starace, “Evidence of the $2s2p(^1P)$ Doubly Excited State in the Harmonic Generation Spectrum of He,” *Phys. Rev. A* **84**, 013404 (2011).
- [6] E.A. Pronin, A.F. Starace, and L.-Y. Peng, “Perturbation Theory Analysis of Ionization by a Chirped, Few-Cycle Attosecond Pulse,” *Phys. Rev. A* **84**, 013417 (2011).
- [7] M. Xu, L.-Y. Peng, Z. Zhang, Q. Gong, X.-M. Tong, E.A. Pronin, and A. F. Starace, “Attosecond Streaking in the Low-Energy Region as a Probe of Rescattering,” *Phys. Rev. Lett.* **107**, 183001 (2011).
- [8] Z. Zhang, L.-Y. Peng, M.-H. Xu, A. F. Starace, T. Morishita, and Q. Gong, “Two-Photon Double Ionization of Helium: Evolution of the Joint Angular Distribution with Photon Energy and Two-Electron Energy Sharing,” *Phys. Rev. A* **84**, 043409 (2011).
- [9] M.V. Frolov, D.V. Knyazeva, N.L. Manakov, A.M. Popov, O.V. Tikhonova, E.A. Volkova, M.-H. Xu, L.-Y. Peng, and A.F. Starace, “Validity of Factorization of the High-Energy Photoelectron Yield in Above-Threshold Ionization of an Atom by a Short Laser Pulse,” *Phys. Rev. Lett.* **108**, 213002 (2012).
- [10] J.M. Ngoko Djiokap, S.X. Hu, W.-C. Jiang, L.-Y. Peng, and A.F. Starace, “Enhanced Asymmetry in Few-Cycle Attosecond Pulse Ionization of He in the Vicinity of Autoionizing Resonances,” *New J. Phys.* **14**, xxxxxx (2012). [*Scheduled for publication in the Focus Issue on “Correlation Effects in Radiation Fields.”*]

FEMTOSECOND AND ATTOSECOND LASER-PULSE ENERGY TRANSFORMATION AND CONCENTRATION IN NANOSTRUCTURED SYSTEMS

DOE Grant No. DE-FG02-01ER15213

Mark I. Stockman, PI

Department of Physics and Astronomy, Georgia State University, Atlanta, GA
30303

E-mail: mstockman@gsu.edu, URL: <http://www.phy-astr.gsu.edu/stockman>

Current year Grant Period of 2011-2012 (Publications 2010-2012)

1 Program Scope

The program is aimed at theoretical investigations of a wide range of phenomena induced by ultrafast laser-light excitation of nanostructured or nanosize systems, in particular, metal/semiconductor/dielectric nanocomposites and nanoclusters. Among the primary phenomena are processes of energy transformation, generation, transfer, and localization on the nanoscale and coherent control of such phenomena.

2 Recent Progress and Publications

Publications resulting from the grant during the period of 2010-2012 are [1-14]. During the current grant period of 2011-2012, the following articles with this DOE support have been published [7-14]. Additionally, the following major articles are currently submitted [15, 16]. This grant has provided major support for the following articles published and submitted during the current period of 2011-2012: [9, 10, 13, 16]. Below we highlight the current-period articles that we consider most significant.

2.1 Ultrafast Dynamic Metallization of Dielectric Nanofilms by Strong Single-Cycle Optical Fields [7]

This is a significant development and generalization of our recent work [1] on the adiabatic metallization. The system under consideration is a dielectric (or, wide-band semiconductor such as diamond, zinc oxide, or gallium nitride) film of several nanometer thickness. Nanofilms of this thickness are used, in particular, as gate oxide insulators in field-effect transistors. In Ref. [7], we have predicted a dynamic metallization effect where an *ultrafast* (single-cycle) optical pulse with a $\lesssim 1 \text{ V/\AA}$ field causes plasmonic metal-like behavior of such a dielectric nanofilm. This manifests itself in plasmonic oscillations of polarization and a significant population of the conduction band evolving on a $\sim 1 \text{ fs}$ time scale. These phenomena are due a combination and mutual influence of both adiabatic (reversible) and diabatic (irreversible) pathways. The underlying adiabatic phenomena are Wannier stark localization and the related formation of Wannier-Stark ladder of electronic states spaced by the Bloch oscillation frequency and the appearance of the localized states (quantum bouncers) at the surfaces of the nanofilm. In ultrafast fields, the metallization is related to anticrossing of the quantum-bouncer levels

originating from the valence and conduction band. This theoretical work stimulated the recently submitted articles [15, 16].

2.2 Nanoplasmonics: The Physics behind the Application [9]

Nanoplasmonics is a relatively young science but it has already but it is reach in phenomena that lead to important applications in physics, chemistry, biomedicine, environmental monitoring and national security. In this feature article [9] in the most widely read professional physics journal, *Physics Today*, we have considered the fundamental phenomena of nanoplasmonics in their relation to the applications that they have inspired and are underlying.

2.3 Spaser Action, Loss Compensation, and Stability in Plasmonic Systems with Gain [10, 11]

This work deals with one of the most important problems in nanooptics and nanoplasmonics: extremely high optical losses in existing plasmonic metamaterials render them practically unusable. One of the ways proposed to mitigate or even completely eliminate those losses is based on adding a gain medium and using quantum amplification to compensate those losses [17, 18]. This approach is based on our idea of spaser [3, 19, 20].

We have developed [10, 11] a general analytical theory of the loss compensation in dense resonance metamaterials, which all the existing optical metamaterials are. We have demonstrated that the conditions of spaser generation and the full loss compensation in a dense resonant plasmonic-gain medium (metamaterial) are identical. Consequently, attempting the full compensation or overcompensation of losses by gain will lead to instability and a transition to a spaser state. This will limit (clamp) the inversion and lead to the limitation on the maximum loss compensation achievable. The criterion of the loss overcompensation, leading to the instability and spasing, is given in an analytical and universal (independent from system's geometry) form.

2.4 Nearfield Enhanced Electron Acceleration from Dielectric Nanospheres by Intense Few-Cycle Laser Fields [13]

This work has been inspired to a significant degree by our recent work on metallization of dielectrics by intense optical fields [1, 7]. It is expected that in the optical fields of magnitude $\sim 1 \text{ V/\AA}$ dielectric may behave, under certain circumstances, as metals – see Sec. 2.1.

Collective electron motion in condensed matter typically unfolds on a sub-femtosecond timescale. The well-defined electric field evolution of intense, phase-stable few-cycle laser pulses provides an ideal tool for controlling this motion. The resulting manipulation of local electric fields at nanometer spatial and attosecond temporal scales offers unique spatio-temporal control of ultrafast nonlinear processes at the nanoscale, with important implications for the advancement of nanoelectronics. In this article [13] we have demonstrated the attosecond control of the collective electron motion and directional emission from isolated dielectric (SiO_2) nanoparticles with phase-stabilized few-cycle laser fields. A novel acceleration mechanism leading to the ejection of highly energetic electrons is identified by the comparison of the results to quasi-classical model calculations. The observed lightwave control in nanosized dielectrics has important implications for other material groups, including semiconductors and metals.

2.5 Optical-field-induced current in dielectrics [15]

The time it takes to switch on and off electric current determines the rate at which signals can be processed and sampled in modern information technology. Field-effect transistors are able to control currents at frequencies beyond ~ 100 GHz, but electric interconnects may hamper progress towards the terahertz (THz) frontier. All-optical injection of currents via interfering photo-excitation pathways or photoconductive switching of THz transients has permitted controlling electric current on a subpicosecond time scale in semiconductors. Insulators have been deemed unsuitable for both concepts, because of the need for either UV light or high fields, which induce either slow damage or ultrafast breakdown, respectively.

In this article [15], we report the feasibility of electric signal manipulation in a dielectric. A few-cycle optical waveform increases reversibly – free from breakdown – the (ac) conductivity of amorphous silicon dioxide (fused silica) by more than 18 orders of magnitude within 1 femtosecond, allowing electric currents to be driven, directed, and switched by the *instantaneous field of light*. This work opens a route to extending electronic signal processing and high-speed metrology into the petahertz domain. (This article has been submitted to Nature and is still being listed as “Under Consideration” as of today. We have received a notification from the Nature editorial office that it is likely to be accepted.)

3 Directions of Work for the Next Period

We will develop the success in the optics of ultrastrong and ultrafast fields on the nanoscale. One of the most important future directions will be the inclusion of phase-controlled femtosecond pulses and attosecond pulses to induce and study the metallization and other strong field phenomena in dielectrics. We are also developing theory of metals in ultrastrong and ultrafast optical fields on the order of several $\text{V}/\text{\AA}$, where we intend to describe sub-optical cycle field-effect control. This research is being conducted in a close collaboration with the group of Prof. F. Krausz of the Max Planck Institute for Quantum Optics (Garching at Munich, Germany). It has a great fundamental potential and promises important applications to ultrafast signal processing with a petahertz rate (bandwidth).

References

1. M. Durach, A. Rusina, M. F. Kling, and M. I. Stockman, *Metallization of Nanofilms in Strong Adiabatic Electric Fields*, Phys. Rev. Lett. **105**, 086803-1-4 (2010).
2. A. Rusina, M. Durach, and M. Stockman, *Theory of Spoof Plasmons in Real Metals*, Appl. Phys. A **100**, 375-1-4 (2010).
3. M. I. Stockman, *The Spaser as a Nanoscale Quantum Generator and Ultrafast Amplifier*, Journal of Optics **12**, 024004-1-13 (2010).
4. M. I. Stockman, *Dark-Hot Resonances*, Nature **467**, 541-542 (2010).
5. M. I. Stockman, *A Fluctuating Fractal Nanoworld*, Physics **3**, 90 (2010).
6. T. Utikal, M. I. Stockman, A. P. Heberle, M. Lippitz, and H. Giessen, *All-Optical Control of the Ultrafast Dynamics of a Hybrid Plasmonic System*, Phys. Rev. Lett. **104**, 113903-1-4 (2010).
7. M. Durach, A. Rusina, M. F. Kling, and M. I. Stockman, *Predicted Ultrafast Dynamic Metallization of Dielectric Nanofilms by Strong Single-Cycle Optical Fields*, Phys. Rev. Lett. **107**, 0866021-5 (2011).

8. I.-Y. Park, S. Kim, J. Choi, D.-H. Lee, Y.-J. Kim, M. F. Kling, M. I. Stockman, and S.-W. Kim, *Plasmonic Generation of Ultrashort Extreme-Ultraviolet Light Pulses*, Nat. Phot. **5**, 677-681 (2011).
9. M. I. Stockman, *Nanoplasmonics: The Physics Behind the Applications*, Phys. Today **64**, 39-44 (2011).
10. M. I. Stockman, *Spaser Action, Loss Compensation, and Stability in Plasmonic Systems with Gain*, Phys. Rev. Lett. **106**, 156802-1-4 (2011).
11. M. I. Stockman, *Loss Compensation by Gain and Spasing*, Phil. Trans. R. Soc. A **369**, 3510-3524 (2011).
12. M. I. Stockman, *Nanoplasmonics: Past, Present, and Glimpse into Future*, Opt. Express **19**, 22029-22106 (2011).
13. S. Zherebtsov, T. Fennel, J. Plenge, E. Antonsson, I. Znakovskaya, A. Wirth, O. Herrwerth, F. Suessmann, C. Peltz, I. Ahmad, S. A. Trushin, V. Pervak, S. Karsch, M. J. J. Vrakking, B. Langer, C. Graf, M. I. Stockman, F. Krausz, E. Ruehl, and M. F. Kling, *Controlled near-Field Enhanced Electron Acceleration from Dielectric Nanospheres with Intense Few-Cycle Laser Fields*, Nature Physics **7**, 656-662 (2011).
14. S. H. Chew, F. Sussmann, C. Spath, A. Wirth, J. Schmidt, S. Zherebtsov, A. Guggenmos, A. Oelsner, N. Weber, J. Kapaldo, A. Gliserin, M. I. Stockman, M. F. Kling, and U. Kleineberg, *Time-of-Flight-Photoelectron Emission Microscopy on Plasmonic Structures Using Attosecond Extreme Ultraviolet Pulses*, Appl. Phys. Lett. **100**, 051904-4 (2012).
15. A. Schiffrin, T. Paasch-Colberg, N. Karpowicz, V. Apalkov, D. Gerster, S. Mühlbrandt, M. Korbman, J. Reichert, M. Schultze, S. Holzner, J. V. Barth, R. Kienberger, R. Ernstorfer, V. S. Yakovlev, M. I. Stockman, and F. Krausz, *Optical-Field-Induced Current in Dielectrics*, Nature, (Submitted) (2012).
16. M. Schultze, E. M. Bothschafter, A. Sommer, S. Holzner, W. Schweinberger, M. Fiess, M. Hofstetter, R. Kienberger, V. Apalkov, V. S. Yakovlev, M. I. Stockman, and F. Krausz, *Controlling Dielectrics with the Electric Field of Light*, Nature, (Submitted) (2012).
17. V. M. Shalaev, *Optical Negative-Index Metamaterials*, Nat. Phot. **1**, 41-48 (2007).
18. S. Xiao, V. P. Drachev, A. V. Kildishev, X. Ni, U. K. Chettiar, H.-K. Yuan, and V. M. Shalaev, *Loss-Free and Active Optical Negative-Index Metamaterials*, Nature **466**, 735-738 (2010).
19. D. J. Bergman and M. I. Stockman, *Surface Plasmon Amplification by Stimulated Emission of Radiation: Quantum Generation of Coherent Surface Plasmons in Nanosystems*, Phys. Rev. Lett. **90**, 027402-1-4 (2003).
20. M. I. Stockman and D. J. Bergman, *Surface Plasmon Amplification by Stimulated Emission of Radiation (Spaser) [US Patent 7,569,188]*, USA Patent No. 7,569,188 (August 4, 2009).

Laser-Produced Coherent X-Ray Sources

Donald Umstadter, Department of Physics and Astronomy, 257 Behlen Laboratory, University of Nebraska, Lincoln, NE 68588-0111, donald.umstadter@unl.edu

Program Scope

In this project, we experimentally and theoretically explore the physics of novel x-ray sources, based on the interactions of ultra-high-intensity laser light with matter. X-rays in the energy range 10 keV – 1 MeV can be produced by Thomson (inverse Compton) scattering of intense laser light with laser-accelerated electrons. Because the x-rays produced from such a source have sub-angstrom wavelength, and femtosecond pulse duration, they can provide information on the structure of matter with atomic-scale resolution, simultaneously on both the spatial and temporal scale lengths. Moreover, because the electron beam is accelerated by the ultra-high gradient of a laser-driven wakefield, the combined length of both the accelerator and wiggler regions is only a few millimeters. Consequently, such a source can have a university-laboratory-scale footprint. Matter under extreme conditions can be studied with pump-probe experiments with any combination of these x-ray, electron, or laser beams.

This project involves the physics at the forefront of relativistic plasma physics and beams, as well as relativistic nonlinear optics. Applications include the study of ultrafast chemical, biological and physical processes, such as inner-shell atomic processes, phase transitions, and vacuum-assisted ionization. Industrial applications include non-destructive evaluation, large-standoff-distance imaging of cracks, and remote sensing.

Recent Results

High-brightness x-ray source with multi-MeV energy and femtosecond duration

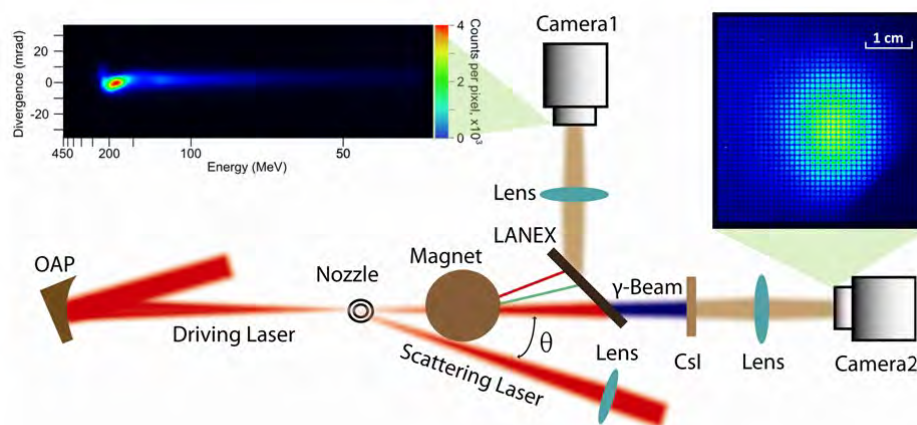


Figure 1: Schematic of the experimental setup for all-optical inverse Compton backscattering. Left inset shows the electron energy spectrum as recorded by a 12-bit CCD camera image of the fluorescent screen (LANEX). Right inset shows the gamma ray profile measured by the CsI(Tl) detector and 14-bit EMCCD camera.

In this latest phase of the project, we succeeded in generating MeV energy x-rays by means of Compton-scattering. Figure 1 shows the schematic of the experimental setup of our all-laser-driven Compton γ -ray source. Our design employs two independently adjustable laser pulses from the same high-peak-power laser system—one to accelerate electrons by driving a high-gradient laser wakefield, and one to scatter. This allowed for independent optimization of both the electron bunch and scattering laser pulse, which

were spatially overlapped (and temporally synchronized) with micron (femtosecond) accuracy. The drive laser system delivers a peak power of > 100 TW at a repetition rate of 10 Hz. The laser-driven electron accelerator delivers beams with energy up to 800 MeV and divergence of 2 mrad.

The total photon number achieved with our source was measured to be 2×10^7 ; the source size was $5 \mu\text{m}$; and the beam divergence angle was ~ 10 mrad. The peak brightness is four orders of magnitude higher than obtained by conventional Compton sources. The x-ray photon energy, peaked at 1 MeV, and reaching up to 4 MeV, exceeds the thresholds for fundamental nuclear processes (e.g., pair production and photodisintegration). The typical experimental parameters of the x-ray beam can be found in Table 1.

Parameter	Sym	Value
Source size	σ	$5.1 \pm 2.6 \mu\text{m}$ (RMS)
Divergence	θ	12.7 mrad (FWHM)
Peak energy	E	1.2 MeV
Total photon number/pulse	N	$\sim 10^7$
Peak on-axis brilliance	B	2.3×10^{19} photons/s- $\text{mm}^2\text{-mrad}^2$ (0.1% BW)

Table 1: Typical experimental parameters for the x-ray beam

Modelling of x-ray source

We developed our own benchmarked numerical code to calculate the angle-resolved γ -ray spectrum, using as input the experimentally measured characteristics of the ω_0 -beam and e -beam. The simulated γ -ray parameters were then used as the input for a Monte-Carlo simulation (MCNPX code) in order to produce a simulated x-ray beam profile image that could be compared to the measured one, shown in Figure 1 (right inset). With the input electron spectrum shown in Figure 1 (left inset), the simulated γ -ray beam profile had a divergence of 11.3 mrad, consistent with the experimentally measured value, 12.7 mrad. The simulation also predicted a total photon number of 2×10^7 , twice the number measured experimentally, which is within the uncertainty originating from fluctuations of the input parameters (degree of overlap, etc.).

Laser-driven electron accelerator

We have continued our effort into improving our understanding of, and control of, electron beam dynamics in laser-wakefield accelerators (LWFA), since the x-ray beam quality depends critically on the quality of the electron-beam driver. As a result of this effort, we have demonstrated a scalable high-energy electron source based on laser wakefield acceleration. The electron accelerator is operated in the blowout regime. We can show that the accelerator produces high-quality, quasi-monoenergetic electron beams in the range 100-800 MeV, using 30-80 TW, 30 fs laser pulses. These beams have low angular divergence of 1-4 mrad, and small energy spread (5-25 %), with a resulting brightness 10^{11} electrons mm^{-2} MeV^{-1} mrad^{-2} . The beam parameters can be tuned by varying the laser and plasma conditions. The use of a high-quality laser pulse and appropriate target conditions enables optimization of beam quality, such that a significant fraction of the charge is contained in the monoenergetic peak. The approach is scalable to multi-GeV energy beams by the use of PW-class laser pulses.

Upgrade of laser system to PW peak power

An upgrade of the DIOCLES laser system to increase its power level from 100 TW to 0.7 PW has been completed. A new amplifier and compressor stage were installed in order to increase the beam energy from 5 J to 25 J and compress the amplified beam to 30 fs. Diagnostics were installed to measure and optimize the laser system characteristics. The original system, used to drive the above-mentioned electron and x-ray sources, was comprised of an oscillator, stretcher, and 4 multipass amplifiers. The latter are comprised of Ti:S crystals pumped by Nd:YAG pump lasers operating at 532 nm. The amplified 5-J energy pulse was compressed to 30-fs pulse duration in a standard two-grating pulse compressor, resulting in a peak power of >100 TW at 10-Hz repetition rate.

The laser pulse is characterized at full power with a multi-stage beam sampling system that enables all diagnostic measurements to be made in real-time. The laser system was fully characterized with respect to pulse parameters (energy, spectrum, pulse duration, spatial profile, and nanosecond contrast) and stability (both energy and pointing angle, from minutes to hours). All measurements were done with the laser operating at full output, and the beam sampled with a wedge, a beam attenuation system comprised of a waveplate and polarizer's, and a final sampling wedge after compression. Contrast measurements on the femtosecond and picosecond time scale employed a scanning third-order autocorrelator. The laser system is also equipped with an acousto-optic spectrum modulator to compensate for gain narrowing and spectral shifting during amplification, which permits optimization of the laser pulse spectral characteristics and control of the temporal pulse profile.

Future Plans:

Further development of the x-ray source

In order to operate in the x-ray photon energy regime that is more relevant to atomic physics, we will demonstrate energy tunability over the range 10 keV to 100 keV. This will be accomplished by tuning the energy of electron accelerator, which we have previously demonstrated. The 10-fs x-ray pulse duration, which is inferred from measurements of the electron bunch duration, is shorter than that produced from x-ray synchrotrons or K-alpha x-ray sources, and is comparable to x-ray free-electron lasers. We also plan to demonstrate repetitive operation of the x-ray source at 10-Hz rate.

Ultrafast pump-probe experiments

We also plan to implement an experimental capability to use the x-ray source for ultrafast science in pump-probe geometry. While any combination of x-rays, electrons, or optical photons is possible in principle, we intend to first demonstrate several simple geometries. By permitting the use of standard cross-correlation techniques, these pump-probe measurements will also serve to verify the x-ray pulse duration. For instance, using an *x-ray pump and laser probe*, we can use the technique of x-ray-induced transient reflectivity cross-correlation.ⁱ Using a *laser pump (at low power) and an x-ray probe*, we can also measure the x-ray pulse duration by means of transient diffraction efficiency changes of crystalline structures induced by laser-disordering.ⁱⁱ

Finally, by using a *petawatt-power laser pump and x-ray probe*, we can merge high-field physics with ultrafast science. Light at the focus of the upgraded laser can reach the highest intensities ever achieved in the laboratory, up to 10^{23} W/cm². At this intensity level, matter can thus be exposed to extreme field strengths: 870 TV/m. This is sufficient to ionize gallium to the hydrogen-like stage by means of over the barrier field ionization.ⁱⁱⁱ In this ultra-high intensity regime, an electron can gain energy in the electromagnetic field—in the form of quiver energy—up to 217 times its rest mass energy. At such intensities, it is expected that not only will the electrons of ionized media relativistically quiver in the laser fields, but protons will also begin to quiver significantly.

DOE-Sponsored Publications (published within last three years)

1. S. Banerjee *et al.*, "Generation of tunable, 100-800 MeV quasi-monoenergetic electron beams from a laser-wakefield accelerator in the blowout regime," *Phys Plasmas* 19 (5), 056703 (2012).
2. B. M. Cowan *et al.*, "Computationally efficient methods for modelling laser wakefield acceleration in the blowout regime," arXiv:1204.0838v1, (Wed, 4 Apr 2012).
3. Ghebregziabher, B. Shadwick and D. Umstadter, "Spectral bandwidth reduction of Thomson scattered light by pulse chirping," arXiv 1204.1068, (2012).
4. S. Y. Kalmykov *et al.*, "Electron self-injection into an evolving plasma bubble: quasi-monoenergetic laser-plasma acceleration in the blowout regime." *Physics of Plasmas* 18 (5), (2011).
5. V. Ramanathan *et al.*, "Submillimeter-resolution radiography of shielded structures with laser-accelerated electron beams," *Phys. Rev. Spec. Top.-Accel. Beams* 13 (10), (2010).
6. S. Banerjee *et al.*, in Conference on Lasers and Electro-Optics/International Quantum Electronics Conference, Anonymous (Optical Society of America, 2009) pp. paper JFB2.
7. D. Umstadter *et al.*, in AIP Conf. Proc. 1099, APPLICATION OF ACCELERATORS IN RESEARCH AND INDUSTRY: Twentieth International Conference, Anonymous (American Institute of Physics, 2009) pp. 606.
8. S. Baghchi *et al.*, in Conference on Lasers and Electro-Optics/International Quantum Electronics Conference, Anonymous (OSA Technical Digest (CD), Optical Society of America, 2009) pp. paper JThE51.
9. N. J. Cunningham *et al.*, in AIP Conference Proceedings; Journal Volume: 1099; Journal Issue: 1; Conference: CAARI 2008: 12. international conference on application of accelerators in research and industry, Anonymous (American Institute of Physics, International Atomic Energy Agency (IAEA), 2009) pp. 638.
10. Banerjee, S., Powers, N., Ramanathan, V., Shadwick, B., Umstadter, D., "Stable, monoenergetic 50-400 MeV electron beams with a matched laser wakefield accelerator," *Proceedings of PAC09, Particle Accelerator Conference 2009 A14 Advance Concepts, (TH4GBC02)*, (2009).
11. V. Ramanathan *et al.*, in Lasers and Electro-Optics, 2009 and 2009 Conference on Quantum electronics and Laser Science Conference. CLEO/QELS 2009. Conference on, Anonymous 2009) pp. 1-2.

ⁱ O. Krupin *et al.*, "Temporal cross-correlation of x-ray free electron and optical lasers using soft x-ray pulse induced transient reflectivity," *Optics Express*, **20**, pp.11396-11406 (2012).

ⁱⁱ A.L. Cavalieri, "Clocking femtosecond x-rays," *Phys. Rev. Lett.* **94**, 114801 (2005).

ⁱⁱⁱ M. Protopapas, C. H. Keitel, *et al.*, "Atomic physics with super-high intensity lasers," *Reports on Progress in Physics* **60**, 389-486 (1997).

New scientific frontiers with ultracold molecules

Jun Ye

JILA, National Institute of Standards and Technology and University of Colorado

Boulder, Colorado 80309-0440

Ye@jila.colorado.edu

On the experimental front cold polar molecules (OH and YO molecules), we have recently achieved two major breakthroughs. The first is the observation of direct evaporative cooling of OH molecules in a magnetic trap. The second is the implementation of the first magneto-optic trap (1D and 2D) for YO. OH molecules are prepared by Stark deceleration followed by loading in a permanent magnetic trap, resulting in a Boltzmann distribution with a 60 mK temperature. We first observed two-body collisions. When we implemented forced evaporation by using a radio frequency knife to selectively remove relatively hot molecules, we observed more than a factor of 10 decrease in the sample temperature, with a corresponding increase in the phase space density by 100. This research direction is extremely exciting, as we expect to be able to further cool the molecules to a much lower temperature. On the other front, extending the magneto-optical trapping technique to diatomic molecules promises to be a general method for the creation of ultracold systems with new, complex interactions. We have demonstrated one and two-dimensional transverse laser cooling and magneto-optical trapping of the diatomic molecule yttrium monoxide (YO). A quasi-closed cycling transition allows us to scatter >1000 photons, resulting in 1-dimensional Doppler cooling of a YO molecular beam from a temperature 25 mK to 5 mK. With the addition of a quadrupole magnetic field we observe additional cooling of the YO beam due to a magneto-optical restoring force and achieve temperatures as low as 3 mK.

In joint work with Debbie Jin and building on the previous success of producing a rovibronic ground-state molecular quantum gas in a single hyperfine state, we have realized long-lived ground-state polar molecules in a 3D optical lattice, with a lifetime of up to 25 s, which is limited only by off-resonant scattering of the trapping light. Starting from a 2D optical lattice, we observe that the lifetime increases dramatically as a small lattice potential is added along the tube-shaped lattice traps. The 3D optical lattice also dramatically increases the lifetime for weakly bound Feshbach molecules. For a pure gas of Feshbach molecules, we observe a lifetime of greater than 20 s in a 3D optical lattice; this represents a 100-fold improvement over previous results. This lifetime is also limited by off-resonant scattering, the rate of which is related to the size of the Feshbach molecule. Individually trapped Feshbach molecules in the 3D lattice can be converted to pairs of K and Rb atoms and back with nearly 100% efficiency.

*Author Index
and
List of Participants*

Agostini, P.	159, 163
Becker, A.	119
Belkacem, A.	30, 65, 66, 75
Ben-Itzhak, I.	23, 25, 26, 29, 30, 31, 53, 54
Berrah, N.	2, 5, 123
Bogan, M.	89, 91, 93, 100
Bohn, J.	127
Bucksbaum, P.	2, 89, 91, 104
Buth, C.	1, 4, 5, 6, 9, 10, 12, 13, 15
Centurion, M.	131
Chu, S.I.	135
Cocke, C.L.	23, 29, 30, 31, 53
Côté, R.	139
Cundiff, S.T.	143
Dantus, M.	147
DeCamp, M.	151
DeMille, D.	155
DiMauro, L.	2, 159, 163
Doumy, G.	1, 2, 3, 4, 5, 7, 8, 9, 10, 13, 14
Doyle, J.	167
Dunford, R.W.	1, 4, 7, 8, 15
Eberly, J.H.	169
Elser, V.	173
Esry, B.D.	23, 25, 26, 33
Feagin, J.M.	1177
Gaffney, K.	89, 91, 108
Gallagher, T.F.	181
Gessner, O.	75, 87
Gould, P.	185
Greene, C.H.	189
Gühr, M.	89, 91, 93, 115
Haxton, D.	65, 70, 75
Head-Gordon, M.	75
Ho, T.S.	261
Jones, R.R.	193
Kanter, E.P.	1, 2, 4, 6, 7, 8, 9, 14, 15
Kapteyn, H.C.	197
Klimov, V.	61
Kling, M.	23, 30, 31, 37, 53, 54
Krässig, B.	1, 2, 4, 8, 13, 15
Kumarappan, V.	23, 41, 42, 58
Landers, A.	30, 201
Leone, S.	75
Lin, C.D.	23, 31, 45
Lucchese, R.	57, 58, 257
Lundeen, S.R.	205
Macek, J.H.	209
Manson, S.T.	213
March, A.M.	1, 4, 7, 8, 9, 10, 14
Martínez, T.J.	89, 91, 93, 112
Matsika, S.	217

McCurdy, C.W.	65, 70, 75
McKoy, V.	221
Miller, T.A.	159
Msezane, A.Z.	225
Mukamel, S.	229
Murnane, M.M.	197, 233
Nelson, K.A.	233
Neumark, D.	75
Novotny, L.	237
Orel, A.E.	30, 241
Orlando, T.M.	245
Ourmazd, A.	249
Pelton, M.	1, 16
Phaneuf, R.A.	253
Poliakoff, E.	57, 257
Rabitz, H.	261
Reis, D.	2, 10, 89, 91, 97
Rescigno, T.N.	30, 65, 70
Robicheaux, F.	265
Rocca, J.J.	269
Rose-Petruck, C.	273
Rudenko, A.	23, 49, 54
Scherer, N.	1, 16
Schoenlein, R.W.	75
Schwander, P.	249
Seideman, T.	93, 277
Seidler, G.T.	281
Southworth, S.H.	1, 2, 4, 6, 7, 8, 9, 10, 13, 14, 15
Starace, A.F.	285
Stockman, M.I.	289
Thumm, U.	23, 53, 54
Trallero, C.A.	23, 42, 57, 58, 59
Umstadter, D.	293
Weber, Th.	30, 65, 66, 75
Weinacht, T.	217
Ye, J.	297
Young, L.	1, 2, 4, 6, 7, 8, 10, 14, 15, 23, 49, 54

Participants

Jamil Abo-Shaeer
DARPA
675 North Randolph Street
Arlington, VA 22203
Phone: 571-218-4399
E-Mail: jamil.abo-shaeer@darpa.mil

Pierre Agostini
Ohio State University
191 W. Woodruff Ave.
Columbus, OH 43210
Phone: 614-247-4734
E-Mail: agostini@mps.ohio-state.edu

Paul Baker
Army Research Office
4300 S. Miami Blvd.
Durham, NC 27703-9142
Phone: 919-549-4202
E-Mail: Paul.M.Baker1@us.army.mil

Andreas Becker
JILA and Department of Physics
440 UCB, University of Colorado
Boulder, CO 80309-0440
Phone: 303-492-7825
E-Mail: andreas.becker@colorado.edu

Ali Belkacem
Lawrence Berkeley National Laboratory
Mail Stop 2R0100
Berkeley, CA 94720
Phone: 510-486-7778
E-Mail: abelkacem@lbl.gov

Michael Bogan
SLAC National Accelerator Laboratory
2575 Sand Hill Road
Menlo Park, CA 94025
Phone: 650-926-2731
E-Mail: mbogan@slac.stanford.edu

John Bohn
JILA
UCB 440
Boulder, CO 80305
Phone: 202-492-5426
E-Mail: bohn@murphy.colorado.edu

Christian Buth
Argonne National Laboratory
9700 South Cass Avenue
Argonne, IL 60439
Phone: 630-252-1397
E-Mail: cbuth@anl.gov

Michael Casassa
Department of Energy
19901 Germantown Rd.
Germantown, MD 20874
Phone: 301-903-0448
E-Mail: michael.casassa@science.doe.gov

Martin Centurion
University of Nebraska - Lincoln
Jorgensen Hall, 855 North 16th Street
Lincoln, NE 68588
Phone: 402-472-5810
E-Mail: mcenturion2@unl.edu

Shih-I Chu
University of Kansas
Department of Chemistry, Malott Hall
Lawrence, KS 66045
Phone: 785-864-4094
E-Mail: sichu@ku.edu

C.L. Cocke
Kansas State University
Physics Dept., 116 Cardwell Hall
Manhattan, KS 66506
Phone: 785-532-1609
E-Mail: cocke@phys.ksu.edu

Participants

Robin Côté
University of Connecticut
2152 ilside Road, U-3046
Storrs, CT 06269
Phone: 860-486-4912
E-Mail: rcote@phys.uconn.edu

Steven Cundiff
JILA
440 UCB
Boulder, CO 80309
Phone: 303-492-7858
E-Mail: cundiff@jila.colorado.edu

Marcos Dantus
Michigan State University
58 Chemistry Building
East Lansing, MI 48823
Phone: 517-881-4562
E-Mail: dantus@msu.edu

Matthew DeCamp
University of Delaware
217 Sharp Laboratory
Newark, DE 19716
Phone: 302-831-2671
E-Mail: mdecamp@udel.edu

David DeMille
Yale University
Physics Dept., P.O. Box 208120
New Haven, CT 06520
Phone: 203-432-3833
E-Mail: david.demille@yale.edu

Louis DiMauro
The Ohio State University
191 W. Woodruff Ave. #4178
Columbus, OH 43210
Phone: 614-688-5726
E-Mail: jackson.1926@osu.edu

Roberto Diener
Booz Allen Hamilton
3811 North Fairfax Drive
Arlington, VA 22203
Phone: 703-248-3406
E-Mail: diener_roberto@bah.com

Gilles Doumy
Argonne National Laboratory
9700 S. Cass Ave.
Argonne, IL 60439
Phone: 630-252-2588
E-Mail: gdoumy@aps.anl.gov

John Doyle
Harvard University
17 Oxford St.
Cambridge, MA 02138
Phone: 617-495-3201
E-Mail: doyle@physics.harvard.edu

Robert Dunford
Argonne National Laboratory
9700 S. Cass Ave.
Argonne, IL 60439
Phone: 630-252-4052
E-Mail: dunford@anl.gov

Veit Elser
Cornell University
426 PSB
Ithaca, NY 14853
Phone: 607 255-2340
E-Mail: ve10@cornell.edu

Brett Esry
J.R. Macdonald Lab, Kansas State
University
116 Cardwell Hall
Manhattan, KS 66506
Phone: 785-532-1620
E-Mail: esry@phys.ksu.edu

Roger Falcone
Lawrence Berkeley National Laboratory
One Cyclotron Road Mailstop 80R0114
Berkeley, CA 94720
Phone: 510-486-6692
E-Mail: RWFalcone@lbl.gov

Jim Feagin
Cal State Univ Fullerton
800 North State College Blvd
Fullerton, CA 92834
Phone: 657-278-4827
E-Mail: jfeagin@fullerton.edu

Participants

Kelly Gaffney
SLAC and Stanford University
2575 Sand Hill Road
Menlo Park, Ca 94306
Phone: 650-926-2382
E-Mail: kgaffney@slac.stanford.edu

Thomas Gallagher
University of Virginia
Department of Physics
Charlottesville, VA 22904
Phone: 434-924-6817
E-Mail: tfg@virginia.edu

Oliver Gessner
Lawrence Berkeley National Laboratory
1 Cyclotron Rd
Berkeley, CA 94720
Phone: 510-486-6929
E-Mail: ogessner@lbl.gov

Phillip Gould
University of Connecticut
Physics Dept. U-3046, 2152 Hillside Rd.
Storrs, CT 06269-3046
Phone: 860-486-2950
E-Mail: phillip.gould@uconn.edu

Chris Greene
Purdue University
Department of Physics
West Lafayette, IN 47907
Phone: 765-496-1859
E-Mail: chgreene@purdue.edu

Daniel Haxton
Lawrence Berkeley National Laboratory
1 Cyclotron Road Mail Stop 2R0100
Berkeley, CA 94720
Phone: 415-412-9508
E-Mail: djhaxton@lbl.gov

Robert Jones
University of Virginia
382 McCormick Road
Charlottesville, VA 22904-4714
Phone: 434-924-3088
E-Mail: bjones@virginia.edu

Henry Kapteyn
JILA, University of Colorado at Boulder
UCB 440
Boulder, CO 80309
Phone: 303-492-8198
E-Mail: kapteyn@jila.colorado.edu

Matthias Kling
Kansas State University
116 Cardwell Hall
Manhattan, KS 66506
Phone: 785-532-6786
E-Mail: kling@phys.ksu.edu

Bertold Kraessig
Argonne National Laboratory
437 7th Ave
La Grange, IL 60525
Phone: 708-482-3891
E-Mail: kraessig@anl.gov

Jeffrey Krause
Department of Energy
19901 Germantown Rd.
Germantown, MD 20874
Phone: 301-903-5827
E-Mail: Jeff.Krause@science.doe.gov

Vinod Kumarappan
Kansas State University
328 Cardwell Hall
Manhattan, KS 66506
Phone: 785-532-3415
E-Mail: vinod@phys.ksu.edu

Allen Landers
Auburn University
206 Allison Laboratory, Physics
Auburn, AL 36849
Phone: 334-844-4048
E-Mail: landers@physics.auburn.edu

Stephen Leone
Lawrence Berkeley National Laboratory
209 Gilman Hall
Berkeley, CA 94720
Phone: 510-643-5467
E-Mail: srl@berkeley.edu

Participants

Chii Dong Lin
Kansas State University
Department of Physics, Cardwell Hall
Manhattan, KS 66506
Phone: 785-532-1617
E-Mail: cdlin@phys.ksu.edu

Robert Lucchese
Texas A&M University
Department of Chemistry
College Station, TX 77843-3255
Phone: 979-845-0187
E-Mail: lucchese@mail.chem.tamu.edu

Stephen Lundeen
Colorado State University
Dept. of Physics, Colorado State Univ.
Fort Collins, CO 80523-1875
Phone: 970-491-6647
E-Mail: lundeen@lamar.colostate.edu

Joseph Macek
University of Tennessee
401 Nielsen Physics Bldg
Knoxville, TN 37996-1200
Phone: 865-675-5541
E-Mail: jmacek@utk.edu

Steven Manson
Georgia State University
Dept. of Physics & Astronomy
Atlanta, GA 30303
Phone: 404-824-0625
E-Mail: smanson@gsu.edu

Diane Marceau
Department of Energy
19901 Germantown Rd.
Germantown, MD 20874
Phone: 301-903-0235
E-Mail: diane.marceau@science.doe.gov

Anne Marie March
Argonne National Laboratory
X-ray Science Division
Argonne, IL 60439
Phone: 630-252-4099
E-Mail: amarch@anl.gov

William McCurdy
Lawrence Berkeley National Laboratory
One Cyclotron Road
Berkeley, CA 94720
Phone: 510-486-4283
E-Mail: cwmccurdy@lbl.gov

Vincent McKoy
California Institute of Technology
120 Noyes, Caltech Chemistry 127-72
Pasadena, CA 91125
Phone: 626-395-6545
E-Mail: mckoy@caltech.edu

Michael Metcalfe
Booz Allen Hamilton - DARPA
3811 Fairfax Drive
Arlington, VA 22203
Phone: 703-248-3492
E-Mail: Metcalfe_Michael@bah.com

Alfred Z. Msezane
Clark Atlanta University
223 James P Brawley DR SW
Atlanta, GA 30314
Phone: 404-880-8663
E-Mail: amsezane@cau.edu

Shaul Mukamel
University of California, Irvine
1102 Natural Sciences II
Irvine, CA 92697-2025
Phone: 949-824-7600
E-Mail: smukamel@uci.edu

Margaret Murnane
JILA, Univ of Colorado at Boulder
UCB 440
Boulder, CO 80309
Phone: 303-492-8198
E-Mail: murnane@jila.colorado.edu

Keith Nelson
Massachusetts Institute of Technology
MIT Room 6-235
Cambridge, MA 02139
Phone: 617-253-1423
E-Mail: kanelson@mit.edu

Participants

Lukas Novotny
University of Rochester
The Institute of Optics
Rochester, NY 14627
Phone: 585-275-5767
E-Mail: novotny@optics.rochester.edu

Ann Orel
University of California, Davis
One Shields Ave.
Davis, CA 95616
Phone: 925-980-9245
E-Mail: aeorel@ucdavis.edu

Thomas Orlando
Georgia Institute of Technology
901 Atlantic Drive
Atlanta, GA 30332
Phone: 404-385-6047
E-Mail: nicole.williams@chemistry.gatech.edu

Abbas Ourmazd
University of Wisconsin
Physics, 1900 E. Kenwood Blvd
Milwaukee, WI 53211
Phone: 414-229-2610
E-Mail: ourmazd@uwm.edu

Enrique Parra
Air Force Office of Scientific Research
875 North Randolph St., Suite 325
Arlington, VA 22203
Phone: 703-696-8571
E-Mail: enrique.parra@afosr.af.mil

Mark Pederson
Basic Energy Sciences
1000 Independence Ave, SW
Washington, DC 20585-1290
Phone: 301-903-9956
E-Mail: mark.pederson@science.doe.gov

Matthew Pelton
Argonne National Laboratory
9700 S. Cass Ave.
Argonne, IL 60439
Phone: 630-252-4598
E-Mail: pelton@anl.gov

Ronald Phaneuf
University of Nevada
Department of Physics
Reno, NV 89557-0220
Phone: 775-784-6818
E-Mail: phaneuf@unr.edu

Jeffrey Pietryga
Los Alamos National Laboratory
MS J567, PO Box 1663
Los Alamos, NM 87545
Phone: 505-667-2484
E-Mail: pietryga@lanl.gov

Erwin Poliakoff
Louisiana State University
Chemistry Department
Baton Rouge, LA 70803
Phone: 225-578-2933
E-Mail: epoliak@lsu.edu

Herschel Rabitz
Princeton University
Frick Laboratory
Princeton, NJ 08544
Phone: 609-258-3917
E-Mail: hrabitz@princeton.edu

Thomas Rescigno
Lawrence Berkeley National Laboratory
1 Cyclotron Rd. MS 2-100
Berkeley, CA 94720
Phone: 510-486-8652
E-Mail: tnrescigno@lbl.gov

Francis Robicheaux
Auburn University
206 Allison Lab
Auburn University, AL 36849
Phone: 334-844-4366
E-Mail: robicfj@auburn.edu

Jorge Rocca
Colorado State University
Dept. of Electrical and Computer Eng.
Fort Collins, CO 80523
Phone: 970-491-8371
E-Mail: rocca@engr.colostate.edu

Participants

Christoph Rose-Petruck
Brown University
324 Brook Street
Providence, RI 02912
Phone: 401-863-1533
E-Mail: crosepet@brown.edu

Artem Rudenko
Kansas State University
Dept. of Physics
Manhattan, KS 66506
Phone: 785-532-1636
E-Mail: rudenko@phys.ksu.edu

Robert Schoenlein
Lawrence Berkeley National Laboratory
1 Cyclotron Rd. MS: 80-114
Berkeley, CA 94720
Phone: 510-486-6557
E-Mail: rwschoenlein@lbl.gov

Tamar Seideman
Northwestern University
2145 Sheridan Road
Evanston, IL 60208-3113
Phone: 847-467-4979
E-Mail: t-seideman@northwestern.edu

Gerald Seidler
University of Washington
Box 351560
Seattle, WA 98195-1560
Phone: 206-427-8045
E-Mail: seidler@uw.edu

Stephen Southworth
Argonne National Laboratory
Bldg. 401
Argonne, IL 60439
Phone: 630-252-3894
E-Mail: southworth@anl.gov

Anthony F. Starace
University of Nebraska
855 North 16th St, 208 Jorgensen Hall
Lincoln, NE 68588-0299
Phone: 402-472-2795
E-Mail: astarace1@unl.edu

Andrew Stickrath
Booz Allen Hamilton
3811 North Fairfax Drive, Suite 600
Arlington, VA 22203
Phone: 703-816-5200
E-Mail: stickrath@gmail.com

Mark Stockman
Georgia State University
29 Peachtree Center Ave
Atlanta, GA 30302
Phone: 678-457-4739
E-Mail: mstockman@gsu.edu

Uwe Thumm
Kansas State University
Dept. of Physics
Manhattan, KS 66506
Phone: 785-532-1613
E-Mail: thumm@phys.ksu.edu

Carlos Trallero
J.R. Macdonald Lab
116 Cardwell Hall
Manhattan, KS 66506
Phone: 785-532-0846
E-Mail: trallero@phys.ksu.edu

Donald Umstadter
University of Nebraska-Lincoln
208 Jorgensen Hall
Lincoln, NE 68588-0299
Phone: 402-472-8115
E-Mail: dpu@hfsserve.unl.edu

Thorsten Weber
Lawrence Berkeley National Laboratory
1 Cyclotron Road
Berkeley, CA 94720
Phone: 510-486-5588
E-Mail: TWeber@lbl.gov

Thomas Weinacht
Stony Brook University
Dept of Physics and Astronomy
Stony Brook, NY 11794-3800
Phone: 631-632-8163
E-Mail: thomas.weinacht@stonybrook.edu

Participants

Linda Young
Argonne National Laboratory
9700 S. Cass Ave
Argonne, IL 60439
Phone: 630-252-8878
E-Mail: young@anl.gov